

Advances in Printing and Media Technology

Vol. XXXV

Edited by Nils Enlund and Mladen Lovreček

Darmstadt
MMVIII

Advances in Printing and Media Technology

Proceedings of the 35th International Research Conference of iarigai

Valencia, Spain
September 2008

Published by the International Association
of Research Organizations for the Information,
Media and Graphic Arts Industries

Darmstadt, Germany 2008

Co-edited by
Nils Enlund, Stockholm, Sweden
Mladen Lovreček, Zagreb, Croatia

The facts published in this book are obtained from sources believed to be reliable. However, publishers can accept no legal liability for the contents of papers, nor for any information contained therein, nor for conclusions drawn by any party from it.

No part of this publication may be reproduced, stored in a retrieval system or transmitted in any form or by any means of eletronic, mechanical, photocopying, recording or otherwise without the prior written premission of the publisher.

ISBN 987-3-9812704-0-2

Printed in Croatia by Sveučilišna tiskara, Zagreb - November 2008

Contents

Introduction

Preface
Advancing the frontiers of printing and media technology research 3
Nils Enlund

Minimizing the environmental impacts of the SMEs:
a challenge for the Graphic Industry 5
Susana Otero, David Pérez, Vicente de Gracia, Juan Carlos Iglesias

Numerical simulation and investigation of processes
present in AC corona charging systems 9
Ingo Reinhold, Stephan F. Jahn, Lutz Engisch, Reinhard R. Baumann

1. Strategic issues: ecology, new media and industry structure

Ecodesign management system adapted
to the graphics arts industry: A case study 19
David Pérez, Vicente de Gracia, Juan Carlos Iglesias, Susana Otero

Changes in sustainability due to
technology development in selected printing processes 27
Pentti Viluksela, Minna Nors, Hanna Pihkola, Katri Behm, Helena Wessman, Tiina Pajula

Organized alliances in the printing industry 37
Thomas Mejtoft, Åsa Nordin

Delivery times and closeness to geographic market:
A comparison between digital and conventional printing houses 45
Thomas Mejtoft, Magnus Viström

Transaction costs and their influence on institutional arrangements
- A comparison between the Swedish and the German printing industry 55
Sven Packmohr, Thomas Mejtoft

Implementing TQM in graphic arts industry by six sigma - A case study 67
Rajendrakumar Anayath, Kiran P Prayagi

Profiling ecosolvent inkjet printers 69
Richard M. Adams II, Mark Gundlach

Distributing and publishing newspaper content on a digital TV-platform 79
Olli Nurmi, Atte Kortekangas

Magazine product structure and workflow control
between a publisher and a printing house 91
Olli Kuusisto, Hannele Antikainen, Janne Pajukanta

Business from hybrid media and printed functionality 101
Ulf Lindqvist, Pertti Moilanen

Typography on web banners 107
Klementina Možina, Romana Horvat

2. Printing and printing materials

Pressroom draw variation and its impact on web breaks
Part I: Newspaper pressroom trials 119
Nina Deng, Frédéric Parent, Tony Manfred, Joe Aspler, Jean Hamel

Extended operating maintenance model for modern printing machines 129
Csaba Horvath, Zoltan Gaal, Katalin Kerekes

Removing the constraints in publication printing. A potential paradigm shift! 137
Anders Bjurstedt

A new test method to measure dynamic contact in a printing nip for rotogravure papers 147
Janet Preston, Roger Bollström, Kenneth Nylander, Martti Toivakka, Jouko Peltonen

Influence of plasma activation on absorption of
ink components and dampening water in sheet-fed offset printing 155
Maiju Pykönen, Hanna Silvaani, Janet Preston, Pedro Fardim, Martti Toivakka

Flexographic print quality of pilot coated paperboard 169
Robert Olsson, Li Yang, Magnus Lestelius

Ink Transfer during flexographic printing to paper 181
Tiothy C. Claypole, David G. Beynon, Simon M. Hamblyn

Evaluation of the ink transfers of prints using low-angle shaving system 189
Yasushi Ozaki, Naoko Fujisawa, Eiji Kawamura

The effects of surface treatment on
digital print quality of extrusion coated paperboard 195
Johanna Lahti, Mikko Tuominen, Jurkka Kuusipalo

Surface properties and UV ink-jet printability of recycled polyolefins 209
Diana Gregor-Svetec, Tadeja Muck, Goraz Golob

Insight into IJ-ink/paper interaction using drop spreading model 213
Marie Kaplanová, Lenka Otáhalová, Tadeja Muck

Theoretical investigation into pigment-resin binding energies and 223
conformations associated with the magenta bodying reaction of water-based inks
Scott Williams

Toner spreading during the fixing stage 231
Elina Hakola, Pirkko Oittinen, Jorma Koskinen, Ulla Forsström

Curing of UV ink and product safety 237
Merja Kariniemi, Anu Ilmonen, Eija Kenttä, Satu Sundqvist, Birgit Aurela

In situ monitoring of the photo polymerization
of UV curable acrylate coatings 245
Elena-Magdalena Casagrande, Andreas Hörner, Achim Wixforth

Considerations for thermally engineered
coated printing papers: focus on electrophotography 249
Philip Gerstner, Patrick A. C. Gane

Highly accurate material characterization of paper
for the simulation of printing processes 263
Thomas Kaulitz, Edgar Dörsam

In situ monitoring of the photo polymerization
of UV curable acrylate coatings 245
Elena-Magdalena Casagrande, Andreas Hörner, Achim Wixforth

Considerations for thermally engineered
coated printing papers: focus on electrophotography 249
Philip Gerstner, Patrick A. C. Gane

Highly accurate material characterization of paper
for the simulation of printing processes 263
Thomas Kaulitz, Edgar Dörsam

3. Special printing

Colour control with dual separation for daylight and daylight/infrared light 273
Ivana Žiljak, Jana Žiljak Vujić, Klaudio Pap

Gravure printing of enzymes and phages 279
Tarik Jabrane, Jawad Jeaidi, Martin Dubé, Patrice J. Mangin

Rotogravure for printed electronics 289
*Alexandra Pekarovicova, Erika Hrehorova, Paul D. Fleming,
Marian Rebros, Margaret K. Joyce*

The impact of conductive carbon properties on print performance 299
E. H. Jewell, T. C. Claypole, S. R. Roberts, D. C. Bould

Security printing for product packaging in industrial printing applications 307
Slavtcho Bonev, Bernhard Wirnitzer

Integration of screen-printed antennas
in plastic body parts using in-mould technology 313
Ingmar Petersen, Gunter Hübner, Markus Pfletschinger

4. Color reproduction and quality

High definition halftone printing - HDHP: background,
current status and challenges of the adaptive screening developments 323
Yuri V. Kuznetsov

Finding optimum screen combinations for
flexible hybrid screening technologies in flexography lithography 333
Yung-Cheng Hsieh, Hui-Wen Cheng

Implementation of global and local thresholding
algorithms in image segmentation of coloured prints 341
Miha Lazar, Aleš Hladnik

Method of objective evaluation the fine detail distortion in process of screening 347
Yuri V. Kuznetsov, Denis E. Zheludev

Colour Management - differences arising
between analogue and digital photo colour reproduction chains 355
Kristiina Saukkoriipi, Päivi Miettinen

Improved gamut boundary determination for colour gamut mapping 365
Arne M. Bakke, Ivar Farup, Jon Y. Hardeberg

Predictability of spot color overprints 373
Robert Chung, Michael Riordan, Sri Prakhya

Quality control and colour assessment for
flexography and gravure printing based on machine vision 381
Andrés Navarro-López, José F. Caballero-Aroca, José J. Esteve-Taboada, Juan Hervás-Juan, Emilio Ribes-Gómez

Developing a test-procedure for newsprint color quality evaluation 389
Fons Put

Use of static and dynamic device link profiles:
incidence on colorimetric accuracy and ink savings 397
Amélie Trichon, Lionel Chagas, Elie Khoury, François Fournié, Nadia Hassissi

Estimating the spectral reflectance of
fluorescent offset papers for varying illuminants 405
Eva Maria Löffler, Phil Green

Improving inter-instrument agreement in colour and density measurement 413
Andrew Williams

Causes of matt/gloss effects ("ghosting") in sheet-fed offset 421
Uwe Bertholdt, Gina Sommer

Measurement possibilities of interference layers on a paper 429
Marta Klanjšek Gunde, Maša Žveglič, Nina Hauptman, Gorazd Golob

Index of authors 437



Introduction

Advancing the frontiers of printing and media technology research

Nils Enlund

Co-editor, Chairman of the Program Committee

KTH - Royal Institute of Technology
Media Technology and Graphic Arts
Stockholm, Sweden

E-mail: nilse@kth.se

Preface

The scientific studies included in this volume provide an overview of current international research in the broad and diverse field of media and printing technology. The book contains the scientific and technical research contributions presented at the 35th International Research Conference of iarigai, the International Association of Research Organizations for the Information, Media and Graphic Arts Industries, held in Valencia, Spain, on September 7-10, 2008. The contributions, selected by a scientific board of international experts through a double-blind review process, present recent scientific work aiming at the advancement of printing and media technology and at a better understanding of the processes and changing conditions of the media industry.

We set the stage for the reviewed research reports by opening this volume with two specially invited contributions. The organization hosting the conference, AIDO, introduces the theme of environmental considerations in the printing industry with a case study on ecodesign management. The theme of special printing technologies is introduced through a paper by a young promising researcher, Ingo Reinhold, who won the award for the best student presentation at the Printing Future Days in 2007.

The printing and media industry faces great challenges as the world in which it operates rapidly changes. In the first section of this book we address questions of high strategic importance: environmental issues, industry restructuring, quality management, alternative content distribution methods and channels, as well as business considerations. In order to remain competitive, the industry must learn from the findings of independent researchers investigating threats and possibilities within these fields.

The second section is concerned with the printing processes and the materials used for printing. The included papers address productivity, printability, runnability, print quality, ink transfer as well as pigments, inks, coatings and substrates. In the third section, the focus is on new developments in special printing techniques and applications: security printing, printed electronics and enzyme printing. There are many exciting new developments in this field.

The final section of the current volume discusses color reproduction and color quality. The included papers report findings on high definition halftone printing, screening techniques, color management, testing and measuring methods, and many other highly topical issues.

Scientific and technical progress is mostly incremental and the results presented here are definitely advancing the frontiers of knowledge. You may find studies that will be of immediate use in your present activities or you may scan the content for future reference. In any case, they will certainly prove valuable both for researchers and practitioners in our field.



Minimizing the environmental impacts of the SMEs: a challenge for the graphic industry

Susana Otero, David Pérez, Vicente de Gracia, Juan Carlos Iglesias

Technological Institute of Optics, Colour and Imaging, AIDO
C/ Nicolás Copérnico 7-13
46980 Paterna, Valencia
E-mail: aido@aido.es

Abstract

Minimizing the environmental impacts is a commitment that we should acquire in all areas of everyday activity with special attention to industrial activity, which should move towards sustainable growth. The Sustainable Development was described by the Brundtland Commission in the Report "Our Common Future" in 1987 as "development that meets the needs of the present without compromising the ability of future generations to meet their own needs". However, traditionally it has been considered that minimizing the environmental impacts, development and industrial growth are not compatible; and most entrepreneur in general feel that to guide their production in a sustainable manner must make large investments, a great economic effort, suffering an apparent loss of competitiveness.

The specificity of the industrial fabric in the printing industry, more than 85% of the industrial structure is composed by SMEs employing less than 20 workers (Intergraf), makes particularly difficult taken the best practices in order to reduce the environmental impact of their activity, basically because the SMEs do not have qualified technical employees for this task to assume the challenge from within the company. Initiatives such as the BREF document from the European Commission are the first step, but the definitive one is to know how to carry the BATs to the SMEs jointly with implementation procedures in order to facilitate its implementation in the printing companies. The real challenge is to establish guidelines that facilitate the adoption of the best environmental practice in daily production while also demonstrating that a lower environmental impact and competitiveness are not incompatible.

Keywords

BATs, best practices, environment, graphic industry, sustainability

1. Introduction

The term **"Best Available Techniques"** is defined in Article 2 of the Directive 96/61/CE as "the most effective and advanced stage in the development of activities and their methods of operation which indicate the practical suitability of particular techniques for providing in principle the basis for emission limit values designed to prevent and, where that is not practicable, generally to reduce emissions and the impact on the environment as a whole".

The BAT (Best Available Techniques) Referent Document (BREF) titled "Surface Treatment Using Organic Solvents (STS)", belongs to this family of documents published by the European Commission, with the collaboration of Intergraf, and affect to the following installations included at the Annex 1 of the **Directive 96/61/CE**: "installations for the surface treatment of substances, objects or products using organic solvents, in particular for dressing, printing, coating, degreasing, waterproofing, sizing, painting, cleaning or impregnating, with a consumption capacity of more than 150 kg per hour or more than 200 tones per year".

In the graphic industry there are three printing processes that use solvents on a large scale: heatset web offset, flexible packaging and publication gravure, in which the BREF are focused, but this represent only medium and big companies and we must take into account that more than 85% of the graphic enterprises are small companies, so they are out the scope of the BREF. But, joining the total emissions of the all small printing companies we can state that the environmental impact is similar or, even, bigger than the one produced by the big companies. However, the main part of the Techniques indicated in the BREF can be extrapolated to SME graphic enterprises which use others printing systems, as Sheet-Fed Offset.

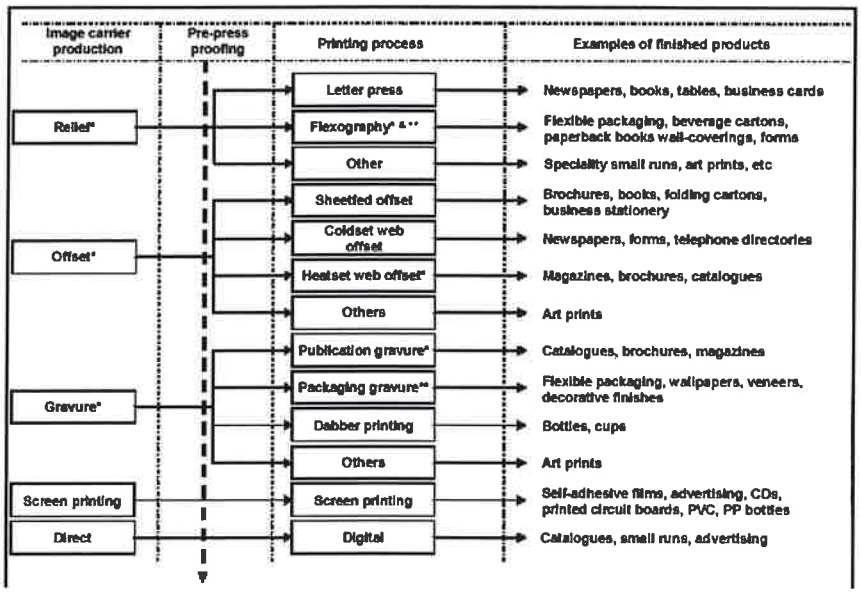


Figure 1: Overview of printing systems
Source: BREF "Reference Document on Best Available Techniques on Surface Treatment Using Organic Solvents"

"The Graphic Industry consists of a minority of large companies and a majority of small family businesses" (Intergraf). The above mentioned industry features a well fragmented sector, with roughly a 85% of enterprises employing less than 20 workers. In the organizational structure of these SMEs it doesn't appear a responsible person in the environmental management. Usually, the production chain manager is the person in charge of the environmental subject. So, it is possible to state that there is a lack of skilled staff about environmental issues (including environmental legislation) in the printing companies.

For that reason, the environmental impact of the Graphic Industry, specially VOCs emissions, requires a technical support which guides easily the SMEs printers to get a proper eco-efficient solution in their production processes without any decreasing of the quality and competitiveness required by the market.

2. Minimizing the environmental impacts of the SMEs: a challenge for the graphic industry

As has mentioned before, the majority of the printing companies in Europe are small companies, most businesses are family-owned, and they have a weak financial structure and less capacity to invest in non productive activities. For that reason, the implementation of BATs in SMEs printers has some added problems, related with their structure. There are three factors which reduce the possibilities of implementing BATS:

- There are a lot printing companies with less than 10 employees and without any technical expert in the environmental management field.
- Nowadays, the market conditions force them to give the costumers a quick service, so they don't have time enough for studying the legislation and developing variations on their processes.
- And, specially, the BREF document does not include any recommendations or procedure about how to implement correctly these BATs in their company.

On the other hand, a lot of prejudice about sustainability and the environmental management are extended across the entrepreneurs. Basically:

- A lot of investment and a big economic effort are needed in the printing houses in order to be respectful with the environment.
- An environmental production decreases the printing quality and the competitiveness of the printing houses.

Finally, the BREF document and other information related with good practices and environment management, usually, don't reach the majority of the printing companies and the whole of SMEs unknown the best way to reduce or minimize the environmental impact of their daily production. There also, obviously, differences in the implementation of BATs depending on the country of the European Union, so nowadays the knowledge about implementing BATs in an efficient way is quite heterogeneous around Europe.

3. Ways to sustainability: BATs, Best practices and Eco-strategies

From the last 15 years new eco-strategies have been developed in order to minimize the environmental impact of the product's life cycle, retaining or increasing the functionality or value of the product, such as design for environment (DfE) or eco-design, defining an eco-efficient product as "a product or process that simultaneously meets cost, quality, and performance goals, minimizes environmental impacts and maximizes conservation of valuable resources". Most of these strategies can be applied to the graphic industry; we can find some studies and initiatives from 1992 applying the DfE methodology to the printing industry. And recently, in the thesis "Developing tools for sustainability management in the graphic arts industry", Maria Enroth has enumerated the most significant aspects for the graphic arts industry and printed product (Widding et al. 1999, Widding and Enroth 2000) to be taken into account for environmental work in the graphic industry:

- The use of printing paper (or other printing substrates);
- The use of non-renewable materials;
- The handling and use of chemical products, including printing ink;
- The use of energy;
- Transportation;
- Emissions of volatile organic compounds (VOC) to the air;
- The handling and use of electronics.

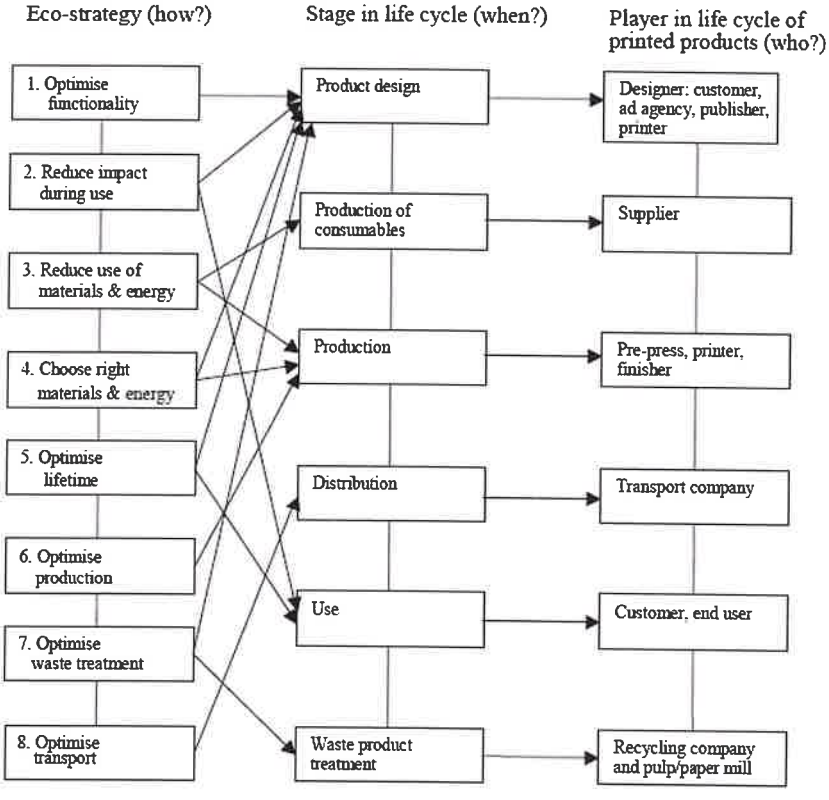


Figure 2: Eco-strategies, numbered here from 1-8, for working with design for environment (DfE)
Source: Enroth, Maria. "Developing tools for sustainability management in the graphic arts industry"

On the other hand, even though some of the printing techniques are outside of the BREF recommendations, there are a lot of BATs which can be applied to the SMEs Sheet-Fed Offset printing houses such as:

- Replacement of conventional inks.
- Reducing emission from the dampening solution.
- Filtering the dampening solution.
- Cleaning.

The challenge is to approximate the information to the whole of the printing companies in an easy and understandably way; giving an outline about how to implement all those eco-strategies that minimize the environmental impact, keeping the quality of the printing product and the competitive of the printing house at the same time. Ultimately, the implementation guideline proposed should be taken easily and should assure the minor extra-cost for the company.

4. BATs-GRAPH: a guideline to minimize the environmental impact of the printing SMEs

The environmental impact of the Graphic Industry, specially VOCs emissions, requires a technical support which guides the SMEs printers to get a proper eco-efficient solution in their production processes without any decreasing of the quality and competitiveness required by the market.

The BATs-GRAPH project is designed to offer the necessary tools to make possible implementing the Best Available Techniques (BATs) for reducing VOC´s emission in the Graphic Arts production while assuring the required level of quality and competitiveness in the final product.

The project will offer to the printing companies a group of actions which will serve as a guide of environmental information directly applied to the company. These actions will allow the companies to overcome the difficulties to access the environmental information and implementing BATs in order of reducing the VOCs emissions.

Objectives:

- To extend the application of BATs included in BREF over the SMEs graphic companies.
- To motivate the European printers to integrate Best Available Technics (BATs) in the industrial graphic processes.
- To minimizes the environmental impact of the printing industry.
- To provide to the European graphic arts industry with a tool which allow them to reduce the Volatile Organic Compounds (VOCs) emissions deriving from using organic solvents.

5. Conclusions

It is necessary to guide the implementation of BATs and eco-strategies over the SMEs printers. The main challenge is to establish guidelines that facilitate the adoption of the best environmental practice in daily production while also demonstrating that a lower environmental impact and competitiveness are not incompatible.

- Minimizing the environmental impacts is not conditioned to large investments, but is adopting best practices that often reflect common sense.
- A cleaner and eco-efficient production means not only a minor environmental impact, but also an optimization of production costs and, therefore, an increase of competitiveness.

References

1. Enroth, M. (2006) "Developing tools for sustainability management in the graphic arts industry". Doctoral Thesis, Royal Institute of Technology in Stocholm (KTH), Sweden
2. Intergraf (2004) "Printing and the Environment". Publication, Intergraf and UNI-Europa Graphical in collaboration with DG Employment and Social Affairs of the EU, Brussels 2004
3. Wessman, H., Leinonen, A., Hiltunen, E., Forsell, M., Hohental-Joutsimo, C., (2007) "Customer oriented and sustainable printed paper". Proceedings from IARIGAI Conference September 2007, Grenoble, France
4. Pira International Ltd (2004) "The Future of European Printing". Publication, Pira International Ltd, United Kingdom
5. European Integrated Prevention and Pollution Control Bureau (2007) The BAT (Best Available Techniques) Reference Document (BREF) entitled "Surface Treatment Using Organic Solvents (STS), European Commission

Numerical simulation and investigation of processes present in AC corona charging systems

Ingo Reinhold[1], Stephan F. Jahn[1], Lutz Engisch[2], Reinhard R. Baumann[1]

[1] Institute for Print and Media Technology, Chemnitz University of Technology
Reichenhainer Str. 70 D-09126 Chemnitz, Germany
E-mail: ingo.reinhold@s2001.tu-chemnitz.de

[2] Queensland University of Technology, School of Physical and Chemical Sciences
GPO BOX 2434, Brisbane, Australia

Abstract

The rapid development of today's commercial printing and graphic arts industry calls for higher throughput and constantly rising imaging quality for a diversity of printing processes and machines. One of the promising technologies for high-speed digital printing is xerography. Furthermore, electro-photographic solid free-from fabrication (ESFF) has been proposed for rapid-prototyping applications [Fay, 2007]. To meet the performance requirements for rapid charging of photoconductors, increased charge current is needed, which is commonly achieved by applying AC corona charging devices, which also reduces the ion energies compared to DC discharges. This paper deals with the fundamental properties of AC corona charging systems. A 2D finite element simulation is conducted to show the space charge development and resulting surface potential of the photoconductor. Mechanisms leading to high current systems and possible drawbacks are outlined.

Keywords

Colour, gamut, newsprint, offset, visual assessment

1. Introduction

High throughput xerographic printing systems face the problem of increased charging times due to insufficient current from conventional charging systems. Therefore new charging devices were introduced to give higher surface potentials on shorter time scales [Gundlach et al., 2002].

DC corona discharge systems have been investigated since the 1920's and are even nowadays a substantial part in many application areas [Goldman et al., 1985]. However, these discharges suffer the disadvantages of low current and high ozone generation at higher operating voltages. Efficiency of these types of discharges may be increased by removal of electron-catching compounds generated during the processes as pointed out in [Kasuga et al., 1997; Yehia et al., 2000]. Furthermore, a strong increase of the applied voltage may lead to breakdown of the gap.

AC discharge systems, in contrast, offer higher charging currents at the expense of a more complicated power supply design. However, the non-deterministic processes occurring as a result of the physical and transient nature are not fully understood on long time scales. The presented paper is aimed at building understanding of the effects leading to a high current AC corona charging device and the possible resulting lateral and temporal deviations resulting from these physical phenomena. A 2D finite element analysis of an extremely simplified model is presented pointing out possible sources of the observed effects.

2. Theory

Corona discharges are based on the properties of charged bodies exposed to a high, externally applied, electric field. Through a sufficient energy gain of electrons through the acceleration resulting from the body force, these may ionize the gas through impact ionization. Ions, due to their low mobility, may not contribute to the process, but reduce the number of the electrons produced in avalanches through recombination and attachment.

Following *Trinh et al.*, corona discharges in DC may be categorized by various modes, resulting in different current characteristics [Trinh, 1995].

2.1 Positive corona

In this case, the stressed electrode is the anode. Therefore the resulting unipolar charge current toward the cathode is made of slow positive ions, while faster traveling negative ions move to the anode. These are not absorbed instantly but travel along the conductor surface (surfacial spreading) until absorption takes place.

Burst corona is a result of the ionization activity along the stressed conductor. Positive space charge produced during the discharge decreases the field on the surface of the electrode, making the discharge stop until positive ions are removed through drift. The potential gradient eventually rises above the critical value and initiates a new avalanche. Onset streamers occur due to the creation of positive space charge in the beginning of the partial breakdown. The positive ions enhance the field and attract surrounding avalanches. Therefore a streamer develops far into the drift zone with the electrons ahead of it. The cumulative effect of positive and negative space charge reduces the potential gradient and abandons the discharge. Glow is observed when the applied voltage is insufficient to create fields that allow the radial development of ionization activity. The discharge is then confined to a small portion of the space around the stressed electrode. A weak kHz contribution to the resulting DC current originates from the lateral movement of the ionization activity along the conductor surface. Breakdown streamers arise when the applied voltage is further increased. The discharge is similar to onset streamers but penetrates deeper into the conductor-surrounding space and exhibits higher intensities. As a result spots of higher positive ion concentrations may be observed along the wire surface.

2.2 Negative corona

In contrast to the aforementioned, current in negatively-coronating devices is mainly made up of negative ions and electrons, traveling the space between the stressed cathode and the substrate.

Trichel pulses have been observed and studied for a long time. The slowly moving positive ions and faster moving negative charges reduce the field around the conductor to below the threshold value, forcing the discharge to stop. A delay time is needed to remove enough positive ionic space charge and raise the surfacial potential gradient above the critical value. Therefore a pulsating current characteristic is observed. A mode often observed is negative pulseless glow and has been extensively treated by *Williams* [Williams, 1993]. This kind of homogenous discharge, especially at higher driving voltages due to the more efficient removal of ionic space charge, exhibits four localized regions: cathode fall region, glow, *Faraday* space and positive column. Negative streamer discharges at higher applied voltages exhibit essentially the same mechanisms as the negative pulseless glow, but with the formation of streamer channels in the positive column.

2.3 Alternating current corona

In AC coronating systems ionic space charge of a certain polarity is generated during the respective half cycle. Here the current comprises two different parts [Amara et al., 1989]. A part synchronous with the frequency of the applied voltage, with low currents from mainly glow discharges, and an impulse current, having high currents from the propagation of streamers. At low amplitudes of the applied voltage, the current of the negative half-wave dominates through the lower value of the onset field. However, with increasing peak-to-peak voltage, positive streamers contribute strongly to the resulting current.

3. Modeling

Many attempts have been made to simulate AC excited discharge processes. As may be seen from the aforementioned modes and physical processes, an overarching model is hard to accomplish. Simplifications have been proposed in the literature to employ various numerical techniques, such as equivalent circuits, charge simulation methods [Abdel-Salam et al., 1989; Adamiak, 1994; Rickard et al., 1991, Zhao et al., 2000] and finite element methods [Karpov, 2005; Ohsawa, 2005] with flux corrected transport [Georghiou et al., 2005, Hallac, 2005] or the method of characteristics [Zhao et al., 1996].

For the undertaken numerical investigations the following assumptions apply:

1. The volume expansion of the ionization zone is neglected and the generated charges appear directly on the conductor surface.
2. The charge injection process is simplified using the studies of *Rajzer* and *Oshawa* [Rajzer, 1991; Ohsawa, 2005].
3. The generated species during a half cycle are of positive polarity in the positive and negative in the other half cycle, respectively.
4. There are no interactions such as recombination within the drift zone.
5. The retroactivity of the deposited charges on the photo conductor is neglected. The deposited charge can be therefore calculated from the charges leaving the contemplated space.

3.1 Transport equation

For this investigation a simple model was used to simulate the movement of the charge carriers from a glow discharge confined to a small region around a stressed, cylindrical electrode. The electron motion was neglected for simplicity and rougher time stepping [Humpert, 2002]. The transport of ions then is controlled by gradients, e.g. diffusion and a volume force, e.g. drift through the electric field. Since we calculate the amount of injected space charge on the basis of the breakdown field at the surface of the stressed conductor, a conservative form of the transport equations may be utilized, as shown by *Karpov* [Karpov, 2005]. The transient problem may be described as follows.

$$\frac{\partial c_{\pm}}{\partial t} + \nabla(-D\nabla c_{\pm} \pm \mu c_{\pm}\nabla\phi) = 0 \tag{1}$$

where c is the concentration for the different ions, t is time, D is the diffusion coefficient, μ is the mobility and ϕ is the scalar electric potential. Since the space charge changes the local field Poisson's equation must be solved simultaneously.

$$\nabla \cdot (\varepsilon_r \nabla\phi) + \frac{c_+ - c_-}{\varepsilon_0} = 0 \tag{2}$$

where e is the elementary charge, ε_0 is permittivity of free space and ε_r is the permittivity of the space around the conductor.

3.2 Charge injection

For convenience we follow the studies of *Rajzer* and *Ohsawa* [Rajzer, 1991; Ohsawa, 2005] and choose a coaxial configuration to assess the amount of injected ionic space charge. According to *Abdel-Salam et al.* [Abdel-Salam et al., 2001] the different onset values are given in kV/cm by

$$E_{\text{onset}_{\pm}} = \delta\left(A_{\pm} + \frac{B_{\pm}}{\sqrt{r_0}}\right) \tag{3}$$

where δ is a surface roughness factor, A as well as B are constants and r_0 the outer radius of the coronating wire. Due to the simple geometry the electric field strength in the system is analytically given by

$$E(r) = \frac{\phi}{r\ln(R/r_0)} \tag{4}$$

where R the distance between the wire and the photoconductor or shield, respectively. Using equation 4 with $r = r_0$ with the equations 3 and 4 gives an expression for the onset value V_c of the applied voltage. Using now the results by *Rajzer* for this simple configuration enables a description of the injected charge in each half cycle.

$$c_{\pm} = \frac{4\varepsilon_0}{R^2}\begin{cases} |V - V_c|, & \text{if } |V| \geq |V_c| \\ 0, & \text{elswhere} \end{cases} \tag{5}$$

3.3 Boundary conditions

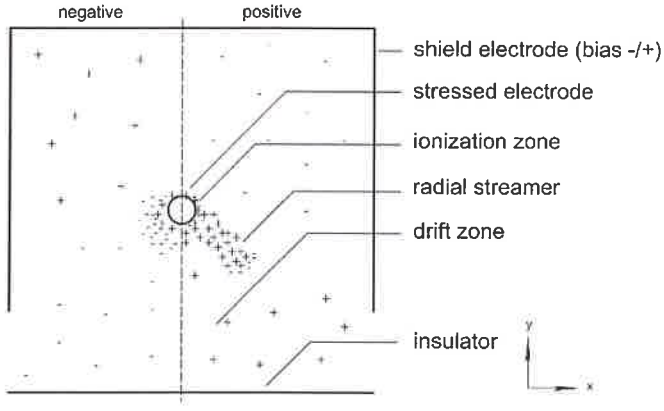


Figure 1: Schematic of the simulated geometry and principal behavior of the different half-cycles

The boundary conditions where assigned to a rectangular domain, as indicated in Figure 1. The shield is set to a certain voltage and the wire loaded with a sinusoidal voltage

$$V(t) = \bar{V}\sin(\omega t) \tag{6}$$

The bottom side of the photoconductor is on ground potential, while the shield and the edges as well as the outlets are considered to have only a normal component in the electric field strength, e.g. $\vec{n}\nabla\phi = 0$. For the charge transport equations we superimpose the concentration from equation 6 on the wire surface, e.g. absorbing wire surface, and convective flux on all other boundaries.

3.4 Fluid mechanics

In order to include the motion of the background gas on the motion of the charged bodies, the evaluation of the incompressible *Navier-Stokes* equations is given by

$$\rho\frac{\partial\vec{u}}{\partial t} + \rho(\vec{u}\nabla)\vec{u} = -\nabla p + \eta\Delta\vec{u} - (c_+ - c_-)\nabla\phi$$
$$\nabla\vec{u} = 0 \tag{7}$$

where ρ is the density of the background fluid, u is the velocity, p is the pressure and η is the dynamic viscosity. In this sense the interaction of the charges with the surrounding air is gives by their charge and the net movement due to the applied field.

The boundary conditions are no slip at the shield and the coronating wire, an inflow of 3 m/s is superimposed at the inlet (cf. Figure 1 (left)), as experiments with forced convection from this side showed an enhancement of the homegeity. The outlet (right) is left neutral.

4. Implementation

The afore explained problem was implemented in Comsol Multiphysics using the standard tools provided by the software package for geometry modeling and meshing.

The values for the different regions were chosen to be consistent with *Karpov* [Karpov, 2005] frequency (f) 7000 Hz, amplitude 7500 V, permittivity of free space (ε_0) 8.85 pF/m, permittivity of the photoconductor (ε_r) 5, mobility of the ions (μ) 2 x 10^{-4} m^2 $(Vs)^{-1}$, the diffusion coefficient (D) 5.3 x 10^{-5} m^2/s, the density of air (ρ_{air}) 1.23 kg m^{-3}, the viscosity of air (η_{air}) 1.8 x 10^{-5} Pa s and a photoconductor velocity (u_{PC}) of 1 m/s. Artificial diffusion was used for the convection-dominated problem to stabilize the solution [Comsol, 2006].

5. Results and discussion

The 2D finite element simulation of the abovementioned model yielded the pictures seen in Figure 2 through Figure 5.

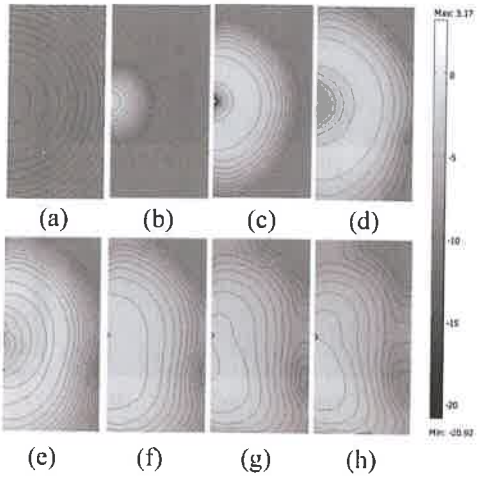


Figure 2: Evolution of the positive ionic space charge with time over the first discharge period

Figure 2 depicts the progress of the positive ion density in the first discharging full period. (a) shows the initial constitution having negligible background ionization and is followed by the field enhancement. Consecutively (b) displays the distribution right after ignition, which, due to the driving electric field is moving outward (c). As the now decreasing applied voltage is incapable of sustaining the critical gradient at the surface of the wire (d) is the point of termination in the positive half wave. The density propagates in a circular shape through the space surrounding the wire, but experiences increasingly dispersion due to the field gradient within the ion cloud and concentration gradients at the outer boundaries. Additionally the highly asymmetric field distribution in y-direction causes the cloud to bulge out into the direction of the higher potential gradient. The local field enhancement of the space charge on connection with the voltage of the shield electrode results into a flux along the region of higher concentration. Thereby the characteristic cross is formed within the shield, leaving a bead shaped remanent positive ionic space charge at the beginning of the next discharging period (see Figure 3).

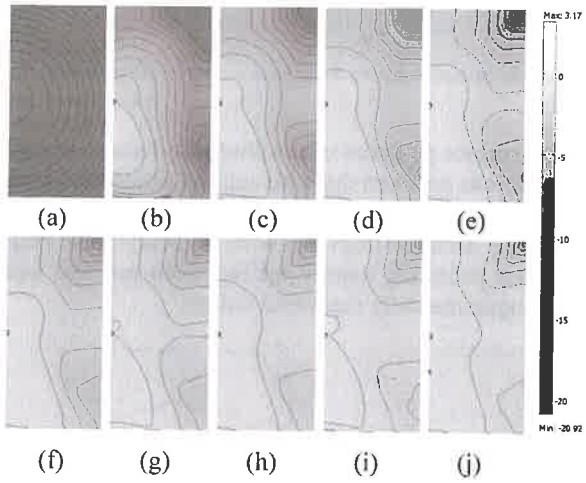


Figure 3: Development of the initial positive ionic space charge distribution (logarithmic depiction)

The development for the negative ion density, as depicted in Figure 4, is similar to the comments made on Figure 2. This time the major potential gradient is between the wire and the shield instead of the photoconductor. Therefore the circular shape bulges into this direction, leaving also a bead shaped remanent negative ionic space charge above the wire (cf. Figure 5). In this case the field enhancement through the

negative space charge in connection with the shielding electrode confines the negative ions almost completely to the upper half of the investigated geometry.

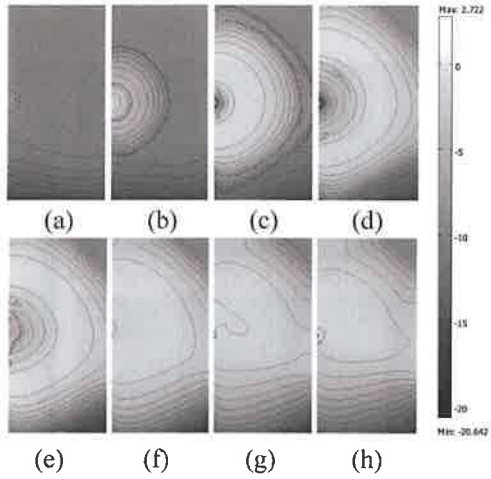


Figure 4: Evolution of the negative space charge in the first discharging period (logarithmic depiction)

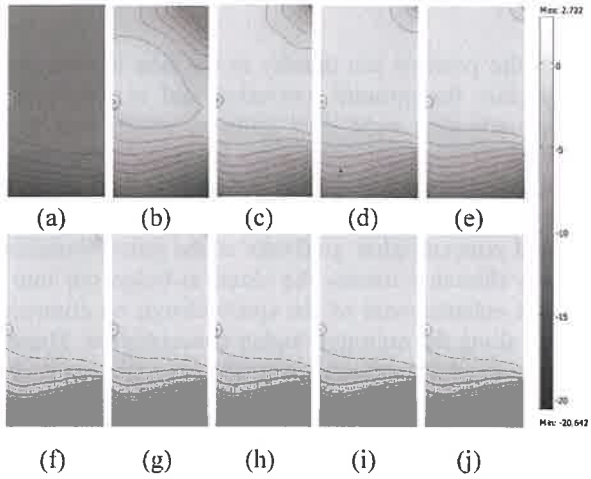


Figure 5: Development of the initial negative ionic space charge distribution (logarithmic depiction)

Additionally current and resulting surface potential of the photoconductor were investigated. Determination of the current density at different positions between the wire and the photoconductor clearly reveal the influence of the shielding electrode. Therefore the current below the wire shows increasingly a positive offset of the synchronous current with increasing distance from the wire, indicating the major current to originate from positive ions. The resulting surface potential, mainly arising from positive ions, therefore settles at +40V being a factor of 8-10 lower than experimentally measured values.

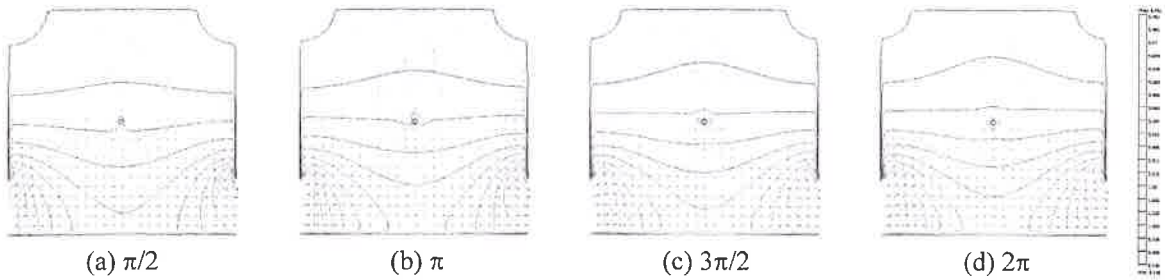


Figure 6: Streamline plot of the air velocity within the contemplated geometry through the first discharging period (isolines show constant velocity, arrows depict the velocity field)

The results from a simulation with the added Navier-Stokes equations may be reviewed in Figure 6. The time dependent simulation shows almost no influence of the velocity of the photoconductor on the contemplated space. Furthermore, an influence from the discharge is not apparent from our simulation, which again corroborates the underestimation of the ionization through a glow discharge and therefore, does not show general "corona-wind" behavior as pointed out by *Feng et al.* [Feng et al., 2001].

6. Conclusion

The paper presents a model for studying an AC corona discharge used in xerographic printing systems. The outlined assumptions define a system, where the main mechanism for ion generation is a glow regime. As shown, the resulting surface potential of the photoconductor is obviously lower, though overestimating charge concentrations, than the measured values, leading to the conclusion that glow discharge is not the major mechanism for charge carrier production.

According to *Amara et al.* [Amara et al., 1989] gains current of the positive half wave, due to additional streamer discharge, in importance with increasing peak-to-peak voltage. *Trinh* [Trinh, 1995] furthermore stresses the importance of remanent space charge, which is obvious from our simulations, for the development of breakdown streamers, which are not fully conductive and do not lead to a breakdown of the gap. As a result of these streamers local differences in ion concentrations are present on the surface of the wire, but lead in the author's opinion to noticeable differences in current. However, similar observations have been made, e.g. spontaneous pattern formation along a high-voltage stressed wire, have been made in investigations on dielectric barrier discharges in coaxial configurations. *Guikerma* et al. [Guikema, 2000] observed a stronger random placement of filaments with increased amplitude of the applied voltage, which may lead to inhomogeneous charging of the photoconductor. Visual evidence of these mechanisms in corona discharges was also given by *van Veldhuizen et al.* [v. Veldhuizen et al., 2001].

The introduction of the motion of the background gas on the discharge did not yield noticeable influences of the discharge on the air velocity in the system and vice versa. This again underlines the underestimation of the currents in the discharge, as conventionally an influence known as "corona wind" is observed. As we propose the strong effect of streamers on the homogeneity of the charging device further investigations may in a first step neglect this motion.

References

1. Abdel-Salam, M., Abdel-Aziz, E. Z., (2001), *Corona power loss determination on multi-phase power transmission lines, Elec. Power. Syst. Res., 58, 2, 123 - 132*
2. Abdel-Salam, M., Abdel-Sattar, S., (1989), *Calculation of corona V-I characteristics of monopolar bundles using the charge simulation method, IEEE Trans. Dielectr. Electr. Insul., 24, 4, 669 - 679*
3. Adamiak, K., (1994), *Simulation of corona in wire duct electrostatic precipitator by means of the boundary element method, IEEE Trans. Ind. Appl., 30, 2, 381 - 386*
4. Amara, K., Goldman, A., Goldman, M., Sigmond, R. S., (1989), *Current imbalance and charge build-up on insulators in AC air coronas, Conduction and Breakdown in Solid Dielectrics, S. 20 - 24, 1989*
5. Comsol AB, (2006), *COMSOL Muliphysics User's Guide, Tech. report*
6. Fay, Jr., J. E., (2003), *Electrostatic Analysis of and Improvements to Electrophotograohic Solid Freeform Fabrication, Master's thesis, University of Florida*
7. Feng, J.Q., Morehouse, P.W., Jr., Facci, J.S., (2001), *Steady-state corona charging behavior of a corotron over a movingdielectric substrate, IEEE Trans. Ind. Appl., 37, 6, 1651-1657*
8. Georghiou G. E., Papadakis, A. P., Morrow, R., Metaxas, A. C., (2005), *Numerical modelling of atmospheric pressure gas discharges leading to plasma production, J. Appl. Phys. D, 38, 20, R303-R328*
9. Goldman, M., Goldman, A., Sigmond, R. S., (1985), *The corona discharge, its properties and specific uses, Pure Appl. Chem., 57, 9, 1353 - 1362*
10. Guikema, J., Miller, N., Niehof, J., Klein, M., Walhout, M., (2000), *Spontaneous Pattern Formation in an Effectively One-Dimensional Dielectric-Barrier Discharge System, Phys. Rev. Lett., 85, 18, 3817 - 3820*
11. Gundlach, R. W., Fornalik, A., Mey, W., (2002), *New Corona Charging System for Low Cost Printers, International Conference on Digital Printing, 18, 41-44*

12. A. Hallac, Georghiou, G. E., Metaxas, A. C., (2005), *Three-dimensional characterization of short-gap streamers in air at atmospheric pressure, IEEE Trans. on Plasma Sci., 33, 2, 268-269*
13. Humpert, C., (2002), *Modellierung des dynamischen Verhaltens von Oberflächen Barrierenentladungen und der Ozonerzeugung, PhD thesis, Rheinisch-Westfälischen Technischen Hochschule Aachen*
14. Karpov, S., (2005), *Electrohydrodynamic flow modeling using FEMLAB, Proc. Comsol User's Conference*
15. Kasuga, A., Hoshino, Y., Omodani, M., Koike, F., (1997), *Air Flow Effect on Corona Discharge Characteristics, International Conference on Digital Printing Technologies, 13, 93-95*
16. Ohsawa, A., (2005), *Modeling of charge neutralization by ionizer, J. Electrostat., 63, 6, 767 - 773*
17. Rajzer, J. P., (1991), *Gas Discharge Physics, Springer*
18. Rickard, D. A., Dupuy, J., Waters, R. T., (1991), *Verification of an alternating current corona model for use as a current transmission line design aid, IET Sci. Meas. Technol., 138, 5, 250–258*
19. Trinh, N. G., (1995), *Partial discharge XX. Partial discharges in air. I. Physical Mechanisms, IEEE Electr. Insul. Mag., 11, 2, 23 - 29*
20. van Veldhuizen, E., Rutgers, W., (2001), *Corona discharges: fundamentals and diagnostics, Frontiers in low temperature plasma diagnosis, 4, 40 - 49*
21. Williams, E. M., (1993), *The physics and technology of xerographic processes, Krieger, Malabar (FL)*
22. Yehia, A., Mizuno, A., Takashima, K., (2000), *On the characteristics of the corona discharge in a wire-duct reactor, J. Phys. D: Appl. Phys., 33, 2807 - 2814*
23. Zhao, T., Comber, M. G., (2000), *Calculation of electric field and potential distribution along non-ceramic insulators considering the effects of conductors and transmission towers, IEEE Trans. Power Delivery, 15, 1, 313 - 318*
24. Zhao, T., Sebo, S. A., Kasten, D. G., (1996), *Calculation of single phase AC and monopolar DC hybrid corona effects, IEEE Trans. Power Delivery, 11, 3, 1454 - 1463*



1

Strategic issues: ecology, new media and industry structure

Ecodesign management system adapted to the graphics arts industry: A case study

David Pérez, Vicente de Gracia, Juan Carlos Iglesias, Susana Otero

Technological Institute of Optics, Colour and Imaging, AIDO
C/ Nicolás Copérnico 7-13
46980 Paterna, Valencia, Spain
E-mail: dperez@aido.es

Abstract

The Ecodesing or Design for Environment (DfE), which is defined as "Design process which considers the environmental impacts in every steps of the design and development of the products, in order to achieve products with the minimum environmental impacts as possible during their life cycle", has appeared in the last years as a response of the increasing environmental conscience in the industrial sectors.

The traditional design process can be adapted to Ecodesign through the integration of some changes, in order to not focusing the environmental improvements only in the production stages but also in the continuous improvement of the environmental behavior of the products and services.

The succesful implementation of Ecodesign in the organizations needs an "Ecodesign Management System", focus on a systematic continuous improvement of the products and services from their design and development, by means of an environmental management system.

The objective of the present research is to define an "Ecodesign Management System adapted to the Graphics Arts Industry".

In order of obtaining real information about the effectiveness of the Ecodesing Management Systems in the Graphic Arts SMEs, there has been developed a practice case with the cooperation of a Spanish company.

Keywords

Ecodesign (design for environment), environment, graphic industry, management

1. Introduction

The organizations are more a more conscious about the significance of the environmental management of the activity, products and services for their competitiveness. The environmental improvement has been carried on a management systems context, but this improvement hasn´t often been focused on the environmental aspects of the products.

Nowadays, the environmental policies related to products and services are more a more important inside the Integrated Policy Product (IPP), developed by the European Commission.

IPP is a public policy whose aim is the continuous improvement of the environmental behavior of the products and services with a Life Cycle criteria

Then, the Ecodesing or Design for Environment (DfE) appeared, which is defined as "Design process which considers the environmental impacts in every steps of the design and development of the products, in order to achieve products with the minimum environmental impacts as possible during their life cycle".

The traditional design process can be adapted to Ecodesign through the integration of some changes, which are summarized in the figure 1.

The succesful implementation of Ecodesign in the organizations needs an "Ecodesign Management System", focus on a systematic continuous improvement of the products and services from their design and development, by means of an environmental management system.

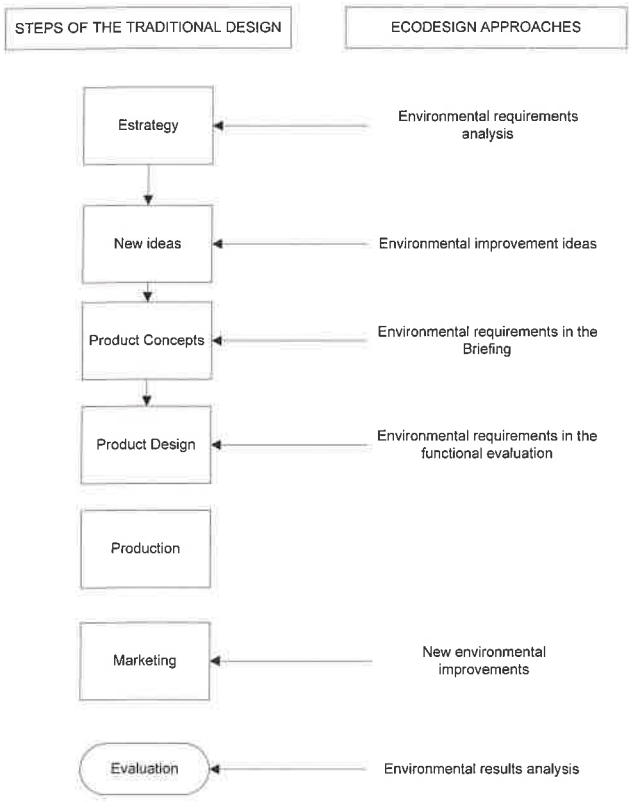


Figure 1:
Relation of the Ecodesign with the Traditional Design Process

The main aspects to be included in this management system are the following:

Analysis of the Environmental Requirements: Depending on the motivations for applying Ecodesign and the objectives of the organization, there will be determined the environmental aspects to include in the new product. A general environmental analysis could be useful to identify the main improvement areas. Normally, the environmental aspects to be considered in this step are related to concepts as durability, recyclability, easy dismount...

Ecodesign Team: The main difference with the traditional design is that now there is included a new kind of professional role: the environmental issues expert. His function will be making environmental analysis and advice during the selection of eco-strategies.

Environmental Analysis: During the development of a new product or service it could be done different environmental analysis to identify the critical aspects to improve or to compare different design alternatives.

Ecodesign Strategies: In this step, the environmental aspects are translated to concrete design actions. The organization must select the most suitable eco-strategie for its product or service, having in minds the results of the environmental analysis and the economical and technological viability.

Environmental communication: The environmental benefits of the new product or service may be communicated to the customers by using different tools.

Analysis of the results of Ecodesign: This evaluation could be used in future actions of environmental improvement.

The implementation of an Ecodesign Management System in a printing company has to be carried out inside the specific characteristics of the Graphic Arts Industry.

European printing industry is highly fragmented and more than 85% of the industrial structure is composed by SMEs employing less than 20 workers, which are not usually specialists in environmental management issues. New significant providers from emerging countries (Eastern and Central Europe, China) force printers to redefine their market position by integrating more services.

Entrepeneurs and managers in medium-sized companies are still much in the rationalisation of internal resources in order to improve margins, so there´s a lack of strategical approach.

In addition to fulfilling legal requirements, printing companies are increasingly confronted with requests from customers to demonstrate their commitments towards ensuring environmental sustainability...

Based on data provided by various studies, environmental protection seems to be an issue of importance for the graphic arts industry. Again, according to an EU study for the forest industry published by Integraf, the international association for the graphic industry, the European Graphic Industry is an industrial branch which has only a marginal impact on the environment. The industry is devoing increased resources to meeting the stricter environmental requirements.

The objective of the present research is to define an "Ecodesign Management System adapted to the Graphics Arts Industry".

2. Research methods

2.1 Literature study

Literature study was based principally on different publications from various organizations which are leading the application of Ecodesing strategies in the industrial sectors of the world.

It has been especially important the study of the standard UNE 150.301:2003 "Environmental Management of the design and development process. Ecodesing", published by AENOR, which is the Spanish body for standardization.

The fulfilment of this standard implies that the organisation has integrated a continuous systematic to identify, control and improve the environmental aspects in their products and/or services. Through this systematic, the organisation can adapt themselves to the technical advances.

2.2 Case study research

In order of obtaining real information about the effectiveness of the Ecodesing Management Systems in the Graphic Arts SMEs, there has been developed a practice case with the cooperation of a Spanish company. There was selected a "typical" European SME printing company:

- ✓ More usual workflows in printing companies (prepress, platemaking, printing, postpress).
- ✓ 20 employees.
- ✓ No environmental technical experts.

In this practice case, there were developed the next actions:
Definition of an "Ecodesign Management System" in a graphic arts company: then, there was defined an "Ecodesign Management System" in the company, adapted to its characteristics.

Implementation of an Ecodesign project over a specific graphic product: the defined "Ecodesign Management System" was implemented.

Eco-strategies application: during the implementation process, some eco-strategies were selected for developing an ecodesigned graphic product

Review of the "Ecodesign Management System" results: after finishing the ecodesigned project, the results were evaluated in order of getting information about the effectiveness of the ecodesing process and future improvements.

3. Summary of the results

An Ecodesign Project in a Graphic Arts Industry needed to implement an "Ecodesign Management System" which included the next steps:

3.1 Analysis of the environmental requirements

The environmental requirements considered were defined depending on the requirements of the product.

- Prepress
- Press
- Post-press
- Raw materials
- Transport
- Duration of the life of the product
- Legal requirements
- Water consumption
- Energy consumption
- There exist other aspects that we can consider
- Customer needs and expectations
- Market situation
- Competitors

3.2 Ecodesign team creation

The Ecodesign Project generates a cooperation activity between several departments in the graphic company. A small and efficient workgroup was needed in order to advancing the market trends and the changes inside the company.

Having in mind the structure of the majority of the graphic companies, the "Ecodesign Workgroup" included members of the next departments:

- Management
- Sales Department
- Purchasing Department
- Prepress Department
- Production Department (press and postpress section)
- Quality, Environmental and Security Department

3.3 Environmental product analysis

The critical environmental aspects to be improved were analysed during the development of the new product. First of all, the environmental aspects were identified. After this, the associated environmental impacts were identified in order to determine the relevant impacts. The environmental aspects which generate a significant environmental impact were considered as a significant environmental aspect.

In the graphic processes there exist some environmental aspects which could be considered when designing a product with the minimum environmental impact:

- Atmospheric emissions: VOCs
- Chemical additives, Cleaning wastes, Dumping solutions ...
- Waste management: paper, board, plastics, ink wastes ...
- Ground contamination
- Raw materials consumptions: inks, paper, board, additives ...
- Natural resources consumptions: water, energy...

In this step some tools were used, like simple checklists for applying DfE to graphic arts products.

3.4 Eco strategies selection

At this moment, the environmental considerations were translated to concrete design actions. Depending on the graphic product type, and their characteristics environmental impacts, some Ecodesign strategies were more suitable than others. Different aspects have to be considering in order choosing the best Ecodesign strategies in each concrete project.

The main Ecodesign strategies groups are shown in the figure 2:

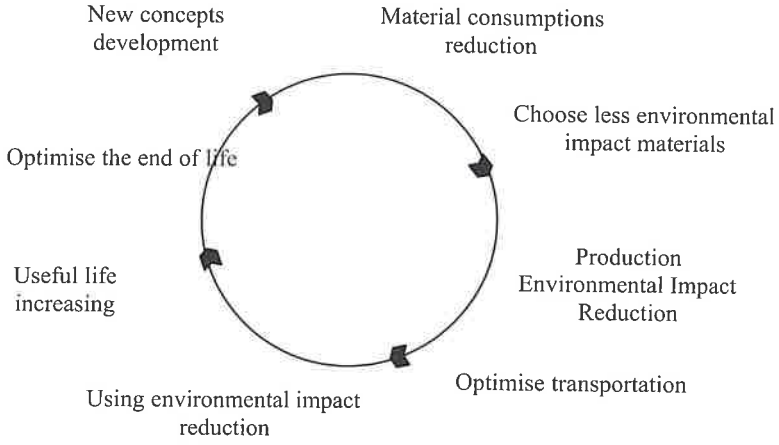


Figure 2: Main ecodesign strategies

When it comes to designing printed products, efforts may be focused on the following current eco-strategies:

- Optimise functionality
- Optimise lifetime
- Reduce use of materials and energy
- Choose right materials and energy sources
- Optimise production
- Optimise waste treatment
- Optimise transportation

3.5 Environmental communication

This step included the communication of the characteristics and benefits of the ecodesigned product, in order to encourage the costumers to acquiring it.

An open, clear and truthful programme of environmental communication is essential. If not, the costumers could be disappointed with the environmental attributes what they could expect.

The communication strategy was based in the next steps:
Objetives definition: in this initial step, it must be defined what are the short and medium term aims of the communication plan and how to measure them.

Public characterisation: To determine the group of customers and what are their priorities?

Strategy definiton: To determine the values and imaging what the organisation wants to transmit and the message to communicate them.

Action Plan: To define the promotion channels to be used, the concrete actions to be done and the way for evaluting the results.

The main actions that were consider are resume in the table I.

The graphic arts products can give an excellent environmental communication by means of printing some extra information in the product. It´s an important advantage in comparison with other kind of products.

Then, there were proposed different ways of environmental communication:
Printed communication on the product: "This printed product has been designed using eco_strategies for reducing its environmental impact".

Table I: Actions to be consider in ecodesign communication action plan

Action	Objetives	Benefits
Advertising	To communicate the specific benefits To transmit the company image to the products	To contact with a high number of persons at the same time To use implicts elements
Public relations	To create a competent image To develope and to strenght the ecological conscience	Personal contact Closeness to the public of the company
Sales promotion	To link the sales to the ecological behavior	To include the sale men in the strategy Visibiliy in the Visibilidad en el punto de venta
Alliances with NGOs	To develope new links between the company and its environment	Higher credibility and acceptability of the message Development of a broad cannel of involvement
Internet	Interaction between the company and its public	Deep of the information Embodiment of the message Feed back Update
Environmental/ Sustainability Memory	To show the environmental compromise of the company To create a competent image	Justification and credibility of the message Evaluation of the results

Printed logo: It was proposed to use a logo (figure 3) created by a consortium of Spanish technological institutes.



Figure 3:
Ecodesign logo created by a consortium of Spanish technological institutes

Internet: It could be an excellente channel for the printing companies what are using their web pages for receiving digital information from the customers (FTP systems).

3.6 Project results analysis

Table II: Ecodesign project results analysis

Ecoestrategy applied	Change in the product	Result
Material consumptions reduction	Printed in paper with A-4 format without bleed.	By means of this modification it has been achieved a decrease in the sheet format. It has changed from 70 x 100 cm to 65 x 90, what means a decrease in the paper consumption of 16,4%.
Material consumptions reduction	Appropiate black generation: GCR	With this technique it was reduced the total ink coverage from 400% to 280% and so the ink consumptions was reduced and the quality of the product it was kept.
Useful life increasing	Independent folders	The products update in the company doesn´t affect all the images include in the catalogue. By means of this independent folders, it was achieved a reduction of the new production. So there was a important decrease in the associated impacts.
Choose less environmental impact materials	Perforated binding	Related with the independent folders, we have achieved also, the elimination of the self-adhesive glue.
To include a company diary	New concepts development	The catalogue was completed with a company diary, so it was eliminated the whole process of printing the company diary. It was an ecoestrategy specially supported from the sales department.

As a result from this eco_strategies application, there were made some changes in a graphic product from the selected company, which are included in the table II.

After the product was marked; we reviewed the project in order to know if the expectations and needs were fulfilled. If not, a new ecodesign project must improve the product.

This information comes from the customers and other interested agents. It is and important source of continuous improvement in the company. It will improve the company products and the design and development process.

An important agent is the company who manage the wastes of the company, because they could inform the company about the consequences of certain changes derived from the ecodesign project.

Is important to share some of this information with the suppliers, because should support the company in this continuous improvement process.

4. Discussion and conclusions

It is possible to develop and implement ecodesign strategies to printed product. However requires a close cooperation between each stage of the production process and the management staff: sales, purchase, design, prepress, printing and finishing, defining an "Ecodesign Management System" for each printing product.

An **"Ecodesign Management System"** may have the next benefits in the graphic arts organization

- Minimization of the environmental impact.
- Reduction of the costs.
- Added value products.
- Involving all the employees in a common environmental project.
- Continuous improvement.
- To systematize the design actions, so the company "know-how" is registered.
- Innovation

Acknowledegments

The authors would like to thank the references authors for their work. Some information and figures from them have been adapted in this papee

References

1. Ernst & Young (2007), *Competitiveness of the European Printing Industry*
2. AENOR (2003), *UNE 150.301:2003 "Environmental Management of the design and development process. Ecodesing"*
3. Enroth M., Widing A. (2006) *Tools for Design for Environment (DfE) - Applications in the Printing Industry*, TAGA Journal Vol 2, pages 205-223
4. Fullana P. (1997) *Principales estrategias de ecodiseño*
5. AIDO (2007) *Como gestionar un proyecto de ecodiseño*



Changes in sustainability due to technology development in selected printing processes

Pentti Viluksela[1], Minna Nors[2], Hanna Pihkola[2], Katri Behm[2], Helena Wessman[2], Tiina Pajula[2]

[1] Helsinki Metropolia University of Applied Sciences
Vanha maantie 6, 02650 Espoo, Finland
E-mail: name.familyname@metropolia.fi

[2] KCL
P.O.Box 70, 02150 Espoo, Finland

Abstract

In the paper, changes in the environmental impacts of the printing processes are discussed. The analysis is focused on the interdependence between technology development and environmental load. Environmental load is analysed based on the annual input and output data that was collected from Finnish printing houses from years 2006 and 2007. Information on recent technical and process development was compiled from the literature and interviews with industry experts.

Energy efficiency and material efficiency are the main topics of the paper. Material efficiency is described by means of material use, waste output and waste sorting. The results are presented regarding sheet-fed offset, coldset web offset and heatset web offset. In addition, the differences between sheet-fed offset and electrophotography printing are discussed.

The results indicate that on a general level the energy efficiency has improved and that the use of chemicals and output of waste have decreased when compared to the levels of 1990's. Paper consumption per tonne of products has remained the same or even increased, likely due to changes in the production. Finally, environmental impacts of electrophotography seem to differ remarkably from other printing methods.

Keywords

Ecobalance data, energy efficiency, material efficiency, printing technology, sustainability

1. Introduction

Environmental loads of the printing processes were for the first time studied in detail in the 1990's. In Finland, a research project was carried out in 1993 - 1994 to define ecobalance of main printing processes and printed products [Juntunen et al. 1994, Rissa 2003, Pösö 1993]. In 1997, a study on the energy efficiency of the printing industry was carried out [Westren-Doll et al., 1997].

Corresponding work was done in other countries. For example, a study on the environmental profiles of several printed products was completed in Sweden in 1995, using a life cycle approach [Dalhielm-Axelsson 1995]. Springer in Germany together with Stora and Canfor carried out a full-scale life cycle assessment (LCA) on newspaper and magazine production [INFRAS 1998]. More recently, a LCA of sheet-fed offset printed products was done in Denmark [Larsen et al. 2006]. In Sweden, environmental performance of printing houses focusing on web offset and gravure printing has been studied by Enroth [2006].

Lately the environmental issues have gained additional importance due to climate change and global warming. For printed products, the attention has traditionally focused on forestry, pulping and papermaking, but the other stages of the lifecycle are also becoming important. Recently, the interest has been directed from papermaking towards printing, end-use and transportation of products, and thus closer to the customer and end-user of the products.

As the awareness of environmental impacts of print production has increased, more attention has been given to the efficient use of raw materials. Since the printing industry processes materials to produce new products, a remarkable portion of the environmental load caused by the print products during their life cycle is caused

outside the printing house, when the raw materials are manufactured [see for example Rissa 2003]. Thus the role of the printing house is important, since efficient use of raw materials is essential to improve the overall sustainability of the products.

Many technology changes have facilitated the move towards more sustainable print products. For example, printing presses have become faster and more automated, film-based platemaking has almost disappeared, digital printing has entered the market and new materials, like vegetable oil based printing inks and cleaning chemicals have become available. Many of these changes have also had an effect to energy and material consumption, and thus affect the ecobalance of printing.

The paper presents some of the first results of a Finnish research project "Lean Development with Renewable Resources [2007 - 2010]". The project is coordinated by Finnish pulp and paper research company KCL. Project partners include Metropolia University of applied Sciences, pulp and paper manufacturers, The Federation of the Finnish Media Industry, several printing houses and other actors related to the print product manufacturing. The overall aim of the project is to assess the environmental impacts of printed products covering the whole life cycle products (from forest to end-use and disposal or recycling). During the project, input and output data from printing and related processes is collected in order to conduct the life cycle inventory (LCI, eco balance) and to calculate the carbon footprint of the products.

The aim of this paper is to discuss the relationship between technology changes and environmental performance of the printing houses. Changes in ecobalance data and trends between the years 1993 - 2007 are assessed. In the paper, the term sustainability refers to environmental sustainability. Although environmental sustainability consists of multiple factors, the discussion in the paper is focused on energy efficiency and material efficiency. In addition, a case example of electrophotography is presented. Analyzed data includes information on sheet-fed offset (SFO), coldset web offset (CSWO), heatset web offset (HSWO) and electrophotography (EPG).

2. Methods

Annual level input and output data was collected from several printing companies participating in the project. In most cases the data was collected from years 2006 and 2007. The input data included printing materials (paper, inks, chemicals etc.), water and energy. Output data consisted of products, different waste fractions and emissions. Company-level accounting and reporting systems provided the basic data, which was verified and, if necessary, complemented. Background information on recent technical and process development was compiled from the literature, technical documentation of equipment and materials suppliers and interviews of industry experts.

3. Results

The data presented here can be regarded as the preliminary results of the research project. Firstly, background information on the recent technical development on the area of energy efficiency is presented. Secondly, trends and changes in the ecobalance data are evaluated. Thirdly, technical changes and development trends in the ecobalance data related to material efficiency are discussed. Finally, an example highlighting the differences between electrophotography and sheet-fed offset is presented.

The results presented in the paper are calculated using one tonne of printed products as the functional unit against which the results (e.g. material consumption) are reported. Tonne of products was chosen as a functional unit since many of the material inputs are generally reported in kilograms. In general, mass based evaluation is the most commonly used approach in life cycle assessment and eco-balance calculations. However, using tons as a functional unit was in some cases challenging since the print production is usually reported based on surface area.

3.1 Energy efficiency

Energy is one of the most important inputs in the printing processes. As a consequence, energy consumption is one of the main indicators when looking at the environmental performance of the printing houses. Due to the climate change, the use of energy becomes even more critical in the future. The growing interest towards

the carbon footprints and carbon labelling of end products will likely increase the demand for energy saving solutions and products. Carbon footprint means the amount of greenhouse gases (e.g. CO_2, CH_4, N_2O) produced during a products' life cycle. Reporting of the footprint is commonly done as CO_2 equivalents.

Generally, the biggest source of greenhouse gases (and thus the biggest contributor to the carbon footprint) in print production is the use of electricity and heating. If the electricity from the grid is partly or mainly produced from fossil energy sources (which is the case in many countries), savings in energy use is the most efficient way to reduce the carbon footprint of the production site.

According to Westren Doll et al. [1997], about 40% of the energy consumed by a Finnish printing company is used for print production, while the building services - heating, ventilation, lighting etc. - stand for the remaining 60%. On a printing press, ink drying, main drive and air supply account for the largest share of the energy consumption [Heidelberg 2008, Jepsen & Tebert 2003, see also Table I].

Table I: Examples of energy consumption of the printing processes

Item	SFO, % of total	HSWO, % of total
Ink drying	35	64
Exhaust gas treatment		3
Main drive	26	21
Air supply	19	
Cooling	8	6
Compressed air	1	1
Others	11	5
Notes	Speedmaster XL 105-5+L sheetfed offset press, data from year 2006. [Source: Heidelberg 2008]	A model German HSWO plant [Source: Jepsen and Tebert 2003]

Technological developments that have contributed to the improved energy efficiency are press technology (such as direct drives) and the incineration of HSWO exhaust gases. Direct drives have more or less replaced earlier systems using gears and belts for drive transmission. This brings about energy savings and reduced installation footprint [PrintCity 2008b]. Modern presses are also equipped with converters that brake energy into electricity and feed it back into the power system [PrintCity 2008b]. In addition, more energy efficient ink drying and cooling systems are being developed [Heidelberg 2008].

During the last decades, HSWO dryer exhaust gas purification technology has developed considerably. Modern installations use a regerative thermal oxidiser integrated into the dryer, instead of an independent oxidiser and recuperative method. The new technology is claimed to result in a significant improvement in both energy efficiency as well as in CO_2 emissions [PrintCity 2008b, p. 12 - 13]. In optimal circumstances, the new integrated oxidisers run with the ink solvents, i.e. without additional gas fuel [Manroland 2008, p. 27], and up to 97% of the energy can be recovered [PrintCity 2008a].

Based on the earlier studies and on the data collected, the energy consumption in printing houses has decreased considerably from the level of early 1990's. However it must be noted that the situation can vary remarkably between different printing houses, and the results of different studies are not totally comparable but rather indicative. It is also important to notice that the energy consumption figures in the printing houses often include the total energy consumption of the production site and thus the type and size of the buildings can affect the figures. To improve the accuracy of the figures, data from several printing houses is included so that an understanding about typical consumption levels can be composed. A summary of the total energy consumption for different printing methods is presented in Figure 1.

Although the downward trend of energy consumption is quite clear, there are differences between the results of the individual studies. This can be explained by differences in the time frame, scope and geographical location of data collection, overall objective of the studies, number of companies involved, etc. A clear example of the differences between companies was reported by Enroth [2006, p. 77]: out of seven quite similar newspaper printers, the one with the highest energy consumption per one tonne of products consumed almost three times more energy than the lowest. The energy consumption levels are to some extent dependent of the production structure and machinery and thus the energy consumption figures should be evaluated also in relation to the infrastructure and production type.

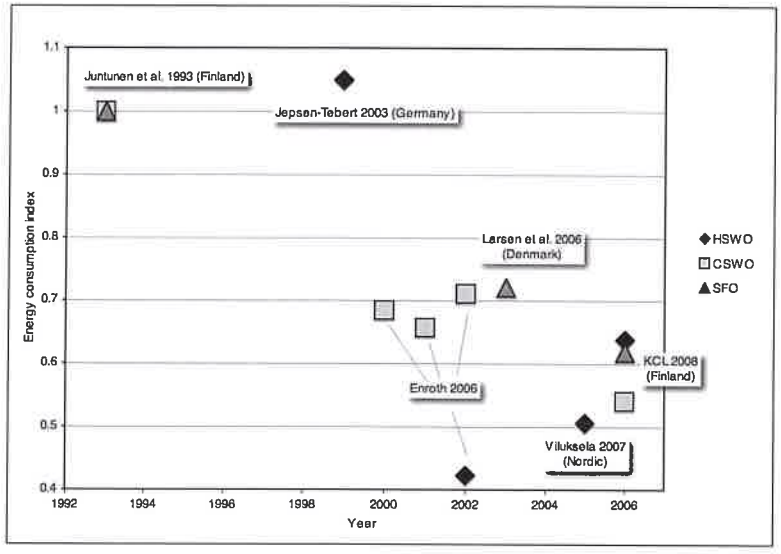


Figure 1: Energy consumption index of printing processes, calculated as total energy consumption per one tonne of printed products (Finnish ecobalance study from year 1993 = 1)

As a conclusion, the technical developments and innovations during the past 15 years are clearly reflected in the improved energy efficiency. Even better performance can be expected in the future, as older production equipment is gradually replaced. At the moment, in SFO and HSWO printing, the most energy consuming process is ink drying (see Table I). Thus it is both likely and preferable that the most significant future improvements could take place in the area of ink drying/curing.

3.2 Material efficiency

Material efficiency refers to the use of printing materials and to the amount of products and waste produced during the process. Material efficiency is usually measured in relation to the production volumes. In the paper, a number of indicators have been chosen to illustrate the development of material use and waste production. Indicators discussed in the paper are the amount of paper, inks and chemicals used in the process and the amount of waste produced (divided into various waste fractions).

Recent technological developments that have contributed to the improvement of material efficiency are e.g. automation of the makeready operations and production and digital workflow. Makeready operations, register control and colour control have all benefited from technical development. Makeready automation includes ink zone and sheet size preset adjustments from prepress data using JDF (Job Definition Format), automatic or semi-automatic plate loading and start-up sequences. Automatic register control has been used in web presses since the 1980's. Closed loop colour control is included in modern web and sheet-fed presses. Automatic blanket washing devices have also become common technology in the last decade. All these developments can lead to improvements in both materials efficiency and productivity. [Heidelberg 2008, Manroland 2008]

As an example of the technology development, the introduction and adoption of Computer-to-Plate technology (CTP) has caused a decline in the consumption of films and film chemicals. In Finland, the share of CTP plates is well over 90% (Figure 2). The change in technology has decreased the developer consumption, the amount of film and developer waste and the energy consumption at the prepress stage.

3.2.1 Material consumption of printing processes

Compared to the clear improvement of energy efficiency presented in chapter 3.1, paper consumption per one tonne of printed products has remained on the same level or shows a slightly upward trend (see Figure 3). The technical and process improvements for makeready and automated quality control, outlined above, should lead to better paper utilisation. On the other hand, shorter print runs and more complicated products (more colour, effects, etc.) may counteract these advantages. Since paper in many printed product groups is the

single most important factor both financially and ecologically, the efficient utilisation of paper remains a major challenge for the printing industry, also in the near future.

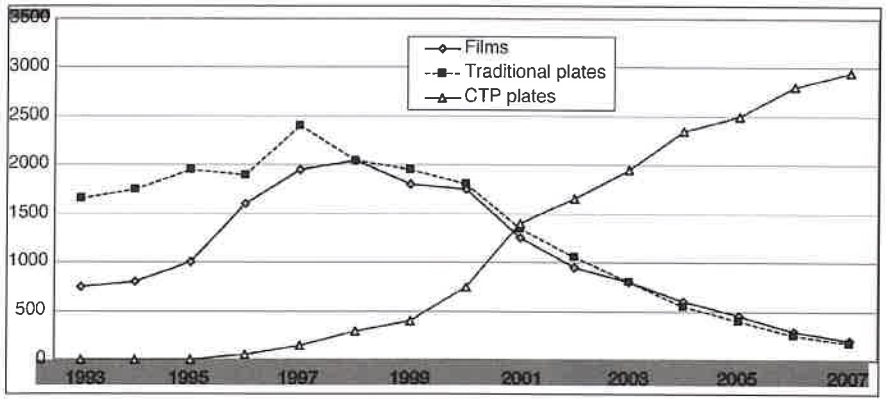


Figure 2: The market of graphic arts consumables in Finland (in millions of m^2) CTP plates have taken over the market while films and traditional plates are phased out [Source: KTA-yhtiöt]

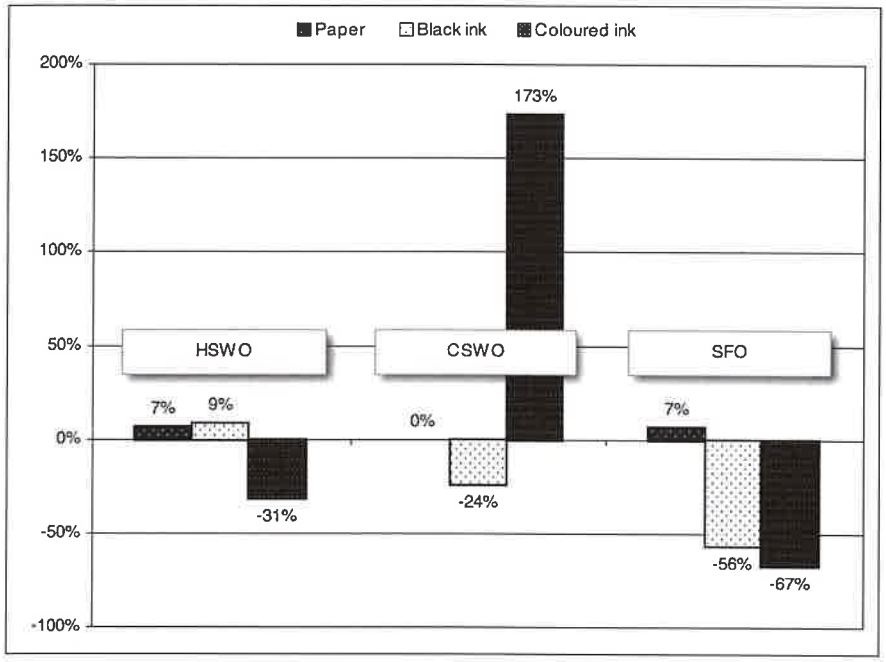


Figure 3: Relative change in the use of paper and ink per one tonne of printed products in Finland, 1993 - 2007 (Reference year 1993 =0)

The changes in ink consumption between years 1993 and 2007 (Figure 3) are interesting. In HSWO, the increase in black and decrease in coloured ink consumption per tonne of products could be explained by more effective under-colour removal or grey component replacement methods. The dramatic increase in coloured CSWO ink consumption seems to come from an increase in four-colour printing of newspapers. The decrease in SFO ink consumption may be caused by the increased use of coated paper grades, which require less ink.

The consumption of other materials has generally decreased from the level of 1993 (Figure 4). Isopropanol, one of the causes of VOC emissions, is being replaced or phased out. Developing and fixing agents decrease with the change from film to digital prepress and to CTP plates - and the recently introduced chemistry-free and processless plates. The consumption of washing agents has decreased with the growing use of automatic blanket washing devices.

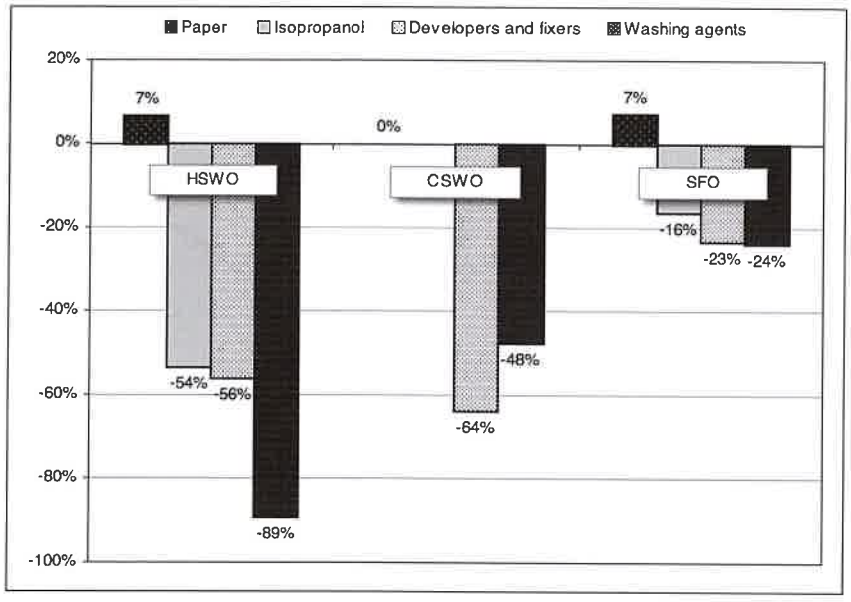


Figure 4: Relative changes in the use of chemicals per one tonne of printed products in Finland, 1993 - 2007 (Reference year 1993 = 0)

3.2.2 Waste output of printing processes

Output of different waste fractions describes on one hand materials and process efficiency, on the other hand waste sorting. It seems that the development has mainly been positive. Both hazardous waste and landfill waste per one tonne of printed products have generally decreased. Waste recovery and sorting seem to have been improved, too: the decrease in landfill waste is partly reflected by the increase in metal and energy waste fractions (Figure 5). The improvements in waste sorting and recovery have been boosted by stricter legislation and increasing waste handling and processing costs.

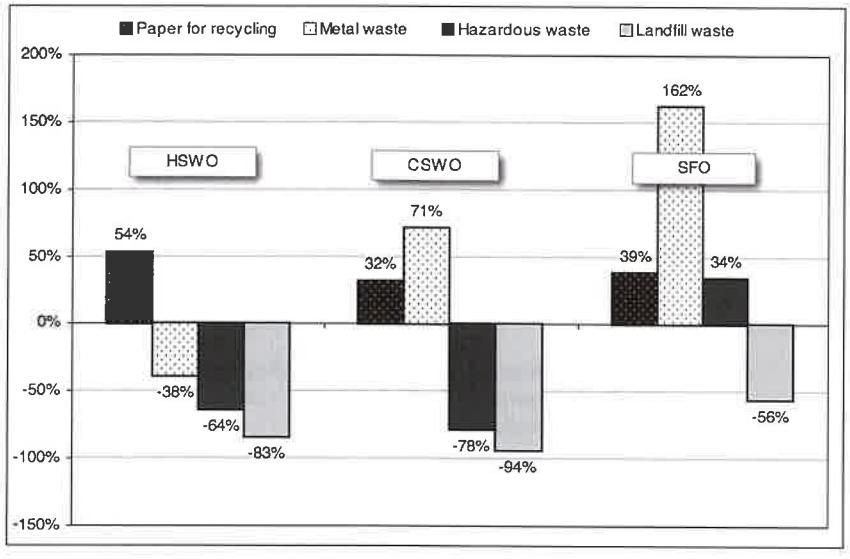


Figure 5: Relative change in the output of waste fractions per one tonne of printed products in Finland, 1993 - 2007 (Reference year 1993 = 0)

Even though the relative change during the last fourteen years gives some indication of the trends in waste output and sorting, it is important to consider also the total amount of waste per one tonne of product. The amount of recovered paper per tonne of product varies between one hundred and few hundred kilograms, but the amount of energy waste, landfill waste, metal waste and hazardous waste usually varies from only few kilos to 20 and up to around 50 kilos (per fraction) per tonne of product. Thus, when the total amount of waste

per tonne of product is rather small, one event or small change can increase in the total amount (e.g. from 1 kg to 2 kg per tonne of product) causing a huge relative change. As a consequence, to have a clearer picture about the long-term trend in waste output, the input and output data should be followed during several years.

When analysing the waste output data, the comparison with other studies is somewhat complex since the sorting of different waste fractions can vary depending of the local waste infrastructure. This should be noted especially when looking at studies conducted in different countries, but some differences in waste sorting can exist even between different municipalities in one country. However, on a general level, the results related to the amount of waste (per tonne of printed product) indicate positive development and improvements in the waste sorting. The most positive indication is the decrease in the amount of landfill waste.

3.3 Case: Electrophotography vs. sheet-fed offset

Digital printing is one of the fastest growing sectors in the printing industry. Electrophotography is currently the main method for producing documents and publications. In the small print run market (around 1000 copies) EPG is challenging sheet-fed offset. Since the volume of EPG is growing, it is very important to look at the environmental impacts and possible challenges related to the method.

First results from a case study focusing on EPG and SFO printing are presented in the following section. Environmental impacts of electrophotography have not been studied widely before and thus the comparison with previous studies is not possible in this context. Since substantially little is known about the impacts, it must be noted that the results can vary between different printing houses, depending on the machinery and on the type of production. Nevertheless, the results presented in this paper provide one indication of the current situation. The results can also provide valuable information on the future research needs concerning EPG.

Based on the data gathered from the printing houses, a comparison of energy and material efficiency between EPG and SFO is presented in Figure 6, and a corresponding comparison of waste output is presented in Figure 7.

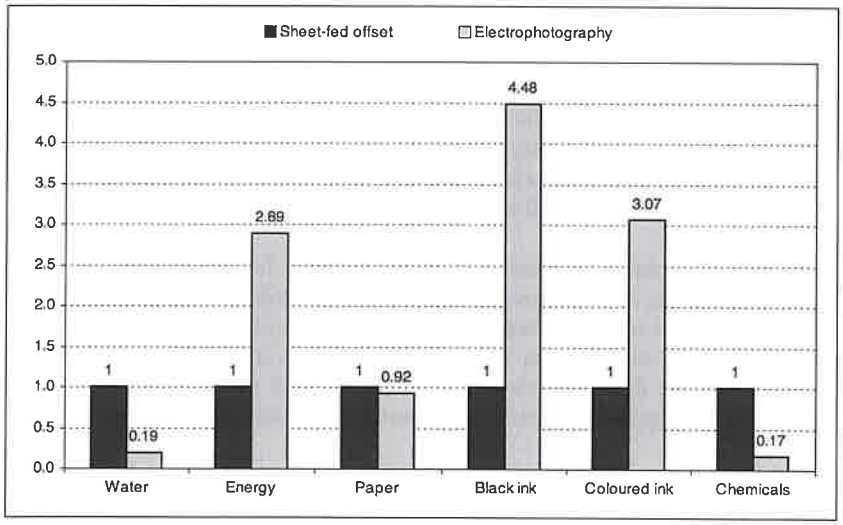


Figure 6: Material and energy consumption index of electrophotography compared to sheet-fed offset per one tonne of printed products. Data from Finland 2007(Sheet-fed-offset = 1)

The comparison of EPG vs. SFO provides some interesting views. Energy consumption of EPG was found considerably higher than that of SFO (see Figure 6). This may partly be explained by electricity consumption in the standby state of EPGs and differences in production scheduling and capacity utilisation. However, more research is required to understand and to improve the energy efficiency of EPG. Ink consumption of EPG is also very much higher than that of SFO, which illustrates the differences in ink formulation of these printing processes.

As expected, EPG has a significantly lower water and chemicals consumption and slightly lower paper consumption than SFO. Similarly, the waste output of EPG is clearly lower than in SFO. One explanation for the differing waste output levels between SFO and EPG could be the recycling of empty EPG toner cartridges which are sent back to the supplier. It is also important to notice that the water consumption figures in the

printing houses often include the total water consumption of the production site and thus many different things (such as the number of personnel) can affect the level of consumption.

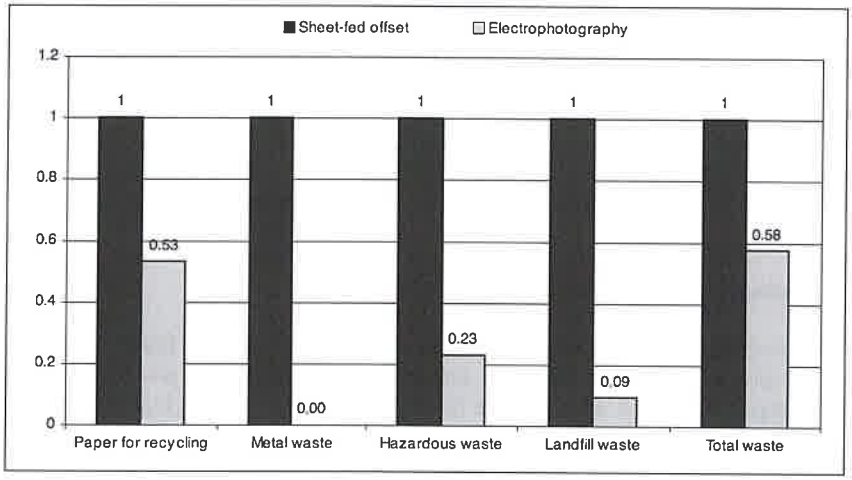


Figure 7: Waste output index of electrophotography compared to sheet-fed offset per one tonne of printed products. Data from Finland 2007 (Sheet-fed-offset = 1)

As a conclusion, the comparison between different printing methods is not simple, but to some extent it provides useful information about the differences between the methods. The results presented here are the first steps of a research which will later focus on the waste output and energy consumption in EPG.

4. Discussion

The paper has presented some of the first results of a wider research project. The data presented in this paper is based on a limited but quite representative number of cases from the Finnish printing industry. Comparisons with earlier studies can be regarded as indicative only, because there may be differences in calculation methods. More data will be collected during the on-going project, which will improve the reliability of the results. Careful studying of the input and output data (LCI, ecobalance) and the impacts of technological changes provides a good starting point for further research and full scale life cycle assessment studies.

In general, studying environmental performance of print products for the purpose of life cycle assessment calculations is a challenging task. A huge amount of data is required, and careful consideration is needed in order to make data from different sources comparable, and to ensure the reliability of the data. In many cases, some generalizations and basic assumptions have to be made no matter how detailed the data collection actually is. Nonetheless, reliable data collection is possible through networking of different actors in forest industry, graphic arts industry, suppliers, logistics companies and actors from the recycling and landfill stages.

In the light of recent understanding of climate change and the scarce resources, both fossil and renewable, the information that can help to improve the sustainable use of raw materials becomes more important all the time. Life cycle inventory calculations that cover the whole value chain of print products can increase the understanding about the overall environmental impacts of print products. The awareness about environmental impacts can help the printing industry to further improve its performance and move towards more sustainable practices. Improved sustainability performance can bring competitive advantage both for the individual companies and for the industry as a whole. In addition, detailed ecobalance data and life cycle assessment calculations can provide valuable information for the printing press manufacturers.

5. Conclusions

According to the findings presented in this paper, the environmental performance of offset printing has clearly improved since the early 1990's. Energy efficiency and decreased waste output can be seen as the most improved areas. On the other hand, paper consumption per tonne of printed product shows slight increase, despite the numerous technical and process improvements, which should improve paper efficiency.

The case example presented in the paper indicated that environmental impacts of electrophotography printing differed significantly from that of sheet-fed offset. Higher energy and ink consumption of electrophotography can be seen as a disadvantage, but lower water and chemical consumption and lower waste output are clear benefits.

Sustainability and eco-balance issues of printing and printed products require further research. Material efficiency, especially the role of paper, is one of the most important topics for continued attention. The other, relatively new area is digital printing. Both electrophotography and inkjet technologies are undergoing strong technical development - sustainability issues should be included in the development processes.

As a conclusion, since changes and advances in printing technology are achieved, information and research about the sustainability impacts of the new technologies and applications are constantly needed. The results presented in this paper related to electrophotography underline that further research is required and that the new technological solutions are not automatically improving the performance. Instead, the relationship between the eco-balance data, sustainability performance and technological developments is multidimensional, and the impacts are not always clear. To really understand the overall environmental impacts of the print products and to find out the most critical factors, the whole production chain and the life cycle from forest until the end use should be considered.

Acknowledgements

The authors would like to thank the companies that are participating in the research project, as well as TEKES and Graafisen teollisuuden tutkimussäätiö (The Research Foundation of the Printing Industry) for financial support.

References

1. Dalhielm, R., Axelsson, U. (1996). Miljöprofilering - Livscykelanalyser av grafiska produkter. Teknikrapport nr 4/95. Institutet för Medieteknik, Stockholm, 1996 [In Swedish]
2. Enroth, M (2001): Tools for Eco-efficiency in the Printing Industry. Licentiate thesis. Royal Institute of Technology, Stockholm, 2001
3. Enroth, M (2006): Developing tools for sustainability management in the graphic arts industry. Doctoral thesis. Royal Institute of Technology, Stockholm, 2006
4. EU (2007): Reference Document on Best Available Techniques on Surface Treatment using Organic Solvents. European Integrated Pollution Prevention and Control Bureau (EIPPCB), Seville, May 2007
5. Heidelberg (2008): Environmental performance of printing presses. DRUPA 2008 presentation material. Heidelberger Druckmaschinen AG, 2008
6. INFRAS (1998): A Life Cycle Assessment of the production of a daily newspaper and a weekly magazine. Short version of the study. A project of Axel Springer Verlag, Stora and Canfor
7. Jepsen, D., Tebert, C. (2003): Best available techniques in the printing industry. German background paper for the BAT-Technical Working Group "Surface treatment using organic solvents" organised by the European IPPC Bureau. Ökopol GmbH
8. Juntunen, S., Helle, T., Vasara, P., Villikka - Storm, J. (1994): Painetun viestinnän ekotase - Loppuraportti (Eco-balance of Printed Media - Final report). Federation of Finnish Media Industry. [In Finnish]
9. Larsen, H. F., Hansen, M. S., Hauschild, M. (2006): Ecolabelling of printed matter Part II – Life cycle assessment of model sheet fed offset printed matter. Danish Ministry of the Environment, Environmental Protection Agency. Working Report No. 24. 2006
10. Manroland (2008): Manroland EcoLogic. Economy through Ecology. Subjects of Print 1/2008. manroland AG 2008
11. PrintCity (2008a): Sustainability, Energy & Environment. Frequently asked questions ... and some answers. PrintCity Special Report. PrintCity GmbH, 2008
12. PrintCity (2008b): Energy Efficiency. Optimisation for Web Offset Printers. Webline Special Report N°4. PrintCity GmbH, 2008
13. Pösö, K., Juntunen, S., Virtanen, J. (1993): Painetun viestinnän ekotase (Eco-balance of Print Media). Federation of Finnish Media Industry [In Finnish]
14. Rissa, K., (2003) Graafisen alan ympäristöopas. (Environmental Guide for the Printing Sector.) 2nd ed. Työturvallisuuskeskus [In Finnish]

15. Westren-Doll, J., Innanen, J. and Väisänen, T. (1997): Teollisuuden energiatehokkuusindeksi: Graafinen teollisuus (The energy efficiency index of the industry: Printing industry). Motivan julkaisuja 2/97 [In Finnish]
16. Viluksela, P. (2007): Environmental sustainability in the Finnish printing and publishing industry. Licentiate thesis. Helsinki University of Technology, Forest Products Department

Organized alliances in the printing industry

Thomas Mejtoft[1], *Åsa Nordin*[2]

[1] STFI-Packforsk/Media Technology and Graphic Arts, Royal Institute of Technology (KTH)
Järnvägsgatan 3, SE-891 18 Örnsköldsvik, Sweden
E-mail: thomas.mejtoft@stfi.se

[2] Digital Printing Center, Mid Sweden University
Järnvägsgatan 3, SE-891 18, Örnsköldsvik, Sweden

Abstract

Franchising has been important in many industries for a long time and organized alliances are a current phenomenon in the Printing Industry, and may be an alternative way for smaller privately owned printing houses to be a part of a larger network to handle rapid changes in the market. The objective of this qualitative case study of three Swedish Organized Alliances is to investigate how companies perceive the importance of organized alliances in the Printing Industry.

This study concludes that there are many different opinions about the use, impact and importance of organized alliances in the Printing Industry. However, the partner companies believe that they acquire value by being part of an organized alliance. The most important advantages are joint purchasing, access to national agreements, large scale advantages and partly access to a franchise brand. The results indicate that different kinds of organized alliances fit different companies because of the focus of the alliance and the difference in support and commitment from the central organization. Both central organizations and many partner companies deem the franchise brand as important for national recognition. Nevertheless, the combination of the franchise brand and the local company brand is a way for printing houses to strengthen both on the local and national market. The major disadvantage of being part of an organized alliance is the high costs compared to the benefits, which has given many respondents a reason to consider leaving the organized alliances.

Keywords

Competitive advantages, organized alliances, printing industry

1. Introduction

Alliances and acquisitions are two alternative ways to create a governance structure to strategically combine different companies' resources and create competitive advantages. Wang & Zajac [2007] show that even though 82% of investigated US companies considered alliance and acquisition as a way to achieve the same growth goal, only 24% considered an alliance before there latest acquisition. Cooperation and different kinds of partnerships are valuable for achieving competitive advantages in business. Harrigan [1986] suggests that due to technological and economic changes, cooperations have been of great importance in international business since the mid 1970's. This importance was strongly indicated during the beginning of the 1990's, when the number of alliances grew by as much as 25% annually [Bleeke & Ernst, 1995]. Cooperation is in many cases very informal and based on a need for solving problems in the daily business, nevertheless, in many industries organized alliances are important to be able to gain and maintain competitive advantages. One example is the structure of the airline industry. By organizing the industry in alliances it is possible for individual airlines to, more efficiently, serve customers with transportation to destinations all over the world. A study from He & Balmer [2006] provides a good example; the airline industry after the September 11 catastrophe, and the rise of low-cost carriers in North America and Europe have resulted in that most well-established airlines see alliances as necessary. Organized alliances are also a current phenomenon in the Printing Industry, and may be an alternative way for smaller privately owned printing houses to be a part of a larger network to handle rapid changes in the market. Lately, much discussion has been focused on the consolidation of the fragmented and highly competitive Printing Industry [Gilboa, 2002; Kipphan, 2001]. Early research on franchising by Caves & Murphy [1976, p. 573] suggests that franchising has been important in many sectors for a long time. In 1973, 13% of the total sales in the printing and copying sector in the US were from companies in franchising [Caves & Murphy, 1976].

Approximately 90% of the European Printing Companies employ less than fifteen people [Smyth, 2006]. Today many printing houses choose to integrate as much as possible of the printing value chain. The Printing Industry no longer only functions as supplier of printed matters, but has to offer full service solutions of media production to ensure their customers' needs. Having to provide customers with full service solutions is, for many small companies, costly. However, the customers also change their behavior., More customer companies choose to produce a major part of their printed matters in house thanks to the higher quality of and larger range of printing equipment available today for home and office use. Due to mergers and bankruptcies [e.g. Intergraf, 2007; Smyth, 2006], it has been foreseen that the Printing Industry will consist of a smaller number of actors in the future.

A newly seen threat for the mature Western Printing Industry is globalization. Non-time-sensitive material can be printed in Eastern Europe, or even further away in China or India, to a lower cost than within the EU. However, time-sensitive materials, such as e.g. newspapers and some food packages, are still printed locally to ensure short lead times [Smyth, 2006]. For an individual company, taking part in an alliance can be a strategy to try to shape the current market or a doorway to new markets and also achieve benefits such as economies of scale, learning and gaining access to other companies' assets [Faulkner, 1995; He & Balmer, 2006]. This means that due to the strong competitive situation in the Printing Industry, organized alliances could be a way for printers to maintain and increase their market share through e.g. gaining access to customers and avoiding a costly and unhealthy capacity expansion.

Previous research on alliances in the Printing Industry has deemed it important to cooperate with other actors to either extend the service offer with complementary resources or extend resource capacity whenever needed [Mejtoft & Nordin, 2007; Mejtoft & Nordin, 2008]. However, this previous research is focused on ad hoc alliances with low or no formal agreements between partners. This paper extends this research further by focusing on organized alliances with a central organization and formal agreements between partners in the alliance.

2. Research objective

The objective of this study is to investigate how companies perceive the importance of organized alliances in the Printing Industry. This study further aims to identify factors that make companies in the Printing Industry join these strategic alliances, what benefits they perceive, both from the individual printers and from the central organisations.

3. Theoretical framework

The importance of forming strategic partnerships is well known [e.g. Child et al., 2005; Faulkner, 1995; Gulati et al., 2000; Jarillo, 1988]. Being part of an alliance is a way to achieve strategic benefits such as economies of scale, learning, gaining access to other companies' assets and a doorway to new markets. Faulkner [1995] further suggests seven common external forces that describe why alliances are formed; turbulence in markets; economies of scale and/or scope; globalization of the industry; regionalization of the industry; fast technological change leading to ever-increasing investment requirements; shortening product life-cycles and high economic uncertainty. Depending on how these forces are met, different companies can engage in alliances, which, according to Bleeke & Ernst [1995] can result in the emergence of six different types of alliances - collisions between competitors, alliances of week companies, disguised sales, bootstrap alliances, evolutions to a sale and alliances of complementary equals. Bleeke & Ernst [1995] claim that only the last type, alliances of complementary equals, is expected to be successful. The first two almost always fail and the others are likely to end up in a merger or a sale. It should be noted that this situation may not be regarded as a failure since a merger or sale could benefit involved partners.

Being part of an alliance is a way to achieve strategic benefits such as economies of scale, learning, gaining access to other companies' assets and a doorway to new markets. Alliances can also be a way to try to shape the market [Faulkner, 1995; He & Balmer, 2006]. By working in organized alliances it is possible for small companies to receive benefits, such as joint purchasing, gaining access to customers, a strong brand etc, that otherwise only larger companies can benefit from.

One organized form of alliance is the so-called franchise, a cooperation form where *"the licensee takes over the personality and brand of a brand name normally for a specified geographical area"* [Child et al., 2005, p.

109]. Basically this means that franchising is an organizational form with a legal agreement between a central organization (franchisor) and a local company (franchisee). Gerlach [1990] illustrates the importance of updated agreements and that alliances based on trust may end in legal disagreements if the alliances evolve over time and the agreements are not updated to handle the new situation and both parts trust the "gentlemen's agreement". The exchange between the franchisor and the franchisee is that the franchisor normally provides for e.g. common marketing, brand, training and a specific product range. The franchisee, on the other hand, usually pays refundable or non-refundable initial deposits, royalties or other fees for being part of the alliance [e.g. Blair & Kaserman, 1982; Norton, 1988]. Furthermore, the franchisor often has contractual power over the franchisee on e.g. business hours, quality standards and supplying products or material [Inaba, 1980; Rubin, 1978]. According to Gassenheimer et al. [1996, p. 68, based on Shepherd, 1991], *"franchisors act as umbrella organizations, orchestrating the efforts of seemingly independent entrepreneurs sharing a common business formula, similar to a lead firm's role in directing product development, image, and marketing strategy in constellations"*.

The extent of integration between the central organization and the franchisee can vary depending on the strength of the franchise brand or the importance of the technology used in production [Caves & Murphy, 1976]. He & Balmer [2006, p. 242] suggest that *"with careful nurturing on the part of marketers, alliance brands have the potential to develop into a valuable strategic resource"*. In the case of the fast food industry, e.g. McDonald's or Burger King's strong brands have a huge influence over the individual restaurants, both in terms of brand and product range. In a similar way companies such as Anheuser-Busch and Coca-Cola have signed license and franchise agreements with companies in different parts of the world to get access to both production facilities and distribution networks for their beverages [Lei & Slocum, 1991]. It should be noted that a franchise differs from a multi-unit company, such as e.g. H&M, since the franchisees operate as independent companies without central ownership [Caves & Murphy, 1976]. Another interesting aspect of franchising is the sharing of intangible assets [e.g. brand and goodwill) between independent companies [Caves & Murphy, 1976]. One big problem in these cases can be that the value of gaining access to these assets must be predetermined, since these reflect the royalty that the franchisee pays to the central organization. There is, however, no doubt about the franchise concept being important and in 1996, 40% of the total retail sales in the US were through companies that were engaged in franchising [Bradach, 1998].

4. Methodology

This study was designed as a qualitative multiple case study [Yin, 2003] of three organized alliances active in Sweden. Respondents have been selected from nine printing houses (three from each organized alliance) that are currently part of different organized alliances. Furthermore, respondents at each of the three central organizations of the organized alliances were chosen for interviews. In addition, interviews with respondents from thirteen printing houses that are not currently involved in organized alliances were conducted to obtain their view on how these organizations affect the Printing Industry. During the interviews open-ended general questions were asked and depending on the answers follow-up questions could be adjusted to the situation [Robson, 2002]. The interviews were carried out either at the case companies or by telephone during winter 2007 and fall 2008. Additional information has been collected by telephone and from the companies' websites.

Since the Printing Industry, both in Sweden and internationally, is a fragmented industry consisting mainly of many small privately owned companies [Caslon & Company, 2005; Gilboa, 2002; Kipphan, 2001; Smyth, 2006], the printing houses were small and medium sized companies with approximately 10 to 90 employees. Collins & Montgomery [2005, p. 3] state that *"because the impact of corporate strategy is so pervasive and long lasting, it has more important consequences than most other managerial decisions. Setting corporate strategy, therefore, is a critical task and responsibility of the CEO"*. Due to the importance of the founder and/or the CEO in small and medium sized companies [e.g. Beal & Yasai-Ardekani, 2000; Harrigan, 1985; Porter, 1996; Schein, 1983], the CEO at each printing house and central organization was chosen for an interview.

Qualitative case studies make it possible to gain deeper knowledge of the behavior behind the strategy used in an industry [Robson, 2002; Saunders el al., 2007]. According to Yin [2003, p. 9], a case study should be considered when *"a 'how' and 'why' question is being asked about a contemporary set of events, over which the investigator has little or no control"*. The lack of being able to form generalized conclusions is a common criticism of case study methodology. However, in a case study, whether it is a single or multiple case study, Stake [2005, p. 460] states that *"the purpose of a case report is not to represent the world, but to represent the case"*. This means that "*case studies, like experiments, are generalizable to theoretical propositions and*

not to populations or universes" [Yin, 2003, p. 10]. This means that even though the results from this study should not be considered general, they give a good indication of the importance of organized alliances in the Printing Industry.

5. Results and discussion

During the last couple of years the number of companies organized in alliances has grown and the results of this study show that the organized alliances in the Printing Industry in Sweden are important, this is the belief of both the partner companies and the central organizations. The three organized alliances in this study all were established (in alliance form) from the late 1970s to the late 1990s. Nevertheless, for all organized alliances the biggest growth was in the late 1990s.

Table I: Summary of organized alliances in the Swedish Printing Industry

	Organized Alliance		
	Alliance 1	**Alliance 2**	**Alliance 3**
Type:	Franchise/ Multi-unit company	Franchise	Equity interest in central organization
Fee base:	Initial deposit + Turnover based fee	Fixed monthly fee + Turnover based fee	Turnover/ no of employees/ location based fee
Size of central organization:	Large	Small	Small
Offer:	Joint purchasing Franchise brand Joint marketing IT support Access to national agreements Large scale advantages Distributed printing and geographic access	Joint purchasing Franchise brand Joint marketing Access to national agreements Large scale advantages	Joint purchasing Franchise brand[1] Joint web sales Access to national agreements Large scale advantages Distributed printing and geographic access
Perceived strength of franchise brand:	Strong	Weak	Medium
Current trend of Organization growth:	Small increase	Small increase	No change

The degree of dependence and control from the central organization on the individual printing houses differ, but generally the influence from the central organizations is quite weak. The three investigated organized alliances have slightly different structure and purpose (Table I). Alliance 1 is based on both the franchise concept and the central organization being a multi-unit company, since the central organization is running several of the individual printing houses. The franchisee pays a fee based on an initial deposit and a variable turnover based fee to the central organization. In contrast to Alliance 1, Alliance 2 and Alliance 3 consist only of privately owned independent companies. In Alliance 3 the partner companies all have an equity interest in the central organization at the same time as they pay a regular fee to the central organization (comparable to a franchise fee). This fee is based on turnover, the size of the company (no of employees) and how dense the populated area around the printing house is. Alliance 2 is based on a classic franchise concept where the central organization is independent from the partner companies and each franchisee pays a fee based on turnover to the central organization. Hence, all organized alliances in this study are based on a variable fee from the partner companies to the central organization. This is also, according to the respondents, one of the major problems of being part of an organized alliance - the cost. The respondents believe that the cost is quite high, and many of the case companies have from time to time considered leaving the alliance since the cost/benefit ratio is too high. This picture is also confirmed by the respondents at companies that are currently not part of organized alliances, as they state that they believe the costs for being part of an organized alliance are higher then the expected benefits.

[1] Even though Alliance 1 is not technically a franchise organization, the term franchise brand will be used to avoid confusion, since the idea behind the branding is similar.

There are differences in the size of the central organizations and this has, according to the respondents, an impact on the services and the support the central organizations can provide their partner companies. Alliance 1 has the most structured and largest central organization, while Alliance 2 and Alliance 3 have smaller central organizations. There is criticism toward both of these forms. Companies within Alliance 1 partly think that they are too controlled by the central organization, whilst companies within Alliance 2 and Alliance 3 believe that their alliances are to "loose" in structure, which affect the commitment to the alliance negatively.

The results show that the main reason for joining an organized alliance is *joint purchasing*, *access to national agreements* and *large scale advantages* through sharing jobs (Table I). Getting access to a *franchise brand* is also a major reason, however, the opinion about the brand differs, and this is why this cannot be regarded as a main reason. Companies within Alliance 1 believe that they acquire access to a strong brand, which also is a part of the organized alliance policy that the brand is displayed and used. In the other alliances this is also a policy, but according to the respondents, the observance is to some extent rather low. This has made those brands less strong. It should be noted that Alliance 2 saw a drop in the number of partner companies when they regulated that all partner companies should use and display the franchise brand. This illustrated the importance of the local brand for companies in the Printing Industry.

Furthermore, the different case companies emphasize other values received from being part of an organized alliance, one example is the possibility of distributed printing due to the nationwide network of printing houses. Even though one of the major benefits mentioned is access to the network itself, the respondents believe that in many cases the members of the organized alliance act more individual than as a group. This has resulted in a situation where the respondents feel that it is hard to work along a common strategic path in the alliances.

5.1 Impact of organized alliances

The primary impact of organized alliances is *internal*, since they mainly contribute to lowering costs and increasing effectiveness for the partner companies. This is a classic way of working in an industry that is under constant price pressure and under tough competition [e.g. Birkenshaw, 2004; Smyth, 2006], where lowering costs are important. The organized alliance provide a possibility for lowering costs by e.g. joint purchasing and sharing costs by e.g. joint marketing, joint development of IT systems etc.

Marketing, however, touches upon the secondary impact of organized alliance - the *external impact*. By getting access to a network it is possible for the partner companies to increase their competitive advantages and provide full service solutions for their customers. Furthermore, the structure of the Printing Industry has historically consisted of many individual companies working mostly on local or regional markets. This has made the individual printing houses' brand strong locally, but, generally, not nationally. The use of the franchise brand of the organized alliance strengthens the company both locally and nationally. Most of the case companies have, however, kept their own company brand and complimented this brand with the brand of the alliance. In this way they feel that they can gain both local and national benefits of having strong brands. Other external impact is the opportunity the organized alliance provides in taking part of large national agreements, which they cannot handle on their own. This is a way for a smaller local company to expand their market and enable increased production at a low cost. As mentioned before, it should be noted that the strength of the different brands of the organized alliances differs, and not all are well known to the general public.

There are many different opinions about the use, impact and importance of organized alliances in the Printing Industry. This has also, according to the respondents, reflected itself in the organizations. Apart from Alliance 1, which is the most structured and controlled, there are many opinions from the partner companies on how the alliances should work. Since all partner companies are individual companies with different opinions and strategic goals, the key to success is still within each of the individual companies. This has, according to the respondents, severely slowed the development of the alliances. Nevertheless, it should be noted that the respondents in general were quite satisfied with their commitment to the organized alliances, otherwise they should have discontinued their participation. Even though companies within organized alliances believe that they get market advantages, companies that are not currently part of organized alliances believe that the alliances' impact on the market is rather insignificant. Some of the non-organized respondents even believed that joining an organized alliance might harm the companies' development, since too much faith is put into the alliance to be the solution to the companies' problems. This to some extent is consistent with the respondents within the organized alliance, as they state that the success of the partner companies is still dependent on each company.

The results from this study on organized alliances differ slightly from earlier studies regarding the use of alliances in the Printing Industry [Mejtoft & Nordin, 2007; Mejtoft & Nordin, 2008]. While other alliances often are formed locally or regionally to complement or extend resources, the organized alliances are more focused on activities such as joint purchasing and creating a network of printers distributed over the country. It is clear that to be able to create a larger network of printers a central organization, which controls the alliance, is needed. In the case of "ordinary" alliances in the printing industry, they are not controlled in the same manner as organized alliances, but rather more of ad-hoc alliances. Even though opinions differ, organized alliances are important and due to the current restructuring of the Printing Industry with mergers and bankruptcies, organized alliances can be a possible scenario for smaller local privately owned companies to remain as individual companies. In the strong competitive situation in the Printing Industry, organized alliances could be a way for printers to maintain and increase their market share through e.g. learning, gaining access to customers and avoiding a costly and unhealthy capacity expansion.

6. Conclusions

During the last couple of years the number of companies organized in the alliances in this study has grown. Partner companies believe that they acquire value by being part of such an alliance. This study, however, also concludes that there are many different opinions about the use, impact and importance of organized alliances in the Printing Industry. The most valuable advantages are *joint purchasing*, *access to national agreements*, *large scale advantages* and partly *access to a franchise brand.*

Different kinds of organized alliances fit different companies because of the focus of the alliance and the difference in support and commitment from the central organization. Both central organizations and many partner companies deem the franchise brand as important for national recognition. Nevertheless, the combination of the franchise brand and the local company brand is a way for printing houses to strengthen both on the local and national market. The major disadvantage of being part of an organized alliance is the high costs compared to the benefits, a fact which has given many respondents a reason to consider leaving the organized alliances.

Acknowledgements

The authors would like to thank *all the anonymous respondents* at the case companies for their participation in this research study. We would also like to show our gratitude to *Prof. Nils Enlund*, KTH, and *Dr. Marianne Klaman* for their valuable comments on this research project. The *Kempe Foundations*, the *EU Structural Fund*, the *industry participants in STFI-Packforsk's DigiPrint project* and *Mid Sweden University's Digital Printing Center* are gratefully acknowledged for their financial support.

References

1. Bleeke, J., & Ernst, D., (1995, January-February), *Is Your Strategic Alliance Really a Sale?, Harvard Business Review, pp. 97 - 105*
2. Beal, R. M., & Yasai-Ardekani, M., (2000), *Performance implications of aligning CEO functional experiences with competitive strategies, Journal of Management, Vol. 26, No. 4, pp. 733 - 762*
3. Blair, R. D., & Kaserman, D. L., (1982), *Optimal Franchising, Southern Economic Journal, Vol. 49, No. 2, pp. 494 - 505*
4. Bradach, J. L., (1998), *Franchise Organizations, Harvard Business School Press*
5. Birkenshaw, J., (2004, April), *The future of print on paper, Prepress and print Technology, Pira International. Retrieved January 26, 2005, from http://pira.atalink.co.uk/pulp-and-paper/163.html*
6. Caslon & Company., (2005), Digital Printers - Growth Leaders of the Printing Market, Caslon & Company
7. Caves, R. E., & Murphy II, W. F., (1976), *Franchising: Firms, Markets, and Intangible Assets, Southern Economic Journal, Vol. 42, No. 4, pp. 572 - 586*
8. Child, J., Faulkner, D., & Tallman, S., (2005), *Cooperative Strategy, Managing Alliances, Network and Joint Ventures, Second Edition, Oxford University Press*
9. Collis, D. J., & Montgomery, C. A., (2005), *Corporate Strategy, A Resource-Based Approach, Second Edition, McGraw-Hill/Irwin*
10. Faulkner, D., (1995), *International Strategic Alliances, Co-operating to Compete, McGraw-Hill*

11. Gassenheimer, J. B., Baucus, D. B., & Baucus, M. S., (1996), *Cooperative Arrangements among Entrepreneurs: An Analysis of Opportunism and Communication in Franchise Structures, Journal of Business Research Vol. 36, pp. 67 - 79*
12. Gerlach, M., (1990), *Trust is not Enough: Cooperation and Conflict in Kikkoman's American Development, Journal of Japanese Studies, Vol. 16, No. 2, pp. 389 - 425*
13. Gulati, R., Nohria, N., & Zaheer, A., (2000), *Strategic Networks, Strategic Management Journal, Vol. 21, pp. 203 - 215*
14. Gilboa, R., (2002), *The Production Digital Printing Market: Opportunities and Trends, Proceedings from IS&T's NIP18, pp. 134 - 138*
15. Harrigan, K. R., (1985), *Vertical Integration and Corporate Strategy, Academy of Management Journal, Vol. 9, No. 2, pp. 397 - 425*
16. Harrigan, K. R., (1986), *Managing for Joint Venture Success, Lexington Books*
17. He, H - W., & Balmer, J. M. T., (2006), *Alliance brands: Building corporate brands through strategic alliances?, Brand Management, Vol. 13, No. 4/5, pp. 242 - 256*
18. Inaba, F. S., (1980), *Franchising: Monopoly by Contract, Southern Economic Journal, Vol. 47, No. 1, pp. 65 - 72*
19. Intergraf, (2007), *Competitiveness of the European Graphic Industry, European Commission, Enterprise and Industry Directorate-General*
20. Jarillo, J. C., (1988), *On Strategic Networks, Strategic Management Journal, Vol. 9, pp. 31 - 41*
21. Kipphan, H., (2001), *Handbook of Print Media, Technologies and Production Methods, Springer*
22. Lei, D., & Slocum, J. W., (1991), *Global Strategic Alliances: Payoffs and Pitfalls, Organizational Dynamics Vol. 19, No. 3, pp. 44 - 62*
23. Mejtoft, T., & Nordin, Å., (2007), *Strategic Alliances in the Digital Printing Industry, TAGA 2007 Proceedings, pp. 38 - 62*
24. Mejtoft, T., & Nordin, Å., (2008), *Cooperation and Resource Flexibility as Competitive Strategy: The Case of the Printing Industry, Submitted for publication*
25. Norton, S. W., (1988), *An Empirical Look at Franchising as an Organizational Form, The Journal of Business, Vol. 61, No. 2, pp. 197 - 218*
26. Porter, M. E., (1996, November-December), *What is Strategy?, Harvard Business Review, pp. 61 - 79*
27. Robson, C., (2002), *Real World Research, Second Edition, Blackwell Publishing*
28. Rubin, P. H., (1978), *The Theory of the Firm and the Structure of the Franchise Contract, Journal of Law and Economics, Vol. 21, No. 1, pp. 223 - 233*
29. Saunders, M., Lewis, P., & Thornhill, A., (2007), *Research Methods for Business Students, Forth Edition, Prentice Hall*
30. Schein, E. H., (1983), *The Role of the Founder in Creating Organizational Culture, Organizational Dynamics, Vol. 12, pp. 13 - 28*
31. Shepherd, J., (1991), *Entrepreneurial Growth through Constellations, Journal of Business Venturing Vol. 6, No. 5, pp. 363 - 373*
32. Smyth, S., (2006), *The Future of European Printing to 2011, Pira International*
33. Stake, R. E., (2005), *Qualitative Case Studies, In N. K. Denzin, & Y. S. Lincoln (Eds.), The SAGE Handbook of Qualitative Research, Third Edition (pp. 443 - 466), Sage Publications*
34. Wang, L. & Zajac, E. J., (2007), *Alliance or acquisition? A dyadic perspective on interfirm resource combinations, Strategic Management Journal, Vol. 28, No. 13, pp. 1291 - 1317*
35. Yin, R. K., (2003), *Case Study Research, Design and methods, Third Edition, SAGE Publications*



Delivery times and closeness to geographic market: A comparison between digital and conventional printing houses

Thomas Mejtoft, Magnus Viström

STFI-Packforsk
Media Technology and Graphic Arts, Royal Institute of Technology (KTH)
Järnvägsgatan 3, SE-891 18 Örnsköldsvik, Sweden
E-mail: thomas.mejtoft@stfi.se

Abstract

Having short delivery lead times has been deemed as a major order winner and a way of creating short term competitive advantages. Short delivery lead times are also important when trying to reduce inventory levels. This study of 136 randomly selected Swedish commercial printing houses, investigates the differences between digital printers and conventional printers with respect to the importance of providing short delivery times and having close geographic distances to customers.

The study concludes that printing houses, using digital printing, are active mostly on a regional market, while printing houses using conventional printing are active mainly on a national market. Further, digital printing contributes to significantly shorter delivery times, which, in general, are deemed important to be kept short. Nevertheless, there are indications of a larger gap, regarding delivery times, between importance and perceived customer satisfaction among digital printers than among conventional printers.

Keywords

Business strategy, delivery time, geographic market, printing industry

1. Introduction

Being able to provide short delivery lead times is in general regarded as an important factor for the success of a company [e.g. Blocher et al., 1999; Johansson et al., 1993; Tan, 1998]. This is also the case in the Printing Industry. One of the drawbacks of printed communication before the introduction of digital printing was the difficulty of achieving time and cost efficiency in smaller production volumes [Kipphan, 2001]. The setting-up of a print run and the start-up of a conventional printing press, before delivery-ready copies can be produced, have been labor and time intensive. According to Smyth [2003, p. 302], *"digital printing has changed a lot of the restraints of delivery times"* due to short set up times. This advantage allows fast completion of the first delivery-ready copy, which makes digital printing suitable for on-demand printing when fast deliveries are important. So-called on-demand printing can, according to Romano et al. [1999, p. 133], be defined as *"short notice, quick turnaround of short, cost-competitive print runs"*. In contrast to conventional printing technologies, that use static printing formes, make-ready times for digital printing are low. Although, the printing speed of digital printing is lower than the speed of conventional printing [e.g. Mejtoft, 2005], the technology behind digital printing makes it advantageous to use when fast deliveries of short print runs are required (Figure 1).

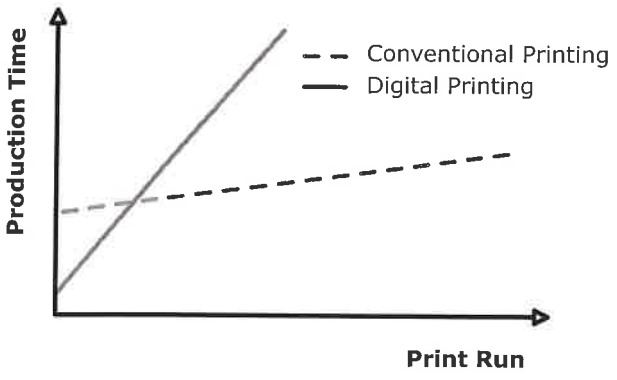


Figure 1:
Digital printing has a shorter make-ready time But a lower print speed than conventional printing technologies [After Kipphan, 2001]

The Commercial Printing Industry is in general considered as a low margin industry, with declining prices, and the competition between companies is regarded as fierce [Birkenshaw, 2004; Mejtoft & Viström, 2007; Smyth, 2006]. Lately, differentiating and adding value to printed products as well as the value of becoming a service provider have become widely discussed issues in the printing industry [e.g. PODi, 2003; PODi, 2006; Romano, 2004]. Providing short lead times are a way for digital printers to differentiate their service from conventional printers.

Previous research [Mejtoft, 2006] has deemed small editions and short lead times for time critical jobs to be the primary added value gained by using digital printing. Providing short lead times is also a factor that printing houses perceive their customers to value very high [Mejtoft & Viström, 2007; Viström & Mejtoft, 2007]. However, failing to meet delivery commitments was, according to Pellow et al. [2002], a reason for customers having doubt about digital printing in the early stages.

1.1 Research objective

This study sets out to investigate the differences between digital printers and conventional printers with respect to the importance of providing short delivery times and having close geographic distances to customers.

2. Theoretical framework

As mentioned earlier, providing short delivery lead times is important for a company if it is to be successful [e.g. Blocher et al., 1999; Johansson et al., 1993; Tan, 1998]. In accordance with Aitken et al. [2002, p. 62], total lead time can be defined as *"the time taken from a customer raising a request for a product or service until it is delivered"*. Having short lead times is important in many logistic systems and has been deemed as a major order winner [Stalk & Webber, 1993]. Reduction of lead times can also be a source of competitive advantages [e.g. Tan, 1998]. Nevertheless, being able to provide a high level of service, such as assuring fast deliveries, is most often done at the expense of having higher costs [e.g. Brandenburger & Nalebuff, 1996; Herer et al., 2002]. Hence, the aspect of cost is very important; however, in this research study the possible increase of cost for providing short delivery times is left for future research.

Reduced lead time is also an important part of the lean manufacturing approach that derives from the Toyota Production System (TPS) [e.g. Liker, 2004; Liker & Morgan, 2006]. In Just-in-Time manufacturing, which is a crucial aspect of lean manufacturing, *"only the necessary products, at the necessary time, in necessary quantity"* are manufactured or ordered [Sugimori et al., 1977, p. 553]. Postponement strategies were first proposed in the early 1950s [Alderson, 1950; Bucklin, 1965] and Stern & El-Ansary [1992, p. 22] states that *"postponement promotes efficiency by moving differentiation nearer to the time of purchase when demand is more certain, thus reducing risk and uncertainty costs"*. In Just-in-Time models, relationships with suppliers are important and Mohr and Spekman [1994, p. 138] propose that *"without high levels of coordination, Just-in-Time processes fail, production stops, and any planned mutual advantage cannot be achieved"*. Because of fast product development and fast price declination of parts, in e.g. the PC industry, short delivery lead times are crucial. By adopting Just-in-Time delivery models it has been possible e.g. for Dell [Selling PCs, 1996] to limit the amount of value that got wasted in the assembly process between purchasing and sales.

Reducing inventory levels is something that is important in many industries. Porter [1990, p. 42] states that *"on-time delivery requires that operations, outbound logistics, and service activities such as installation should function smoothly... good coordination allows on-time delivery without the need for costly inventory"*. As a result of customers keeping low stock of finished goods, many customers demand guarantees of delivery reliability to reduce their risk in the just-in-time approach [Hill & Chambers, 1990]. Being able to deliver at the actual time and date promised, having high delivery reliability, is accordingly increasingly important, since this makes it possible for customers to plan their actions more accurately. Wang et al. [2002, p. 988] suggest that *"introduction of service differentiation based on demand-lead-time, manufacturers can reduce system-wide stock levels, and pass the savings on to their customers"*. If a delivery is, however, not made on time, it can disrupt a customer's production process and force a last minute rescheduling of the customers' deliveries [Hill & Chambers, 1990].

Geographical distances between supplier, producer and customer have traditionally been an important issue in many industries and working with a specific geographic market is common when customer's location is

important for business success [Anderson & Narus, 2004; Axelsson et al., 2005]. However, new information technology and efficient logistics systems have made this issue less important in some industries. In general, expanding towards new geographic markets is a way of expanding the business within the current industry [Collis & Montgomery, 2005]. Nevertheless, country boundaries are usually the most influential factor since government regulation and logistics are more difficult to handle [Day, 1990].

Aitken et al. [2002] states that a company providing short lead times and high delivery reliability can improve its customers' cash flow due to the possibility for the customers to reduce their stock levels. By offering this advantage a company can compete against low prices. Hill & Chambers [1990] deem delivery reliability as an important order winner along with having short delivery times. Inability to meet delivery schedule with the right quantity and quality is according to Dobler & Burt [1996] the single greatest supplier failure.

3. Methodology and study design

This paper is based on a subset of data from a larger survey study of 136 Swedish commercial printing houses carried out during the spring and early fall of 2006. The questionnaire was sent out by letter to 300 companies, which were randomly selected Swedish commercial printing houses from the members' list of the Swedish Graphic Companies' Federation (GFF). It should be noted that this list is not a complete list of all commercial printing houses in Sweden, which limit the possibilities to generalize the results to the whole Swedish commercial printing industry. An alternative to this list could be e.g. extracted from the telephone directory or a financial information database. However, these other alternatives did not, according to the authors, provide a list with sufficient accuracy. Consequently, the authors believe the list used to be the best directory to constitute the basis for this survey investigation of Swedish printing houses. Although the used list is not complete, it does, according to GFF, include companies covering at least 80% of the volume of invoiced sales of printed commercial products in Sweden [K. Flick, *GFF*, personal communication, January 25, 2007]. Hence, the results should give a good indication of the situation in the Swedish commercial printing industry. CEOs or vice managing directors made up 82% of the respondents. The rest of the respondents were persons responsible for marketing, production or logistics.

The data in the study has been separated and analyzed in different categories depending on the printing technology used at each company. The categories used were: *all commercial printing houses*, *commercial printing houses with digital printing* (39%) and *commercial printing houses with only conventional printing* (61%). The other categories *printing houses with only digital printing*, *printing houses with both conventional and digital printing* and *printing houses with conventional printing* were also analyzed, but without any interesting results. For a printing house to be regarded as using a specific printing technology in production, it should constitute at least 10% or more of the total production.

3.1 Questionnaire design

The questionnaire was designed to obtain information about the respondents' opinion on the importance of delivery time, importance of delivery reliability, perceived customer satisfaction, future changes and actual performance in terms of geographic market and delivery time. The questionnaire was mostly based on closed questions, with the purpose of measuring opinions. Data was collected using numeric rating scales where the end categories were labeled with appropriate options [Saunders et al., 2007]. Two different scales were used, a 10-point numeric rating scale from 1 to 10 when rating opinions about e.g. importance. When rating opinions about e.g. future changes, an 11-point rating scale from -5 to +5 (including 0) was used to capture positive and negative changes. However, it is important to remember that respondents may have different perceptions about numerical values [Churchill and Brown, 2004]. Furthermore respondents may tend to set high values when they are evaluating their own performance [Robson, 2002]. However, since the purpose was to evaluate different factors or groups of the same factor against each other the problem identified by Robson [2002] was not an issue in this case.

All questions were in Swedish, since the questionnaire was completed by Swedish printing houses. To ensure the validity of the questionnaire, an initial pilot testing [Saunders et al., 2007] was performed with three printing houses. Some questions were changed and new questions were formulated according to comments made by the respondents in this pilot test.

3.2 Data collection and analysis

Since this survey was constructed as a self-administrated survey, a covering letter, explaining the survey, was enclosed in the letter to each respondent [Saunders et al., 2007]. The respondents had the choice of responding either by post or through a web interface. The companies that did not respond to the initial survey were reminded by email and/or telephone. While collecting data from the sample, it was found that some of the companies did not meet the research requirements of this study as they did not at the time of the study own any printing equipment, and they were subsequently omitted. Hence, the response rate was calculated, in accordance with the Council of American Survey Research Organizations [CASRO, 1982; Wiseman & Billington, 1984] requirements. Out of a total of 300 companies, 46 were found to be ineligible and 136 eligible companies responded, which constituted a total response rate of 54%. Out of all companies, only six were not possible to reach by personal communication (i.e. telephone or email), implying that practically all ineligible companies in the sample have been identified. The reason for having so many as 46 ineligible companies was that the database contained some companies that went into bankruptcy, sold their printing units or did not currently own any printing equipment, but were interested in the Commercial Printing Business. In most cases the latter companies were working with activities closely related to this business, such as prepress, finishing or sales of printing equipment. About half of the answering respondents posted their answers without any reminder, whereas the other half sent their response after being given a reminder. According to Armstrong & Overton [1977] people who respond late are assumed to be comparable with non respondents. No major differences between the two groups were found, thus giving an indication of no significant differences between respondents and non-respondents.

The sample (136 companies) was large (>30) and approximately normally distributed [Keller, 2005], whereby the t-distribution was used to calculate confidence intervals and p-values. Since the sample also covered a large portion of the studied population (428 companies) a Finite Population Correction Factor (FPCF) was used when calculating the standard deviations for the mean values [e.g. Andersson et al., 2002; Keller, 2005]. The significance between different categories in the dataset has been analyzed using an independent sample t-test using a 95% confidence level. The significance of differences between factors was determined using a paired sample t-test. SPSS 15 and Microsoft Excel 2003 were used for the statistical analysis.

A survey study typically gives a good overview over a large population (e.g. an industry), while it is more difficult to get a deeper understanding of specific research questions. To get deeper understanding it is preferable to use in-depth case studies of a few selected companies. However, since the aim of this study was to investigate the positioning of the commercial printing industry, the use of a survey should be regarded as the preferable method. As mentioned earlier, the aim of this survey was to capture opinions of the respondents. Peoples' opinions are, however, always subjective and do not necessarily correspond to reality, which is a limitation of any study concerning the capture of opinions.

4. Results and discussion

4.1 Customers and geographic market

The companies in this study had, on average, 549 different customers that placed orders annually (Table I). There was a significant difference ($p = .000$) between printing houses with digital printing technology (digital printers) and printing houses using only conventional printing (conventional printers) in number of annually returning customers. Digital printers had, on average, 601 annual returning customers, while conventional printers had 512. One reason for digital printers having more reoccurring customers than conventional printers is that order sizes in digital printing are usually smaller than orders in conventional printing. Consequently, since the volumes are lower, digital printers may need to have more customers to increase their total volume. This strengthens the propositions from e.g. Corr et al. [2005] that providing digital printing services may help printing houses to acquire new customers.

Table I: Annual returning customer base for companies within the Printing Industry

	All Printers	Digital Printers	Conventional Printers
Mean value:	549	601	512
Std. deviation:	558	547	649
95% conf. interval	100	156	152
No. of respondents:	122	50	72

Regarding delivery time, the geographic market of the companies is important, since shorter distances may decrease delivery times. There is a significant difference ($p = .038$) between digital printers and conventional printers in how they define their maximal geographic market (Figure 2). While conventional printers work primarily on a national level, digital printers are mainly active on the regional market. Segmentation and working with a specific geographic market are common when the location of the customers is important for business success [Anderson & Narus, 2004]. This strengthens the view on digital printing being a technology for short delivery times, as digital printers try to work with shorter geographic distances [Mejtoft, 2006].

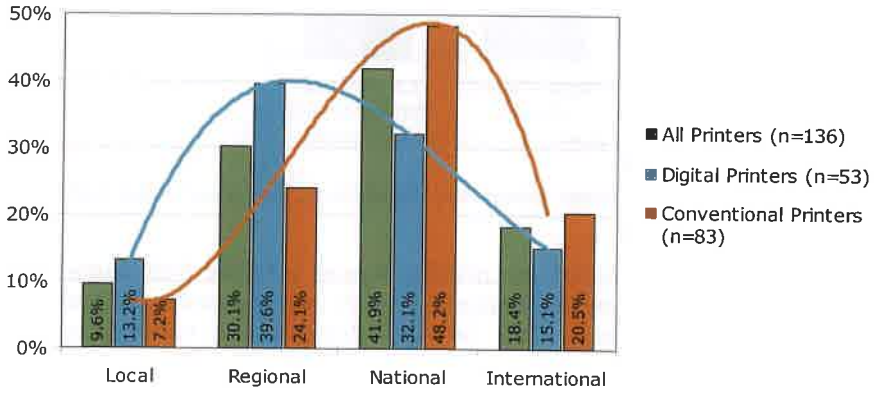


Figure 2: Geographic market of the printingiIndustry

Regarding working with international customers, there were just small differences between the two categories. Concerning geographic boundaries, country borders are also usually the most influential since government regulation and logistics are more difficult to handle internationally [Day, 1990].

Accordingly, digital printers deem it significantly ($p = .000$) more important to have customers in close vicinity than conventional printers do (Figure 3).

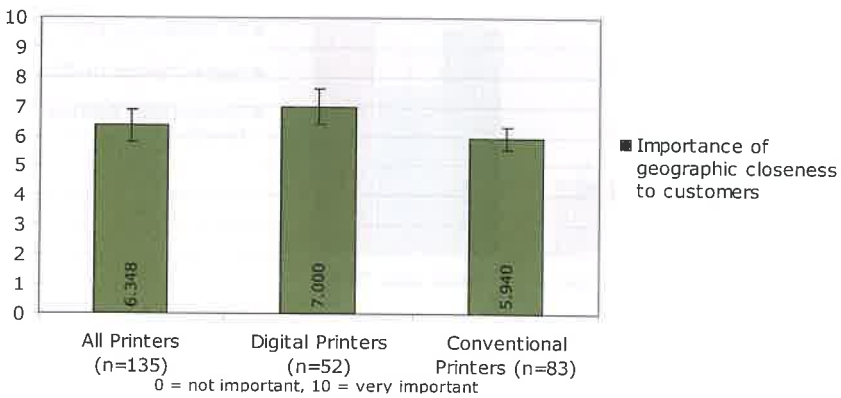


Figure 3: Importance of geographic closeness to customers (mean values with a 95% conf. interval)[1]

4.2 Delivery Times

Short delivery times are, as mentioned earlier, important in the Printing Industry in general and particularly in the Digital Printing Industry, as the short setup times of digital printing are suitable for quick order fulfillment. In Figure 4 it can be noted that the grading of the importance of short delivery times is high and there are just small differences between conventional and digital printers. Even though no significant differences can be detected, digital printers tend to grade the importance of short delivery times slightly higher than conventional printers do.

[1] Survey question: *"How important is it to have geographic closeness to customers?"*

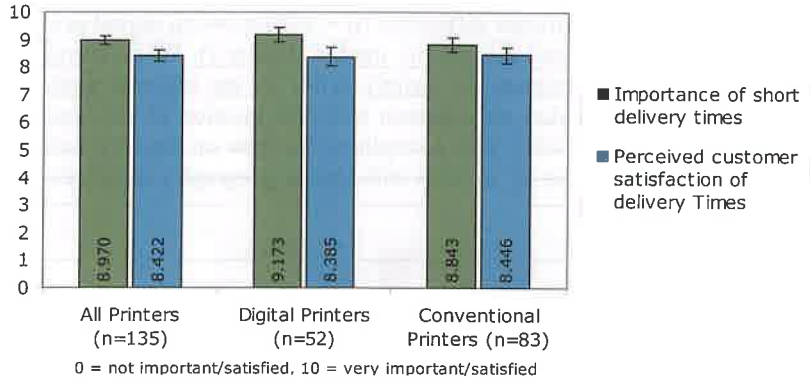


Figure 4: Importance of and perceived customer satisfaction with delivery times (mean values with a 95% conf. interval)[2]

However, the gap between how satisfied the printing houses perceive their customers to be and the importance of short delivery times is greater for digital printers than conventional printers. Hence, there is a difference in importance and performance. This can signal that customers have higher demands on digital printers than conventional printers regarding providing short delivery times, which is further strengthened by this study's result regarding actual internal lead times[3]. Digital printers provide significantly shorter lead times, both in terms of mean and shortest lead time (Figure 5). The shortest lead time for digital printers was on average 0.82 days, while conventional printers used twice the time, 1.69 days, on average. A similar pattern can be noticed regarding mean lead times (Figure 5). As expected there is a large correlation effect (r = .716) between average and shortest lead times provided [in accordance with Cohen, 1977]. Even though lead times are in fact shorter when using digital printers, the gap between importance and perceived customer satisfaction is greater.

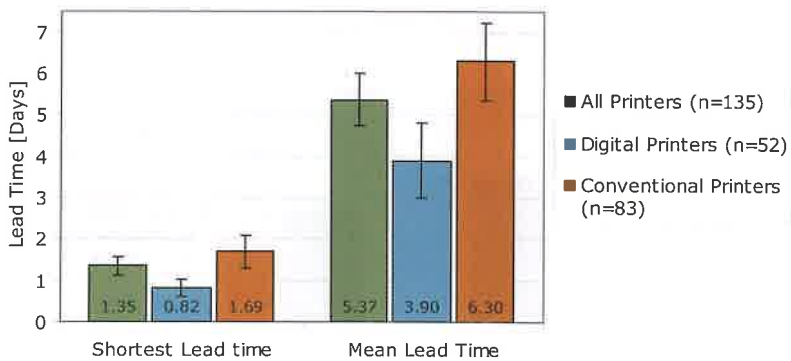


Figure 5: Shortest and mean lead times[3] *(mean values with a 95% conf. interval)*

Furthermore, the share of digital printing used in production has been measured, and a negative medium correlation [in accordance with Cohen, 1977] of r = -.347 can be detected between the share of digital printing used in production and average lead time. This implies that a higher share of digital printing used in a printing house results in a shorter average lead time.

When analyzing the actual delivery times, it is important to keep in mind that not only the printing technology will influence the delivery times, but also the geographic distance to the customers. Even though deliveries over national distances are relatively fast, it is hardly possible to achieve delivery times shorter than one day if any major parcel distributor, such as the national postal services should be used. Hence, it seems like digital printers choose to work locally or regionally to be able to provide really short delivery times. As stated earlier,

[2] Survey questions: *"How important is it to provide short delivery times? How do you perceive the customers satisfaction of your delivery times?"*
[3] Lead time from finished original to delivery ready prints.

digital printers had a closer geographic market (Figure 2) and consequently this contributes to keeping total delivery times short for digital printers.

Johansson et al. [2006] stress that digital printers believe that competition from conventional printers on providing short delivery times has strengthened. Figure 6 illustrates that this competition may be strengthened further since conventional printers believe that their delivery times will be shortened even more than digital printers believe. However, in general, digital and conventional printers agree that delivery times will be even shorter in the near future (within a three year period).

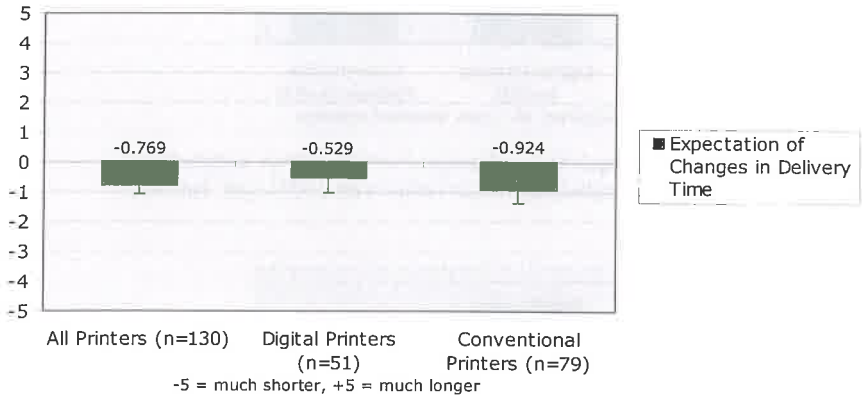


Figure 6: Future expectations regarding changes in delivery time within a three year period (mean values with a 95% conf. interval)[4]

Not surprisingly, only a small part of the printing houses expect the delivery lead times to increase within a three year period (Figure 7). Meanwhile about half of the respondents expect the delivery lead times to decrease. In general there is no correlation between current shortest or average delivery times and the expectations about the future. This indicates that the expectations about shorter delivery times are unanimous within the Printing Industry.

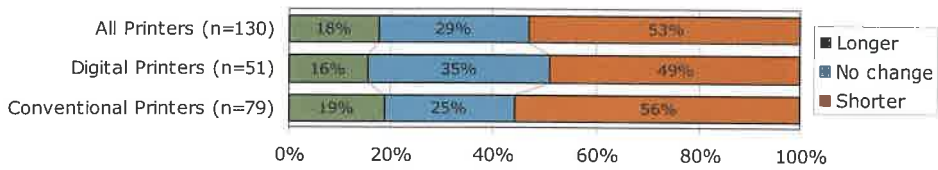


Figure 7: Distribution of companies regarding future expectations on delivery times

4.3 Delivery reliability

In addition to the fact that providing short delivery times are deemed important (Figure 4), it is also considered important to have high delivery reliability, i.e. deliver on time promised (Figure 8).

It is also possible to notice a positive medium correlation [in accordance with Cohen, 1977] of r = .343 between the grading of importance of short delivery times and the grading of importance of high delivery reliability.

4.4 The importance of digital printing for delivery times and delivery reliability

The results from this study indicated that digital printing is regarded as important for achieving both short delivery times and high delivery reliability (Figure 9). There was a significant (p = .000 in both cases) difference between digital printers and conventional printers, and, as expected, digital printers are more confident in digital printing being the solution for short delivery times and high delivery reliability.

[4] Survey question: *"How do you believe that the delivery times will change within a three year period?"*

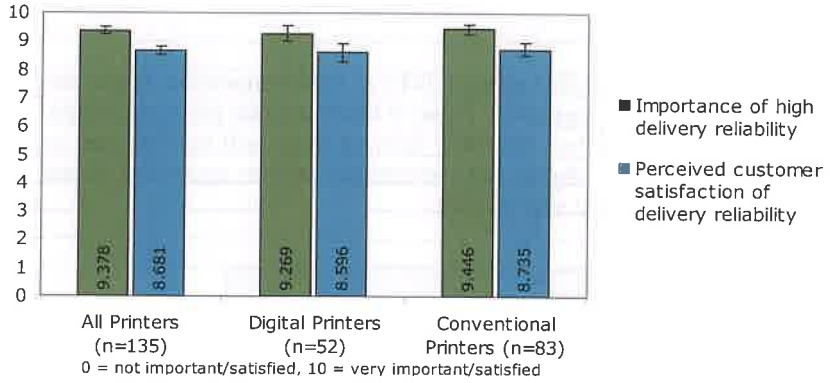


Figure 8: Importance of and perceived customer satisfaction with delivery reliability (mean values with a 95% conf. interval)[5]

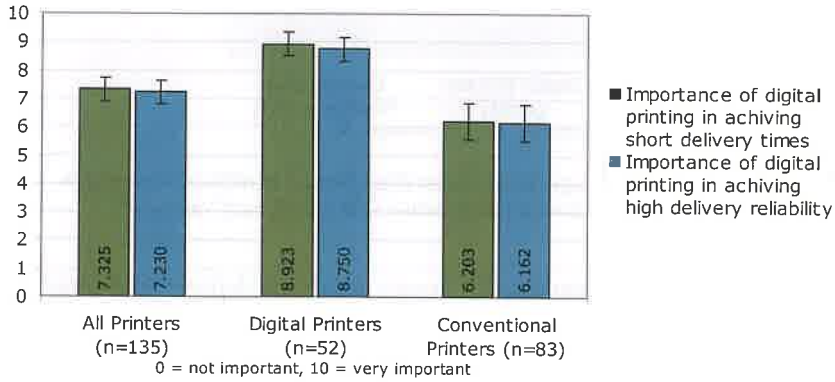


Figure 9: Importance of digital printing in achieving short delivery times and high delivery reliability (mean values with a 95% conf. interval)[6]

5. Conclusions

This study concludes that digital printers are active mostly on a regional market, while printing houses using conventional printing are active mainly on a national market. Further, digital printing contributes to significantly lower delivery times, which, in general, are deemed important to be kept short. Nevertheless, there are indications of a larger gap, regarding delivery lead times, between importance and perceived customer satisfaction among digital printers than among conventional printers.

Digital and conventional printers agree on that delivery times will be shorter in the near future. However, there are indications that the competition between digital and conventional printing regarding delivery times will further strengthen in the future since conventional printers believe that their delivery times will be shortened even more than digital printers believe that theirs will be.

Acknowledgements

The authors would like to thank *Ola Karlsson*, *Kaj Flick* and *Hasse Johansson* at the *Swedish Graphic Companies' Federation (GFF)* for valuable input to this survey investigation and sharing their members list. Furthermore, the authors express their gratitude to *the respondents* for their participation in this survey investigation and *Prof. Nils*

[5] Survey questions: *"How important is it to have high delivery reliability? How do you perceive the customer satisfaction of your delivery reliability?"*

[6] Survey question: *"How important do you regard digital printing for providing short delivery times/high delivery reliability?"*

Enlund, KTH, *Dr. Marianne Klaman*, STFI-Packforsk and *Dr. Ester Appelgren*, formerly at KTH, for valuable comments regarding this research project, *André Odeblom* for providing a really fast proofreading of the first version of the abstract and *Anna Lundberg*, Mid Sweden University, for helping out with the data collection.

The *Kempe Foundations* and the *industry participants in STFI-Packforsk's DigiPrint project* are gratefully acknowledged for their financial support.

References

1. Aitken, J., Christopher, M., & Towill, D., (2002), *Understanding, Implementing and Exploiting Agility and Leanness, International Journal of Logistics: Research and Applications, Vol. 5, No. 1, pp. 59-74*
2. Alderson, W., (1950), *Marketing Efficiency and the Principle of Postponement, Cost and Profit Outlook, Vol. 3, No. 4, pp. 15-18*
3. Anderson, J. C., & Narus, J. A., (2004), *Business Market Management, 2nd ed., Pearson Education International*
4. Andersson, D. R., Sweeney, D. J., & Williams, T. A., (2002), *Statistics for Business and Economics, 8th edition, South-Western*
5. Armstrong, J. S., & Overton, T. S., (1977), *Estimating Nonresponse Bias in Mail Surveys, Journal of Marketing Research, Vol. 14, No. 3, pp. 396-402*
6. Axelsson, B., Rozemeijer, F., & Wynstra, F., (2005), *Developing Sourcing Capabilities: Creating Strategic Change in Purchasing and Supply Management, John Wiley & Sons, Ltd*
7. Birkenshaw, J., (2004, April), *The future of print on paper, Prepress and print Technology, Pira International, Retrieved January 26, 2005, from http://pira.atalink.co.uk/pulp-and-paper/163.html*
8. Blocher, E. J., Chen, K. H., & Lin, T. W., (1999), *Cost Management: A Strategic Emphasis, Irwin/McGraw-Hill*
9. Brandenburger, A. M., & Nalebuff, B. J., (1996), *Co-opetition, Currency Doubleday*
10. Bucklin, L. P., (1965, Feb.), *Postponement, Speculation, and the Structure of Distribution Channels, Journal of Marketing Research, Vol. 2, No. 1, pp. 26-31*
11. CASRO, (1982), *On the Definition of Response rates, A Special Report of the CASRO Task Force on Completion Rates, Retrieved April 4, 2007, from http://www.casro.org/resprates.cfm*
12. Churchill, G. A., & Brown, T. J., (2004), *Basic Marketing Research, 5e, South-Western*
13. Cohen, J., (1977), *Statistical Power Analysis for the Behavioral Sciences, Revised Edition, Academic Press*
14. Collis, D. J., & Montgomery, C. A., (2005), *Corporate Strategy, A Resource-Based Approach, Second Edition, McGraw-Hill/Irwin*
15. Corr, C., Gordin, A., & Hamilton, J., (2005), *Satisfaction Level of Production Digital Color Printer Owners, Proceedings from IS&T's NIP21, pp. 661-666*
16. Day, G. S., (1990), *Market Driven Strategy, Processes for Creating Value, Free Press*
17. Dobler, D. W., & Burt, D. N., (1996), *Purchasing and supply management, Sixth Edition, McGraw-Hill*
18. Herer, Y. T., Tzur, M., & Yücesan, E., (2002), *Transshipments: An emerging inventory recourse to achieve supply chain leagality, International Journal of Production Economics, Vol. 80, pp. 201-212*
19. Hill, T., & Chambers, S., (1991), *Flexibility - A Manufacturing Conundrum, The International Journal of Operations & Production Management, Vol. 11, No. 2, pp. 5-13*
20. Johansson, H. J., McHugh, P., Pendlebury, A. J., & Wheeler, W. A., (1993), *Business Process Reengineering: Breakpoint Strategies for Market Dominance, John Wiley & Sons*
21. Johansson, K., Lundberg, P., & Ryberg, R., (2006), *Grafisk Kokbok 3.0, Guiden till Grafisk Produktion, Arena*
22. Keller, G., (2005), *Statistics for Management and Economics, Seventh Edition, Thomson Brooks/Cole*
23. Kipphan, H., (2001), *Handbook of Print Media, Technologies and Production Methods, Springer*
24. Liker, J. K., & Morgan, J. M., (2006), *The Toyota Way in Services: The Case of Lean Production Development, Academy of Management Perspectives, Vol. 20, No. 2, pp. 5-20*
25. Liker, J. K., (2004), *The Toyota Way: 14 Management Principles from the World's Greatest Manufacturer, McGraw-Hill*
26. Mejtoft, T., & Viström, M. (2007). *Positioning in the Printing Industry - Differentiation in Terms of Price, Lead Time, Print Quality and Flexibility.* In N. Enlund, & M. Lovreček (Eds.), *Advances in Printing and Media Technology, Acta Graphica Publishers, Vol. 34, pp. 327-336. Acta Graphica Publishers*

27. Mejtoft, T., (2005), *The Cost of Digital Printing in Newspaper Production, Report 111, STFI-Packforsk*
28. Mejtoft, T., (2006), *Strategies for Successful Digital Printing, Journal of Media Business Studies, Vol. 3, No. 1, pp. 53-74*
29. Mohr, J., & Spekman, R., (1994), *Characteristics of Partnership Success: Partnership Attributes, Communication Behavior, and Conflict Resolution Techniques, Strategic Management Journal, Vol. 15, pp. 135-152*
30. Pellow, B. A., Frey, F., & Sorce, P., (2002, Sep.), *Digital Color - Where is the Market?, Research Monograph No. PICRM-2002-02, RIT Printing Industry Center*
31. PODi, (2003, Jan.), *Best Practices in Digital Printing, Third Edition, Caslon & Company*
32. PODi, (2006), *Best Practices in Digital Print, Sixth Edition, Caslon & Company*
33. Porter, M. E., (1990), *The Competitive Advantage of Nations, Macmillan*
34. Robson, C., (2002), *Real World Research, Second Edition, Blackwell Publishing*
35. Romano, F. J., (2004, May 27), *Designing for Digital, Speech presented for GFF, Stockholm, Sweden*
36. Romano, F. J., Lee, B., Rodrigues, A., & Sankarshanan, (1999), *Professional prepress, printing, and publishing. Prentice-Hall*
37. Saunders, M., Lewis, P., & Thornhill, A., (2007), *Research Methods for Business Students, 4th Ed, Prentice Hall*
38. *Selling PCs like bananas,* (1996, October 5), *Economist, Vol. 341, No. 7986, p. 63*
39. Smyth, S., (2003), *The Print and Production Manual, 9th edition, Pira International*
40. Stalk Jr., G., & Webber, A. M., (1993, July-Aug.), *Japan's Dark Side of Time, Harvard Business Review, pp. 93-102*
41. Stern, L. W., & El-Ansary, A. I., (1992), *Marketing channels, Fourth Edition, Prentice-Hall*
42. Sugimori, Y., Kusunoki, K., Cho, F., & Uchikawa, S., (1977), *Toyota production system and Kanban system Materialization of just-in-time and respect-for-human system, International Journal of Production Research, Vol. 5, No. 6, pp. 553-564*
43. Tan, B., (1998), *Agile Manufacturing and Management of Variability, International Transactions in Operational Research, Vol. 5, No. 5, pp. 375-388*
44. Viström, M., & Mejtoft, T. (2007). *The Importance of Agility in the Packaging Printing Industry,* In Á. Halldórsson, & G. Stefánsson (Eds.), *The 19th Annual NOFOMA Conference Proceedings, pp. 1111-1123, University of Iceland/Reykjavík University*
45. Wang, Y., Cohen, M. A., & Zheng, Y-S., (2002), *Differentiating customer service on the basis of delivery lead-times. IIE Transactions, Vol. 34, No. 11, pp. 979-989*
46. Wiseman, F., & Billington, M., (1984), *Comment on a Standard Definition of Response Rates, Journal of Marketing, Vol. 21, No. 3, pp. 336-338*

Transaction costs and their influence on institutional arrangements - A comparison between the swedish and the german printing industry

Sven Packmohr[1], *Thomas Mejtoft*[2]

[1] Business Studies, Organizational Theories and Information Systems (BOW), University of Osnabrück
Media Technology and Graphic Arts, Royal Institute of Technology (KTH)
SE-100 44 Stockholm, Sweden
E-mail: sven.packmohr@uos.de

[2] STFI-Packforsk / Media Technology and Graphic Arts, Royal Institute of Technology (KTH)
Järnvägsgatan 3, SE-891 18 Örnsköldsvik, Sweden

Abstract

The printing industry is undergoing a lot of structural changes. One way to deal with these changes is by institutional arrangements like hybrid organizations made possible by modern digital communication technologies. The aim of this qualitative case study with four Swedish and four German printing houses is to examine if and how these arrangements are used to lower transaction costs and increase competitive advantages. The results indicate that the companies in this study face the need to integrate for different reasons to increase their competitive advantage. Nevertheless, due to strong competition and to lower their need for investments, the companies in this study cannot integrate all capacity and resources needed in the production. Due to fear for opportunism, the preferred way is to create cooperation with a few close partners. This suggests that the companies have chosen a hierarchical intuitional arrangement (integration) with a hybrid character (cooperation).

Keywords

Institutional arrangements, printing industry, qualitative case study, transaction costs

1. Introduction and objectice

The printing industry is an old industry that, during the last decade, has faced new challenges due to introduction of substitute products, such as electronic documents, and new production technologies, such as digital printing, to handle customers' demands of increasingly shorter run lengths. However, regarding the status of print being a commodity, there has been no change. This has put pressure on companies in the printing industry to be both efficient in production and deliver high customer value. One way to deal with these changes are hybrid organizations made possible by modern digital communication technologies. Other institutional arrangements that a company can choose are vertical integration of activities in the value chain or buying complementary activities on the market. Neo-Institutional Theories concentrate on a macro level on institutional arrangements and their rules *"that define the appropriate ways to manage organizations and to structure relations"* [McAuley et al., 2007, p. 450]. Having efficient institutional arrangements (market, hierarchy or network) is important to be able to maximize a company's profitability. Strong efforts are made by companies to be more efficient regarding production costs. However, as long as a company does not produce everything internally, there are costs associated with the interaction with other companies, so-called transaction costs. Transaction costs are costs for e.g. information, initiation, agreement, processing, control and adjustment of contracts. Depending on the degree of integration the transaction costs differ and it is important for a company, independent of its integration path, to try to lower the transaction costs. One example is the use of information and communication technology (ICT). In many industries ICT helps to lower the transaction costs, which makes it possible for companies to change their degree of integration to a lower level and to specialize more, leading to more sourcing or networked companies. On the other hand, there might be other factors, such as gaining competitive advantages, which force companies to vertically integrate activities in the value chain more intensely [Coase, 1937; Williamson, 1975].

Previous research has focused on the competitive posture of being vertically integrated when working in the printing industry, especially when trying to sell digital printing [Mejtoft, 2006a; 2006b]. This paper further extends this research by regarding the importance of lowering transaction costs and increasing competitive advantages in the Printing Industry and to identify possible cultural differences. The aim is to focus on a comparison between the institutional arrangements made by Swedish and German printing houses.

2. Theory

The Transaction Cost Theory is a neoclassical theory expounding the efficiency oriented static framework [Nooteboom, 1993] and belongs to a family of organizational theories called Neo-Institutional Theories. These theories are supposed to give hints for the design of different institutional arrangements, such as companies [Bea & Göbel, 2006]. Transaction costs (TAC) are defined as cost for information and agreement both before and after a contract is signed [Fritsch et al., 1996]. Transaction costs were introduced in the literature by Coase [1937] in his groundbreaking work *The Nature of the Firm*, but have been implicitly considered before in other organizational theories, such as Taylorism. Taylor proposes the distinction between production and administration by introducing blue and white collar employees [McAuley et al., 2007].

Vertical integration occurs when a company chooses to produce its own input or take care of its own output, in order to increase the company's power in the marketplace [Porter, 1985]. That is an expansion of the company's business into areas that are at different points on the same production path. Harrigan [1983] suggests two major reasons why a company should consider vertical integration; internal benefits and costs, and effects on competitive posture. Scherer [1970] claims that the most obvious motive for vertical integration is to reduce transaction costs. When integrating activities companies are facing production costs (PC) for these, which could be lowered if a company specializes on a few tasks, because of learning curve effects. On the other hand transaction costs will increase, the greater the degree of specialization is, because of the necessity to contract with external partners. Because of this trade-off, the aggregated overall cost curve (TC = PC + TAC) is u-shaped and has a minimum which represents the companies optimal degree of specialization [Picot et al., 1998]. An alternative to integrating activities is to purchase on the market to get access to value added activities necessary to produce the end product. According to Transaction Cost Theory, costs associated with performing a transaction on the market occurs when a company chooses to purchase instead of producing internally. Instead of buying on the market, it is possible to create close cooperation with selected partners and create strategic alliances to perform certain tasks that the company needs to have performed. Strategic alliances can be described as a long-term, purposeful work between legally independent players to create and/or preserve competitive advantages against the surrounding world [Gulati et al., 2000; Jarillo, 1988; Todeva & Knocke, 2005]. An opportunity of cooperations are gaining control of resources and knowledge without direct ownership [Håkansson & Johansson, 2002] and thus, increasing the flexibility and dynamics in resource control and the organization. Furthermore, through cooperation companies are able to lower their transaction cost and focus even more on their highly specific core activities of their value chains or in other words can choose higher degrees of specialization. A shift in the transaction cost can be provoked i.e. by integrated ICT-systems (information and communication technology) which make it easier to observe actions of partners. A shift in transaction costs will also have impact on the minimum of the TC curve and therefore on the degree of specialization companies choose [Picot et al., 1998]. The problem is of course to measure the exact shifts and the exact optimal point. Such ICT-systems were e.g. built up in the automotive industry where suppliers are connected via supply-chain-management systems to the entity-resource-planning-systems of the main company [Geraedts, 2007].

Nevertheless, even though there are possibilities to lower transaction costs and make it attractive to buy on the market or collaborate with partners, there are factors like opportunism and bounded rationality between cooperating partners that increases transaction costs [Williamson, 1991]. Strategies to lower these costs can be e.g. screening and signaling [e.g. Spence, 1973]. For example, a person applying for a job hands over documents and certificates that signal what to expect from the applicant. The documents can be screened by the human resource manager at the employer. Factors like opportunism and bounded rationality will consequently lead companies to integrate more activities in-house and specialize less. In general, it is possible to contract every product or service a company needs via the market. In some cases these market transactions will cause very high costs until the contract is signed due to a high specificity. Therefore, transaction costs in relation to specificity could be used to define the borders of a company.

Specificity is defined as the loss a resource experiences if used in another context than planned. There are different forms of specificity for locations, equipment, purchaser or human capital. Other activities or results of activities with a low specificity and therefore low transaction costs should be bought via the market. Parts of the value chain which have a high specificity should, according to the theory, be integrated vertically into the company, because the internal control through hierarchy causes lower transaction costs. Today, modern ICT in combination with standards help to lower the transaction costs mostly for middle specific activities. This leads to the possibility to break up integrated value chains and the borders of companies up to a certain degree, leading to hybrid organizations like network companies or alliances. Thus, having a given degree of

specificity for a process a company could choose the optimal institutional arrangement. The area between the dashed lines in Figure 1 represents activities with a certain middle specificity. For these a hybrid arrangement i.e. via an alliance of partners seems to be advantageous. As a market's products and resources evolve and develop over time, it is possible that the specificity of processes or products also transform over time.

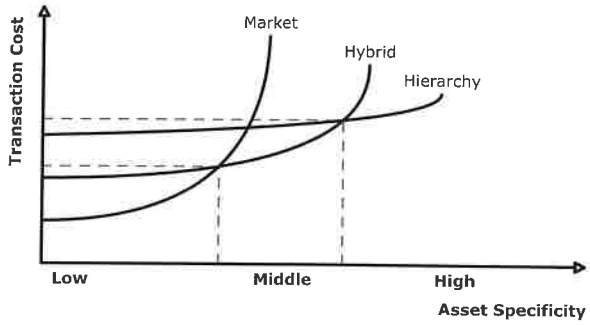


Figure 1: Different institutional arrangements [Williamson, 1991, p. 284]

Jarillo [1993] suggests that it is the transaction costs that determine when these different strategies are used. If the internal cost (IC) for performing an activity is lower than the price for an external producer (EP) plus the transaction cost, then the activity should be integrated in-house (i.e. IC < EP + TAC). However, since in many cases other companies produce certain parts of a value chain less expensively than the cost for producing internally (EP < IC), it is the level of the transaction cost that is important. If transaction costs are low, buying over market is preferred and if transaction costs are high vertical integration is to be considered as the most successful strategy. However, when selective companies can offer low transaction costs, then strategic alliances arise. Furthermore, Gulati [1998] states the need for a social network as a prerequisite for a company network, because personal relations between individuals and positions within these social groups lower the transaction costs when implementing a network.

Although the Transaction Cost Theory and its argumentation seems to be obvious and easy applicable for companies it has some difficulties. Firstly, transaction costs instead of production costs with their elements such as specificity, its cost curve or the degree of specialization, can hardly be measured in a metric way [Dow, 1993]. Another problem touches upon those of vertical integration [Gadiesh & Gilbert, 1998] and affect how the transaction costs are distributed between the partners when collaborating around certain activities [Blois, 1990]. Nevertheless, according to Dow [1993], an integration of activities does, unfortunately, not only avoid certain transaction costs, but also generate new ones. One example is that when performing more activities internally, more employees are needed in production and this can be regarded as "cooperation" between the company and its employees, since the employer can hardly have total control of the human capital. Therefore, wages could be seen as transaction costs as well, leading to the conclusion that companies themselves are a set of transaction costs. Of course production costs still exist, but the cost of keeping together the company as an entity can be regarded as a set of transaction costs.

3. Research methodology

This research paper is based on a qualitative multiple case study [Yin, 2003] with eight case companies, four Swedish and four German cases. The Swedish cases have previously been presented in a pre-study [Mejtoft & Packmohr, 2008]. Qualitative case studies make it possible to gain deeper knowledge of the complex behavior behind the strategy used in an industry [Robson, 2002; Saunders et al., 2007; Yin, 2003]. Qualitative studies are used to examine general tendencies and not an overall empirical generalization [Bortz et al., 2003]. According to Stake [2005, p. 445] case studies are conducted as intrinsic, instrumental or collective studies. Following this classification this study is a collective one with the aim *"to provide insights into an issue"*, where the cases serve as supportive material. It is important to choose a selection of cases which represent the population of all possible cases. To assure the possibility to learn the most from the cases and to look on the research question from different perspectives it is necessary to include some kind of variety. The case companies were selected to be as representative for the Printing Industry in Germany and Sweden as possible. Between the Swedish and the German cases the perspective differs in terms of number of employees. The German companies (10-80 employees) in this study had slighter more employees than the Swedish companies

(10-50 employees). Nevertheless, it is important to remember that *"the purpose of a case report is not to represent the world, but to represent the case"*. Because the time spent in a market can have impact on the social networks, which are a prerequisite for a company network [Jarillo 1988], variety was built in by selecting companies with different dates of establishment. The oldest German printing house was established 140 years ago. Business strategy and organizational culture in a company are often a direct reflection of the founder and/or the CEO, because they are responsible for the business development in the organization [e.g. Beal & Yasai-Ardekani, 2000; Collins & Montgomery, 2005; Porter, 1996; Schein, 1983]. Therefore, the CEO or equivalent at each printing house was chosen for an interview.

The data collection was conducted with interviews either at the printing house or by telephone during late fall 2007 and spring 2008. The interviews were focused on questions regarding the following areas: degree of specialization/integration, level of competition, specificity of resources/capabilities and influence of digitalization. Direct questions e.g. about the height of transaction cost were avoided due to difficulties for companies in measuring these.

4. Case Studies

This chapter summarizes the results from the case studies. For the analysis, please refer to the discussion.

4.1 German Company A

Company A is a family company with a business tradition spanning 140 years. This seems to play a major role as far as price setting is concerned. Company A is a classic commercial printing house working with sheet fed offset. Company A employs approximately 80 people, working in three shifts. Company A does not normally produce original work and the added value begins when the customers have delivered the original work. The company handles 99% of all prepress internally, and very seldom is prepress done by external companies. Printing is accomplished in-house with 95% and 5% via partners. Regarding finishing, about 90% occurs internally and the remaining 10% is mostly production peaks and bulks that are produced at partner's facilities. Stock keeping of finished goods is done both in-house and via the market. Distribution is mostly contracted via the market with the aid of logistics companies. A reason for the high integration of certain steps of the value chain is the temporal flexibility. It is the respondent's opinion that confidence and trust in their partners plays a major role concerning the cooperation with partners. This is very important in order to assure reliability as well as quality, and thus prevent the risk of damaging their reputation.

Company A believes that the technological changes within the Printing Industry hold fewer advantages for the producers and more advantages for the customers, as customers expect shorter and shorter production times. Furthermore, the respondent mentions that each order is a single production and that printing products are not standardized products due to different data qualities. According to the respondent, the Graphic Market and the Printing Industry respectively is one of few industries in which the customer is involved in the production process by data preparation and delivery. Due to the wide spread use of PCs and the possibility for almost anyone to produce simple original material, the respondent believes that the material delivered by the customers is partially of insufficient quality. In the opinion of Company A, production costs have not decreased from digitalization, quite contrary to administration costs. According to Company A, the digitalization do not make customers rely more on Company A to provide full service solutions as customers continue to consult agencies or their own departments for the original work. Company A rather emphasis the strong competition in the Printing Industry as the main reason for integration. However, Company A believes that digitalization has greatly influenced printing as far as prepress is concerned. Contacts between Company A and other printing houses are weak. The respondent assumes an overcapacity of 30% on the German market, which according to, the respondent makes a consolidation of the market probable. This assumed consolidation is the main reason for low communication between printing houses, however, of course there is communication between cooperative partners in their own network. However, there exist some contacts beyond the Printing Industry in order to exchange technological experience.

Company A attaches great importance to focusing on time efficiency because time-critical orders often require short production times and higher flexibility. They believe that the development towards jobs being time critical is even more extreme when using digital printing. This flexibility in the Printing Industry is well-known by the customers and it is the respondent's opinion that the strong competitive situation and the

overcapacity also play their part in this situation. This can be noticed for example by the fact that orders in many cases are changed just before going to print. Regarding the importance of the time aspect, Company A believes it to be very important. For Company A, printing is the core competence, however services, which provide the customer with benefits in the value chain of printing, become more and more important.

4.2 German Company B

Company B was founded 60 years ago, originally as a printing house specialized on printing books. A major co-proprietor of the company is a trade-union, which influences pricing. Today the company has 80 employees and production normally runs in two shifts. As far as printing methods are concerned, the company primarily uses offset and for the last 10 years they have also used toner-based digital printing. Within the value chain of print media, 95% of the original work and all prepress are handled internally within the company. Regarding printing, 95% of the printing is done internally, the additional 5%, which concerns special printing methods which can not be produced in-house, are contracted out to partners. Within finishing Company B works internally with 50% of the volumes, 40% with partners and 10% via the market. All stock keeping and distribution is handled internally. In addition they offer a complete solution for letter printing and mailing service and develop software for web-to-print solutions.

The vertical integration from printing into the other levels and the additional fields is justified with the increased market power provoked by the consequences of digitalization. With the aid of ICT it is possible to send data quickly to a supplier who offers more favorable printing prices. Therefore Company B decided to offer their clients not only printing but also a total service solution. This should, according to the respondent, reduce the customers' costs of process and create a balance to printing suppliers with more favorable prices. In the opinion of Company B digitalization influences customers more than digitalization influences the printing houses. Digitalization results in a reduction of production costs for example as far as CTP is concerned, however the general administration costs have increased. This is a consequence of an increase in the number of customer enquiries for calculation of offers, nevertheless, due to the use of ICT it is simpler for customers to address more contractors. According to Company B digitalization initially enabled customers to procure each level of the value chain individually. However, the different steps had to be coordinated, either by the customer or by a separate agency. Therefore, Company B pursued the strategy to coordinate all activities in-house and offer their customers a full service solution. Hence, the respondent believes that digitalization in the Printing Industry initially caused single solutions which have been displaced by full service solutions. Company B certainly feels the effects of tough competition. According to the respondent, each offer is undercut by competitors. Therefore printers usually proceed with caution concerning contact with colleagues and Company B does not have much exchange with other printing houses. Nevertheless, other actors in the value chain such as paper merchants have a larger exchange. According to the respondent, printing houses owned by and integrated with total publishing houses are considered as an exception on the market, as they have no direct competitors.

Time is considered as a very important factor by the respondent and the delivery date is very important to keep. According to the respondent, Company B uses both digital printing and offset to fulfill customers' orders, and according to the time aspect, Company B believes that the customers do not care about the technology used as long as the delivery times are kept. There are other specific resources like time, the respondent emphasis the employees and their know-how. Thus by the know-how and flexibility of the employees it is possible to absorb temporary surges in demand by going from two to three shifts. Concerning the production facilities, these are regarded as relatively inflexible.

4.3 German Company C

Company C is a full service printing house, but their main product is printed matter. The company was founded 30 years ago as a collective of a number of individual persons and is directed by its incorporators. Company C has 15 employees and predominantly uses offset printing technology and for a year and a half now also toner-based digital printing. Even though Company C offers original work internally, it is only a small part of the total value chain. Nevertheless, all prepress and printing are handled internally. In exceptional cases, as far as special printing technologies are concerned, partners are contracted. Regarding finishing, all simple finishing is done in-house such as cutting and folding, however, other finishing as binding is contracted though partners. Due to cramped facilities they resort to a network of partners concerning stock keeping and distribution. Company C has recently integrated finishing internally, mainly

because they believe that quality assurance is much more difficult when using cooperative partners. Another argument for vertical integration is that know-how for e.g. finishing was already present in the company. Furthermore, Company C wants to be regarded by its customers as the place for full service solutions concerning print productions, with the possibility to offer total prices to customers. With respect to production and contract placing, Company C talks about a massive structural change due to digitalization. As approximately 98% of all orders are received as digital files, it is easy to get orders via the market using the internet as the channel. However, there are many orders that are more complex and need more consulting from the printing house's side, these are usually handled on-site at the printing house. Regarding communication with customers, the major part still occurs verbally and "by hand", this since reviews and subsequent transformation in data still demands much effort until the start of the technical production. Herein Company C believes that they are separated from internet printing shops. Therefore, the challenge for Company C is to try to keep the costs at a low level while offering consulting at a high level of quality. The general production costs for Company C have decreased and administration costs have had a declining tendency but there is still, according to the respondent, more potential.

In the opinion of Company C, digital printing is in general no reason for the fact that one has to offer overall solutions. In the Printing Industry one could notice different degrees of integration before digitalization started. However, due to the implementation of digital technologies there is a tendency for printing houses in developing digital printing pre-stages. According to the respondent, the competition within the industry is very strong and causes high pressure on prices, as the market is subjected to consolidation. To handle this situation, some actors try to reduce overcapacities by low prices. This means that certain value added services have to be offered for free to the customers in order to make sure that a company gets an order. In general, there is a low exchange within this Printing Industry. Company C only has limited contacts with other companies within the Industry and the company is not organized in any Industry associations. However, they are members of general discussion circles for technology which have occurred through long-standing personal contacts. According to the respondent, the customer puts great importance in Company C being able to provide short lead times. This expectation is an argument for using digital printing. When Company C talks about flexibility caused by time constraints in order to respond to customer requests, they talk about a specific resource. The production facilities are also considered as flexible, thanks to continuous expansion investments.

4.4 German Company D

Company D was founded 80 years ago and it is a family company in the third generation that has ten employees. Company D is a classic offset printing house and one year ago Company D started with toner-based digital printing. They believe that digital printing can handle smaller orders in a much more cost-efficient way. About 99% of the original work is received from the customers. Even though they offer this service in-house, the use of desktop publishing and orders from advertising agencies contribute to fewer customers demanding original work services from Company D. Hence, the value chain for the Company D begins with prepress and data control, composition f printed sheets and production of printing plates using CTP. All this (100%) is accomplished internally. The printing stage is produced in-house with formats of up to A2, which equals approximately 99% of the printing needed. Concerning orders which require special printing techniques, partners are contacted. About 80% of the finishing occurs internally, and partners handle more advanced finishing, such as perfect binding. Company D keeps a small stock of finished products and ordering and delivery occur according to Just-in-Time. Due to the order volume, the printing products are usually delivered directly after production and 90% of distribution is offered in-house with the rest through partners. It is the experience of Company D that most of its profits are made when as much as possible of the customers' orders are handled internally, that is, less use of partners and other external companies. Company D mentions the development of its printing prepress as an example: At first the exposures for the photo composition were contracted through external companies and this caused high expenditures. Thus they acquired their own system of exposure. When this system was defect, they made an investment in CTP. In other words, the company was engaged steadily with make-or-buy decisions. In this connection they noticed that the alternative of in-house production is much more cost-efficient.

In the opinion of Company D digitalization caused a structural change within the industry. Before digitalization, printing houses were known as handicraft enterprises offering a service, that the customer could not produce on his own. The proceeding digitalization dissolves this classification. Today everyone is able to print smaller editions at home and this fact results in a loss of added value concerning the know-how in the domain around printed media. The customers deliver data which can immediately go into printing. As far as

the costs are concerned, Company D notices advantages as well as disadvantages. On one hand ICT makes costs decrease for example by administration systems but on the other hand the smaller orders cause higher expenditure. Thus the exchange of data has become easier to handle, however at the same time the data delivery which has to be dealt with, has increased. The respondent believes that digitalization causes the value chain to be split up between designers and printing houses. According to Company D the market is highly competitive. Prices are under constant pressure among other things due to the digital printing technologies and the printing houses working mainly through the Internet. There are less regular customers because price consciousness is high and according to Company D it is very important to find and establish a market niche. The time factor is considered as very important and it is possible to assure flexibility by e.g. working overtime. Even though the printing machines are considered rather inflexible, digital printing has caused a reduction of time in the Printing Industry. According to the respondent the customers expect that the printing machine will start directly when the data are delivered, which is not possible since most printing houses need to schedule their orders.

Company D has few contacts within the Industry. According to the market situation each printing house works independently, as it is important to find and protect the current market niche.

4.5 Swedish Company E

Company E is a privately owned typesetting company founded in the 1970's and they define themselves as a prepress company that has acquired digital printing. Their first investment in printing was a web-fed digital printing press in the mid 1990's, and they were one of the pioneers in digital printing in Sweden. Even though they did not fully believe that the market for digital printing was ready in the mid 1990's, they felt that the market was increasing and they wanted to take part in creating the market. During the fall of 2006 Company E acquired a new sheet fed digital printing press. A sheet fed press was chosen due to the higher flexibility than a web fed press. Having both web and sheet fed printing presses are, according to the respondent, important for increasing flexibility in production. Also having more than one printing press is important to ensure delivery.

Company E tries to work with the complete value chain from original work to distribution (except for stock-keeping). Currently they perform all prepress and about 30% of the original work internally. Regarding printing they perform all digital printing needed and use partners for other printing technologies, mostly offset. They handle all finishing and most of the distribution for the print production in-house. Finishing and distribution are integrated due to the shorter lead times when performing the total forward value chain in-house. In general, the respondent deems the time aspect very important for their company. The combination of digital printing and the shorter start up time for offset has made the general lead times in the printing industry shorter. In general, the respondent regards it crucial to offer full service solutions. It is the respondent's view that if the company had chosen to specialize on a certain task it would not have survived as an independent company. Different business units, such as printing, prepress, original work etc, have served as cash cows during build-up and hard times for other business units. Regarding general digital development, Company E believes that they have during the last few years started to loose more and more of the digital printing jobs to the Internet and to in-house copy-printers at customers' companies. This is, according to the respondent, an increasing problem for the digital printing industry as many simpler previously digitally printed matters are now distributed over the internet. The general competition is regarded as very hard and they feel a relatively strong competition even with the printing houses they regard as partners. Prices are set on the basis of actual production cost and the markup is determined with benchmarking of competitors. They do not have any formal agreements with companies they work with, but instead they work with companies they trust will perform a good job and not try to steal their customers.

Company E is currently a member of the National Federation for Graphic Companies and a regional network for companies from many different industries. However, they do not regard themselves as active members in these networks and organizations.

4.6 Swedish Company F

Company F was founded in the early 1990's and its growth has mainly been organic. The business model has, from the start, been based on handling the whole chain from original work to print to distribution. Regarding printing they have both sheet fed digital printing and offset printing in-house to be able to offer the customer a

wide selection of printing options. Regarding web offset, they collaborate with another printing house to provide this option.

Basically they are active in, and try to do as much as possible, within the value chain of print media. However, they balance the level of integration in each step to the cost. To ensure a *"backup situation"* they at all time have at least 3 - 4 different printing houses they collaborate with to ensure customers' deliveries at all times. The backwards integration is strong and today only about 10% of the orders come from advertising agencies. The idea is to do the original work for the customers, unless they have an in-house advertising agency. The trend towards customer companies integrating their own department for making advertising material is, according to Company F, strong. All forward activities in the value chain are integrated. However, regarding e.g. finishing, Company F collaborates with 2 - 3 partners for more advanced finishing and larger volumes. One of the main reasons for integrating a full value chain is, according to the respondent, to lower costs. Even though Company F emphasis lowered costs when integrating vertically, they also believe that the increased market power and reduced lead times are as important as the lowered costs. The general digital development has helped Company F to construct a more efficient production work-flow. Integrating software for handling orders, invoicing etc. is important for Company F, and they regard having such a system as a competitive advantage. Short lead times and efficient production are two important factors when active with print media production. This is due to the strong competition and poor advanced planning from customers. The respondent emphasized the importance of having close ties and collaboration with other actors, both other printers, to complement and extend capacity of their printing units and with other steps to be able to offer a complete solution to their customers. Company F is also active in the regional employers' association, but believes that many such networks are not as important any more. This is mostly, according to the respondent, due to the strong competition between the members in the networks, which makes it hard to work together and find common goals.

Company F has always aimed towards a high level of flexibility in their production equipment by using both sheet fed offset and digital printing. By further investing in a new work-flow, they have lowered costs for production (by decreased ink usage), increased print quality and decreased the total lead time by approximately 35%. By being flexible it is possible, according to the respondent, to provide a complement to Internet and not lose volume, as many of the larger printers have during the last couple of years.

4.7 Swedish Company G

Company G is a merger between two equally sized privately owned printing houses a couple of years ago. The two original companies complemented each other regarding printing technology as one had offset printing technology and the other digital printing technology. Company G regards themselves as a printing house serving mainly local and regional customers.

Regarding integration in the value chain, they have integrated a total prepress department and most of the finishing work. They have created cooperations with other companies to handle stock keeping and distribution. Original work is usually delivered by the customer, and is not something Company G has in-house. According to the respondents, it was important to offer a complete range of products and services, since their customers wanted full service solutions from their supplier of printed materials. The current integration strategy has resulted in, according to the respondent, that approximately 80% of all jobs can be handled internally in the integrated steps. Furthermore, the respondent emphasis the shorter lead times when integrating activities close to the printing and a majority of the jobs are time critical. Delivering full service solutions gives competitive advantages and it is the respondents view that if Company G would not have been an integrated company today, they would not have survived. For the activities that are not performed in-house, they have a couple of different companies they have close cooperation with. Company G has tried to find a suitable level of integration and cooperation to create a flexible production system for print media, which they deem important. They believe that by having a high level of flexibility with both offset and digital printing, it is possible to switch between the two technologies and always keep the customer *"indemnified and happy"*. Company G believes that the general digital evolution has been positive for the printing industry. However, *"you have to take advantage of new markets that are created by new technology"*, since the Internet revolution has resulted in that the *"marketing money is spread [between even more and different actors]"*. In general, the largest single influence from digitalization is that the lead times have been reduced significantly, which means that more jobs can be accomplished during the same time. This is also an effect digital printing has had on the industry as customers have grown accustomed to short lead times. Time is, according to the respondent, always important for ad hoc production, which is an increasing part of the total production.

Company G is currently a member of the National Federation for Graphic Companies and the regional employers' association. They believe these networks to be an important contact arena and the respondent believes cooperation in these networks to be good.

4.8 Swedish Company H

Company H is a privately owned medium sized company founded in the mid 1960's as a publishing house. Due to some tuff times, the company was bought by a local newspaper in the end of the 1990's. The current owners acquired the company in the beginning of the 2000's, but the current CEO (that is also one of the owners) has worked in the company since the 1980's. Company H offers their customers full service solutions regarding a complete value chain and offset printing technology as well as black and white digital printing.

Company H has the complete value chain for print production in their production facility and they try to satisfy customers' needs from original work to addressing and distribution. They have a strong backwards integration and approximately 70% of all original work and prepress are performed in-house. However, since their printing presses are not suitable for longer production, they use partners when this becomes an economic advantage. Those productions constitute about 10% of the total print production. One major reason for having both a complete value chain and different printing technologies internally is the ability to provide short delivery times and have a high level of flexibility. The time aspect of printing is very important and has become a prerequisite and it is very hard to make money just by having short delivery times today. In other words, ownership of resources is important to keep the delivery times and consequently keep customers satisfied. A negative consequence of ownership of resources is, according to the respondent, that it is hard to find monetary assets to keep up with new investments. As mentioned earlier, Company H chooses to cooperate in some cases to keep the production costs and the need for investments low. Their current printing equipment is due for an upgrade, however, as a smaller company it is hard to cope with investments. The digital development has lead to increased investment needs in the steps before printing, and without having cutting edge software and hardware, it is hard to be competitive in the printing industry today. Even though the respondent feels that the general digital development has created *"communication problem"*, since anyone can create original to a printed matter, one major advantage is the pdf format. The general use of the pdf format has made *"life a little easier (as a printer)"*. Even though the development in prepress is fast, the respondent feels that the development in printing is mainly in speeds and to some extent quality, but nothing revolutionary. The business model of Company H is to both offer "ordinary" print jobs to local, regional and in some cases national customers. However, a substantial part of their business is to offer some niche products, in the form of magazines to different organizations. In this service they can offer organizations a magazine to their members at a low cost. They try to do as much as possible in these productions and in many cases they even sell ads to the magazine, which pays for parts of or the whole magazine. Even though they feel that the general competition is hard within the printing industry, having differentiated their product with specific services to organizations makes them unique and Company H does not feel such strong competition in these areas.

5. Discussion

The results show that the companies in this study have a high level of integration and it is the respondents' opinion that this increases the competitive advantages in terms of decreased delivery lead times and the possibility to offer full service solutions [cf. Mejtoft, 2006a; 2006b]. The respondents believe that by having resources, such as both conventional and digital printing technology, internally based they have created a very high flexibility in the production equipment which enables them to decrease delivery lead times and increase the service offer. Nevertheless, to decrease the transaction costs, the companies have chosen to partly work with external companies and have a so-called taper integrated approach [e.g. Kessler & Stern, 1959; Porter, 1980; Harrigan, 1983; 1984], that is that there is not a complete internal transfer between each integrated step in the value chain. In other words, jobs are both received from and delivered to external companies.

The respondents believe that they experience a very high level of competition [cf. Birkenshaw, 2004; Mejtoft & Viström, 2007; Smyth, 2006], which has made contact with external companies, regarding production, to be mainly with cooperation partners. The reason for creating close cooperation with certain companies is to avoid the risk of opportunistic behavior and loosing clients to partners. Due to the low specificity of the flexible production resources and the high specificity of providing short delivery lead times, there is a mixture of two effects. One effect (flexible production) favors buying from the market and the other effect (short

delivery lead times) favors the hierarchy (integration). The theoretical implication of this is that these companies are active in the borderland between high asset specificity and middle asset specificity (Figure 2). Nevertheless, it is not possible to isolate and give a clear answer to whether only a hierarchical or a hybrid institutional arrangement (cooperating through alliances) is the most successful method in the Printing Industry. The results show that the general integration is high and the case companies in some cases use partners to gain cost advantages. This suggests that the companies have chosen a hierarchical institutional arrangement with a hybrid character (Figure 2).

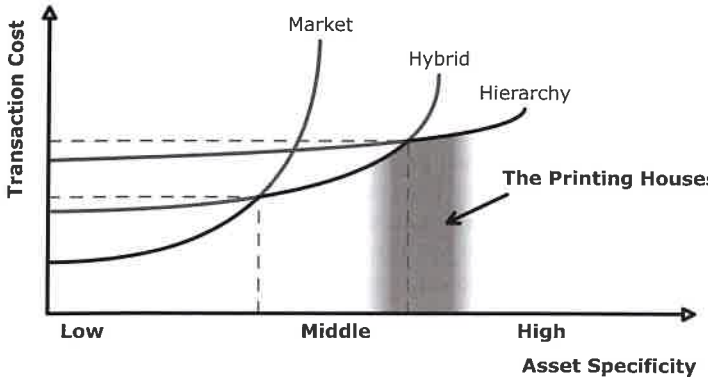


Figure 2:
Companies in this study have adopted a hierarchical intuitional arrangement with a hybrid character (the grey area). [After Williamson, 1991, p. 284]

In this sense there is no difference between the Swedish and the German companies. Both choose to integrate due to the same reasons: time, flexibility, and a fear of opportunism. The fear of opportunistic behavior has lead to minimal communication between different printing houses but to a high communication to other actors close to the Industry, e.g. paper suppliers. Even though the German case companies are larger than the Swedish case companies, the German printing houses seem to choose a slightly lower degree of integration than the Swedish printing houses, e.g. by not performing original work internally or by having only a small portion of finishing in-house. This is motivated by trying to focus on core competencies. Nevertheless, the German case companies also need to partly integrate to differentiate their businesses and to avoid the strong competition in printing in order to get the same profits by adding additional services. Although the German case companies have been established for a longer period than the Swedish ones, there were no differences in the extension of their social networks. For example, even though one of the German printing houses was established 140 years ago they do not have a social network that was notably larger than the Swedish printing houses. Furthermore, there are differences in the use of printing technologies between the printing houses in the two countries. The Swedish printing houses seem to adopt new technologies, such as digital printing, faster. German printing houses still focus on offset printing or have adopted digital printing just recently. This is in accordance with Hofstede & Hofstede [2006], they state that Sweden has lower degree for fear of uncertainty than Germany, which may lead to more openness to new technologies. The printing houses focusing on offset instead, try to increase their production flexibility by organizational means, since offset printing is less flexible than digital printing. The results in adoption of printing technologies concurs with the investigation by Pira [Smyth, 2006], where the growth in digital printing both had been higher during the 2000s and was expected to grow faster until 2011 in Sweden than in Germany. Although, the transaction cost theory states that a high availability of technology will have a positive influence, printing houses in both countries seem to have the same reasons to integrate. Therefore, this seems to be more of a cultural question, to adopt new technologies, than a question of transaction cost theory if one assumes the same availability of technology worldwide. The cultural concept of implicit organizations by Hofstede & Hofstede [2006] suggest that market transactions should be more common in Sweden than in Germany, since the cultural traditions in Germany favors hierarchies unlike in Sweden. Nevertheless, the results in this article show no differences in the need of integrating activities. Consequently, coming from different cultural positions but confronted with the same market conditions make companies in both countries to have the same tendency to vertically integrate activities.

6. Conclusion

By combining integration with cooperation, the respondents believe that they have created flexible resources at a reasonable cost within the companies' control and this strategy is a way for the companies to level the competitive advantage of being integrated with the lower transaction costs (compared to market transfer) of

cooperation. This paper concludes that from a transaction cost perspective the high level of competition within the Printing Industry decreases the possibilities to partner with other companies which at the same time leads to less focus on core competencies due to the need of integration. This might lead to cost inefficiency and as a result of reduction in specialization. Even though Swedish and German companies coming from different cultural positions, when confronted with the same market conditions companies in both countries tend to have the same need to vertically integrate activities. These results could be used by large printing houses with a high market power or by industrial organizations to build up the needed social networks.

Acknowledgements

The authors would like to thank *the anonymous respondents* at the case companies for their participation in this research study. Further, we would like to show our gratitude to *Prof. Nils Enlund*, KTH, valuable comments. The *Kempe Foundations*, the *EU Structural Fund*, the *Swedish Institute*, the *industry participants in STFI-Packforsk's DigiPrint project* and the *German Research Foundation* are, acknowledged for their financial support.

References

1. Bea, F. X. & Göbel, E., (2006), *Organisation: Theorie und Gestaltung, 3rd Edition, Lucius & Lucius*
2. Beal, R. M. & Yasai-Ardekani, M., (2000), *Performance implications of aligning CEO functional experiences with competitive strategies, Journal of Management, Vol. 26, No. 4, pp. 733 - 762*
3. Birkenshaw, J., (2004, April), *The future of print on paper, Prepress and print Technology, Pira International, Retrieved January 26, 2005, from http://pira.atalink.co.uk/pulp-and-paper/163.html*
4. Blois, K. J., (1990), *Research Notes and Communications: Transaction Costs and Networks, Strategic Management Journal, Vol. 11, pp. 493 - 496*
5. Bortz, J. & Döring, N., (2003), *Forschungsmethoden und Evaluation: für Human- und Sozialwissenschaftler, 3rd edition, Springer*
6. Coase, R. H., (1937), *The Nature of the Firm, Economica, Vol. 4, No. 16, pp. 386 - 405*
7. Collis, D. J. & Montgomery, C. A., (2005), *Corporate Strategy, A Resource-Based Approach, 2nd Edition, McGraw-Hill/Irwin*
8. Dow, G. K., (1993), *The Appropriability Critique of Transaction Costs Economic, In C. Pitelis (Ed.), Transaction costs, markets and hierarchies (pp. 101 - 132), Blackwell*
9. Fritsch, M., Wein, T. & Ewers, H-J., (1996), *Marktversagen und Wirtschaftspolitik: Mikroökonomische Grundlagen staatlichen Handelns, 2nd revised and updated Edition, Vahlen*
10. Gadiesh, O. & Gilbert, J. L., (1998, May-June), *How to map your industry's profit pool, HBR, pp. 149 - 162*
11. Geraedts, S., (2007), *Diffusion des Supply Chain Management : Ermittlung von Einflussfaktoren und Ableitung von Gestaltungsempfehlungen; eine Untersuchung am Beispiel der Automobilindustrie, Kovač*
12. Gulati, R., (1998), *Alliances and Networks, Strategic Management Journal, Vol. 19, pp. 293 - 317*
13. Gulati, R., Nohria, N. & Zaheer, A., (2000), *Strategic Networks, Strategic Management Journal, Vol. 21, pp. 203 - 215*
14. Harrigan, K. R., (1983), *A Framework for looking at vertical integration, The Journal of Business Strategy, Vol. 3, pp. 30 - 37*
15. Harrigan, K. R., (1984), *Formulating vertical integration strategies, Academy of Management Review, Vol. 9, No. 4, pp. 638 - 652*
16. Hofstede, G., & Hofstede, G. J., (2006). *Lokales Denken, globales Handeln: interkulturelle Zusammenarbeit und globales Management, vollst. überarb. Aufl., München*
17. Håkansson, H. & Johanson, J., (2002), *A model of industrial networks, In D. Ford (Ed.), Understanding Business Marketing and Purchasing, An interaction approach, 3rd Edition (pp. 145 - 149), Thomson Learning*
18. Jarillo, J. C., (1988), *On Strategic Networks, Strategic Management Journal, Vol. 9, pp. 31 - 41*
19. Jarillo, J. C., (1993), *Strategic Networks, Creating the Borderless Organization, Butterworth-Heinemann*
20. Kessler, F., & Stern, R. H., (1959), *Competition, Contract, and Vertical Integration, The Yale Law Journal, Vol. 69, No. 1, pp. 1 - 129*
21. McAuley, J., Duberley, J. & Johnson, P., (2007), *Organization theory: Challenges and perspectives, Prentice Hall*
22. Mejtoft, T. & Packmohr, S., (2008), *Transaction Costs and Their Influence on Institutional Arrangements in the Swedish Printing Industry, Paper presented at the 8th World Media Economics and Management Conference, 18th - 22nd May 2008, Lisbon, Paper accepted for publication*

23. Mejtoft, T., & Viström, M., (2007), *Positioning in the Printing Industry - Differentiation in Terms of Price, Lead Time, Print Quality and Flexibility, In N. Enlund, & M. Lovrecek (Eds.), Advances in Printing and Media Technology, Vol. 35, pp. 327 - 336*
24. Mejtoft, T., (2006a), *Strategies for Successful Digital Printing, Journal of Media Business Studies, Vol. 3, No. 1, pp. 53 - 74*
25. Mejtoft, T., (2006b), *Strategies in the Digital Printing Value System, Licentiate Thesis, KTH, Sweden*
26. Nooteboom, B., (1993), *Networks and Transactions: Do they connect?, In J. Groenewegen (Ed.), Dynamics of the Firm: Strategies of Pricing and Organisation (pp. 9 - 26), Edward Elgar*
27. Picot, A., Reichwald, R. & Wigand, R. T., (1998), *Die grenzenlose Untemehmung: Information, Organisation und Management; Lehrbuch zur Unternehmensführung im Informationszeitalter , 3rd revised Edition, Gabler*
28. Porter, M. E., (1980), *Competitive Strategy: Techniques for Analyzing Industries and Competitors, Free Press*
29. Porter, M. E., (1985), *Competitive Advantage: Creating and Sustaining Superior Performance, Free Press*
30. Porter, M. E., (1996, November-December), *What is Strategy?, HBR, pp. 61 - 79*
31. Robson, C., (2002), *Real World Research, 2nd Edition, Blackwell Publishing*
32. Saunders, M., Lewis, P. & Thornhill, A., (2007), *Research Methods for Business Students, 4th Edition, Prentice Hall*
33. Schein, E. H., (1983), *The Role of the Founder in Creating Organizational Culture, Organizational Dynamics, Vol. 12, pp. 13 - 28*
34. Scherer, F. M., (1970), *Industrial Market Structure and Economic Performance, Rand McNally & Company*
35. Smyth, S., (2006), *The Future of European Printing to 2011, Pira International*
36. Spence, M., (1973), *Job Market Signaling, The Quarterly Journal of Economics, Vol. 87, No. 3, pp. 355 - 374*
37. Stake, R. E., (2005), *Qualitative Case Studies, In N. K. Denzin, & Y. S. Lincoln (Eds.), The SAGE Handbook of Qualitative Research, Third Edition (pp. 443 - 466), Sage Publications*
38. Todeva, E. & Knocke, D., (2005), *Strategic alliances and models of collaboration, Management Decision, Vol. 43, No. 1, pp. 123 - 148*
39. Williamson, O. E., (1975), *Markets and Hierarchies: Analysis and Antitrust Implications, Free Press*
40. Williamson, O. E., (1991), *Comparative Economic Organization: The Analysis of Discrete Structural Alternatives, Administrative Science Quarterly, Vol. 36, No. 2, pp. 269 - 296*
41. Yin, R. K., (2003), *Case Study Research, Design and methods, 3rd Edition, SAGE Publications*

Implementing TQM in graphic arts industry by six sigma - A case study

Rajendrakumar Anayath[1], *Kiran P Prayagi*[2]

[1] Print Media Academy-Heidelberg India
333,GST Main Road, Jameen Pallavaram
Chrompet, Chennai-600044, Tamilnadu State, India
E-mail: rajendrakumar.anayath@heidelberg.com

[2] Graphic Arts Technology & Education, Mumbai

Abstract

This research is mainly focused on the study of the of Indian graphic arts industry, its history, current status, upcoming technologies and the feasibility of implementing six sigma in the Indian print industry. The phase one study was done by extensive reviews from various sources such as publications from Ministry of Industry and Commerce (Govt. of India), AIFMP(All India Federation of Master Printers), PIRA, IFRA, GATF,INS (Indian Newspaper Society-India) and many other research publications on printing, TQM and Six sigma. This is a case study based research to implement six sigma and was conducted at leading commercial press to reduce printing plate wastage. The DMAIC (Define, Measure, Analyse, Improve and Control) model was used during the six sigma implementation which was developed and implemented successfully in Motorola. Later a study has been conducted to assess the feasibility of six sigma implementation in the Indian graphic arts industry by personal interviews and questionnaires.

Keywords

Six sigma, TQM, DMAIC, plate wastage

1. Introduction

Even though Six sigma methodology is a well proven TQM tool to many industries unfortunately this is not much used in print industry in India. A study says even globally very few printing companies have adopted this methodology to standardize processes, production and reduce variation from the target value.

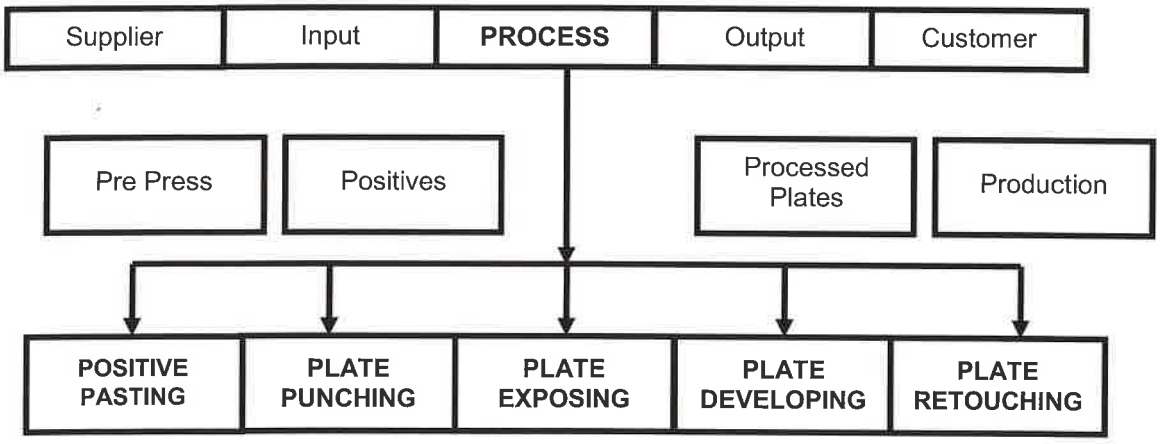


Figure 1: CTQ drill down tree and data collection sheets:

In a commercial offset printing plant, plate wastage being a key constituent in overall wastage and needs to be taken care off. The main objective of this research is to understand practicality of Six sigma implementation and to reduce the plate wastage at least by 10% from the existing level. Area of study includes only X-company web offset machines (Two cold set m/c's & one heat set) and all other machines are excluded from the study. The

project was implemented at Press X- a leading printer in the Indian sub continent .The methodology applied was DMAIC (Define, Measure, Analyze, Improve & Control) for implementing Six sigma.

The project started on 1st May of 2007 and the problem is defined as "The plate wastage is to be reduced by 10% from the existing level by the end of August 2007". Core group is identified and roles are assigned. The typical SIPOC (Supplier, Input, Process, Output & Customer) tree is drawn. Critical to qualities (CTQ) are identified and relevant data's are collected.

DATA COLLECTION PLAN							
Measure	Type	Data type	Operational definition			Collecting	Sampling
			What	When	Who		
Plate wastage On-X machines	Output	Continuous	Plate Waste	Plate analysis from the month of May 07	Team members for their respective shifts	As per the format	Entire population

DATA COLLECTION FORMAT														
Daily extra plates recording sheet					No. of extra plates									
Issue date														
Sno	Edition	Page Label	Color page	Mc. No	Std plate consumption	Edit mistakes running changed	Advt. Probs.	Pre pres probs.	Wrong punching imaging Processing	Improving registration	Worn plates	Mfg faults	Total	%
1														
2														
3														
Daily Total														

Figure 2: Customized data collection formats are designed as shown

2. DPMO Calculation and other analysis

All the X's for wastage generation are identified such as, edit correction, Advertisement, Punching, Clamping, registration, worn out etc. To know the sigma level of the existing system "Defects Per Million Opportunities" (DPMO) is calculated for the month of May 2007 and found 76,638. Then defect percentage is calculated which was 7.66. Later Yield through put percentage is found (92.34%).Then process sigma is calculated (2.93).

DPMO - 76,638
Defect % - 7.66
Yield % - 92.34
Process sigma - 2.93

To study the vital fews a cause and effect diagram(Pareto) is drawn and three important parameters have been identified as given below.

1. Registration
2. Worn out
3. Plate bending/clamping/cracking

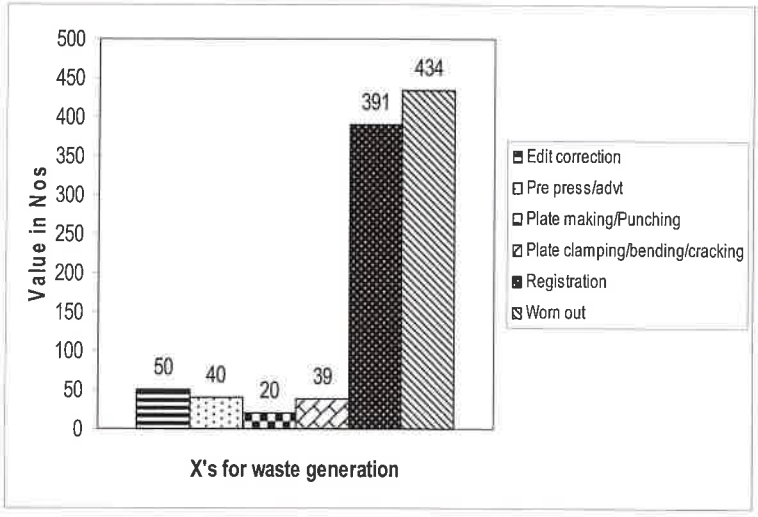


Figure 3: Plate wastage data for May 2007

In the Analysis phase following points are identified:

- Operational mistake due to carelessness of the Plate Punching.
- Checking of only the Registration marks of Pasting.
- General Carelessness in Plate Bending.
- Plates getting damaged during mounting due to clamping problem.
- Plate clamps not in required position.
- Dampening solution not being cooled during circulation.
- Plates with improper regn. not being rectified and re-used.

Based on this study certain suggestions were given to the respective department and they performed the following task for the improvement.

- General awareness in Plate Making Dept./M/c for Plate Punching / bending / clamping respectively.
- Thorough checking of the positives/pasting instead of registration marks only.
- Weekly checking of Exposure and Vacuum of the Plate Exposures.
- Plate clamps adjusted.
- Regular cleaning of the plate clamping bars by metal strip and air.
- Chilling unit attached with M/c-I&II.
- Filter cloth being changed daily.
- Colour plates being re-used after filing or shifting plate on the cylinder itself.
- New formats put in use to ensure proper cleaning of the M/c.

End of August (4^{th} month) the wastage is assessed and sigma level of the project is calculated.

DPMO	- 40,316
DEFECT %	- 4.03
Yield %	- 95.97
Process Sigma	- 3.25

We could clearly see an improvement in sigma level from the earlier 2.93 to 3.25.

To control whatever achieves additional Checking List, New Data Collection Format, Data Summary Sheet and Control Format are designed and implemented. The total savings calculated for a year which amounts to US$ 75,000/-.

The whole project was very successful and additionally 3 more projects are decided to start. The best feature of six sigma is that, there is no extra investment after the initial training. To be competitive in the market the only option in front of us is to reduce wastages as much as possible. Money saved is money earned.

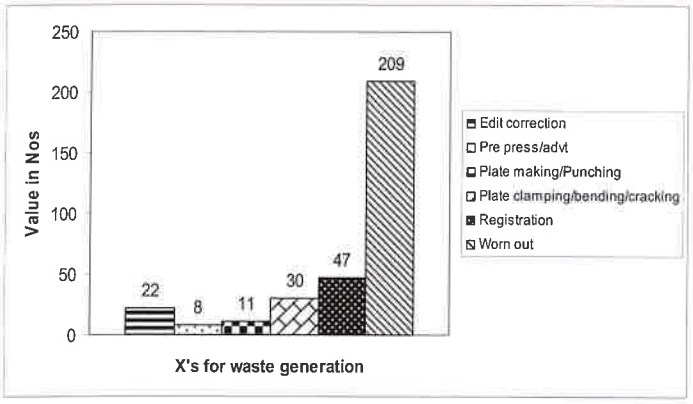


Figure 4:
Plate waste data for August 2005

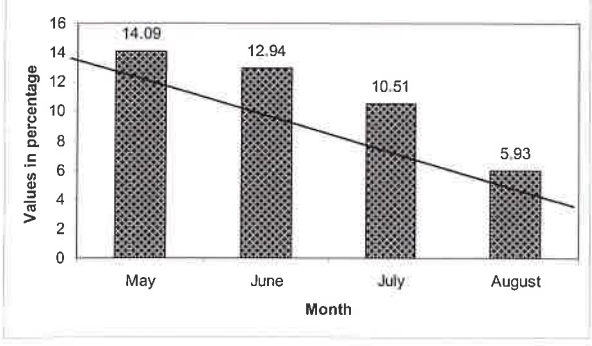


Figure 5:
Plate waste analysis

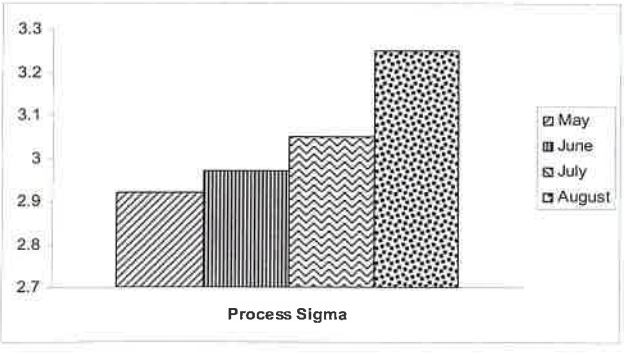


Figure 6:
Process sigma per month

2.1 Feasibility analysis

Based on the case study implemented and feedback taken from the industries we have made a detailed analysis on the feasibility of implementing six sigma in Indian graphic art industry and it is explained below.

Even though the financial savings of the projects are very evident most of the top management who represent the major printing industries have expressed their negative attitude in going for this. To assess the feasibility of the 6 sigma implementation in Indian Printing Industries the following parameters are considered.

2.2 Perception of owner

Most of the A class printing press owners in the country were not in favour of going for Six sigma in their printing presses. Reasons were very simple. The initial investment for a black belt project is very high

according to them (7.5 million INR) for which they were interested to go for a new printing machine or a CTP system. They opinioned that our industry is not matured enough to go for a highly professional and expensive projects like Six sigma. The second reason being pointed out was the profit margins are very very low compared to other parallel industries. Competition is cut-throught. Any other simple methods are sufficient such as Kaizen, Quality circle etc. One of the funniest observation about Indian Print industry is that there is no scientific costing system is followed. Each press has got their own ways. Normally a when a customer goes to a press to execute a job the press owner's first question to him is how much price his immediate competitor offered for the job. Whatever the amount may be he will agree for a less price without costing. This is unjustifiable.

2.3 Affordability/Economy

The initial investment for implementing a green belt or black belt project is a huge amount for an Indian printer. The only industries which can really afford couple of projects is news paper industry. Then may be six or seven printing presses in India can invest on this.(Even they are not interested).

Most presses believes that instead of investing on a TQM project let us invest on a technology. Since the profit margins are very low compared to other industries still that financial barrier is visible in Indian graphic arts industry.

2.4 Sustainability

From my last five years of observation the only printing press in India (Organizations manufacturing machineries and systems for pre press/press/post press are not included) which sincerely put all the effort to implement six sigma was Hindustan Times. They implemented couple of projects and almost continued their enthusiasm for three years and later they gave up. Other projects they started are in between and later it has come down to something like a JQI projects. Any system to sustain the commitment from top management is important and the retention of trained man power was also found difficult. ITC Printing and Packaging division is implementing JQI projects not exactly six sigma.

2.5 Manpower availability

Since this country has got sufficient qualified hands with good computational skills it is quite possible to generate man power for six sigma implementation. But retaining them is a Herculean task. It so happened to one of the leading print industry in India, after developing sufficient man power to undertake new projects (Invested huge amount on them) their all trained, value added manpower shifted to software and other similar BPO industries. The remuneration package offered was very high which none of the existing printing industry can afford. Since I was in touch with this organization I could witness how they deserted the six sigma programme in their parental company. So the problem we face in India is retaining the trained manpower in printing organization is nearly impossible.

2.6 Training availability

There are sufficient training concerns in India and sufficient trained people in different industries. Availability of trainers is not at all a problem. The main advantage in this country is that most of the top six sigma practicing companies like motorolla, GE, Philips etc have their R&D centres in India. They normally train their own people (every body has to undergo six sigma training) and often train outsiders. Organisations like FICCI had tied up with ASQ and running regular training programmes other than the government training centers.Among all the points discussed here training availability is fully satisfied.

3. Conclusion

This research study concludes the following points.

- Since the study is primarily focused on offset industries the Six sigma implementation is done at off set technology plants.

- The research gives us a conclusion that Indian printing industry is not matured enough to go for Six sigma implementation.(Refer questionnaire in appendix).
- 95% of the employees in Indian graphic arts industry are just skilled employees and not knowledge workers.
- Basic TQM techniques using SQC techniques are sufficient to streamline most of the problems, which are very cost effective and easy to implement.
- Feed back survey taken from the industries which are implemented six sigma projects during this research study it is evident that they are not interested to go for further projects for the time being.
- All are well versed with modern technologies and they opeined that buying the most modern equipment is more sensible for them rather than going for a very expensive six sigma project.
- None of the industries are interested in reducing paper after certain level since it is already included in the customers costing.
- Our import policy allows us to buy paper in an extremely low rate. To retain the status-co, companies have to continue printing the same quantities which allows them to import the same quantity.
- Few industries even with out printing they just get the paper and sell it in the market with a price that alone bring them profit.
- This situation is quite funny and it happens only in print industry.
- Waste paper is unaccounted money and most presses make a good profit out of it.

3.1 Best practice for Indian graphic arts industry

The profit margins are the lowest compared to many parallel industries and products are not so critical like hospital equipment, space systems or nuclear industry, customer expects a very reasonable price. Probably that could be the reason why this industry is 26th in turn over but size wise 3rd (AIFMP report July 2001). Basically a study conducted by Quality Council India says 93% of the printing industries are below 3 sigma level and they must adopt fundamental quality management practices to lift themselves to at least three sigma level. For the time being the best practice for general print industry shall be to practice systems such as 5S, Kaizen, ISO and SQC tools like Quality Circles, Pareto Analysis, Control charts, FMEA and QFD for measurement and quantification.

Acknowledgement

1) Prof. Dr. Sreekumaran Nair, Head, Department of Statistics, Manipal University, India
2) Mr. B. Shesh, Hindusthan Times, New Delhi
3) Mr. Amrutharaj Harikrishnan, Print Media Academy, Chennai, India

References

1. Abernathy, D. P. (2001), "Avoiding unintended consequences: Managing "Anti-Ys" in a Six Sigma project", Annual Quality Congress Proceedings, Milwaukee
2. Adams, L. (2002), 'Whom do you trust?', Quality, Vol.41, No.13
3. Alvarez, M., Binkley, E., Bivens, J., Highers, P., Poole, C., & Walker, P (1990). Case-based instruction and learning: An interdisciplinary project. Proceedings of 34th Annual Conference , College Reading Association. Reprint
4. Amelsberg, J. (2002), "Systematic performance and cost management: A management framework for organisational excellence", Annual Quality Congress Proceedings, Milwaukee
5. American National Standard: Definitions, Symbols, Formulas, and Tables for Control Charts Milwaukee, WI: American Society for Quality Control, 1987
6. Rasis, D., Gitlow, H. S., and Popovich, E. (2003), "Paper organizers international: A fictitious Six Sigma Green Belt case study II", Quality Engineering, Vol. 15, No.2
7. Senapati, N. R. (2004), "Quality and reliability corner: Six Sigma: myths and realities", The International Journal of Quality & Reliability Management, Vol. 21, No.6/7
8. The ASQC Basic References in Quality Control: Statistical Techniques. Milwaukee, WI: ASQC Quality Press, 1986 - 89

* Many publications from AIFMP the apex body of Indian Printers

Profiling ecosolvent inkjet printers

Richard M. Adams II[1], *Mark Gundlach*[2]

[1] Ryerson University, School of Graphic Communications Management
350 Victoria Street, Toronto, Ontario M5B 2K3, Canada
E-mail: richard.adams@ryerson.ca

[2] X-Rite, Inc.
4300 44th Street SE, Grand Rapids, MI 49512, USA

Abstract

Since 2004, solvent-based inkjet printers have come to replace aqueous dye- and UV-based pigmented inkjet printers in the production of outdoor signs and banners. These printers use aliphatic and aromatic hydrocarbon-based ink to print mostly on polyvinyl chloride (PVC) and other media. They produce graphics with superior fade-resistance and weatherability. However, the ink vehicle emits volatile organic compounds (VOCs), requiring that the printer be ventilated.

In 2005, a new type of inkjet printer, the so-called ecosolvent printer, was introduced to produce outdoor graphics with superior fade-resistance and weatherability. Ecosolvent printers use ethylene glycol-based ink, which has similar weatherability characteristics to solvent-based inkjet, but does not emit significant quantities of VOCs, so they can be used in office and plant environments without ventilation.

Unlike aqueous inkjet printers, both solvent and ecosolvent printers require that media be heated to facilitate ink absorption and drying. Determining the optimum print heater settings adds another dimension to profiling these printers for color management.

This paper presents experimental results to document an empirical procedure for profiling solvent and ecosolvent printers. In addition to the steps that precede profiling of aqueous inkjet printers (determining optimum ink density, linearization of tone values, and setting total ink coverage), solvent and ecosolvent printers require an additional step to determine the optimum heater settings for the media and ink used.

Keywords

ICC profiling, printer profiling, ecosolvent inkjet printing, large-format printing, wide-format printing

1. Introduction

ICC profiling characterizes the color reproduction capabilities of printers and ensures accurate and consistent color output. First introduced in the 1990s for lithographic printing, ICC profiling became popular with inkjet printers introduced in the late 1990s as a way to get accurate color with many different printers, media, RIPs, and settings such as resolution and screening. [Adams, Sharma, and Suffoletto, 2008].

To make an ICC printer profile, the user begins by printing a test chart of approximately 500 - 2,000 color patches with the printer's color management turned off. The test chart is then read with a spectrophotometer and generates the profile with a profiling application. The profile is used by ICC-compliant applications (e.g., image-editing or page-layout software) or the printer's raster image processor (RIP) to convert image data or pixel values for an accurate match to the original file upon output.

Since printer profiling merely captures the printer's color reproduction characteristics at the time the color test chart is printed, the user generally wishes to set up the printer to optimum output and to calibrate it to a known specification before profiling. Thus two steps preceding the profiling process, along with profiling and the color conversion process for which the profile is used, are known as the "4 Cs" of color management (Figure 1). These optimization and calibration processes are particularly important with inkjet printers, which can use more ink and reproduce higher print densities than lithographic presses. The "4 Cs" are particularly challenging with ecosolvent and solvent inkjet printers (Figure 2), which heat the media prior to, during, and after printing to ensure good ink penetration and fast drying.

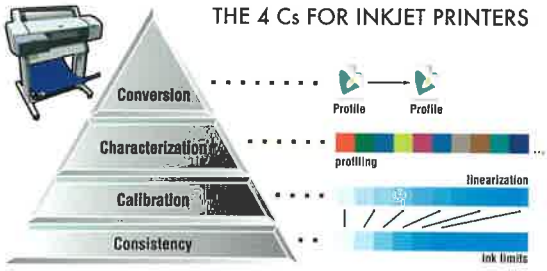


Figure 1: The "4 Cs" of color management is a convenient way to think about printer optimization ("consistency"), linearization ("calibration") and ICC profiling ("characterization"). Applications "convert" image data to ensure a match on different devices



Figure 2: The Roland SolJet Pro III is one of a new type of "ecosolvent" inkjet printers that began to be developed in the early part of this decade. It uses ethylene glycol-based ink that is fade- and waterproof for outdoor signs and banners

Over the course of two years, the authors developed a procedure for profiling ecosolvent inkjet printers that they used to make many profiles for media manufacturers [Adams and Gundlach, 2004, 2007]. Many of our procedures were based on empirical observations and trial-and-error. The purpose of this study is to present the procedure and document it with experimental observations. Specifically, we wanted to answer the following questions:

1. What settings are important in optimizing print quality on an ecosolvent inkjet printer, beyond those on an aqueous-based inkjet printer?
2. Does the heater temperature of an ecosolvent printer affect the printed ink density and color gamut?
3. Do print density and color gamut vary with the manufacturing method (cast or calendered) used to make PVC media?

2. The "4 Cs" for inkjet printers

Consistency. Consistency, or optimization, establishes upper density limits on inkjet prints. Unlike lithographic presses, inkjet printers print by ejecting ink droplets from print heads. The amount of ink printed is a function of the printhead, printer resolution, and the media's ability to hold ink. When profiling an inkjet printer, the first step is to determine the optimum amount of ink required. This usually means identifying the maximum density achievable with the minimum amount of ink. Known technically in lithography as "ink mileage," as the amount of ink is increased, ink density rises to a certain point, after which it may level off and even decline (Figure 3).

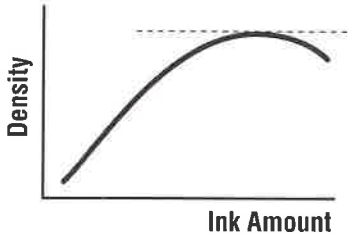


Figure 3:
An "ink mileage" graph shows how, as the amount of ink is increased, density increases to a point where it levels off, then actually declines

On inkjet printers, the amount of ink printed is generally determined by the RIP. Most RIPs have an optimization routine and test chart (Figure 4) that allow the user to print a test chart of increasing ink amounts and then determine optimum ink limits. After printing the test chart at maximum ink output, the user selects the highest density achievable with the minimum amount of ink, either visually or with a densitometer.

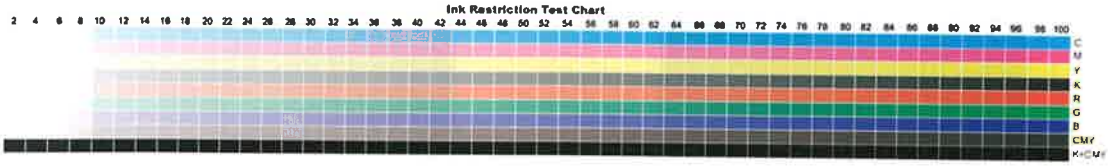


Figure 4: The first step in optimizing an inkjet printer is to establish the optimum ink density, which is generally done through the RIP. Using a target such as this ink restrictions target from Onyx Graphics, the RIP prints increasing amounts of ink. The operator evaluates the chart visually to see where density levels off and can select the optimum ink amount

A second stage of ink density optimization is to determine the value of total ink coverage that produces the maximum density with the minimum amount of ink. This procedure, which is usually performed after calibration (described below), involves printing a test chart of multiple, increasing ink amounts (Figure 5). The user evaluates the chart, visually or with a densitometer, and selects the dot area combination, on a scale of 0 - 400%, that produces the maximum density with the minimum amount of ink.

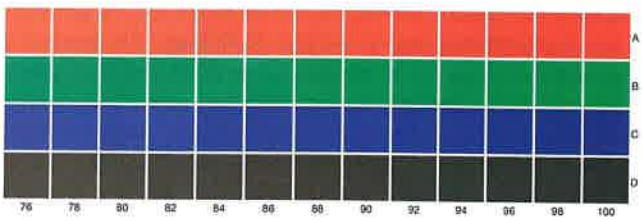


Figure 5: The second step in printer optimization, usually done after linearization, is to determine total ink coverage. This is the sum of CMYK inks needed to produce black

Calibration. After establishing upper ink density limits, calibration, also known as linearization, spaces intermediate tones evenly throughout the tone reproduction curve. Inkjet printers tend to be non-linear because they print stochastic screening with the same-size dots, which depending upon the screening pattern could tend to clump together at different dot percentages. To linearize the printer, the user prints a linearization target, consisting of tones from 0 - 100% in increments of 5 or 10% (Figure 6). He or she then reads the printed tones with a densitometer. The RIP calculates the dot area for each tone, and computes a smooth linearization curve that spaces the tones out between the minimum and maximum values (Figure 7) this process provides better data for the characterization process that attempts to create a correlation between CMYK instructions and CIE L*a*b* measurements

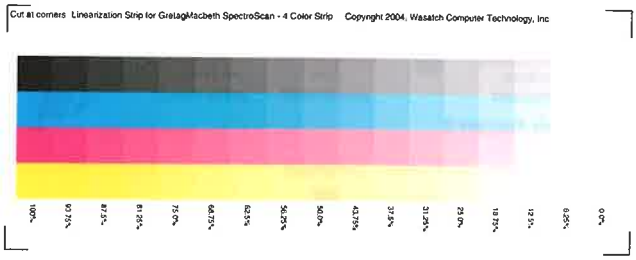


Figure 6: After setting ink limits, the operator linearizes the printer. Linearization spaces tones evenly from light to dark

Characterization. Characterization refers to the actual profiling process. To profile the printer, the user prints a test chart on the optimized, linear printer, with color management turned off. As described in the introduction, the test chart is read with a spectrophotometer, and a color profile is computed with an ICC profiling application. What does the ICC profile store?

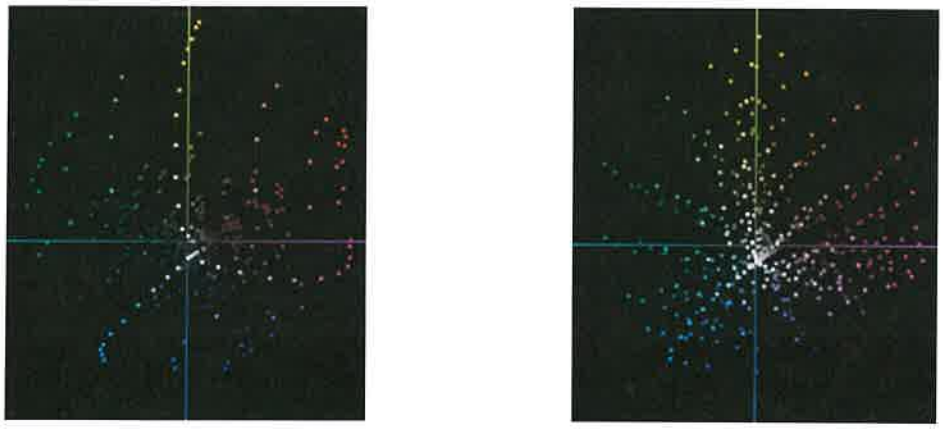


*Figure 7: This diagram shows an L*a*b* plot of a printer profiling target before (left) and after (right) linearization. Note that, in the linearized printer, tones are more evenly spaced*

3. The challenges of ecosolvent and solvent inkjet printers

Inkjet printers popular in desktop publishing, photography, graphic arts proofing, and indoor graphics use aqueous-based ink. These printers use paper-, plastic, and cloth-based media that has been especially coated for ink receptivity. The ink is not weatherproof and is subject to fading. The outdoor sign and durable graphics market uses a new type of printer that began to be developed in 2004 and uses solvent-based ink. This ink can print on plastic media that has not been specially coated, and it is more weatherproof and fade-resistant than aqueous ink. However, since solvents give off harmful volatile organic compounds (VOCs), these printers must be used in a specially ventilated environment. A more recent variant of the solvent printer is the so-called ecosolvent printer that was first commercialized in 2005 and uses ethylene glycol-based ink. Ecosolvent ink emits fewer VOCs than solvent ink, and the printers can be used in a normal office environment.

Both solvent and ecosolvent printers are most commonly used with polyvinyl chloride (PVC) media to produce outdoor signs and banners. While solvent-based ink penetrates, or "etches," the media so the ink can penetrate the surface, an ecosolvent printer requires special heating to make the media more receptive to the ink and to assist in drying.

An advantage of uncoated PVC media is that it is cheaper than coated media used with aqueous-based printers. Also, uncoated media can often be stretched slightly without damaging the image, whereas the coating on aqueous media is prone to cracking when stretched. Also, because coatings are subject to wear and physical abrasion, uncoated media is more resistant to chemicals, solvents, water, scratching, and ultraviolet fading. Even without protective lamination, it will hold up against moisture and sunlight better than most coated aqueous inkjet media.

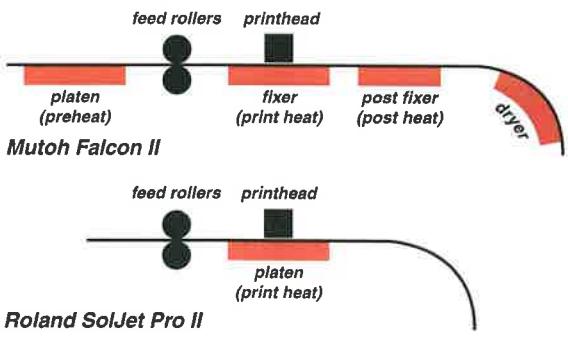


Figure 8: Ecosolvent printers heat the media to facilitate ink penetration and drying. This diagram compares printers from two manufacturers, one of which has a 4-stage heating system (Mutoh), while the other has a single-stage system (Roland)

On ecosolvent printers, heat helps the ink penetrate the surface of the media and accelerates drying. If ink cannot penetrate the media, it spreads out on the surface, causing ink bleed and an artifact known as "dot-gain

banding." Ecosolvent printers employ one to four heaters (Figure 8) that optimize media temperature before, during, and after ink application. Heating stages include pre-heat (applied before printing), platen-heat (applied at the print stage), post-heat (applied after the print stage) and drying (applied after post-heat to speed up drying). Heaters range in maximum setting from 50 - 70°C.

4. Experimental procedure

An experiment was conducted to determine the extent to which the color gamut of an optimized ecosolvent printer is affected by heater settings and the resulting ink restrictions that were achievable.

1. To create a two-by-two experimental matrix, two media, Avery MPI 1005EZ calendered and MPI 3100 cast PVC media, were printed at different heater temperatures on two printers, an HP 8000 (25, 35, 45 and 55°C) and a Roland SolJet Pro III (25 and 50°C, this printer's maximum setting).
2. Using the Onyx ProductionHouse software RIP, the built-in Onyx ink limit target was printed with color management turned off and ink limits set to maximum (100%) in the RIP.
3. To implement the first "C," consistency, of the "4 Cs" of color management, the printer was optimized for ink density limits by visually evaluating the target for maximum density without mottling, dot-gain banding, vertical banding, or other artifacts. Also, after linearization (step 4 below), the RIP's proprietary total ink coverage target was printed and visually evaluated to select the maximum total ink coverage, which was generally around 300%.
4. To implement the second "C," calibration, the density-optimized printer was linearized using an X-Rite i1 iO x/y-scanning spectrophotometer connected to the Onyx RIP, using the RIP's linearization routine.
5. After optimizing density and linearizing the printer, a 2000-patch ECI 2002 test chart was printed at the ink density set in step 3.
6. The target was measured with an X-Rite/GretagMacbeth i1 iO x/y-scanning spectrophotometer.
7. An ICC profile was made from the printed target.
8. Using Chromix ColorThink Pro software, the color gamut of the profile was graphed in CIE xyY color space to determine its size.
9. Density was measured with a color reflection densitometer and graphed as a function of ink application.
10. Print samples of 20% black ink from the 25° and 55°C ink restriction targets were examined with a scanning electron microscope to look for signs of ink penetration and other physical behavior on the surface of the media.

5. Results

Maximum density and color gamut. Maximum densities achieved in the printer optimization step are shown in Tables I and II and graphed in Figure 9. From the data it appears that solid density does not vary widely between the cast (MPI 3100) and calendered (MPI 1005EZ) PVC media used in the study. Also, densities are about the same at different print temperatures. Likewise, color gamut (Figure 10) does not appear to vary widely among the different print temperatures.

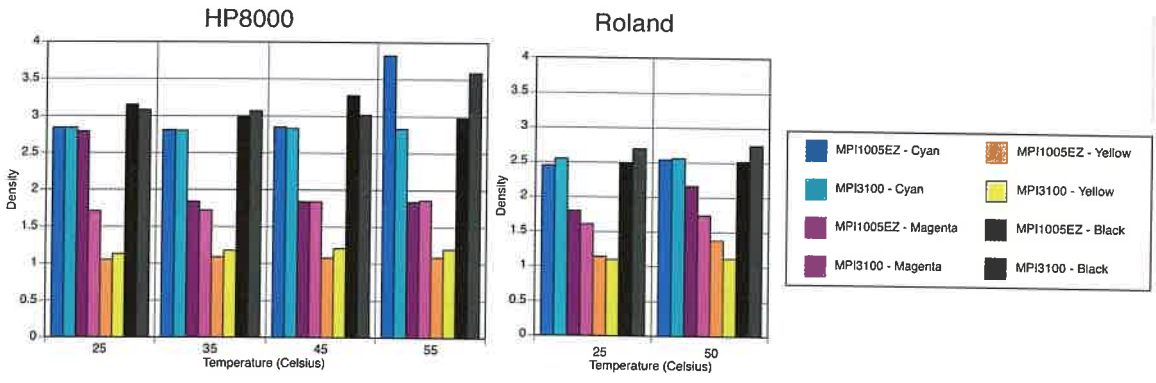


Figure 9: This graph shows CMYK ink densities on Avery MPI1005EZ (calendered, left bar) and MPI3100 (cast, right bar) media printed on the HP 8000 and Roland SolJet

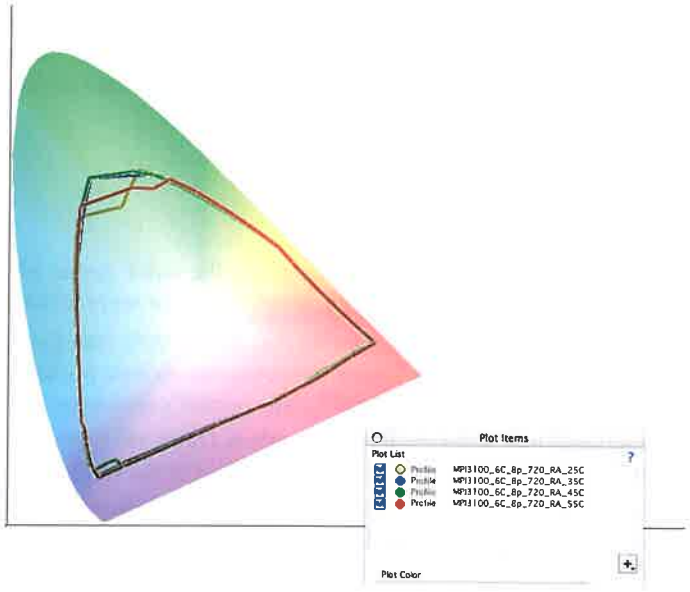


Figure 10: This CIE xyY plot shows the color gamuts of 4 ICC profiles made on an HP 8000 printer on Avery MPI 3100 cast media at 4 different temperatures. The graphs show that color gamut does not vary significantly with print temperature

In general, only a slight increase in density is apparent with increasing printer heater temperatures. This slight density increase also results in a marginal increase in color gamut. However, scanning electron micrographs at around 100x magnification (Figure 11) clearly show the ink's tendency to spread out on the media's surface with insufficient print heat. At optimal print temperatures, however, ink penetrates the media surface and remains in well-defined droplets.

Micrographs of the two media at approximately 500x (Figure 12) show the difference between calendered media, which appears to have a rougher surface, and cast media, which is smoother.

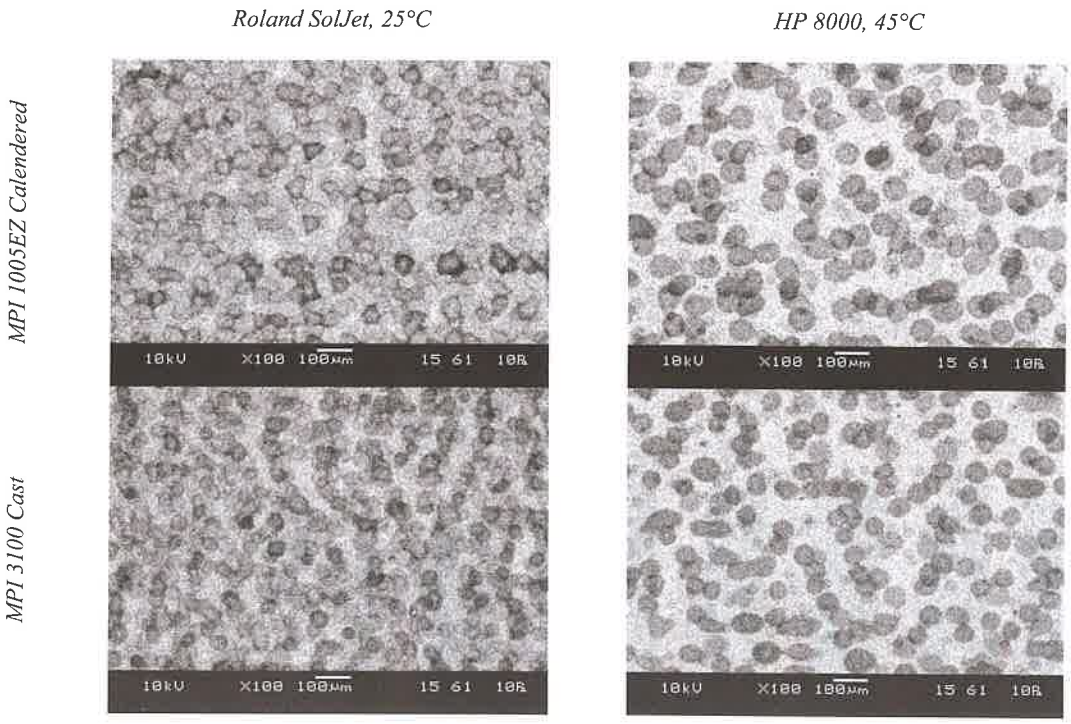


Figure 11: Scanning electron micrographs (originally 100x) of prints on MPI 1005EZ (top row) calendered and MPI 3100 cast (bottom row) media, printed at 25°C (left column) and 45°C (right column). Note that dots printed at 25°C are not well-formed and spread out over the media, while those printed at 45°C form nearly round circles with well-defined edges

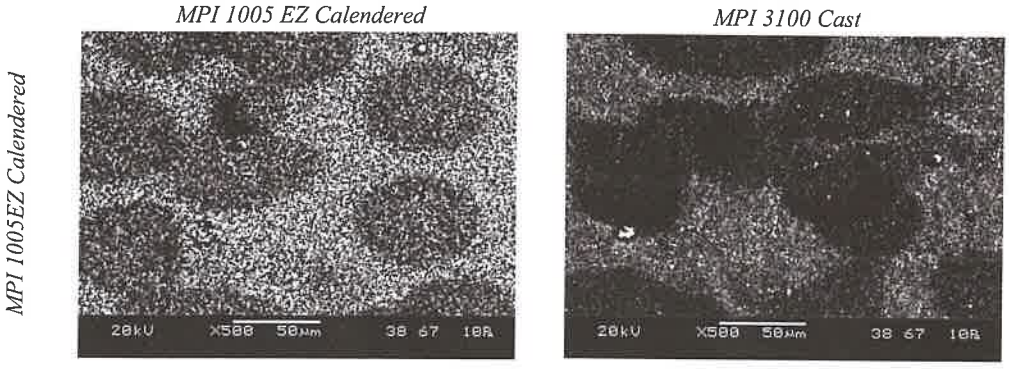


Figure 12: Originally 500x micrographs of MPI 1005 EZ calendered and MPI 3100 cast PVC media. The cast media is considered to have a higher quality but is more expensive. Its surface appears smoother

In our study the MPI 1005EZ media on the Roland exhibited a clear ink-mileage relationship. As more cyan and black ink was applied, density leveled off and then began to drop (Figure 13).

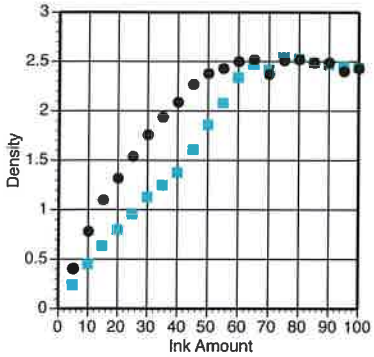


Figure 13:
This graph of Avery MPI1005EZ on the Roland printer at 50°C shows a clear ink-mileage relationship in black and cyan inks. As more ink is applied, density increases, levels off, and drops. The optimum ink amount, before the point where density levels off, here is 60% of the maximum amount

Based on the tradeoff between horizontal dot-gain banding and vertical temperature-based banding, the optimal heater temperature for both media on the two printers was approximately 45°C. At lower temperatures (25 and 35°C), ink remained wet on the surface and took much longer to dry (Figure 14) than at the optimal 45°C. At 55°C, both media buckled slightly and showed signs of vertical banding (Figure 15).

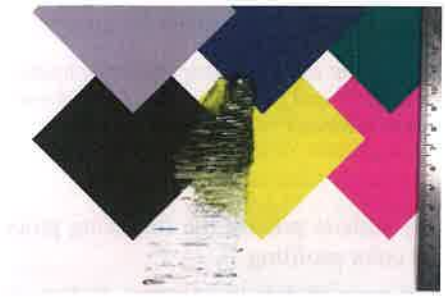


Figure 14:
A test chart printed at 25°C on the Roland SolJet printer shows how insufficient printer heat results in slow ink drying, which can enable the ink to smear after printing



Figure 15:
Excessive heat (70°C) on the HP 8000 causes this media to buckle and lift off the surface of the printer platen. When media lifts high enough it contacts the print heads, ruining the print and possibly damaging the printheads. Even if media does not contact the print heads, the buckling can cause banding in the direction of media travel

Table I: Maximum densities for both media printed on the HP 8000 and Roland SolJet printers

HP 8000 Printer					
	Substrate	**25°C**	**35°C**	**45°C**	**55°C**
Cyan	MPI1005EZ	2.84	2.81	2.85	2.82
	MPI3100	2.84	2.80	2.83	2.83
Magenta	MPI1005EZ	2.79	1.84	1.84	1.84
	MPI3100	1.71	1.72	1.84	1.86
Yellow	MPI1005EZ	1.05	1.09	1.08	1.09
	MPI3100	1.13	1.18	1.21	1.20
Black	MPI1005EZ	3.15	3.00	3.28	2.98
	MPI3100	3.08	3.07	3.02	3.59
Roland SolJet III Printer					
	Temperature	**25°C**	**50°C**		
Cyan	MPI1005EZ	2.46	2.54		
	MPI3100	2.55	2.56		
Magenta	MPI1005EZ	1.80	2.16		
	MPI3100	1.61	1.74		
Yellow	MPI1005EZ	1.14	1.38		
	MPI3100	1.10	1.12		
Black	MPI1005EZ	2.49	2.52		
	MPI3100	2.7	2.75		

6. Discussion

Print temperature, ink density and color gamut. As a result of this study, the authors concluded that the heat level on an ecosolvent printer plays a greater role in ink drying and elimination of artifacts from prints than it does in ink density and color gamut.

Ecosolvent printing involves a tradeoff between heat, ink density, and print speed [Adams and Gundlach, 2004; Figure 16]. High heat levels enable faster printing at greater ink densities. However, excess heat may cause the media to buckle, which in turn causes vertical banding. It may also cause the media to rise above the platen to a sufficient height to contact the print heads, which ruins the print and may cause a print head crash. As a result, the user, who wants high quality and high speed, may not be able to achieve both.



Figure 16:
Profiling an ecosolvent inkjet printing involves a tradeoff between color (density and gamut), quality (smoothness and freedom from artifacts), and speed (throughput)

Printer optimization. Based on the foregoing conclusions, the authors present the following procedure for optimizing an ecosolvent inkjet printer prior to linearization and color profiling.

1. Inkjet printers use multi-nozzle print heads that print several rows of dots in one pass. Before optimizing the printer, the operator should ensure that all ink nozzles on the print head are ejecting ink. Many printer manufacturers have special test patterns to check nozzle firing. If, after printing a nozzle-check test pattern, one or more nozzles are found to be not printing, the operator should perform a print head cleaning, which is usually an automated procedure on the printer.

2. Setting Heaters. The optimal heater setting differs for each media and depends on its composition, thickness, and transport speed through the printer. To find the optimal heater setting for a media, start at a moderate level, such as 35°C. Print a test chart, such as a heater test chart supplied by the manufacturer (Figure 17), or the generic chart illustrated in Figure 18.

3. Check media feed compensation. After printing the heater test chart, first check that the ink dried. Ink should dry within 5 min. of printing. Next, look for horizontal banding in the direction of print head

travel. Such banding could be a sign of excessively low temperature, or it could also indicate that the media feed compensation is too high or too low. Media feed compensation (Figure 19) adjusts print head overlap between passes to compensate for media thickness and slippage during printing. If set too low, horizontal banding will occur as the print heads overlap each other. If set too high, horizontal banding will also occur due to excessive distance between print passes.



Figure 17:
Mutoh supplies this test chart of CMYK solids and overprints for use in selecting the proper print temperature for new media

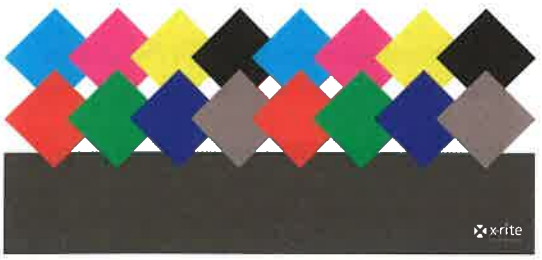


Figure 18:
The second author developed this test chart for evaluating print quality on ecosolvent printers

4. Check for dot-gain banding. Once the proper media feed compensation has been verified, examine the print for dot-gain banding, which is horizontal banding in the direction of print head travel. Dot-gain banding occurs as ink spreads out over the media surface due to insufficient temperature. If necessary, increase the heater setting until dot-gain banding is eliminated.

5. Check for high-temperature banding. Once dot-gain banding has been eliminated, also check for high-temperature banding, which is vertical banding in the direction of media travel (perpendicular to the direction of print head travel). High-temperature banding occurs when media buckles and lifts off the surface of the print platen to form waves. The banding effect is created by differences in ink application to the front and back sides of the media "wave".

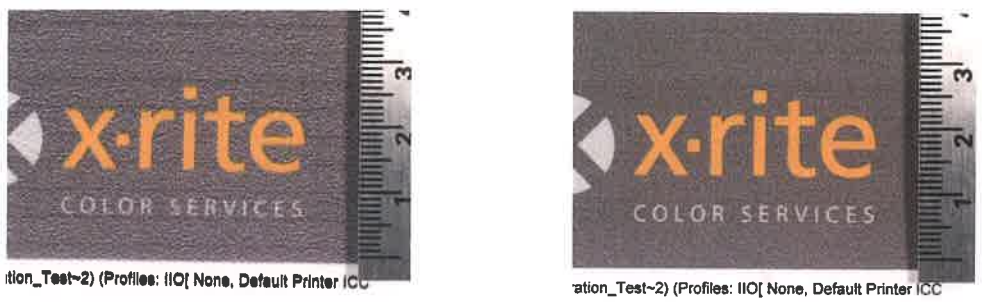


Figure 19. Ecosolvent printers generally have a setting for media feed compensation, which is used to compensate for varying media thicknesses and rates of slippage in the transport mechanism. The setting affects the distance between subsequent passes of the print head. If set too low, print passes overlap and create dark banding (left). If set too high, the gap between print passes results in light banding (right)

Using the above procedure, the operator can generally find a satisfactory print heater level that eliminates both dot-gain and temperature banding. If it is not possible to eliminate both types of banding, the operator may need to reduce print speed. Reducing print speed, like increasing print temperature, promotes faster ink drying by allowing more time between applications of ink by the print heads.

7. Ideas for further research

These studies could be done with additional printers and media to see if the same relationships between temperature and print quality are true. Also, more study is needed to assess the print quality and printability of PVC media used for ecosolvent printing. Specifically, manufacturers formulate small batches of media using different additives that affect printability, so a method or protocol to predict printability based on surface properties would be useful in the manufacturing process.

Acknowledgments

The authors would like to thank Tom Durner from Avery-Dennison for donating PVC media for these experiments; Chris Gwinn from X-Rite, Inc., for his help in running printer tests; and Evelyn To, fourth-year student at Ryerson University's School of Graphic Communications Management, assisting with preparation of the paper.

References

1. Adams, R. M., A. Sharma, & J. Suffoletto. (2008). *Color Management Handbook.* Sewickley PA: PIA/GATFPress
2. Adams, R. M., & Gundlach, M. (2007, March). Profiling ecosolvent inkjet printers. *TAGA Proceedings*
3. Adams, R. M., & Gundlach, M. (2004, October). Tech talk: profiling media for mild solvent printers. *Digital Graphics*
4. Berns, R. S., A. Bose, & D. Y. Tzeng. (1996). The spectral modeling of large-format ink-jet printers. *RIT Munsell Color Science Laboratory*
5. Desie, G., G. Deroover, F. DeVoegt, & R. Claes. (2004, October). Fundamental mechanisms in ink media interaction for aqueous, UV-curing and solvent based inks. *IS&T's NIP20: International Conference on Digital Printing Technologies*, Salt Lake City, UT, 774 - 779
6. Forrest, D. J., Briggs J. C., Tse, M.-K. & Barss, S. H. (1998, October). Print quality analysis as a QC tool for manufacturing inkjet print heads. *IS&T's NIP 14: International Conference on Digital Printing Technologies*, 590 - 594
7. Gundlach, M. (2004, August). Tech talk: mild solvent profiling - where do you start? *Digital Graphics*
8. Kline, E. A. (2005). Rate of fading of large format inkjet prints on synthetic substrates. M.S. thesis proposal, *Rochester Institute of Technology*
9. Noble, S. (2004, October). Inkjet Printing and the Clean Air Act. *IS&T's NIP20: International Conference on Digital Printing Technologies*, 802 - 804
10. Wang, J. (2003, September). Soft-solvent based inkjet inks for uncoated vinyl printings. *IS&T's NIP19: International Conference on Digital Printing Technologies*, 265 - 267
11. Wilhelm, H. (2006, September). A 15-year history of digital technology and print permanence in the evolution of digital fine art photography: from 1991 - 2006. *IS&T's NIP22: International Conference on Digital Printing Technologies*, 308 - 315
12. Wilhelm, H., J. Holmes, & M. McCormick-Goodhart. (1998, October). The important roles of inks and media in the light fading stability of inkjet prints. *IS&T's NIP 14: International Conference on Digital Printing Technologies*, 122 - 122

Distributing and publishing newspaper content on a digital TV-platform

Olli Nurmi, Atte Kortekangas

VTT Technical research centre of Finland, Media and Internet
P.O. Box 1000, FI-02044 VTT, Finland
E-mail: Olli.Nurmi@vtt.fi

Abstract

In this paper we study and evaluate DVB-T broadcasting of newspaper content and user interface on a digital TV platform. The objective of the research was to study a) the data transmission reliability and efficiency, b) user interface and c) the user experience of the DigiTV Newspaper. The study was conducted in two stages. Fist a facsimile copy of the newspaper content was generated daily and transmitted in three geographical regions in Finland to test the service for three local newspapers. After this the layout was modified to improve the usability and user tests were conducted. The results show that the facsimile representation of the content can be enhanced by using wide format layout, video material and navigational aids. This kind of publishing channel can be a supplementary service especially when the newspaper distribution faces geographical challenges.

Keywords

Data transmission, digiTV, newspaper distribution, user experience

1. Introduction

In Finland, newspaper distribution is carried out by early-morning home delivery, which covers about 80 % of the households. In some areas the distribution faces major challenges (like the archipelago and some rural areas). In these areas the distribution is costly and time consuming. To save the costs and time the printed newspaper could be complemented or in some cases even replaced by the digital newspaper.

Because fast internet connections do not cover whole Finland we must consider other networks to distribute digital newspapers. One option is to use DVB-T-networks which are designed to broadcast data for large geographical areas. The DVB-T- infrastructure also has free capacity during the nights and business models suitable for freesheets and subscription based newspapers. The alternatives to digital right management are:

1) The user has free access to the data without any limitations. This is suitable for freesheet business model which is based on advertisement income.

2) The access is checked at the beginning of the data capture. If the user has proper rights the encrypted material can be decoded and captured to the memory of the reading platform without any further limitations. This model can be implemented by incorporating a slot for a smart card in a DVB television or set-top box with the appropriate hardware facility to view conditional access content that has been encrypted using a conditional access system.

The layout for online newspaper published in internet in not optimal for the digital TV platform. The TV sets typically have aspect ratio of 9:16 different from the broadsheet format commonly used for newspapers in Finland. The user interface can be improved by navigational aids and wider layout that doesn't require scrolling.

In this study we conducted empirical tests with three local newspapers in two stages. In the first stage the reliability and efficiency of the DVB-T distribution was tested for a test period in three geographic regions in Finland. The content was derived from the editorial system, packed and error correction encoded after which a *transport stream* was generated. The data was broadcasted during night time via the DVB-T network. PC- clients with an external DVB-T receiver captured the data and users read the digital newspaper on a HDTV-screen.

A specially designed transport protocol was developed which allowed error free reception of the data even in cases where some of the data packets were missing in the first place. The log files for the data transmission and reception were analysed and the network efficiency calculated.

In the second stage the user interface was modified to suit better into 16:9-format. Indexes in two levels were included and navigation aids introduced. The newspaper was enriched by videos.

The usability of the service was evaluated collecting information by observations and questionnaires. The data included comparison of the target product with a newspaper in printed form and in online form.

2. Navigation aids in online newspaper

Newspaper design pattern is in most cases based on the front page design. Familiarity and recognition are strongly related to the front page design, making positioning of objects and visual patterns important. On the front page of online newspapers, headlines are often the representation of stories that are valued most interesting, resembling the printed format that also presents the top stories on the front page [Ihlström & Åkesson, 2004].

Newspaper sections enable the reader easy access and guidance to information. It does not take much effort to find a particular section e.g. the sport section or the business section, inside a newspaper. The newspaper indexing is the most effective "navigational" tool in newspapers and headlines are the main entry points to text. According to Garcia [Garcia, 1997] all publications, printed or digital, should minimize the number of items that appear as navigational tools. In online newspapers, readers scroll the front page to get an overview of the contents of the news site, which could be compared to browsing and flipping through the printed newspaper.

Two reader patterns for newspaper can be identified. The first one is so called browsing pattern where the reader wants to get an overview of the information. This kind or readers typically read the newspaper linearly by turning the pages sequentially. The other reading pattern is more task-oriented where the reader actively seeks some information by using typically sections (for example politics, sports etc.).

Based on this theory following design principles for digital newspapers have been reported [Ihlström Eriksson, et al, 2006]:

- Index - e.g. in three levels (front page, index of sections, index per section);
- Menus - for an easy way of going back and forth to sections and pages;
- Turning page - support for both traditional page by page browsing and skimming (browsing through multiple pages very quickly);
- Page indicators - strong indicators that gives an overview of where you are in the total newspaper and support the feeling of an beginning and an end, e.g. page 27/52;
- Visual cues concerning which section the reader is currently in - e.g. colour coded sections (sport - pink);
- Headlines - different headlines that helps the user orient themselves on a page;
- Hyperlinks - support fast navigation to a specific article without having to browse.

3. DigiTV Newspaper tests

We made an experimental evaluation of versions of the *DigiTV Newspaper* where the content was derived from various web-versions of the daily newspaper at three sites, i.e. the Hämeenlinna, Jyväskylä and Turku regions during spring and summer 2006. The voluntary testers were surveyed prior to the experiments including demographic data and habits of media consumption. We urged the testers to keep a diary of daily experiences and opinions on the *DigiTV Newspaper*. At the final review the testers were interviewed for experiences during the whole test period. There was also a group interview for the whole test group with each of the three distinct test sites. The following report and analysis of reader perception is based on these questionnaires and interviews.

The total number of testers was 26, with 38% of them female and 62% male. The age distribution had one quarter of the population below the age of 29; 12 percent in the age group 30 - 39 and 20 percent in the age group 40 - 49. The largest population, one third of the total, was with the age group 50 - 59 whereas the age group of 60 or older had 12 percent of the participants.

3.1 Contents transmitted, transmission and reception technology

A standard web-based publication product, essentially a hybrid of a facsimile representation of the daily newspaper and a web-based html edition of the same contents was used as the content source. Some local newspapers have marketed such an online newspaper to subscribers while some other papers have employed similar device for internal editorial work. Technically, the product is based a set of relatively low-resolution facsimile images for each page, where links to text-based representation of individual articles and high-resolution images of photographs, advertisement and graphic-oriented objects are inserted at corresponding positions on the facsimile image. The articles are represented as html mark-up. Links to images and graphics are also represented html-based links from rectangular boxes corresponding to double coordinate pairs on the facsimile canvas. The principle also readily adapts to inclusion of other types of media like videos or audio recordings.

The compilation of the *DigiTV Newspaper* mainly relied on the standard newspaper production process for the online newspaper. Insertion of video links was an experimental process done manually with a dedicated tool. The contents of the *DigiTV Newspaper* were represented as a hierarchical tree-like collection. The root of this information also included pointers to application-specific utility software and generic support contents

The national Finnish DVB-T network (terrestrial digital TV broadcasting network) operated by the national operator *Digita* was used as the delivery channel. While there was no existing infrastructure for the delivery of file-like packaged contents to be cached locally at the receiving end for this network, an *ad hoc* solution was devised for the purpose. Digita assigned a dedicated *DVB elementary stream* with a specific constant transfer rate to be used a Private datacast stream during a certain period of each night. There was a transmission server at Digita premises. The *DigiTV Newspaper* was compiled off site into a *zip*-based archive and copied to the transmission site right before the on-the-air period. The archive package was also supplemented with *error detection* and *error correction* information (*Reed-Solomon encoding*). Full advantage was also taken of the available transmission slot by repeating the same transmission as many times as there happened to be time based on the size of the daily archive.

The transmission slot typically started at 2am and ended at 6am each night. However, with the last of the three experiments in the Turku region the time slot was available around the clock, but a considerably lower transfer rate. The success of reception was dependent on recording the transmission throughout one complete transmission cycle. However, the included error detection and error correction information allowed for random transmission errors of a few percent of the total number of bytes. In addition, the scheme was able to collect data from subsequent records so that loss of portions of the recorded archive could be compensated by subsequent successful transmission of the missing parts. However, the starting point of the whole concept was to have the receiver on and making any efforts for successful reception throughout the available transmission time slot.

The design of the experimental reception system was based on a laptop computer equipped with a digital TV reception adapter and application-specific software. The laptop could serve as the reading display, but intended way of reading the *DigiTV Newspaper* was an external 32 inch lcd-based TV monitor. The application software could also be controlled by a dedicated IR controller so that the viewing and reading environment resembled that of a standard digital TV reception setup. However, a wireless mouse was offered as an extra user interface device, since the material from the original online newspaper was intended for mouse-based browsing and changing this would be too cumbersome.

3.2 Technical transmission protocols

A specific *DVB-T Private Transport Stream* was developed for the experiments with simplicity and robustness as the primary targets, since there was no established infrastructure to support delivery of media content files over the digital TV transmission network. The solution could be simplified by not placing emphasis on support for multiple operators and content providers nor making provisions for extensions mechanisms for a multi-actor operating environment. Issues related error recovery and security were also left for the responsibility of the application layers. Figure 1 illustrates the structure of the data transmission packet.

The protocol specifies the following structure for each packet of the stream, i.e:

- DVB-TS header,
- CRC32 checksum,

- name of file,
- location of record,
- partial payload (all that fits in; no padding).

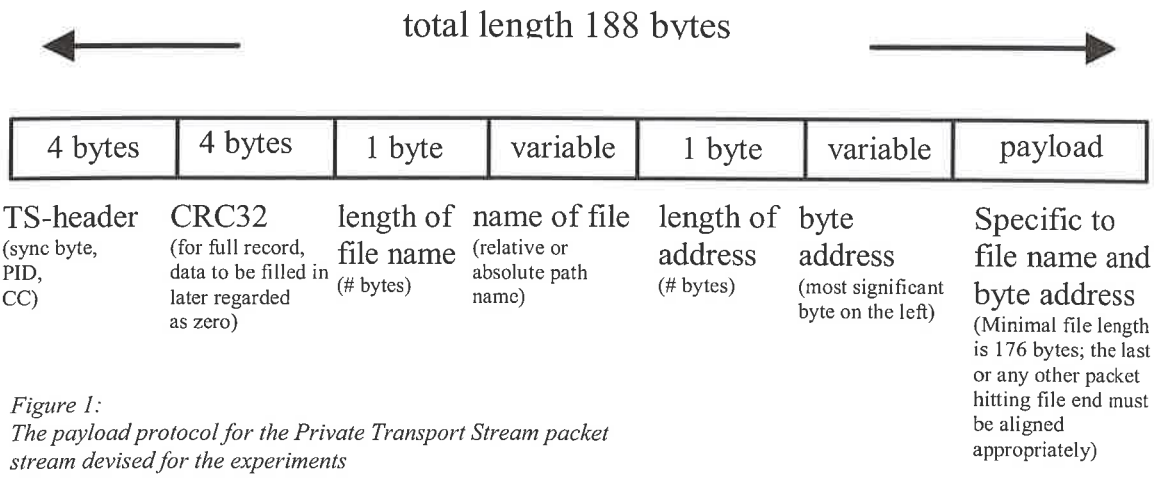


Figure 1:
The payload protocol for the Private Transport Stream packet stream devised for the experiments

The protocol specifies the following structure for each packet of the stream, i.e:

- DVB-TS header,
- CRC32 checksum,
- name of file,
- location of record,
- partial payload (all that fits in; no padding).

The CRC32 is used for detecting the majority of distorted packets (the DVB-TS layers already have stringent error detection mechanism to drop erroneous packets before reaching this stage). As a third layer of error detection and correction, there is an application layer RS (*Reed-Solomon*) coding layer. This was realised using the open source *par2* software, which organises the error correction information as several separate files to be carried separately via the same file delivery mechanism as the contents of the *DigiTV Newspaper* itself. Roughly said, the error correction mechanism is able to correct any number of errors with the media record up to the total number of erroneous blocks corresponding to the cumulative size of the extra error correction information files. In addition, the repetition of the complete data cast transmission record is able to provide still another layer of error tolerance. However, this option has not been exploited up to its full potential, even though missing pieces are automatically filled in when the contents can be recovered from subsequent transmission phases. The relatively strong error detection mechanism is able to filter out almost all distorted packets leaving the result within the capacity of the application layer RS error correction mechanism.

4. Results

4.1 Reliability and transfer rate of transmission

The following discussion relates to the transmission experiments with the DVB-T network in the Turku region. The bandwidth reserved for broadcasting of the *DigiTV Newspaper* was 345 kbit/s available around the clock. The coastal line near Turku is fragmented with numerous islands (inhabited at least during the summer season). This will make the delivery of daily newspapers highly challenging. The map of Figure 2 illustrates the approximate locations where the testers had their receivers for the majority of their experiments.

Table I summarises the success rates of the transmission experiments. Some receivers had rather many failures with reception (e.g. devices 8, 5 and 3). However, the error recovery scheme often succeeded to correct the situation, even though the margin remained low. It is typical to observe such problems at remote locations with inadequate filed strength (cf. Figure 2.) or when there are problems with local antenna setup, shading terrain or construction elements etc.

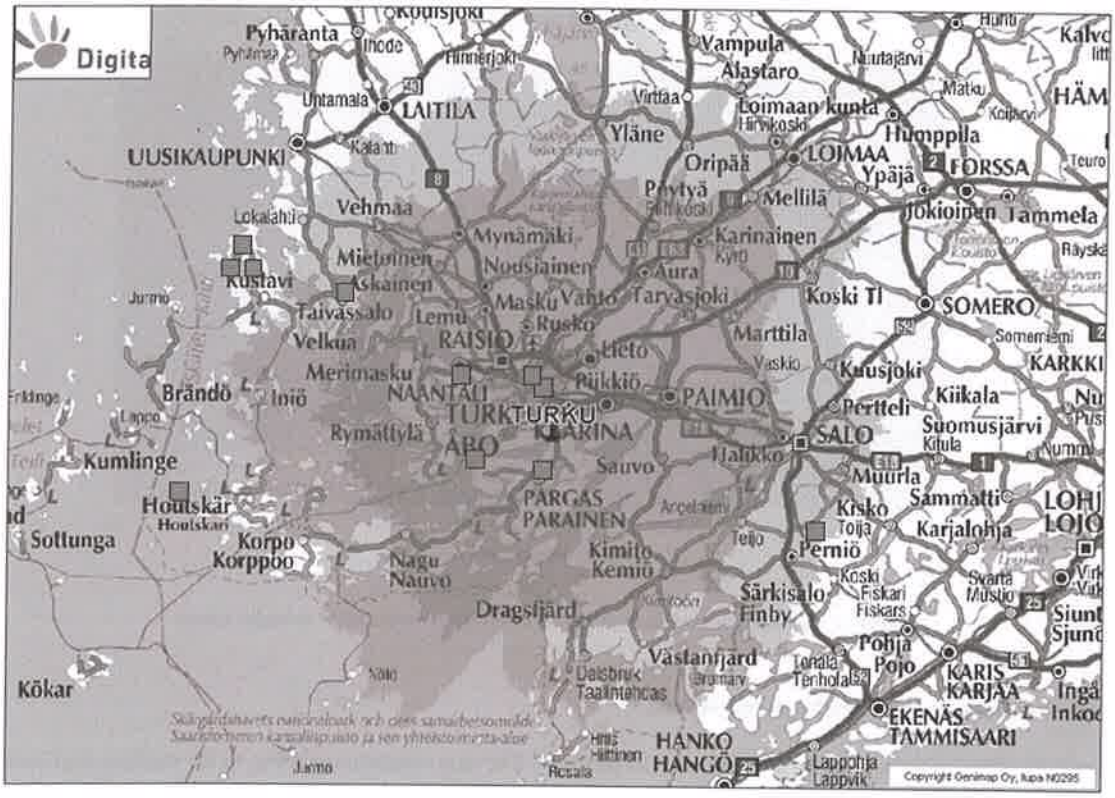


Figure 2: Locations of receivers for the experiments in the Turku region. The area in blue is the area where the field strength is expected to be adequate for digital TV reception according to the transmission network operator (Digita)

Table I: Summary of transmission success rate (DigiTV Newspapers received / not received that day)

Device index	Days succesfully received	Days failed to receive
1	51	1
2	25	0
3	23	5
4	25	4
5	19	11
6	55	0
7	38	0
8	20	18
9	34	3
10	31	0

Devices 6 and 7 proved to be more reliable receivers because of their favourable location site. Figure 3 shows that time for successful data transfer depends linearly on file size during period of 27.6.2006 - 10.8.2006 for these two receivers.

The net transfer rate can be calculated from the recorded number of successful reception and available transfer slot (determined by the receiver alone in this case, while the transmission was continuously on the air in this case). The net transfer rate was 288 kbit/s. Compared with the available bandwidth of 345 kbit/s, this suggest an efficiency of 84%. The rest of the capacity is wasted as protocol overhead, error correction overhead and as truncation errors at the beginning and end of the time window for reception, since transmission and reception begin and end unsynchronised. Real transmission errors were so rare in this case time that the error correction layers are capable of doing full recovery without any loss of net transmission bandwidth.

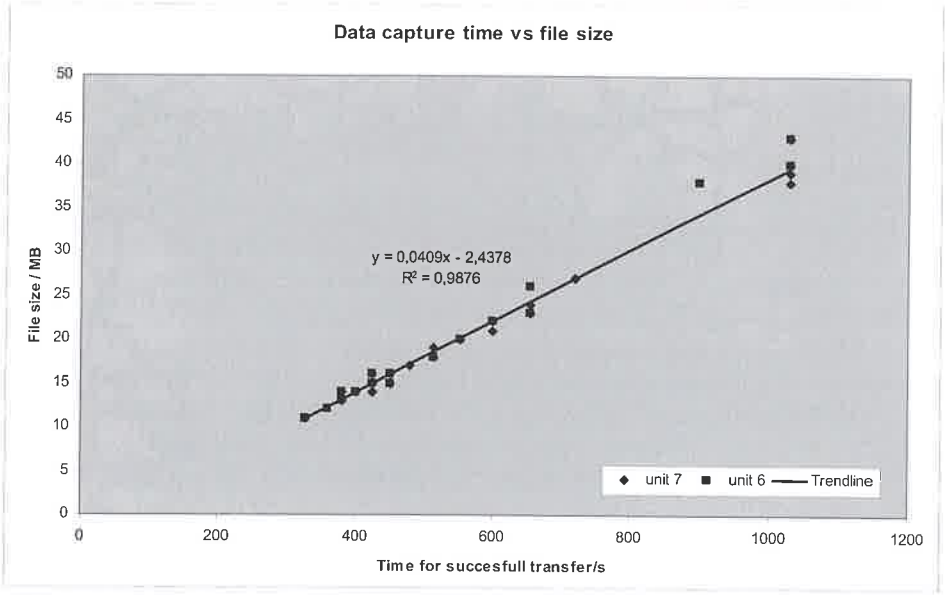


Figure 3: Data capture time vs file size showing constant data transfer speed

4.2 The reading experience from lcd-screen

The user feedback for the reading experience was positive. The expectations regarding to the reading and browsing of the content were mostly met. Especially the readers located in the Archipelago of the Turku appreciated the service because in many cases the distribution of the paper based newspaper was impossible or delayed.

The 32-inch lcd-screen was regarded as suitable platform for reading newspaper material. The screen size, format, readability, resolution of the images and videos and the speed for browsing were considered satisfactory.

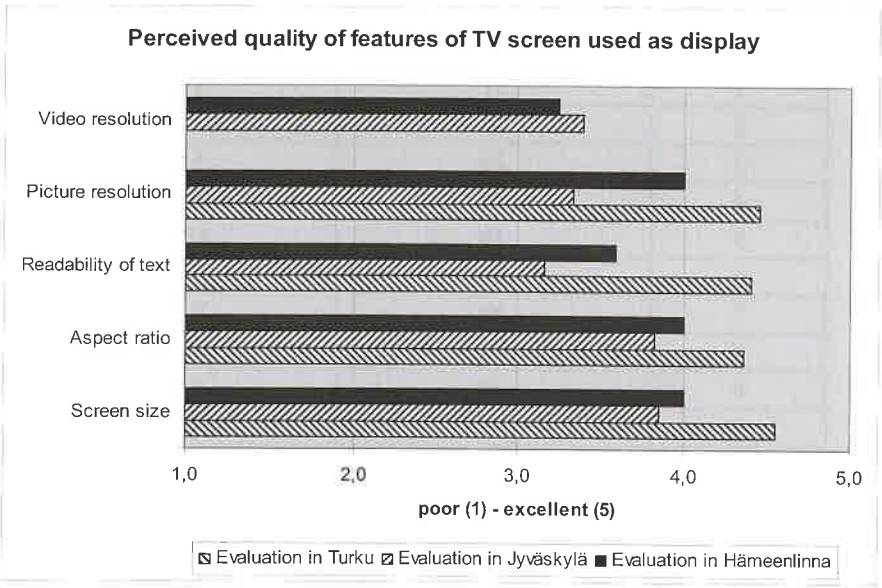


Figure 4: User evaluation about the suitability of lcd-screen to read DigiTV Newspaper

Majority of the users regarded the reading the newspaper from lcd-screen unnatural and less convenient than reading the paper based newspaper. However some of the younger user gave opposite feedback and read even material that they normally skip in the paper based newspaper.

The readers criticised the lack of portability of TV screen compared with the paper based newspaper.

4.3 An enhanced user interface evaluation

In this part the user interface was redesigned to fit into 16:9 format screens for a fixed resolution of 1280 x 768. One of the already published e-newspaper was redesigned with Adobe InDesign, the facsimile images for each page produced and the navigation with browser was done with HTML- and JavaScript.

The usability was improved using chapters and layout where scrolling is not necessary. Page turning buttons were introduced to support the linear reading. Long articles were divided into parts. Each page had page number to help the reader to identify his location in the e-newspaper.

Indexes in two levels were used. The first level index showed the main article in each section. The section level index showed all of the articles in each section and ingresses. The section index can be reached from main index or menu.

The test persons evaluated the usability of the new layout by answering a questionnaire. They were asked to compare the 19:6 format *DigiTV Newspaper* to the other media formats. According to the result the paper based newspaper is the most convenient format to read the newspaper. The next in the ranking were online newspaper followed by 16:9-format *DigiTV Newspaper*. The mobile news got the lowest ranking.

The redesigned user interface received mostly positive feedback. The user appreciated the fast and easy browsing of the material. Also the video material and the possibility to archive the material were appreciated.

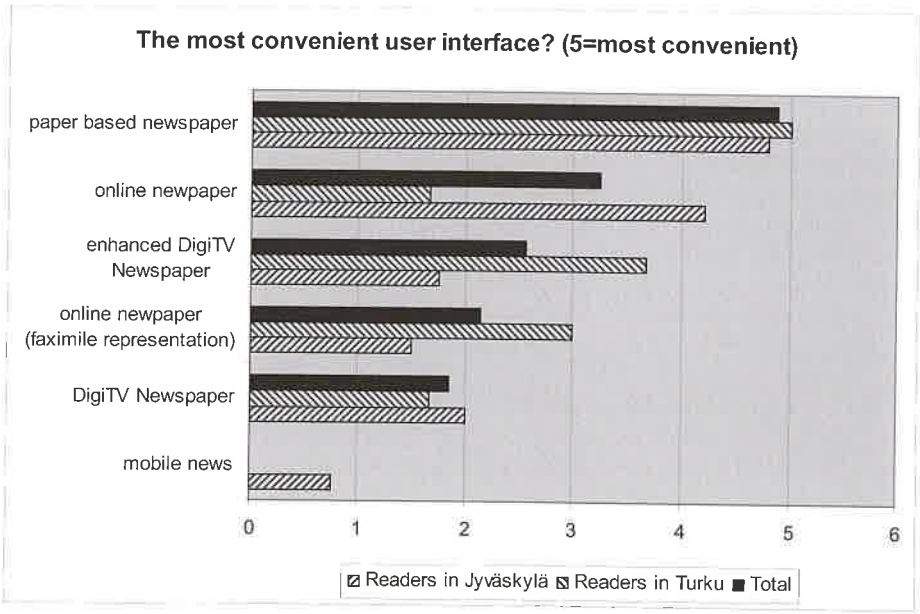


Figure 6: Results from the evaluation of the user interface to the news

5. Conclusions

The reliability of the developed DVB-TS Private Tranport Stream protocol was high when the client was within the range of the local sending station. In these cases the data was received reliably by the clients.

The data transmission was tested by sending one newspaper at a time to one geographical location. Technically it is possible to configure the system to distribute and capture several newspapers. Conceptually this model resembles so called joint distribution model where the same carried distributes several newspapers regionally. The DVB-T-distribution can save costs especially when we consider that the distribution capacity allows 10-40 local newspapers to be distributed at the same time.

Technically reading from lcd-screed with hdtv-resolution was evaluated as suitable for *DigiTV Newspaper* but the reading experience is not at the same level as with the paper based newspaper. With the paper based

newspaper the user controls totally the interface and he can also take the newspaper anywhere he wants. When reading the *DigiTV Newspaper* the user has to stay quite near the lcd-screen without the ability to move.

The newspaper content can be published in digital TV but it need to be modified for this publishing channel. The first generation of the product can be the same version that is published in the internet. However the product should be developed further to include also video and up-to-date material.

One interesting result was that during the test period the received newspapers created a personal digital newspaper archive which was regarded useful. In the *DigiTV Newspaper* it is possible to include interactivity like search and calendars.

This service can be regarded as a supplementary service for paper newspaper and it can save distribution costs.

References

1. Ihlström Eriksson, C., Svensson, J, Åkesson, M. Sammanfattning av DigiNews projektet 2004 - 2006. 66p. Available at www.diginews.se
2. Ihlström, C., Åkesson, M. & Nordqvist, S. (2004). From Print to Web to e-paper - the challenge of designing the e-newspaper. In Proceedings of ICCC 8th International Conference on Electronic Publishing (ELPUB 2004), Brasilia, pp. 249-260.
3. Garcia, M. R. (1997) Redesigning Print for the Web. Hayden Books.
4. http://www.dvb.org/

Magazine product structure and workflow control between a publisher and a printing house

Olli Kuusisto, Hannele Antikainen, Janne Pajukanta

VTT Technical Research Centre of Finland
P.O. Box 1000, FI-02044 VTT, Finland
E-mail: olli.kuusisto@vtt.fi

Abstract

This paper describes the work done in a project which focused on the product structure and production data communication between a magazine publisher and a printing house and the possibilities offered by JDF in it. Besides long-term printing contracts, the information needed for an issue of a magazine are communicated using email, phone, fax and even mail. Furthermore, many practices are company- or person-specific and the information is divided to many separate systems in different departments. Data communication using JDF vocabulary was examined, and was found to be suitable for most of the magazine structure information. This was also tested with a web-based demonstration system. The project included a cost-benefit analysis model including the key factors. Gathering of all the information needed to produce the print job at a printing house and sending it in electronic form would greatly benefit both publishers and printing houses. It would reduce dramatically the inquiries between the parties and also streamline the process, as all relevant data could be found in one place at each company.

Keywords

JDF, magazine printing, magazine publishing, magazine workflow

1. Background

Magazine publishers and printing houses use several channels and involve several persons in temporally different occasions in order to exchange information about the contents of an issue of a magazine. This results in overlapping and multiple contacts between the parties when communicated information - possibly repeatedly in different channels with more detailed data - needs to be cross-checked by either party. The communication process also depends on company - and person-specific conventions. Versioning of the contents makes it even more vulnerable to errors. Both parties have several systems containing job-specific information. Usually there is no central system at publishers site for converging the different pieces of information needed for the production of a print job.

At big publishing houses, the information needed by a printing house to produce a magazine issue is located in different systems that are different peoples' responsibility. The information on a long-term contract with a printing house is often not known or not easily accessible to all people at the publishing house who need the information. When publishers use different printing houses with different opportunities for the product structure, misunderstandings may and will emerge of e.g. what product structures can or cannot be implemented at a certain printing house.

JDF (Job Definition Format) is an XML-based vocabulary designed to simplify information exchange between different applications and systems in and around the graphic arts industry. The vocabulary ensures standardized integration, where JDF-based information about the product and production can be communicated between different systems. CIP4 organization is responsible for the creation and development of the JDF specification.

The main objectives of the project were:

- to model and define the information flow (product structure and production data) between a magazine publisher and a printing house;
- to compare the different needs to the possibilities offered by JDF and to communicate proposed amendments and comments to CIP4;

- to demonstrate publishers' product control and procurement system;
- to create Finnish terminology and operations model for JDF-based workflow in magazine production.

2. Implementation

2.1 Magazine production

The main actors in the magazine production chain consist of publishers, advertisers, printing houses and distribution organisations. Figure 1 shows actors in the magazine production.

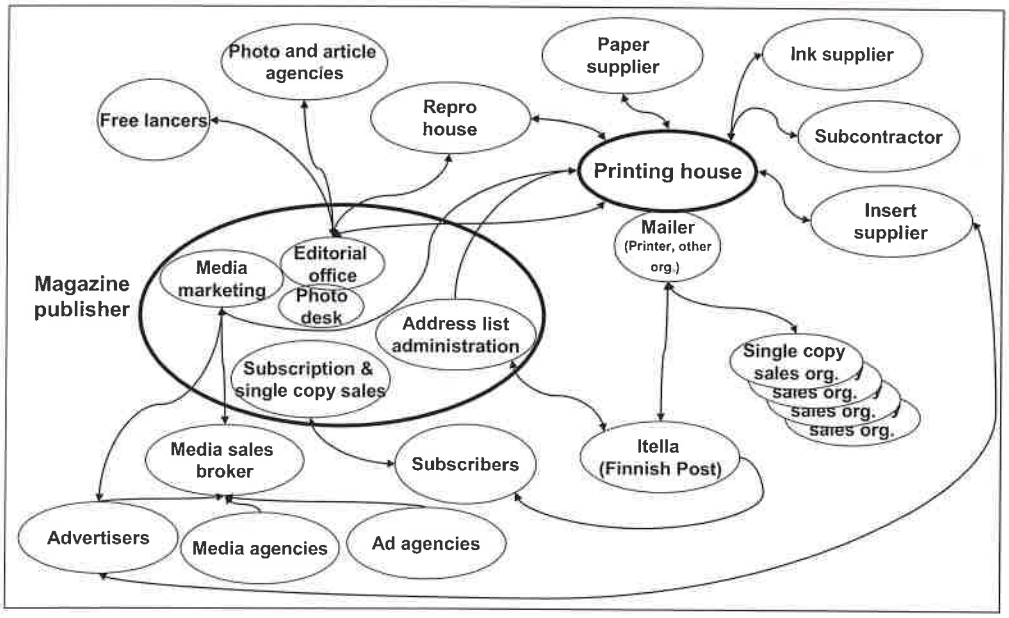


Figure 1: A simplified diagram of the actors in magazine production. The project focused on data communication between a publisher and a printing house

The production of an issue of a magazine was studied based on case products, and a more general process model with data and material flow diagram was created. Process analysis on the information flow between a magazine publisher and a printing house was made including defining of the data communication needs of the product structure and production data between the parties.

Interviews and open discussion were held with publishers' and printers' personnel to establish the present operations model. Most of the information needed for the production and delivery of an issue is generated by the publisher who then communicates it to printing house and distribution companies. Some of the information has been specified in the long-term contract made between a publisher and a printing house. The rest of it is generated and gets gradually more detailed during the production process. There is usually a schedule for communicating different pieces of information to the printing house. However, as it is not always followed, and the information is communicated in temporally different occasions between several persons at both the publisher and the printing house, the process is in practice person-dependant and error-prone.

2.2 Product structure and production data

An issue of a magazine is usually divided into subscription and single copy issues, which both can be divided into countless versions having different covers, blocks, pages (editorial or ad material) or inserts. With just a few component versions the number of different end product and delivery versions can rise very high. Versioning of the pages makes the situation even more complex.

Figure 2 shows an example of a magazine product structure. Wrapped product consists of a perfect bound magazine with glued and loose inserts, and two wrapped inserts. The various product and delivery versions

are assembled from the separate components. Besides the product structure and production information, a printing house or a mailing company also needs the subscribers' addresses.

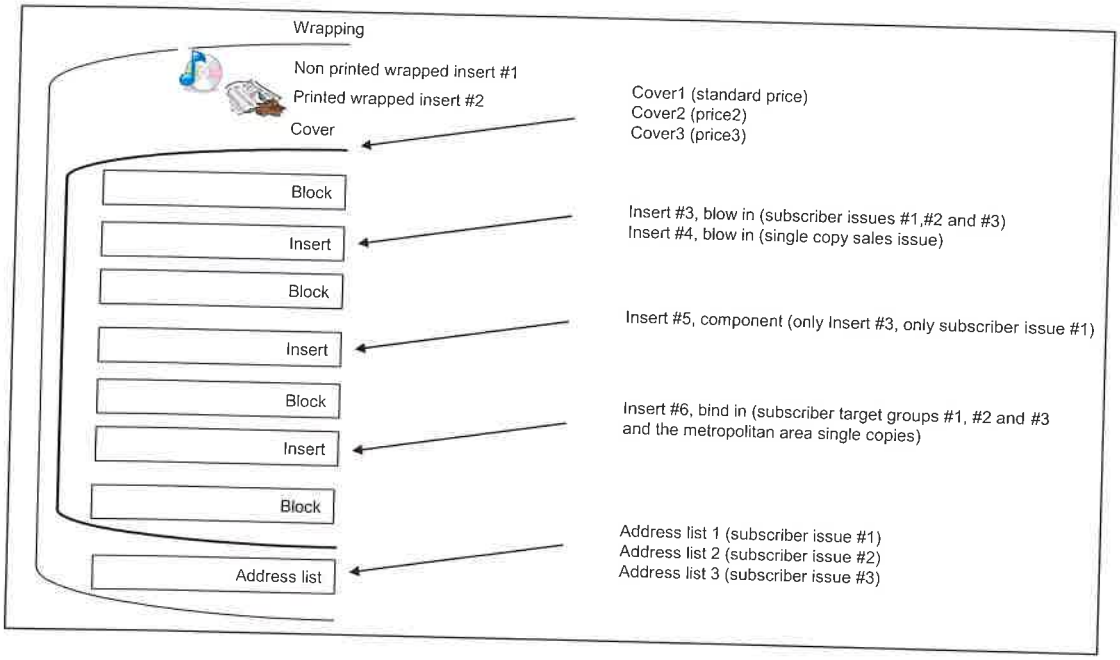


Figure 2: A simple example of the structure of a magazine

3. The applicability of JDF vocabulary in magazine production

JDF is an industry standard designed to facilitate information exchange between different applications and systems in and around the graphic arts industry thus allowing integration of heterogeneous products from diverse vendors to create seamless workflow solutions (see figure 3). It is a comprehensive XML-based file format and proposed industry standard for end-to-end job ticket specifications combined with a message description standard and message interchange protocol. It is intended to enable the entire industry, including media, design, graphic arts, on-demand and e-commerce companies, to implement and work with individual workflow solutions. /CIP4, www.cip4.org/

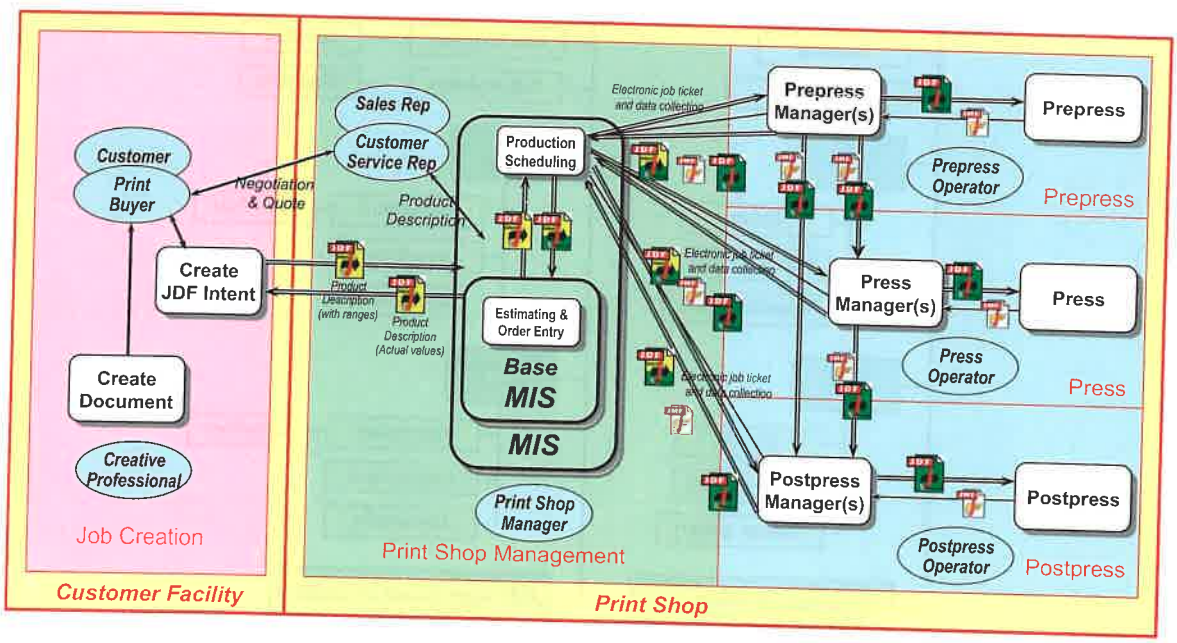


Figure 3: CIP4 Reference model

At present, JDF contains the most commonly used structures. However, especially more complicated structures may not be supported or need complicated JDF structure. By defining the minimum requirements in various application areas, the creation of the ICS (Interoperability Conformance Specification) documents has helped system providers to implement JDF (see www.cip4.org). Furthermore, its has helped in setting up certification procedures for JDF-compatibility in these areas.

3.1 Product structure

JDF specifies almost 200 different resources, which describe the parameters needed to execute the process or the end result of it.. Most of the resources are linked to printing processes and to other products than magazines. In the communication between the publisher and the printing house mainly intent resources are needed, as they define the product structure, and it is mainly the printing house which specifies the production methods (process resources in JDF). There are together 17 intent resources in the JDF, of which following seven were used in the project:

- ArtDeliveryIntent (original content, artwork),
- BindingIntent (binding),
- ColorIntent (colour),
- DeliveryIntent (delivery),
- InsertingIntent (inserting),
- LayoutIntent (layout),
- MediaIntent (materials to be used).

The structure of a magazine can be specified with JDF nodes and the characteristics of the different components with intent resources. Figure 4 shows a magazine as JDF-structure. The top JDF node defines the outcome of the process eg. how a finished magazine is assembled. BindingIntent describes the parameters needed in binding e.g. the binding type. The input of the top node consists of all the components that are bound together i.e. the cover, possible different blocks, inserts to be bound, loose and glued inserts and possible wrapping and the inserts inside the wrapping.

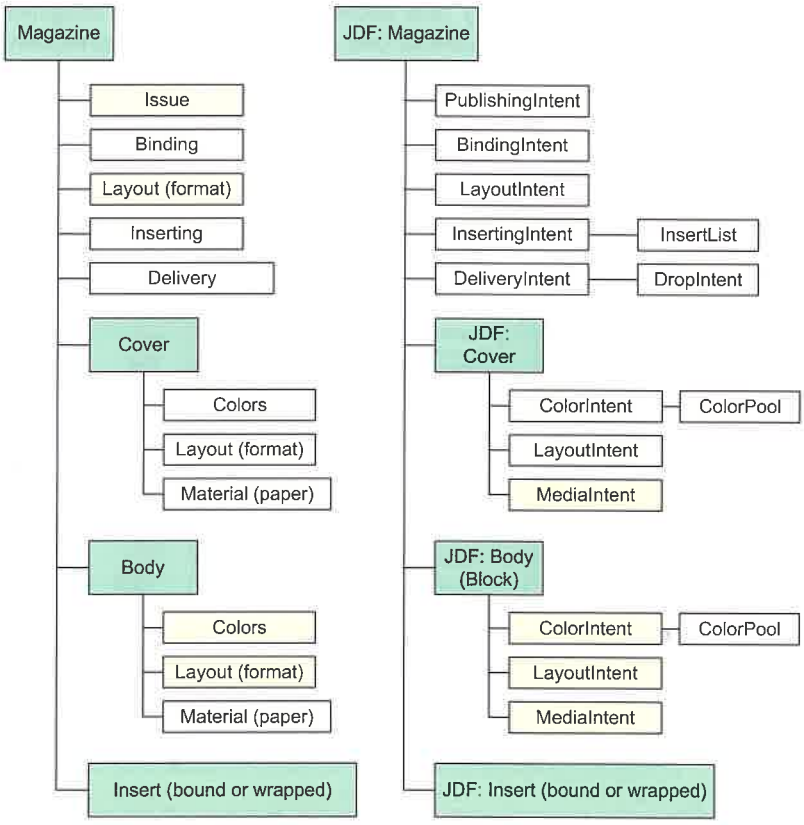


Figure 4: The structure of a magazine and the corresponding structure of a JDF file

The input components for the top node are output components of lower level nodes. The lower level nodes include information about the components they need to be made from. For example describing which component is to be printed on which media i.e. material (MediaIntent) or what is the format of the component (LayoutIntent).

Figure 5 shows a more detailed description of the previous structure diagram. The top level component has been divided into various edition versions by the use of PartIdKeys attribute. The different versions consist of partly or totally different cover, block and insert components. In each node the ComponentLink defines with AmountPool element how much of each component is needed for each version. The figure shows only one-level versioning.

Even more detailed structure includes Intent Resources of all the elements. In DeliveryIntent element the different edition versions are assembled into delivery lots (DropIntent), which comprise of a certain amount of one or several edition versions (DropItemIntent).

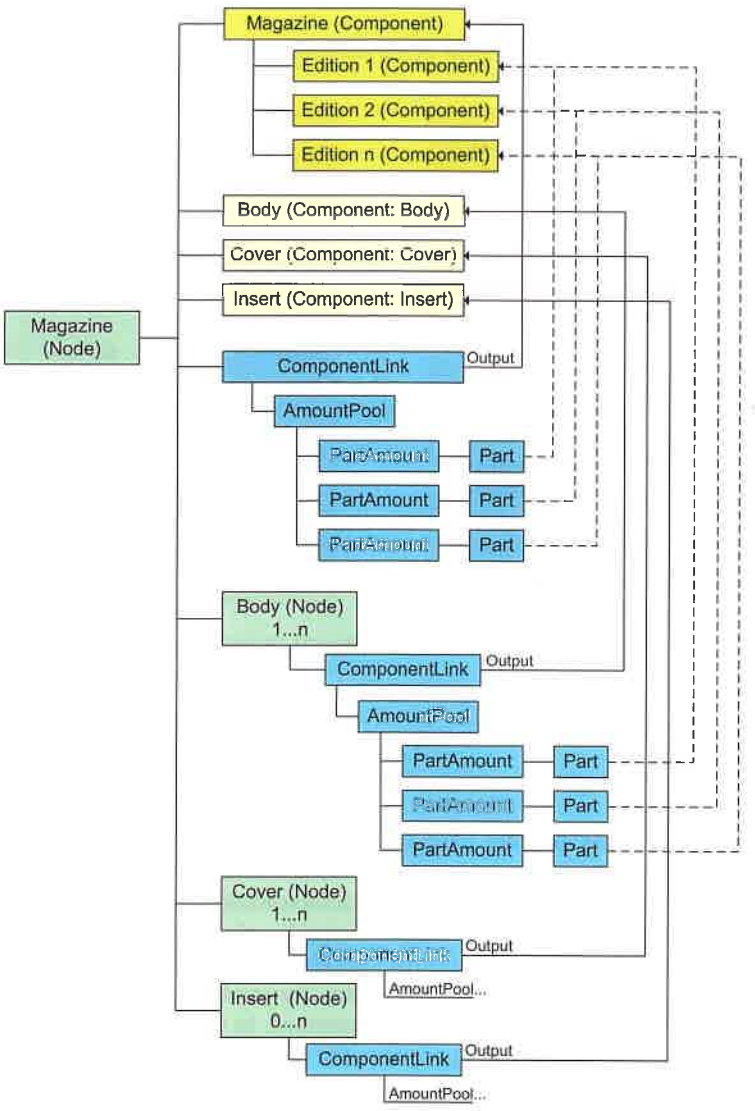


Figure 5: The structure of a versioned (cover, block, inserts) magazine

3.2 Challenges

There were some challenges in describing the magazine structure with JDF. Firstly, the versioning of different components and even their sub-components (pages), and the editions versions assembled from them. Secondly, there were no Intent element for wrapping. Thirdly, there were no custom to describe the inserts

outside the magazine but inside the wrapping. Fourthly, the amount attribute was not allowed to be used but for a few Intent elements which complicates the allocation of the different edition versions.

The versioning challenge was overcome by using PartIDKeys attribute.

Wrapping could be described by using process resources, but it would mean that the publisher's system has to describe the assembly process of the whole product step-by-step, for every edition version (see figure 8). This is because inserting must have only one parent and one child element, and each process phase before wrapping should also be specified consecutively. Therefore, a WrappingIntent element has been suggested to be included in the JDF specification.

Describing the wrapped inserts (outside the magazine but inside the wrapping) was discussed with CIP4. It was suggested to add a new method ("stack") for Insert element. That would be well in line with specifying the other insert types.

The AmountPool and Amount attribute were used in the demonstration system with InsertingIntent/Insert.

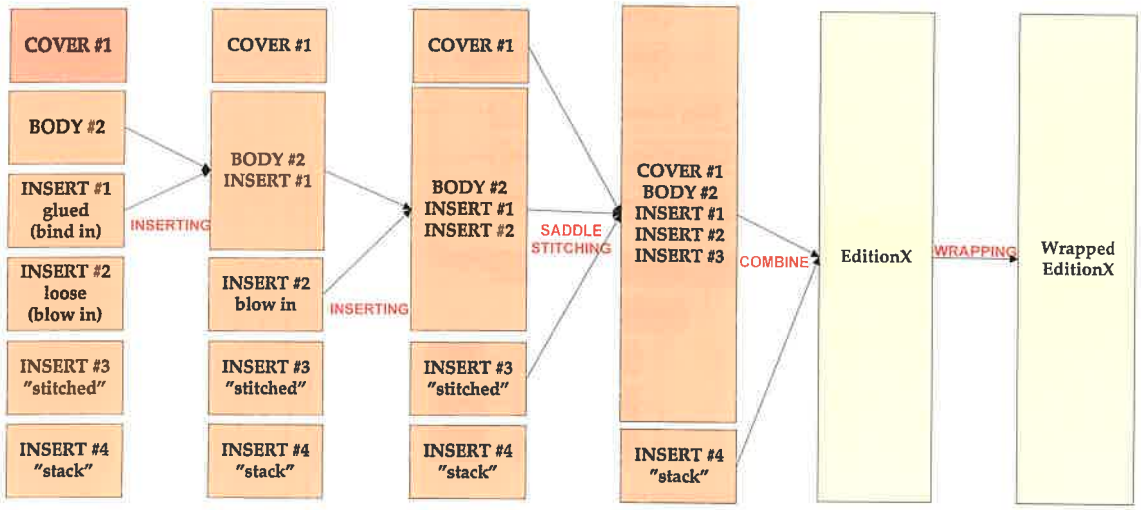


Figure 8: Phases of describing a wrapped edition with process resources based on JDF specification v1.3

4. Demonstration system

4.1 Setting up the demonstration system

A small-scale web-based publishers product control and procurement demonstration system applying JDF specification for communicating the information needed for manufacturing a specific issue of magazine between a publisher and a print house was set up by VTT. A demonstration system was made because the pilot companies didn't have MIS systems which could have been used in the piloting. The demonstration system was made to be used only for demonstrating that all information could be fed in, and that it would be able to produce a valid JDF file from the data. Furthermore, some elements for publishers' product data management and a possibility to print out a human readable version were implemented. In the demonstration system, all information was fed manually. It didn't include the versioning of pages nor wrapping as it was suggested to be created a new WrappingIntent element to ensure more appropriate way to communicate it than using process resources. In the demonstration system wrapping information is communicated in comment field.

The focusing of inserts was done with same custom as with covers and blocks ie. by using the Amount attribute. Wrapped insert was specified by using value "stack" with the Method of Insert element. That was also used to implicitly mean that wrapping is needed.

```
<InsertingIntent Class="Intent" ID="ID_InsertingIntent" PartIDKeys="Edition" Status="Unavailable">
 <InsertList>
 <Insert DescriptiveName="Insert #1" Method="Stack">
```

```
<AmountPool>
<PartAmount Amount="20000">
<Part Edition="Subscriber edition" />
</PartAmount>
<PartAmount Amount="20000">
<Part Edition="Single Copy edition" />
</PartAmount>
</AmountPool>
</Insert>
</InsertList>
</InsertingIntent>
```

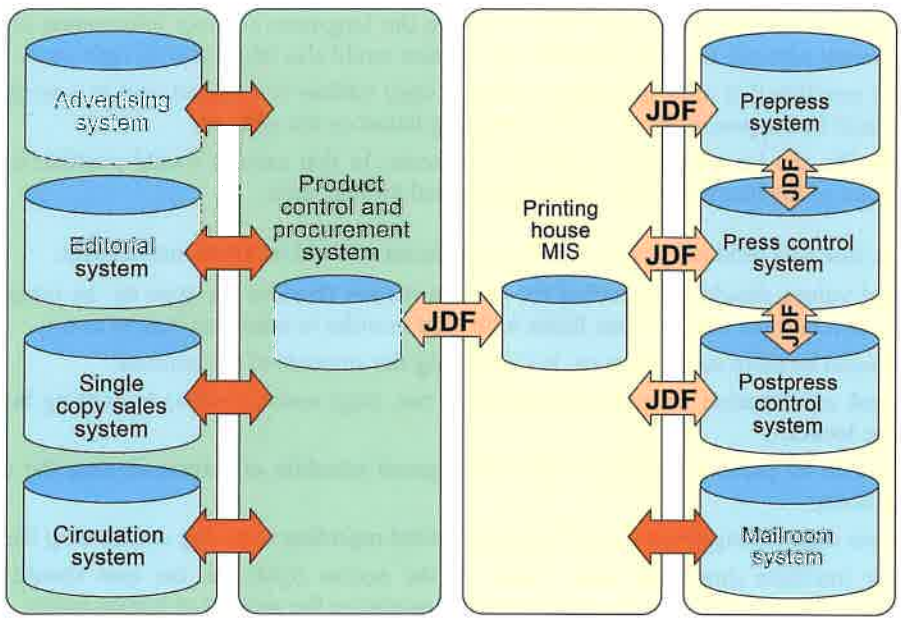


Figure 9: A diagram of the systems engaged in the magazine production information flow with demonstrated publishers' product control and procurement system. Big publishing companies would create and maintain the system themselves. Printing house could offer same kind of service for the smaller publishing houses

In the demonstration system, edition versions and delivery lots having different cover and block versions together with focused inserts leading into several edition versions and delivery lots can be specified and a corresponding JDF-file printed (see Figure 10). There may be more delivery lots than edition versions.

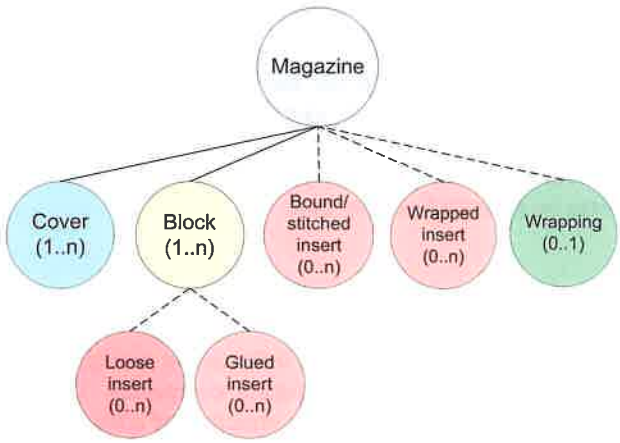


Figure 10: The structure of a magazine with potential amounts of each component

Change order management of the job can be dealt with either by sending each individual complimentary information with JMF messages or by sending the JDF file containing all information of the product and production. The safest way is to send the entire description each time when there are changes.

4.2 Feedback and comments of the demonstration system

The validity of the JDF file created by the demonstration system has been checked with CheckJDF Server of CIP4. Error messages were naturally created by the use of a novel custom with wrapped inserts and the AmountPool with Amount attributes used in focusing the amount of inserts in InsertingIntent resource.

The demonstration system was presented to the participating companies and let to be piloted. Consecutively, following feedback was received:

- Such system would be useful especially in letting the long-term contract information to be accessible to all relevant persons, the issue-specific information could also be accessible right away.
- It is also possible that only subscriber or single copy edition is wrapped, and in a production system there should be the possibility to choose wrapping based on the editions.
- The JDF file can be referenced in Adobe's systems. In that case, it would possible to compare the information of the incoming PDF files to the agreed product data.

Furthermore, in case of a production system, following factors should be taken into account:

- Permitted values should be specified for all information (besides the type eg. an integer or decimal number, also rational min and max limits with alert in order to minimize human errors.
- There should be more automation eg. in calculating the amounts of the editions.
- After final confirmation the product data (print run, page count, inserts) to printing house, that data should be locked .
- There should be proactive alerts based on the agreed schedule of communicating the information to printing house.
- The access right management should be implemented regarding to seeing and sending the information.
- The user interface should be made based on the access rights, ie. the user should see only the information that is relevant to him/her in order to minimize the amount of human errors.

5. Cost-benefit calculation

The factors in the workflow affecting the costs and benefits in JDF implementation were examined and listed. Benefits can arise from direct working time savings, better production planning, reductions in correction of the errors and in reclamations including the extra material usage. In present state surveys, the share of the latter ones has often been surprisingly substantial. Direct working time savings lead either to lesser labour costs with the same amount of jobs or being able to use the released working time for acquiring extra revenues. All benefits i.e. the effects of separate factors must be estimated company-specific based on their current workflow.

Cost factors include requirements specification of the system properties and the information to be communicated, product data control/procurement system (own or purchased implementation project), integration with other systems in the company, user training and updates (JDF, product data control/procurement system, other systems. Costs depend even more on the companies' size and current infrastructure, and must always be estimated case by case.

6. Results

The magazine production process was modelled and the information needed for the production of a magazine issue was determined in co-operation with the participating companies. The appropriate JDF counterparts were documented with some proposed amendments. The structure of a basic magazine turned out to be quite easy to define with JDF. A more complex situation with customized editions and printed or non-printed inserts with last minute changes was more challenging. Area, sales channel or target group -specific editions

may extend up to tens, hundreds or even more customized edition versions. In some cases even the same block can have different versions with page changes.

Development suggestions for JDF specification were made. It should be possible to describe wrapped inserts and the wrapping using the JDF Intent elements. Furthermore, the Amount attribute should be allowed for all Intent elements which would ease the allocation of the different edition versions.

A web-based application was made to demonstrate the determination and communication of the product structure and production data of a magazine consisting of different covers, blocks and inserts that make different editions and delivery lots. It used standard JDF except for the development suggestions mentioned before. In addition, a cost-benefit model was created for business-based analyses of JDF integration.

Pilot user feedback was gathered which indicated the usefulness of such system. A product manager of a magazine spends a significant amount of his/her time in clarifying the deviations in the printing or delivery process. A tool like the demonstration system would reduce dramatically the inquiries between the parties and streamline the process, as all relevant data could be found in one place at each company. Furthermore, all product data would be real-time, the communicated data documented, and it could be used in calculations of magazine- and printing house -specific key figures. The system would also work as communication channel inside the publishing house. The limitations and possibilities of different printing houses could be fed in to the system where they could be easily checked when needed.

The use of product control and procurement system would reduce the communication channels to one central one which is not person-dependant. The system would help especially with changes and special situations. It would reduce the need to check the information from the printing house to the situations where the publisher wants to deviate from the agreed schedules or product data. It enables automatic alerts, comparisons to long-term contracts and remarks when the product data is not within the limits of it.

In the printing house especially customer contact persons would benefit from such a system. They would no longer have to hunt for the missing or clarify invalid information. At the same time the information would be documented and accessible to all other personnel who needs it. This would save costs and efforts when the information wouldn't have to be inquired for and retyped to various systems in the printing house. Besides, the examining of deviations would speed up.

7. Conclusions

At present, the information needed for the production of a magazine issue is situated scattered in the various software systems of the publisher. This leads into problems in the flow of information within the functions of the publisher, which reflects also to the partners of the publisher from prepress to delivery. With present diversified communication methods between the publisher and the printing house, the data on product structure and production data is not consistent. Gathering of all the information needed to produce the print job to a single place and sending it in electronic form to a printing house would benefit greatly both parties. It should also include the information about who has sent the information and when it was sent to a printing house. A cost-benefit analysis model helps for company-specific estimations of the magnitude of the financial effects of JDF integration.

The small-scale demonstration indicated that needed product structures and production data can be composed by using JDF. A publisher and a printing house have the basic information based on long-term contracts e.g. paper and binding information. When the production proceeds, a publisher sends JDF files about more defined information, for example, on the print run, page count, inserts and delivery lots.

The next step would be to implement the demonstrated system in practice to communicate the product structure and production information to printing house. The software demonstration showed that it is possible to implement an IT system for magazine product structure and production data control by using JDF vocabulary. After that, following target for development would be in exchanging information with the distribution companies.

The factors affecting benefits and costs have been documented in the cost-benefit calculation model. The values of each factor can deviate very much from case to case. Nonetheless, based on the interviews and estimations,

especially big publishers would most certainly get the invested capital back very fast. However, the benefits will fully be realized only after the people have changed their way of action according to new process.

Acknowledgements

The authors wish to thank the (Finnish) Foundation for Graphic Arts Industry, VTT and the participating companies: publishers Sanoma Magazines Finland and Yhtyneet Kuvalehdet, printing houses Scanweb and Acta Print, MIS-provider Logica (formerly WM-data) and a virtual prepress provider Flowman.

References

1. Antikainen, H., Bäck, A., Melin, M., Pachoulis, G. XML-vocabularies for control and communication within company networks. 22 p. + appendix 63 p. VTT Research Report TTE4-2003-33. Espoo 2003. (in Finnish)
2. Antikainen, H., Siltanen, P., Bäck, A. Electronic data communication in the book industry: PrintTalk-process, JDF-pilot, ISBN13 and ONIX. 30 p. + appendix. 12 p. VTT Research Report VTT-R-06423-06. Espoo 2006. (in Finnish)
3. Kuusisto, O., Antikainen, H., Koivumäki, K. Applying JDF in the integration within the systems of a sheet-fed offset printing house. 28 p. + appendix 19 p. VTT Research Report. Espoo 2005. (in Finnish)
4. Kuusisto, O. Applying JDF in the integration within the systems of a web offset printing house. 32 p. + appendix 17 p. VTT Research Report VTT-R-07618-07. Espoo 2007. (in Finnish)
5. Kuusisto, O., Antikainen, H., Pajukanta, J. Applying JDF in the integration of the systems between a magazine publishing house and a magazine printing house. To be published. (in Finnish)

Business from hybrid media and printed functionality

Ulf Lindqvist, Pertti Moilanen

VTT
Vuorimiehentie 3, P.O. Box 1000
FI-02044 VTT, Finland
E-mail: firstname.surname@vtt.fi

Abstract

Printed functionality means adding new functionalities into flexible substrates like paper or plastic by using printing methods. It has been the scope of this study to define innovative new applications of printed functionality, to study the required technology and to create business models for these applications. Special attention has been paid to the new role of conventional printing plants in the value chain of printed functionality.

Roadmaps were created for the different technologies for printed functionality. Business models for the additional services available through printed functionality are complex because of the variety of earning logics and the number of players in the value chain. Each player has the opportunity to overtake new roles and functions.

New applications of printed functionality were innovated in brainstorming seminars. Some of them were tested in pilot scale, business models were created for them, and they were also analysed regarding environmental aspects and usability.

Keywords

Business models, hybrid media, printed functionality, roadmaps

1. Introduction

Printed functionality means adding new functionalities into flexible substrate like paper or plastic by using printing methods. Printed functionality can be codes with links to additional information, visual effects, multi-layer structures, electronics, optics, displays, sensors and indicators. The codes, in turn, can be 1- or 2-D optical barcodes, hidden, embedded, reactive or electronic codes.

Hybrid media is defined as the integration of different media, contents and functionalities - especially convergence between fiber-based products and digital media.

It has been the scope of this study to define some innovative applications of printed functionality, and to create business models for these applications. In the first step the printed functionality production has been classified and typical innovations have been defined within each cathegory. After this, the production processes for the new applications were analysed and the sufficiency of traditional printing plants to meet the technical requirements was estimated. Finally, general business models were developed for the most important types of applications.

The final aim has been to define the new role of the printing plants in the value chain of printed functionality. Special attention was paid to the performance of traditional printing plants, which types of new services are within their ability and what kind of material and immaterial investments are needed. This should involve an evaluation of existing know-how and technology compared to new requirements and investment needed in human resources and equipment.

2. Research methods

Roadmaps were created for the different technologies for printed functionality. For each technology the year of first availability was determined, and the time to first commercial pilot, first established use and commercial solutions in wide use was estimated. All the technologies have been available at least on a research scale for some time.

Business models for the additional service available through printed functionality were calculated. New applications of printed functionality were innovated in two brainstorming seminars. More than sixty innovation embryos were created, of which the most promising ones were tested on a laboratory scale and finally in production printing tests. Business models were developed for these applications. Finally, also the recyclability and usability aspects of printed functionality were analysed.

3. Technology roadmaps

Codes can usually be printed along with other graphic content using regular inks. Personalisation of the codes requires digital printing, and for physically small codes high-quality substrates are needed to prevent ink spreading. Codes always require a reading technology, as do sensors whereas indicators can be detected with human senses. Sensors and indicators require special inks and extra printing units. In this case the on-press performance of the ink and its compatibility to the substrate must be checked in addition to the required special properties. If the sensors or indicators are printed on a label, a special attachment unit is needed.

Printed electronics, finally, are fabricated from conductive, semi-conductive or dielectric materials using printing technology. They require separate printing units for the special inks and often also curing by heat or UV beam. Printed electronics require much higher accuracy than traditional graphic applications, and moving from laboratory scale to industrial scale always results in loss of performance. The inks for printed electronics are considerably expensive, and since many components consist of several different ink layers also the compatibility between the different inks must be adjusted.

Special inks for indicators and displays based on different technologies have been available for some time, but their established use is just ahead. Many new technologies are also expected to have their breakthrough. Printed power sources are needed for many displays and printed electronics, but are still expected to become common later than the technologies relying on them.

The roadmaps for the most critical technologies for printed functionality and hybrid media are summarised in Table I and Figure 1.

Table I: Printed functionality technology roadmap globally

Technology	Available	First commercial pilot	First established use	Commercial solutions in wide use
Hybrid media: optical codes	Japan 2003 (1) Others 2006 (2)	2003 (1)	Japan 2005 (3) Others 2009	2010
Hybrid media: hidden/embedded codes	2004 (4)	2005 (5)	2007	2010
Indicators and sensors	2003 (6)	2003 (7)	2003 (8)	2011
Special effects	1980's-1990's	Late 1990's	Early 2000's	2005
Electronic codes/RFID	Codes: 1990's RFID: 1959 (9)	Codes: Early 2000's RFID: 1970's (9)	Codes: 2008 RFID: 1990's (9)	Codes: 2010 RFID: 1990's
Printed electronics and optics	Early 2000's	2006 (10)	2008	2012
Displays integrated into printed products	Early 2000's	2004	2005	2008
Power sources	2001 (11)	2007 (12)	2010	2012

(1) Teleoperators NTT DoCoMo and Vodafone pre-install decoding software into camera phones
(2) February 2005: 64% have used hybrid media codes at least once, 89,1% have seen codes in publications/packages
(3) Nokia pre-installs decoding software to N9X Series camera phones
(4) Mobot in USA
(5) ELLEgirl magazine tests Mobot technology
(6) Swedish BioEtt: printed time-temperature indicator
(7) Findus tests Bioett indicator for transportation of meat balls to IKEA in Finland
(8) Swedish Skånemejeriet has used BioEtt since 2003
(9) RFID tags invented 1959, RFID tags for theft prevention introduced 1970's and become popular 1990's
(10) The first simple games and electronic books including printed electronic come to market
(11) Power Paper introduced the first printed power source
(12) Japan: Toppan Printing installed information displays into sub-way stations with printed power source

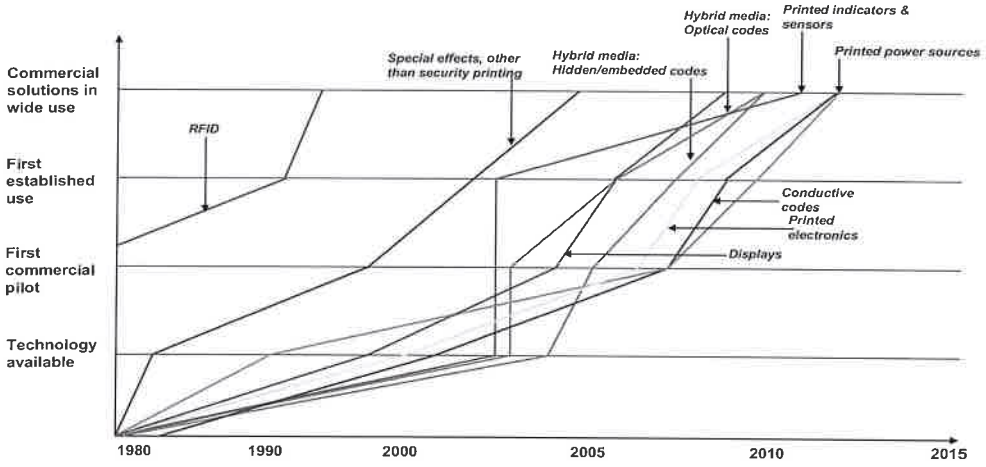


Figure 1: Printed functionality technology roadmap globally

4. Market and business models

The business models for the additional service available through printed functionality are complex because of the variety of earning logics and the wide value chain. The earning logic can be based on direct sell, AD sales, access and subscription, royalties and licences, selling of brands, management of logistics or e-Business. The business chain also contains many players: publishers, advertisers, technology providers, printers, materials suppliers, data base providers, content providers and the end users. The publisher seems to have the best prerequisit to manage the value chain but each player, including the printer, has the opportunity to overtake new roles and functions.

The global market of printed electronics is expected to grow up to 40 billion euros until 2017 (Figure 2). In the same time we expect the global market for printed functionality suitable for conventional printers to grow from 200 millions to 17 billions. The corresponding figures for Finland are 3 and 250 millions respectively [Lindqvist 2008].

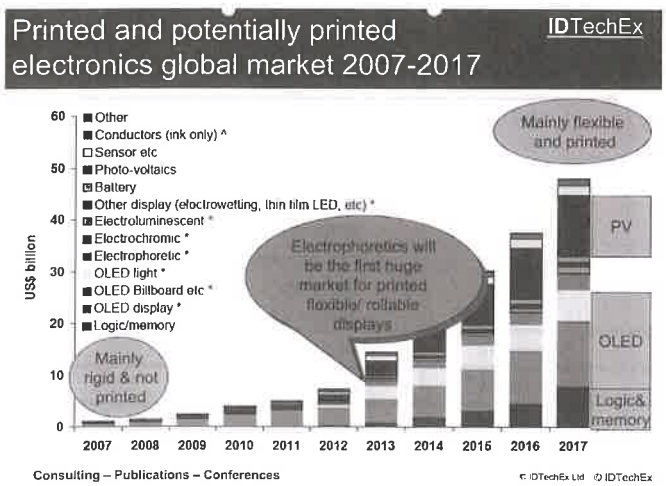


Figure 2:
Market forecast for printed and potentially printed electronics during 2007 - 2017 (Source: IDTechEx) /Harrop 2007/

5. New applications of printed functionality and hybrid media

The following new innovation embryos were tested in pilot scale: Weather sensors in newspapers, UV-fluorescent security elements, UV-indicators and Conductive codes. All these application were rather easily realised and functioned well on the laboratory scale. Printed UV-indicators and UV fluorescent security elements were also successfully made in full scale printing in two different sheet-fed printing houses. However, full scale printing of sensors in newspapers was not carried out since the inks required were not available commercially for offset newspaper printing.

Basically, the flexo process offers more flexibility and more sensible applications than offset. The possibilities to use a huge offset rotation press for producing printed functionality are rather limited, so it is assumed that versatile narrow-web printing lines with several units for printing and converting will take the leading position. Attachments with printed functionality may then be inserted as an integrated part of the main product.

Business models were calculated for the following hypotetical applications of printed functionality for the national market: Weather sensors in newspapers, Conductive identifier for individualisation, UV-indicators in newspapers or on sun lotion bottles, Inexpensive conductive codes to replace RFID, Security elements in event passes, Anti-counterfeiting by RFID, Combination of RFID and sensors to control the value chain. For all the cases profitable applications were found, though the market potential varied a lot and was most promising for identifiers in books and for anti-counterfeiting. However, it should be noted that today only the antenna of an RFID tag can be printed and the chip must be attached to the antenna in a separate stage.

In Table II the products of printed functionality are analysed from the user aspects. The table describes the applications, their producers, the end users and the probability of realisation within the next five years.

Table II: The applications, the producers and the users of a given technology; the probability of the application within five years

TECHNOLOGY	APPLICATION	WHERE	FOR WHOM	P (within 5 years)
Hybrid media: Optical codes	Additional info	Newspapers	Publishers	100%
	Additional info	Tickets	Customers	100%
	Additional info	Packages	Manufacturers	90%
	Effects	Advertisements	Many companies	70%
Hybrid media: Invisible codes, Embedded codes Printed indicators and sensors	Brand logo etc.	Packages, labels	Brand owners	40%
	Brand logo etc.	Newspapers	Publishers	40%
	Brand logo etc.	Advertisement	Brand producers	50%
	UV sensors	Labels	Tan oil mfrs	70%
	Thermometer	Packages	Food industry	70%
	Freshness indicator	Packages	Food industry	60%
	Humidity indicator	Packages	Food industry	30%
	Alcometer	Newspaper	Publisher	30%
	Alcometer	Packages	Consumers	20%
	Time indicator	Fast food bar	Fast food chains	30%
Special effects reactive inks	Thermometer	Packages, drinks	Beverage mfrs	100%
	Flashing label	Discos	Beverage mfrs	100%
	Lottery score indica	Lottery	Lottery company	50%
Conductive codes RFID	RFID for shops	Logistics	Product mfrs	80%
	RFID on products	Labels	Product mfrs	70%
	RFID on prints	Books etc.	Publishers	40%
	RFID in mailing	Logistics	Logistic companies	50%
	RFID baggages	Airports	Aircompanies	70%
	RFID in mfr	In plant	Industry companies	70%
Optics & electronics	Components	Consortia	Consumers	30%
Printed displays	Many applications	Consortia	Consumers	30%
Energy sources	Many applications	Consortia	Consumers	50%

6. The role of the printing plant

To build up a working 2D-code solution requires both willingness and commitment from all the partners involved. It should be noted that in certain cases the copyright owners may prevent the implementation of a new 2D-code application.

Printing special effects with special ink has been a stable technique for quite some time. These cases always require a customer willing to pay for the additional value of such effects in the printed product. Unfortunately, special inks are not available for all production processes.

From a printer's view the production of conductive codes is similar to printing with special inks. Again the ink properties are the key factor. Even if the production of the code could be easily solved, a large-scale use requires a great number of specific readers. Therefore, one possible application could be a specific sector, where all the users have access to readers. Another apparent application area is product identification. When comparing costs, a simple printed conductive code is cheaper than an RFID tag.

RFID chips cannot yet be produced in normal mass-volume printing presses. Ready-made chips may be attached to printed sheets, labels or packages in a special printing and converting process line. After this the printed sheet (with the RFID) is processed in the bindery machine.

If the antenna of the RFID tag is printed in the same printing line as the main product, the silver ink requires a closed chamber in the printing unit. However, it may be difficult to modify an existing printing unit to a closed chamber system. One example of an integrated flexographic press for producing RFID labels is shown in Figure 3. One printing unit is of a closed chamber type for printing the antenna.

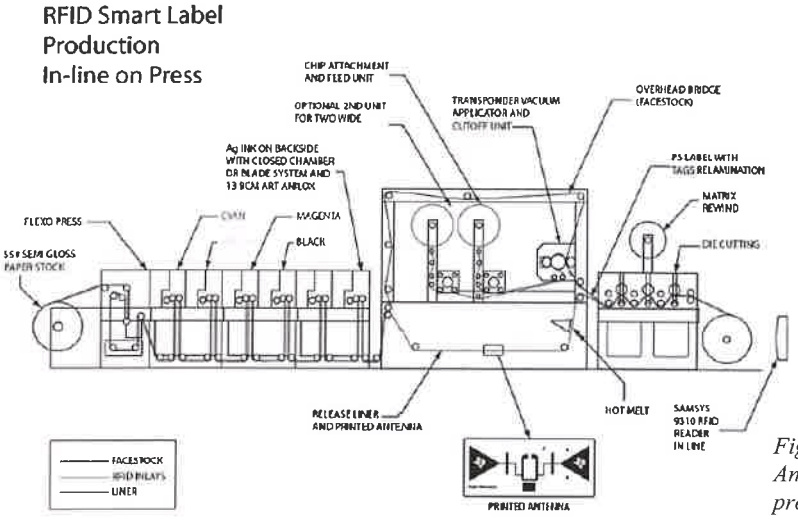


Figure 3:
An integrated flexo press line for producing RFID labels [Neilson 2005]

It is obvious that conventional printing plants may carry out two main strategies in their production: 1) to specialize to a certain functionality or 2) to carry on with conventional volume production and ally with a specialist on printed intelligence. The first option may be complicated since totally new production equipment are likely to be needed - at least in the case of printed electronics. Another complex area may be the need of special environment. To build a new clean room is much more expensive than to stick to existing premises.

The second strategy is to stay in volume production but at the same time utilize the inserting capacity. In principle, the inserting process may offer great versatility. The functionality element to be inserted can be printed at a limited speed in a special printing line in advance without reducing the production speed of the main product. For example, one magazine printer allows the maximum thickness of 2 mm and a maximum weight of 20 g for a tipped (glued) insert. This gives flexibility for the choice of base material of the insert. One restriction is, however, that the insert must bear a load of 1000 kg caused by the finishing process. Of course, a printed sheet can be inserted as a loose insert or as a permanent part of a magazine (bind-in insert).

In case of a newspaper the porous and relatively weak newsprint may hinder the use of special inks. Therefore again, the insert enables the use of smooth substrates and higher grammages. It should be noted that many special inks require UV curing, and this is not common standard in conventional heatset and coldest printing lines.

7. Usability and recyclability

Usability is a non-functional quality of a product describing ease of use, learnability, accessability and the interface between product and user. Hybrid media, tags and barcodes extend the world wide web to the physical world. Usability refers mostly to the interactions with mobile phone cameras and RFID readers. The usability aspects of a sensor or an indicator refer to effective reading and interpreting of the indicator, since

the user can only read it, not affect it. The key questions in visualising the indicator are location, environment, physical phenomenon measured, visualising the change and the meaning of the change.

The evaluation of recyclability and de-inkability of a printed product is very case specific and with new type of printed products no specific answer is available previously. Generally bonding the substrate material to other materials, which are difficult to remove and/or harmful to production, can diminish recyclability. A nonpaper component is suitable for recycling if it can be separated from the recovered paper by recognized technical processes and recycled or disposed without damage to the environment.

8. Conclusions

In summary printed functionality is an opportunity for the printing industry to create an additional value and service for their products. The value chain of printed functionality offers many new roles and opportunities for the printer. Barcodes, indicators and sensors can rather easily be innovated and realised without big investments in technology. For more complex products, such as printed electronics however, an exact application of material compatibility and process application is needed in co-operation with other stakeholders.

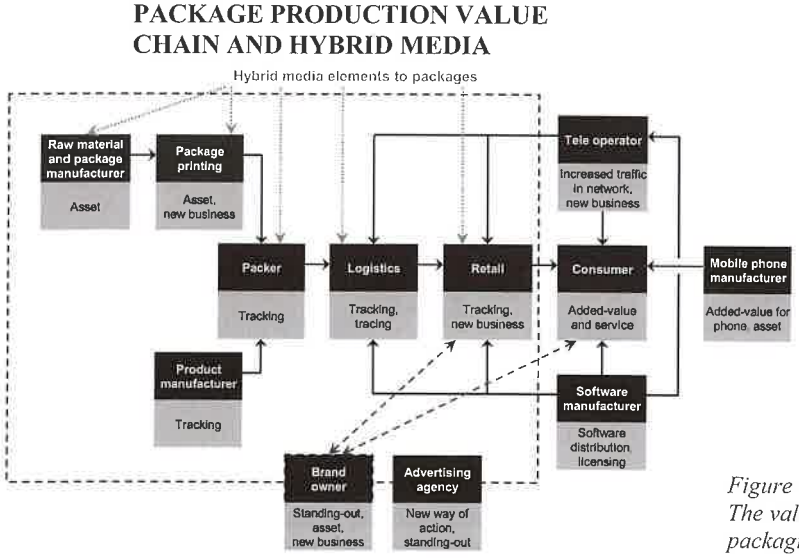


Figure 4:
The value chain of hybrid media in the packaging industry

Further research will concentrate on hybrid media in packaging, where intelligent applications offer a huge additional market for printed functionality. The value chain of hybrid media in the packaging industry is shown in Figure 4.

References

1. [Hakola 2007] Hakola, L., Lindqvist, U., Linna, H., Siivonen, T., Södergård, C., Roadmap on printed functionality and hybrid media. Advances in Printing and Media Technology Vol. 33, ed.: Nils Enlund, Acta Graphica Publishers, Zagreb, 2007. p. 103 - 110
2. [Harrop 2007] Harrop, Peter. The global market for printed electronics, Printed Electronics USA 2007 Conference
3. [Lindqvist 2008] Lindqvist, U., Eiroma, K., Hakola, L., Jussila, S., Kaljunen, T., Moilanen, P., Rusko, E., Siivonen, T., Välkkynen, P., Technical innovations and business from printed functionality. VTT Research Notes 2436, Espoo, 2008, 73 p.
4. [Lindqvist 2008a] Lindqvist, U., Hakola, L., Linna, H., Moilanen, P., Siivonen, T., New business models for printed functionality. Proceeding of the 34th IARIGAI Conference, Grenoble, France, 2007. To be published in Advances in Printing and Media Technology Vol. 34, ed.: Nils Enlund, Acta Graphica Publishers, Zagreb, 2008
5. [Neilson 2005] Neilson, James. Flexo Printing with Conductive Ink: An overview of Printed RFID Antenna & Intelligent and Active Packaging Applications. PIRA Printed Electronics 2005. London, September 14 - 15, 2005. 20 p.

Typography on web banners

Klementina Možina, Romana Horvat

University of Ljubljana, Faculty of Natural Sciences and Engineering
Chair of Information and Graphic Technology
Snežniška 5, SI-1000 Ljubljana, Slovenia
E-mail: klementina.mozina@ntf.uni-lj.si

Abstract

The Internet has clearly become an active medium for advertising, and as a result, web pages are often full of adverts. Therefore, these adverts should be designed in such a way as to attract and motivate users. For the present study, we evaluated the effectiveness of web banners among Internet users (n=106) with a multiple-choice questionnaire composed of "closed" questions. We considered various aspects of web banners: their form, size and position on web pages, with emphasis on typography, colour and legibility. The choice of typographic elements depends on the size and form of the banner. Of primary importance is the proper combination of type size and type design, according to text length. We considered numerous typographic issues: type style, x-height, ascender and descender, distinctive character features, counter shape, type size, letter and word spacing, leading, line length, setting, mixing different typefaces, typeface colour and background. All these factors greatly influence the legibility of an advert, and it is important to make good use of limited web banner space, with the proper balance of graphic elements. In addition to graphic design, we also addressed the issue of age, for example the probability that older users are more annoyed by illegible banners than younger users, and thus how to provide the best legibility (e.g. high contrast), particularly for users over 45 years of age. Knowing these factors is essential for planning effective advertising.

Keywords

Banner adverts, colour, Internet advertising, typography

1. Introduction

Internet advertising is known to have begun in 1994, when the first web banner on Hotwired, the first commercial web magazine, was sold. This kind of advertising greatly attracted readers' interest, with more than a 5% response [Chapman, 2000; Skrt, 2006]. These days, however, only two to five Internet users out of a thousand click on web banners [Chapman, 2000; Outing, Ruel, 2007]. Web banners represent paid advertising, and thus advertisers have a substantial interest in their usefulness and whether they attract and motivate Internet users.

In our research, we were interested in the factors which influence the effectiveness of web banners: the website itself, the position of the advertisement, the chosen typeface(s) and type size. In addition to graphic design, we also addressed the issue of age, for example the probability that older users are more annoyed by illegible banners than younger users, and thus how to provide the best legibility (e.g. high contrast) for older users, particularly those over 45 years of age.

2. Legibility of typography

Communication through a web page or screen demands that the reader translate symbols into meaning. Legibility refers to how easily this process is performed. To make reading possible, the text must fulfil three essential properties [Reynolds, 1979]:

- The property of visibility, in which a clear image of adequate size is received by the retina. Visibility requirements will of course depend to a certain extent on the acuity of the viewer's eyesight.
- The recognisability or perceptibility of the letters and words making up the text. This will be affected by factors such as type style and form as well as the reader's skill.

- The property of comprehensibility. Comprehension will be affected not only by the content of the text but also by its visibility and perceptibility and by the verbal capacity and intelligence of the reader.

It is important to know how readers move their eyes around a page: In Western cultures the eyes most often fixate first in the upper left part of the page and hover in that area before scanning left to right. Only after perusing the top portion for some time do viewers' eyes explore further down the page (Figure 1). It has been observed that readers' instincts are to first look at the upper left part of a website [Outing, Ruel, 2007]. It is important to remember that viewing patterns are affected by the page elements that exist in particular locations, e.g. logos and headlines should be in the upper left.

People often ignore web adverts, depending to a great extent on their placement; good placement and the right format can improve readers' interest. Research has shown [Outing, Ruel, 2007] that banners in the left column (68%) and on the top of the page (55%) are viewed most. Right-side banners (34%) did not do as well, and banners at the bottom of the page were seen by only a small percentage of people – 14%.

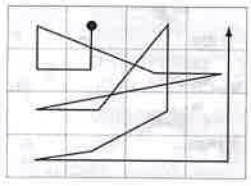


Figure 1: The most common eye-movement pattern across a page

For successful advertising, proper positioning of a web banner on a page is not the only criterion; well designed banners will attract readers' attention, with their gaze tending to stop on web banners with the greatest legibility. Legibility has been studied using different methods [Možina, 2001; Reynolds, 1979]: visibility, perceptibility in peripheral vision, speed of perception, ocular movement, rate of work, readers' preference and other factors. Readers' preferences cannot be relied upon as an accurate indication of the relative legibility of a text, however. According to different studies of legibility, researchers concluded that readers prefer those typefaces which they can read most easily, and they are able to read most easily those typefaces which they find most pleasing [Reynolds, 1979]. Still, reader preferences possibly have greater significance in the investigation of ways of representing information structure.

The large number of studies on legibility highlights its importance. The results are in broad disagreement as to what makes text legible, but it is possible to determine certain general guidelines that can help to create legible text. There are a number of typographic characteristics to be observed to make text more legible:

DISTINCTIVE CHARACTER FEATURES, COUNTER SHAPE: Legibility is greater in typefaces with strongly distinctive character shapes. The upper half and the right side of the letter seem to be the most important for letter recognition and thus are good places to highlight distinctive characteristics [Gaultney, 2001; Reynolds, 1988]. Counter and shape of the letter are very important. Results of studies show that a larger space between letters increases legibility. Counters give the eye important clues in letter recognition, and varying their shapes can also help increase distinctness and legibility [Gaultney, 2001; Možina, 2001; Tracy, 2003].

ASCENDER, DESCENDER, X-HEIGHT: Letters with ascenders or descenders are critical for word shape and letter recognition [Spencer, 1969]. Long ascenders and descenders help to distinguish characters from one another. A smaller x-height increases the white space between lines. Nevertheless, typefaces with larger but moderate x-heights are generally more legible at small sizes and with certain reproduction methods. Increased x-height gives the impression of the increased legibility of the next larger type size [Gaultney, 2001; Možina, 2001; Tracy, 2003].

SERIFS: The common wisdom is that serif faces are inherently more legible than sans-serif faces. Many studies support this view, although their validity is sometimes questioned [Lund, 1997; Wheildon, 1995]. The shape of serifs can influence legibility. Some analyses indicate that the legibility of letters is diminished by the use of thin lines or long or heavy serifs [Reynolds, 1979; Spencer, 1969]. In certain production environments and in certain media (e.g. TV, web), bracketed serifs retain their shape best, increasing letter distinction and legibility [Možina, 2001; Reynolds, 1979]. Non-print media and digital products (e.g. digital

phone with a display) have clearly revived sans-serif typefaces [Možina, 2003]. Owing to low screen resolution and/or the use of many different colours, sans-serif typefaces tend to be very effective in improving legibility in digital media [Götz, 1998; Kommer, Mersin, 2002].

CONTRAST, COLOUR AND STROKE WEIGHT: Little research has been done about contrast and its relationship to legibility; nevertheless, some results indicate that increased contrast does not enhance legibility – on the contrary, thin lines can actually diminish it [Gaultney, 2001; Možina, 2001].

TYPE SIZE: For a normal reading distance, the optimum type size for continuous text is usually between 9 and 11 points [Reynolds, 1988], or even between 8 and 12 points [Možina, 2001]. The precise size will depend on the x-height of the typeface. Of course, these sizes are not big enough for computer screens. It is suggested that sizes between 12 and 14 points be used for continuous text, and between 14 and 20 points for titles/headlines [Kommer, Mersin, 2002].

LEADING: For legibility, the white space between lines must be greater than the word spacing. For continuous text it is an advantage to use a line feed one or two points greater than the size of the type, or the leading should be set to 120% of the type size. This is especially important for typefaces with a relatively large x-height and sans-serif typefaces [Možina, 2001; Reynolds, 1988]. For computer screens, greater leading is suggested – about 150% [Götz, 1998].

LINE LENGTH: For sustained reading the optimum line length is about 60 to 65 characters and spaces. Lines with more than 80 or less than 30 characters and spaces will reduce legibility [Carter, 1997; Možina, 2001; Reynolds, 1988]. For computer screens, a much shorter line length is recommended – about 50 characters and spaces [Pring, 2000]. Some authors [Götz, 1998] suggested even shorter line lengths: 35 characters per line or even less.

SETTING: Researchers have been unable to show any significant difference in the legibility of fully justified and flush-left setting of text. It is critical to pay attention to letter and word spacing and hyphenation to avoid white "rivers" (especially with justified setting) and assure good continuation of the lines [Možina, 2001; Reynolds, 1988]. For computer screens, a ragged-right setting is recommended given the limited possibility to arrange very good letter spacing [Kommer, Mersin, 2002].

COLOUR AND TYPOGRAPHY: For good legibility, it is important to have sufficient contrast between background and typography. The colour properties of hue, value and saturation are important concerns when choosing colours for type and background. It is suggested that colours be chosen according to their value and saturation first, and then according to hue [Carter, 1997; Možina, 2001; White, 1996].

Based on the typical design of typefaces, they are grouped according to variation in stroke width, such as Old-style, Transitional and Didone; or in groups without (or minor) a variety in stroke width, such as Slab serif and Sans-serif.

OLD-STYLE TYPEFACE: The principal features of old-style typefaces are the slight contrast between the thick and thin strokes of the characters and an oblique emphasis. An early version (Humanist) of these typefaces has steeply sloping serifs and an angled crossbar of the lowercase *e*. A later version (Garalde) of old-style typefaces has a more pronounced contrast between thick and thin strokes. The crossbar of the *e* has become resolutely horizontal; the serifs are finer and more horizontal [Možina, 2003]. Generally, old-style typefaces are legible as body text in print media.

TRANSITIONAL TYPEFACE: The contrast between thick and thin strokes of the characters is much more marked. The emphasis of the curved letters is vertical. Serifs have become even more horizontal. The crossbar of the *e* is horizontal [Možina, 2003]. Generally, transitional typefaces are still very popular for book, journal and magazine print work, also because of their good legibility in body text.

DIDONE (MODERN) TYPEFACE: The contrast between thick and thin strokes of the characters has been reduced to hairlines. Serifs have become extremely thin lines and hairlines, which are unbracketed. Right angles predominate between strokes and serifs. The crossbar of the *e* is horizontal [Možina, 2003]. Didone typefaces are generally used nowadays as display typefaces and newspaper headlines, etc., but because of the lack of legibility they are not used as body text.

SLAB SERIF TYPEFACE: The contrast between strokes of the characters is limited; slab serif typefaces have a small (or even nonexistent) difference between thick and thin strokes. Serifs are unbracketed and very heavy. The crossbar of the *e* is horizontal [Možina, 2003]. In general, slab serif typefaces are used as display typefaces; because of their poor legibility as body text they are not used for print work. However, in certain new media (e.g. TV, web), the shape of the characters and serifs of slab serif typefaces increases legibility.

SANS-SERIF (LINEAL) TYPEFACE: As is evident from the designation of this category of typeface, sans-serif (lineal) typefaces do not have serifs. The contrast between strokes of the characters is limited; sans-serif typefaces have little or no difference between thick and thin strokes. The crossbar of the *e* is horizontal [Možina, 2003). Generally, sans-serif typefaces tend to be used in display roles, such as for titles, although some sans-serif typefaces are used as body text, especially in certain new media (e.g. fax, web). Nowadays, certain new sans-serif typefaces have been designed in such a way as to increase their legibility.

The design of a typeface is not the only important criterion for legibility, but also the population of readers to whom a certain text is going to be shown. According to the results of research [SURL, 2006], young web users prefer the Comic Sans typeface in 12- and 14-point sizes and Arial in 14-point size. Less popular typefaces are Courier and Times New Roman, however these typefaces tend to be very popular in the group of much older Internet users.

3. Experimental

We evaluated the effectiveness of web banners among Slovenian Internet users with a multiple-choice questionnaire composed of "closed" questions. Two questions involved ranking possible choices by order of preference. Our study of typographic legibility on web banners was performed according to the method known as reader preference. The method is subjective, but convenient and good enough for testing the legibility of short/informative (not continuous!) text, such as the content of banner adverts. Before the main investigation, a pilot study was made. Data from properly completed questionnaires that were returned (*n=106*) were processed using SPSS [Field, 2005; Klemenčič, 2005], (version 13 for Windows). For analysing the calculation of frequency, an average with standard deviation according to the normal distribution was derived.

In our research, we had assumed that: the effectiveness of a web banner is most influenced by its graphic design, chosen website and banner position on the page; a web banner on the top of the page attracts and motivates users more than banners in any other position on the page; users above 45 years old tend to be more annoyed by less legible banners than younger generations; the highest contrast between text and background gives the highest legibility.

Among the respondents in the study, 66% were female and 34% male; 11.32% were 19 years old or younger, 59.44% were between 19 and 30, 18.87% were between 31 and 45, and 10.37% were older than 45; according to education level, most of the participants had completed secondary school (58.49%), 31.13% had a higher (bachelor or higher) degree, 3.78% had attended vocational school, and 6.60% were primary school pupils.

4. Results and discussion

For the question "What factor has the greatest influence on the effectiveness of web banners?", out of a possible six answers almost half of the participants (Figure 2, Tables I and II), i.e. as Internet users (48.11%), among them about half female and half male, between 19 and 45 years of age, chose "creativity of graphic design". Second (17%) and third (16%) rankings were "recognition of a trademark" and the "website itself". Among males, "website" took second position, also rating the "shape of the advert" (13.89%) and the "position of the advert" (11.11%) as more important than the "trademark" (8.33%). Only 4.29% of females valued the importance of the "position of the advert", and even fewer (2.86%) the "shape of the advert"; they (7.14%) stressed more the "size of the advert".

Users were then asked to "Arrange the position of a banner (marked from *a* to *e*) from the most noticeable to the least noticeable". Banners were placed in five different positions: on the top of the web page (*a*), on the left side (*b*), on the right side of the page (*c*), in the middle embedded in the text (*d*), and at the bottom of the page (*e*). Results showed (Figure 3, Table III) that a banner at the top of the web page is the most noticeable

(84.90%, average 1.29, standard deviation 0.792), being least noticeable at the bottom of the page (70.75%, average 4.52, standard deviation 0.875). Users ranked the right-side position of an advert on a web page as second most noticeable (average 2.85, standard deviation 1.049), with the left-side position and a position embedded in the body of the text ranking third and fourth, respectively.

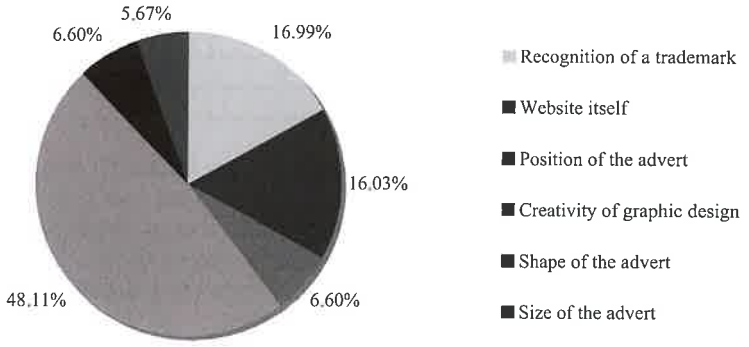


Figure 2: Influence on the effectiveness of web banners

Table I: Influence on the effectiveness of web banners - by sex

Sex	Male		Female	
Influence of the effectiveness	f	%	f	%
Recognition of a trademark	3	8.33	15	21.43
Website itself	6	16.67	11	15.71
Position of the advert	4	11.11	3	4.29
Creativity of graphic design	17	47.22	34	48.57
Shape of the advert	5	13.89	2	2.86
Size of the advert	1	2.78	5	7.14
SUM	36	100.00	70	100.00

Table II: Influence on the effectiveness of web banners - by age

Age	up to 19 years		19 - 30 years		31 - 45 years		46 - 65 years	
Influence of the effectiveness	f	%	f	%	f	%	f	%
Recognition of a trademark	4	33.30	9	14.29	4	20.00	1	9.09
Website itself	2	16.70	10	15.87	1	5.00	4	36.36
Position of the advert	2	16.70	2	3.17	2	10.00	1	9.09
Creativity of graphic design	4	33.30	35	55.56	9	45.00	3	27.28
Shape of the advert	0	0.00	3	4.76	3	15.00	1	9.09
Size of the advert	0	0.00	4	6.35	1	5.00	1	9.09
SUM	12	100.00	63	100.00	20	100.00	11	100.00

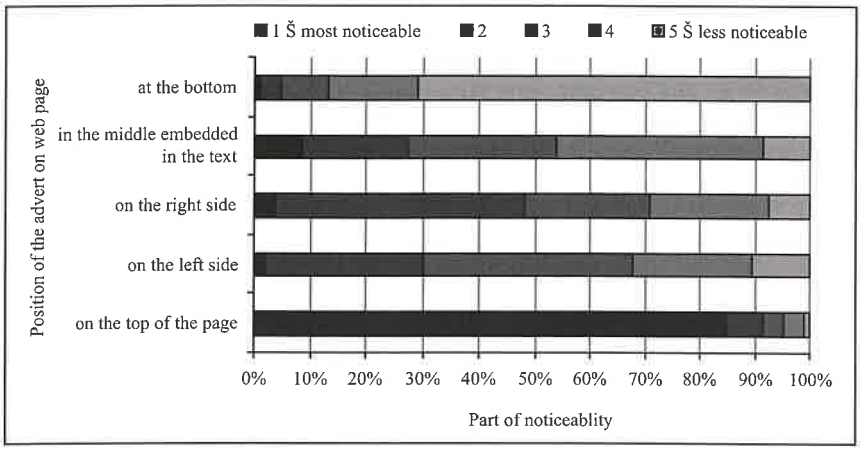


Figure 3: Noticeability of the position of a banner

Table III: Estimation of noticeability of banners

Noticeability of adverts on a web page	Rank	Min	Max	Average	Standard deviation
a - on the top of the page	1	1	5	1.29	0.792
b - on the left side	2	1	5	3.10	0.995
c - on the right side	3	1	5	2.85	1.049
d – in the middle embedded in the text	4	1	5	3.19	1.105
e - at the bottom	5	1	5	4.52	0.875

To the question "How many different typefaces could be used in one banner?", four possible answers were given: one, two, three, or more than three. Figure 4 shows that more than half (52.83%) of the respondents answered that two different typefaces could be used, with 20.76% of users answering three. An average of 14.15% opted for one typeface, highest in the oldest group (over 45) of users – 27.27%. 12.26% of users agreed that three or more typefaces could be used. The results pointed to a big difference in sex (Table IV): 25% of males agreed with this possibility, but only 5.71% of females.

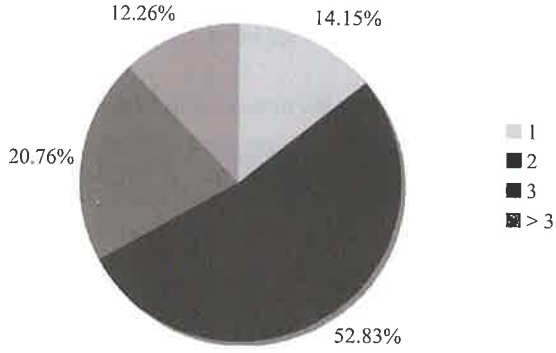


Figure 4: Different numbers of typefaces used in a single banner

Table IV: Different numbers of typefaces used in a single banner - by sex

Sex	Male		Female	
Different numbers of typefaces	f	%	f	%
One	5	13.89	10	14.29
Two	15	41.67	41	58.57
Three	7	19.44	15	21.43
More than three	9	25.00	4	5.71
SUM	36	100.00	70	100.00

When asked "How many different type sizes could be used in one banner?", four possible answers could be selected: one, two, three, or more than three. Figure 5 shows that almost half of the users (47.17%) concluded that three different type sizes would be appropriate. Only the oldest group (Table V) of users (over 45) did not agree, with 54.55% preferring only two type sizes. Second (27.36%) and third (24.53%) ranking were given to two type sizes and to more than three sizes. Users older than 30 agreed with this rating, but younger (up to 30) users opted for more than three different type sizes and less for two type sizes. Males (Table VI) ranked more than three type sizes second (30.56%), and two type sizes third (22.22%); however, among females less than one and a half percent (1.43%) chose the use of one type size in an advert. It is interesting that this possibility was not chosen by the oldest group of users, but by the group between 19 and 30 years old.

Table V: Different numbers of type sizes used in a single banner - by age

Age	up to 19 years		19 - 30 years		31 - 45 years		46 - 65 years	
Different numbers of type sizes	f	%	f	%	f	%	f	%
One	0	0.00	1	1.59	0	0.00	0	0.00
Two	1	8.33	16	25.40	6	30.00	6	54.55
Three	9	75.00	28	44.44	9	45.00	4	36.36
More than three	2	16.67	18	28.57	5	25.00	1	9.09
SUM	12	100.00	63	100.00	20	100.00	11	100.00

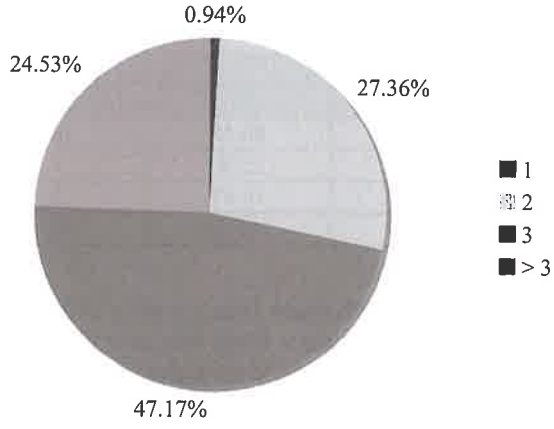


Figure 5: Different numbers type sizes used in a single banner

Table VI: Different numbers of type sizes used in a single banner - by sex

Sex	Male		Female	
Different numbers of type sizes	f	%	f	%
One	0	0.00	1	1.43
Two	8	22.22	21	30.00
Three	17	47.22	33	47.14
More than three	11	30.56	15	21.43
SUM	36	100.00	70	100.00

Users were asked: "Are you annoyed by illegible banners?". Figure 6, Tables VII and VIII show that most (86.79%) were irritated by poor legibility, especially the older population (whole group – 100%). 5.66% did not care about poor legibility. All users who gave this answer were younger (up to 30 years old). 7.55% of users were undecided (more males than females).

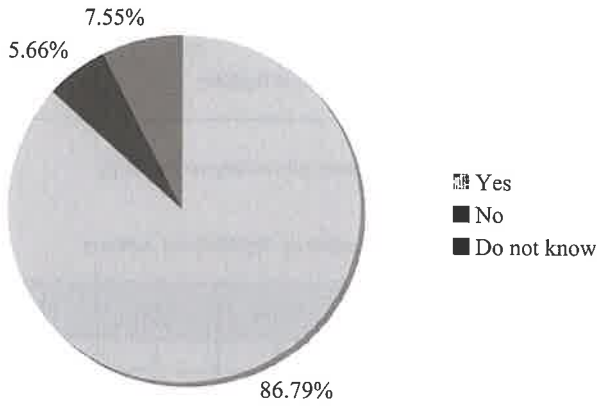


Figure 6: Illegible banner

Table VII: Illegible banner - by age

Age	up to 19 years		19 - 30 years		31 - 45 years		46 - 65 years	
Illegible banner	f	%	f	%	f	%	f	%
Yes	8	66.67	56	88.89	17	85.00	11	100.00
No	3	25.00	3	4.76	0	0.00	0	0.00
Do not know	1	8.33	4	6.35	3	15.00	0	0.00
SUM	12	100.00	63	100.00	20	100.00	11	100.00

Table VIII: Illegible banner - by sex

Sex	Male		Female	
Illegible banner	f	%	f	%
Yes	29	80.55	63	90.00
No	1	2.78	5	7.14
Do not know	6	16.67	2	2.86
SUM	36	100.00	70	100.00

Finally, users were asked to "Arrange different banners (marked from *a* to *f*) according to legibility from best to worst". Adverts were designed as: inverse/cameo – white text on a black background (*a*), black on a grey background (*b*), black on a white background (*c*), black on a grey textured background (*d*), yellow on a red background (*e*), and yellow on a dark blue background (*f*); in all examples sans-serif typeface was used. The results (Figure 7, Table IX) confirmed that black text on a white background is most legible (34.90%, average 2.27, standard deviation 1.276). Slightly less legible was white text on a black background – 32.07% of users even ranked it as the best solution. In third place was a black and grey combination for text and background. An equal number of users (31.13%) ranked this combination second and third. The remaining combinations were considered less legible, especially black letters on a textured background (62.26%, average 5.22, standard deviation 1.219). The yellow and blue combination, and yellow and red combination were ranked fourth and fifth.

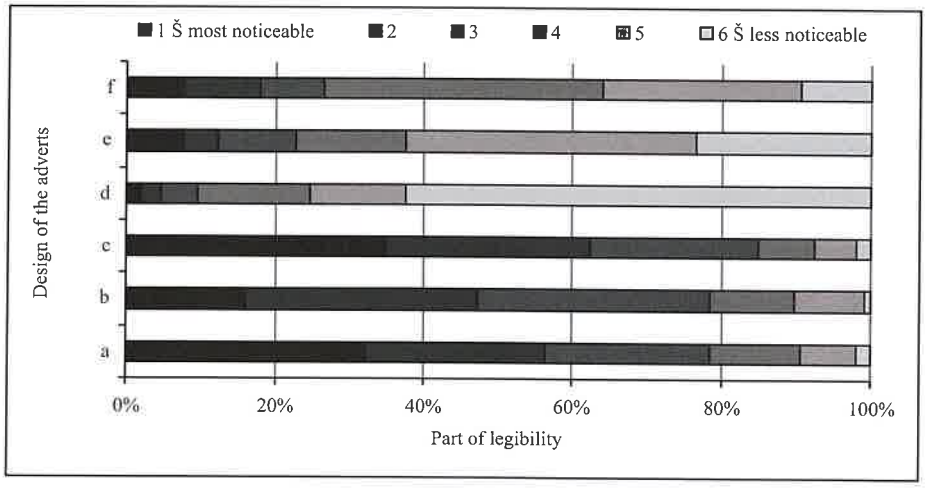


Figure 7: Banners according to legibility

Table IX: Estimation of legibility of banners

Legibility of adverts	Rank	Min	Max	Average	Standard deviation
a - white text on a black background	2	1	6	2.44	1.353
b - black text on a gray background	3	1	6	2.70	1.205
c - black text on a white background	1	1	6	2.27	1.276
d - black text on a textured background	6	1	6	5.22	1.219
e - yellow text on a red background	5	1	6	4.43	1.461
f - yellow text on a dark blue background	4	1	6	3.93	1.354

5. Conclusions

The results of the research indicated that the creativity of graphic design has a powerful influence on the effectiveness of web banners, but the influence of the actual web page on which the banner appears is not as important as we had suspected. Quite a bit importance was given to the "recognition of a trademark", especially among females. As previous studies have established which position on a web page is the most noticeable, these

results were confirmed in our research – the top of the web page is the most important place for adverts, but it is a bit surprising that the right side of the web page seems to be preferred over the left. Information about typefaces used in banners is important, especially if the advert is targeted to a specific group of users, e.g. more than three different typefaces could be suitable in advertising for males. Generally, most users prefer only two typefaces in an advert. The results also showed that three different type sizes in an advert would be the right solution, but older people prefer just two different type sizes in a single banner. Most users (especially older than 45) are annoyed by poor legibility, with users preferring black text on a white background, which yields the highest contrast. With lower contrast, legibility is poorer. For the use of different colour combinations, larger type sizes, bold letters or combination would be required for proper legibility.

The results of this study would be useful in planning and designing web banners – the more a banner appeals to a target population, in all likelihood the better the response to the advert will be.

References

Print sources

1. Carter, R., (1997), *Working with Computer Type 3, Color & Type*, Crans, RotoVision
2. Chapman, M. R., (2000), *The Product Marketing Handbook for Software*, Atlanta, Aegis Resources
3. Field, A., (2005), *Discovering Statistics Using SPSS*, London, Sage Publications
4. Gaultney, V., (2001), *Balancing Typeface Legibility and Economy: Practical Techniques for the Type Designer,* research essay, Reading, University of Reading
5. Götz, V., (1998), *Color & type for the screen*, Crans, RotoVision
6. Klemenčič, M. M., (1995), *Pa ne spet SPSS!*, Ljubljana, University of Ljubljana
7. Kommer, I., Mersin, T., (2002), *Typografie und Layout für digitale Medien*, München, Carl Hanser
8. Lund, O., (1997), *Why Serifs are (still) Important, Typography Papers, No. 2, pp. 91 - 104*
9. Možina, K., (2001), *Zgodovinski razvoj knjižne tipografije,* doctoral thesis, Ljubljana, University of Ljubljana
10. Možina, K., (2003), *Knjižna tipografija*, Ljubljana, University of Ljubljana
11. Pring, R. (2000), *www.type*, New York, Watson-Guptill
12. Reynolds, L., (1979), *Progress in Documentation - Legibility Studies: Their Relevance to Present-Day Documentation Methods, Journal of Documentation, Vol. 35, No. 4, pp. 307 - 340*
13. Reynolds, L., (1988), *Legibility of Type, Baseline, International Typographic Journal, No. 10, pp. 26 - 29*
14. Spencer, H., (1969), *The Visible Word*, London, Lund Humphries
15. Tracy, W., (2003), *Letters of Credit: A View of Type Design*, Boston, David R. Godine
16. Wheildon, C., (1995), *Type & Layout: How Typography and Design Can Get Your Message Across - or Get in the Way*, Berkeley, Strathmoor Press
17. White, J. V., (1996), *Color for Impact*, Berkeley, Strathmoor Press

Web sources

18. Outing, S., Ruel, L., (December 2007), *Eyetrack III*, <http://www.poynterextra.org/eyetrack2004/main.html>
19. Skrt, R., (September 2006), *Oglaševanje s spletnimi pasicami*, <http://www.nasvet.com/doc/pasice.php>
20. SURL, Wichita State University, (September 2006), *Services*, <http://psychology.wichita.edu/surl>





2

Printing and printing materials

Pressroom draw variation and its impact on web breaks Part I: Newspaper pressroom trials

Nina Deng, Frédéric Parent, Tony Manfred, Joe Aspler, Jean Hamel

Nina Deng, Frédéric Parent, Tony Manfred, Joe Aspler and Jean Hamel
FPInnovations-Paprican
570 Boul. St. Jean, Pointe Claire, Quebec, Canada H9R 3J9
E-mail: nina.deng@fpinnovations.ca

Abstract

Web breaks in pressrooms are affected not only by paper properties, but also by pressroom conditions. Recent research at Paprican has identified the key paper properties controlling web breaks. However, the impact of pressroom conditions has not been clarified. In this study, we used a synchronized pair of Laser Doppler sensors to measure high frequency draw variations of newsprint webs, and examined the relationship between draw variations and web breaks in five different newspaper pressrooms. The results show that the draw variation is related mainly to press configuration, operating conditions, and maintenance, while the contribution of the paper was found to be small. In certain cases, the draw variation can be very high (close to 1%) at press start-up and stop, as well as at pasting. We also found that severe out-of-roundness in newsprint rolls did have an impact on draw variations. Using frequency analysis, we showed that the sources of draw variations can be identified and linked to press variables. Finally, a correlation between pressroom draw variation and web break rate was found, with a higher draw variation causing a higher break rate. These results suggest that in addition to improving paper properties, it is important to minimize draw variation through better control of the press.

Keywords

Pressroom, runnability, tension variation, web break

1. Introduction

Web breaks have always been a major problem in the pressrooms. Large efforts have been expended by the paper industry to improve pressroom runnability, such as increasing the average tensile strength of paper, improving the uniformity of paper strength, reducing the number of physical flaws in the sheet, and improving winding controls.

Today, 1 break per 100 rolls is considered to be good performance in North America, while for Japanese pressrooms, less than 1 break per 1,000 rolls is the target. What is surprising is that North American newsprint can run at this demanding break level in Japan [1], but not in North America. It is therefore evident that opportunities exist to improve North American runnability.

Earlier work suggested that physical flaws in the sheet (shives, holes, calender cuts, etc.) were responsible for a large proportion of web breaks [2, 3]. Recent work has shown that the concept of the physical flaw in the sheet may be overstated, since such flaws are found in only a small minority of today's web breaks [4, 5].

In a classic paper, Page and Seth [6] showed that both paper and pressroom have a major influence on runnability. They pointed out the random nature of web breaks, which they described in terms of press variations such as tension surges meeting with flaws in the sheet.

For this reason, understanding tension variations in both the web and the press is critical. Uesaka [7] provided a quantitative model of the strength uniformity of the sheet. Even a sheet that is apparently without visible defects will be more likely to break if it has a broad strength distribution. The classic view of a tension surge on the press meeting a weak spot on the sheet may still apply, but the "weak spot" now indicates a zone of lower average tensile strength rather than a visible flaw. Uesaka's model assumed random variations in tensile strength. As far back as 1977 [8] it was also recognised that *systematic* MD variations could also cause strength variations that could influence runnability.

Pressrooms routinely use load cells to measure tension. However, the measurement frequency is very low (typically once per second), so that higher frequency variations are not picked up. Therefore, Meinander and Marttinen [9] described an instrument in which higher frequency tension variations in the moving web were determined with a non-contact acoustic sensor. Using this device, Larsson [10] showed that tension surges on the press coincided with events such as roll changes and acceleration/deceleration of the press.

In this study, we use the technique of laser Doppler velocimetry to determine high frequency draw variations on newspaper offset presses. These draw variations are then related to pressroom runnability statistics. Frequency analysis is used to relate the draw variations to moving elements of the presses.

2. Experimental

2.1 Laser speed sensor

The LaserSpeed 1100 System (Figure 1) was used in this study. It measures the velocity of a moving web without contact by utilizing the Doppler frequency shift technique. The optical sensor produces two laser beams that cross at an angle, creating an interference pattern. The velocity is measured in the area where the beams cross. The light scattered by the material moving through the measurement area contains velocity information in the form of a Doppler frequency shift. The optical sensor collects this scattered light, which is sent to a signal processor and converted to velocity data. This sensor can measure the velocity at a very high frequency (every 2 ms or 500 Hz), which allows the detection of high frequency speed variations. The accuracy of this device is 0.05% [11].

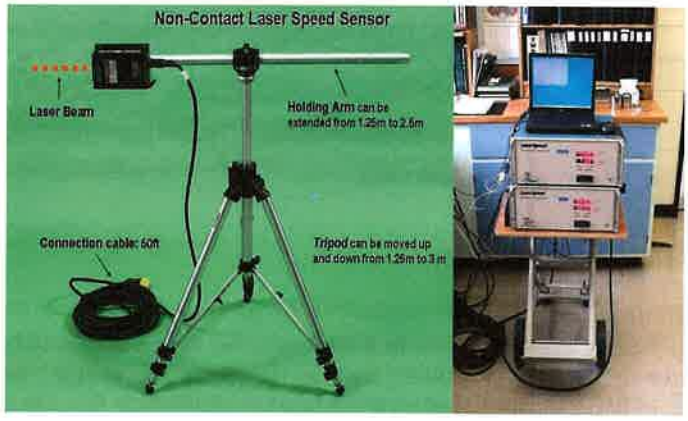


Figure 1: Laser Speed 1100 System

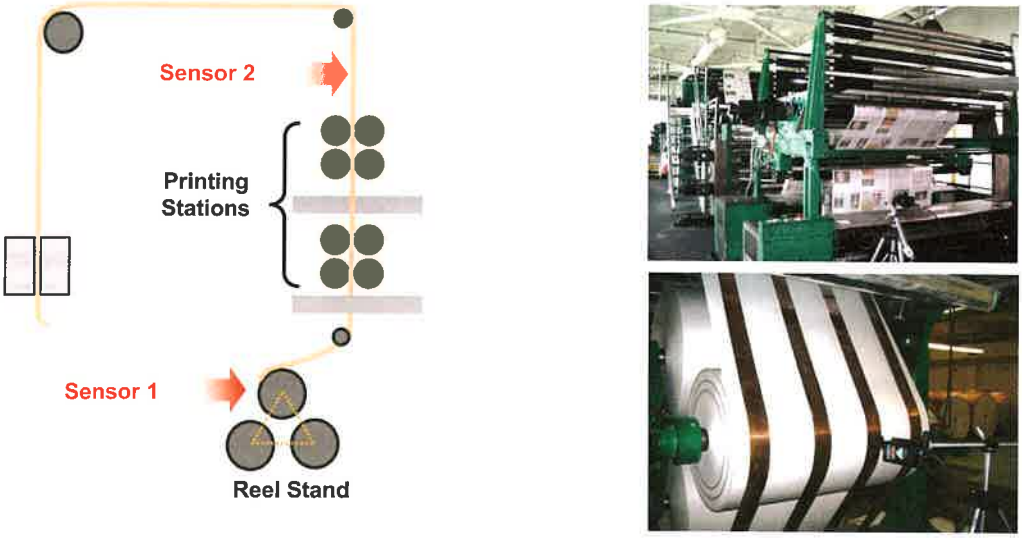


Figure 2: Locations of laser speed sensors on coldset offset newsprint press

To measure the draw variation on a printing press, two synchronized laser Doppler sensors are installed at different locations (Figure 2). For the newspaper pressroom trials, one sensor was usually installed at the reel stand; while the other sensor was installed after the last printing station. Because the newsprint presses are usually enclosed, it is difficult to install the sensor between the printing units.

For each test, a velocity signal was obtained from each sensor. The signals from the two sensors were synchronized so that the two sensors were able to start the measurements at the same time. Therefore it was possible to calculate the draw between the two points of measurements. By definition, the mechanical draw is equal to the relative speed difference between the two points (Equation 1). To evaluate the draw variation, the standard deviation of the draw was calculated.

$$Draw(t) = \frac{V_2(t) - V_1(t)}{V_2(t)} \quad (1)$$

2.2 Description of pressrooms and paper samples for the trials

We carried out trials in five newspaper pressrooms with different presses and operating conditions. The break rate in each pressroom varies considerably, from 0.8 to 3.0%. The break rates, supplied by each pressroom, were the yearly break rates of the tested presses and were based on the overall statistics including different paper suppliers. Information on the pressrooms is listed in Table I.

Table I: Pressroom information

Trials	Pressrooms	Press Type	Press Speed	Break Rate (yearly)
Trial 1	Pressroom 1	Goss Metro	450 m/min	2.0%
Trial 2	Pressroom 2	Goss Metro	350 m/min	3.0%
Trial 3	Pressroom 3	Geoman	500 - 600 m/min	0.8%
Trial 4	Pressroom 4	Wifag	500 - 600 m/min	1.0%
Trial 5	Pressroom 5	Goss Metro	400 m/min	2.75%
Trial 6	Revisit Pressroom 2	Same press as Trial 2	400 m/min	2.0%

Papers from different suppliers were tested. We also tested the papers from the same supplier (Mill B) in three different pressrooms (Pressrooms 2, 3 and 4) to separate the contributions of paper and press. The newsprints are listed in Table II.

Table II: Description of newsprint samples

Trials	Pressrooms	Paper Supplies	Grades
Trial 1	Pressroom 1	Mill A	48.8 gsm Newsprint
Trial 2	Pressroom 2	Mill B	45 & 48.8 gsm Newsprint
Trial 3	Pressroom 3	Mill B, C & D	45 & 48.8 gsm Newsprint
Trial 4	Pressroom 4	Mill B & E	45 & 48.8 gsm Newsprint
Trial 5	Pressroom 5	Mill F	45 gsm Newsprint (with different deinked pulp content)
Trial 6	Pressroom 2 (re-visit)	Mill B	48.8 gsm Newsprint

2.3 Pressrooms and paper factors examined during the trials

During each trial, the following factors were evaluated: the draw variation at different press conditions and for different papers in order to examine the effect of pressroom and paper factors affecting the pressroom draw variation. The pressroom and paper factors examined are listed in Table III.

Table III: Pressroom and paper factors examined

Pressroom factors	Paper factors
Compare the draw variation in different pressrooms	Paper from different suppliers and made with different furnish (TMP vs. DIP)
Draw variation at steady state	45 gsm vs. 48.8 gsm newsprint
Draw variation at press start-up and stop	Out of roundness of the roll (OoR)
Draw variation during pasting cycle	Paper rolls from different CD position
Draw variation at different press speeds	Narrow roll (25") vs. wide roll (50")

3. Results and discussion

Previous studies [12] have shown that the majority of web breaks (> 60%) are either press-related or result from "unknown" causes. This implies that pressroom tension variation may play a key role in web breaks. In the present study we have focused on the draw variations and its impact on web breaks.

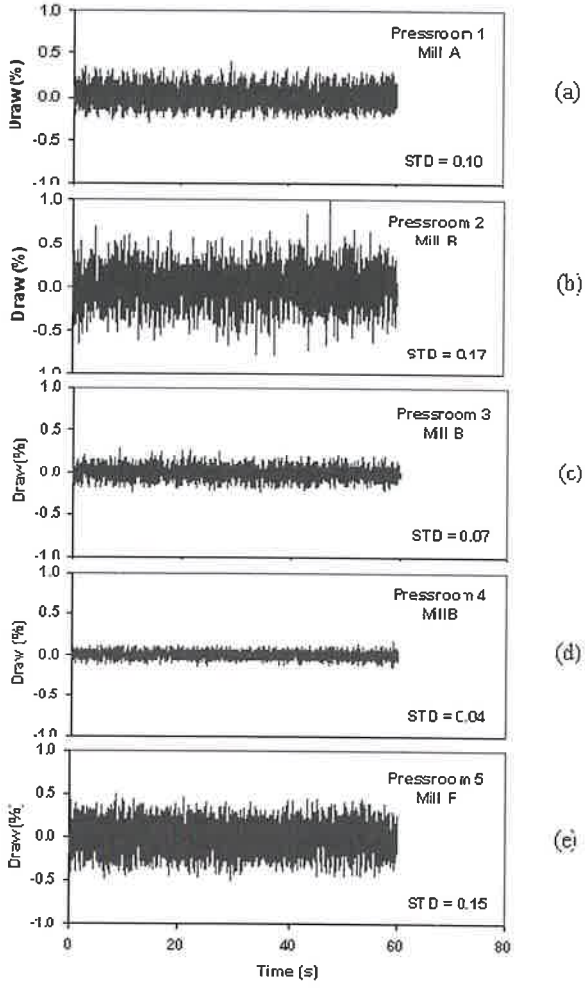


Figure 3: Draw variation in different pressrooms

3.1 Draw variation in different newspaper pressrooms

Figures 3a to 3e show the draw variations between the unwind stand and after the last printing unit in five different newsprint pressrooms. As can be seen, the draw variation occurs at very high frequency and is quite different from one pressroom to another. The draw variation is given as the standard deviation of the draw and ranges from 0.04% to 0.17%.

In Pressrooms 2, 3 and 4, the newsprint was produced on the same paper machine, in Mill B. However, the draw variation in Pressroom 2 (Figure 3b) is much higher than in Pressrooms 3 and 4 (Figures 3c and 3d). This indicates that draw variation is affected strongly by pressroom conditions.

3.2 Sources of draw variations

In order to identify the sources of draw variations, Fast Fourier Transform (FFT) analysis was performed to related draw variations to rotating elements on the press, and to identify the proportion of random vibrations on the press.

Figures 4a to 4e show the frequency analysis results for each pressroom. Pressrooms 1, 2 and 5 demonstrate there are peaks with characteristic frequencies (Figures 4a, 4b and 4e), but no characteristic frequencies are found in Pressrooms 3 and 4, which also have very low draw variation (Figures 4c and 4d).

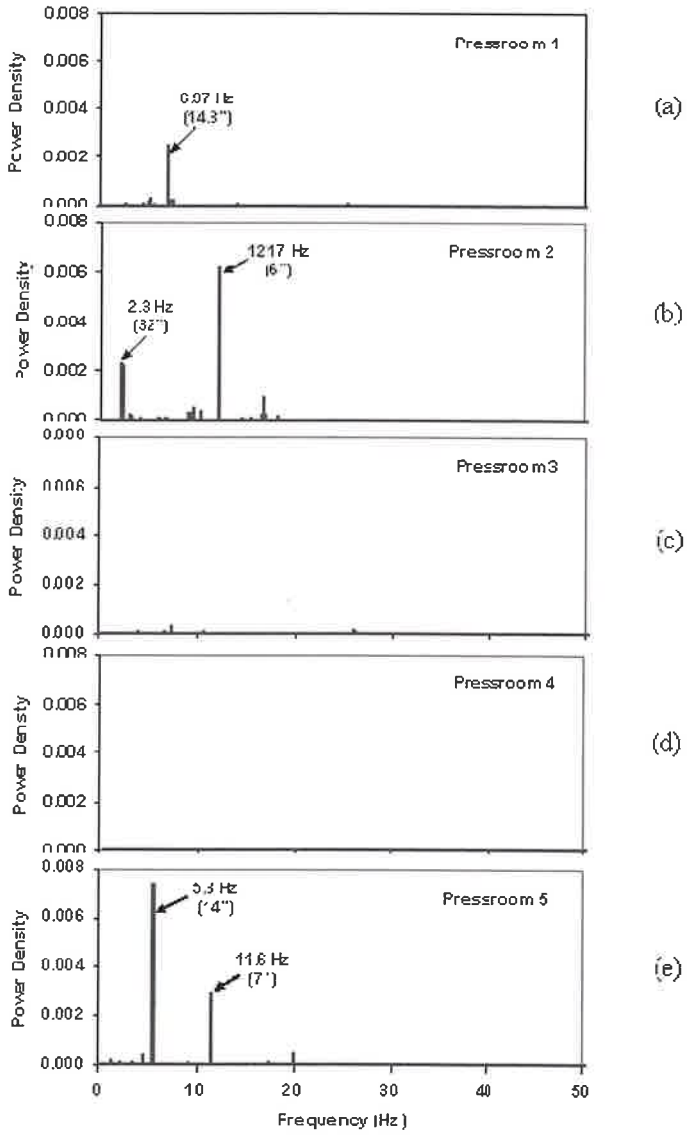


Figure 4:Frequency analysis of draw variation

When revisiting pressroom 2, it was found that the main peak at 12.7 Hz which created 30% of the total variance was related to the dancing roll (6" or 15 cm in diameter). The other smaller peak found in this pressroom corresponded to the paper roll diameter, and might be caused by roll out-of-roundness (OoR). The effect of OoR on draw variation will be discussed in a later section.

3.3 Draw variation during press star up and stop

In pressroom 4, it was noticed that there are more breaks during press start-up or stop, so we measured the draw variation at press start up and stop during this trial. As shown in Figures 5 and 6, draw variations at press start-up and stop are very high, close to the critical level of 1%, which is close to the limit of paper stretch for newsprint. This explains the higher web break rate often observed at press start up and stop.

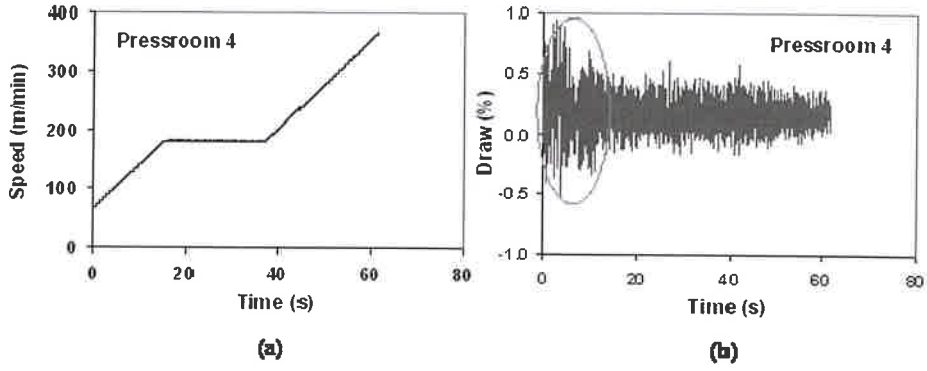


Figure 5: Speed increases (a) and corresponding draw variation (b) during press start up

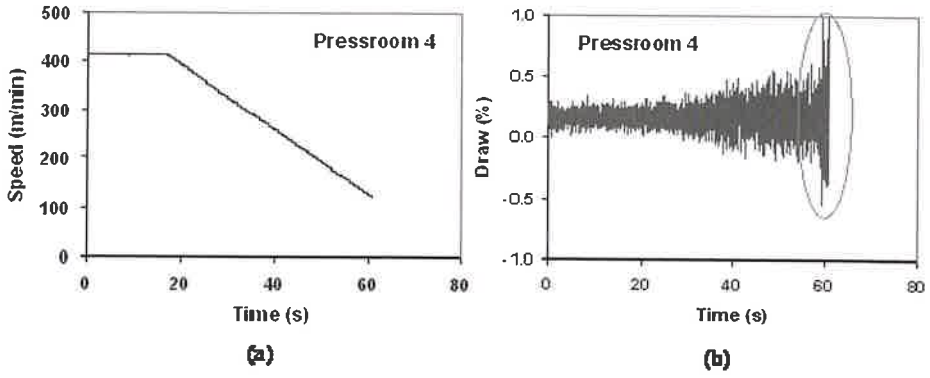


Figure 6: Speed decreases (a) and corresponding draw variation (b) during press stop

3.4 Draw variation during pasting cycle

The draw variation was monitored during pasting cycles in three pressrooms in which the presses and pasting patterns are different. Due to pressroom confidentiality, we cannot describe their paste patterns here. The paper rolls tested in these three pressrooms are from the same paper machine.

As shown in Figure 7a, the draw variation was very high during the pasting cycle in Pressroom 2. However, in Pressroom 3, only a small increase in draw variation was observed during pasting (Figure 7b). In Pressroom 4, the draw variation was very small, but there was a spike at the paste (Figure 7c).

These results indicate that pasting certainly affects draw variation, but the extent of its impact depends on the press configuration, paste patterns, and also on how the press is operated and maintained.

3.5 Draw variation at different press speeds

To examine the effect of press speed, we measured the draw variation at three different speeds (180, 410 and 550 m/min) on the same press in Pressroom 4. As seen in Figure 8a, press speed has a significant effect on draw variation. It is somewhat surprising to see that at a high press speed, the draw variation is lower. We also observed the same trend in other pressrooms (Pressrooms 2 and 6). By examining the frequency analysis results, we found that at lower speed, there are several peaks, which are related to the rotating elements on the

press (Figure 8b). However, at high speed, these peaks disappeared. This may be explained by the fact that for each press, there is probably an optimum design speed. Therefore, a lower speed does not necessarily mean a lower draw variation.

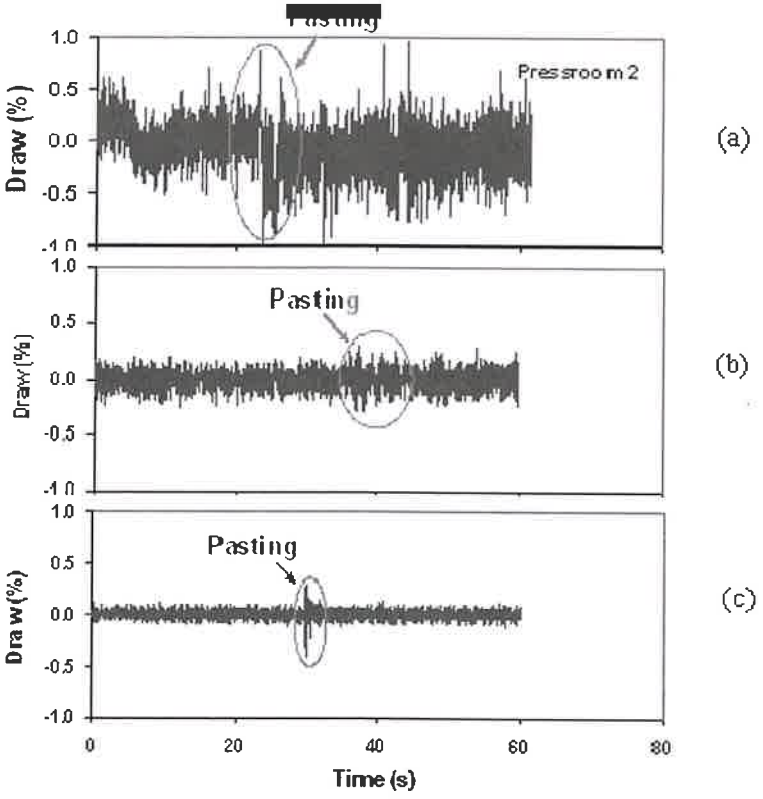


Figure 7: Draw variation during pasting

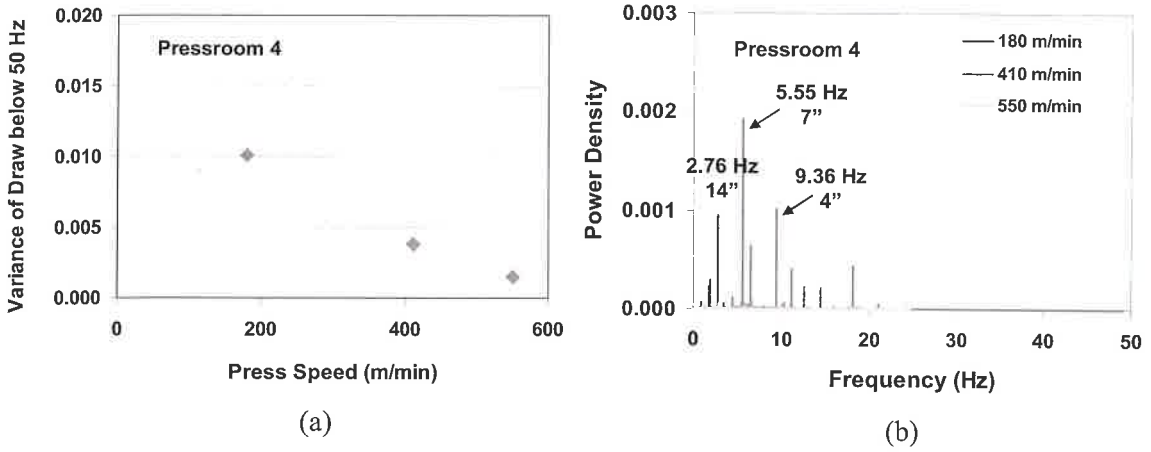


Figure 8: Effect of press speed on draw variation

3.6 Draw variation for the papers from different mills

To see how paper affects draw variations, newsprints produced at different mills (all with basis weight of 48.8 gsm) were run on the same press and the draw variations were monitored.

As shown in Figure 9a and 9b, there is no significant difference in the draw variation among papers from different mills in both Pressrooms 3 and 4. However, a significant difference in draw variation was observed between Pressrooms 3 and 4, indicating that the draw variation is controlled mainly by the press.

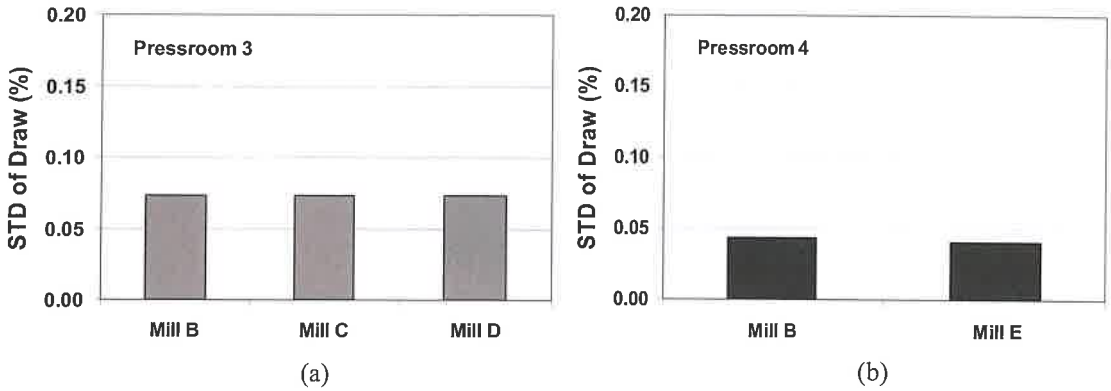


Figure 9: Draw variation vs. paper supplies in pressroom 3 (a) and 4 (b)

3.7 Draw variation: 45 vs. 48.8 gsm newspaper

To see whether the basis weight of paper will affect the draw variation, we measured the draw variation of 48.8 gsm to 45 gsm papers which were produced with the same furnish and on the same paper machine.

We found that there was no significant difference in the draw variation between 45 and 48.8 gsm newsprints in the same pressroom (Figure 10). However, for the same paper, there is a significant difference in draw variation among three pressrooms, with Pressroom 2 having three times greater draw variation than Pressroom 4. This confirms again that the draw variation is controlled mainly by the press.

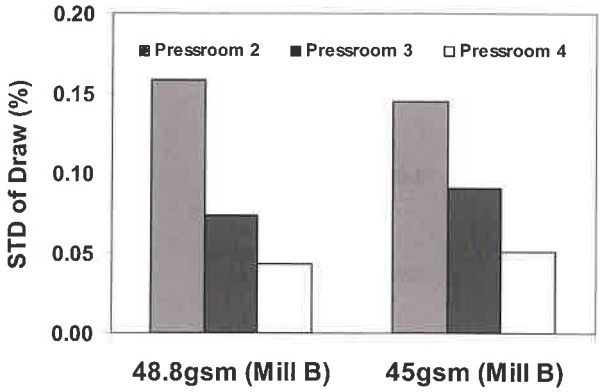


Figure 10: Draw variation of 45 gsm vs. 48.8 gsm newsprint paper

3.8 Effect of roll out-of-roundness (OoR) of paper roll on draw variation

A paper roll can be deformed during handling and transportation which may cause problems when the roll is unwound for printing. It could increase the web breaks due to increases in tension variation.

Figure 11 shows the draw variation of paper rolls from the same newsprint machine, with and without out-of-roundness (OoR). As can be seen, the roll with OoR (6 mm on the radius) caused a significantly higher draw variation compared to the normal roll. However, the impact of OoR on draw variation was found to depend on the magnitude of the OoR and also on the pressroom conditions. For example, the OoR roll in Pressroom 3 even had a lower draw variation than the roll without OoR in Pressroom 2.

3.9 Effect of other paper factors on draw variation

We also examined the effect of other paper factors on draw variation, including edge roll vs. center roll, narrow roll (25") vs. wide roll (50"), draw variation at different roll diameters, and draw variation of papers

made with different deinked pulp (DIP) content. The results showed that these paper-related factors have very little effect on draw variation.

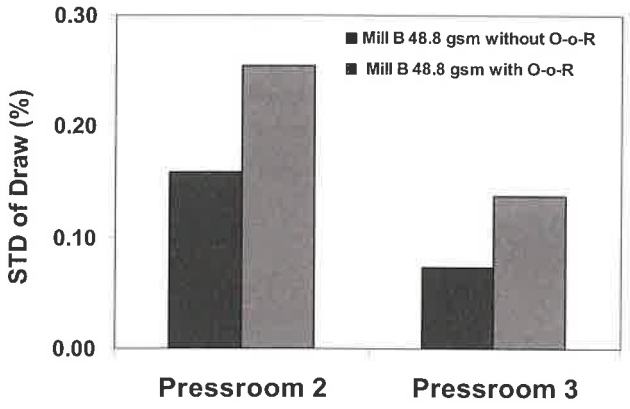


Figure 11: Effect of roll out of roundness on draw variation

3.10 Draw variation vs. break rate

Figure 12 shows the correlation between the break rate and draw variation (i.e. the standard deviation of the draw) is shown in Figure 12. As can be seen, considering that several pressrooms operating under different conditions were examined in this study, there is a good correlation between the break rate and draw variation: a higher draw variation leads to a higher break rate. Note that the rolls tested in Pressroom 2, 3 and 4 are from the same paper machine and have the same basis weight (48.8 gsm), yet the draw variations in different pressrooms are very different. This explains a well-known fact that the same paper can have very different break rates in different pressrooms [6]. The papers used in pressrooms 1 and 5 are from different suppliers.

It should be pointed out that web break rate is also affected by paper properties such as MD tensile strength, MD stretch and the tensile strength uniformity [4]. Therefore, the data points in the plot of web break rate against draw variation do not necessarily fall on the same line.

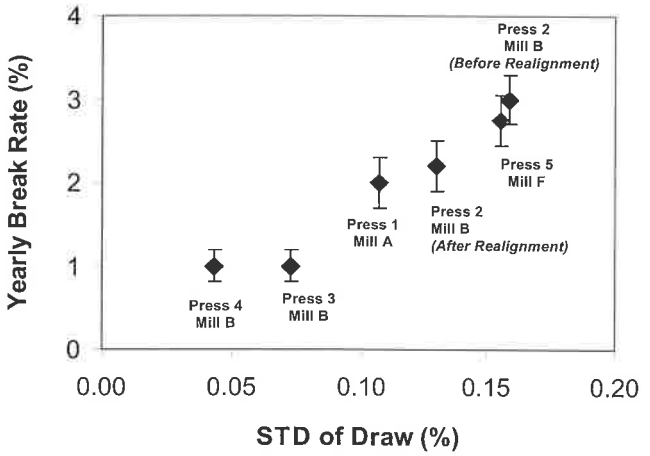


Figure 12: Web break rate vs. draw variation

3.11 A case study

In pressroom 2, the draw variation was much higher than the other pressrooms. It also had a higher web break rate. The frequency analysis showed that about 30% of the draw variation is related to the dancer roll, which was found to be not properly aligned. After the realignment, the draw variation was reduced (Figure 13). The pressroom later confirmed that the break rate was also reduced from 3% to 2.2% based on six months of web break statistics after the realignment.

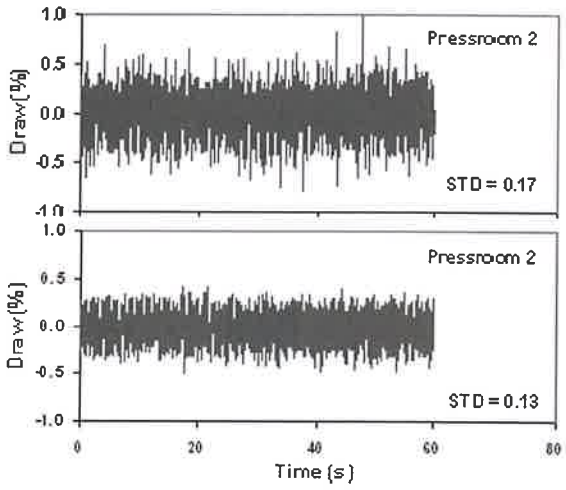


Figure 13:
Draw variation before (a) and after (b) realignment in pressroom 2

4. Conclusions

High frequency draw variations in five offset newspaper pressrooms were quantitatively characterized using the technique of Laser Doppler Velocimetry. The draw variation is controlled mainly by the pressroom conditions and operation. For example, at press start-up and stop, the draw variation can reach a value of nearly 1%, which is close to the critical value for generating web breaks. Using frequency analysis, we showed that draw variations could be related to press-related variables. The contribution of the paper to the tension variation is rather small. However, paper roll out-of-roundness can have a measurable effect on draw variation. Finally a correlation was found between the pressroom tension variation and web break rate, demonstrating the importance of better monitoring and control of press conditions in reducing web breaks.

Acknowledgements

The authors would like to thank Paprican's Member Companies and the pressrooms that assisted us in carrying out the pressroom trials and provided information on printing press and web break data.

References

1. Kamanga, H., *One in a 1000 - Canadian newsprint mill meets Japanese quality standard*, Paper Technol. 35:10, 16 (1994)
2. Snider, E. H., *Why does the web ever break*, Pulp and Paper Canada 80:T-238 (1979)
3. Adams, R. J. and Westlund, K. B., *Off-line testing for newsprint runnability*, 1982 International Printing and Graphic Arts Conference, CPPA, Montreal, 13
4. Uesaka, T. and Ferahi, M., *Principal factors controlling pressroom* breaks, Proceedings of the 1999 Tappi International Paper Physics Conference, Tappi Press, Atlanta, 229 - 245
5. Moilanen, P. and Linqdvist, U., *Web defect inspection in the printing press - research under the Finnish technology program*, Tappi 79(9): 88 - 94 (1996)
6. Page, D. H. and Seth, R. S., *The problem of pressroom runnability*, Tappi 65:8, 92 (1982)
7. Uesaka T., Ferahi M., Hristopulos D., Deng N., and Moss C., *Factors controlling pressroom runnability of paper,* The science of papermaking, 12th Fundamental research symposium, Oxford, UK, 17-21, Sept. 2001, 2:1423
8. Epton, J. B., *Pulsation and vibration studies at the wet end of a paper machine*, Paper Technol. Ind. 18, no. 4: 114-117 (April 1977)
9. Meinander, S. and Marttinen, T., *Measuring of web tension using contactless tension meter*, Graphic Arts in Finland, 11:34 (1982)
10. Larsson, L. O., *What happens in the press to cause web breaks?* Pulp and Paper Canada 85:T249 (1984)
11. TSI Incorporated, *LaserSpeed 1100, Speed and Length Measurement System, Instruction manual* (2001)
12. Deng, N., Ferahi, M. and Uesaka, T., *Press Room Runnability: A Comprehensive Analysis of Pressroom and Mill Database*, Proceedings of PAPTAC, C: 217 (2005)

Extended operating maintenance model for modern printing machines

Csaba Horvath[1], Zoltan Gaal[2], Katalin Kerekes[3]

[1] Nyomda-Technika Kft.
H-4027 Debrecen, Boszormenyi ut 6, Hungary
E-mail: csaba.horvath@nyt.hu

[2] University of Pannonia, Department of Management
H-8200 Veszprem, Egyetem ut 10, Hungary

[3] Alfoldi Nyomda Zrt.
H-4027 Debrecen, Boszormenyi ut 6, Hungary

Abstract

The authors outlined an extended model to examine the modern printing machines' unexpected breakdowns. They had been analisyng the different downtimemes for years. The results of the research helps to organize the pro-active maintenance at the graphic arts industry.

Keywords

breakdown, operating of printing machines, predictive and pro-active maintenace

1. Introduction

Maintenance techniques have changed over time from correction (breakdown) to prevention to prediction and pro-active continuous improvement. Effective maintenance is a series of progressive steps to improve operational effectiveness and the key step in this process is the transition of pro-active working. Companies that optimize their maintenance select and combine the techniques that match the needs of their equipment and operations. Moving up the maintenance stairway requires a planned approach that brings together the right procedures, tools, training and the knowledge the feature and history of our machines' breakdowns.

2. The objectives of the research

The results of authors' survey - covering 25 leading Hungarian printing offices - suggest that the major cause (46%) of maintenance issues is events of unexpected breakdowns. Consequently, the high ratio is the most influential factor of the design and management of maintenance tasks. The objective of the research is to critically map and discover the characteristics of unexpected breakdowns of printing machines in order to facilitate proper maintenance management.

3. Research methods - Operating maintenance model

Despite the possible big differences between printing machines we treat them with a united approach based on their fundamentally common characteristics. One of the major reasons for the synthesis originates from maintenance practice. Generally, the printing offices perform the maintenance duties with staff small in number. Consequently, there is a little chance to gain special knowledge and subdivide the maintenance approach and practice. The machines, which are different in structure and technological tasks, have a lot of common characteristics from the operational and maintenance point of view in case of printing office applications, which makes the united approach acceptable.

The technological elements of modern printing machines unite two equally important operations. The major operation, which performs informational types of formation on the product, is based on a highly accurate transmitting operation of the processing material (mostly paper). Therefore, the input and the output units are

very important elements of printing machines. These elements ensure the assembly of machine systems. Moreover, if the bigger systems were divided into elements we would always get division three, in the model. The units of operation, management and supply set the same claims up for the technological units regarding their structural form, complexity and especially their maintenance requirements.

The authors outlined a model (*Figure 1*) to examine the unexpected breakdowns of modern printing machines. The model reflects the general structure of printing machines, which is needed to analyse the features of maintenance and maintenance management. The modeling analysis focused on various types of downtimes of 65 different printing machines representing the previous, current and future generations.

The data of unexpected breakdowns were derived from an extensive period of time .

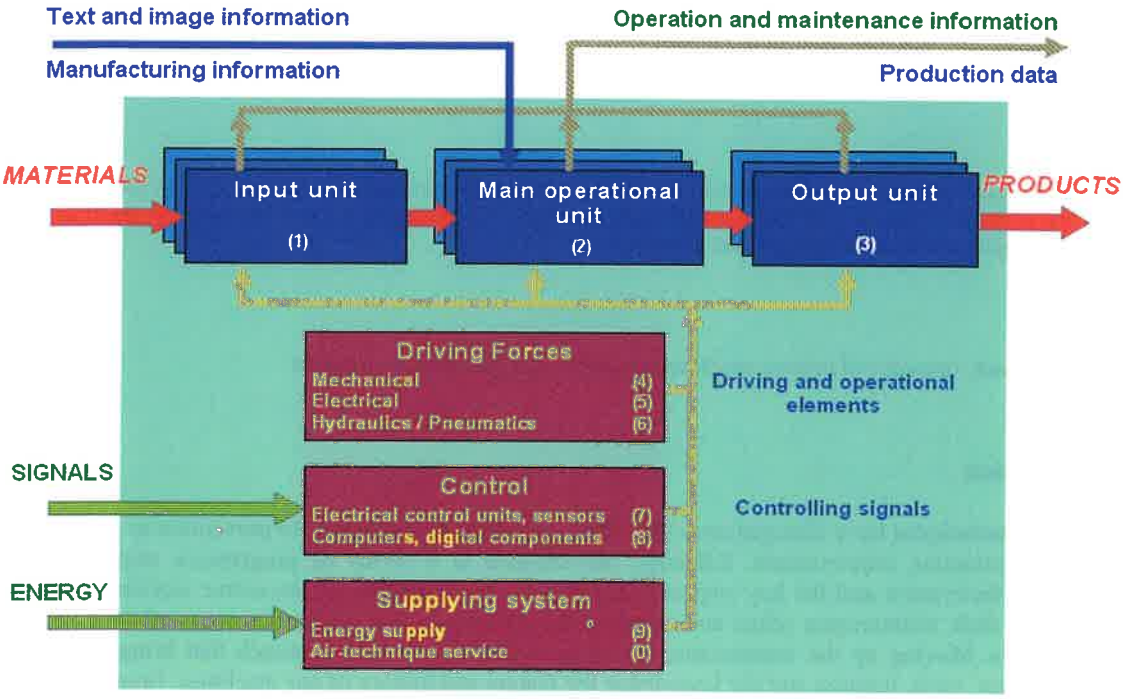


Figure 1: Extended operating maintenance model for the printing machines

4. Maintenece features of printing machines

While providing analysis for the typical features of the troubleshooting and detailed information of repairing operations, the results of the researches outline the maintenance characteristics of the modern printing machines' unexpected breakdowns.

The similarities between the manufacturing processes, raw materials and products of printing machines result in similar defective, corrective and maintenance features, which should be considered during management and organizational tasks. Therefore, thoroughly analyzed those sources of faults and damaging processes, with which we struggle during the operation of printing machines.

The authors collected data on unexpected breakdowns of printing machines for a long period of time at Alfoldi Printing Plant Plc., Hungary's largest book printing plant. A computer-assisted system could continuously record the basic data of the important processing machines. The historical datasets were set as the starting point for our analysis. The continuous data collection was carried out on the most important processing machines of Alfoldi Printing Plant Plc. During the monitoring the machines were replaced from time to time following the technological development. We monitored 65 printing machines. These represent the previous, current and following generations. Their age varied between 1 and 27 years and 22 completely new machines were purchased during our monitoring. Every machine was operated at a specific site, the centre site of Alfoldi Printing Plant.

The data of unexpected breakdowns what they used are from a wide period of time (data of 17 years of full operation between 1988 and 2004).

The extent of generalization based on the characteristics of printing machines might obviously raise a few questions from the reader. The printing machines and the relatively complex technology of Alfoldi Printing Plant and their loading give an extensive cross-section of today's typical printing machines. It was a limiting factor that there were only a few similarly detailed and accessible historical databases even for a shorter period of time. However we could make a comparison with the data of similar Hungarian printing plants; like Szikra Lapnyomda., Revai. and Petofi Printing Plant. The data on downtime and reparation time showed similarities with the calculations from our database.

Table I shows the major conclusions and the calculated characteristics. The 65 printing machines ran nearly 1.7 million operating hours, while 58317 maintenance events originated from unexpected breakdowns were recorded. The reparation of the machines caused more than 105,000 operational hours of dropout in the production and more than 130,000 reparation hours.

Table I: Most relevant data characterizing the unexpected breakdowns of printing machines (Examination period: 1. January 1988 - 31. December 2004)

The calculated mean values	**Mean**	**Standard deviation**
Restoration time	**1.80 hours**	0.47 hours
Reparation time of a breakdown	**2.24 hours**	0.54 hours
Characteristic data of printing machine		
Operational time in a year	**2 883 hours**	**617 hours**
The expected number of unexpected breakdowns during the operational period (rounded values)		
yearly	**87 occasions**	**24 occasions ***
monthly	**7 occasions**	**3 occasions ***
weakly	**2 occasions**	**1 occasions ***

* Rounded values for the easier understanding

The development of maintenance efficiency obviously has a great impact on unexpected breakdowns. The change in average values during the past few years show a slightly decreasing tendency as shown on *Figure 2*, conforming that the maintenance efficiency has also improved at Alfoldi Printing Plant. The slowly changing tendency of downtimes however proves that the fundamental maintenance characteristics are originated from structures and technological conditions. These are independent from the quality of maintenance. The number of machines used after 2000 did not modify the average values of downtime and reparation times significantly.

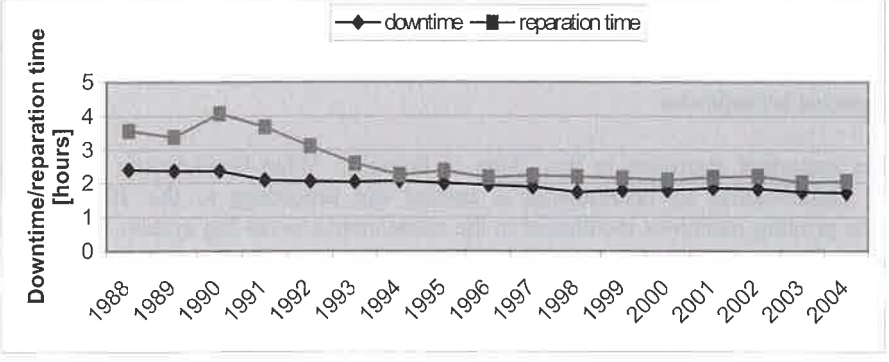


Figure 2: Time dependence of the average downtime and reparation time

The data also shows that the maintenance characteristics of pressing and bounding machines don't differ significantly. The values (shown at *Table II)* confirm the correctness of the principle; these should be treated together, like I haven't distinguished them in the maintenance model either.

Table II: Characteristics related to the troubleshooting of unexpected breakdowns for different types of printing machines

Calculated mean values	Pressing machines	Bounding machines
Time of troubleshooting:	*1.84 hours*	*1.77 hours*
Reparation time of a breakdown:	*1.97 hours*	*2.38 hours*

The unexpected breakdowns of printing machines are quickly reparable; these generally require small maintenance events. The downtime, which is not more than two hours, caused by operational failure is more than 80 %, which generates more than 50% of this kind of troubleshooting. The originated reduction of losses requires concentration to details and predictive organization. The relatively low average value might just well have a great influence on the future developmental concepts of maintenance systems. The relatively short reparation times typically contain several elements that are not actual professional work (reaction time, approaching the reparation scene, information transfer etc.). The relative frequency of values characterizing the reparation times of unexpected breakdowns is shown on a histogram of *Figure 3.* These data contain extremely important information for maintenance managers.

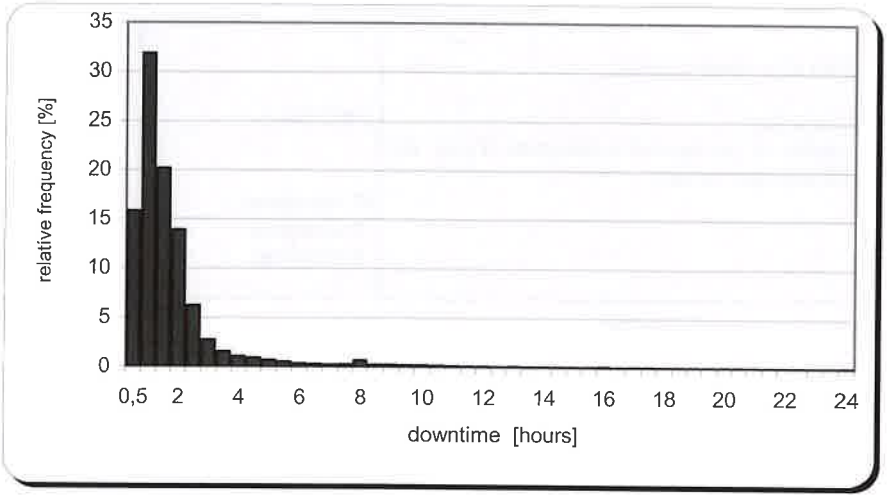


Figure 3: Histogram of the relative frequency of time needed to troubleshoot the unexpected breakdowns of printing machines

5. Typical breakdown of printing machines

While providing analysis for the typical features of the troubleshooting and detailed information of repairing operations, the results of the researches outline the maintenance characteristics of the modern printing machines' unexpected breakdowns.

There is another important approach in this chain of thoughts. What breakdowns are typical for printing machines? The classification of breakdowns is carried out according to the 10 big structural groups characterizing the printing machines mentioned in the maintenance event log system, based on the previously presented model.

Figure 4 shows the breakdown proportion of the distinguished parts.

The input and output units - the units of the above-mentioned transmitting machines - give the 39% of all breakdowns.

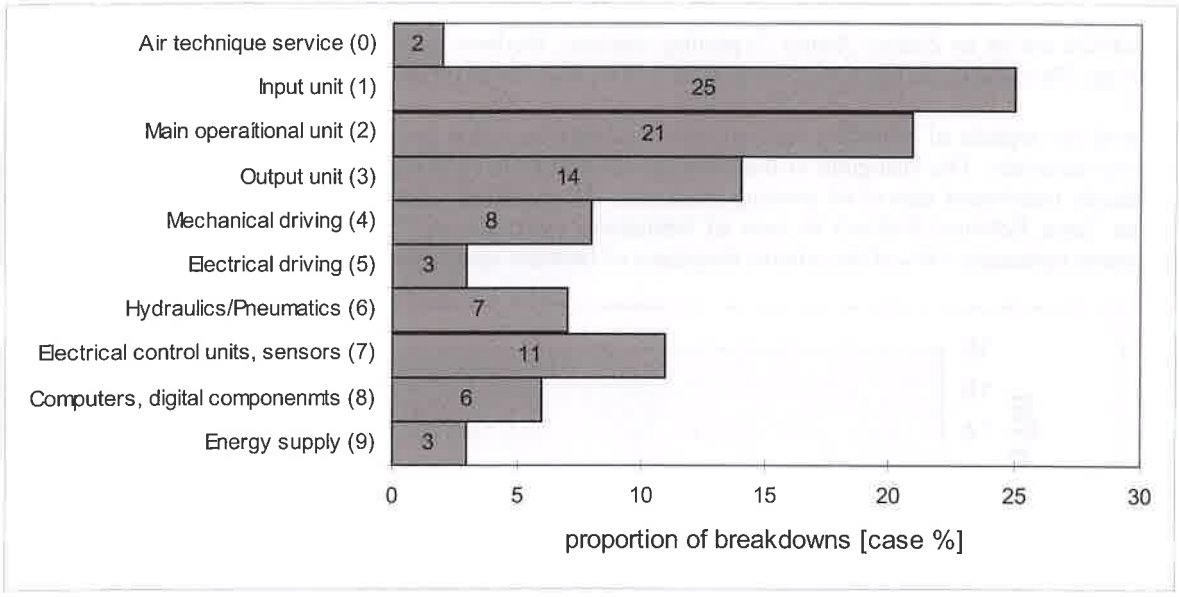


Figure 4: Distribution of unexpected breakdowns of printing machines between the given main units

There is a high occurrence of breakdowns due to failures of mechanical propulsion, sensors and beacons. Units performing technologically important operation have relatively smaller breakdown proportion compared to their importance in the machinery. The breakdown proportion of the electrical parts is 20% as shown on the diagram. The proportion of the electrical type of unexpected breakdowns is 29% including electrical faults of any part. The knowledge of proportions is especially important preparing for condition-assessment and modernization.

6. Reliability analysis

An adequately designed and managed historical maintenance database was needed to determine the above presented maintenance characteristics. In this part we wish to prove that the determination of breakdowns occurring in printing machines is possible through methods based on examples using databases. The methods of predicting breakdowns and the increase in reliability are also possible in the phase of application and operation.

The maintenance of high capacity production lines in the printing industry raises the issue of the application of maintenance-management from the reliability point of view. The user of several expensive machines (mostly magazine and newspaper printers) not only expects to have a fault-free system for a given time period, but also wants to have a lasting system complying with the instructions of operation, maintenance and reparation. This demand yet covers the complex understanding of reliability.

By definition reliability is the complex characteristic and the ability of an equipment that carries out a given function depending on its purpose and terms of operation for a given time period. It might include faultlessness, durability, and reparability respectively or all together [Tsang, 2002].

During the reliability approach of maintenance-management the type of maintenance strategy must be chosen based on the intended operational purpose, technical and economical characteristics of the machine, moreover the optimal tactical methods and activity system must be also determined. [19]

As a first step, the operational reliability of the maintained machines must be determined though. These reliability analyses are carried out on mathematical and statistical bases. It is only possible when possessing the number of maintenance events related to a given machine. We have only found one printing industry application of reliability theory in the literature. The authors [Malzhan, K. and Hofmann, S., 1972] published three summaries from their dissertation (Technical University of Dresden).

Maintenance strategy was developed for an offset roll printer following reliability theory basis. The actual analysis was carried out on an Zirkon Ultraset 72 printing machine. We have the historical data of 3 identical machines' event log. The distribution function of breakdown probabilities can be parameterised by Weibull distribution.

We took the aspects of reliability analysis into consideration when analysing the unexpected breakdowns of printing machines. The histogram of fault-free operation periods is illustrated on *Figure 5* calculated from the previously mentioned data of 65 printing machines. The expected value of the fault-free operational periods (Mean Time Between Failure) in case of continuous operation is 75.25 hours. The last column of the histogram represents 16% of the relative frequency of faultless operational periods exceeding 168 hours.

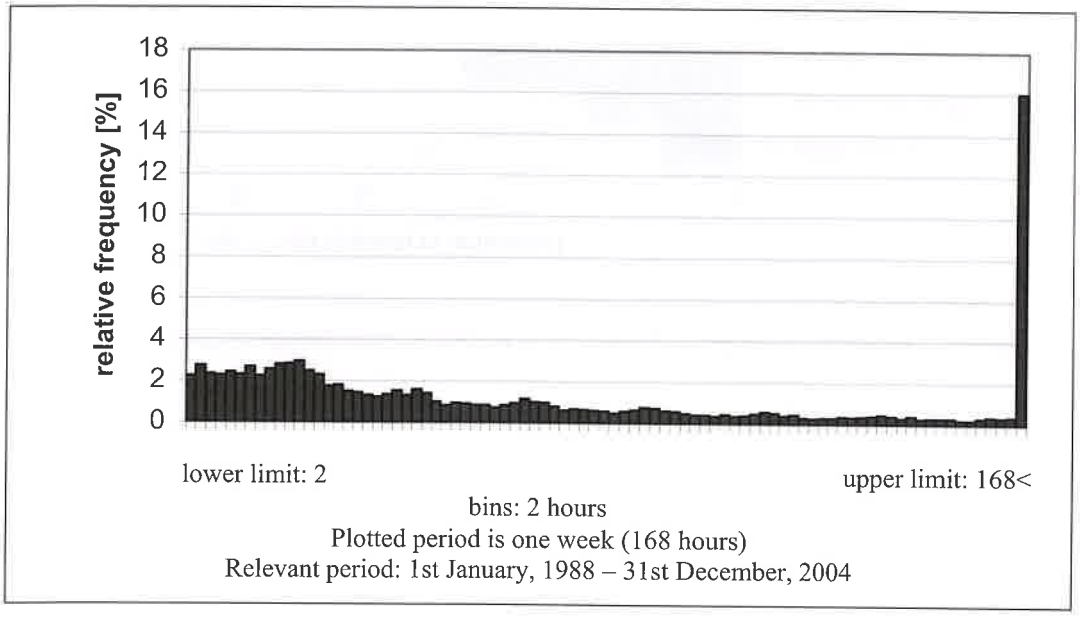


Figure 5: Histogram of relative frequencies related to fault-free operational periods of printing machines

The existing historical databases allow us to develop reliability models for several types of printing machines. Our main purpose was to assemble a toolbox of maintenance management, so we only presented the new ways of development after processing the results. The actual application of reliability analyses can only be expected after the wide use of computer-assisted systems, which we think is going to be one of the major professional challenges of future.

7. Process integration efforts

The data provided by the machine monitoring system at Alfoldi Printing Plant allow us to explore the connections between operation and maintenance.

The experts of maintenance have a natural human relationship with the workers of the plants due to the smaller plant sizes of the printing industry. The routine and experience many times bridge over the failures, which occur due to unexplored correlations. It is essential for the maintenance management to clarify the reasons and the time periods of high occurrence of reparations and it is also important to know the time period and location of low occurrence of reparations.

The following analyses show that the breakdown events don't just depend on the technical condition of machines. Specific time dependence can also be recognised.

We analysed the unexpected breakdowns of the above mentioned 65 printing machines of Alfoldi Printing Plant during the given time period, and we also analysed the distribution of the resulting downtimes for a working day.

The results of the analyses are illustrated on *Figure 6.*

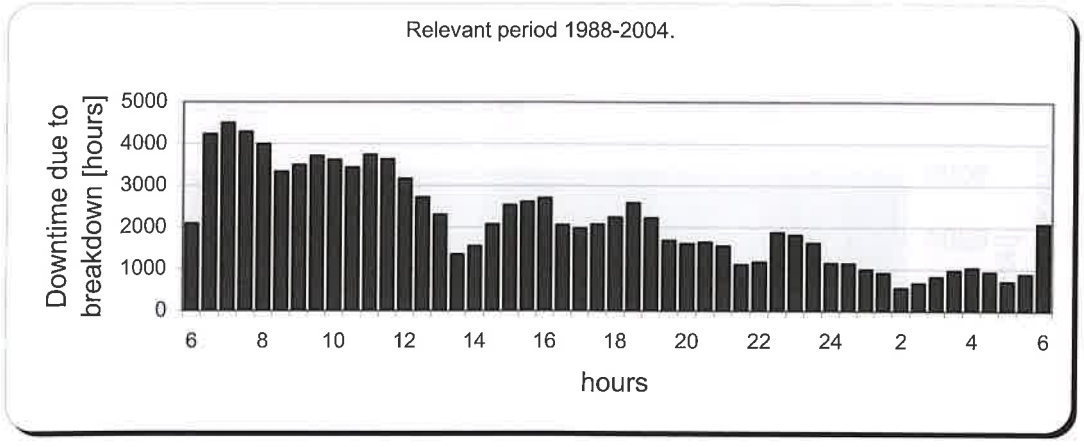


Figure 6: Daily distribution of downtimes due to unexpected breakdowns

There is a fundamental correlation in the number of operating machines. The proportions of the operating machines in the analysed period were the followings: 72% in the morning shift, 54% in the afternoon shift and 31 % in the night shift. The proportions of downtimes reflect nearly the same result. While the proportion of operating machines hardly changes, a well-observed pulsation occurs (in the first and second halves of the shifts) in the downtimes.

This phenomenon is a bit better observable on *Figure 7*, where the probability of downtimes due to the breakdown of at least one printing machine out of 65 during a day is plotted. In this case the way of calculation was the following: we related the data to operating machines at a given time. Therefore, the probability of downtimes related to breakdowns is independent of the number of operating machines. It is observable that the proportions of reparation needs in given shifts are different but not in a bigger extent. The critical time period is the beginning of morning- and nightshifts. The double hump or maximum peaks clearly appear in the 2 - 3rd and the 5 - 6th hours of each shift. It is important, without further analysis, for the maintenance managers to know these results for the sake of uniform loading of the workers and for the requirements of the reparation.

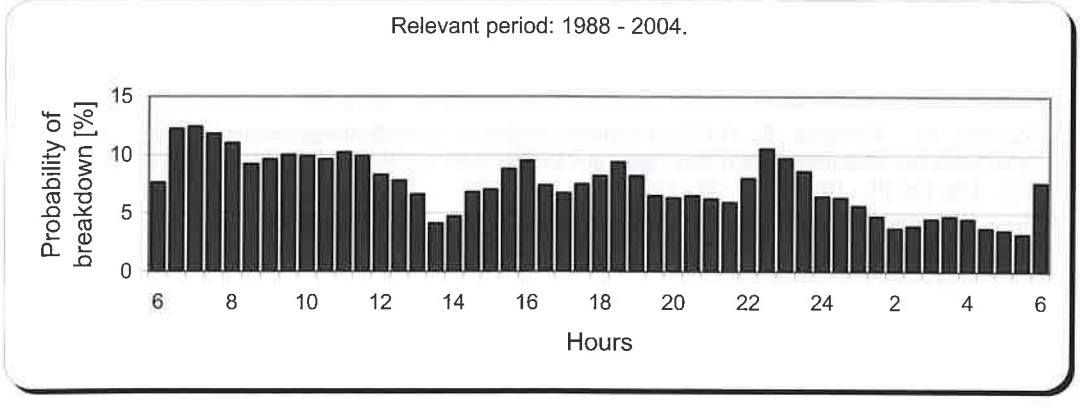


Figure 7: Frequency of downtimes due to the breakdown of at least one printing machine during a day referring to the operation of 65 printing machines

It should be also informative to carry out an analysis on each working day of the week, as shown on *Figure 8.* The tools of work psychology can explain the low breakdown rate in Monday mornings and Friday evenings. It is well observable that the week starts with reparations and the number of breakdowns is relatively high even in the second shift. The operators want to "bring a good machine together" in the beginning of the week. The number of breakdowns, after the reparation, during the week is continuously decreasing. The Friday morning is the "time of preparation" for the weekend overtime, but that night, if it is possible, they don't bother with reparations.

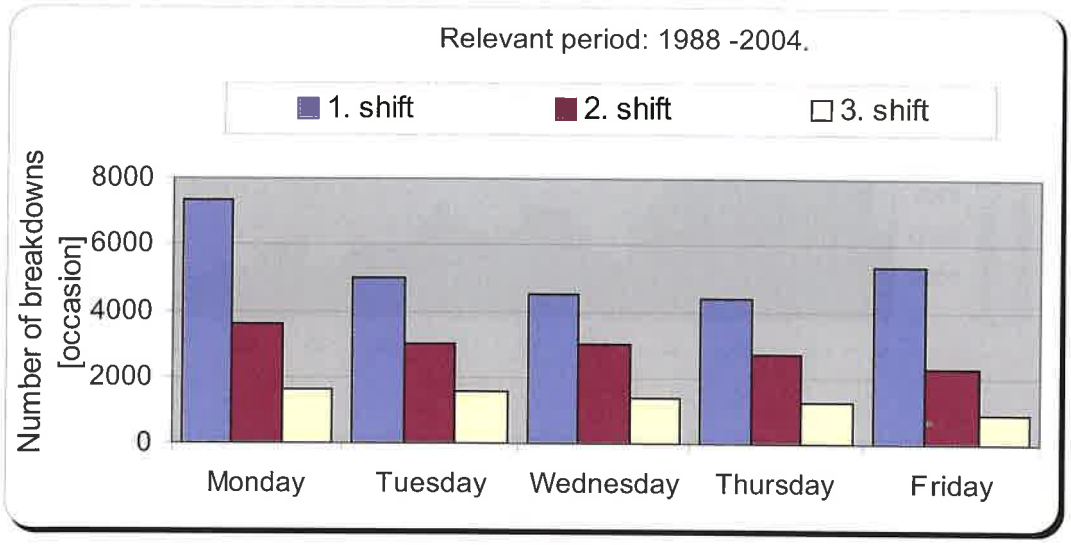


Figure 8: Distribution of unexpected breakdowns projected to working days of the week

The proportions, the demands of afternoons and nights during a week, the occurrence and the handling of demands are also useful information for the maintenance manager.

8. Conclusions

For maintaining the productivity of printing machines, the detailed knowledge of relations between failures is crucial. Aversion of unexpected breakdowns generally requires short/reactive reparative action. The knowledge about the typical failure rates of major parts of printing machines is the fundamental pillar to apply pro-active maintenance management.

References

1. Claypole, T. - Wells, N., (2005), Productivity Maintenance in the UK Printing Industry - Final report, Vision in Print, March 2005, p. 84 - www.visioninprint.co.uk
2. Gaal Z., (2007), Karbantartas-menedzsment, Pannon Egyetemi Kiado, p. 236
3. Malzhan, K. - Hofmann, S., (1972), Ermittung optimaler Instandhaltungstrategien für polygrafischen Maschinen und Maschinenfliessreihen Papier und Druck, Teil I. - 7/1972, p. 100 - 101, . Teil II. - 9/1972, p. 133 - 136, Teil III. - 10/1972, p. 149 - 152
4. Printweek, (2005), Best Practice: Maintenance, Vision in Print, December 2004, p. 24 - www.visioninprint.co.uk
5. Tsang A., (2002), Strategic Dimension of Maintenece management, Journal of Quality in Maintenance Engineering, 2002/1, p. 7 - 39
6. Web Offset Champion Group, (2002), Productivity Maintenance - how to run longer, leaner and faster, p. 33

Removing the constraints in publication printing - a potential paradigm shift

Anders Bjurstedt

Bjurstedt Management Consulting AB
Karlavägen 1, SE-114 24 Stockholm, Sweden
E-Mail: anders.bjurstedt@bmcab.se

Abstract

During the last decade, there have been many changes in the European media market. In particular, during the last 2-3 year, advertising money has been reallocated in many national markets from the traditional printed media to the web. This will also undoubtedly affect the publication printing markets, as has been pointed out by both Bjurstedt [2006] and Leckner [2007].

Although the manufacturing cost for the process has normally been the deciding parameter when choosing a printing process, the technical work-flow process is equally important. The latter factor has not previously been taken into account, but it was shown by Bjurstedt [2007] that it is a very important aspect when determining the minimum average print run (MAPR) of any printing process.

The MAPR is dependent only on the turn-around time or cycle time for a set of printing forms, either offset plates or gravure cylinders, because no printer is willing to have idle press room units waiting for new cylinders or plates to be delivered. Modern CTP devices (Computer-To-Plate) have very short turn-around cycles for eight plates in relation to gravure cylinder processing (for the same number of processed pages), and this enables the user-printer to produce very short runs if the market so demands. This makes commercial web-offset almost independent of the plate-making process in this context.

This paper analyzes the various parameters in the gravure cylinder process and what can be done to significantly enhance the turn-around cycles. If the turn-around cycle and costs (calculated per m^2) comparing a gravure cylinder and a web-offset plate would become very close, it would constitute a paradigm shift in the publication printing industry.

Keywords

Commercial web-offset, gravure cylinder engraving, offset plate-making, publication gravure, the minimum average print run (MAPR)

1. Introduction

During the last decade, there have been many changes in the European media market. In particular, during the last 2-3 years, advertising money has been reallocated in many national markets from the traditional printed media to the web. This will also undoubtedly affect the publication printing markets, as has been pointed out by both Bjurstedt [2006] and Leckner [2007]. The larger publication gravure printers have been suffering from lower volumes and shorter runs for a considerable time, but those printers working in the smaller circulation segments of the market seem to perform better.

All forecasts put forward by larger publishers and catalogue producers state that the market is becoming more and more fragmented. Any publication printer must be able to handle shorter runs with high demands on both print quality and much tighter turn-around schedules. The needs and demands of the customers have to be very carefully studied and comprehended by all publication printers.

In a previous investigation by Bjurstedt [2007], some ideas for improving the Minimum Average Print Run (MAPR) for publication gravure printing were put forward. The object was to find solutions where gravure cylinders could be processed so fast that the MAPR would be almost equal to that of commercial web-offset. This means that in real terms the turn-around cycle should be equal (or very close) to the make-ready process time in the press room. Contemporary studies indicate that investments for offset plate-making equipment is less than 15-20% of that of cylinder processing comparing similar volumes and sizes. Yet, the final factor to consider for a publication printer is the financial aspect when deciding on alternative equipment.

To overcome some of these constraints, Puri [2001] suggested the use of service providers (trade houses) for procuring and processing gravure cylinders in publication printing. This concept has not been used, with very few exceptions, in the European markets because of timing and other logistical constraints. If such services houses , using the most modern engraving equipment in combination with new light weight cylinders, improving both external and internal logistics and handling, the turn-around cycle might nevertheless be short enough even for the most topical products.

If some publication printers were to share such a service house, the volumes could be large enough to give piece costs (calculated per m2) very close to that of a lithographic plate. The marginal cost (per m^2) of producing a gravure cylinder is quite low, only about 15 - 20% of a lithographic plate [Bjurstedt 2005], because the marginal cost of processing offset plates can never be lower than the price of the plate itself. This might lead to a second chance for this concept, provided that the economic and time factors are taken care of.

2. Research methodology and concept

2.1 Methods in collecting data from the industry

The research methodology used in this paper is both quantitative and qualitative, based on a survey approach extended with personal interviews. The interviewees have been selected among the most leading publication printers and suppliers to the industry. Today, there are not more than about 6 - 8 leading suppliers to the industry (plate and printing cylinder processing equipment manufacturers). In 2005-2007, a number of European publication printers and most of the suppliers in plate and cylinder making equipment were approached and some of the results were published by Bjurstedt [2005, 2006 and 2007]. Nevertheless, the data used in this paper have not been previously published. A few complementary interviews with the suppliers in plate- and cylinder-making equipment were conducted during Drupa 2008 - probably the most important exhibition in the printing and allied industries - held in Düsseldorf between May 29th and June 11th. The data collected have been used in several simulation models developed by the author.

2.2 Objectives of the research

In determining the factors which are important when using a particular publication printing method, wether commercial heat-set web-offset printing or publication gravure, it has been customary only to take into account the number of copies. Recent research [Bjurstedt 2006, 2007] has shown that there are other factors to consider, i.e. the physical size of the signatures, the choice of paper grade and the number of pages in the signature.

Another important factor, very often neglected, is the technical work-flow process controlling the turn-around time or cycle time for a set of offset plates or gravure cylinders. The turn-around cycle for processing eight cylinders or offset plates determines the MAPR in any printing process, because no printer is willing to have idle press room units waiting for new cylinders or plates to be delivered. Modern Computer-to-Plate (CTP) devices are supposed to have a very short turn-around cycle for eight plates in relation to gravure cylinder processing (for the same number of processed pages) allowing the user-printer to produce very short runs if the market so demands. This constitutes flexibility in commercial web-offset and it makes the user almost independent of the plate-making process in this context.

2.3 Research questions

The research questions in this paper are as follows:

- If the turn-around cycle is shorter than the make-ready process in the press room, what is then the MAPR?[1]
- May the turn-around cycles for the processing of publication gravure cylinder be drastically reduced, to an extent that the first research question also would be relevant?

[1] However, there might be an economical constraint, which limits the length of the print run and/or the choice of printing method.

2.3.1 Delimitations

This work is an investigation of the publication printing industry in Europe. Previous work has been concentrated to members of the European Rotogravure Association, but this is no longer the case. It has, nevertheless, become apparent that there is very little scientific literature available related to the industry. Some of the references have been extracted from the general printing industries, because they are close to publication printing

3. Results

3.1 Background

Web-offset plate making has made great strides in developments during the last few years. One reason is the rapid growth of the installed base of commercial web-offset presses in Europe [Bjurstedt 2007], in particular wider, faster and hence more demanding press characteristics. Plates for commercial web-offset are of course also used in other lithographic applications, such as sheet-fed offset and newspaper printing. This means that the total market for these offset applications can be counted in many thousands of companies in Europe alone, whereas there are only about 50 gravure plants in operation in Europe (run by 20 different companies) having about 250 - 275 engraving units (in addition there are about 25-30 service houses for packaging applications in Europe).

The supply of publication gravure cylinder engraving and plating equipment is limited to two competitors [Bjurstedt 2007].

The European market for CTP-devices has become very competitive during the last 10 - 12 years, when the first installations were made by Creo and Scitex (since then both companies have been bought by Kodak). Agfa recently announced that its American manufacturing of CTP-devices will soon be closed, and all Agfa models will be outsourced to a third party. During the Drupa exhibition, it was announced that Dai Nippon Screen (DNS) will be manufacturing the Agfa CTP product range. Fuji film will also outsource its larger CTP products to DNS making this company one of the largest manufacturers, in strong competition to Kodak.

DNS announced that it will shortly ship its 12.000th CTP device, and earlier this year Kodak announced its 10.000th shipment. There are no public figures available concerning the total CTP market, but Kodak and DNS claim each that they have about 25 - 30% of world market. However, in Europe most manufacturers suggest that the market is saturated, and new sales are based on refurbishing and/or expansion units only. The market for very large CTP-devices (exposing plates of 32 A4 pages or more) is concentrated to only three companies, Kodak, DNS and Luescher AG (Switzerland). However, in the market for smaller sizes there are at least 5 - 6 additional companies worldwide.

3.2 CTP devices and offset plates

The laser technology of CTP-devices is closely connected to the offset plates available, and for larger runs (150.000 - 200.000 impressions) thermal plates (some preheated) are dominating. Baking (post-exposure heating) is used with print runs up to a million impressions. Luescher AG, however, has recently launched a CTP-device which can expose standard UV-sensitive plates, and claims that such a device is profitable above 20.000 m^2 annually, because standard plates are 15 - 20% cheaper per m^2 than thermal plates. But, even UV-sensitive plates have to be baked for longer runs.

The trend in small-size offset plates and newspapers plates is moving towards process-less plates. However, these plates are presently limited to some 50.000 - 100.000 impressions, and are more expensive than both thermal and standard plates. One reason is that these plates are supposedly environment-friendly, because there is no developer/replenisher in the process to be taken care of. Digital water-less plates have noticed a come back, in particular in newspaper production, but also for small-size sheet-fed offset printing.

This means that these plates will be cut perpendicular to today's standard grain. Bending these plates in the wrong direction might become a problem, and one manufacturer stated that these plates have to be thicker (40 μm) than the present standard (30-35), and this accordingly leads to a higher price per m^2.

Gravure technology

There was very little news about publication gravure engraving and plating systems at the Drupa exhibition. The equipment for the cylinders applicable for publication printing is very large and heavy and, hence, not suited for exhibitions. Nevertheless, Hell Gravure Systems (HGS) showed one K6 (multi-head engraver), and claimed that the calibration procedure was reduced by 50% (from 2 minutes per head to one minute). HGS seemed to be concentrating on the packaging market, showing an upgraded mechanical engraving unit as well as a laser engraving device (Cellaxy) and the whole range of plating equipment.

Max Dätwyler AG was also concentrating on the packaging market with a complete range of engraving and plating equipment including overhead cranes connecting the various devices. Those interested in publication gravure laser engravers were invited to its closest customer, bauer druck in Cologne, for private visits. The latest developments in using alternative alloys for gravure cylinders were not, however, shown but they were discussed with selected customers. The enhanced cycle times when using these new processes were discussed in great detail (see below).

Table I shows a summary of the cycle times when using the most modern equipment for producing a 32 page A4 format (approx 2.5 m^2 plate/cylinder size) printing form in both gravure and web-offset. It should be noted, however, that the cycle times for mechanical engraving are improved by approx. 10% because of a new and faster calibration process according to information given at the Drupa exhibition by Hell Gravure System.

The cycle times have been calculated using a simulation model developed by the author, allowing ample slack between the operations. This is of course mostly applicable to the gravure process where rather heavy cylinders have to be moved between each of these by means of an overhead crane system. Web-offset plates are, even with larger sizes, light but sensitive to scratches. These plates can easily be moved on conveyer belts from the CTP-device to the developing, further to the baking (when necessary) ovens and plate-bending units.

Table I: Update of the lead-time for a 32 A4 page printing form

Processes (incl. developing/gumming of plates degreasing/chromium plating/polishing gravure cylinders)	***Cycle time for 8 cylinders/plates (hrs)***
CTP - web-offset - dual lines	< 0.5
Mechanical engraving - 7.5 kHz - dual lines	5.0 - 5.5
Mechanical engraving - 7.5 kHz - three lines	4.5 - 5.0
Mechanical engraving - 7.5 kHz - four lines	3.5 - 4.0
Direct Laser engraving - dual lines	3.5 - 4.0
Direct Laser engraving - three lines	3.0 - 3.5

Sources: Hell Gravure Systems, Max Dätwyler AG, Agfa, Kodak, Fuji Film

In Table I it is obvious that publication gravure printers are facing a serious problem ith regard the achievable MAPR. There are several bottlenecks in the cylinder processes, and one obvious bottleneck is that the K-cylinder (text/LW) must be engraved with a higher resolution (about 100-110 # screen to avoid ragged text and head-lines) than the colour cylinders (70 # screen) with proportionally longer engraving times. Yet another bottleneck is the current standard procedure of chroming all cylinders regardless of the print run.

Chromium plating adds three more processes, i.e. the post-engraving process includes degreasing, chromium-plating and finally polishing to achieve a smooth wiping surface. In this context it should be added that all plating is basically process-dependent, i.e. the design of the plating bath, immersion, electrolytes etc. determine the cycle time, whilst all other processes, such as engraving (both mechanical[2] and laser) and mechanical (turning and polishing/honing) processes are area-dependant (in both directions, length and circumferential, i.e. how many pages are imaged on the cylinder). Similarly, the exposure and development of offset plates are also area-dependent.

[2] In mechanical engraving one engraving head is used for each page (landscape) around the cylinder which constitutes a semi-area dependent process (however, the calibration process depends on the number of heads)

3.3 A new concept

Recent circulation statistics from FIPP[3] shows that about 95% of the European magazines have a print circulation of less than 500.000 impressions. Recent statistics [Bjurstedt 2007] from the German magazine market show that about 80 - 85% of all registered titles have a circulation of less than 0.5 million copies (the printed number of impressions, however, is about 25 - 30% higher because of returns from the sales outlets). Many leading suppliers are of German origin, i.e. solutions are developed for their home market and its needs. Germany is by far the largest magazine market in Europe, and what is happening in this market is of great importance for all other publishers and suppliers. Hence, an analysis of these numbers suggest that it is not quite rational to process cylinders which may withstand many millions of revolutions (= impressions) when you are only printing maybe 0.5 million or less.

Many gravure printers up to the end of the 1970's were still etching, and some preferred printing on copper surface for small to medium runs (< 200.000 impressions) and for products which were not quality-critical for the publishers. The doctor blades in use at the time were sharply ground which occasionally caused streaking and other quality problems. Chromium-plating of gravure cylinders became standard procedure in the early 1960's and became widely in use in a few years' time. When the electromechanical engraving was introduced in the early 1970's, the copper surface had to be much harder than before (otherwise the cutting properties are not suited for copper), and, hence, chromium-plating was unavoidable.

Laser engraving methods were investigated by ERA[4] already 50 years ago, but the result of the investigation at that time was negative. Unfortunately, no further investigations of alternative metals or alloys were conducted. Alternative attempts to improve both the quality and turn-around engraving times were made by Dr Hell (the origin of Hell Gravure Systems) with the Electron Beam Gravure (on copper cylinders) and Crosfield Electronics Ltd with Lasergravure (on epoxy surfaced cylinders) in the 1980's, but both failed for various reasons.

Not until the direct laser engraving on zinc was introduced almost 15 years ago, did a viable alternative to mechanical engraving become available. However, the zinc surface had to be chromium-plated to withstand the wear (zinc is softer than copper). This new combination has had a great success in gravure packaging applications with about 20 installations worldwide, because of the much improved printability of both halftones and text which is important in the packaging market. In publication gravure, however, the installations are fewer and only four companies (in total 8 engraving units are installed) have invested in this technology. They all report much improved printability and turn-around cycles in comparison with the conventional mechanical engraving technology.

Recent advancement in laser technology (single mode fiber lasers[5]) makes it possible to engrave both much faster (up to 100 kHz per head) and with a laser power up to 1.5 - 2.0 kW. These developments would make it possible to engrave on other metals or alloys than zinc, and to market a new process where the surface could withstand at least 500 - 600 000 metres of run length[6] without having to be chromium-plated. Ideally, the new process would be a Ballard skin[7] type which, after printing, could be stripped off and recycled. It is also very important that the post-engraving polishing/honing is kept to a minimum. For some time, various attempts have been made in this direction, one of which is marketed by Hell Gravure Systems (HGS) with the Cellaxy engraving unit, but only for packaging application. HGS is, however, using a solid chromium layer (40-50 μm) and claims that very little post-engraving polishing is needed. One of the disadvantages is that the chromium layer has to be chemically removed after printing, and yet another is that the engraving process is rather slow (0.8 m^2/hr) and hence not suitable for publication gravure printing.

A more promising alternative is currently being developed by Max Dätwyler AG. The new process (tests up to now have reached a 95% confirmation level) is based on a different metal, most probable nickel, although

[3] FIPP – Federation International des Presse Periodique (International Federation of Magazine Publishers) - publishes annual statistics from all member states

[4] In 1963, the European Rotogravure Association asked the Battelle Institute in Geneva to investigate the possibility of using laser for the engraving of copper gravure cylinders

[5] Fiber laser, i.e. manufacturers such as IPG Photonics Corp. and SPI Lasers (information from corporate web-sites).

[6] As gravure cylinders may vary in circumference, a meter in length is more appropriate (500 000 meters corresponds to 580 000 revolutions for an A4 format (landscape size)

[7] Ballard (named after the American inventor Ernest Ballard, who invented this method in the 1920's) skins are today common practise among European gravure printers

not yet 100% confirmed by MDC. Nickel is already in use today as a very thin separation layer between the solid copper base cylinder and the copper Ballard skin (plated to about 85 µm thick).

One of the main advantages of nickel would be if it could be applied as a Ballard skin but much thinner (40 µm) than the normal copper skin. Nickel is much harder than both copper and zinc, but it is a very expensive metal. Hence, a precise recycling process (as the Ballard process allows) is very important, otherwise it would not be economical to use. Further it can be assumed that the post-engraving polishing/honing processes[8] are of the same magnitude as after chromium plating (or preferable shorter). When using the new laser technology, according to my sources, the engraving time will be independent of the resolution chosen, which means that the K-cylinder (text and black printer) can be engraved at the same speed as the process colours (similar to CTP plate exposure where all plates in a four colour set have the same exposure time). With these important factors in mind, the same simulation model as in Table I has been applied on the new process - see Table II.

Table II: Summary of the new enhanced processes - 32 page A4 printing form

Engraving/polishing gravure cylinders - new process technology -	***Cycle time for 8 cylinders/plates (hrs)***
CTP - web-offset - dual lines (as comparison)	< 0.5
Direct Laser engraving - dual lines (as comparison)	3.5 - 4.0
Direct Laser engraving - three lines (as comparison)	3.0 - 3.5
Direct Laser engraving - **no chromium** - one line	3.0 - 3.5
Direct Laser engraving - **no chromium** - dual lines	2.0 - 2.5

Source: Max Dätwyler AG

The approximate marginal costs of materials for the different surface combinations in publication gravure printing can be computed, see Table III (the current world market prices for metals have been used).

Table III Marginal costs for 1 m^2 printing form (€/m^2)

Materials	***Net cost (approx)of materials (€/m^2)***
Copper and Chromium	2.5
Zinc and Chromium	0.8
Nickel	1.0
Nickel and Chromium	1.5
Offset plates[9]	8 - 12

The next to the last line in Table III suggests that for long runs (above 500.000 - 600.000 metres) Ni-plated cylinders can be post-treated like standard copper or zinc cylinders, i.e. chromium-plated. The marginal cost is twice the cost of zinc/chromium alternative but still cheaper than the present copper/chromium. Another advantage would be that a single new device has an annual capacity of processing cylinders (in a 24/6 usage, 24 hrs in 6 days) comparable with three lines using mechanical engravers, Table IV.

Table IV: Weekly capacity based on a 32 page A4 printing form

Processes	***Weekly capacity***
CTP - web-offset - dual lines	> 1.500
Mechanical engraving - 7.5 kHz - dual lines - chromium	180
Mechanical engraving - 7.5 kHz - three lines - chromium	270
Mechanical engraving - 7.5 kHz - four lines - chromium	360
Direct Laser engraving - dual lines - chromium	360
Direct Laser engraving - three lines - chromium	540
Direct Laser engraving - one line - **no chromium**	270
Direct Laser engraving - dual lines - **no chromium**	540

[8] The speed of engraving and polishing is area-dependent, but plating is only process-dependent.
[9] Depending on the type of plate (standard, thermal, process less etc.) and volume of sales.

It is evident from Table IV that the new process without chromium would give the publication printer a much needed price/performance boost in cylinder-making. The total investment cost is probably at least 35 - 50% less than that of the present equipment comparing similar volumes. With only two lines, almost all European publication gravure printers would gain sufficient capacity (approx 25.000 - 27.000 cylinders annually), and for those printers having print runs above the present limitations of 600.000 impressions, chromium plating may still be used. There are, of course, other advantages of the laser technology, and one option is the ability to match exactly the needs and/or minimize the cycle time by choosing a suitable laser frequency of the engraving head.

4. Discussion

A break-through in developing a completely new process for gravure cylinders would indicate a significant reduction in the number of processes and, not least, a significant reduction in the turn-around time for processing four or eight cylinders. With this new promising process, the turn-around cycle might come much closer to the make-ready time in the press room and hence allow the MAPR to be further reduced. Combined with a Double Ender (DE) gravure press [as described by Bjurstedt 2007] using only four printing units, this would allow a gravure printer to print any job he might find profitable.

A 64-page signature, however, has to be printed 8U (eight around in landscape mode) in gravure, whilst in commercial web-offset the available press configuration is 4U in portrait mode (or long grain). A modern DE gravure press might run 28 - 30 000 revs/h in 8U mode in comparison to the web-offset press which would run about 40.000 revs/h. The cycle time for a set of four cylinders using a DE - gravure press is shown in Table V.

Table V: Summary of lead-times for a set of four cylinders - 64 pages A4 (printing 8U in a DE gravure press)

Processes (incl. developing/gumming of plates degreasing/chromium plating/polishing gravure cylinders)	***Cycle time for 4 8U-cylinders and 8 plates (hrs)***
CTP - web-offset - dual lines (as comparison)- no baking	*< 0.5*
Mechanical engraving - 7.5 kHz – dual lines - chromium	5.0 - 4.5
Mechanical engraving - 7.5 kHz – three lines - chromium	4.0 - 4.5
Mechanical engraving - 7.5 kHz – four lines - chromium	2.5 - 3.0
Direct Laser engraving - dual lines 140 kHz - chromium	3.5 - 4.0
Direct Laser engraving - three lines 140 kHz - chromium	3.0 - 3.5
Direct Laser engraving - one line 200 kHz - **no chromium**	3.0 - 3.5
Direct Laser engraving - dual lines 200 kHz - **no chromium**	1.5 - 2.0

Note that the cycle time with the new gravure process processing four cylinders in 8U is shorter than that for eight cylinders in 4U, which makes it ideal for the DE-concept and with a considerable advantage in particular for short to medium runs up to 500.000 - 600.000 copies. (The other engraving processes with chromium-plating have cycle times which are almost identical for 8U and 4U). With a dual installation of the new faster laser engravers, the cycle time would be rather close to the make-ready in the press room, and a theoretical MAPR would be 40.000 - 50.000 copies. These numbers give publication gravure new and enhanced possibilities to be competitive on all print runs, from the small to the multi-million.

In terms of further enhancements, there are many more options available in the gravure cylinder process, because in offset plate-making much has already been accomplished. One remaining area for further improvements of offset-plates might be the current run length limitation of the process-less plate, which is still to be worked on.

In the gravure cylinder process many more options are available particularly with regard to choosing the optimum laser sources, such as going from pulsed lasers to solid state fiber lasers. These also have other advantages:

- further enhancement of the laser frequency (presently 35 kHz) to maybe 50 - 100 kHz.
- competition between laser-developing companies might improve the price performance of the laser sources.
- much longer MBTF (mean-time between failures) suggests lower maintenance costs.

- Much improved power ratio (ratio of laser output power to input of electrical power) suggests lower running costs - particularly important with rising energy costs. Today the rate is about 1:20 but new lasers may come to 1:5 or less.

Finally, the final process prior to printing is polishing/honing. With an optimized relation between the laser power and the properties of the metal surface, this process should be minimized with respect to process time and the use of consumables (honing stones etc.). Presently, in the simulation model, this process is as long as the engraving modes as both are area-dependent. This constitutes a real bottle neck in the cycle time for producing cylinders. Last but not least, much work needs to be done to find the optimum combination of the wiping conditions of the cylinder surface and the doctor blade.

5. Conclusions

A paradigm shift in the publication printing markets may be under way as defined by Kuhn [1962]. The developments described in this paper would be extremely important for the future of the publication gravure industry as well as for the only publication gravure press manufacturer now left on the market.

In commercial web-offset, the first research question is affirmative and the MAPR is equal to 1 (one) copy. It has been shown that the technical constraint concerning the run lengths is limited to the plate itself. The only limitations are the economic constraints with the relevant break-even levels (depending on the pagination and paper grades chosen).

The answer to the second research question can not, however, yet be affirmative. The present engraving processes are still way off. Nevertheless, as indicated in the Tables IV and V, there is certainly a strong potential for improvements to the present cylinder processing methods. Will it be possible to improve the gravure cylinder processing to such an extent that the MAPR levels for publication gravure are in the same order as that of commercial web-offset plate making? New developments in laser technology indicate that this may not be unlikely, but there is still a lot more work to be done as well as finding the optimum metal surface (which does not need to be chromium plated).

Developing a new alloy for use in publication gravure would also lead to further developments in light-weight cylinders. It is not technically impossible to produce gravure cylinders of 260 cm face width weighing maybe less than 1/3rd of the current design. At the Drupa Exhibition this year, shaft-less cylinders up to 200 cm face width and very low weight were shown. Low-weight cylinders would ease the logistics of cylinders, both internally and not least externally. This would also open up a potential structural change in the industry, such as housing third party suppliers of gravure cylinders to be located in the printing houses, and then allowing very short delivery cycles.

What strategies should a publication gravure printer use in order to survive in a most competitive European or North American print market? The printing variables in gravure are very few (when the cylinder-making process is optimized as it is when using laser- engraved cylinders) and the variations in print quality and/or print density are in general very low in comparison to those in lithography. It is a well-known fact that the mechanical construction of a gravure press unit is very simple in relation to the blanket-to-blanket web-offset unit. The flexibility in product format, however, makes the gravure press folder the most expensive part of a gravure press. Nevertheless, the DE publication gravure press has a very competitive price level compared to commercial web-offset presses made for similar formats and signature sizes. In some markets, the DE concept has other comparative advantages, such as low manning and low foot-print (if the press room size is a limiting factor). The gravure process has also other advantages such as very low waste and trimmings, and it may use low-cost paper grades and yet give superb print/image quality.

But, the question remains, does the publication gravure industry really want this to happen? The gravure packaging industry seems to be more entrepreneurial and keen on new technology with more than 20 Direct Laser systems installed (not to count the indirect Laser systems for autotypically etched cylinders with more 200 units installed world wide).

This paper has considered what could happen when and if these changes in technology occur; and it would constitute a real paradigm shift in the publication printing industry.

Acknowledgements

Author would like to thank all those companies who have actively been taken part in this study, and in particular many thanks to all the gravure and web-offset printers who have supplied data and most valuable input and commitment. Without their work it would never has been possible to write this article.

Finally many thanks goes to Hell Gravure Systems GmbH, Max Dätwyler AG, Agfa Sweden, Fuji Film, Sweden and Kodak Polychrome Graphics AB in Sweden for most valuable input and comments as well as in-depth technical discussions.

References

1. Bjurstedt, A., 2006. *Benchmarking gravure cylinders vs. web-offset plates*. Advances in Printing and Media Technology, Vol. XXXII, Zagreb, 2006, pp. 71 - 89
2. Bjurstedt, A., 2007. *Is there a future for the European Publication printing industry*? TAGA 2007 Proceedings, Sewickley, 2007, USA
3. Bjurstedt, A., 2007. *Gravure vs. Web-offset. A changing world in publication printing 1986-2006.* Doctoral Thesis, Royal Institute of Technology, Stockholm, Sweden
4. Leckner, S., 2007. *Is the media the message? The impact of digital media on the newspaper concept.* Doctoral Thesis, Royal Institute of Technology, Stockholm, Sweden
5. Puri, K. K., 2001. *Cost-Competitive, Short-Run, Narrow-Web Rotogravure for Publications*. TAGA 2001 Proceedings, Rochester, New York, USA
6. Kuhn, T. S., 1962. *The Structure of Scientific Revolutions*, University of Chicago Press, Chicago, USA

Appendix - Technical constraints in printing - some definitions

The Minimum Average Print Run (MAPR)

This is defined as the minimum average print run achievable without having idle press room units and it is only dependent on the lead-time for producing eight (or four) printing forms (plates/cylinders). Hence, the cycle time or lead-time for the image carrier can easily be defined.

Printing processes

There are basically two different printing processes available today. One is the traditional analogue process represented by lithography and gravure printing. Nevertheless, in these cases the prepress processes are basically digitally driven, although the image carrier cannot be changed once it has been imaged or exposed. Hence, without changing the printing form (plate or cylinder) the image cannot be changed. The digital printing process is totally digitized and every image can be continuously changed - totally or in part.

Analogue printing - lithography or gravure

The MAPR is dependent on the cycle time. If the cycle time is equal to or less than the make ready process, there are no technical but only economic constraints for the manufacturing process to be chosen (gravure or web-offset). The MAPR is then 1 (one) copy.

Digital printing or Print on Demand (POD)

The MAPR is equal to one (1) copy. The lead-time for the image carrier can be seen as a "virtual" plate or cylinder, and hence the smallest integer is one copy (or impression). The cycle time is less than the "make-ready process" in the digital press, i.e. in a copying machine or digital press. The fastest digital press available for commercial printing is the Kodak Versamat high speed inkjet running at 1000 fpm, but not yet available for a commercially acceptable lithographic quality. For such an application producing an A4 page (portrait) the lead-time or cycle time per page can be estimated to about be 0.01 seconds and the only limiting factor is actually the speed of the digital press itself. There are no other constraints except for economic considerations when choosing the right manufacturing process.

A new test method to measure dynamic contact in a printing nip for rotogravure papers

Janet Preston[1], Roger Bollström[2], Kenneth Nylander[2], Martti Toivakka[2], Jouko Peltonen[2]

[1] Imerys Minerals Limited, Par, Cornwall, UK, PL24 2SQ
E-mail :Janet.Preston@imerys.com

[2] Laboratory of Paper Coating and Converting, Åbo Akademi University, Turku, Finland

Abstract

In rotogravure printing a common problem is the non-transfer of ink from cells to the paper, resulting in "missing dots". This is often because of rough or incompressible papers, which do not make good enough contact with the printing cylinder. A novel method for studying dynamic contact between the paper and the print cylinder whilst in the printing nip was developed. In the method, a blue carbon paper is contacted with the test papers and passed through a printing nip at different pressures. The resultant setoff pattern on the test paper was captured using a scanner and then analysed using image analysis software. A Fast Fourier Transform (FFT) was applied to the set-off pattern to quantify the degree of variation occurring at different length scales. A range of different common coating pigments were assessed, which had been coated onto a ULWC basepaper at three different solids concentrations. When compared to the percent missing dots on the laboratory printed coatings a significant correlation between degree of contact variation and the missing dots was found.

Keywords

Compressibility, printing nip, rotogravure printing, topography, test method

1. Introduction and objectives

Freedom from speckle or missing dots in a rotogravure printing process depends on the ability of the substrate to contact the inked printing cylinder cells as the paper passes through the printing nip. Poor transfer of the ink from the cells to the substrate is often seen with rough or incompressible papers [Popil, 1998 and Jackson *et al* 1964]. Thus compression of paper has been studied for many years and reported by a wide range of authors, [e.g., Jackson & Ekstrom 1964, Hsu 1964, Roehr 1955 and Mangin *et al* 1994]. Mangin *et al* used confocal microscopy with a novel compression attachment to study the local static compressibility of uncoated papers calendered with different processes. They showed that the compressibility after calendering depended on both the calendering conditions and the furnish.

A model for the compressibility of paper under applied load is given by Schaffrath & Gottsching 1991. This considers that the total sheet is compressed initially with applied load, followed by fibre collapse and finally deformation of the fibre wall. The total compressibility is a combination of both surface and bulk compressibility; the surface being the most important at low applied loads but the bulk becoming more significant as the load increases. Jackson & Ekstrom showed that addition of a coating to the surface reduced the compressibility, and that higher coat weights reduced it to a greater extent. Lorusso 2001 found that SC (super-calendered) papers, which had a larger void volume of pores greater than 1.5 μm in size, were more compressible, and required less pressure to achieve a surface smoothness of 1μm. She also observed that lower pressures were required by the smoother side of the paper to reach the target smoothness, (despite the fact that this had been calendered to a greater extent and would therefore be considered to be less compressible).

More recently, 1997, Heikkila modelled paper smoothness under a dynamic load. The percentage contact area as a function of applied pressure and time was studied, and a non-linear viscoelastic model for coated paper contact smoothness was proposed. The elastic and viscoelastic properties of paper at very short times (milliseconds) were found to be of importance, and these dwell times are of a similar duration to that of a paper passing through a printing nip.

Paper compressibility has been measured in the past using the Parker Print Surf, but has been reported as rather inaccurate [Lorusso 2001 and Wanske *et al* 2006]. The need for a dynamic measurement of smoothness under the printing nip, rather than a static measurement has been proposed by Heikkila *et al* 1994. Wanske *et al* have recently [2007] reported an updated version of the FOGRA contact area tester, in which a high-precision distance measuring system was connected to a digital image processing system. With this apparatus the development of surface structure as a function of paper deformation under compression load was studied and correlated with rotogravure print quality. Bery 1985 reported a technique designed to assess the smoothness of paper under compression. In this method a graphite rod is drawn down across the test paper at different pressures, depending upon the paper characteristic to be studied and under controlled conditions. The graphite rod produces a set off pattern on the paper depending upon the density, topography and compressibility of the sheet in a similar manner to this work. This method is different from that reported in this paper, in that the set off pattern is achieved by passing the paper through a printing nip, which is similar to a rotogravure press.

The influence of pigment size and morphology on the rotogravure printability of coated papers has also been widely reported [Brociner & Beazley 1980; Sennett *et al* 1982; Gane & Hooper 1992, Hiorns *et al* 1997, Hassell 1984]. High aspect ratio pigments such as platy kaolins and talc have been shown to give smooth surfaces, when the particles are well aligned, leading to low levels of missing dots [Kent & Lyne 1989, Gane *et al* 1995, Elton *et al* 1990]. The platy nature of these particles also gives a tortuous path for ink imbibition and maintains the ink on the surface of the substrate. Hiorns *et al* 1997, suggested that a smooth paper on a length scale of around 100μm is important for low missing dots.

The aim of this study was two-fold; firstly to develop a simple test which would give a measure of contact occurring in a printing nip, and secondly, to determine whether the coating formulation plays an important part in the dynamic smoothness and compressibility of coated paper, and therefore contributes to rotogravure printability.

2. Materials and methods

In this study four different coating colour formulations were separately coated onto a ULWC basepaper. All colours included 35 percent talc combined with 65 percent of platy kaolin, blocky engineered kaolin, coarse platy engineered kaolin or narrow PSD carbonate.

The pigments were combined with 4.6 pph rotogravure latex and 0.5 pph stearate. The pH was adjusted to 9 and the coatings were applied to the ULWC basepaper using a laboratory Helicoater at 800 m/min. The coat weight was 7.5 g/m² for every paper except for the series with varied coat weights with weights from 5.1 - 8.1 g/m². Each colour was diluted twice and run at 3 solids content levels. The coatings were calendered under standard laboratory rotogravure conditions (10 nips, 65°C, 36 m/min at 750 psi pressure).

2.1 Paper and print testing

A DataColor Elrepho 3300 was used to measure the optical characteristics of the papers; brightness and opacity (D65 illumination with 400 nm UV filter). A Parker Print Surf was used to measure roughness at a pressure of 1000 kPa. TAPPI 75° gloss was measured using a Hunter glossmeter. A Spectroeye densitometer was used to measure the print densities.

2.2 Burnout test

The burnout test is a method used for analysing coat weight distribution [Dobson 1975]. The coated sheet is saturated with an ammonium chloride solution (25 g ammonium chloride / litre in 50 / 50 water / ethanol), air dried and then heated in oven (200° C for 5 minutes). When heated the organic fibres carbonize and turn black but the coating layer consisting of inorganic pigments appears as a grey film on the black background. The samples were scanned with an Epson Perfection V750 pro scanner and an area of 2 x 2 cm was analysed and the greyscale correlated with the optical coverage of the coating layer. A lighter area has received more coating colour than a darker (Figure 1).



Figure 1: Scanned images of base paper to the left and coated paper to the right after burnout test (2 cm x 2 cm)

2.3 Missing dots

The sheets were printed in the laboratory with a Winstone printing press. The samples were printed at a speed of 37 m/min and a nip pressure of 600 N. Immediately after the nip the samples were dried with a hot air drier and passed under a camera where images were taken. The percent missing dots in the halftone area was determined with image analysis. The dot size in the printing cylinder was 65 - 70 μm in diameter and a commercial printing ink was used. The printing was made without electrostatic assist (ESA). In reality the use of ESA, and the much higher printing speed, would decrease the differences observed between the different pigment coatings significantly. However the Winstone press has been shown by experience to give a ranking of the missing dots relating to different paper structures, which can also be observed in a commercial printing trial.

2.4 Dynamic contact test

In the new test developed in this work, the paper to be tested was contacted with a sheet of carbon paper (Pelikan plenticopy 200 H), which was passed through a printing nip (IGT Ac-2 printability tester) at a known pressure and speed, resulting in transfer of some of the carbon copy paper ink. The tests were made using a 20 mm aluminium roll against an enlarged sector with a constant speed of 0,5 m/s. The sector was enlarged with a polystyrene film of 1,5 mm thickness. Polystyrene is an incompressible polymer which stands high pressures without deforming. When this procedure is repeated at a range of pressures, a blue coverage/ pressure relationship can be established, as shown in Figure 4. The degree of blue ink transfer was determined by scanning a portion of the test paper (15 x 2 cm area), and carrying out image analysis on the scanned image. The original unprinted papers were also scanned and analysed in the same way and used for normalising the greyscales measured from the printed areas in order to avoid differences caused by differences in paper brightness.

A band pass filter is a mathematical procedure that passes frequencies within a certain range and rejects frequencies outside that range. In this study a filter was created by combining a low-pass and a high pass filter. The ranges analysed in this study to look at variations in the greyscale data, were 0,25 - 0.5, 0.5 - 1, 1 - 2, 2 - 4, 4 - 8 and 8 - 16 mm. The coefficient of variation (standard deviation / mean) shows the amount of variation occurring in each size range.

2.5 Optical confocal microscopy images

The images (1.6 x 1.6 mm) were taken with a 10x lens using NanoFocus μSurf equipment and planarized. The waviness off the paper was filtered away with an ISO Gaussian filter, then the images were analyzed with the *Scanning Probe Image Processsor* from *Image Metrology*.

3. Results

3.1 Paper and print results

The paper and print properties are included in Table I. The blocky minerals were coated at higher solids contents than the platey pigments. The highest brightness and opacity and lowest sheet gloss, were obtained with the most porous carbonate containing coatings, which also had the lowest Gurley values. The coarse platey

engineered kaolin coating gave the lowest macro-roughness, but only the second highest sheet gloss. The finer blocky engineered kaolin coating had the highest sheet gloss.

Table I: Paper and print properties

	Solids level	H-Gloss-75°	PPS1000	Bness-F8	Opacity	Gurley	Print Results		
	wt.%	%	µm			s	Missing Dots %	Print density	Print gloss %
Talc 35	57	45.5	0.95	72.6	87.9	1025.0	2	1.94	66
P Kaolin 65	55.5	46.0	0.84	72.7	87.8	1060.0	1.7	1.93	67
	54	44.5	0.88	72.7	87.7	1060.0	1.7	1.94	68
Talc 35	60	55.0	0.76	73.8	87.8	775.0	1.7	1.95	71
B Eng Kaolin 65	58.5	53.5	0.80	73.7	87.4	825.0	1.9	1.95	70
	57	51.5	0.78	73.7	87.6	825.0	1.9	1.94	68
Talc 35	60	45.5	0.82	77.0	88.2	675.0	2.9	1.86	64
Narrow PSD Carb 65	58.5	43.5	0.85	76.9	88.1	650.0	3.5	1.85	61
	57	44.0	0.84	76.9	88.1	675.0	3	1.84	62
Talc 35	58	47.5	0.74	72.9	87.0	780.0	0.9	1.9	65
C P Eng Kaolin 65	56.5	48.5	0.73	72.9	87.2	800.0	0.9	1.92	68
	55	47.0	0.74	72.8	87.3	840.0	1.2	1.91	65

The coarse platey engineered kaolin coatings had the lowest missing dots while the carbonate containing colour had the highest (Figure 2). The percent missing dots was independent of the coating solids. For this reason, in the subsequent figures, the values used were those interpolated to 57% solids.

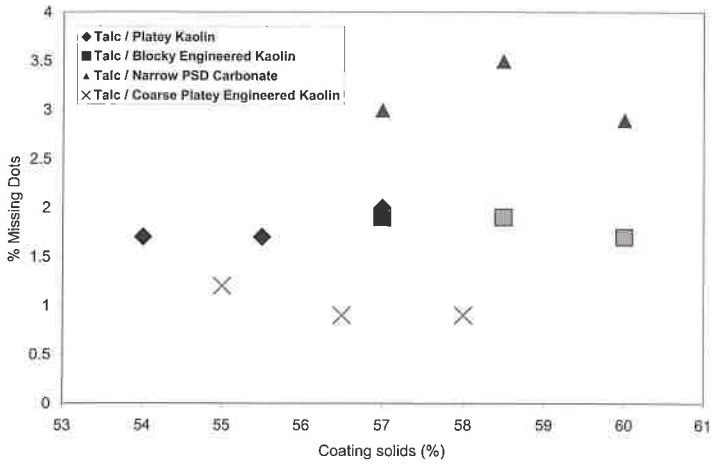


Figure 2: Percentage missing dots as a function of coating solids amount for the studied coatings

The missing dots were not solely related to the static smoothness of the papers as measured by PPS (R^2 value only 0.27); the platey kaolin resulted in the roughest coating but gave intermediate levels of missing dots. The optical profilometry results showed somewhat better correlation with the print results (Figure 3). A higher RMS roughness gave higher percent missing dots.

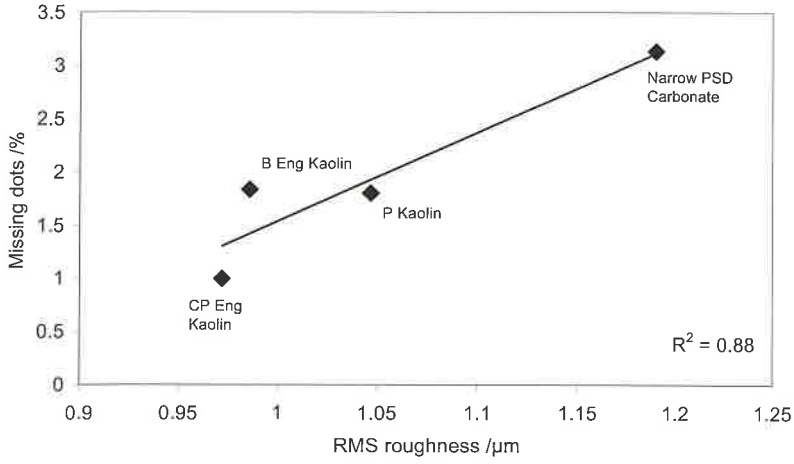


Figure 3: Missing dots plotted as a function of RMS roughness from confocal optical profilometry

3.2 Dynamic contact test

A typical result from the dynamic contact test for a calendered coated paper is shown in Figure 4. The set off patterning of the sample visually appears the same as the formation of the paper. The curve in Figure 4 shows that for forces beyond 600 N the blue transfer is becoming non-linear, and less dependent on load, approaching an asymptotic limit value.

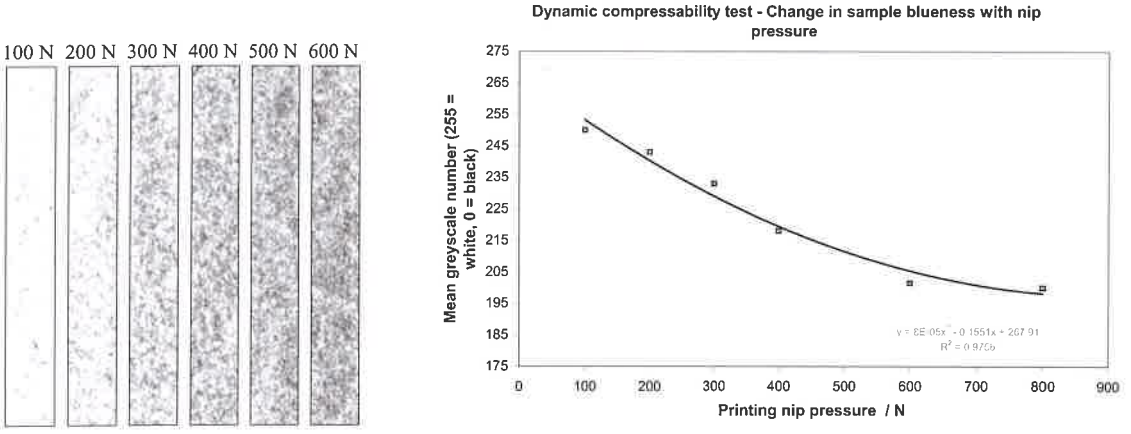


Figure 4: Images of ink transfer at different nip pressures and the curve showing average greyscale value as a function of nip pressure

"Greyscale" images were obtained by scanning the sets of blue set-off patterns. The images are composed of 255 shades of grey, varying from black (zero intensity) to white (255). In Figure 5, the average greyscale is plotted for each of the pigments at different solids contents as a function of the percent missing dots, after the data had been normalised to account for differences in the original paper brightness. A higher greyscale value, i.e. a decrease in the contact area between cylinder and blue carbon paper, results in a higher percent missing dots.

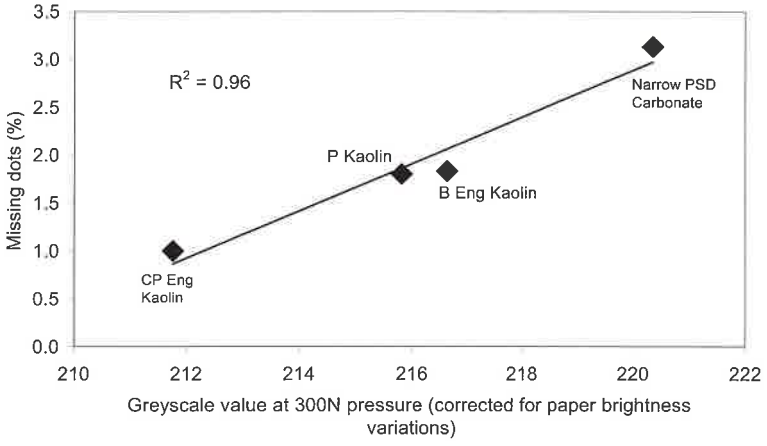


Figure 5: Correlation between corrected greyscale value for 300N nip pressure and percent missing dots

The degree of variation occurring at different length scales was analysed with the band pass method [Johansson, 1993 and Nylund 2007]. A significant correlation with the coefficient of variation (COV) of the small ranges and the missing dots was found. Figure 6 shows the COV for the ranges of 0.25 - 0.5 mm and 0.5 - 1 mm. The larger ranges did not give any correlation for the studied samples.

A comparison of the scale of variation in the basepaper (optical reflectance), coating layer (burn-out) and blue set off pattern was made by comparing the COV at each length scale (Figure 7). The basepaper images showed that the greatest degree of variation was occurring in the smallest length scales measured, up to 0.5 mm in size. This variation was reproduced in the subsequent coating burnout analysis and also in the variations in the blue set off pattern.

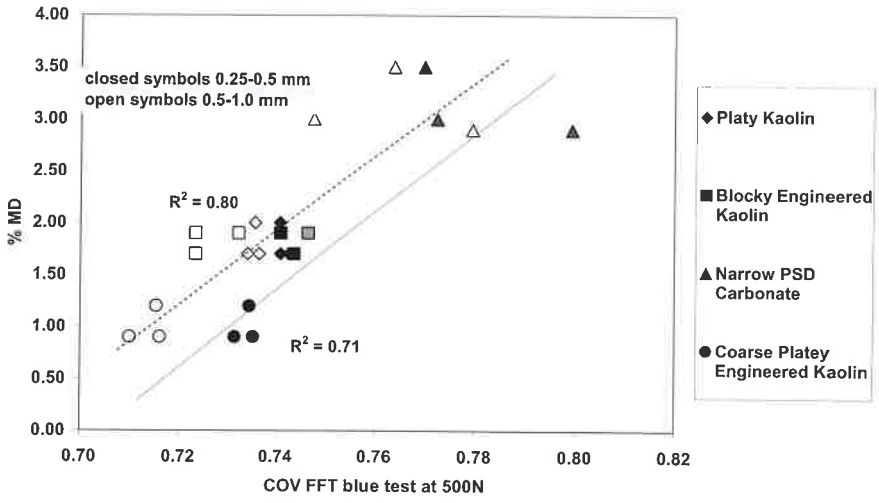


Figure 6: Correlation between FFT band pass analysis for 500 N pressure and percent missing dots

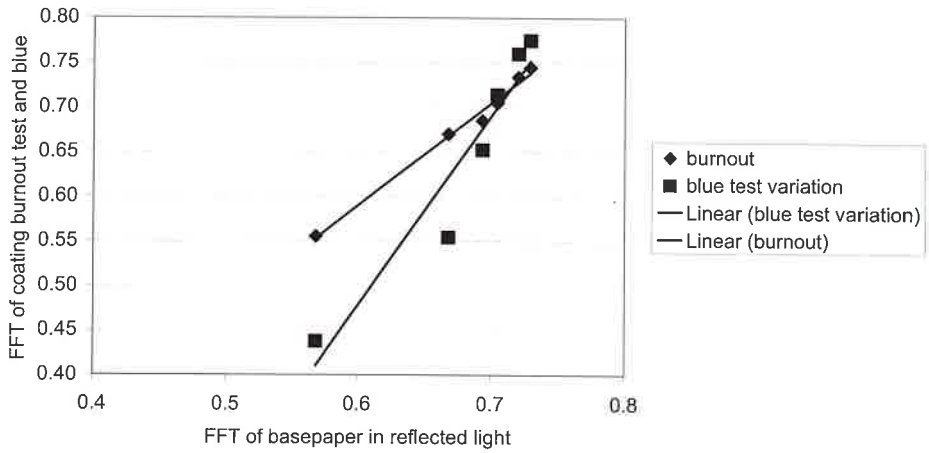


Figure 7: Coefficient of variation (COV), occurring at each length scale in the basepaper formation, the coating coverage as determined by burnout, and the blue set-off pattern

4. Conclusions

This work has shown:

1. Roughness as determined by RMS optical profilometry gave some correlations with percent missing dots for a series of papers coated with different pigments and at a range of solids. Higher roughness gave higher percent missing dots. PPS gave a poor correlation.

2. A novel dynamic contact test was developed to see the degree of contact between the coated papers and a carbon paper when passing through a nip. The set off pattern could then be analysed using image analysis. A paper with a higher degree of contact (lower greyscale number) gave better printability. When a FFT was applied to the data the important length scales were found to be between 0.25 and 1 mm. A lower degree of variation at these length scales gave lower percent missing dots.

3. The scale and amount of variations occurring in the basepaper formation, was mirrored by the variations occurring in the coating coverage as determined by the burnout test. The same variations were also seen in the blue contact patterning, obtained by passing the paper and the carbon paper through a printing nip. Variations in the paper dynamic smoothness are likely to originate from the formation of the basepaper.

References

1. Bery Y. A., Wash T., *"Structural and Surface Properties Tester for paper" US Patent 4, 541, 273, Sept 1985*
2. Dobson R. *L., "Burnout, A Coat Weight Determination Test Re-examined", Preprints of 1975 TAPPI Coating Conference, TAPPI PRESS, Atlanta, Georgia, pp 123*
3. Brociner, R. E. and Beazley, K. M., *"The influence of the coating pigment on missing dots in LWC gravure paper", TAPPI J., 63 (5):55 1980*
4. Elton, N. J., Gate, L. F., Hooper, J. J., *"Texture and orientation of kaolin in coatings", Clay Minerals, 34, 89 - 98, 1999*
5. Gane, P. A. C., and Hooper, J. J., *"The influence of coating structure on rotogravure print gloss and print density", Proceedings of EUCEPA Symposium, Budapest, Oct. 1992, p. 296 - 317*
6. Gane, P. A .C., Hooper, J. J., Grunwald, A., "Coating pigment orientation", TAPPI 1995 Coating Conf. Proceedings, pp. 383 - 390, TAPPI Press, Atlanta
7. Hassell M. V., *"The effect of the mechanical properties of the pigment coating structure upon print performance" Proc. 1984 Tappi Coating Conf., pp 45 - 53*
8. Heikkila I., *"Paper contact smoothness under static and dynamic pressures", Graphic Arts Finland, vol 23, no. 3, 1994, pp 9 - 15*
9. Heikkila I., *"Viscoelastic model of paper surface compressibility", Pap. Puu vol. 79, no.3, 1997, pp 186 - 192*
10. Heikkila I., Oittinen P., Saarelma H., Tuovinen P., *"Measurement of dynamic contact smoothness", Pap.Puu vol 76, no. 6-7, 1994, pp 399 - 402*
11. Hiorns, A. G., Coggon, L., Renals, M. S., Elton, N. J., McGenity, P. M., "Effect of color solids and blade angle on rotogravure coatings", PITA 1997 Coating Conference proceedings, pp. 19 - 25, PITA, Bury, Hsu Brit. J. Appl. Phys., Vol 15, 1964
12. Jackson M, Ekstrom L., *"Studies concerning the compressibility of paper. Svensk Pap., 67 (20): 1964, 807 - 821*
13. Johansson P.-Å. *"Print mottle evaluation by band-pass image analysis", Advances in Printing Science and Technology, Vol 22, 1993*
14. Kent, H. J., and Lyne, M. B., *"On the penetration of printing ink into paper", Nordic Pulp Paper Res. J., 2, 141 - 145, 1989*
15. Lorusso M., PhD Thesis UMIST *"Experimental study of the influence of mineral structure on the void structure and printing characteristics of supercalendered papers", 2001*
16. Mangin P. J., Beland M-C., Cormier L. M., *"Paper Surface Compressibility and printing" Proc 1994 Int Printing & Graphic Arts Conf. pp 19 - 31*
17. Nylund, N., *"Bildanalys för pappers- och tryckkvalitet", MSc-thesis, Åbo Akademi, 2007 (In Swedish)*
18. Popil R. E., *"Observations of dynamic paper compressibility", Proc 1998 Progress in Paper Physics, Vancouver, Canada, Sept 1998, pages F1 - F2*
19. Roehr W. W., *"Effect of Smoothness and Compressibility on the Printing Quality of Coated Paper" Tappi, Vol 38, No.11 Nov 1955*
20. Schaffarth H-J, Gottsching L., *"The behaviour of paper under compression in the z direction", Proc Int. Pap. Phys. Conf., Volume 2, pages 489-510, Kona, Hawaii, Sept 1991*
21. Sennett, P., Massey, H. L., Morris, H. H., *"Effect of kaolin pigment particle size and shape on rotogravure print quality", TAPPI J., 65, 5, 95 - 99 1982*
22. Wanske M., Klein R., Grossmann H., *"Assessing the Surface Structure of Printing Papers under Pressure",TAGA 58th Annual Technical Conference, March 19-21 2006, Vancouver, Professional papermaking 78 - 82 (2006) 2*
23. Wanske M., Klein R., Grossmann H., *"Measuring and Evaluating the Surface Quality of gravure Papers", Proc 2007 PITA Coating Conference, March 27-28th, Cambridge pp 129 - 137*



Influence of plasma activation on absorption of ink components and dampening water in sheet-fed offset printing

Maiju Pykönen[1], Hanna Silvaani[1], Janet Preston[2], Pedro Fardim[3], Martti Toivakka[1]

[1] Laboratory of Paper Coating and Converting and Center for Functional Materials
Åbo Akademi University. Porthaninkatu 3, FI-20500 Turku, Finland
E-mail: maiju.pykonen@abo.fi

[2] Imerys Minerals Ltd., Par Moor Centre
Par Moor Rd, Par, Cornwall, United Kingdom. PL 24 2SQ

[3] Laboratory of Fibre and Cellulose Technology
Åbo Akademi University, Porthaninkatu 3, FI-20500 Turku, Finland

Abstract

The influence of plasma activation on offset printability was investigated. Four different model pigment coated papers were treated with corona, experimental pilot scale argon plasma, and laboratory scale nitrogen plasma. Surface characterization was made by contact angle measurements, X-ray Photoelectron Spectroscopy (XPS) and Time-of-Flight Secondary Ion Mass Spectrometry (ToF-SIMS). Five different model inks with different portions of linseed and mineral oils, and one commercial ink were used in ink setting evaluation with Ink Surface Interaction Tester (ISIT) and laboratory scale printing. In addition, samples were printed in a pilot scale sheet-fed printing press using the same commercial ink as in laboratory scale. According to results, plasma activation increased surface wettability and polarity due to oxidation of high molecular weight dispersion chemicals of pigment and latex particles. Therefore, the dispersion system of different pigments seemed to influence the effectiveness of the plasma treatment: Talc containing paper had the greatest change in O/C ratio determined by XPS, whereas ground calcium carbonate (GCC) containing paper had the smallest. Plasma treatment had a clear impact on ink setting with all the papers, but the response depended on the ink composition. The ink setting rate decreased with linseed oil dominating inks, probably due to increased acid-base interaction between ink oil and polar plasma treated coating. With mineral oils ink setting accelerated. Pilot scale plasma treatments did not have an impact on print density and gloss, but the laboratory scale plasma treatment led to a significant print density variation. Ga focused ion beam (FIB) and optical microscope images, showed that micro-picking was occurring in the surface layers of the coating, leading to a decrease in the print density with laboratory plasma treated samples.

Keywords

Dampening water, ink components, pigment coated paper, plasma treatment, sheet-fed offset printing, surface chemistry

1. Introduction

Plasma is a state of ionized gas, consisting of excited atomic, ionic, molecular, and free-radical species. Non-thermal or cold plasma treatment can be used for surface modification, also for organic surfaces, because the overall temperature of plasma remains near room temperature even if the temperature of electrons can reach 30.000 - 100.000 K [Cernacova *et al.* 2006]. Plasma-solid interactions can be divided into three sub-categories: The first is plasma-induced etching or ablation, in which material is removed from the solid surface. The second is a process, where material is added to the surface in the form of growing thin film deposition. In a third process, material is neither added nor removed, but the surface is chemically and/or physically modified [d'Agostino *et al.* 2005]. This is often termed plasma treatment or activation. Atmospheric plasma modification has raised interest in recent years because non-thermal plasma processing provides a possibility to develop new dry surface modification methods based on roll-to-roll processing.

In the paper industry so-called corona treatment has been used already for decades, for example to improve the adhesion between polymer and paper in extrusion processes, and printability of low surface energy polymer substrates. The so-called corona treatment is also one kind of dielectric barrier discharge (DBD) plasma; however it has some drawbacks, such as poor uniformity and backside treatment of the substrate [Cernacova *et al.* 2006; Roth 2001]. It has frequently been tried to improve these drawbacks of corona treatment, for example by changing electrode arrangement or by adding a treatment gas in the plasma.

Plasma modification has potentially many advantages compared to more conventional surface modification methods. Plasma modification is a dry process, which makes it more environmentally friendly compared to wet processes. It produces hardly any by - or waste-product chemicals, and it does not demand an energy-consuming drying step in the process [Roth 2001]. Plasma deposition enables extremely thin defect-free coating layer formation, which adheres to the substrate. Therefore, only a small amount of starting material is needed. While it is commonly believed that plasma affects only the outermost surface of a material [e.g. Sahin *et al.* 2002; Navarro *et al.* 2003], it has also been reported that in the case of porous surfaces inner structures are also affected [Mukhopadhyay *et al.* 2002].

Ink-paper interactions, including the ink setting and drying processes, have an important role in print production, since they influence both print quality and runnability issues [Ström 2005; Preston *et al.* 2001]. For instance, piling or low print gloss may result from too fast ink setting, whereas smearing and scuffing can be caused by too slow ink-setting [Preston *et al.* 2003; Marttila *et al.* 2004]. If ink setting is uneven, it may lead to back trap mottling [Preston *et al.* 2008]. In sheet-fed offset printing, ink drying can be divided into two phases: the first is separation of ink oils from the ink film by absorption into the substrate, which can be referred to as ink setting and leads to touch-proof ink layer, the second phase is chemical curing, i.e. polymerization of residual drying oils and alkyd resin initiated by oxygen [Ström 2005]. Even if the ink transfer occurs in a nip under high pressure, it is known that the separation and absorption of the low viscous fluids of the ink occur after the printing nip [Oittinen 1976; Rousu *et al.* 2001]. The time frame in ink setting is between one to ten minutes, whereas the chemical curing may last several days [Ström and Gustafsson 2006]. The main components in sheet-fed offset ink are colorant, binder and ink oils. In addition, it contains catalytic dryers, antioxidants, wax particles and other additives [Ström 2005]. Typically, colorant is hydrophobic organic pigment [Rousu *et al.* 2001], and binder consists of alkyd and hard resins. Ink oils can be classified into mineral and vegetable oils. The mineral oil is a mixture of hydrocarbons from petroleum distillates, whereas vegetable oils are typically esters, for example linseed, soya, tung and castor oils are glycerol esters. Based on their ability to polymerize during drying, the vegetable oils can be classified as drying, semi-drying and non-drying oils. The drying oils polymerize at room temperature, semi-drying oils require heat, and non-drying oils do not polymerize at all. Linseed oil is a triglyceride containing linoleic and linolenic acids, and it is referred as a drying oil. The drying oils may act also as a binder during the chemical curing, however most of it absorbs into the coating [Ström and Gustafsson 2006].

There have been several studies concerning separation of different ink components during ink setting on coated paper [Rousu 2002; Ström *et al.* 2001; Koivula *et al.* 2008]. It is well known that coating pore structure and latex type and amount play a key role in ink setting on coated paper [Ström 2005; Preston *et al.* 2001a]. It has also been shown that ink setting rate increases, when the ratio of surface tension to viscosity of the ink oils is increased [Rousu 2002]. The vegetable oil separates less efficiently from the ink film, when compared to mineral oil, and the absorption of the latter into paper is also faster [Ström *et al.* 2001; Rousu 2002]. This, in combination with the low viscosity of mineral oil, leads usually to a faster ink setting in comparison to high viscosity oils, such as linseed oil. The acid-base interactions between polar vegetable oil and ink film are stronger when compared to dispersion forces between non-polar mineral oil and ink film. Rousu [2002] showed that hydrophilic dispersed coating pigment surfaces act as sites for adsorption, thereby slowing down the absorption of polar vegetable oils and letting the non-polar mineral oils absorb further. Polarity difference is claimed to be the main property for ink, when contributing to oil separation, because molecular size and viscosity difference is not a factor when considering species in a miscible dissolved state [Rousu *et al.* 2005]. Higher solubility and greater compatibility of linseed oil with resins results also in an increased retention of the oil in the ink, which is an additional factor slowing down the absorption of linseed oil [Rousu 2000].

The effect of substrate surface energy on ink setting has been evaluated, but usually in relation to changes in surface chemistry, where also coating structure changes impact the results. Rousu *et al.* [2001] compared dispersed and undispersed carbonate pigment in order to evaluate the influence of surface energy on ink oil separation and wetting rate. Ink oil separation increased clearly with the dispersed system, which had higher polar surface energy due to polyacrylate dispersant. Even if the particle size distribution was the same, the pore size distribution differed significantly due to flocculation of the undispersed system. Therefore, the results showed not only the effect of surface energy on ink oil separation, but also the change in pore size distribution. According to Rousu *et al.* [2001], surface energy did not have an important role in wetting rate measured by contact angles. Ridgway and Gane [2006], however, compared the absorption rates of polar water and non-polar hexadecane on polyacrylate dispersed GCC pigment tablets. They found that both surface chemistry and pore structure influenced the rate of absorption: non-polar liquid had faster initial absorption, whereas with longer time scale polar water absorbed faster. Latex surface energy and polarity has been shown to have clear influence on ink setting due to changes in diffusive interactions between ink solvent and latex. Generally, it can be said that higher surface energy or polarity decreases the ink setting rate [Ström 2005; Van

Gilder and Purfeest 1994; Van Gilder and Smith 2001; Fouchet *et al.* 2004; Fouchet *et al.* 2006]. Van Gilder and Purfeest [1994] found that high surface energy and polarity of latex polymer led to significantly less absorption of ink solvent, which resulted in a slower rate of ink-tack build. This behavior showed also improved press runnability, associated with observably longer time before coating failure and less picking, when compared to low surface energy and polarity latex containing paper. Van Gilder and Smith [2001] managed to reduce picking also in waterless offset by increasing the polarity of latex polymer. This caused resistance to mineral and linseed oil diluent absorption and slowed down the rate of ink tack build-up. Rousu *et al.* [2001] showed that vegetable oils are more prone to oil-latex diffusion than non-polar mineral oils. However, the latex-oil diffusive interactions did not affect print quality, even if there were significant differences in interactions and ink setting dynamics. In addition, they also found that styrene butadiene latex in the coating structure increased imbibition rate of polar linseed oil, and after ~ 4 pph addition by weight the oil separation in favour of mineral oil transport in comparison to linseed oil was no longer seen.

This paper is a continuation to our earlier work [Pykönen *et al.* 2008], where we noticed that plasma activation had an impact on ink and dampening water absorption. Ink setting was accelerated on pigment coated paper, and print gloss and density reduced in laboratory scale printing, when pre-dampening was used. In pilot scale printing trials, strong laboratory scale plasma treatment resulted in reduced print density. With surface sized paper, plasma activation reduced the water interference mottle, probably due to more even dampening water absorption. The objective of this work was to understand how different ink components and dampening water react to surface chemistry and energy changes as created by plasma activation. In addition, the aim was to understand how different pigments and binders react to plasma activation.

2. Materials and methods

2.1 Papers

A 45 g/m^2 fine paper base was coated with simple model pigment coatings with a minipilot scale roll-to-roll blade coater (web width 300 mm, speed 15 m/s, IR- and hot air-drying). The target coat weight was 15 g/m^2. The coating formulations and results from mercury porosimetry are presented in Table I and Figure 1, respectively. Paper 2 had the largest pores but very broad pore size distribution, whereas paper 4 had the smallest pores and a small pore volume. Addition of starch increased pore size and widened the pore size distribution, seen when comparing paper 1 to paper 3. Here, only the pore sizes relevant to the coating layer in the range of 30 - 500 nm were considered.

Table I: Coating formulations and total pore volume for model coatings

	Paper 1	Paper 2	Paper 3	Paper 4
Kaolin (Capim SP, Imerys)	70		70	
GCC (Hydrocarb 90, Omya)	30	50	30	
GCC (Setacarb HG, Omya)				100
Talc (FinnTalc, Mondo Minerals)		50		
SB-latex (Styronal D 809, BASF)	10	10	6	10
Starch (Raisamyl 01151, Ciba Specialty Chemicals)			6	
Total Pore Volume, cm^3/g	8.0	6.9	7.6	4.6

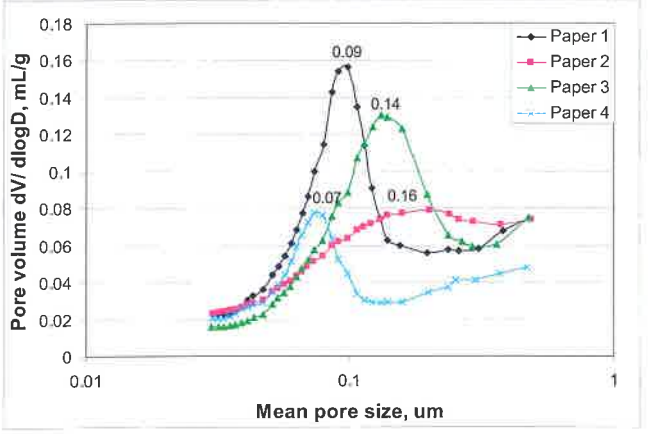


Figure 1:
Pore size distribution for the coatings

2.2 Plasma surface treatments

The coated papers were treated with plasma in pilot (argon) and laboratory scale (nitrogen). In addition, experimental pilot scale plasma treatment was compared to conventional corona treatment. The details of the treatment parameters are in Table II. The experimental plasma apparatus has been further developed since our previous publication [Pykönen et al. 2008], and therefore the current results are not directly comparable to those in that work.

Table II: Treatment parameters for corona, pilot scale argon plasma, and laboratory scale nitrogen plasma

Parameter	Corona treatment	Pilot plasma treatment	Laboratory plasma treatment
Treatment power	1.3 kW	1 kW	300 W
Voltage	22.5–25 kV	22.5–25 kV	1 kV
Frequency	21.5–25 kHz	21.5–25 kHz	16–20 kHz
Treatment width	0.50 m	0.35 m	10–35 mm
Air gap	2 mm	1 mm	15 mm
Treatment speed	20 m/min	20 m/min	0.6 m/min

2.3 Surface characterization

Contact angle measurements were performed using a KSV CAM 200 Optical Contact Angle Meter applying the following liquids: water, ethylene glycol (EG), diiodomethane (DIM), dampening water used in pilot scale printing trials, and mineral and linseed oils used in the inks. In addition, contact angle titrations [see e.g., Berg 1993] for paper 1 were made with nine liquids by changing the pH of water was changed with NaOH and HNO_3. A minimum of four parallel measurements were done on each sample.

Changes in chemical surface composition were determined by X-ray Photoelectron Spectroscopy (XPS) using a Physical Electronics Quantum 2000 ESCA instrument, equipped with a monochromatic Al Kα X-ray source and operated at a power of 25 W. Three different spots were measured in each sample. The pass energy for the survey spectra was 184 eV, and the measurement time was five minutes. For high resolution carbon spectra, C1s, the pass energy was 23.5 eV and measurement time 10 minutes. Curve fitting (deconvolution) of high resolution C1s peaks was performed using a Shirley background, Gauss-Lorentzian character and full width at half-maximum (FWHM) of 1.3 - 1.7 eV. Binding energy (BE) of all spectra was related to C1 (C-C, C-H) at 285 eV. The following chemical shifts relative to the C1 position were employed for the respective groups; 1.7 ± 0.2 eV for C2 (C-O), 3.1 ± 0.3 eV for C3 (C=O, O-C-O), 4.6 ± 0.3 eV for C4 (O=C-O) and 5 eV for C5 (CO_3^{2-}).

The Time-of-Flight Secondary Ion Mass Spectrometry (ToF-SIMS) analysis was carried out using a PHI TRIFT II spectrometer. Mass spectra and images of paper surfaces in both positive and negative ion mode over the mass range of 2 - 2 000 Da were acquired using a Ga primary source on a raster size of 200 µm x 200 µm with applied voltage of 25 kV and a primary ion current of 600 pA. The acquisition time was 5 min. The spectra and images were acquired also with area of 2.5 mm x 2.5 mm, when the voltage of primary ion source was 15 kV, and acquisition time was 10 min. At least three different spots were analyzed on each sample.

A FEI FIB201 gallium focused ion beam instrument was used for sectioning and high-resolution imaging. The instrument is capable of producing a gallium ion beam of between 7 nm and 300 nm in diameter at 30 keV energy. A platinum organometallic gas injector allows ion beam assisted deposition of platinum over selected areas of the sample. This facility was applied to the sectioning shown here in order to protect the top of the surface of the sample during ion milling. For sample sectioning, a large ion current was used initially to remove a staircase-shaped trench. A finer beam of lower current was then used to "polish" the larger vertical face of the trench by scanning the beam in a line and moving it progressively up to remove further material. The sample was then tilted to 45° and the polished face imaging using the same ion beam generally at a much lower beam current to achieve high resolution.

The optical microscopy was carried out on a Polyvar Optical Microscope. The prints were embedded in epoxy resin and sectioned using a glass knife followed by an ultramicrotome.

2.4 Offset printability

Offset printability was studied both in laboratory and pilot scale. Ink on paper tack was measured with the Ink Surface Interaction Tester (ISIT), in which three parallel measurements were analyzed on each sample.

Laboratory scale printing was performed with an IGT unit (IGT GST2) according to SCAN-P86:02. Both ISIT and IGT printings were performed with five model inks, where the proportion of the mineral and linseed oils was changed, as shown in Table III. In addition, a commercial ink; *SiegWerk Tempo Max Soft*, was used for both laboratory and pilot scale printing. This ink contained both the mineral and linseed oils, which were also used in the model inks. Properties of the inks are presented in Table 3. Ink tack and stability, i.e. change of tack with time, increased as a function of the linseed oil. Vegetable oils have typically better stability due to higher boiling point when comparing to mineral oils. Pilot scale printing was performed on a sheet fed offset press (Heidelberg Speedmaster CD 74). Print density, print gloss and mottle were measured. In addition, the effect of plasma activation on surface strength of the coated paper was studied with respect to pick resistance (SCAN-P 63:90).

Table III: Ink properties

	Ink1	Ink 2	Ink 3	Ink 4	Ink 5	Ink 6
Portion of the mineral oil [%]	100	75	50	25	0	
Portion of the linseed oil [%]	0	25	50	75	100	
Viscosity [Pas]	160	186	195	156	180	207
Tack [N]	115	171	207	215	242	136
Stability [N]	177	189	237	255	294	188
Ink flow, 30 min [cm]	24	29	58	40	62	80
Ink flow, 60 min [cm]	28	32	70	48	74	91

3. Results

3.1 Surface properties

The general trend was that all the treatments reduced the contact angle for water, EG, DIM and dampening water (Table IV). However, the contact angle values of polar liquids did not decrease on the GCC and latex containing paper 4. The high standard deviation in laboratory plasma treated test points indicates non-uniformity of the treatment. The treatments did not have an influence on contact angles with mineral and linseed oils. Talc containing paper 2 had the highest water contact angle, which is probably due to the intrinsic hydrophobic nature of the talc pigment surface. Starch and/or latex reduction seems to decrease the contact angles for water, EG and dampening water, and thus inducing some polarity on the surface.

Table IV: Contact angles [°] of water, EG, DIM, dampening water, mineral and linseed oils for papers 1 - 4

		Water	StDev.	EG	StDev.	DIM	StDev.	Damp. Water	StDev.	Mineral Oil	StDev.	Linseed Oil	StDev.
Paper 1	Untreated	58.1	0.8	36.7	1.6	36.8	1.8	39.2	3.9	11.9	0.5	23.3	1.8
	Pilot plasma treated	47.3	1.6	30.5	1.0	35.2	0.9	27.3	2.0	12.0	0.7	26.0	0.7
	Corona treated	50.7	2.1	36.5	1.5	30.7	3.5	32.2	1.6	11.5	0.3	23.5	0.8
	Lab. plasma treated	30.8	3.4	29.5	1.6	28.4	0.7	28.6	0.5	12.6	0.6	23.6	0.8
Paper 2	Untreated	68.0	1.2	35.9	1.2	40.7	2.3	40.6	1.7	9.8	0.6	19.3	1.0
	Pilot plasma treated	65.9	1.7	30.3	0.7	37.1	1.5	36.6	1.7	9.9	0.3	16.6	0.8
	Corona treated	68.9	2.5	33.3	1.9	35.3	2.0	36.2	1.3	10.0	0.2	15.9	1.3
	Lab. plasma treated	61.0	3.8	30.5	1.5	37.3	2.1	38.4	3.3	10.2	0.7	18.5	1.4
Paper 3	Untreated	50.7	2.2	30.5	2.8	37.9	1.4	34.6	1.1	8.6	2.4	23.1	0.7
	Pilot plasma treated	41.6	1.9	24.0	1.1	35.4	2.5	29.2	2.4	9.2	0.3	22.8	0.5
	Corona treated	45.9	0.2	27.1	0.5	32.5	2.1	31.5	0.7	7.9	1.4	21.0	1.4
	Lab. plasma treated	30.2	0.8	28.0	1.0	34.7	2.0	30.7	1.6	10.6	0.7	23.7	1.2
Paper 4	Untreated	55.1	2.2	29.3	2.2	30.6	1.6	28.0	1.1	10.3	0.5	19.3	0.5
	Pilot plasma treated	47.0	2.7	21.7	1.2	29.1	0.3	36.2	4.2	10.5	0.4	17.0	1.1
	Corona treated	53.8	2.5	27.6	1.5	26.7	3.1	36.1	1.7	10.6	0.0	17.7	1.2
	Lab. plasma treated	56.4	8.0	30.9	1.4	25.0	2.6	32.6	6.8	10.3	0.8	18.5	1.3

The contact angles in Table IV were taken after two seconds, when the contact angle values were as static as possible given the nature of the porous, rough and heterogeneous paper substrates. Even if plasma treatment did not have an influence on the contact values for ink oils, presented in Table IV, it influenced the initial change of contact angles with time with linseed oil, as can be seen in Figure 2. The initial contact angles were significantly smaller for plasma treated surfaces.

The contact angle titrations and works of adhesion were determined for paper 1 to clarify the nature of the polarity. In our previous studies, adopting the van Oss equation indicated an increase in base character [Pykönen *et al.* 2007]. However, it is well known that the van Oss equation emphasizes the base component [Berg 1993; Lee 1996]. According to the present results, plasma treatments have clear impact on polar component (W^{AB}), which has contribution of acid-base interactions and hydrogen bonding. However, pH has no clear effect, which indicates that there are no strong acidic or basic groups on the surface including also

that the plasma treatment did not introduce large amounts of COOH groups. Laboratory plasma treatment had the clearest impact on contact angles and polarity due to the longest treatment time. Pilot scale plasma treatment had the stronger influence on contact angles in comparison to the corona treatment.

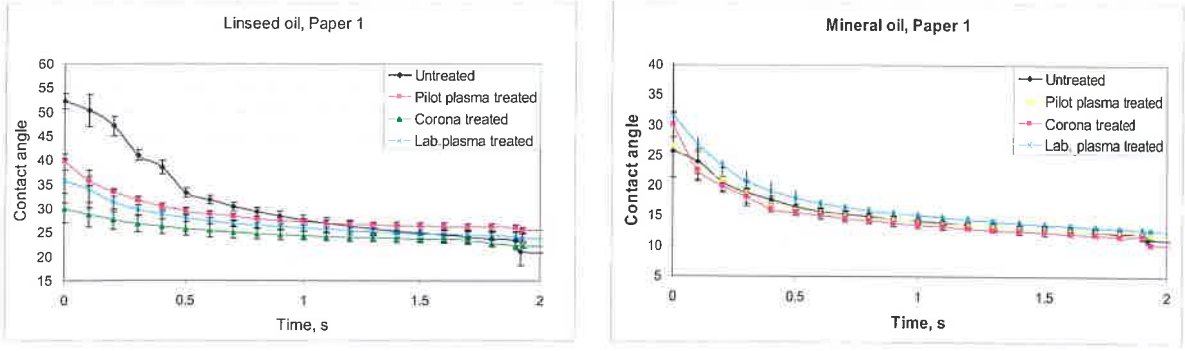


Figure 2: Change of contact angles with time from 0 to 2 seconds with linseed oil (left) and Mineral oil (right) for paper 1

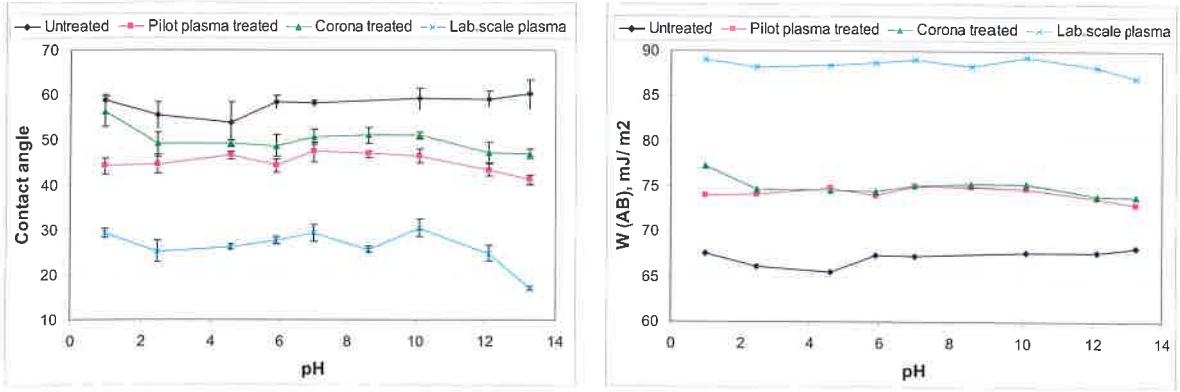


Figure 3: Contact angle titrations [°] (left) and work of adhesion values to acid-base interactions (right) as a function of pH for paper 1

The polar oxygen containing molecular groups explain the increase in polarity (W^{AB}). The O/C ratio calculated from the XPS measurement data was highest with laboratory plasma treated samples due to longest treatment time, as can be seen in Table V. The pilot plasma activation was slightly more effective than the conventional corona. With C1 - C5 groups, it is possible to see more accurately which oxygen containing molecular groups were formed. The C1 peak is related to hydrocarbon chains and aromatic compounds, in which carbon is not bonded with oxygen. The C2 peak corresponds to ethers and alcohols, which are typically from polysaccharides (e.g. starch) and polyacrylic latex in paper samples. The C3 peak is related to ketones and aldehydes, which may come from polysaccharides. The C4 peak includes carboxyl and ester groups, which may result from latex and polysaccharides. The C5 peak indicates carbonate groups from calcium carbonate pigment [Ström, Carlsson 1993; Vyörykkä *et al.* 2006]. The behavior was similar to that in our previous study [Pykönen *et al.* 2008]: The relative portion of C1 related molecular groups was reduced by all the treatments, and the portion of C2-C4 peaks increased due to pilot scale treatments. However, the long treatment time with the laboratory plasma method led also to a conversion of C2 groups to C4, and especially the C4 peak increased. It seems that the composition of the pigment coating had an influence on the effectiveness of the plasma activation: the talc containing paper 2 had the highest delta O/C values, while the GCC containing paper 4 had the lowest values. Starch did not seem to influence the tendency to oxidize under experimental conditions applied here. Talc containing paper 2 also had a higher portion of the C4 after pilot scale treatments when compared to the other papers.

ToF-SIMS was used to provide detailed chemical information to see where the plasma treatment takes place. Changes in ToF-SIMS spectra occurred between 200 - 700 Dalton (Da), whereas between 0 - 200 Da no changes could be detected. Therefore, it can be said that the plasma activation seems to influence high molecular weight paper chemicals, such as dispersion chemicals and surfactants, instead of pigment or latex particles itself. Since the spectra were measured also from the coating components (dispersed pigments and

binders), most of the peaks at coated paper spectra could be identified to be connected to some coating component. In Table VI is listed the characteristic peaks for each coating component, and showed which peaks were identified also in the coated paper spectra. It seems that addition of starch eliminated all the kaolin peaks from the spectra and brought GCC peaks visible, when comparing paper 1 to paper 3. However, any peaks from starch could not be seen on the coated paper spectra. The characteristic peaks of talc component were clearly identified on the talc and GCC containing paper 2 spectra, even if any GCC peak could not be identified. Only GCC containing paper 4, characteristic peaks for GCC were clearly visible.

Table V: XPS results; O/C ratio and C1-C5 groups

		O/C	Std.	C1 [%] C-C, C-H, C=C	C2 [%] C-O, C-OH C-O-C	C3 [%] C=O O-C-O	C4 [%] O-C=O	C5 [%] CO32-
Paper 1	Untreated	1.24	0.10	90.0	4.4	0.0	2.5	2.7
	Pilot plasma treated	1.41	0.13	77.4	10.6	3.0	7.3	1.9
	Δ Pilot plasma	**0.17**		**-12.6**	**6.2**	**3.0**	**4.7**	**-0.8**
	Corona treated	1.43	0.09	77.7	10.9	2.7	5.5	2.9
	Δ Corona	**0.20**		**-12.3**	**6.6**	**2.7**	**3.0**	**0.2**
	Lab. plasma treated	2.96	0.27	68.0	8.8	2.5	17.9	3.2
	Δ Lab. Plasma	**1.72**		**-22.0**	**4.4**	**2.5**	**15.4**	**0.6**
Paper 2	Untreated	1.27	0.04	74.8	13.4	0.8	4.3	6.9
	Pilot plasma treated	1.62	0.10	62.4	15.4	4.3	12.2	4.6
	Δ Pilot plasma	**0.35**		**-12.4**	**2.0**	**3.6**	**7.9**	**-2.3**
	Corona treated	1.50	0.06	66.3	14.8	3.6	10.7	4.6
	Δ Corona	**0.23**		**-8.5**	**1.4**	**2.9**	**6.3**	**-2.4**
	Lab. plasma treated	3.43	0.14	52.3	9.3	2.8	30.2	5.5
	Δ Lab. Plasma	**2.16**		**-22.5**	**-4.1**	**2.0**	**25.9**	**-1.4**
Paper 3	Untreated	1.19	0.11	83.0	9.3	0.6	3.4	3.7
	Pilot plasma treated	1.44	0.10	70.6	14.2	5.0	9.8	0.4
	Δ Pilot plasma	**0.25**		**-12.5**	**4.9**	**4.4**	**6.4**	**-3.3**
	Corona treated	1.39	0.11	70.3	15.8	4.6	7.4	1.8
	Δ Corona	**0.20**		**-12.8**	**6.6**	**4.0**	**4.0**	**-1.9**
	Lab. plasma treated	2.68	0.08	70.8	7.7	2.4	17.3	2.1
	Δ Lab. Plasma	**1.49**		**-12.3**	**-1.6**	**1.8**	**13.9**	**-1.6**
Paper 4	Untreated	0.70	0.01	72.1	6.7	0.1	3.4	18.4
	Pilot plasma treated	0.85	0.02	57.6	14.0	3.5	8.8	15.5
	Δ Pilot plasma	**0.15**		**-14.4**	**7.3**	**3.5**	**5.5**	**-2.9**
	Corona treated	0.82	0.03	60.7	13.5	3.2	9.7	12.7
	Δ Corona	**0.12**		**-11.4**	**6.8**	**3.1**	**6.4**	**-5.7**
	Lab. plasma treated	1.52	0.11	47.2	3.8	5.0	32.9	12.0
	Δ Lab. Plasma	**0.82**		**-24.8**	**-2.8**	**4.9**	**29.5**	**-6.4**

Table VI: Characteristic peaks for coating components and identified peaks from coated paper in positive ToF-SIMS spectra

	0–100 Da	100–700 Da
GCC (HC90)	23 *(Na+)*, 40 *(Ca+)*	113, 327, 355, 383, 411, 439, 467, 495, 536
GCC (Setacarb)	23 *(Na+)*, 40 *(Ca+)*	113, 327, 355, 383, 411, 439, 467, 495, 536
Kaolin	23 *(Na+)*, 27 *(Al+)*, 28 *(Si+)*	245, 301, 414, 442
Talc	23 *(Na+)*, 24 *(Mg+)*, 28 *(Si+)*	139, 156, 256, 272, 288, 300, 314, 330, 344, 356, 372, 388
Latex	23 *(Na+)*, 77 *(C6H5+)*, 91 *(C7H7+)*	115, 128, 259, 566
Starch	23 *(Na+)*	105, 143, 206, 223, 268, 404, 330, 450, 478, 502, 528
Paper 1	23 *(Na+)*, 27 *(Al+)*, 28 *(Si+)*, 40 *(Ca+)*	**115, 128 *(latex)*, 245, 414, 442 *(kaolin)*, 467 *(GCC)***
Paper 2	23 *(Na+)*, 24 *(Mg+)*, 28 *(Si+)*, 40 *(Ca+)*	**115, 128 *(latex)*, 139, 156, 256, 272, 288, 300, 314, 330, 344, 356, 372, 388 *(Talc)***
Paper 3	23 *(Na+)*, 27 *(Al+)*, 28 *(Si+)*, 40 *(Ca+)*	**115, 128 *(latex)*, 411, 439, 467 *(GCC)*, 566 *(latex)***
Paper 4	23 *(Na+)*, 40 *(Ca+)*	**115, 128 *(latex)*, 355, 383, 411, 439, 467, 495, 537*(GCC)***

Most changes caused by the treatments were detected in positive spectra. With kaolin, GCC and latex containing paper 1, a new 259 Da peak from latex spectra occurred after laboratory scale plasma treatment. Peaks from dispersed GCC (467 and 495 Da) were missing after pilot scale treatments. With talc containing paper 2 spectra the locations of the peaks originating from dispersed talc were changed by the surface treatments. With kaolin, GCC, latex and starch containing paper 3, peak 566 Da from the latex spectrum were missing after all the treatments. Peak 259 Da also from the latex spectrum occurred as a new peak due to laboratory scale plasma treatment. With GCC and latex containing paper 4, the peak intensities from the GCC spectrum were changed by all the treatments. The ToF-SIMS spectrum of GCC and paper 4 had peaks 355, 383, 411, 439, 467, 495, 536 Da with a peak separation of 28 Da corresponding to molecular fragments $C_2H_4^+$ (Figure 4). This fragmentation pattern suggested the presence of long chain hydrocarbon on the surface of paper 4 that originated from the GCC. The long chain hydrocarbon peaks disappeared after laboratory scale plasma treatment and indicated a surface modification process.

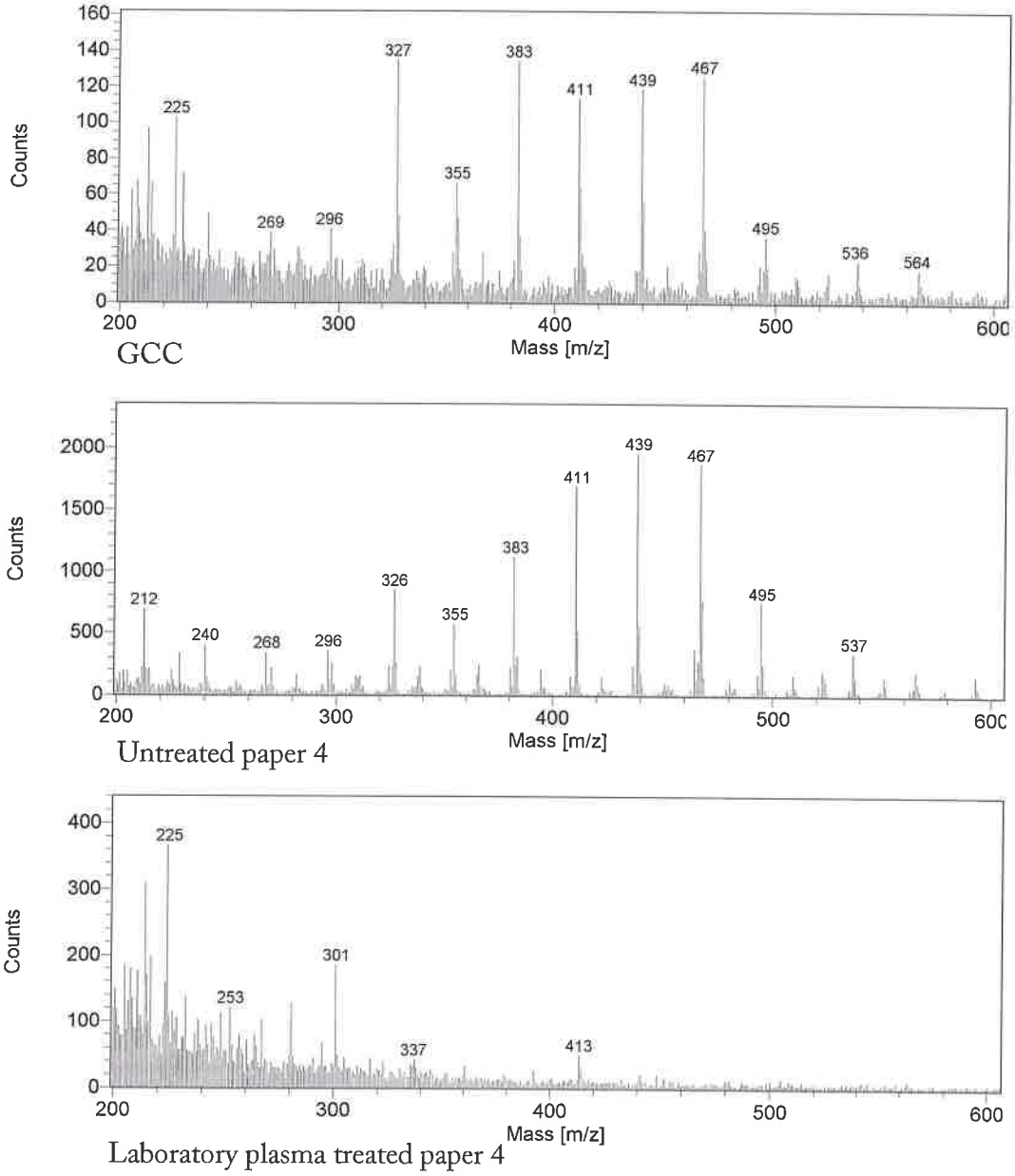


Figure 4: Spectra for dispersed GCC (Setacarb) pigment, untreated paper 4 and laboratory plasma treated paper 4

In the negative spectra, the peaks from the latex spectrum (119, 183, 265, 417 and 519 Da) could be detected from all spectra of coated papers. Clear changes for these peak intensities and also missing peaks could be detected especially after laboratory plasma treatment. As a conclusion, it can be said that plasma activation affects chemicals, which appear on pigment and latex particle surfaces. However, all the papers had differences in spectra between 200 - 700 Da, i.e. different surface chemistry. With papers 1 and 3, plasma activation seemed to influence dispersion chemicals of both pigments and binders, whereas with paper 2 and 4 it influenced mostly the dispersion chemicals of pigments. The ion bombardment causes fragmentation, and thus we are detecting only indicative fragments of the polymers, and not the whole polymer. The actual polymers have high molecular weights, which are outside the detection limit of the ToF-SIMS.

According to earlier results [Pykönen *et al.* 2008], intensive plasma treatment may affect, in addition to surface chemical properties, also surface roughness. In this study, simple gloss measurement was used to indicate the effect on surface roughness. As can be seen in Figure 5, the laboratory scale plasma treatment decreased gloss, which indicates an increase in roughness. However, the pilot scale treatments did not seem to have an influence on gloss. Surface strength was also determined, since it is an important property in offset

printing. Results clearly show that strong laboratory plasma treatment decreases surface strength. However, pilot scale treatments did not have an influence on surface strength, as shown in Figure 5.

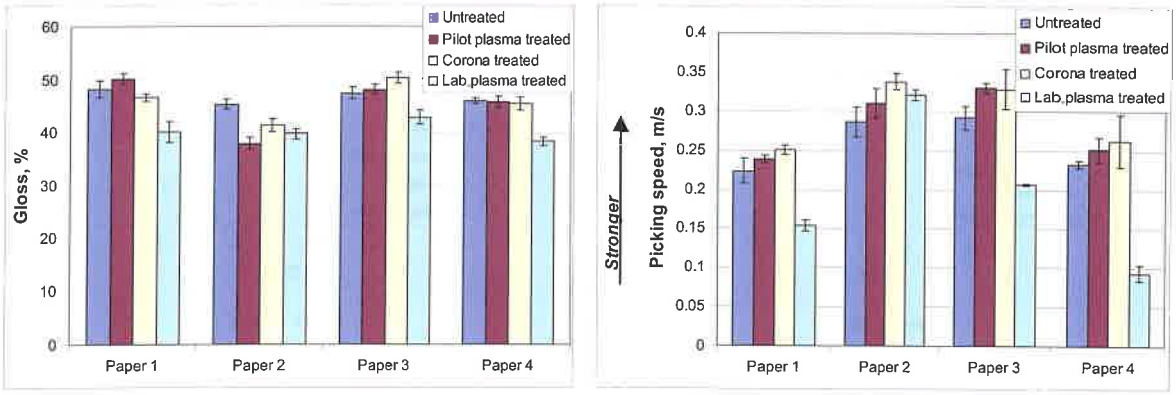


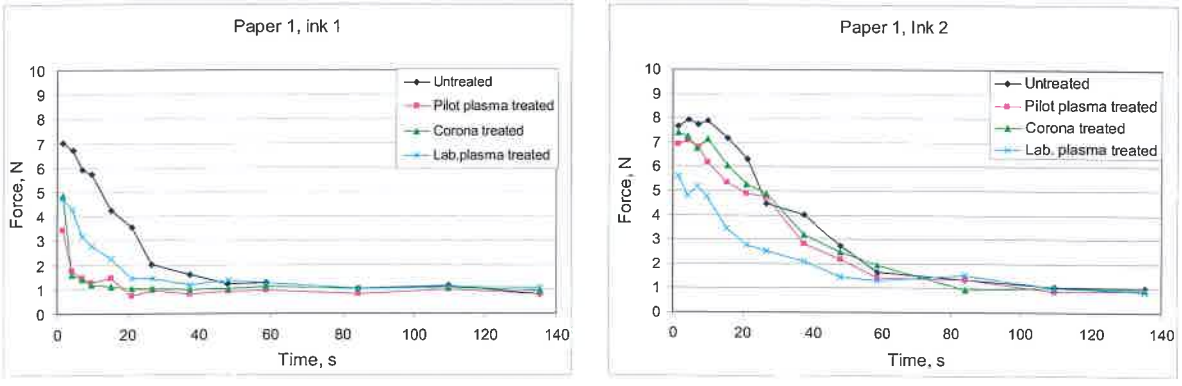
Figure 5: Gloss (left) and surface strength (right)

3.2 Ink setting

The ratio of the linseed to mineral oil had a clear impact on ink setting rate; an increased portion of linseed oil slowed down the ink setting with all papers. This result is in agreement with previous studies [Ström 2005]. GCC containing paper 4 was the fastest setting paper with all the inks. This is probably due to it having the highest frequency of the small pores, and thus probably also a greater number of pores compared to the other paper coatings. The slowest ink setting paper coating was kaolin, GCC, latex and starch containing paper 3, on which ink setting was clearly slower compared to the starch-free kaolin, GCC and latex containing paper 1. Starch containing paper 3 had a larger pore size, and the amount of binder composition in total was two parts greater than with paper 1, which may explain the slower ink setting.

The plasma activation had an impact on ink setting, as can be seen in Figure 6. Plasma activation accelerated the ink setting and decreased tack, when the ink contained for the most part mineral oil. However, the response to plasma treatment was the opposite, when ink contained for the most part linseed oil. This may result from increased acid-base interactions between polar linseed oil and the polar paper surface. Plasma treatment increased the polarity of the surface, and the portion of the dispersive forces decreased. Therefore, the interactions of treated surface and non-polar mineral oil may have reduced, and thus causing absorption of mineral oil to be accelerated.

The laboratory scale plasma treated sample differed clearly from the pilot scale treated samples. In addition, the standard deviation was clearly larger compared to untreated and pilot scale plasma treated samples. Gloss measurements indicated that the strong laboratory scale plasma treatment increased also the roughness of the paper. Therefore, maximum tack force may have decreased due to reduced thin film contact between the print and the tack disc, which occurs as a result of increased roughness.



Continued on page 164

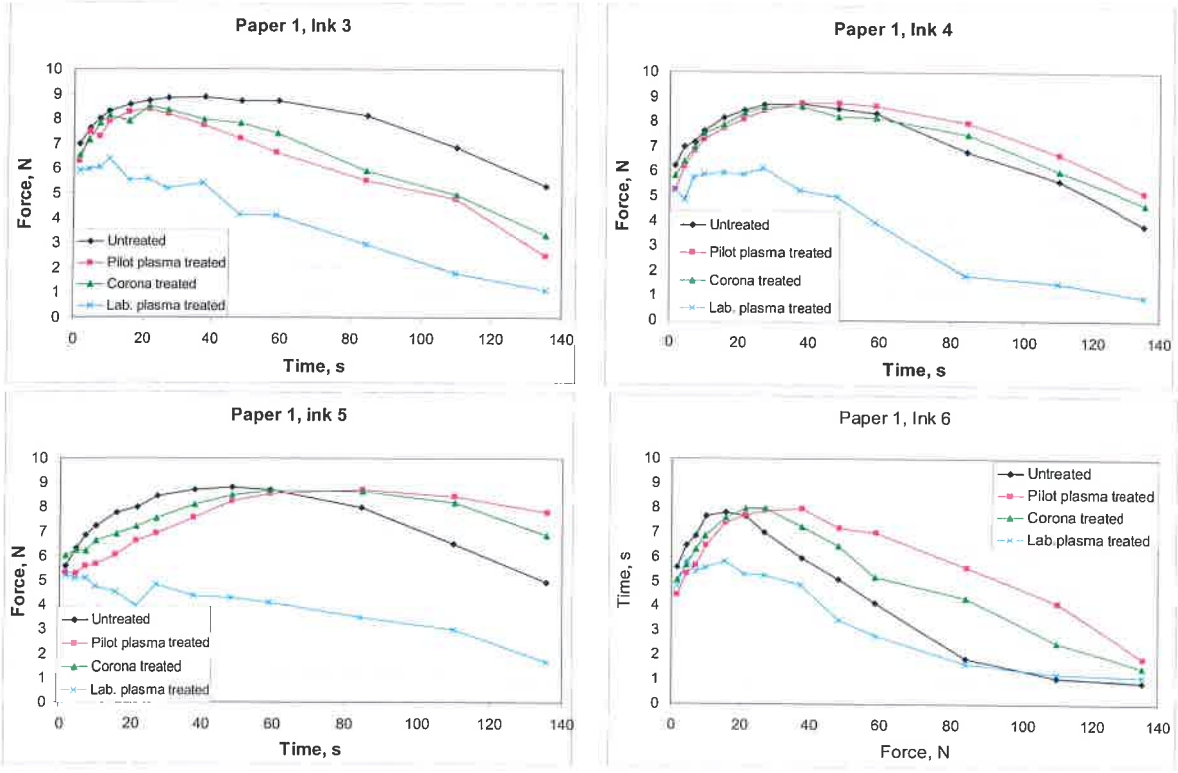


Figure 6: Effects of plasma treatments on ink setting (tack response) for kaolin, GCC and latex containing paper 1 with inks 1 - 6

3.3 Print quality

According to the laboratory scale printing, ink composition had a clear influence on print quality; print gloss increased as a function of linseed oil amount. This is probably caused by a reduced ink setting speed, which allows ink-filaments caused by the film split in the printing nip to level out. However, pilot scale treatments did not have an impact on density, print gloss, set-off or mottling of pigment coated papers either on laboratory or pilot scale printed samples. This correlates with our earlier study [Pykönen *et al.* 2008], where we saw changes in print quality only with surface sized paper. Similarly also to our previous study, laboratory scale plasma treatment caused significant print density variation with all papers. The print density was clearly lower in spots where plasma treatment had the strongest influence. The print density variation could also be seen in laboratory scale printing, which confirms that it is not caused by variation in dampening water absorption. It seems, however, that plasma treatment has an influence on dampening water absorption, but it is more crucial with hydrophobic surface sized papers than with pigment coated papers. According to FIB and optical microscopy images the density variation with laboratory plasma treated samples is likely caused by micro-picking. It appears that only the top layer of the coating fails, and not the whole coating layer as can be seen in Figure 7.

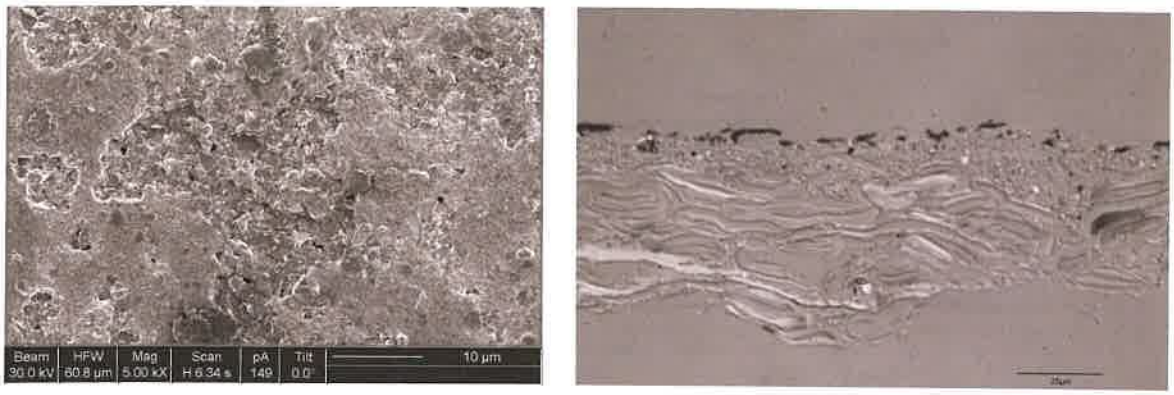


Figure 7: FIB (left) and optical microscopy (right) images of printed laboratory plasma treated samples to show micro-picking to be a likely explanation for density variation of laboratory scale plasma treated samples

4. Discussion

Plasma activation modified the surface of coated papers by inducing polar oxygen containing molecular groups. Coating composition seemed to have an impact on the response to plasma treatment. This was probably due to different dispersion chemicals as the ToF-SIMS results showed that plasma treatment modified the high molecular weight chemicals on the surface of pigment and latex particles. The contact angle values for polar liquids did not decrease on the GCC and latex containing paper 4, as they did with all the other papers. The paper 4 also had the lowest O/C ratio after the treatments. Talc containing paper 2 had the greatest change in O/C ratio, and plasma treatment seemed to create more carboxylic acid and/or ester groups when compared to the other papers. Using of the model pigment coatings and measuring also spectra of the coating components, the ToF-SIMS results enabled to recognize that plasma treatment had impact especially on the dispersion chemicals of the pigment and latex particles. However, the identification of the exact chemical nature of these dispersion chemicals from the spectra was not still possible. However, for most clays and carbonate pigments the dispersants are based on sodium polyacrylates, but sometimes also inorganic polyphosphates are used [Järnström 1992].

In this study experimental plasma treatment seemed to result in slightly higher impact on the surface properties compared to corona treatment. Too intense and long treatment time during laboratory plasma treatment caused also an increase in surface roughness, in addition to chemical changes. This resulted in a significant print density variation, and a decrease in gloss, surface strength and maximum tack force in ISIT curves. The density variation caused by the intensive laboratory scale plasma treatment was also noticed in our earlier study [Pykönen *et al.* 2008], but not until know the micro-picking was confirmed to be the reason for that.

It seems that the surface of coating is weakened by the laboratory plasma treatment. The explanation for the weakening could be that plasma causes some chemical changes to dispersion chemicals of latex and pigments, which may cause the loss in surface strength of the coating. The plasma treatment can also potentially cross-link any remaining double-bonds in SB latex and change its mechanical properties.

The changes in ink setting due to pilot scale plasma treatment can be considered as resulting only from surface chemistry changes, because the changes in gloss or surface strength could not be detected. The ink setting slowed down with polar linseed oil dominated inks, and accelerated with non-polar mineral oil dominated inks. The slower setting with linseed oil dominated inks was probably due to increased polar interactions between polar ink oil and plasma treated coating. Work on adhesion values showed clearly that plasma treatment increases the polarity of the surface. The linseed oil had clearly (up to 20°) lower initial contact angles after plasma treatment, which indicated also that plasma treatment increased the interactions between coated paper and linseed oil. In previous studies the chemical interaction between ink and coating has been shown to have an influence on ink setting. For instance, it is well known that ink setting is slower with linseed oil based inks compared to mineral oil based inks, and one given explanation for this has been the acid-base interactions between polar linseed oil and coating [Ström 2005; Rousu 2002]. In addition, by increasing latex polarity the rate of increase for ink-splitting force has been reduced [van Gilder and Purfeest 1994; van Gilder and Smith 1999]. van Gilder and Smith [1999] have concluded that the reduced rate of increase for ink-splitting force caused by increased latex polarity was associated with greater resistance to both mineral and linseed oil diluents.

However, in this study the ink-setting was accelerated with mineral oil based inks, probably because the portion of the dispersive component in proportion to total surface energy decreased due to plasma treatment. Therefore, chemical interactions, i.e. dispersive forces between treated paper surface and non-polar mineral oil, were reduced and the absorption was even more dominated by capillary forces.

The surface chemistry changes by pilot plasma activation did not influence the offset print quality of pigment coated paper. In our previous study [Pykönen *et al.* 2008] plasma treatment had influence on print gloss and density of surface sized paper in laboratory scale printing, when pre-dampening was used. In addition, plasma treatment reduced water interference mottle with surface sized paper. Even if the plasma treatment was shown to influence contact angles of dampening water with pigment coated papers, it seems that the role of the dampening water is more crucial with hydrophobic surface sized papers. Ink oil type had a clear impact on ink setting and print quality with all papers: ink setting rate decreased with linseed oil inks and, as a result, print gloss increased. This is in agreement with earlier studies, where has been shown that vegetable oils reduce the ink setting speed compared to mineral oils [Ström 2005], and slower ink setting yields greater ink leveling and higher print gloss [Preston *et al.* 2001b]

5. Conclusions

- Since plasma treatment caused changes mainly in respect to dispersion chemicals of pigment and latex particles, different dispersion systems of coating pigments seemed to influence how the surfaces respond to plasma treatment. For example, the chemical changes reflected in contact angle values and oxidation ratio indicate that the plasma treatment had the most intense effect on talc containing paper coating (paper 2), whereas the influence on GCC containing paper coating (paper 4) was the smallest.

- The surface energy and degree of polarity of coated paper had an influence on ink setting. However, the effect was dependent on ink oil type; increased substrate surface polarity decreased the setting rate of linseed oil based inks, whereas for the mineral oil based inks the ink setting accelerated, possibly due to the reduction of the portion of the dispersive component.

- Too intensive plasma activation (evidenced on the laboratory scale) reduced the surface strength of pigment coated paper, which caused density variation due to micro-picking. The coating failure occurred only on the topmost layer of the coating, leaving rest of the coating intact.

- Pilot scale plasma activation enables ink setting adjustment by modification only of the surface chemistry properties without affecting coating structure. For instance, a slower rate of ink tack build with vegetable oil based ink could be induced, which could reduce picking and/or piling tendency. Vice versa, with slow setting papers ink setting could be accelerated if mineral oil based ink is used.

Acknowledgments

This work was funded by the Finnish Funding Agency for Technology and Innovation (Tekes). The Authors would like to acknowledge Development Manager Hannu Laine from Siegwerk for planning the ink recipes for this work and for offering materials and instruments for ink preparation. We would like to acknowledge also Research Scientist Juha Saari from Technical Research Centre of Finland (VTT) for his help with preparing the model inks, and thank VTT also for the access to the laboratory scale plasma apparatus. Research Scientist Mikko Tuominen from Tampere University of Technology is acknowledged for performing the pilot scale plasma and corona treatments, and Laboratory Technician Pauliina Saloranta for performing the contact angle measurements at Åbo Akademi University. Peter Heard from University of Bristol is thanked for performing the FIB measurements.

References

1. Berg, J. C., (1993), *The Importance of Acid-Base Interactions in Wetting, Coating, Adhesion and Related Phenomena*, Nordic Pulp and Paper Research Journal, 1, pp. 75 - 85
2. Cernakova, L, Stahel, P., Kovacik, C., Johansson, K. and Cernak, M., (2006), *Low-Cost High-Speed Plasma Treatment of Paper Surfaces,* 9th TAPPI Advanced Coating Fundamentals Symposium, Turku, Finland 8 - 10 February, pp. 7 - 17
3. d'Agostino, R., Favia, P., Oehr, C. And Wertheimer, M. R., (2005), *Low-Temperature Plasma Processing of Materials: Past, Present and Future, Plasma Process.* Polym., 2, 7 - 15
4. Fouchet, B., Noirot, P.-A., Desjumaux, D. and Van Gilder, R. L., (2004), *Diffusion dynamics of offset ink components in very thin latex films of different structure and composition.* In proc. Tappi 2004 International Printing and Graphic Arts Conference, pp. 43 - 58
5. Fouchet, B., Noirot, P.-A., Desjumaux, D. and Van Gilder, R. L., (2006), *Absorption Dynamics of Offset Ink Components in Thin Film of Different Structures and Compositions,* Journal of Pulp and Paper Science, 32 (3)
6. Järnström, L., (1992), *The Polyacrylic demand in Suspensions Containing Ground Calcium Carbonate*, Nordic Pulp and Paper Research Journal, no. 111993, pp. 27 - 33
7. Koivula H., Preston J. S., Heard P. J., Toivakka M., (2008), *Visualisation of the distribution of offset ink components printed onto coated paper,* Colloids & Surfaces A: Physiochem.Eng. Aspects 317, pp. 557 - 567
8. Lee, L-H., (1996), *Correlation between Lewis Acid-Base Surface Interaction Components and Linear Solvation Energy Relationship Solvatochromic α and β Parameters,* Langmuir, 12, pp. 1681 - 1687
9. Marttila J., Preston J. S., Parsons D. J., (2004), *Ink scuff of Matt and silk papers,* Proc 2004 Tappi IPGAC Vancouver Oct 2004, pp 11 - 18

10. Mukhopadhyay, S. M., Joshi, P., Datta. S. and Macdaniel, J., (2002), *Plasma Assisted Surface Coating of Porous Solids,* Applied Surface Science, 201, pp. 219 - 226

11. Navarro, F.; Davalos, F.; Denes, F.; Cruz, L. E.; Young, R. A.; Ramos, J., (2003), *Highly Hydrophobic Sisal Chemithermomechanical Pulp (CTMP) Paper by Fluorotrimethylsilane Plasma Treatment,* Cellulose 10(4), pp. 411 - 424

12. Oittinen, P., (1976), *Fundamental rheoligical properties and Tack of Printing Inks and their Influence on Ink Behaviour in a Printing Nip.* Dissertation, Helsinki University of Technology, Helsinki, Finland

13. Preston J. S., Elton N., Hiorns A. G. Strom G., (2008), *Application of Imaging Reflectometry to Studies of Print Mottle on Commercially Printed Coated papers,* Tappi J, vol.7 No. 1, January 2008 pp. 11 - 18

14. Preston J. S., Elton N. J., Legrix A. and Nutbeem C., (2001a), *The role of pore density in the setting of offset printing ink on coated paper,* TAPPI Advanced Coating Fundamentals May 2001, San Diego

15. Preston, J. S, Nutbeem, C., Parsons, J. and Jones, A., (2001b), *The Printability of Coated Papers with Controlled Microstructure*, Paper Technology, Vol 42, no. 2, pp.33 - 41

16. Preston, J. S, Parsons, D. J., Gate, L. F., Husband, J.C., Legrix, A. and Jones, M., (2003), *Ink gloss development mechanisms at short time-scales after printing- Part 1 - The influence of ink film thickness,* Journal Graphic Technol. Vol 1, No. 2, p.29 - 37

17. Pykönen, M., Hakola, L., Eiroma, K., Lahti, J., Sundqvist, H., Kaukoniemi, O.-V., Tuominen, M., Järnström, J., Peltonen, J., Fardim, P. and Toivakka, M., (2007), *Effects of Atmospheric Pressure Plasma Activation on Inkjet Print Quality,* 23rd International Conference on Digital Printing Technologies (NIP), September 16th - 21st 2007, Anchorage, Alaska

18. Pykönen, M., Sundqvist, H., Tuominen, M., Lahti, J., Preston, J., Fardim, P. and Toivakka, M., (2008), *Influence of Atmospheric Plasma Activation on Sheet-Fed Offset Print Quality.* Nordic Pulp and Paper Research Journal, 2

19. Ridgway, C. J. and Gane, P. A. C., (2006), *Correlation Pore Size and Surface Chemistry during Absorption into a Dispersed Calcium Carbonate Network Structure,* Nordic Pulp and Paper Research Journal, 21, 563 - 568

20. Roth, J. R., (2001), *Industrial Plasma Engineering. Vol. 2: Applications to Nonthermal Plasma Processes, IOP, Bristol and Philadelphia, 645 P*

21. Rousu, S. M., Gane, P. A. C. and Eklund, D. E., (2001), *Influence of Coating Pigment Chemistry and Morphology on the Chromatographic Separation of Offset Ink Constituents,* 12th Fundamental Research Symposium of the Pulp & Paper Fundamental Research Society, September 17 - 21 2001, England

22. Rousu, S., (2002), *Differential Absorption of offset Ink Constituents on Coated Paper.* Doctoral thesis, Åbo Akademi University, Painotalo Gillot Oy, Turku, 102 p

23. Rousu, S., Gane, P. and Eklund, D., (2005), *Print Quality and the Distribution of Offset Ink Constituents in Paper Coatings,* Tappi Journal, 4, 9 - 15

24. Rousu, S. M., Gane, P. A. C., Spielman, D. C. and Eklund D. E., (2000), *Differential Absorption of Offset Ink Components on Coated Paper,* 2000 Tappi International Printing & Graphic Arts, 55 - 70

25. Sahin, H. T., Manolache, S., Young, R. A. & Denes, F., (2002), *Surface Fluorination of Paper in CF_4-RF Plasma Environments,* Cellulose, 9(2). pp. 171 - 181

26. Ström, G., (2005), *Interaction between Offset Ink and Coated Paper - A Review of the Present Understanding,* 13th Fundamental Research Symposium, Cambridge, September 2005, pp. 1101 - 1137

27. Ström, G. and Carlsson, G., (1993), *Chemical Composition od Coated Paper Surfaces Determined by means of ESCA,* Nordic Pulp and Paper research Journal, 1, pp. 105 - 112

28. Ström, G. and Gustafsson, J. (2006), *Physical and Chemical Drying in Sheet-fed Offset Printing on Coated Paper,* Professional Papermaking, 2, 72 - 77

29. Ström, G., Gustafsson, J. and Sjölin, K., (2001), *Printing Papers Separation of Ink Constituents during Ink Setting on Coated Substrates,* Coating and Graphic Arts Conference and Trade Fair, San Diego, CA, United States, May 6 - 9 2001, pp. 269 - 279

30. Van Gilder, R. L. and Purfeest, R. D., (1994), *Latex binder modification to reduce coating pick on six-color offset presses.* Tappi J, 77(5, 230 - 239

31. Van Gilder, R. L. and Smith, D. A., (2001), *Development of a high polarity latex polymer for waterless sheet fed offset paper coatings.* Paper Technology, March 2001, p. 50- - 56

32. Vyörykkä, J., Fogden, A., Daicic, J., Ernstsson, M. and Jääskeläinen, A.-S., (2006), *Characterization of Paper Coatings – Review and Future Possibilities,* 9th TAPPI Advanced Coating Fundamentals Symposium, Turku, Finland, February 8th - 10th 2006, pp. 41 – 66



Flexographic print quality of pilot coated paperboard

Robert Olsson[1,2], *Li Yang*[2,3], *Magnus Lestelius*[2]

[1] Holmen Paper AB, Hallsta Paper Mill
SE-763 81 Hallstavik, Sweden
E-mail: Robert.Olsson@holmenpaper.com

[2] Karlstad University, Department of Chemical Engineering
SE-651 88 Karlstad, Sweden.

[3] Holmen Paper AB, Holmen Paper Development Center
SE-601 88, Norrköping, Sweden

Abstract

The study addresses how paperboard coating structures and ink properties (waterbased) affect print quality in flexography, from an ink setting perspective. Pilot coated paperboards with different pigment blends and lattices in the coating were printed with a pilot flexographic printing press. The inks used are one solution polymer binder based (SPB) ink and one emulsion polymer binder based (EPB) ink. The study showed that the type of ink affects all of the measured print-quality parameters: print density, print gloss, and dot gain, and is of the greatest importance to achieve the best print-quality. The portion of clay pigment in the coating has great influence on the dot gain. Increasing the clay content in the coating leads to a higher dot gain. Changing coating binders from soft to hard latex results in increased paper gloss and print density.

Keywords

Coated paperboard, clay pigment, binders, print quality

1. Introduction

The printability of a substrate depends on several parameters. Some of them are common parameters for all printing technologies, such as paper porosity and ink absorption, while the rest are more printing-technology-specific, such as paper smoothness and deformable printing forms. Flexographic printing has, traditionally and primarily, been applied to package printings. The type of material used within the package industry is traditionally paper of different grades such paperboard, liner and corrugated board as well as foils, plastic films and cellophane [Hallberg Hofstrand 2006]. All these types of materials have a wide range of properties that influence the printing process as well as the print. The subject of interest of this study is coated paperboard which has a smooth and porous coating on the top surface, most frequently used for gravure printing but even to a certain extent for flexographic printing.

The coating porosity and pore radius have significant influence on the ink absorption rate and hence the final print quality, [Gane et al. 2000, Leskinen 1987, Preston et al. 2002]. The type of pigment used in the coating will influence the coating smoothness, gloss and porosity. Mixing pigments of different shapes and types will, also, strongly influence the coating structure, due to different packing characteristics, and hence its ability to absorb ink [Alince and Lepoutre 1983, Leskinen 1987]. In flexographic printing rapid absorption of the ink vehicle by porous substrates (i.e. paper, paperboard and corrugated board) is required to enable fast drying especially in multi colour printing. This property can be achieved by coating, using pigments that result in coatings with a high capillarity, i.e., fine pores, which absorb fluid rapidly [Gane 2004].

The absorption rate of inks into a coating strongly affects the print gloss. It have been shown that inks with higher resistance to dewatering results in higher final print gloss [Olsson et al. 2007a]. Preston et al. [2003] showed that the final print gloss was influenced both by ink film levelling and the absorption of the ink resin (offset). The higher the absorption rate, the shorter the ink-levelling time, which results in a rougher ink film that leads to a lower print gloss.

In the 1950's Walker and Fetsko [1955] introduced an empirical equation describing the amount of ink that will be transferred from a printing nip. The equation is based on the possibility of ink-immobilization, the ink

thickness on the printing plate and the fraction of the wet ink-layer to be transferred. The possibility of the ink-immobilization is dependent on the character of the substrate. A thicker layer of immobilised ink increases the amount ink transferred and hence the total print density. De Grâce and Mangin [1983] found that the surface roughness of the substrate influenced the ink transfer in offset presses so that a rougher surface accepts more ink. When the surface gets too rough, however, it will lead to reduced contact area and then reduced ink transfer. For newsprint, on the other hand, the print density is little affected by the surface roughness. Concerning the printing pressure they found that a higher pressure forces more ink into the substrate (newsprint); but too high pressures may close some of the pores, thereby, reduce ink transfer.

The transferred amount ink flows not only into the substrate but also laterally on the substrate resulting in an expansion of the tone values, i.e., dot gain. In flexography besides the ink spreading on paper surface, deformation of the printing form also contributes to the physical dot gain, which are defined as the difference between the size of the printed dot and that on the printing form (without pressure). Bould et al. [2004b] suggested two mechanisms of print-form-deformation, causing dot gain: either the dot surface on the print form expands laterally during compression or a "barrelling" effect occurs where part of the dot sides becomes a part of the printing area. Investigating physical dot gain, Olsson et al. [2006b] found that at higher applied printing pressure the physical dot gain exhibit a nonlinear characteristic. In a separate study Bould et al. [2004a] found that the ink spreading also had a significant effect on the final dot size.

The major objective of the present study is to extend our understandings and findings obtained from the lab-scale studies [Olsson et al. 2006a, b, 2007a, b] into a more production-like situation i.e., pilot scale. In addition, how the inks' and substrates' characteristics affect on ink transfer, ink-setting and in turn the final print quality, are also studied.

2. Materials and methods

2.1 Pilot coating

Eight coating colours, denoted from A to H in *Table I*, were used for the pilot coating trials. The trials were conducted at UMV Coating AB, Säffle, Sweden, with a coating speed of 400 m/min, at temperature of 23°C. Coating colour of 10 - 12 g/m^2, with 63 - 65% solids content, was applied. A commercially produced (Stora Enso Skoghall, Sweden) pre-coated board, 185 g/m^2, with a coat weight of 13 g/m^2 (as a pre-coating for the pilot coatings) was used as substrate. The pigments used were fine particle clay (Capim DG from Imerys, USA) and ground calcium carbonate (GCC, Hydrocarb 90, from Omya AG, Switzerland). A soft (Litex P6115) or a hard (Litex PX9142) latex with T_g of 8 or 30°C, respectively, supplied by Eka Polymer Latex, Sweden, was added to the coating colour formulation. A thickener for the coating colour, CMC (FinnFix 10 from Noviant), was used in all coatings.

Hg-porosimetery, at MoRe Research, Örnsköldsvik, Sweden, together with a L & W Gloss Tester, AB Lorentzen & Wettre, Sweden, were used for characterizing the pore size distribution and Tappi gloss (75°), respectively, of the substrate and of the pilot-coated papers. The roughness of the substrate and the coated paper were measured with a PPS (Parker Print Surface) instrument from AB Lorentzen & Wettre, Sweden, with a measuring pressure of 10 kg/m^2 (SCAN-P 76:95). Printing was performed on the substrate and the pilot-coated paperboards.

Table I: The coating colour formulations (pph is parts per hundred part of dry pigment)

	A	B	C	D	E	F	G	H
GCC [pph]	0	50	70	100	0	50	70	100
Clay [pph]	100	50	30	0	100	50	30	0
Soft latex [pph]	16	16	16	16	0	0	0	0
Hard latex [pph]	0	0	0	0	16	16	16	16
CMC [pph]	1	1	1	1	1	1	1	1

2.2 Printing

Two water-based flexographic inks (with different binders, see *Table II*) were printed with a Windmöller & Hölscher Soloflex flexographic printing press at Brobygrafiska, Sunne, Sweden, on the pilot coated boards

and the base substrate (pre-coated board, 185 g/m^2). The two inks were printed at two different printing units in the printing press. The employed anilox roll was a ceramic coated roll with 315 l/cm screen ruling and a cell volume of 3.5 ml/m^2. The printing press setup, nip pressure, drying fans (50°C), etc., were the same throughout the trial and the print speed was set to 70 m/min. The printing plate, DuPont DPI-45 with a thickness of 1.14 mm, was produced by Brobygrafiska, Sunne, Sweden, and mounted on the plate roller using a 0.55 mm mounting tape, 1020M, from 3M, Sweden. The print form layout was composed of a large full tone area and smaller areas (25 cm^2) of tone values from 0 to 90%, in steps of 10%, situated next to each other. The screening ruling of the printing forms of 10 to 90% areas was 42 lines/cm. The ink viscosity, for both inks, was adjusted to 20 s with a DIN-4 cup prior printing.

2.3 Ink properties

Two inks containing identical type and amount of ink pigment, cyan, but different binders were prepared. While both binders are of acrylate type, one is solution polymer binder (SPB), another is emulsion polymer binder (EPB), *Table II*. A FibroDAT 1100, FibroSystems AB, Sweden, was employed for surface tension analysis (pendant drop) of the inks. For the viscosity character of the inks we refer to our previous work [Olsson et al. 2007b]. The binders and pigments were supplied by Sun Chemical Inks A/S, Skovlunde, Denmark. Generally, the acrylic EPB based ink has a lower polarity which contributes to faster water release and thereby higher drying speed than the SPB based ink [Laden 1997]. The EPB inks are usually used for low cost inks for porous substrates when print gloss is not required.

Table II: The ink characteristics

	SPB	EPB
Type of binder	**SPB**	**EPB**
T_g of binder [°C]	**101**	**-23**
Solid content [%]	**43,5**	**46,4**
pH	**8,2**	**7,7**
Surface tension [mN/m]	**35.6 ± 0.2**	**38.8 ± 0.2**

2.4 Print characterization

After printing, the prints were stored for several months in a climate controlled room (23°C and 50 % RH) prior analysis. Different measurements were performed on the prints to evaluate the print quality. The print density and overall dot gain were evaluated with a GretagMacbeth densitometer. The physical dot enlargement of the prints 50% nominal tone value in both the printing direction and cross printing direction, were estimated by employing an interference profilometer (WYKO NT3300 from Veeco Instruments Inc., AZ, USA). The optical magnification of the profilometer was 20 and the scanning depth, the distance from top to bottom of the vertical scan, was 75 µm. 10 randomly selected sampling points within a scanning area of 1.49 x 1.14 mm^2 were measured, with a scanning resolution of 2 µm/pixel. The size of the image was 736x480 pixels. The roughness values were calculated using the in-built software, Vision 32 (version 2.303, Veeco Instruments Inc., AZ, USA) of the profilometer. The Tappi gloss values of the prints were measured at 75° with a glossmeter from Zehntner GmbH Testing Instruments, Switzerland. A Perkin Elmer atomic absorption spectrophotometer 3300, (Perkin Elmer, Wellesley, MA, USA) has been employed to measure the relative ink (cyan) transferred, the copper amount, for all printing conditions according to SCAN-CM 38:05. To collect data for evaluating mottling, a scanner, Duoscan T2500 from AGFA, was used with a scanning resolution of 300 dpi. Mottling was evaluated on the solid tone areas employing a STFI Mottling v.2.41 software (Swedish Pulp and Paper Institute, Stockholm, Sweden).

3. Results and discussion

3.1 Characterisation of the pilot coated paper

Fig. 1, shows the pore characteristics of the pre-coated substrate and the pilot-coated papers. The pore distributions exhibit remarkable dependence on both the type of the lattices as well as clay vs. calcium-carbon portions. When the soft latex is used, the clay-based coating (100% soft) has approximately a similar average

pore radius to that of the calcium-carbonate-based coating (0% soft). While with the hard latex is used, the clay-based coating (100% hard) has a smaller average pore radius compared to the calcium-carbonate-based coating (0% hard). A synergy is observed for the coatings of 30% clay and 70% calcium-carbonate, as the coatings have a similar (hard latex) or a smaller (soft latex) average pore size than those of the 100% clay coatings. The average pore radius is important in liquid absorption as it has been shown that smaller pore radiuses correlate to faster ink setting [Xiang et al. 2004]. The coating pore sizes and porosity are strongly dependent on the pigments packing ability [Leskinen 1987]. It is also worth noticing that the 100% calcium carbonate (0% clay) coating display a significantly lower but broader peak than the rest of the pilot coated paperboards. This leads to a greater average pore radius as shown in *Table III.* Nevertheless, the positions of the peaks seem to alternate with the amount calcium carbonate in the coating as suggested by the profiles of 0%, 30%, 50% and 100% clay-contents. The average pore radius is therefore also alternating, as shown in *Table III.* This may imply that the blending of clay with calcium carbonate produces a denser structure for some material-ratios. The using of soft latex in coating generates smaller accumulated pore volume but slightly large averaged pore radius than those of using hard latex. Larsson et al. [2007a] has described it as the clay achieves a house of card structure, when not calendered, and thereby achieves a higher pore volume than calcium carbonate. It is however surprising that no synergy effect on pore volume is visible when mixing clay and calcium carbonate. Studies have shown that mixing of pigments can result in smaller pore volume [Larsson et al. 2007b, Vidal et al. 2004].

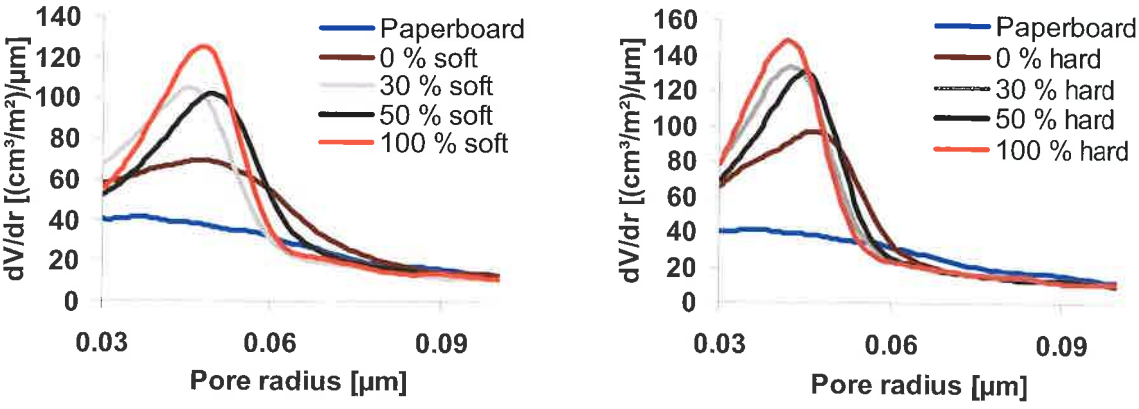


Figure 1: The coating pore characteristics of the paperboard substrate and the pilot coated paperboards measured with Hg-porosimetry. The index represents percent of clay in the coating (clay-calcium carbonate) and the type of latex applied, i.e., soft or hard, respectively

With increasing clay content, roughness of the coating surface decreases as a consequence of the platy structure of clay pigments, *Fig. 2.* As explained by Chinga et al. [2002] the platy clay particles orient themselves during the coating and the consolidation process of the coating layer to lie flat on the coating surface and thereby form a smoother more glossy surface, see *Fig. 5* below. With spherical calcium carbonates, on the other hand, it is not capable to form a smooth surface as clay does.

Table III: The average pore radius and cumulative volume (of the coating (0.03 - 0.3 µm) as extracted from the Hg-porosity measurements

Coating (clay content and latex type)	Average pore radius [µm]	Cumulative pore volume [cm³/m²]
0 % hard	0.048	4.42
30 % hard	0.043	4.74
50 % hard	0.046	4.72
100 % hard	0.043	4.80
0 % soft	0.049	4.25
30 % soft	0.046	4.31
50 % soft	0.051	4.55
100 % soft	0.048	4.69

The improvement of the surface roughness has a non-linear relationship with the increasing clay-content, see Fig. 2. The PPS roughness decreases rapidly with only a small portion of clay, for example 30%, in the coating. However, a further addition of clay results only in very small changes in roughness, as indicated by *Fig. 2*. A possible scenario is that the clay pigments locate more frequently on/near the surface rather than in the bulk of the coating when mixed and thereby capable of forming a smoother surface than expected from a simple mixing rule. Al-Turaif [2006] using pigment blends of clay and PCC found that the content of clay at the surface was indeed higher than expected by a simple mixing rule. He also found that the PCC induced a higher latex concentration at the surface. It is worthy to notice that it is not the increased latex concentration at the surface that produces a reduction in roughness to the level of the clay coating. Nevertheless, the mechanism producing a higher degree of latex content at the surface with PCC explains why the type of latex has an impact on roughness. Compared coatings of 100% GCC, higher roughness is obtained with the soft film forming latex than with the hard latex. The base substrate has, as expected, significantly rougher surface, as it was coated with more coarse pigments, traditionally used for pre-coated paperboard.

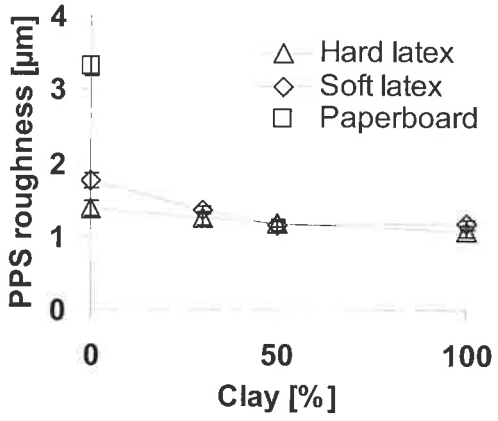


Figure 2: The PPS roughness of the paperboard and the pilot coated paperboard, the error bars are standard deviation calculated from 10 measurements

3.2 Print evaluation

The print density measurement, *Fig. 3,* reveals differences both in respect to different inks and different lattices used in the coatings. There are, at least, two possible causes: different amounts of ink transferred onto the substrates and/or different ink distribution in the substrates. Lindholm and Ström [1995] have earlier shown that the ink transfer in a flexographic press varied with the inks properties. The transfer from the anilox to the printing form was affected to a higher degree by the ink properties, compared to ink transfer from the printing form to the paper. However, clear differences between the studied inks have been observed in both positions. A similar argument may also apply to our system as suggested by *Fig. 3,* i.e. the print density depends strongly on the type of ink used: the SPB ink produces higher print density than the EPB ink. The type of latex has also significant influence on the print density and the hard latex results in a higher print density than the soft. From ink-coating interaction point of view, both ink properties and coating chemistry affect the print density [Olsson et al. 2006a, b]. For example, coatings comprising higher polar latex promote penetration of ink vehicles. This affects the build-up of the ink layer structure since pigment particles are pulled together and form a tighter and denser ink layer. This led to higher print density. Olsson et al. [2006a] studied the imbibition of fluids with different viscosities, dipole moments and surface tensions into different model coatings. They showed that the polarity of the fluid influenced the depth of penetration of the fluid. As shown by others [Yang et al. 2006], ink penetration results in reduced print density due to strong light scattering of the substrate.

From the atomic absorption spectroscopy measurements, *Fig. 4,* only the difference in transferred amount of ink (estimated through amount Cu) generated by the different lattices used are seen. Amount of Cu, or the amount of ink transferred (Cu containing ink), decreases sharply at the beginning as clay content increases when the hard latex is used, while for the soft latex the amount of Cu increases. Why these two measurements, print density and amount of Cu differ is unclear since the print density should be largely influenced by the amount of ink pigment on/in the coating.

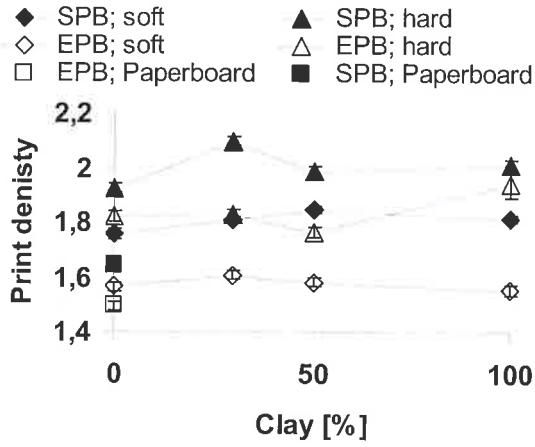


Figure 3: The print density of the prints on the pilot coated paperboards and the substrate. Error bars indicate 95% confidence interval calculated from 25 measurements

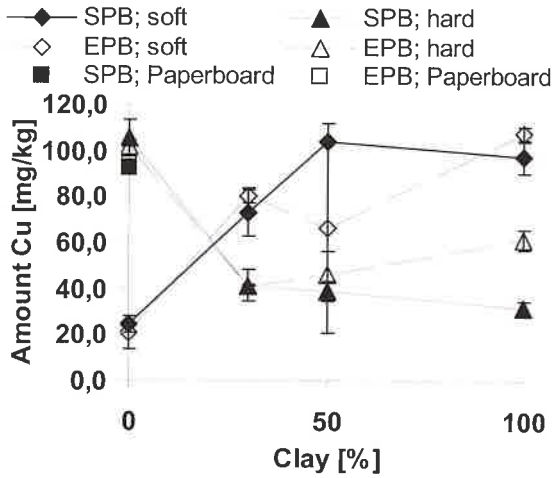


Figure 4: Amount Cu on coated paperboard as a function of on coating clay content for the different inks. Error bars are absolute errors from 2 individual measurements

The paper gloss is improved by coating. *Fig. 5* displays a greater paper gloss for paperboard with the hard latex than with the soft latex, which is in concordance with the roughness data, *Fig. 2.*, because the soft latex causes shrinkage upon film formation [Al-Turaif and Bousfield 2005]. With increasing clay content in the coating colour, gloss difference between the hard and the soft lattices decreases. Generally, the paper gloss improves as the clay content increase in the coating regardless of the type of latex used. There are two mechanisms for the increased paper gloss as clay is introduced to the coating [Al-Turaif 2006]. First, the coating experiences slower dewatering, leaving more time for the particles to pack denser to produce a smoother surface. Second, the platy structure of clay particles produces a surface of higher reflectance than that of the more spherical calcium carbonate (GCC).

The gloss is significantly increased when printed as seen from *Figs. 5* and *6*. For the prints, *Fig. 6*, the trend of increased gloss with clay content of the coating is not as prominent as for the unprinted surfaces (*Fig. 3*). However the delta gloss, difference between print gloss and paper gloss, is higher for the 100 % calcium carbonate coatings than for the 100% clay coatings. This means that the ink has the capability to fill out the rougher surface of the calcium carbonate coating while for the clay coating levelling of the initial roughness is less important to the delta gloss. Print gloss for the soft latex is significantly increased when introducing clay into the coating formulation. An addition of only 30% clay leads to significant enhancements of the print gloss. Further addition of clay does, however, not significantly extend the impact since the roughness of the coating is not decreased by further addition of clay, decreasing the demand for levelling by the ink.

The difference between the inks is also seen in *Fig. 6*. The print with the EPB ink has a lower gloss than with the SPB ink. As previously reported [Olsson, et al. 2007], the water-retention capacity of the ink plays an important role for the time during which the ink has to level. A slower levelling-out process promotes a smoother ink film with a higher gloss. As the EPB inks generally have lower polarity and faster water release they produce lower print gloss.

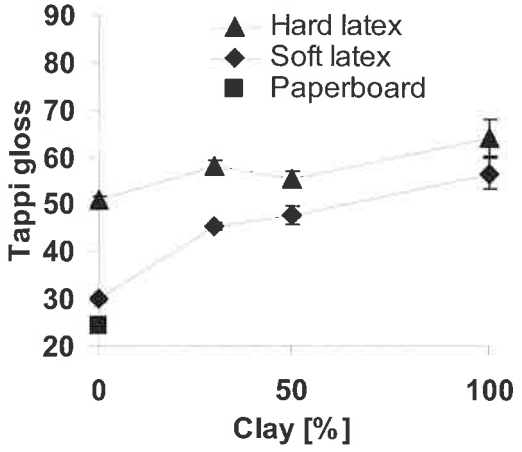


Figure 5: The Tappi gloss (75°) of the paperboard and pilot coated paper as function of clay content

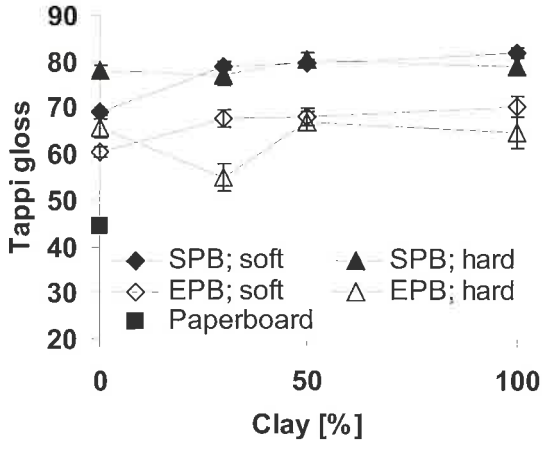


Figure 6: The Tappi gloss (75°) of the printed paperboard substrate and pilot coated paperboard as a function of clay content

The physical dot gain of the 50 % tone value measured with an interference profilometer, *Fig. 7 and 8,* show significantly lower dot gain for the pilot coated samples than for the precoated paperboard substrate. This is probably due to the rougher surface of the substrate as seen in *Fig. 2*. There exists an ambiguity in the contribution of roughness to spreading, and higher roughness (in a sufficiently high size scale capillary driven lateral motion is hindered whereas in lower size scales it is promoted [Gerdes et al. 1997, Gerdes and Ström 1996]) could limit the inks possibility to spread on the surface after the impression in the printing press. In addition higher roughness induces a lower degree of contact during the impression which lowers the ink transfer [De Grâce and Mangin 1983], whereas the opposite could also occur as increased roughness could mean a smaller area for pressure distribution. With increasing clay content in the coating, i.e., smoother surface, there is a very weak tendency for decreased physical dot gain when printing with the SPB ink. However, for EPB ink there is a correlation between the (increasing) physical dot gain and (increasing) clay content. No general trend is observed that differentiate the physical dot gain in the printing direction (MD) from the cross printing direction (CD), as it was the case in the laboratory-scale trail [Olsson et al. 2006b]. This may be attributed to the higher speed and smaller size of half tone dots used in the larger scale printing as compared to the laboratory scale printing.

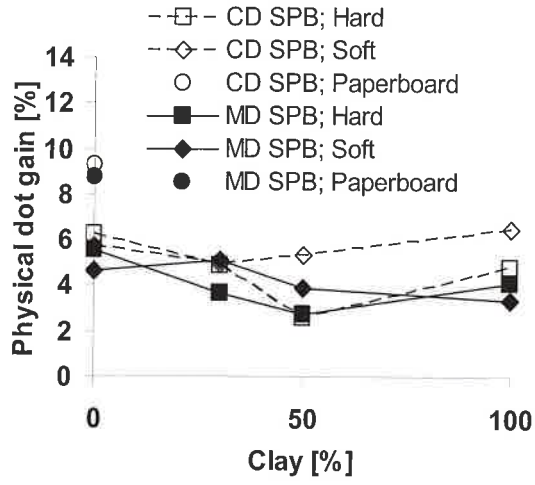


Figure 7: The physical dot gain of the 50 % tone value employing the SPB ink, as a function of clay content of pilot coated paperboard

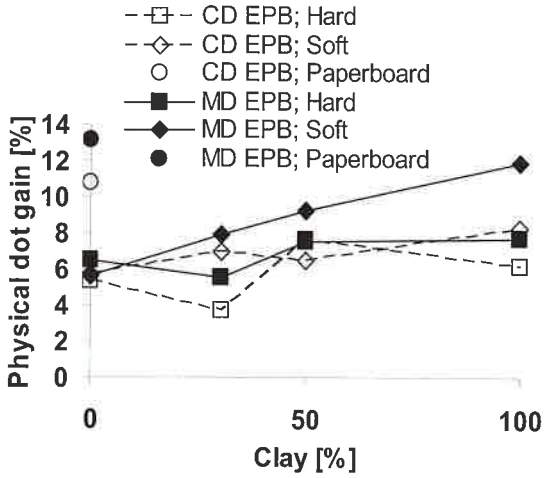


Figure 8: The physical dot gain of the 50% tone value employing the EPB ink, as a function of clay content of pilot coated paperboard

There is a distinct difference between the dot gain measured with the interference profilometer (physical dot gain), shown in *Fig. 7 and 8,* and the overall dot gain (physical plus optical dot gain) measured with a densitometer, *Fig. 9*. The overall dot gain increases for both SPB and EPB ink, with increasing clay content in coating. For prints with SPB ink, dot gain decreases drastically as the tone value increases, the dot gain at 80% tone value is nearly half that of 30%. The situation for prints with EPB ink is less drastic although a decrease in dot gain is also significant as tone value increases. It seems that the prints with EPB ink are more influenced by the substrates than with SPB ink, which may indicate that the chemical interaction between the substrates and the ink or the water retention capacity is more important to EPB ink. The influence of chemical interaction on ink setting has earlier been shown to influence both spreading and absorption of inks (fluids) in flexographic printing [Lagerstedt and Kolseth 1995, Olsson, et al. 2006a]. It is important to notice that it is not only the ink-setting speed, higher for finer pores, that reduces the dot gain because the coatings of 30% and 100% clay content exhibit roughly the same average pore radius. Another important aspect may be the effect of ink pigment penetrating into the substrate. With the larger pores dominating the calcium carbonate coating the ink may also penetrate into the coating matrix and thereby influence the light scattering which in turn reduces the dot gain [Yang and Kruse 2000, Yang et al. 2001]. The type of coating pigment also affects the light scattering, as clay (kaolin, 1.57-1.58) has a lower refractive index than calcium carbonate (1.66 - 1.68) [Engström and Rigdahl 1992]. The larger scattering power of the calcium carbonate coatings may contribute to a shorter lateral scattering length thereby reducing the optical dot gain.

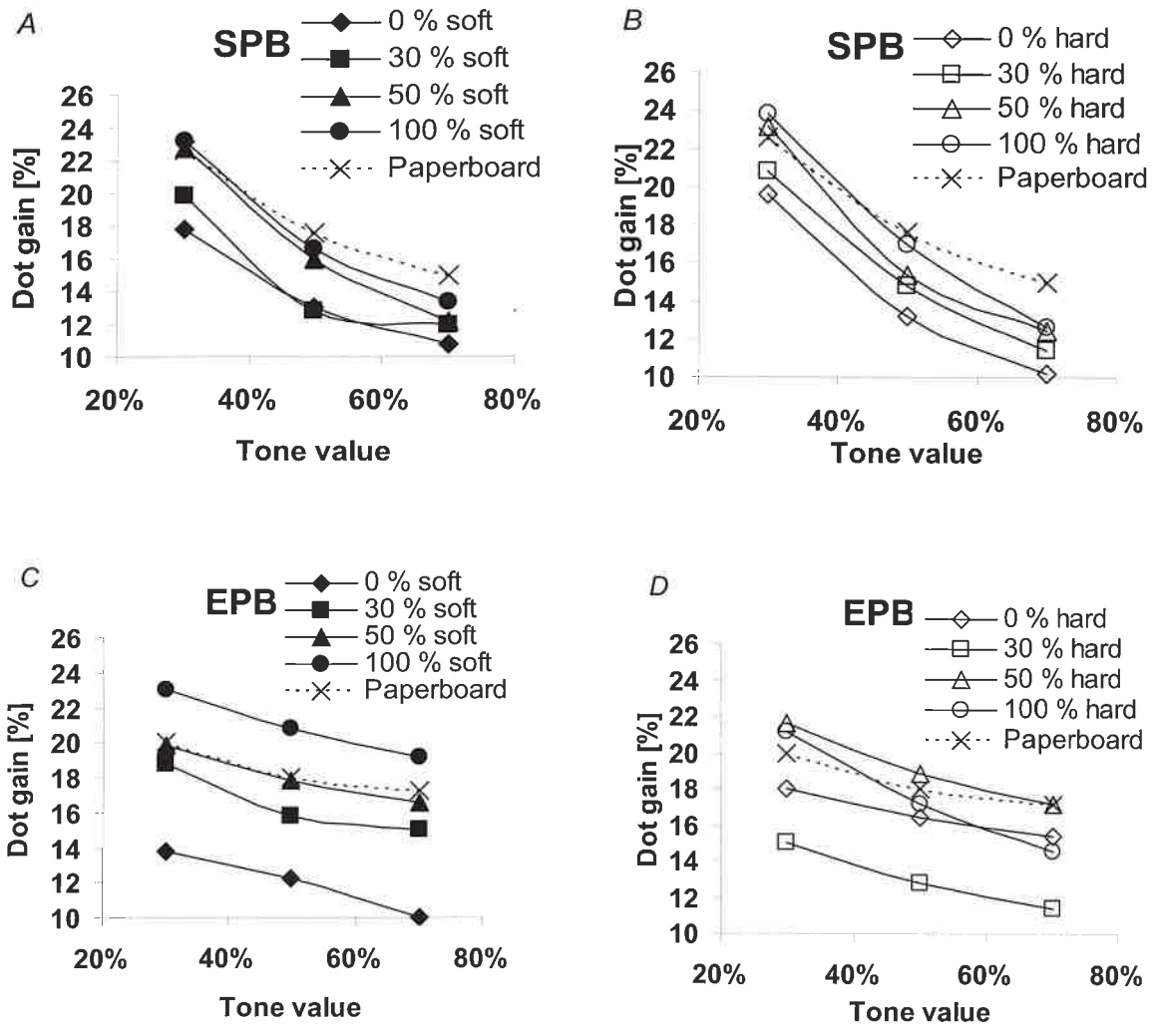


Figure 9:
The overall dot gain measured with a densitometer for SPB ink and EPB ink, for the various pilot coated paperboards consisting of different portion of clay (percentages given) and the different latex types:

A) and C) - soft
B) and D) - hard

Mottling describes the optical heterogeneity of a print and is closely related to ink transfer and absorption [Hallberg Hofstrand 2006, Johansson and Norman 1996]. Ink transfer and absorption are affected by the substrate, ink and printing press conditions. Mottling is usually evaluated with image analysis methods based on frequency analysis where the optical signal is divided into various spatial frequencies.

Mottling of the prints, *Fig. 10,* in general reduces with increasing clay content for all wavelengths. The degree of mottling is higher for prints with EPB ink than those with SPB. The results of EPB ink with the hard latex coating are somewhat irregular. The shorter wavelengths of mottling, *Fig. 10 B and C,* show a clear decrease with increasing clay content, which may reflect the inks' increased possibility to level out as the coating gets smoother. Overall, this ties in to the behaviour of dot gain and gloss where it appears that the EPB based ink is more susceptible to coating penetration and thus also to variation in the coating pore structure. The SPB based inks generally display a lower degree of mottling: This behaviour was previously reported [Rentzhog and Fogden 2006]. They attributed this phenomenon to an increase in low shear viscosity and a decreased surface tension for the SPB. It is also worth noticing that there are generally small differences in mottling, probably due to the relatively smooth and homogenous substrate printed upon.

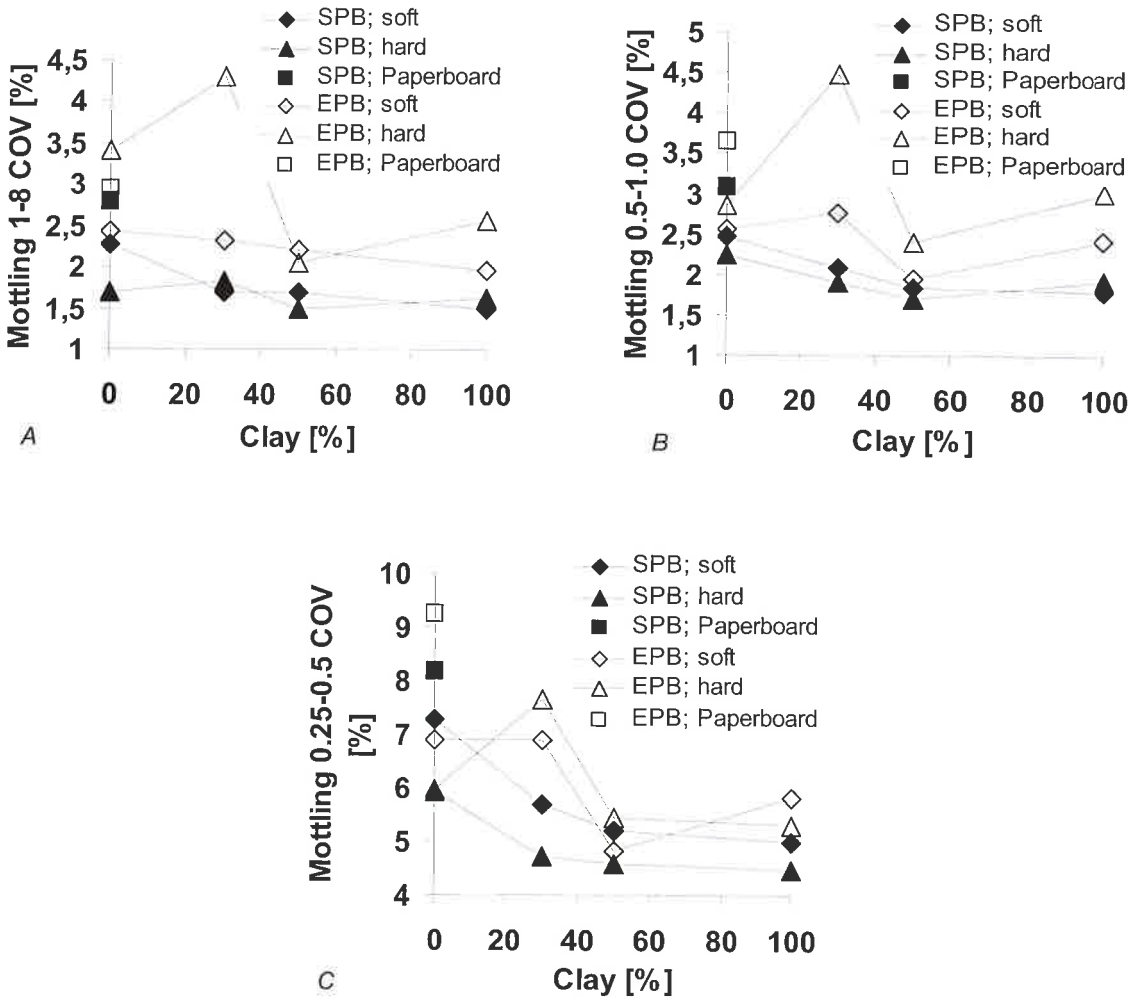


Figure 10: The mottling of different wavelengths for both inks, SPB and EPB inks. Soft and hard represent the type of latex used for the coatings

4. Conclusion

Print quality analysis for prints with different inks on pilot-coated paperboards, consisting of different pigment blends of clay and calcium carbonate, has been performed. Depending on the relative portion of the pigments, coating layers of different pore volumes, average pore diameters, and ink absorption rates were obtained. It shows that the choice of ink influences all print quality parameters (density, dot gain, mottling etc.), thus again emphasising the importance of understanding the actual mechanisms governing the ink-substrate interaction when choosing ink (for a certain type of substrate) to achieve favourable print quality and runnability. From the coating point of view, the amount of clay in the coating influences the pore characteristics, *Fig. 1*, and thereby the absorption speed. When comparing the inks, it appears that the solution polymer binder based ink has a tendency to reside to a greater extent on the surface of the substrate whereas the emulsion polymer binder based ink penetrates more into the coating as evidenced by gloss and dot gain measurements.

Verifications of earlier results were made possible by this study. The importance of surface chemistry on dot gain when printing has to some extent been indicated; due to chemical interaction the spreading may be reduced. The influence on dewatering of inks on gloss seems to hold, although, this parameter has not especially been measured within this study. The mottling tendency depending on the ink system, emulsion and solution polymer binders, is again observed within this study. Unlike observations from laboratory-scale tests, no significant difference was observed in dot-deformation (MD vs. CD).

Acknowledgments

The financial support from the Swedish Pulp and Paper Research Foundation, the Knowledge Foundation and the Swedish Agency for Innovation System (VINNOVA) is gratefully acknowledged. We would also like to thank Sun Chemical Inks A/S, Denmark for supplying the flexographic inks and Stora Enso Skoghall AB, Sweden, for providing the paperboard. UMV coating, Säffle, Sweden, is also thanked for the pilot coating. Additionally Mikael Larsson at Karlstad University, Sweden, is acknowledged for the help during setup of the trail and valuable discussions. Additional thanks go to MoRe research, Örnsköldsvik, Sweden for the mercury intrusion measurements and Irene Olsson at Stora Enso Skoghall AB, Sweden, for performing the surface tension measurements of the inks.

References

1. Al-Turaif, H. (2006): The Effect of Pigment Blends on the Surface Structure and Chemistry of Pigmented Latex Coatings, Tappi Journal, 5(8), 24
2. Al-Turaif, H. A.; Bousfield, D. W. (2005): The Influence of Pigment Size Distribution and Morphology on Coating Binder Migration, Nordic Pulp and Paper Research Journal, 20(3), 335
3. Alince, B.; Lepoutre, P. (1983): Flow Behavior of Pigment Blends, Tappi Coating Conference, San Fransisco, USA
4. Bould, D. C.; Claypole, T. C.; Bohan, M. F. J. (2004a): An Experimental Investigation into Flexographic Printing Plates, Journal of Graphic Technology, 1(3), 1
5. Bould, D. C.; Claypole, T. C.; Bohan, M. F. J.; Gethin, D. T. (2004b): Deformation of Flexographic Printing Plates, 56th Annual TAGA Technical Conference, San Antonio, TX, USA
6. Chinga, G.; Helle, T.; Forseth, T. (2002): Quantification of Structure Details of LWC Paper Coating Layers, Nordic Pulp and Paper Research Journal, 17(3), 313
7. De Grâce, J. H.; Mangin, P. J. (1983): A Mechanistic Approach to Ink Transfer Part I: -Effect of Substrate Properties and Press Conditions, 17th International Conference of Printing Research Institutes, Saltsjöbaden, Sweden, Banks, W. H., Ed. Pentech Press, London: p 312
8. Engström, G.; Rigdahl, M. (1992): The Use of Some PCC Grades as Coating Pigments, Nordic Pulp and Paper Research Journal, 7(2), 90
9. Gane, P. A. C. (2004): Absorption Properties of Coatings: A Selected Overview of Absorption Criteria Derived from Recent Pore Network Modelling, Journal of Dispersion Science and Technology, 25(4), 3889
10. Gane, P. A. C.; Schoelkopf, J.; Spielmann, D. C.; Matthews, G. P.; Ridgway, C. J. (2000): Fluid Transport into Porous Coating Structures: Some Novel Findings, Tappi Journal, 83(5), 1
11. Gerdes, S.; Cazabat, A.-M.; Ström, G. (1997): The Spreading of Silicone Oil Droplets on a Surface with Parallel V-Shaped Grooves, Langmuir, 13, 7258
12. Gerdes, S.; Ström, G. (1996): Spreading of Oil Droplets on Silicon Oxide Surfaces with Parallel V-Shaped Channels, Colloids and Surfaces A: Physicochemical and Engineering Aspects, 116, 135
13. Hallberg Hofstrand, E. (2006): Flexographic Post-Printing of Corrugated Board. Dissertation, Karlstad University, Karlstad, Sweden
14. Johansson, P.-Å.; Norman, B. (1996): Methods for Evaluating Formation, Print Unevenness and Gloss Variations Developed at STFI, Tappi Process & Product Quality Conference Proceedings, Cincinnati, OH, USA, TAPPI Press: p 139
15. Laden, P. (1997): *Chemistry and Technology of Water Based Inks*. Blackie Academic and Professional: London, UK, p 345
16. Lagerstedt, P.; Kolseth, P. (1995): Influence of Surface Energetics on Ink Transfer in Flexo Printing, Advances in Printing Science and Technology: proceedings of the 23rd research conference of IARIGAI, p 269, Paris, France
17. Larsson, M.; Engström, G.; Vidal, D.; Zou, X. (2007a): Impact of Calendering on Coating Structures, Nordic Pulp and Paper Research Journal, 22(2), 267
18. Larsson, M.; Vidal, D.; Engström, G.; Zou, X. (2007b): Paper Coating Properties as Affected by Pigment Blending and Calendering, Tappi Journal, 6(8), 16
19. Leskinen, A. M. (1987): Layer Structure in Model Coatings, Tappi Journal, 70(12), 101
20. Lindholm, G.; Ström, G. (1995): On-Line Measurements of Ink Film Thickness in a Flexo Press, Advances in Printing Science and Technology: proceedings of the 23rd research conference of IARIGAI, p 337, Paris, France
21. Olsson, R.; van Stam, J.; Lestelius, M. (2006a): Imbibition into Model Calcium Carbonate Coatings of Fluids with Different Dipole Moments, Appita Journal, 59(6), 471

22. Olsson, R.; Yang, L.; Lestelius, M. (2007a): Water Retention of Flexographic Inks and Its Influence on Final Print Gloss, Nordic Pulp and Paper Research Journal, 22(3), 287
23. Olsson, R.; Yang, L.; van Stam, J.; Lestelius, M. (2006b): Effects on Ink Setting in Flexographic Printing: Coating Polarity and Dot Gain, Nordic Pulp and Paper Research Journal, 21(5), 569
24. Olsson, R.; Yang, L.; van Stam, J.; Lestelius, M. (2007b): Effects of Elevated Temperature on Flexographic Printing, Advances in Printing and Media Technology: proceedings of the 34th research conference of IARIGAI, Grenoble, France
25. Preston, J. S.; Elton, N. J.; Legrix, A.; Nutbeem, C.; Husband, J. C. (2002): The Role of Pore Density in the Setting of Offset Printing Ink on Coated Paper, Tappi Journal, 1(3), 3
26. Preston, J. S.; Husband, J. C.; Nutbeem, C.; Parsons, D. J. (2003): Ink Gloss Development Mechanism after Printing. Part 2: The Influence of Substrate, Proc. 8th Advanced coating fundamentals symposium, p 15, Chicago, IL, USA
27. Rentzhog, M.; Fogden, A. (2006): Correlation between Properties of Water-Based Flexographic Inks and Their Print Uniformity on PE-Coated Boards, Nordic Pulp and Paper Research Journal, 21(3), 403
28. Walker, W. C.; Fetsko, J. M. (1955): A Concept of Ink Transfer in Printing, American Ink Maker, (December), 38
29. Vidal, D.; Zou, X.; Uesaka, T. (2004): Modelling Coating Structure Development: Monte-Carlo Deposition of Particles with Irregular Shapes, Nordic Pulp and Paper Research Journal, 19(4), 420
30. Xiang, Y.; Bousfield, D. W.; Hayes, P. C.; Kettle, J. (2004): A Model to Predict Ink-Setting Rates Based on Pore Size Distributions, Journal of Pulp and Paper Science, 30(5), 117
31. Yang, L.; Fogden, A.; Pauler, N.; Sävborg, Ö.; Kruse, B. (2006): Studying Ink Penetration with Microscopic and Spectroscopic Techniques, Journal of Imaging Science and Technology, 50(4), 327
32. Yang, L.; Kruse, B. (2000): Ink Penetration an Its Effects on Printing, IS&T/SPIE Conference on Color Imaging: Device-Independent Color, Color Hardcopy and Graphic Art V, p 365, San Jose, California
33. Yang, L.; Lenz, R.; Kruse, B. (2001): Light Scattering and Ink Penetration Effect on Tone Reproduction, Journal of Optical Society of America, image science and vision, 18(2), 360

Ink transfer during flexographic printing to paper

Timothy C. Claypole, David G. Beynon, Simon M. Hamblyn

Welsh Centre for Printing and Coating, School of Engineering, University of Wales Swansea
Singleton Park, Swansea SA2 8PP, UK
E-mail: t.c.claypole@swansea.ac.uk

Abstract

As part of an on going study of the process physics of flexographic printing, a comprehensive study has been undertaken of the effect of ink viscosity, engagement, line ruling and anilox volume on the ink transfer to paper. The viscosity of the ink was varied in two manners, one by dilution with solvent thus reducing pigment concentration as well as the viscosity and the other reducing the viscosity at constant ink strength. The anilox volume was found to have the greatest effect on the ink transfer in the solid coverage areas. However, an interaction was found between the coverage, the line ruling and the anilox cell size. This can be attributed to the deformation of the half tone areas of the plate into the anilox cells and in part explain the inconsistency found by previous researchers in highlight regions on the plate. The engagement was found to increase the ink transfer as more ink was impressed into the substrate.

Keywords

Flexography, ink transfer, paper

1. Introduction

In order to get prints right first time with the minimum wastage and to improve consistency through the print run, there is a need to understand the affect of process parameters on the ink transfer and print quality. There are three main points of ink transfer in the flexographic printing process; inking of the anilox roll, transfer of ink from the anilox to the plate and from the plate to the substrate. There have been previous studies on the transfer of ink in letter press printing onto an absorbent substrate; the majority of the work on ink transfer in flexography had studied the transfer to non absorbent substrates, such as film, as this allows the study of the ink splitting in isolation. This paper focuses on the ink transfer from the plate to paper, a porous substrate. This introduces the absorption into the substrate and its consequent affect on the ink transfer.

There have been several studies of ink transfer in letterpress from plate to substrate, from which parallels can be drawn to flexographic printing. In their series of works on ink transfer in letter press, De Grace and Mangin separated ink transfer into ink Immobilisation and Split fraction [De Grace et al 1983, 1987, 1991]. Increases in substrate roughness and porosity, increase in printing pressure and decrease in speed were found to increase ink transfer due to increased immobilisation. As both polymer film and paper substrates were used, the authors were able to determine which component of ink transfer was being affected by changing parameters. This was possible as ink transfer to film takes place by splitting alone where as transfer to paper is by both immobilisation and split fraction. Increases in ink transfer brought about by higher substrate roughness, porosity, pressure increase or speed reduction was attributed to an increased amount of ink immobilised within the substrate. As the ink film thickness on the plate was increased the split became more asymmetric with respect to total ink film thickness. The position of ink splitting was affected by printing speed. A lower speed allows more time to allow filament flow to even out the splitting position between plate and substrate, therefore a lower speed gives an increase in ink transfer. It was suggested that cavitation due to air entrainment at the nip entry was followed by bubble migration, filamentation and filament rupture. The splitting mechanism of cavitation to filament rupture where ink transfer is to uninked substrate was invstigated through magnified photography at the nip exit. Filament length at rupture is affected by ink film thickness and speed. These investigations into ink transfer in the letterpress process have only examined the solid coverage patches where an uninterrupted rolling nip contact is set up. The ink transfer mechanisms involved may therefore only be appropriate for high coverage areas in flexo printing where dots on the plate are joined.

The effect of flexo process parameters was investigated the NPIRI task force [NPIRI]. The investigation measured optical density of the solid. However, the optical tone gain was only measured for the 2% and 70%

patches. UV ink was printed onto polyester substrate with varying anilox volume and press speed. The viscosity of the ink was also varied with the pigment concentration held constant so that results reflect only the effect of viscosity. Increase in speed decreased solid density and had no effect on tone gain, while increasing the anilox volume was found to increase the solid density and tone gain. Decreasing viscosity of the ink increased solid density. The effect of ink viscosity on tone gain depended upon the line ruling of the anilox roll and the plate dot size. With viscosity decrease there was tone gain decrease at 70% coverage for a 250 lpi anilox roll, the results were "variable" for the 2% coverage patch. For a 400 lpi anilox the results for 70% coverage was found to be variable and the 2% coverage showed a reduction in tone gain with viscosity decrease. Viscosity was found to have no effect on tone gain for a 700 lpi anilox. The viscosities used were high as were the anilox volumes. The authors were unable to explain the inconsistent results.

The effect of pressures at different positions in the flexographic printing process on printed density and tonal reproduction has been studied by Bohan et al. The ink chamber to anilox pressure was the only parameter found to have an effect on the solid density of the prints. This was explained by an increasing pressure increasing deflection of the reverse angle doctor blade allowing more ink to flow to the anilox. The optical tone gain was most affected by the plate to impression cylinder pressure with the tone gain increasing with increasing pressure. This is due to the squeezing action in the nip increasing the dot size through ink squeeze and expansion and barrelling of the dot on the printing plate [Bould].

The investigations into ink transfer from plate to the substrate show that the majority of investigations ignore physical dot gain, as opposed to optical dot gain as a quality parameter. This is important as density and hence optical dot gain measurements do not accurately represent mechanical effects on ink transfer. There are 2 notables exception to this Bould and Hamblyn, this research has been conducted using non porous film substrate where ink transfer takes place by film splitting only. Previous research has indicated the significance of the plate/substrate interaction in ink film splitting process.

It is common commercial practise during printing to control the viscosity of ink by the addition of solvent. This both reduces the viscosity of the ink and reduces the pigment concentration. Thus changes attributed to viscosity may be due predominantly to changing pigment levels not the ink transfer. This paper reports a study undertaken to compare the effect of changing viscosity at constant ink strength with changing viscosity by dilution with solvent. A full factorial experiment was undertaken to study the effects of viscosity change on the ink transfer of printing onto paper, an absorbent substrate for a variety of process parameters. The engagement (impression pressure), anilox volume and line ruling were varied while the printing speed and temperature were kept constant. The printing of half tones was also investigated for the full tonal range as the deformable nature of the plates, lower pressures and interruptions in the rolling nip contact by holes in the plate (approx 70 % + coverage) also have an effect on the ink transfer.

2. Methodology

The trials were undertaken on a narrow web packaging press (a Timsons T-Flex 508). This is a fully equipped in-line press with 4 print units which is used for research and development (Figure 1). The print units are equipped with a chambered ink delivery system. Each unit is equipped with an independently controlled UV dryer allowing optimised performance for each ink printed. The design of the press enabled the engagement between anilox roll and plate cylinder and between the plate cylinder and engagement cylinder to be altered independently. The printing nip engagement could be altered in 1thou inch (25.4 μm) intervals. Three engagements (4, 5 and 6thou) were used while the press was run at a constant speed of 415 ft/min for all the trials.

The experiment was split into two trials to allow the effect of changing viscosity with constant pigment strength to be compared with the change of pigment level and viscosity obtained by dilution by solvent. A water based cyan ink was used. The inks for trial 1 had conventional viscosity reduction by thinned using reducer to produce three viscosities (Table I). The inks for trial 2 had viscosity reduction at constant ink strength. This was achieved by producing three inks each made up of 50% neat ink with the other 50% made up of varying amounts of tinter and reducer (Table II).

The use of a banded anilox roll that incorporate six bands of varying volume and line ruling, together with the a repeat image that contained six different line rulings for each anilox band, allowed a comprehensive study to be made. The anilox roll was engraved to incorporate six bands of varying volume and line ruling. The anilox

roll was measured using a WYKO Rollscope white light interferometer at 5x magnification. Each anilox band was measured 4 times and analysed using WYKO Rollscope software, the line ruling and average volumes are presented in Table III.



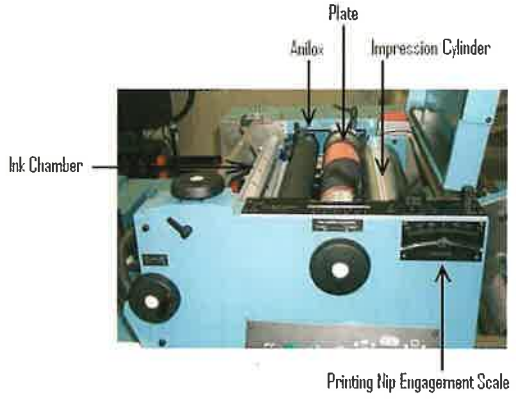


Figure 1: Timson T500 flexopress

Table I: Viscosity reductions for Conventional viscosity reduction

Level	Viscosity (Zhan 2)	% Neat Ink	% Reducer
1	54	100	0
2	32	75	25
3	23	66	33

Table II: Viscosity reductions at constant ink strength

Level	Viscosity (Zhan 2)	% Neat Ink	% Reducer	% Tinter
1	48	50	0	50
2	34	50	15	35
3	24	50	30	20

Table III: Anilox band volumes and line ruling

Anilox Band	Line Ruling (lpi)	Volume (cm^3/m^2)
1	1003	2.54
2	752	3.45
3	610	3.25
4	501	4.18
5	302	6.97
6	252	9.27

The plate used was a digital 1.14 mm thick McDermott CBU plate, this is a solid photopolymer plate. The image was designed to print coverage strips at six different line rulings (85, 100, 120, 133, 150 and 175 lpi) for each anilox band. Each coverage strip consisted of tone patches from 1 - 100% coverage as shown in Figure 2. The plate was mounted onto the plate cylinder using 3M Cushion-Mount 1115 mounting tape, a low-density foam tape intended for halftone printing. The substrate was Clan Standard paper suitable for high gloss ink with a Grammage range of 60 - 150 g/m^2.

In order to ensure that there was consistency between prints before and after stopping the press a confirmation trial was run. The press was run up to a speed with an engagement of 3thou, a one minute run was timed and the press stopped for six minutes. The press was then run up to speed and a second run timed. The temperature of the ink and ambient temperature was measured throughout. Sixteen consecutive samples

measured for density using a Gretag SPM 50 hand held spectrodensitometer. There was found to be a density difference of approximately 0.03 between the runs. This was thought to be due to the ink being 6°C colder than ambient temperature. The confirmation trial was repeated after the ink temperature had stabilised to ambient. The second confirmation trial was conducted in the same manner as the first. Thirty-two consecutive samples were measured for each run. The density measurements were found to be consistent between the two runs either side of stopping the press. This indicated that the temperature stabilisation of the inks is an important factor in the production of consistent prints.

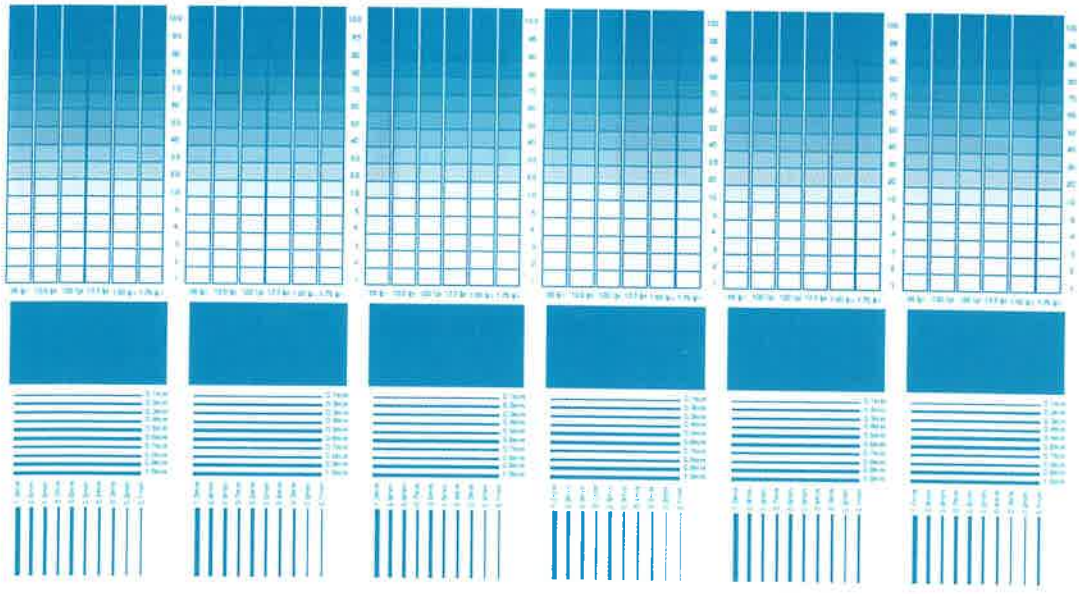


Figure 2: Test image

The sequence of each trial followed the same format with three viscosities and three engagements used in both trials. The press was run up to speed with the first viscosity ink and the lowest engagement. A one minute run was timed with start and finish indicated by tags placed on the web. The engagement was then increased and a second one minute run timed. The engagement was again increased to the highest engagement and another one minute run timed. The engagement was then reduced to the first engagement and the press stopped. The second ink viscosity was then introduced into the ink chamber and the process repeated. Finally the same sequence of engagement changes was conducted with the third viscosity ink.

3. Results and discussion

Increasing anilox volume has been found to increase the printed density in agreement with previous studies. The effect of increasing anilox volume on the printed density was plotted against nominal coverage (Figure 3). Increasing anilox volume increases density for all coverages at 85 lpi, the size of this density increase increases with increasing coverage. The greater volume of the anilox cells transfers a greater volume of ink to the plate and when the ink splits in the plate to substrate nip a greater volume of ink is transferred to the substrate. The 175lpi data shows an increase in density with anilox volume increase, this however an anomaly in the trends is seen in the 175lpi tonal strips at low coverage. There was no increase in density with anilox volume increase from 2.54 to 4.18 cm^3/m^2 from 1 - 5% coverage and no density change from 1 - 20% coverage with anilox increase from. With further anilox volume increase (4.18 to 6.97 cm^3/m^2) there is no density increase for 1 - 20% coverage patches. This is due to dot dipping. The size of the low coverage dots on the plate at 175 lpi are smaller than the cell opening on the anilox roll.

The dots therefore enter the anilox cell and pick up extra ink on the shoulder of the dot, the dots are therefore carrying the maximum amount of ink they can hold and therefore transfer a maximum amount of ink to the substrate. When the anilox volume increases the opening of the cells of the anilox roll also increases and therefore dot dipping can occur for larger dots. At the lowest volume anilox band of 2.54 cm^3/m^2 and 100 lpi the dots up to 5% coverage can dip into the cells, at the higher anilox volume of 4.18 cm^3/m^2 and 150 lpi dots up to 20% coverage can enter the cells. There is then no increase in density for these patches as at all anilox volumes the dots are carrying the maximum volume of ink they can hold.

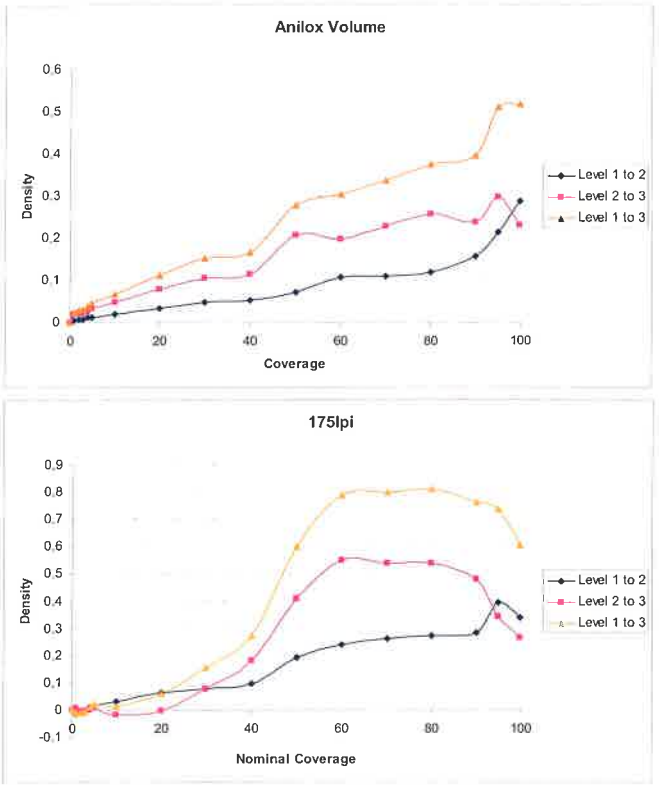


Figure 3:
Effect of anilox volume on density for 85lpi and 175lpi

The line ruling of the tonal strip was found to affect the size of the density increase with increasing anilox volume (Figure 4). With the exception of 175 lpi at coverages below 40% increasing line ruling increases the density increase due to anilox volume increase. The 175 lpi low coverage density increase is affected by dot dipping as described above. The larger density increase with higher line ruling is due to the larger dot perimeter to area ratio of the higher line ruling dots. As the anilox volume increases the greater volume of ink is squeezed outwards in the printing nip. As there is a larger perimeter for spreading to occur on the higher line ruling dot a higher coverage is produced and therefore a higher density.

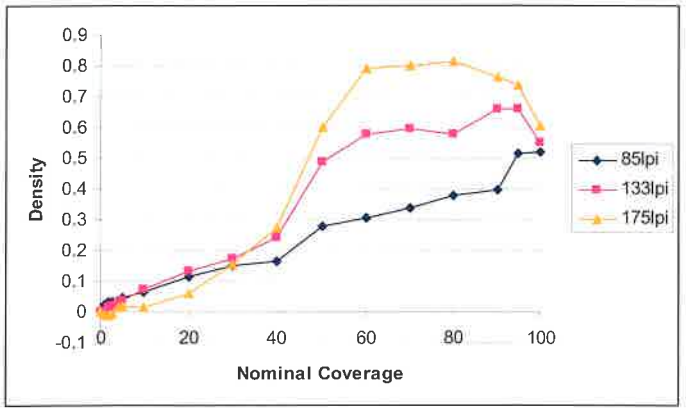


Figure 4:
Effect of 2.54 - 6.97cm^3/m^2 anilox volume increase on density

The density is increased with increasing engagement, with the density increase increasing with increasing coverage up to 90% coverage (Fig. 5). The increased engagement increasing dot deformation against the substrate [Bould, Hamblyn] and ink squeeze in the nip. This increases ink spreading and therefore increases density. The size of this density increase increases with coverage as the larger dots have a larger perimeter therefore there is more spreading of the ink. Above 60% coverage, the topography of the half tone changes from a series of independent dots to a solid with a regularly spaced pattern of holes that become smaller with increasing coverage. There is still an increase in density with increased coverage due to the smaller holes requiring a lower coverage gain to bring about a larger increase in density. As with anilox volume the density

increase increases with increased line ruling, this is also due to the larger perimeter to area ratio of the smaller dots allowing for greater spreading of the ink.

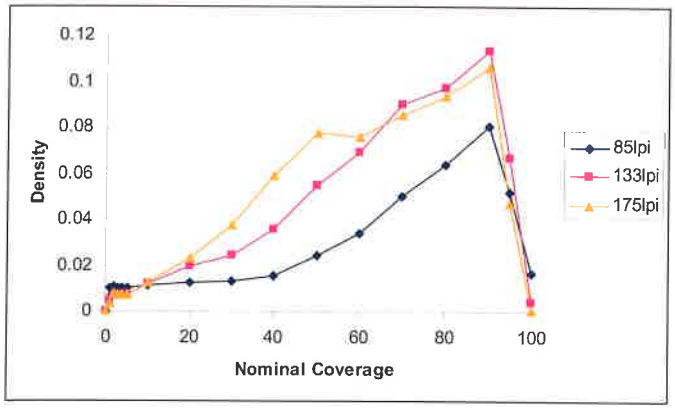


Figure 5:
Density change with 2thou increase in engagement

Figure 6 presents the 133 lpi tonal strip density change with viscosity reduction. The viscosity reduction causes a reduction in density. There are small density decreases from 1 - 80% that increase with increasing coverage. Above 80% coverage the density decreases become larger, increasing with coverage until the largest decrease in density with viscosity reduction is seen at 100% coverage.

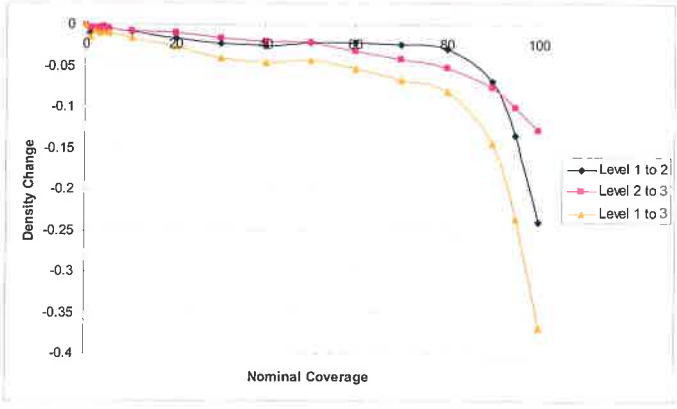


Figure 6:
133 lpi density change with viscosity reduction

The 85 lpi, 133l pi and 175 lpi tonal strip density reduction with reduction of viscosity from level 1 to level 2 is shown in Figure 7. There are small differences between the line rulings in the 40 - 90% coverage region with 175 lpi showing the largest density reduction and 133 lpi the smallest. Reducing the viscosity of the ink reduces the density of the printed samples with the density reduction increasing with increasing coverage. This could be caused by a reduction in release of ink from the anilox roll, a reduction in the transfer from the plate to the substrate or a combination of both. Alternatively the density reduction could be due to the reduction of pigment concentration when reducing the viscosity. The reduced pigment concentration would produce lower densities with the same level of ink transfer.

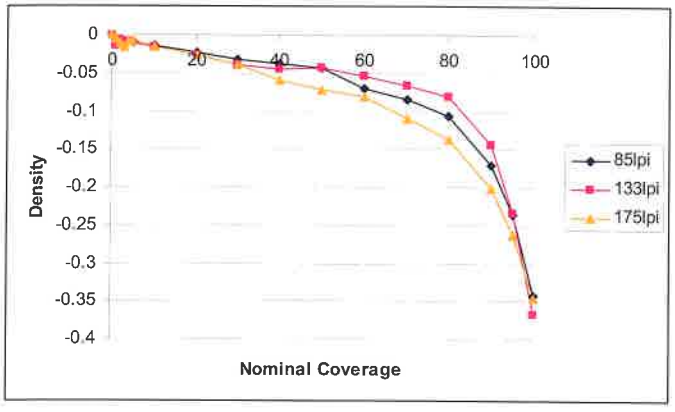


Figure 7:
85, 133 and 175 lpi Density change with 31s viscosity reduction

The effect of altering viscosity with constant pigment concentration is shown for the 133 lpi tonal strip in figure 8. From 1 - 40% coverage reducing the viscosity reduces density with the size of the reduction decreasing with increasing coverage. Above 40% coverage and up to 80% coverage there is a small increase in density with decreased viscosity. From 90% coverage to 100% coverage there is a decrease in density with reduced viscosity that rapidly increases with increasing coverage.

The viscosity reduction with constant ink strength isolates the effect on the viscosity alone. As with the effect of viscosity with conventional reduction there is a reduction in density from 1 - 40% coverage. This shows that for isolated dots the ink transfer is reduced. The viscosity probably affects the release of the ink from the anilox roll, the reduced viscosity reduces the transfer of ink to the plate dots and therefore the reduced volume is not able to be spread as far reducing the density.

Above 40% coverage the dots on the substrate join as the dots touch ink from the adjoining dots flows into each other reducing the viscosity increases the flow of ink therefore increasing the density. At 70% coverage the dots on the plate have joined, at this point a rolling nip contact is set up, the reduced viscosity of the ink would increase ink build up in the nip entrance and therefore increases ink squeeze into the holes between dots As the coverage increases the reduced release from the anilox has a greater effect and the density is reduced due to the reduction in the amount of pigment transferred to the substrate.

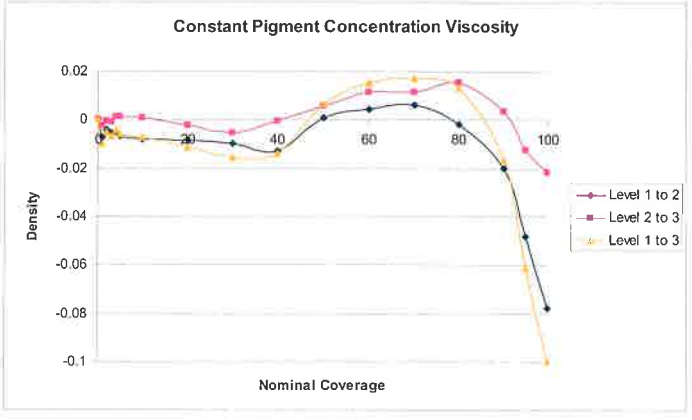


Figure 8: 133 lpi effect of constant pigment concentration viscosity change on density

4. Conclusions

The anilox volume has the largest effect on ink transfer. The larger volume of ink transferred to the plate spreads further on the substrate increasing coverage and consequently increasing density for all coverages. Increasing engagement increases coverage and this increases the optical density of the samples.

The effect of viscosity reduction is to reduce ink transfer to the printing plate. In the plate to substrate nip the individual dots show reduced coverage and density due to this lower ink transfer. Where the dots join however the ink spreading into the dots is increased by the lower viscosity this increased coverage increases the density up to 80 % coverage when the pigment concentration is held constant. Above 80% coverage the reduced ink volume acts to reduce the density of the samples.

For the density small interactions are observed between the viscosity and engagement for the high viscosity ink due to reduction in the hydraulic impression into the substrate pores increasing pressure and therefore increasing ink squeeze. There is an interaction between the anilox volume and the ink viscosity caused by the line ruling of the anilox roll. The ink transfer from anilox to plate is affected by the anilox cell walls. As the line ruling of the higher volume anilox is lower the open area is larger the drag is reduced and therefore the effect of increased ink transfer with increased viscosity is reduced.

The ink transfer was also found to be dependent both on line ruling and coverage. This was attributed to the phenomena of dot dipping, i.e. when half tone dots on the plate are smaller than the anilox cells and therefore can completely enter the anilox cells, thus picking up more ink.

Acknowledgments

The authors wish to acknowledge the financial support of EFTA (European Flexographic Technical Association, UK) for this work. Dr. David Beynon also acknowledges the financial support of EPSRC (Engineering and Physical Sciences Research Council, UK)

References

1. Bohan M. F. J, Townsend. P, Hamblyn S. M, Claypole T. C. and Gethin D. T., "Evaluation of Pressures in Flexographic Printing". TAGA 2003
2. Bould D. C. "An investigation into quality improvements in Flexographic Printing". PhD Thesis University of Wales Swansea 2001
3. De Grace J. H. and Mangin P. J, 1983 "A mechanistic approach to ink transfer. Part 1: Effect of substrate properties and press conditions". Advances in Printing Science and Technology, Proceedings of the 17th International Conference of Printing Institutes, Sweden, 1983
4. De Grace J. H. and Mangin P. J, 1987. "A mechanistic approach to ink transfer. Part 11: The splitting Behaviour of inks in printing nips". Advances in Printing Science and Technology, Volume 19, 1987
5. De Grace J. H. Dalphond J. E. and Mangin P. J, 1991. "A mechanistic approach to ink transfer. Part 111: Properties of Ink Filaments in Printing Nips". Advances in Printing Science and Technology, Volume 21, 1991
6. Hamblyn S. "The Role of the Plate in the Ink Transfer Process in Flexographic Printing", PhD Thesis, University of Wales Swansea, December 2004
7. NPIRI "The effect of UV Flexo ink viscosity, anilox cell volume, and press speed on print density and dot gain, NPIRI Task force", TAGA Proceedings, p 86 - 101, 1996

Evaluation of the ink transfers of prints using low-angle shaving system

Yasushi Ozaki, Naoko Fujisawa, Eiji Kawamura

Research Institute, National Printing Bureau of Japan
6-4-20 Sakawa, Odawara-shi, Kanagawa 256-0816 Japan
E-mail: yozaki@res.npb.go.jp

Abstract

In order to estimate ink transfers of multicolor offset and flexo printing, Surface and Interface Cutting Analysis System (SAICAS) was used to make slopes of ink layers by ultra-low-angle shaving. The slopes of the ink layers obtained were observed with optical microscope (OM), scanning electron microscope (SEM) and scanning probe microscope (SPM), and the ink transfers were characterized using Raman spectroscopy.

Ink transfers of multicolor printing using the low-angle shaving technique of SAICAS could be observed with OM and SEM. Raman spectroscopy could also be applied to the low-angle shaving slope because we were able to expand the thickness of the ink layer using SAICAS. In the case of prints in which each colored ink layer overlaps the previous each ink layer before it has cured, each color ink was not formed as a separate ink layer, instead mixed together. In addition, ink layers of commercial offset and flexo prints could be observed from the slope of prints obtained by SAICAS.

Keywords

Flexo ink, ink transfer, offset ink, SAICAS, shaving technique

1. Introduction

Evaluation of ink setting and ink transfer is an important part of improving printing quality for many kinds of prints. Each ink transfer of multicolor prints directly affects the printing color. In the case of oil-based offset multicolor printing, the second and third layers of ink transfer before the first ink sets. Finally, colors at the boundary between ink layers change due to the mixture of inks during ink curing. Recently, UV curable offset or flexo inks are often using for the commercial printing. There are two types of UV curing systems used on the printing machines. One uses UV lamps behind the last color printing unit and the other utilizes UV lamps behind each color printing unit [Dancan, 2007]. It was expected that the printing quality, such as coloring properties and color densities would differ between the two.

However, a technique to observe ink transfers of multicolor prints has not yet been established. An ink layer can be observed only from a cross section of two-color prints by SEM (Fig.1(a)). Alternatively, cross sections of prints can also be observed using an optical microscope, but the color layers can not be discriminated due to the limitations of light resolution (Fig.1(b)).

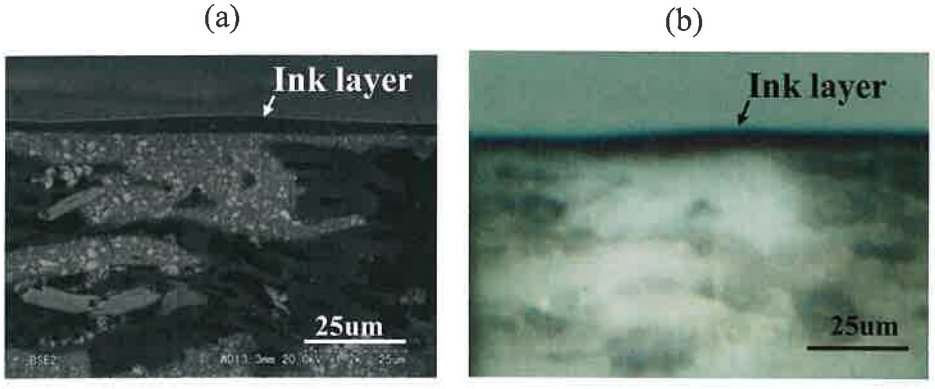


Figure 1: SEM image (a) and optical image (b) on the same cross section of offset prints

In the past, we have observed the three dimensional ink transfer and penetration on the dye and pigment types inkjet prints with a confocal laser scanning microscope (CLSM) [Ozaki, 2006]. Magenta ink could be observed as a fluorescence image, but the other inks, such as blue and black, could not be observed because they have no fluorescence. Specifically, ink transfers of multicolor prints can not be observed by CLSM. As a technique for the low-angle shaving, Yasui et al. used an ultra-microtome for analyzing thermal recording sheets [Yasui, 2007]. The slope of sample prepared by the ultra-microtome was analyzed using ATR (Attenuated Total Reflectance) technique. When using a microtome, however, it is very difficult to control the shaving angle exactly because the axis of movement of the cutting blade is in the direction of the shaving angle. In consequence, the ultra-microtome has not been used for the shaving of offset and flexo prints.

In order to estimate ink transfers of multicolor offset and flexo printing, a Surface and Interface Cutting Analysis System (SAICAS), in which the cutting blade drives to horizontal and vertical directions as two motions, was used to make slopes of ink layers by low-angle shaving. The slopes of ink layers obtained were observed with some microscopes, and the ink transfers were analyzed by Raman spectroscopy.

2. SAICAS

Figure 2 shows the photo of the main body of SAICAS (NN-20, Daipla Wintes Co.). SAICAS is composed of drive of cutting blade, sample stage, CCD camera for position adjustment, horizontal controller of sample stage and computer for control of shaving speed and data processing. Figure 3 shows a schematic of the SAICAS shaving technique. The cutting blade can move at an independent speed both horizontally and vertically. The shaving angle can be accurately controlled at the speeds of both movements. When the velocity of horizontal and vertical movements are respectively A and B nm/s, tan θ is B/A, where θ is the shaving angle.

Two methods of measurement can be chosen in this system: one is shaving with a constant vertical weight, and the other is a constant velocity shaving mode. The former is used to measure shear strength, peel strength and degree of adhesion. In the constant vertical weight mode, the interfacial adhesion of a sealant on polymer substrates was evaluated [Nakauti, 2000], and the density of poly-lactic acid and polystyrene irradiated with positron beam was estimated as a resistant force [Saito, 2004, 2007, 2007]. The constant velocity shaving mode is for preparing the long distance slope of samples. The depth profile of the long distance slope of ion-implanted photoresist was investigated by infrared spectroscopy [Nagai, 2001, 2002]. As the Z-direction of NN-20 type SAICAS is controlled by a piezo unit, a high vertical resolution (2nm) can be obtained. As a result, ultra-low-angle shaving slopes are possible. Blades are made of sintered alloy or solitary crystal diamond.

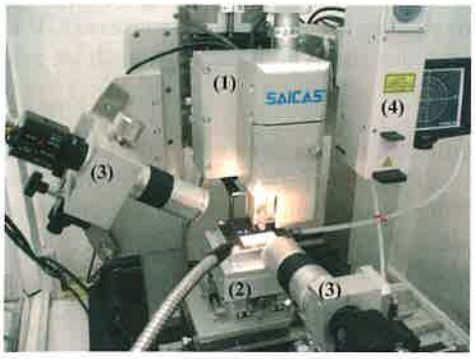


Figure 2: Photo of SAICAS (Main body)
(1) drive of cutting blade, (2) sample stage
(3) CCD camera, (4) horizontal controller of sample

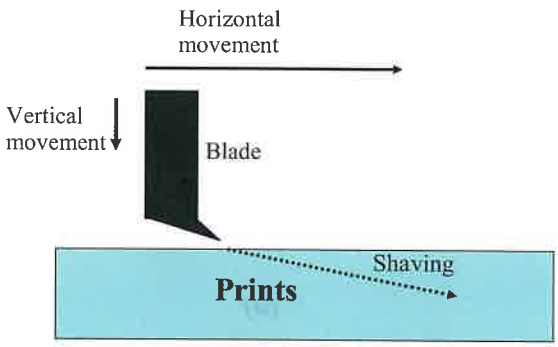


Figure 3:
Schematic of SAICAS shaving technique

3. Experimental

3.1 Samples

Magenta ink (Daicure Septer DT Magenta N, Dainippon Ink Co.) and Cyan ink (Daicure Septer DT Cyan N, Dainippon Ink Co.) were used for offset printing. The coated paper (NPi COAT: Nippon Paper Co., Basis weight 84.9 g/m^2) was used as the printing substrate. Two-color offset printings were carried out with a laboratory print tester (KRK Co.) at a printing speed of 1m/s and printing pressure setting of 40 kgf. UV

curable magenta ink was first printed on the coated paper, and UV curable cyan ink was printed on magenta prints. The thickness of the ink layers was adjusted to approximately 2 μm. Table I indicates the UV curing states of Sample A and B. In Sample A, each printed ink was cured with a UV lamp after each printing, while in Sample B the printed inks were cured with a UV lamp after the second printing. UV curing energy was adjusted to 90 mJ/cm^2. In addition, commercial oil-based offset prints and commercial UV curable flexo prints were also prepared as low-angle shaving samples.

Table I: UV curing states of Sample A and B

	After magenta printing	After cyan printing
Sample A	-	o
Sample B	o	o

o: With UV curing, -: Without UV curing
Offset printing was carried out in order of magenta and cyan

3.2 Low-angle shaving method

SAICAS (NN-20; Daipla Wintes Co.) was used as the low-angle shaving system. A diamond blade with a width of 1mm was selected to shave the prints. The samples were fixed on the sample stage using static electricity. In the case of Sample A and Sample B, the vertical and horizontal velocities were 5 nm/s and 500nm/s, respectively. As tanθ was 0.01, the shaving angle (θ) was approximately 0.58 degrees. In the case of commercial offset and flexo prints, the vertical and horizontal velocities were 3 nm/s and 500 nm/s, respectively. The shaving angle (θ) was approximately 0.34 degrees. The vertical velocity was decided on the basis of ink layer thickness. As a result, the vertical velocity of commercial offset and flexo prints having thinner ink layers was set as slow as possible (3 nm/s). Although a cryo-stage could also be equipped with SAICAS, the printing samples were shaved without cryo-stage.

3.3 Analytical instruments

The shaving slopes of the prints were observed using a digital microscope (VH-8000, KEYENCE Co.). In order to check the distribution of cyan ink on Sample B, Raman spectroscopy (in Via Raman Microscope, RENISHAW Co.) was measured in the confocal mode. An excitation wavelength of 785 nm was used, and the detected wave-number ranged from 1189 cm^{-1} to 1696 cm^{-1}. The slope prepared was also observed with a scanning electron microscope (SEM:S3000-N, Hitachi Co.). The electron beam was supplied at an acceleration voltage of 15 kV and the working distance was 18.5 mm. In addition, the roughness of the slope surface was measured with a scanning probe microscope (SPM:SPA-400, SII Co.). The SPM measurement was carried out with the dynamic force module. Canchilever was DF-20 (Frequency: 162 kHz, Spring constant: 22 N/m). A topographic image was obtained for the region of 5 μm X 5 μm.

4. Results and discussion

4.1 Magenta-Cyan double colors prints

Figure 4 shows the optical image on the low-angle shaving slope of Sample A. Shaving was carried out from top to bottom in the figure. Some streaks on the shaving slope were created by SAICAS. The distribution of cyan and magenta was irregular because shaving conditions varied due to the uneven printing surface. In the case of Sample A, however, the magenta ink layer could be observed clearly. As a result, the slopes of ink layers on the offset prints could be obtained sufficiently without cryo-stage.

Figure 5 shows the optical image on the low-angle shaving slope of Sample B. The magenta ink layer could barely be observed from the low-angle shaving slope. The width of the magenta ink layer was approximately 3 μm in Figure 5. In the case of Sample B, it was supposed that cyan ink would mix with magenta ink because the cyan ink, after printing, was overlapped with the non-cured magenta ink layer. To confirm this phenomenon, the shaving slope of Sample B was analyzed by Raman spectroscopy.

Figure 6(a) shows the analytical positions on a dotted line along the shaving slope. Measurements were carried out at 1.0 μm intervals on the line, and Raman data on 30 points were obtained. Figure 6(b) shows that

the change of Raman intensity at 1530 cm^{-1} depended on the cyan pigment. Point 26 was located on the boundary between the cyan and magenta layers, while point 29 was located on the boundary between the magenta layer and the coated paper. Although Raman intensities were observed to fluctuate, Raman intensities decreased from within 5 μm of the boundary between cyan and magenta. As a result, it was evident that the mixture layer of cyan and magenta inks was formed in Sample B. In addition, as the resolution of Raman spectroscopy was 1μm, this analytical technique could not be applied to analyze the thin ink layer on the cross section of the printing sample. However, Raman spectroscopy could be applied to the low-angle shaving slope because SAICAS could expand the thickness of the ink layer. This is one of advantages for the low-angle shaving technique of SAICAS.

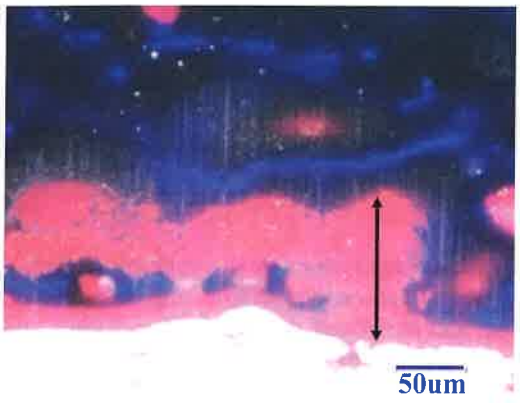


Figure 4: Optical image one the low angle shaving slope of Sample A. Arrow shows the region of magenta layer

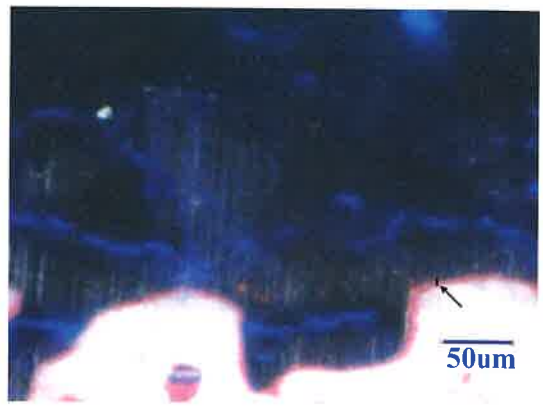


Figure 5: Optical image on the low angle shaving slope of Sample B. Arrow shows the region of magenta layer

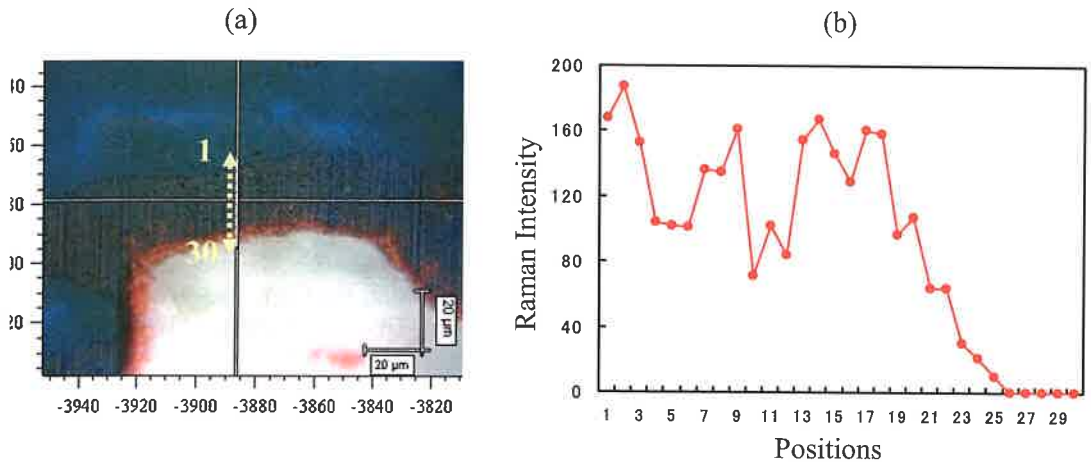


Figure 6: Distribution of cyan ink on the low-angle shaving slope using Raman spectroscopy (a) Analytical positions 30 points on the dotted line were analyzed (1um/step). (b) Change of Raman intensity at 1530 cm^{-1} depended on the cyan pigment

Figure 7 shows the SEM image on the area in Figure 6 (a). Although it was difficult to observe the interface between the ink layer and the coated paper from cross section of prints, the interface could be observed from SEM image of the low-angle slope shaved by SAICAS. The penetration of magenta ink into the coated paper could not be verified by the optical microscope images (Fig.4 and Fig.5). However, it was confirmed in the SEM image that the magenta ink layer only transferred to the surface of the coated paper because the boundary between the ink layer and the coated paper on the SEM image (Fig.7) accorded with that between the magenta ink layer and the coated paper on the optical image (Fig.6(a)). Moreover, the streaks on the shaving slope were also observed on the SEM image. In order to measure the depths of the streaks on the shaving slope, SPM was used. Figure 8(a) shows a topographical image of the slope of the ink layer by SPM, and Figure 8(b) shows the depth profile on the line in Fig.8 (a). The maximum in the depths of streaks was measured as only 80 nm. As a result, a smooth surface of the shaving slope could be obtained by the solitary crystal diamond blade.

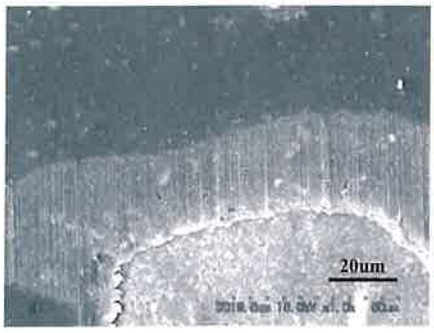


Figure 7: SEM image of the shaving slope

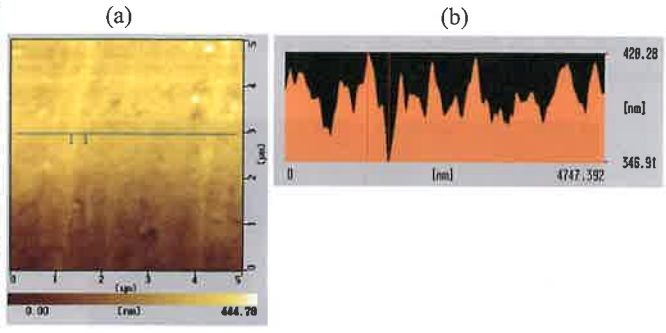


Figure 8: SPM image of the shaving slope of the ink layer (a) topographical image; (b) depth profile of line on topographical image

A risk of ink bleeding together with the diamond blade during shaving would be expected. However, it was considered that ink bleeding didn't occur because the results of observation by optical microscope were consistent with that of Raman spectroscopy. Hattori et al. analyzed the composition of submicron polymer thin film using TOF-SIMS and SAICAS [Hattori, 2007]. Even when TOF-SIMS having high sensitivity on the shaving slope was used, the shaving components never reattached. Eventually, the change of ink layers on multi colors could be estimated from the low-angle shaving slope of the prints prepared with SAICAS. In addition, it was found that the low-angle shaving slope could be easily made by inputting horizontal and vertical velocities into the computer.

4.2 Commercial oil-based offset prints

Figure 9 shows the optical image on the low-angle shaving slope of the oil-based offset prints. As shaving was carried out from the upper side to the bottom side, the white area showing the coated paper appeared at the bottom. Black color portions could be observed up to the boundary of the coated paper. These black areas would indicate the mixed inks. In the case of the oil-based inks, it was anticipated that the mixture of inks would start just when different colors contacted and continue until ink curing.

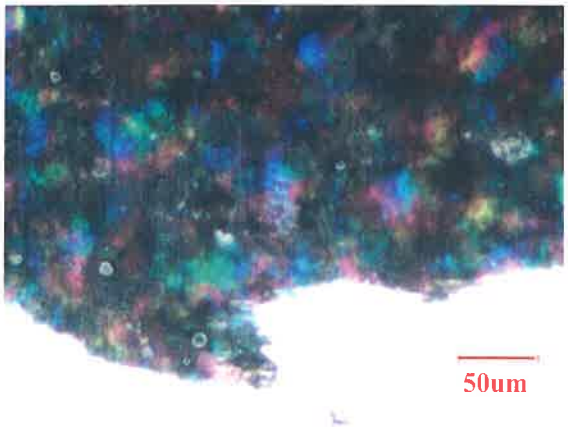


Figure 9: Optical image on the low-angle shaving slope of the oil-based offset prints

4.3 Commercial UV curable flexo prints

Figure 10 shows the optical image on the low-angle shaving slope of the UV curable flexo prints. Compared with the oil-based offset prints, black areas disappeared on the way to the shaving slope, and cyan and magenta ink layers could be clearly observed. The printing machine that produced the flexo prints was equipped with an individual UV lamp on each color unit. Therefore each color ink layer could cure just after printing, and each ink never mixed. As a result, it was expected that each ink layer could be observed on the low-angle shaving slope with SAICAS.

Intermixing as a function of UV exposure and studying the reactive depth profile in the ink will be possible using SAICAS. In addition, the relationship between the mixture of ink colors and color density can also be discussed using this technique.

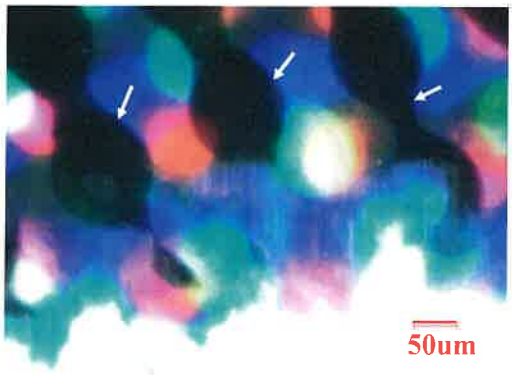


Figure 10:
Optical image on the low-angle shaving slope of the UV curable flexo prints. Arrows show black areas

5. Conclusions

We were successful at estimating ink transfers of multicolor printing using the low-angle shaving technique of SAICAS for the first time.

As a result, in the case of prints in which each color ink layer overlaps the previous each ink layer before it has cured, each color ink was not formed as a separate ink layer, but rather mixed together. Moreover, the magenta ink layer printed first on the double-color prints did not penetrate the coated paper, but only transferred to the surface of coated paper. When commercial UV flexo prints were cured with a UV lamp on each color unit, individual color ink layers could be observed clearly.

References

1. Dancan D. P., (2004), Printing with energy-curable inks - high energy chemistry, high energy business, TAGA proceedings, 76
2. Hattori H. and Yamasaki H., (2007), Compositional analysis of submicron polymer thin film using TOF-SIMS and ultra-low-angle microtomy, NITTO DENKO Tech. Report, 45(88)68
3. Nagai N., (2001), Depth profile analysis by infrared spectroscopy, Anal. Sci.,17, i671
4. Nagai N., Imai T., Terada K., Seki H., Okumura H., Fujino H., Yamamoto T., Nishiyama I. and Hatta A., (2002), Depth profile analysis of ion-implanted photoresist by infrared spectroscopy, Surf. & Int. Anal., 34, 545
5. Nakauti H., Takizawa T., Saito S. and Ono T., (2000), A new method of evaluating the interfacial adhesion of a sealant using a micro-blade cutting system, Proceedings of 3rd Int. RILEM Sym.
6. Saito F., Yotoriyama T., Nagashima Y., Suzuki Y., Ito Y., Goto A., Iwaki M., Nishiyama I. and Hyodo T., (2004),Study of ion irradiated poly-lactic acid using slow positron beam, Material Sci. Torum,Vols, 445-446, 340
7. Saito F., Yotoriyama T., Fujii Y., Nagasima Y, Nakao A., Iwaki M., Nishiyama I. and Hyodo T., (2007), Study of ion-irradiated polystyrene using slow positron beam, Radiation Phys. & Chem., 76, 200
8. Saito F., Fujii Y., Yotoriyama T., Nagasima Y, Nakao A., Suzuki , Iwaki M. Y., Nishiyama I. and Hyodo T., (2007), Density change of ion irradiated polystyrene studied by positron annihilation and SAICAS, Phys. Stat. Sol., 4, (10), 3718
9. Ozaki Y., Bousfield D.W. and Sharer S.M., (2006), Observation of the ink penetration into coated paper by confocal laser scanning microscope, *TAGA J.*, vol. 3, 50
10. Yasui K., Omatsu M. and Kishimoto M., (2007), The analysis of ingredients in paper coatings by the micro-ATR imaging technique, Proceedings of 74th Pulp Paper Res. Conf. in Japan, 160

The effects of surface treatment on digital print quality of extrusion coated paperboard

Johanna Lahti, Mikko Tuominen, Jurkka Kuusipalo

Tampere University of Technology, Paper Converting Technology
P.O.Box 541, FI-33101 Tampere, Finland
E-mail: johanna.lahti@tut.fi

Abstract

The most important function of a packaging material is to shield the product inside the package. Extrusion coated paperboard is generally used in food, medical and cosmetic packages. Extrusion coatings give a barrier against water, water vapour, aroma, grease, oxygen, etc. In addition to barrier properties, heat sealability and printability are important properties in packaging applications. From point of view of printing, the dense and impervious structure of extrusion coatings is challenging: printing inks and toners do not penetrate into the coatings. The durability of the printed image is significant, because the image must withstand various converting operations when the package is constructed. The most common method for obtaining good ink adhesion is to oxidise the surface. Surface treatments are used to change the chemical composition, increase the surface energy, modify the crystalline morphology and surface topography, or remove the contaminants and weak boundary layers. Two widely used methods are electrical corona discharge treatment and flame treatment. These processes generally cause physical or chemical changes in a thin surface layer without affecting the bulk properties. Treatments will increase surface energy and also provide polar molecular groups necessary for good bonds between ink and polymer molecules. In addition to these two methods, a lot of research work has focused on atmospheric plasma treatment. This paper compares these different surface treatments and presents their effects on surface properties of extrusion coating and furthermore, on digital print quality.

Keywords

Adhesion, atmospheric plasma treatment, corona treatment, digital printing, electrophotography, extrusion coating, flame treatment, packaging, paperboard, surface energy

1. Introduction

Polymer and paperboard structures have been applied successfully in several fields, especially in packaging industry. However, making such a packaging product requires special surface properties from the materials used in the manufacturing process. For instance, when the extrusion coated materials are printed, the adhesion of printing inks and toners is essential. Polymers and paperboards very often do not possess such a surface properties, because of low surface energy, incompatibility, chemical inertness, or the presence of contaminants and weak boundary layers. Surface treatments are used to produce special functional groups at the surface for special interactions with other functional groups, increase the surface energy, introduce surface cross-linking, modify surface morphology by increasing or decreasing surface crystallinity or roughness, and remove the contaminants or weak boundary layers. Many processes have been developed to modify substrate surfaces, including flame, corona, and plasma treatments. These processes generally alter physical or chemical properties of a thin surface layer without affecting bulk properties.

Flame treatment is a basic plasma method, which can be used for improving printability of surfaces. For flame treatment of web material the typical arrangement consists of a burner which flames onto the web guided by a cooling roll. In the combustion reaction different thermally activated atoms, molecules free electrons, including O, OH, NH, NO and CN are formed [Garbassi et al. 1987; Gaydon, 1974]. These react with the surface of substrate composing adhesion promoting functional groups. Briggs et al. [1979], Garbassi et al. [1987, a & b] and Sutherland et al. [1991] identified hydroxyl, carbonyl, carboxyl and amide groups on the surfaces of flame treated polyethylene and polypropylene. The surface chemistry is an important factor, i.e. the chemical groups (carbonyls- and hydroxyl-groups) on the surface for adhesion rather than the total quantity of oxygen [Pijpers et al. 2001]. Flame treatment oxidises a thin layer of substrate surface. With polyethylene the depth of oxidation is estimated to be between 4 and 9 nm [Briggs et al. 1979], whereas for example with polypropylene the depth of oxidation is estimated to be between 5 - 20 nm. The estimation depends on the research and measurement technique [Garbassi et al. 1987, a & b; Sheng et al. 1994]. Several

studies in literature concern the effects of flame treatment on surface of polymers, such as polyethylene or polypropylene. Evidently, formation of functional groups, cross-linking, chain scission, breaking of the long-chain molecules and micro roughening occurs in the surface of polymer [Garbassi et al. 1987, a & b; Pijpers et al. 2001; Sheng et al. 1994]. Generally, it is agreed that flame treatment increases polarity and oxidation of the surfaces which leads to improved printability and adhesion [Briggs et al. 1979; Garbassi et al. 1987, a & b; Junnila et al. 1989; Pijpers et al. 2001; Savolainen et al. 1991, Leech 1991, Tuominen & Lahti 2007, Kuusipalo 2008].

Corona discharge is probably the most widely used industrial surface treatment for polyolefin films [Brewis 1982; Chan 1994, Eckert 2003]. Corona phenomenon takes place when a high voltage is applied across electrode and grounded metal roll to induce ionisation of air. In the corona discharge process the surface of substrate is bombarded with high-speed electrons. The energy level of these electrons is high enough to break the molecule bonds of the most substrate surfaces. These oxidants present in corona i.e. ozone, atomic oxygen and oxygen free radicals create oxidised groups with free radicals present on the surface [Cramm et al. 1981; Sun et al. 1998]. At least carbonyl (ketones and aldehydes), carboxylic acid groups, ester, alcohol and ether are identified on the surfaces of polyethylene or paper [Hansen et al. 1993; Junnila et al. 1989]. Even small amount of these reactive functional groups incorporated into polymers can be highly beneficial to improving surface characteristics and wettability. The corona discharge treatment increases surface energy by introducing polar groups on the surface. This improves wetting and the adhesion properties of the surface. Generally, the most of enhanced adhesion is attributed to the oxidation of substrate surface [Brewis 1982; Chan 1994; Cramm et al. 1981; Lahti 2005; Leech 1991, Sun et al. 1998, Briggs et al. 1982]. The treatment oxidises effectively a thin layer of the surface (~30 Å) [Brewis 1982]. The other adhesion improving mechanisms include cross-linking of surface regions and increasing the cohesive strength of the substrate by elimination of LMW fractions from the surface [Cramm et al. 1981; Lahti 2005; Sun et al. 1998], the changing of the surface morphology and increasing surface micro roughness [Junnila et al. 1989; Lahti 2005; Sun et al. 1998] and the formation of electret on the surface (polymers) Brewis 1982; Lahti 2005]. Severe corona treatment increases the risk of adhesion failure through overtreatment. On the surface of polymer corona treatment cuts the chains into smaller fractions. In general, these low-molecular-weight (LMW) oxidised materials are not firmly bound to the substrate and could be a source of adhesion failure [Chan 1994; Lahti 2005]. However, in some cases LMW-materials have not weaken the adhesion [Crolius et al. 1962] but they can cause roll blocking problems [Lahti 2005; Maxwell et al. 1987]. In the studies of Lahti [2005] and Lahti et al. [2004], it has been shown that surface energy level and surface charges control both spreading and adhesion of toner particles. Corona treatment increases surface energy, as well as improves the adhesion properties and bonding ability of PE-LD through surface oxidation and formation of functional reactive groups. Corona treatment can also induce permanent electrical charges in a polymeric surface that contributes to toner adhesion even after a long period of time. Increased surface oxidation and surface energy is highly beneficial for toner adhesion with PE-LD surfaces. Several researchers [Chan 1994; Hansen et al. 1993; Lahti 2005; Maxwell et al. 1987] have verified that the corona treatment effect decays over time along with the adhesion properties of the surface. The main reason for this decay is that during the aging in air, the oxygen concentration at the surface is reduced, either because the functional groups migrate to the bulk or since the surface-active additives or LMW-fragments migrate from the bulk to the surface [Strobel et al. 1991].

In plasma treatment various process gases like argon, helium or nitrogen are fed through an electric field creating plasma, which is a state of ionised gas, consisting of excited atomic, ionic, molecular, and free-radical species. In other words, in plasma treatment a continuous flow of ionised gas is blown on the substrate surface. Plasma treatment can be used to modify or tailor the surface properties of various substrates e.g. to improve adhesion or printability properties. Other applications include plasma polymerisation, etching and cleaning of surfaces [Cernakova et al. 2006, Kuusipalo 2008]. Plasma treatment has been studied for many years, however, mainly in vacuum conditions. Plasma treatment has various benefits over traditional corona as indicated in Table I. The target in TUT's research has been to develop an atmospheric pressure plasma treatment, which can be used to alter the outermost surface (< 10 nm) of various roll-to-roll substrates in-line at high line speeds in normal atmosphere [Tuominen et al. 2008]. Atmospheric process is essential for large-scale processes in paper and printing industry. Furthermore, the target is to solve some of the drawbacks occurring with traditional corona, like backside treatment and decay of surface energy.

The effects of surface treatments like flame and corona have usually been examined as a pre-treatment method. Several researchers [Junnila et al. 1989; Savolainen et al. 1991] have investigated how strongly flame and corona treatments affect adhesion, surface energy and oxidation properties of paper or paperboard. In some studies [Junnila et al. 1989] the corona treatment improves adhesion more than the flame treatment,

while in other investigations [Junnila et al. 1989; Savolainen et al. 1991] the effects are quite equal. In the previous studies done at TUT [Junnila et al. 1989; Savolainen et al. 1991; Tuominen et al. 2005, Kuusipalo 2008], it has also been detected that the corona treatment increases the polarity and oxidation of surface more than the flame treatment. The aim of this study is to map out the role of surface modification in print quality formation of extrusion coated substrates. The surface chemistry of PE-LD coated paperboard has been modified with corona, flame and atmospheric plasma treatments. The effect of treatments on surface energy has been evaluated with contact angle measurements. In addition, the effects on oxidation and printability of the surface are evaluated. This study has concentrated on digital printing, particularly on dry toner-based electrophotographic printing process.

Table I:. The benefits and the limitations of vacuum plasma and corona treatment

VACUUM PLASMA	CORONA
+ possibility to select treatment gas → tailored surface chemistry	+ operates in atmosphere → on-line, no vacuum or chambers
+ high energy densities → effective treatment	+ relatively low costs and high speeds
+ longer lasting treatment	+ simple and acknowledged method
+ more uniform treatment	– operates in atmosphere → fixed chemistry (air)
+ no reverse side treatment	– reverse side treatment → blocking problems
– vacuum process →increased costs	– decay of treatment level (aging)
– batch process → increased costs	– relatively low energy densities
– very complex process → difficult to controll and scale up	– limited treatment uniformity, possible pin holes

2. Methods

Low-density polyethylene (PE-LD) was applied (15 - 20 g/m^2) on commercially available liquid packaging board (205 g/m^2) and pigment coated paper (90 g/m^2) in extrusion coating pilot line at Tampere University of Technology (TUT)/ Paper Converting Technology (PCT) (Figure 1). Corona, flame and atmospheric plasma treatments were used to modify the surface of PE-LD coating.

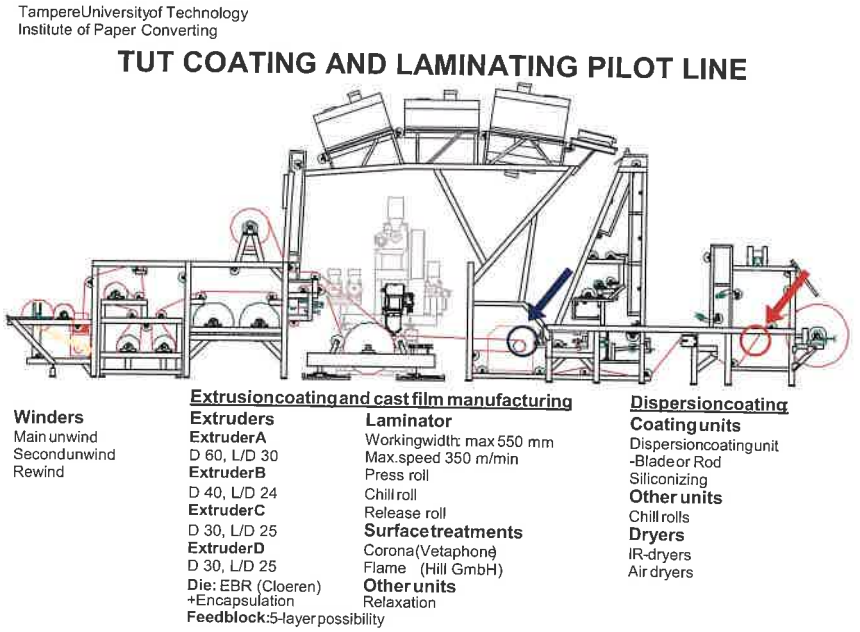


Figure 1: TUT/PCT Pilot line with surface treatment units
(left arrow indicating corona/plasma unit; right arrow indicating flame unit)

Flame treatment gas was propane (C_3H_8), air/gas-ratio was 24.5:1 and the distance between burner and substrate was 2.0 cm. The gas output was 600 l/min. APT (atmospheric plasma treatment) unit (Figure 2) at TUT/PCT pilot line operates in normal atmosphere at line speeds between 10-350 m/min. APT unit can be used to modify the surface properties of various roll-to-roll substrates, e.g. paper, paperboard, laminates, plastic films, and non-wovens. APT unit operates with similar parameters as industrial corona; power range: 400 - 2000 W, voltage range: 22.5 - 25.0 kV, frequency range: 21.5 - 25.0 kHz, treatment width: 380 mm. However, the electrode design of APT differs from industrial corona. Helium and argon can be used as treatment gases. In addition, helium and argon based gas mixes can be used (N_2, CO_2, air). TUT's APT unit can operate as a plasma unit or as a traditional corona unit. The difference is in electrode design, which in plasma treatment prevents breakthroughs that can occur in corona treatment.

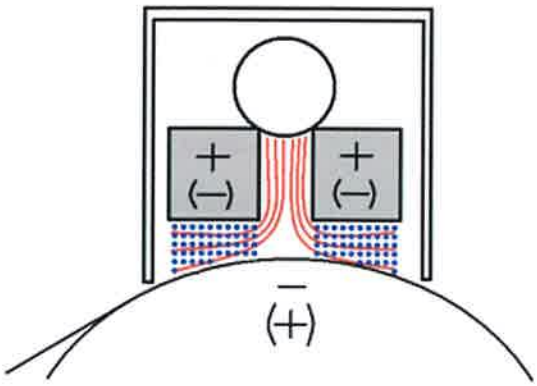


Figure 2: Configuration of the APT unit of TUT/PCT

Surface energies of the samples were defined with contact angle measurements, which were made with Pocket Goniometer PG-3 device 24h after the treatment. The samples were stored in constant laboratory environment (23°C, 50 % RH). Surface chemical composition and oxidation were defined with ESCA (Electron spectroscopy for chemical analysis) 24h after the treatment. Analysis depth of ESCA is 5 - 10 nm. The samples were printed with a Xeikon 5000 XL digital printing machine. The printing method in the Xeikon is based on a dry toner web-fed electrophotographic process. Toner adhesion was defined with a rub-off measurement. Rub-off means the abrasion durability of the dry printing image. It is determined by rubbing the image against an unprinted surface. The amount of toner that has been transferred is measured by change in brightness (%). Print quality, mainly print mottle, was analysed both visually (ranking list) and numerically (mottle value). The visual evaluation was made by six different persons trained for these kind of evaluations. Numerical evaluation was done with Umax PowerLook II scanner and analysed with Mottling Viewer -software.

3. Results and discussion

3.1 Surface energy

The surface energy levels of PE-LD coating after flame, corona and plasma treatments were observed 24h after the treatment. The results are presented in the following Figure 3. Contact angle measurements show that all surface treatments increase the surface energy of the PE-LD surface and the levels of surface energy are quite equal. Corona treatment increases the surface energy more than flame treatment. This is detected also in previous researches [Junnila et al. 1989, Savolainen et al. 1991, Tuominen et al. 2006]. However, argon plasma is the most effective. It must also be noted that compared to corona, with plasma treatments the same surface energy level can be achieved already with ca. 50% lower efficiency.

One drawback with traditional treatments has been the decay of the treatment, i.e. decay of surface energy [e.g. Lahti 2005, Lahti et al. 2004, Kuusipalo 2008]. This can be a problem in printing, especially with low energy surfaces like PEs. The decay of surface energy varies between these different treatments [Tuominen & Lahti 2007]. It has been stated that plasma treatment possesses higher durability of the treatment effect compared to corona [Chan 1994, Chan et al. 1996]. Already, some results are available relating to paper substrates [Pykönen et al. 2008].

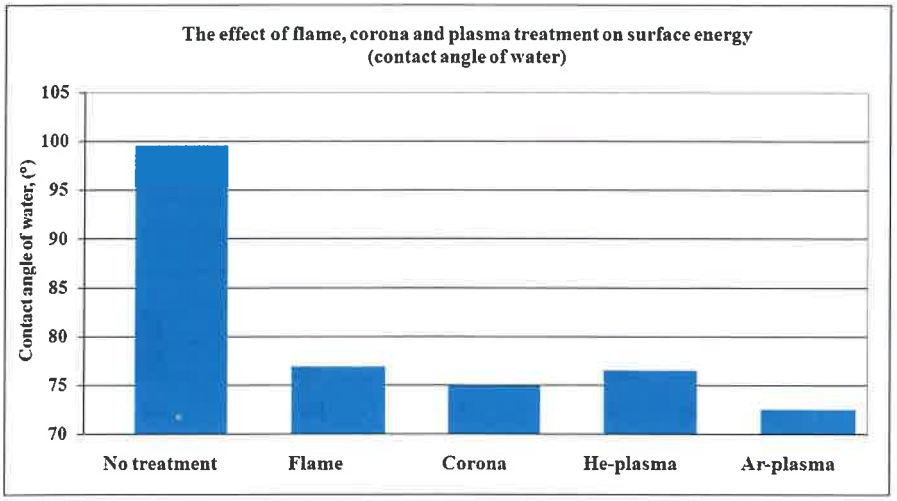


Figure 3: The effect of flame, corona and plasma treatments on surface energy of PE-LD coated paperboard. The efficiencies of the treatments are: flame 774.3 Wmin/m^2 (43.8 BTU/m^2), corona 52 Wmin/m^2, He-plasma 32 Wmin/m^2, and Ar-plasma 28 Wmin/m^2

3.2 Oxidation and chemical composition

The oxidation of PE-LD surfaces after flame, corona and plasma treatments was measured 24h after the treatments. The oxygen content of the surfaces is presented in Figure 4. The oxygen content on the surface of flame and corona treated surfaces is quite equal, whereas the oxygen content on the surface of plasma treated test points is higher, and with argon plasma around 30% higher than with flame and corona. It must be noticed that with plasma treatments the efficiency was only half of that of corona.

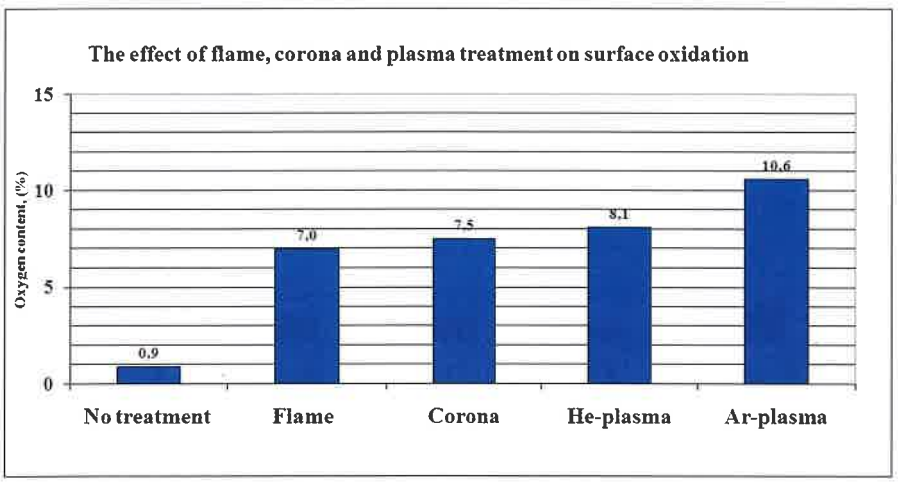


Figure 4: The effect of flame, corona and plasma treatments on surface oxidation of PE-LD coating

3.3 Printability

Printing trials were made within a week after treatment. Print quality, particularly print mottle, was analysed both visually (ranking list) and numerically (mottle value). Print mottle reflects the uniformity of the print. Figure 5 shows the effects of surface treatments on visual print quality. Visual quality of the treated samples is not good compared to the untreated sample. This indicates that the treatments are not uniform. The numerical mottling measurement ascertains the visual evaluations. The unevenness is reflected also in the mottling values, which are higher after treatments. However, if traditional treatments, i.e. flame and corona, are compared to plasma, it can be seen that plasma gives more uniform treatment, and thus lower print mottle and better visual quality. The argon plasma treated sample was ranked the best of the treated samples.

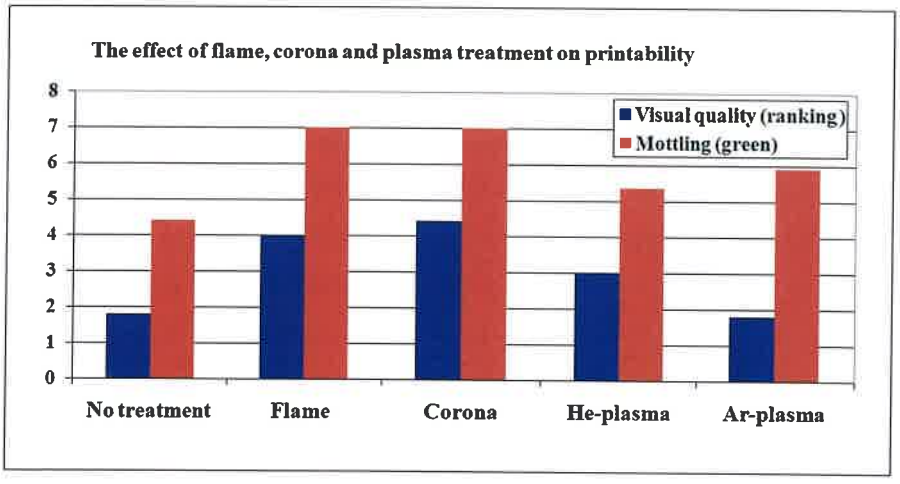


Figure 5: The effect of flame, corona and plasma treatments on printability of PE-LD coated paperboard. Visual quality is evaluated based on ranking (1 is the best and 5 is the worst). The lower the mottling value, the better print quality

Toner adhesion was defined with a rub-off measurement. It describes the abrasion durability of the dry printed image. As Figure 6 demonstrates, surface treatments clearly increase the abrasion resistance of the printed images measured as rub-off values. Abrasion resistance is very important for instance during converting operations of the printed material. With both, magenta and cyan colours, the rub-off values of the treated test points are better than that of the untreated sample. This is due to the increased surface oxidation and high enough surface energy. Lahti [2005] and Lahti et al. [2004] have noted that when the surface energy of the PE-LD surface is higher than that of the toner, adequate toner adhesion can be achieved.

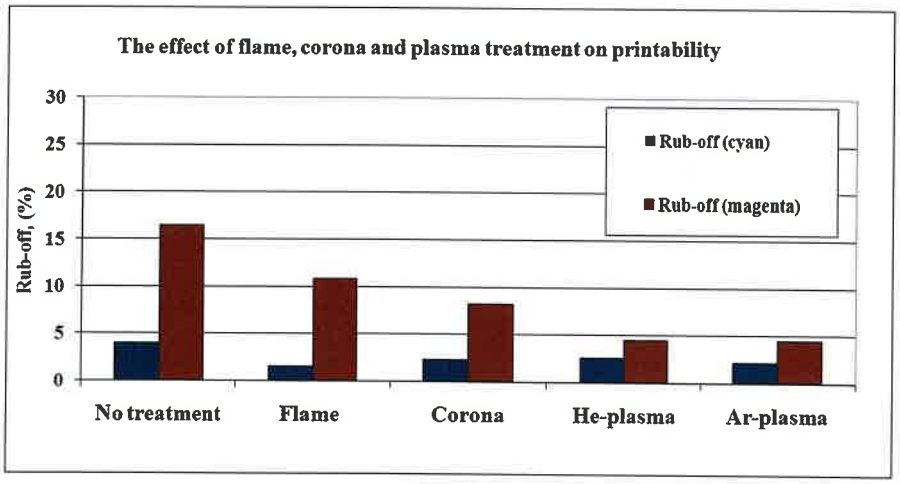


Figure 6: The effect of flame, corona and plasma treatments on printability of PE-LD coated paperboard. The lower the rub-off value, the better abrasion resistance the printed image has

4. Conclusions

Converting processes of packaging boards set quite high demands for extrusion coating surfaces and the printed images. Adequate toner adhesion is essential when extrusion coated packaging applications are concerned. In packaging applications, the visual print quality is also an important element. High enough surface energy and functional chemical groups are necessary for uniform print quality and toner adhesion. Some extrusion coatings have the required surface energy level without the surface treatments, but for example PE-LD needs surface modification in order to succeed in a digital printing process.

Based on the study, the following conclusions can be made:

- Surface treatments clearly increase surface energy of PE-LD coated paperboard by oxidising its surface. Argon plasma is the most effective method based on the contact angle measurements.
- Also surface analysis with ESCA clearly shows the oxidising effect of all surface treatments. Plasma treatments are more effective than traditional flame and corona.
- Plasma treatments are generally speaking more effective compared to corona. Same or even higher effect can be achieved with 50% lower efficiency compared to corona and flame.
- All surface treatments evidently improve toner adhesion, which is very important in packaging applications. Plasma treated surfaces have the lowest rub-off values.
- The effects on print mottle are not yet advantageous. Some more development work is clearly needed with the treatment uniformity in order to improve print evenness. However, compared to corona and flame, plasma treatments are more uniform giving more even print with lower print mottle, and hence better visual quality.

Acknowledgements

This work was partly funded by the Finnish Funding Agency for Technology and Innovation (TEKES). The authors are grateful to Borealis Polymers Oy, Stora Enso Oyj Consumer Boards, Stora Enso InnoCentre and the lab staff of TUT/PCT and Stora Enso for measurement and trial support.

References

1. Brewis, D. M. Applied Science, Publishers Ltd., Essex, 1982, 268 p.
2. Briggs, D., Brewis, D. M., Konieczko, M. B. Journal of Material Science, Vol. 14 (1979), pp. 1344 - 1348
3. Briggs, D., Kendall, C. R. International Journal Adhesion Adhesives, Vol. 2, No. 13 (1982), pp. 13 - 17
4. Cernakova, L., Stahel, P., Kovacik, C., Johansson, K. 9th Tappi Advanced Coating Fundamentals Symposium, Turku, Finland, 2006, pp. 7 - 17
5. Chan, C. M. Hanser Publishers (1994), 285 p.
6. Chan, C.-M. 1994. Polymer surface modification and characterization, Carl Hanser Verlag, Munich Vienna New York, pp. 35 - 76
7. Chan, C. M., Ko, T. M., Hiraoka, H. 1996. Polymers surface modification by plasmas and photons. Surface science reports 24, No. 1 - 54, 54 p.
8. Cramm, R. H., Bibee, D. V. Paper Synthetics Conference, Chicago 1981. Tappi Press (1981), pp. 1 - 11
9. Crolius, V. G., Ebeling, W. E., Parsons, R. C. Tappi Journal, Vol. 45, No. 5 (1962). pp. 351 - 356
10. Eckert, W. European Tappi Polymers, Laminations and Coatings Conference, Rome, Italy, 2003
11. Garbassi, F., Occhiello, E., Polato, F. Journal of Materials Science, Vol. 22 (1987), pp. 207 - 212 (a)
12. Garbassi, F., Occhiello, E., Polato, F., Brown, A. Journal of Materials Science, Vol. 22 (1987), pp. 1450 - 1456 (b)
13. Gaydon, A. G. 2nd edition, Halsted Press, New York, 1974, 412 p.
14. Hansen, H. M., Finlayson, M. F., Castille, M. J., Goins, J. D. Tappi Journal, Vol.76, No. 2 (1993), pp. 171 - 177
15. Junnila, J., Savolainen, A., Forsberg, D. Polymers, Laminations and Coatings Conference, Orlando 1989. Tappi Press (1989), pp. 353 - 360
16. Kuusipalo, J. (ed.) Paper and paperboard converting, 2nd edition, Finnish Paper Engineers' Association/Paperi ja Puu Oy, Jyväskylä, 2008, 346 p.
17. Lahti, J. Ph.D. Thesis, Tampere University of Technology, Publication 523, Finland 2005, 125 p.
18. Lahti, J., Savolainen, A., Räsänen, J. P., Suominen, T., Huhtinen, H. Polymer Engineering and Science 44, 11, pp. 2052 - 2060, 2004
19. Leech, C. S. Screen Printing, January (1991), pp. 52 - 55
20. Maxwell, J. W., Markgraf, D. A., Salvati, L. S. Jr., Ferris, M. Charleston 1987. Tappi Press (1987), pp. 153 - 158
21. Pijpers, A. P., Meier, R. J. Journal of Electron Spectroscopy, Vol. 121 (2001), pp. 299 - 313
22. Pykönen, M., Sundqvist, H., Kaukoniemi, O-V., Tuominen, M., Lahti, J., Fardim, P., Toivakka, M. Surface and Coatings Technology 202 (2008), pp. 3777 - 3786
23. Savolainen, A., Kuusipalo, J. Düsseldorf 1991. Tappi Press (1991), pp. 897 - 904

24. Sheng, E., Sutherland, I., Brewis, D. M., Health, R. J. Applied Surface Science, Vol. 78 (1994), pp. 249 - 254
25. Strobel, J. M., Strobel, M., Lyons, C. S., Dunatov, C, Perron, S., J. Journal of adhesion science technology, Vol. 5, No. 2 (1991) pp. 119 - 130
26. Sun, Q. C., Dong, D. D., Zhang, D., Wadsworth, L. C. Tappi Journal, Vol. 81, No. 8 (1998), pp. 177 - 183
27. Sutherland, I., Brewis, D. M., Health, R. J., Sheng, E. Surface and Interface Analysis, Vol. 17 (1991), pp. 507 - 510
28. Tuominen, M., Kuusipalo, J., Bothor, R., Lankinen, T. Polymers, Laminations and Coatings Conference, Vienna 2005. Tappi Press (2005), 8 p.
29. Tuominen, M., Lahti, J., Kuusipalo, J. 10th Advanced Fundamentals Coating Symposium, Montreal, Quebec, Canada, 2008
30. Tuominen, M., Lahti, J. Tappi 9th European PLACE Conference, Athens, Greece, 2007

Surface properties and UV ink-jet printability of recycled polyolefins

Diana Gregor-Svetec, Tadeja Muck, Gorazd Golob

University of Ljubljana
Faculty of Natural Sciences and Engineering
Snežniška 5, SI-1000 Ljubljana, Slovenia
E-mail: diana.gregor@ntf.uni-lj.si

Abstract

The goal of the research was the investigation of printability of thin plastic plates, produced from the 100% recycled polypropylene (PP), 100% recycled low-density polyethylene (LDPE) and 100% recycled high-density polyethylene (HDPE) chips, made from the separatelly colected waste packaging in Slovenia. Surface roughness, coefficient of friction, surface energy and chemical composition of polymeric plate surface were analysed. Polymeric plates were printed with the UV inks on the large format digital UV inkjet printers TeckSmart and Arizona. Optical density, colour of plates and quality of prints were determined. The results have shown that the lowest optical density has the PP, the highest HDPE, which has also the darkest grey colour and that the uniformity of the surface colour is higher at the PP than at LDPE and HDPE. Prints on the PP are more uniform, and the colour saturation is the highest. The best printability was obtained for polypropylene, as PP has the most uniform surface, the lowest contact angle and the highest surface energy with the prevailing part of the polar component resulting in better wetability of surface.

Keywords

Polyolefins, printability, recycling, UV inkjet printing

1. Introduction

The preservation of non-renewable natural resources is an issue which has assumed great importance in modern society. Our throw-away culture, characterised by a linear treatment of assets which begins with natural resources and ends in waste, is perceived as being guilty of wasteful squandering of precious natural resources [Lunquist, L et.al., 2001] The polymer industry is particular under fire due to the short lifespan of many plastic-based consumer products, the high visibility of polymers in municipal solid waste and the rapid increase of plastic consumption. For further sustainable economic growth we have to improve the efficiency of resource consumption and reduce the waste output [Hahn, B., 1992]. Improvements should occur at all stages of the life cycle of a product, from raw material production, product manufacture and its use to recycling or disposal of a product. Life cycle engineering provides a methodology of haw to design, manufacture, use, maintain and recover materials and products with the aim of optimising resource use and minimising enviromental impact [Tischner, U., Nickel. R., 2003]. Also at the development and design of packaging, made from polymers, the ecological view is becoming very important.

Eco-design is a part of the long-term development strategy of the Eupean Union till year 2014 and includes efficient use of the materials, reduce use of energy, reduce use of enviromentally hazardous matrials, optimization of the lifecycle of product and increase use of recycled materials [Vickers, J. J., Boyle, C. A., 2007].

As the use of polymers for production of packaging is constantly increasing, among them polyolefins, the recycling of pololefins is becoming more and more important, as well as the knowledge upon the influence of the structure and properties of recycled polyolefins on the quality of packaging. The national Slovene research project is dealing with the eco-design of packaging made from the recycled polyolefins and printing of them with different inks and different printing techniques. Research includes following polymers: polypropylene (PP), low-density polyethylene (LDPE) and high-density polyethylene (HDPE). In present paper printability of thin plastic plates made from recycled polyolefins was investigated. As printing technique UV-inkjet digital printing was considered.

2. Experimental

2.1 Materials and testing methods

As the knowledge about the polymer properties is the basis of the product development, the starting point of our research was the determination of recycled polymers properties: melt index, softening and melting temperature, melting enthalpy and crystalinity degree. On the basis of those results, border frames were determined upon which polymer melt extrusion and injection moulding was carried out. Thin plastic plates were produced from the 100% recycled polypropylene, 100% recycled low-density polyethylene and 100% recycled high-density polyethylene chips, made from the separatelly colected waste packaging in Slovenia.

In the next step printability of recycled polymeric materials was investigated. Because printability mainly depends from the surface properties of printing material surface roughness, coefficient of friction, surface energy and chemical composition of surface were analysed. Surface roughness was determined with an air leak method using the Bendtsen tester (Noviprofibre). The rate at which air passes between the flat land and test piece surfaces under the specified conditions of the test is used as a measure of the roughness/smoothness of the sample surface. Dynamic and static coefficients of friction were determined on an Instron tensile testing machine equipped with the Coefficient of friction test fixture testing device. Contact angle and surface energy measurements were performed on a FibroDAT apparatus.

Surface of polyolefin plates was captured with the scanning electron microscope Jeol. Chemical composition of the surface was determined with the ATR-FTIR technique on a FTIR spectrometer PerkinElmer SpectrumGX. With a densitometer GretagMacbeth D19C the optical density of plastic plates and with a spectrophotometer GretagMacbeth Coloreye XTH the colour of plates was measured.

2.2 Printing and evaluation of prints

Plastic plates were printed with the UV inks on the large format digital UV inkjet printer TeckSmart UV 1600 (Tepede) and on Arizona (Océ). The printed samples were evaluated at first visually and than the pictures captured with the optical microscope Leica EZ 4D equipped with a CCD camera and with the Nikon Stereoscopic Zoom microscope SMZ800 by image analysis with the program ImageJ.

Printer Tepede TeckSmart UV 1600 is a universal hybrid large format printer with either 1600 mm or 2500 mm print width. It uses 7 colours (C, M, Y, K, Lm, Lc and the option white colour) and Xaar printheads. It prints with maximal print resolution 1440 dpi. The printer is based on UV curing technology and able to print on flexible media as well as on rigid media. The maximum media weight could be about 5 kg/m^2 and the maximum media thickness of up to 15 mm. Print speeds (high print quality 26 m^2/h at 4 pass, the highest print quality 13 m^2/h at 8 pass).

Printer Océ Arizona uses 8 printing heads, 2 for each color. It produces exceptional quality prints with the Océ VariaDot™ (the drop volume; from 6 to 42 pl) imaging technology. It uses piezoelectric inkjet technology and can be used for printing on rigid and flexible media. The samples are fixed with vacuum table, which holds media stationary for precise printing. The highest media thickness could be max. 48 mm. Print speeds of up to 16.7 m^2/hour (high print quality 12 m^2/h, the highest print quality 8 m^2/h).

3. Results and discussion

3.1 Analysis of polymeric plates

In the first part of the investigation the polyolefin plates were analysed. In Figure 1 the surface roughness of plates is shown.

The analyses of surface roughness made with the airflow measurement with the Bendtsen tester have shown that all three plates have similar roughness (Figure 1). The highest value reached the PP, only for 1% lower LDPE and for 3.4% lower HDPE. If we take into account the measurement accuracy, the obtained difference in mean value for the PP and LDPE is negligible, as the mean values are within the limits of the accuracy of the flow transducer. If we consider the standard deviation of measurements, which is at the polyethylene plates over 200 ml/min, also the difference in mean values obtained for the HDPE in comparison to the PP and LDPE is within

the error bars. The high value of standard deviation means also that the unevenness of the surface of the plates is high, especially at the LDPE and HDPE, where the coefficient of variation is over 10%.

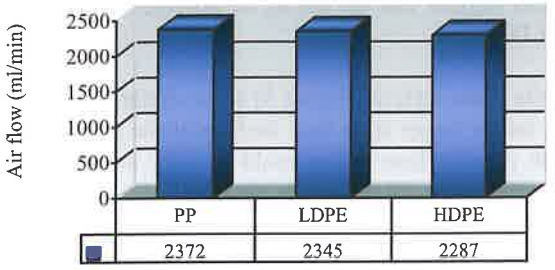


Figure 1:
Surface roughness of polyolefin plates (PP, LDPE, HDPE) determined with the Bendtsen tester

Table I: Coefficient of friction (static, dynamic) and force at friction (mean, maximum) for polyolefin (PP, LDPE, HDPE) plates

Sample	Coefficient of friction (/)		Force (cN)	
	dynamic	static	mean	maximum
PP	0.0875	0.0907	18.3	25.4
LDPE	0.1248	0.1318	22.1	26.1
HDPE	0.0596	0.0659	7.6	13.8

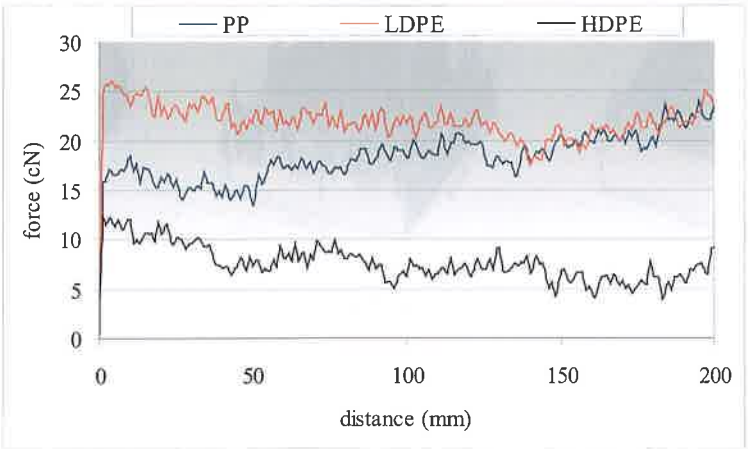


Figure 2: Friction force of polyolefin (PP, LDPE, HDPE) plates

Polyolefin plates differ more in the coefficient of friction (Table I). Static friction is the force that resists initiation of movement of one surface sliding over another surface. Dynamic or kinetic friction is the force that resists maintained sliding of one surface over another surface. The highest dynamic and static coefficient of friction, determined between the plastic plate and metal (aluminium) plate was obtained for the LDPE. Around 40% lower coefficients were obtained for the PP and much lower, i.e. 2.2-times for the HDPE. LDPE has higher force needed to keep the sled moving and almost the same maximum force as the PP, as seen from Figure 2. The mean resisting force that arises when a surface of the polymer plate slides over the surface of the aluminium plate and the maximum force atained during sliding reached at HDPE are also low in comparison to the other two polymers, meaning that the HDPE has higher smoothness than the PP and LDPE.

Table II: Contact angle (water, formamide) and surface energy of polyolefin (PP, LDPE, HDPE) plates

Sample	Contact angle (°)		Surface energy (mN/m)		
	water	formamide	dispersive part	polar part	total
PP	77.9	72.2	12.1	19.7	31.8
LDPE	92.5	71.6	20.7	7.8	28.5
HDPE	81.4	72.4	13.4	16.8	30.2

As seen from the Table II the lowest contact angle with the water droplet, the highest surface energy and the polar component of the energy has the PP. The contact angle with the water droplet greater than 90°, the lowest surface energy and smallest part of the polar component has the LDPE, whereas the HDPE has values between the PP and LDPE, closer to the PP. These results suggest that the ability of polymers to accept and retain ink will be the highest at the PP and lowest at the LDPE.

In the scanning electron microscope pictures of polyolefin plate surface (Figure 3) some differences are also seen. The surface at both polyethylene plates is rougher on the larger scale than surface of the polypropylene plate. If we consider an area of few microns large both polyethylene plates could be very smooth or very rough, whereas the polypropylene plate has similar micro-roughness on the whole surface.

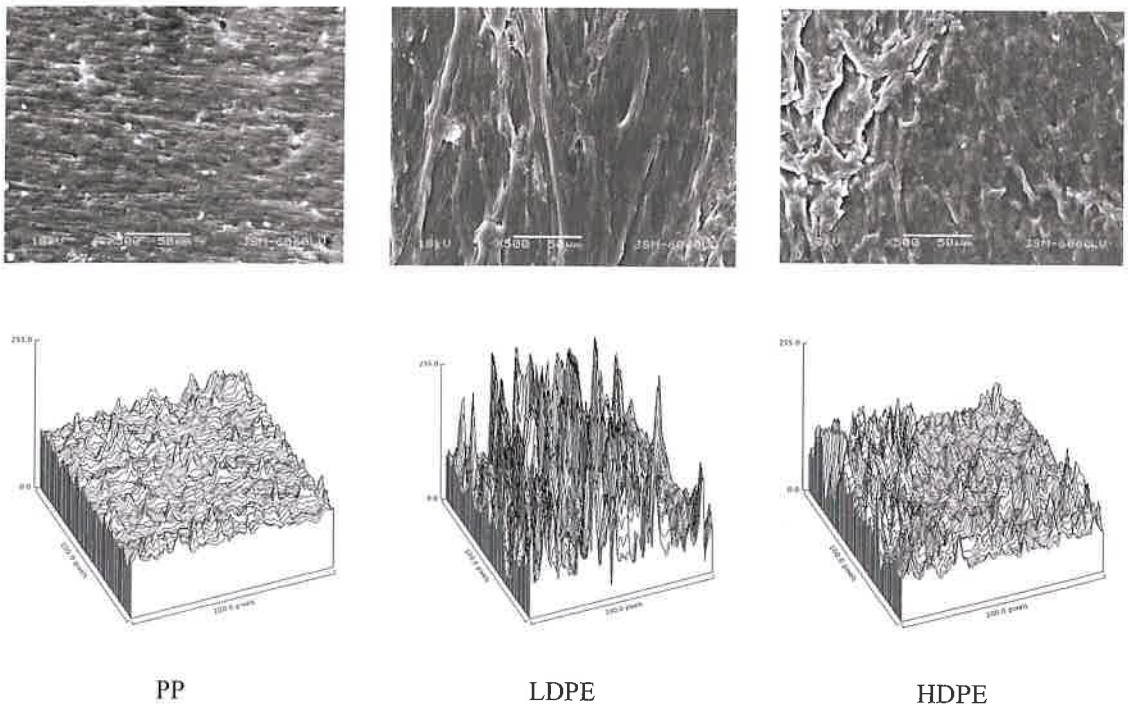
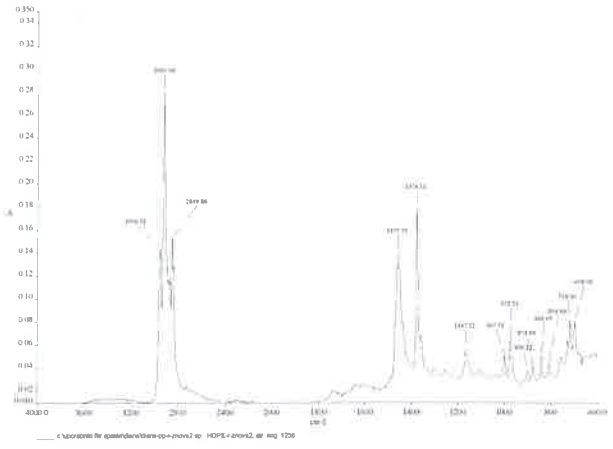


Figure 3: SEM pictures of polyolefin plate surface:
PP (left), LDPE (middle), HDPE (right) and their surface plot diagrams

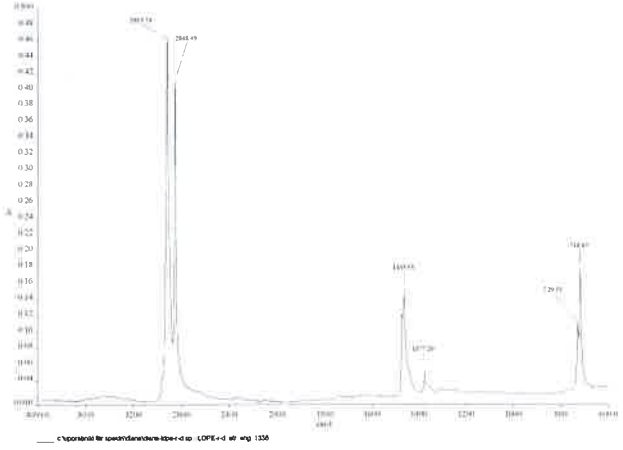
For objective evaluation of SEM images the ImageJ was used. Tiff files were transformed into 8bit images. Images were cropped into the end area 100 x 100 pixels. Topography of samples was evaluated with Surface plot macro. 3D diagrams support visual evaluation of roughness on the SEM images. 3D Surface plot diagrams show the highest level of non-uniformity for the LDPE plate and the highest uniformity for the PP.

Infrared spectroscopy provides the ability to study the interactions of the vibrational and rotational energies of atoms or groups of atoms within molecules. Thus, the spectrum can be used to indentify the presence of a specific chemical compound or mixture of compounds and advise us if there`s any change in the production chain [Sanchez-Alandi, A. et.al., 2007]. The infrared spectrum of polyethylene has strong bands near 2950 cm^{-1} and 1460 cm^{-1} and a band of medium intensity, a doublet, near 725 cm^{-1}, due to the CH stretching, deformation and rocking vibrations. The band at 970 cm^{-1} at HDPE is due to the CH out-of-plane deformation vibration for trans-vinylene group [Socrates, G., 2004]. The infrared spectrum of polypropylene has strong band near 2950 cm^{-1}. The band vibration for methly group is a doublet 1450 cm^{-1} and 1375 cm^{-1}. Bands of medium intensity are observed near 1155 cm^{-1}, 970 cm^{-1}, due to the CC stretching and CH_3 rocking vibration and a number of sharp bands in the region 1250-835 cm^{-1} [Socrates, G., 2004].

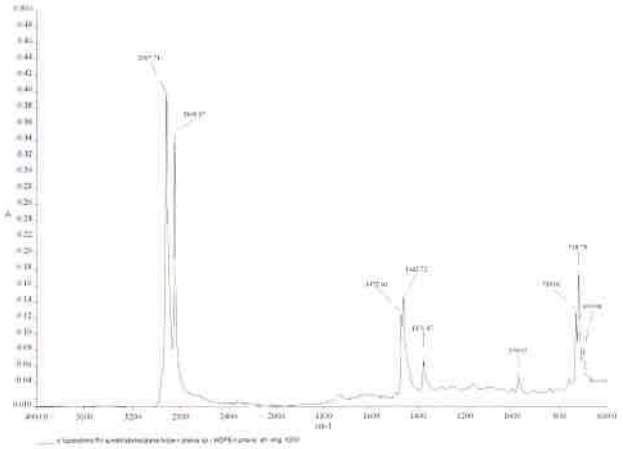
From Figure 4 is seen that the spectra of analysed polyethylenes (LDPE and HDPE) are typical for this two polymers, whereas at polypropylene some peaks not typical for PP are also present. Peaks at 2849, 729 and 719 cm^{-1} in the spectrum of polypropylene mean, that plates made of recycled polypropylene contain also a fraction of polyethylene.



PP



LDPE



HDPE

Figure 4: FTIR spectra of polyolefin (PP, LDPE, HDPE) plates

With the spectroscopic and densitometry measurements the colour and optical density of polyolefin plates were determined. The non-uniformity of plates was determined with the measurements based on the image analyses (histogram) and with the calculation of standard deviation of optical density on each single plate. The lowest optical density has the PP, the highest the HDPE, which has also the darkest grey colour. The

lowest value of standard deviation was determined at the PP, the highest at the HDPE, meaning that the uniformity of the surface colour is higher at the PP than at the LDPE and HDPE (Table III). In Figure 5 the surface of polyolefin plates is shown.

Table III: CIE $L^*a^*b^*$ value and optical density of polyolefin (PP, LDPE, HDPE) plates

Sample	L^*	a^*	b^*	Optical density	Standard deviation
PP	31.74	-1.54	-0.17	1.26	0.03
LDPE	18.73	0.59	2.38	1.69	0.05
HDPE	24.12	0.06	-2.38	1.76	0.07



PP LDPE HDPE

Figure 5: OM pictures of polyolefin plates: PP (left), LDPE (middle), HDPE (right)

The results of densitometry measurements were confirmed with the image analysis of surface of polyolefin plates. With the image analyse the non-uniformity of plates was determined and as an analyzing tool a histogram was used. The histograms are shown in Figure 6. The histogram of the PP surface has the lowest area and is the most narrow among all three histograms. At the PP also the lowest value of the standard deviation was obtained and the highest value on the grey scale, meaning that the colour of the PP surface is brighter and more uniform than at the LDPE and HDPE.

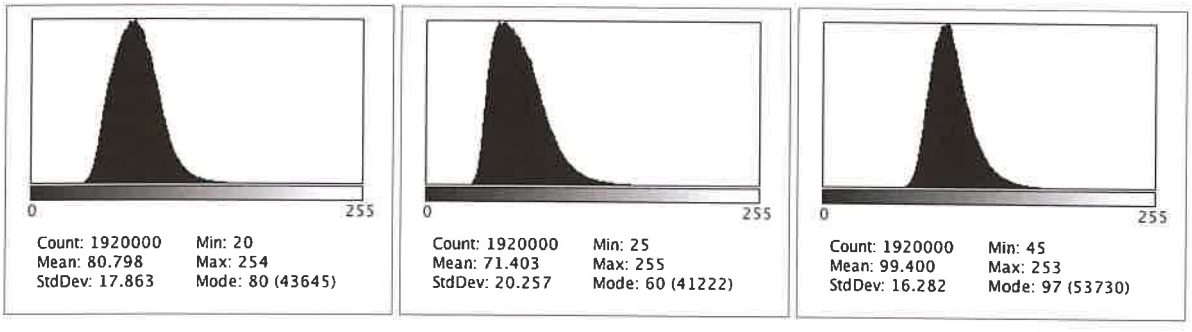


Figure 6: Histograms of polyolefin plates: PP (left), LDPE (middle), HDPE (right)

3.2 Print quality evaluation

The visual assessment (Figure 7) and the image analyses of printed areas of the prints made with the UV-inkjet printer TeckSmart (Tepede) have shown that the best quality of prints was obtained at the PP, followed by the LDPE and HDPE. Prints on the PP are more uniform, and the colour saturation is the highest. Prints on the LDPE have inferior quality, colours are less saturated and halftone dots are not sharp enough. Similar picture is seen at the prints on the HDPE, colours are less saturated and halftone dot is not clear enough. The plate surface is not continuously covered with the ink, on 100% raster tone value the surface of the polymer plate is also sometimes seen.



Figure 7: OM pictures of prints on polyolefin plates: PP (left), LDPE (middle), HDPE (right), made with the UV-inkjet printer TeckSmart

The Optical microscope with 20x magnification was used for capturing images of printed areas with the sign %, which were than evaluated as the percent of surface covered by ink.



Figure 8: The binary images of captured samples after evaluation with the ImageJ program: PP (left), LDPE (middle), HDPE (right)

For better evaluation we upgraded the macro for Measure Area Fraction. In the upgraded macro the following steps were used:

- transformation of captured images into 8 bit images;
- cutting of images (crop) on the end area (600 x 600 pixels);
- reducing background noise with the median filter;
- automatic threshold setting and transformation in binary image;
- analysis of ink covering surface by the use of macro; Measure Area Fraction.

Table IV: The area of ink coverage on polyolefin (PP, LDPE, HDPE) plates

Sample	Area of ink coverage (%)
PP	39.2
LDPE	43.3
HDPE	46.8

From the results presented in Table IV it is clearly seen, that the lower ink coverage on the surface and also the lowest wicking phenomena is achieved on the PP. The higher wicking and higher area of ink coverage was obtained for the LDPE and HDPE. At HDPE and especially at the LDPE the deformation of the dot is seen on the surface, the droplet is extended - bleeds, because it was dried in the state of sliding on the surface.

Polyolefin plates printed with the UV inks on the large format digital UV inkjet printer Océ Arizona were evaluated with following methods: densitometric dot gain evaluation by gradation curves (measuring of raster tone values (A%) on printed strips with 20%, 40%, 60% and 100% A) and evaluation of captured images of printed number (20%) by image analysis

From Figure 9 is seen, that the highest dot loss was obtained at the HDPE at the raster tone value of 20%. Other printed areas (40% and 60% raster tone value) also show high dot loss. A little better results, with less dot gain, was obtained at the LDPE, though the dot loss for all measured patches is also present. The best results, almost an ideal dot gain was achieved at the PP, meaning that the print quality of PP is better in comparison to polyethylenes.

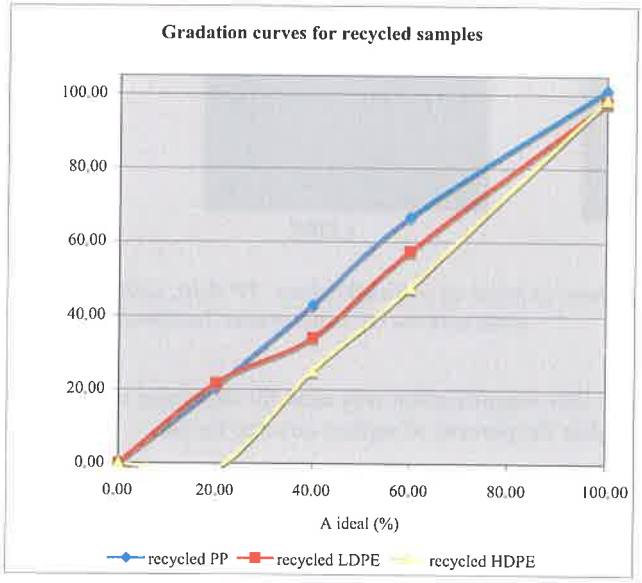


Figure 9: Gradation curves for printed polyolefin (PP, LDPE, HDPE) plates

Printed samples were captured with the use of reflection light at 8x magnification with Optical microscope and at 20x magnification with Stereomicroscope. The images are shown on the Figure 10 and 11.



Figure 10: OM pictures of printed number on polyolefin plates: PP (left), LDPE (middle), HDPE (right) plat

The images of printed number are shown in Figure 10. The contrast on the HDPE is very low, because of its dark background. At the LDPE high reflection of printed ink is present, probably because the ink stayes completely on the plate surface. The good print quality with good print contrast was obtained at the PP. At the PP also the lowest wicking occurred, at both polyethylenes this negative phenomena was more present.

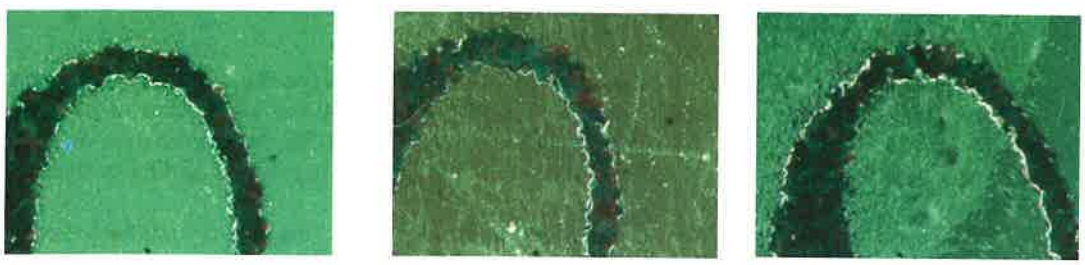


Figure 11: Printed number on the polyolefin plates: PP (left), LDPE (middle), HDPE (right) – image captured with the stereomicroscope

From the images, which were captured by stereomicroscope (Figure 11), the statements from previous evaluations could be confirmed. At the PP the lowest wicking is seen, whereas at both other samples this negative phenomena is more pronaunced.

4. Conclusions

In our study, no direct comparison of prints, made with two different printers was made, because of different UV ink, different printing conditions and print parameters applied. Only the prints, made on different materials with one kind of printer (TeckSmart or Arizona) could be compared, as they were performed at the same time and the same printing conditions applied. The print quality estimation coincides with the results of measured surface characteristics of plastic plates made from 100% recycled polymers. The best printability was obtained for polypropylene (regardless of printer used), as PP has the most uniform surface, the lowest contact angle and the highest surface energy with the prevailing part of the polar component resulting in better wetability of surface. At PP the best formation of halftone dots and the lowest dot gain was obtained.

The research has shown that UV inkjet technology copes quite well with the PP, as this recycled polyolefin could be printed without surface pre-treatment with corona or plasma. Other two tested recycled polyolefin plates, LDPE and HDPE, show lower UV inkjet printability at same conditions. Results of these printing trials show, that the digital UV inkjet printing could be applied for printing recycled polypropylene plastic materials, used for disposable low cost packaging products.

Acknowledgements

This research was financially supported by the Slovenian Research Agency.

References

1. Hahn, B., (1992)Films reduce waste. Packung Transp., No. 10, p. 26 - 28
2. Lunquist, L., Letterie, Y., Sunderland, P., Manson, J. A. E., (2001) Life Cycle Engineering of Plastics. Elsevier Science Ltd.
3. Sannchez-Alandi, A., Otero, S., Gracia, V., (2007) Wavelet automatic classification system of substrates in flexography.Advances in Printing and Media Technology, Ed. Enlund, N., Lovreček, M., IARIGAI, Vol. 34, Acta Graphica Publishers, Zagreb.
4. Socrates, G., (2004) Infrared and Raman Characteristic Group Frequencies. John Wiley & Sons, Ltd.
5. Tischner, U., Nickel, R., (2003) Eco-design in the printing industry. The Journal of Sustainable Product Design, no.3, p.19 - 27
6. Vickers, J. J., Boyle, C. A., (2007) The Changing Face of Environmental Legislation: New Policy Directions in the European Union. Proceedings of the 2nd International Conference on Sustainability Engineering and Science, Auckland, NZ, Feb 21 - 23, 2007, http://nzsses.auckland.ac.nz/conference/2007presentations.htm



Insight into IJ-ink/paper interaction using drop spreading model

Marie Kaplanová[1], *Lenka Otáhalová*[1], *Tadeja Muck*[2]

[1] University of Pardubice, FCHT, Department of Graphic Arts and Photophysics
Pardubice, Czech Republic
E-mail: marie.kaplanova@upce.cz

[2] University of Ljubljana, Faculty of Natural Sciences and Engineering, Ljubljana, Slovenia

Abstract

In non-impact printing the interaction of ink drop with substrate after impacting the paper surface is important process that determines the print quality. Theories that describe the initial stage of wetting usually assumes ideal solid surface that are far from real surfaces encountered in the printing industry and thus leaving some questions concerning the interaction between inks and substrates opened.

The primary interest of this investigation is to study the behaviour of the liquid-paper interaction in the event of ink drop impaction on a sized paper surfaces. Relation of rate constant and surface tension on surface roughness using both the standard liquids and the IJ inks were observed and an alternated model for description of drop spreading of liquids was proposed and verified on a range of coated papers.

Correlation of spreading rate and imbibition and characteristics of drops formed by inkjet printer were further evaluated. UV-curable inks showed almost no absorption process on tested papers. So the drop characteristics are mainly determined by the spreading to equilibrium, unless the print-to-cure time is short enough the freeze the moving droplet.

Keywords

Contact angle measurement, coated paper, inkjet ink, ink/paper interaction, surface tension, UV inks

1. Introduction

In non-impact printing processes (e.g. inkjet) ink properties like viscosity, surface tension, particle size distribution, good jettability and long-term storage stability are crucial for good performance and print quality. Surface tension characteristics are important parameters especially influencing the drop spreading rate, ink penetration and consequently the print quality. The process of interaction of ink drop with substrate after impacting the paper surface can be divided into few stages and includes spreading and penetration. The initial phase of wetting is dynamic, eventually leading to the final equilibrium situation. UV curable digital inks cure rapidly, often before completely wetting out on the substrate. Contact with substrate followed by UV curing is very rapid, on the order of micro or milliseconds. It is influenced by drop velocity, reactivity of the ink to UV lamp and distance of printheads to UV lamps. To achieve higher resolution in paper transport direction, multiple printing passes are used. Today printers are able to send different sizes of ink droplets as small as 1 pl. While the ideal spot shape is circular, in reality it is rather elliptic followed with small droplets, so called satellites [*Mercier, 2007*].

Wetting equilibrium measurement is useful tool for the characterization of printing substrates. The theory of wetting started many years ago by considering an ideal solid surface that is perfectly smooth, chemically homogeneous, rigid, insoluble and nonreactive [*Erbil, 2006*]. However, real surfaces that are encountered in the printing industry are very far from being ideal. Thus, there are some open questions concerning of the interaction between inks and substrates in wetting processes partly due incapability of the experimental technique to follow quick wetting at the microscopic level of contact between the liquid and the solid and theoretical analysis for three-dimensional situations that are essential when considering real surfaces.

When real surfaces are considered, one should distinguish between the actual and the apparent contact angles [*Marmur, 2000*]. The actual contact angle is defined as the angle between the tangent line to the liquid-fluid interface at that point. The usual optical methods for measuring contact angles yield the apparent contact angle, which is the angle between this tangent line to the seemingly smooth solid surface. The contact angle on an ideal solid surface, called the intrinsic contact angle, is calculated from the Young equation and

represents the state of minimum free energy of the drop on ideal surface. On perfectly smooth solid surfaces, the apparent contact angle is identical with the actual and intrinsic one. On rough surfaces they may be very different. The fundamental question is the relationship between the intrinsic contact angle, which is characteristic of the material properties of the system, and the measurable (apparent, actual, pseudo-equilibrium, static) contact angle.

Nowadays, the surface energy of solids is mostly assessed by using computer imaging technology to measure contact angle of liquid drop placed on a solid sample. Although this method of solid surface characterization appears as simple, the interpretation of measurement of real solids and liquids could be very complicated. The measurable contact angle of liquids on real substrates usually decreases in several seconds after drop impact on substrate. Contact angle becomes an excellent approximation to the apparent contact angle, corresponding to the global minimum in free energy, where the size of the drop becomes very large with the scale of roughness.

The wettability of the solid surface is a characteristic material property and strongly depends on both surface energy arising from the surface chemical structure and the surface roughness. A simple model to characterize the influence of the surface roughness on the wettability of a solid was proposed by Wenzel [*Wenzel, 1936*]. In that model the roughness factor r is defined as the ratio of the area of the actual surface to that of a smooth surface and the ratio of cosines of contact angle on rough surface and on the smooth one. This theory is only valid on the condition that the droplet is in perfect contact with the surface over their mutual interface. Wenzel's theory has to be refined, when the geometry of the surface is made in such a way that this requirement is not met. An example for such a surface is a porous or a very rough surface [*Cassie and Baxter,1944*]. In this case the droplet has interfaces with the air being in the pores of the surface, because the droplet sits on the peaks of the surface feature and so bridges the gaps. It states that the cosine of the contact angle on a heterogenous surface is the weighted average of the cosines of the contact angles on the various heterogenous fields on the surface. Therefore if one uses a sufficiently large drop, it may in principle, be possible to identify the most stable situation on a heterogeneous surface. The apparent contact angle corresponding to this state is the average of the intrinsic contact angles characterizing the surface. Contact angle becomes an excellent approximation to the apparent contact angle, corresponding to the global minimum in free energy, where the size of the drop becomes very large with the scale of roughness.

The primary interest of this investigation is to study the behaviour of the liquid-paper interaction in the event of ink drop impaction on a sized paper surfaces. Recently the surface energy components of inkjet papers [*Järnström, et al.; 2007, Kannangara et. al., 2006*] and dynamic surface tension of UV curable inks were studied [*Madhusoodhanan, et al., 2008*] and the print quality of inkjet prints in relation to substrate characteristics, using different destructive and non destructive methods were evaluated *[Drzkova et al., 2004; Muck et al. 2005; Drzkova et al., 2006; Kaplanová, et al., 2006*]. However, detailed insight into process that takes place when an ink drop comes into contact with the substrate surface is missing.

2. Methods

We used four types of coated papers: standard gloss coated APCO paper (150 g/m^2), two-side matt coated G-Print paper (115 g/m^2), two-side triple satin-matt coated Hello Silk paper (115 g/m^2) and double-coated on both sides voluminous matt paper BIOMATT (150 g/m^2). The composition of coatings of tested materials varies: APCO and Hello Silk paper coating includes mainly the kaolin pigments whereas the matt coating of G-Print involves calcium carbonate pigments. Paper PPS roughness was measured with Parker Print Surf, Messmer Bücher.

The pigment inks that were used in this study were commercially available inks: inkjet water-soluble Magenta and light Magenta inks (HP C9426A and HPC9429A respectively) and Sunjet UV ink (Crystal UFX 4574 Magenta).

For contact angles measurement PC controlled KSV CAM 100 USB video camera at resolution of 640 × 480 pixels was used. The image of "sessile" liquid drops was captured immediately after the droplet of liquid had been placed on the sample surface and further every second during 20 s or 30 s interval. Simultaneously the height of segment h and the radius of drop contact circle ρ were measured. At least three independent measurements were made for every sample and standard liquid. Contact angle measurements were carried out at room temperature 20 - 22°C with pure standard liquids: formamide (γ_L = 58.20 mN/m, γ_L^d = 39.50 mN/m), diiodomethane (γ_L = 50.80 mN/m, γ_L^d = 50.80 mN/m), ethylene glycol (γ_L = 47.70 mN/m, γ_L^d = 29.42 mN/m), water (γ_L = 72.8 mN/m, γ_L^d = 21.8 mN/m).

Spreading experiments require a special attention to the condition at which they are being carried out. Using the same microsyringe for all liquids, the volume of the drop self-forming at the end of needle varies according to the density and cohesion energy of liquid. The distance from the porous substrate to the tip of the dosator ranged from 1 to 2 mm. A small standard liquid drop deposited on a surface formed on tested papers a spherical cap. Depending on the liquid, we used drops from 3 to 10 μl.

For the investigation of drop formatted on the substrate during the process of printing a test target with solid and tone values (20, 40, 60, 80 and 100%) was printed on APCO and BIOMATT paper on UV IJ printer GRAPO Octopus I (printing head Xaar XJ 500/400, ink Sunjet Crystal UFX, drop volume 40 pl).

The UV ink and paper interaction and penetration of ink into the paper structure was examined on 20% magenta prints with a Zeiss confocal microscope (LSM 510, Jena). An approximately 5 by 5 mm sample were wetted by immersion oil and enclosed in between glass slide and cover slip. Two lasers: HeNe laser 543 nm (1 mW) at power of 100% and Ar laser 498 nm (30 mW) at power 62.4% were used for the excitation. The emitted fluorescent light was recollected by plan-apochromatic objective (63 × /1.4 OilDIC) and detected in 2 channels: CH1 560 nm and CH2: 505 - 530 nm.

The scaling for all images was the same: x = 0.4 μm, y = 0.4 μm, z = 0.42 μm. The sizes of stacks were the same for all samples in x and y direction (x = 206.83 μm, y = 206.83 μm), but different in z direction.

The contact angle was evaluated in image analysis software ImageJ. First sagittal and coronal stack were exported in OrtView, then a drop projection was created as a sum of the slices in the stack. In the projection edges of the drop were detected and contact angle was measured.

The magenta color prints on APCO and BIOMATT papers were captured with Optical microscope Leica EZ 4D and CCD camera at 8× and 35× magnification. Two different kind of sample lightening were used: light from the top and the side and light only from side of sample.

3. Results and discussion

3.1 Model of liquid spreading process on paper substrate

The spreading of liquid drops has been studied in time interval 20 or 30 second after the drop lands on surface. The drop motion over a dry paper appears to be caused by the interplay of two processes: growth of the drop base (spreading) and the imbibition of the liquid from the drop into the substrate. Typical time dependency of liquid drop contact angle θ, $\cos\theta$ and h/ρ ratio for water drop on one of the tested papers demonstrates Figure 1.

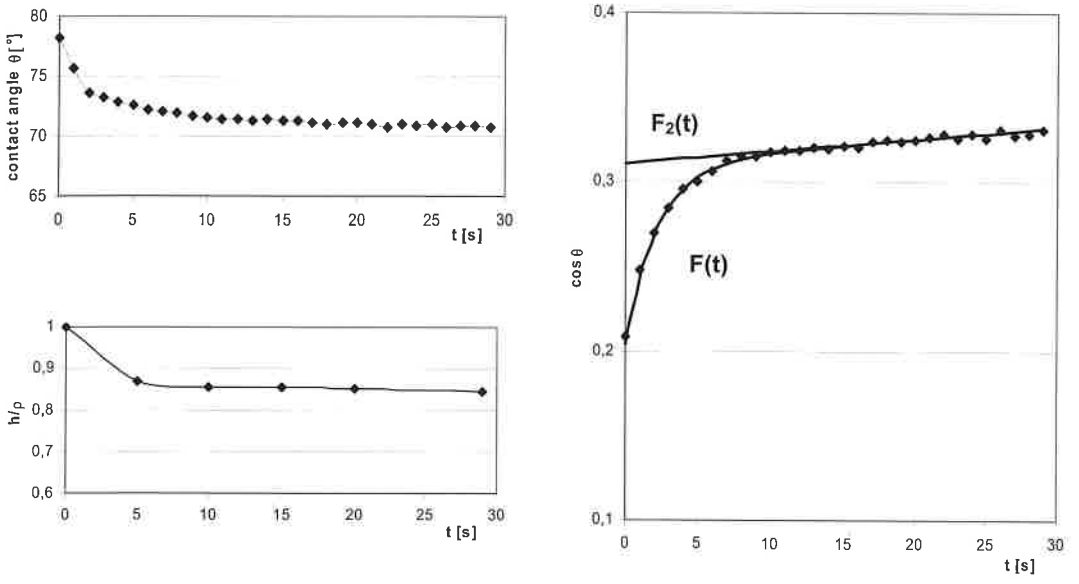


Figure 1: Water drop on APCO paper A2F (PPS 0.918) contact angle θ, $\cos\theta$ and relative h/ρ ratio time dependency

The whole spreading process can be then subdivided into two stages:

- First stage of fast drop spreading over first seconds until the maximum radius of the drop base is reached. During the first stage the contact angle rapidly decreases. Droplet volume remains practically unchanged, the ratio of the height of the spherical cap *h* and the radius of drop contact base ρ decreases.

- Second stage, when the radius of the drop base and h/ρ remain practically constant and the contact angle decreases slowly with time. Droplet volume is slowly decreasing due to the process of liquid imbibition into paper volume and partly due to evaporation (very low for all used liquids in the time interval 20 second).

We supposed that on coated papers with micro capillary surface layer the slow imbibition process starts immediately after the drop impact on paper. The advancing contact angle θ_a was defined as the pseudo-equilibrium contact angle θ_e at the moment, when the drop stopped to spread (the radius of the drop base reached its maximum value).

Spreading of liquid over a solid depends on components of the interfacial tensions acting parallel to the solid surface at the line of contact. The triple interface will move in the direction dictated by spreading pressure π

$$\pi = \gamma_S - \gamma_{LS} - \gamma_L \cos\theta, \tag{1}$$

until the θ_e value is reached at which $\pi = 0$, giving equilibrium. Several studies revealed that the kinetics of liquid wetting of smooth solid surfaces could be well characterized by a simple power law. However, Apel-Paz and Marmur showed [*Apel-Paz and Marmur,1999*] that using a simple power law model to describe liquid spreading on a rough surface was empirical. We observed, that simple power law fits insufficiently to our experimental data and providing the $\cos\theta$ as the best describing parameter of spreading process, we suggested the model describing the drop spreading and imbibition process on coated papers by means overall function of $\cos\theta = F(t)$. The two stages of the spreading process could be described as superposition of exponential (for spreading) $F_1(t)$ and linear $F_2(t)$ functions (for slow imbibition), where (B-A) responds the cosine of initial contact angle, parameter k_1 the rate of spreading and k_2 characterizes the process of liquid penetration into substrate

$$\begin{aligned} \cos\theta &= F(t) = F_2(t) + F_1(t) \\ F_1(t) &= -A\exp(-k_1 t) \\ F_2(t) &= B + k_2 t \end{aligned} \tag{2}$$

We assume that the state of minimum free energy will be reached at the end of spreading stage when $F_1(t) \rightarrow 0$. The equilibrium contact angle θ_e was then estimated as a point where the $F_1(t)$ decreased to 1% of the B-A value.

3.2 Calculation of surface tension of papers

Contact angle methods are frequently used for measuring surface energetics of a solid. A common approach adopted in various mathematical models for calculating the components of surface energy is to first using Eq. 1, which assures that the spreading pressure due to vapour adsorption on the solid surface is negligible. Fowkes proposed that the surface free energy (or surface tension) can be expressed as the sum of two components of intermolecular interactions [*Erbil, 2006*]. The molecular interactions arise from different kinds of forces, which means that the surface tension γ arises from sum of a dispersion γ^d and other polar γ^p forces $\gamma = \gamma^d + \gamma^p$. By incorporation the rule of the "geometric mean" which was initially proposed by Fowkes and Mostafa and later expanded by Owens and Wendt [*Owens and Wendt, 1969*] into Eq. 1, we have

$$\gamma_L(1+\cos\theta) = 2\left(\sqrt{\gamma_L^p \gamma_S^p} + \sqrt{\gamma_L^d \gamma_S^d}\right), \tag{3}$$

where indexes $_{L,S}$ represent the solid-vapour and liquid-vapour interfaces, respectively.

The course of time dependence of $\cos\theta$ of tested liquids on coated papers reveals differences in both the k_1 and k_2 rate constants, as demonstrated Table I for two tested coated papers and two liquids.

Table I: Rate constants of spreading of water and diiodomethane drops on two coated papers APCO and G-Print (for specifications see Tab. II) together with evaluated equilibrium contact angles θ_e

Paper	water			diiodomethane		
	θ_e [°]	k_1 [s^{-1}]	k_2 [s^{-1}]	θ_e [°]	k_1 [s^{-1}]	k_2 [s^{-1}]
A2F	71.4	0.609	0.0010	47.3	*	0.0004
H2F	63.5	0.602	0.0024	50.7	0.187	0.0012
BF	71.6	0.561	0.0030	45.8	*	0.0010
G2F	68.8	0.446	0.0018	33.8	0.441	0.0017

* spreading was finished in time interval shorter than 1 s

Calculated surface tensions for different substrates for both the face and reverse side are demonstrated in Table II and Figure 2.

Table II: Surface tension γ, dispersion γ^d and polar γ^p components of tested coated papers (F - face side, R- reverse side of papers)

Paper			Surface tension [mN/m]		
		PPS [μm]	γ^p	γ^d	γ
APCO	A1F	0.86 ± 0.03	7.27	37.54	44.81
	A2F	0.918 ± 0,011	7.92	35.80	43.72
	A2R	0.946 ± 0,019	8.13	35.82	43.95
Hello Silk	H1F	1.84 ± 0.06	13.17	31.15	44.32
	H1R	2.01 ± 0.04	12.30	34.63	46.93
	H2F	2.074 ± 0.06	12.70	33.91	46.61
	H2R	2.29 ± 0.036	13.03	36.07	49.10
BIOMATT	BF	2.94 ± 0.14	7.59	36.59	44.18
G-Print	G1F	3.244 ± 0.084	4.06	43.05	47.11
	G1R	3.566 ± 0.121	3.25	44.59	47.84
	G2F	3.41 ± 0.15	7.01	42.88	49.89
	G2R	3.87 ±0.25	5.66	43.02	48.68

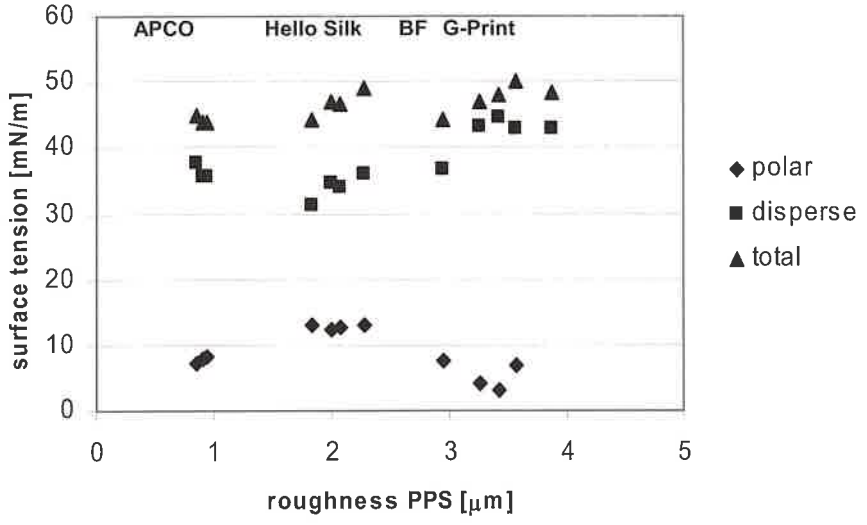


Figure 2: The influence of PPS surface roughness on surface tension of coated papers

3.3 Ink spreading on coated papers

The behaviour of different inkjet inks drops on paper surfaces has been studied at the similar experimental condition. Figure 3 illustrates difference in drop spreading and ink penetration rate on APCO paper surface and reveal dramatically different interaction between inks on this material.

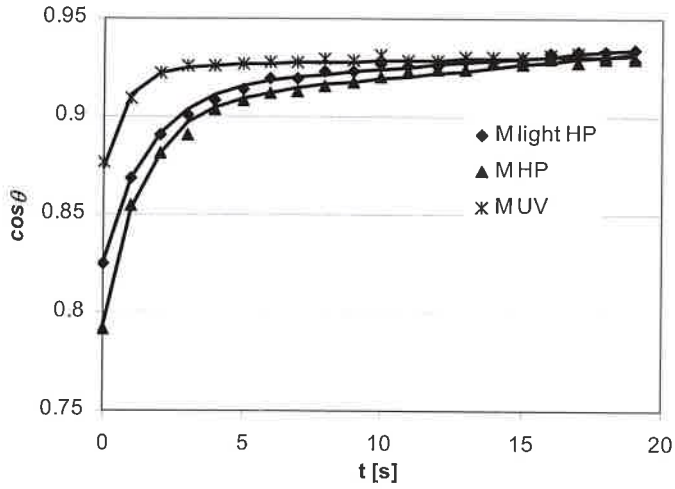


Figure 3: Time course of cos of contact angle of ink drop on APCO paper (A2F, see Tab. II)

The picture shows that the spreading rate is strongly affected not only by different density and viscosity of water based and UV inks, but also by ink penetration (see spreading and penetration rate parameters k_1, k_2 in Table III).

Table III: The parameters of ink and coated paper interaction for the proposed model of spreading

Paper			M UV			M HP		
		PPS	θ_e [°]	k_1 [s^{-1}]		PPS	θ_e [°]	k_1 [s^{-1}]
APCO	A2R	0.946	22.82±0,54	APCO	A2R	0.946	22.82±0,54	APCO
Hello Silk	H2F	2.074	17.87±0,25	Hello Silk	H2F	2.074	17.87±0,25	Hello Silk
BIOMATT	BF	2.94	22.02±0,33	BIOMATT	BF	2.94	22.02±0,33	BIOMATT
G-Print	G2F	3.41	18.39±0.83	G-Print	G2F	3.41	18.39±0.83	G-Print

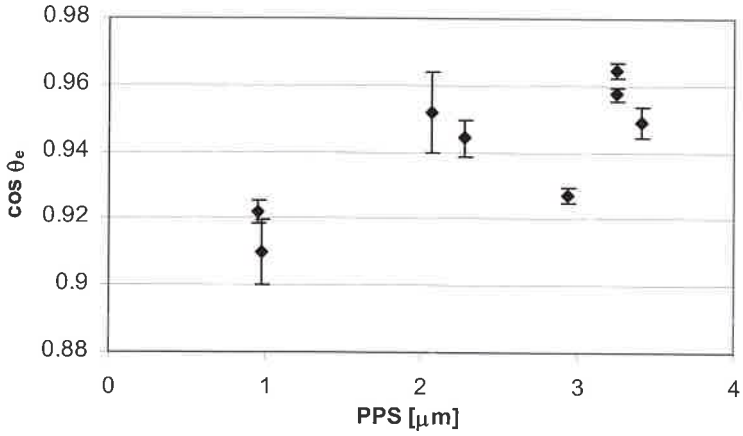


Figure 4: The relation of cos θ_e of UV ink on coated paper PPS roughness

The cos of the contact angle θ_e of UV ink on papers increases with PPS roughness as shown in Figure 4, which reminds the similar trend as observed by Wenzel for cos of contact angles of liquids on rough substrates. The composition of paper coating layer play also important role in this process as well, and consequently contribute to the non-ideal linear tendency.

The cos of the contact angle θ_e of UV ink on papers further depends on difference between paper and ink surface tension as demonstrates Figure 5. Surface tension of tested UV Magenta was 21.84 mN/m.The spreading rate of ink drop on paper characterized by rate parameter k_1 show the decreasing tendency with PPS roughness.

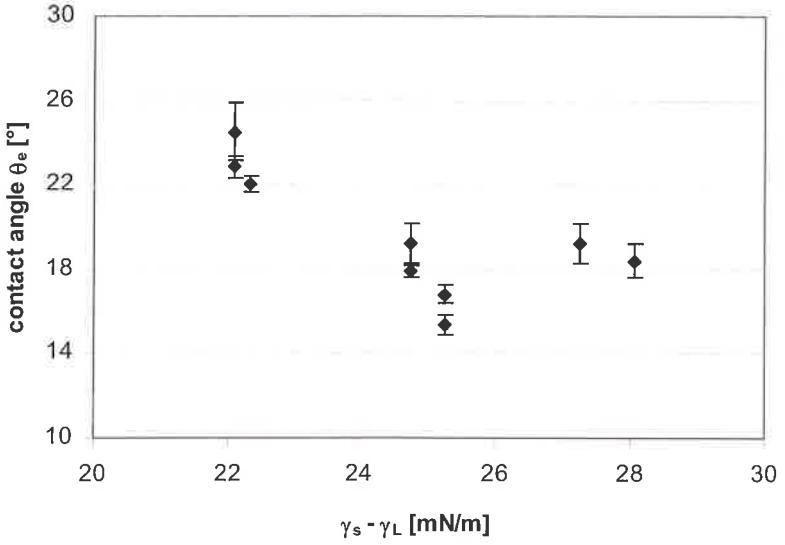


Figure 5: The relation of $\cos\theta_e$ on ink and paper surface tension difference

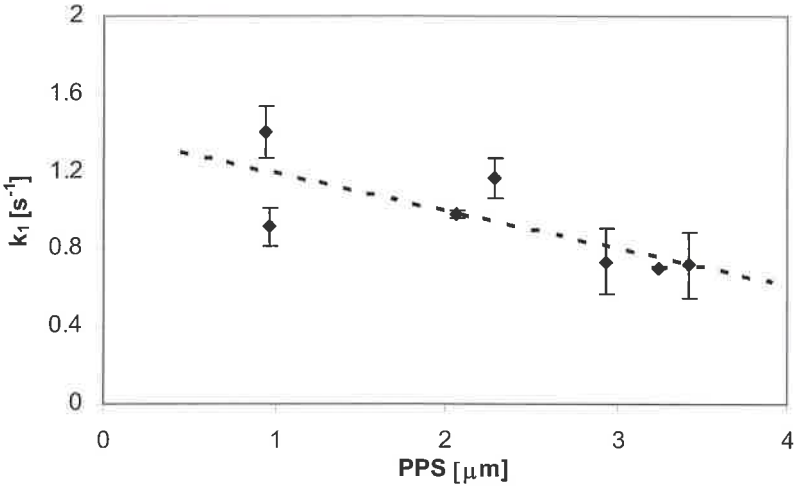


Figure 6: The spreading rate parameter k_1 in relation to PPS roughness

Paper is a porous substrate but as concern of the coated papers, the microporous structure is defined by the coating material and coating technique. In non-impact printing ink penetration into substrate structure is slow process as can be seen from k_2 parameter in Table 3 and could be neglected in case of UV inks.

3.4 UV inkjet prints

Since in inkjet printing the spreading rate determines the final drop base resp. dot size, we demonstrated the correlation between ink spreading behaviour and characteristics of drops formed by inkjet printer on the two substrates (APCO PPS 0.946 μm and BIOMATT 2.94 μm). The print quality measures (like dot gain, dot circularity...) were evaluated on final prints by means of CSLM and optical microscopy.

Dot area was determined on images captured by optical microscope with CCD camera and side light (because only this kind of illumination eliminated the reflection from the ink) at 35x magnification. At first the picture was transformed into 8 bit image and then cropped on the centre of the image due to the nonhomogenity light - exposure. The image dimension decrease from the initial 3125 x 2343 μm, to 1500 x 1500 μm after cropping. For transforming in binary image Auto - Threshold was used. For each evaluation 3 - 6 measurements were averaged. The results of dot gain determination on 20% and 40% tone value were as follows in Table IV.

Table IV: Calculated values of dot area and dot gain for selected papers

Paper	Intended dot area [%]	Measured dot area [%]	Measured dot gain [%]
APCO	20	29.02	9.02
	40	50.51	10.51
BIOMATT	20	42.65	22.65
	40	65.55	25.55

The connection of spreading rate coefficient k1 and dot area and dot gain on for 20% and 40% tone value prints shows Figure 7.

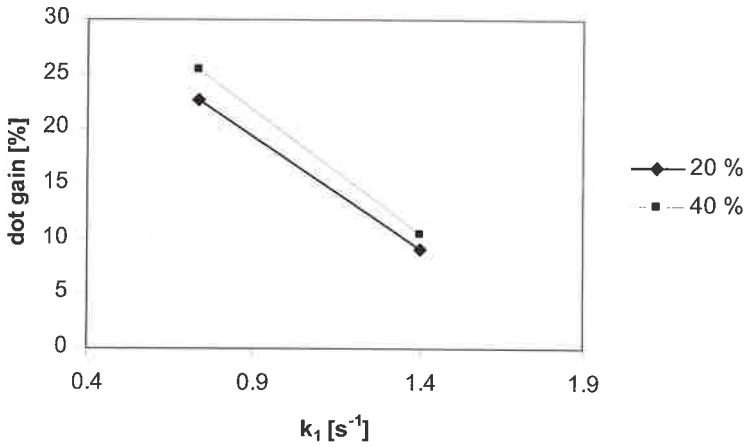


Figure 7: Dot gain on inkjet prints and spreading rate k_1 of magenta UV ink on coated paper APCO and BIOMATT (20% and 40% nominal value)

From the optical microscopy images single dots have been further evaluated for circularity and Ferret diameters which characterize the highest diameter. The results were as follows:

Table V: Calculated dot circularity and Ferret diameter

Paper	Circularity	Ferret diameter [μm]
APCO	0.999 ± 0.002	69.531 ± 22.235
BIOMATT	0.931 ± 0.038	113.740 ± 5.930

The differences in dot shape are clearly illustrated on images from CSLM analysis.

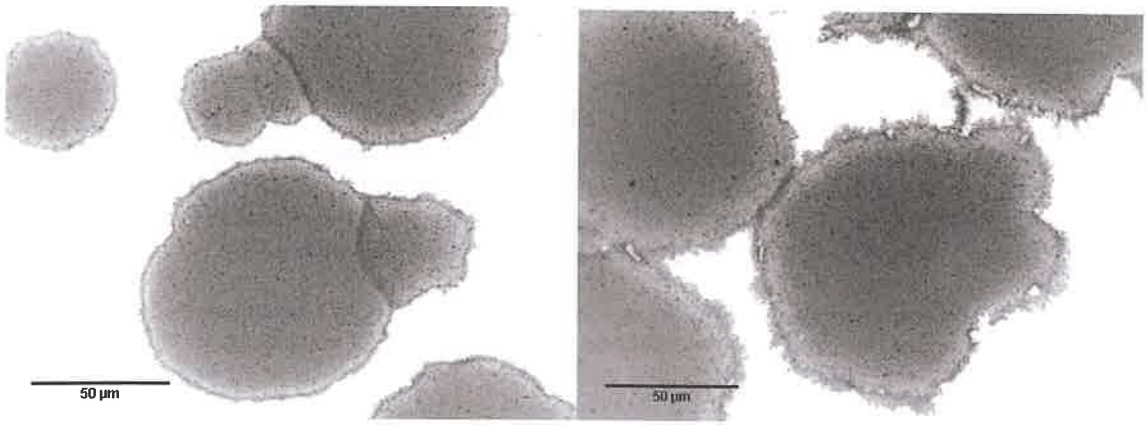


Figure 8: CSLM Z- projection of 20% magenta prints on APCO (left) and BIOMATT (right)

Further projection of final printed dot into *xz* and *yz* plane was prepared and analyzed. For APCO paper contact angle from such image was measured to be 35.7° ± 3.6° for the main drop. Evaluation of contact angle of cured ink on other media will be subject of future work since the analysis in such cases is being complicated by the drop shape that differs significantly from the spherical cup.



Figure 9: CSLM xz (coronal) projection of 20% magenta prints on APCO

By comparison of the contact angle of cured ink measured on prints by analysis of CSLM images and contact angle measured on the drop of uncured ink it can be assumed that the ink drop in the UV IJ printing process is being almost cured before it reaches the equilibrium state. The initial and equilibrium contact angles of "wet" ink on the same substrate was 30.2° and 24.5° respectively.

Both the optical and the CSLM reveal differences in the printed dots circularity in relation to substrate. APCO substrate featured droplet in the shape of spherical cup with minimum structured circumference, on the other hand drops formed on BIOMATT have irregular shape with very rough profile. These differences in shape from ideal sphere cup together with the drop outline structure show sensitivity to substrate micro roughness. Thus suggests that it is also important to study the droplet shape not only the contact angle. However such evaluation is impossible on samples with open structure commonly used in UV IJ printing like textile since on such materials the ink does not form droplet but it's rather being completely scattered inside the macro porous.

4. Conclusions

The study assessed the IJ-ink/paper interaction and provides understanding of the process of inkjet droplet impaction on paper surfaces by means of drop spreading model. Results of this study are useful in the understanding of inkjet droplet impaction on paper surfaces which sets the initial condition for ink spreading and penetration into paper after impaction. The suggested model was tested on a range of standard liquids, common IJ inks and mostly offset lithography substrates and was proved to be suitable for description of spreading kinetics on non-ideal surfaces. This approach represents an easy way of characterizing materials by four simple parameters A, B, k_1, k_2.

Spreading characteristics and penetration rate of the ink are important parameters in IJ printing since they determine the final drop base resp. dot size. UV-curable inks showed almost no absorption process on tested papers. So the drop characteristics are mainly determined by the spreading to equilibrium, unless the print-to-cure time is short enough the freeze the moving droplet.

For UV-curing inks there is almost no absorption process in tested papers. The dot characteristics are mainly determined by the spreading to equilibrium, unless the print-to-cure time is short enough the freeze the moving droplet.

Acknowledgements

This work was supported by Ministry of Education, Youth and Sports of the Czech Republic research project No. MSM 0021627 501and Contact project 9-06-23.

References

1. Apel-Paz, M. and Marmur, A. (1996), *Spreading of liquids on rough surfaces*, Colloids Surf. A, Vol.146, pp 273 - 279
2. Cassie, A. B. D. and Baxter, S. (1944), *Wettability of porous surfaces,* Trans. Faraday Soc. Vol. 40, pp 546 - 551

3. Drzkova M., Otahalova L. and Kaplanova, M. (2004), *Photoacoustic study of printed samples*, Proceedings of CGIV 2004, April 5-8, 2004, Aachen, Germany, pp 307 - 310
4. Drzkova, M., Otahalova, L. and Muck, T. (2006), *Methods for halftone prints quality investigation*, Conference Proceedings of 2nd International Symposium on Novelties in Graphic, 15-17 June 2006, Ljubljana, Slovenia, p 134
5. Erbil, H. Y. (2006), *Surface chemistry of solid and liquid interfaces*, Blackwell Publishing, ISBN 1-4051-1968-3
6. Järnström, J., Granqvist, B., Järn, M., Tag, C.-M. and Rosenholm, J. B. (2007), *Alternative methode to evaluate the surface energy components of ink-jet paper*, Colloids and Surfaces A: Physicochemical and Engineering Aspects, Vol. 294, No. 1-3, pp 46 - 55
7. Kannangara, D., Zhang, H., and Shen, W. (2006), *Liquid-paper interactions during liquid drop impact and recoil on paper surfaces*, Colloid and Surfaces A: Physicochemical and Engineering Aspects, Vol. 280, No. 1-3, pp 203 - 215
8. Kaplanova, M., Valis, J. and Holicka, H. (2006), *Surface tension measurement and ink/paper interaction*, Conference Proceedings of 2nd International Symposium on Novelties in Graphic, 15-17 June 2006, Ljubljana, Slovenia, ISBN 961-6045-37-7, p 146
9. Marmur, A. (2000), *Wetting on Real Surfaces*, J. Imaging Sci. Technol., Vol. 44, No.5, pp 406 - 409
10. Mercier, Ch., Peralba, M., Dubé, M., Bloch, J.-F. and Mangin, P. J. (2007), *Effect of drops interactions on ink-jet print quality,* Advances in Printing and Media Technology, Vol. 34, ed. N. Enlund, M. Lovreček, Acta Graphica Publishers, Zagreb MMV, ISBN 978-953-7292-04-1, pp 221 . 229
11. Muck, T., Lozo, B., Otahalova, L., Drzkova, M., Kaplanova, M. (2005), *Non-destructive methods in the study of IJ ink-substrate interaction*, Advances in Printing and Media Technology, Vol. 32, ed. N. Enlund, M. Lovreček, Acta Graphica Publishers, Zagreb MMV, ISBN 953-7292-01-0, pp 225 - 232
12. Owens, D. K. and Wendt, R.C. (1969), *Estimation of surface free energy of polymers,* J. Appl. Polym. Sci, Vol. 13, pp 1741 - 1747
13. Wenzel, R. N. (1936), *Resistance of solid surfaces to wetting by water*, Industrial and Engineering Chemistry, Vol. 28, No. 8, pp 988 - 994

Theoretical investigation into pigment-resin binding energies conformations associated with the magenta bodying reaction of water-based inks

Scott Williams

Rochester Institute of Technology, School of Print Media
69 Lomb Memorial Drive, Rochester, NY 14623 (USA)
E-mail: sawppr@rit.edu

Abstract

A MNDO/PM3 semi-empirical method for computing the enthalpy of association, dipole moment, and preferred conformation between model ink resin oligomers and the aromatic surface face of 2,9-dimethylquinacridone (C.I. Pigment Red 122) was performed. We earlier reported that inks prepared with this pigment and styrene-acrylic polymer resin systems would undergo rapid viscosity thickening, or bodying, greatly decreasing the useful shelf-life of this ink. The pigment aromatic surface was modeled using known x-ray crystallographic coordinates, and further optimized using an Amber geometry optimization protocol. Two resin oligomer models, diacrylic acid and styrene-triacrylic acid, were also modeled and geometry optimized for this study. Whereas interaction between the negatively charged acrylic acid subunit and the pigment surface was found to be very weak, the addition of a single styrene subunit substantially increased the ability of the styrene-triacrylic resin oligomer to stably complex with the pigment surface. Strong π - π dispersive interactions were found to drive this complexation reaction over dipolar or hydrogen bonding mechanisms.

Keywords

CI Pigment Red 122, intermolecular interactions, MNDO/PM3, styrene-acrylic resin

1. Introduction

We recently reported findings of a bodying reaction, an increase in the resting ink viscosity, associated with CI Pigment Red 122 and styrene-acrylic resin systems[1]. Rheology and thermal analysis on a model ink system indicated that a strong association between the pigment and resin system would occur immediately upon mixing resulting in a doubling of the solution viscosity within a few hours. CI Pigment Blue 15:3, for example, does not exhibit this type of unstable viscosity change over time. In an effort to predict what types of interactions may cause the bodying effect, the enthalpy of association was calculated between CI Pigment Red 122 and two model oligomers of the resin system. In order to resolve a theoretical basis for our experimental observation, MNDO/PM3 calculations were performed to obtain key conformation, charge distribution and thermodynamic information about the system. MNDO/PM3 is a computational method selected for its robust capabilities in estimating the enthalpy of formation parameterized (PM3) by an extensive survey of well-established experimental data[2,3].

CI Pigment Red 122 (DMQA) has the chemical name 2,9 dimethylquinacridone or 5,12-dihydro-2,9-dimethyl quino[2,3-b]acridine-7,14-dione ($C_{22}H_{16}N_2O_2$). This pigment is commonly selected as the magenta pigment of choice for both commercial and digital printing applications. The x-ray crystallographic data illustrated an extensive hydrogen-bonded two-dimensional network which gives rise to its color and colorfast properties[4-6]. In the solid state, strong cohesive forces between chromophore ring planes stabilize the crystal structure[7]. DMQA has a crystal structure comprised of molecular sheets, stacked one on top of another with a slight slip angle, whereby one chromophore is hydrogen bonded to two neighbors. Each DMQA molecule is anchored by four N-H-O hydrogen bonds with a bond angle of about 150[4]. Aggregation, therefore, has been found to result from the propensity to extend the hydrogen bonded network[8].

Pigment-polymer resin interactions have been studied in an effort to characterize and obtain stable pigment dispersions in a variety of media[9,10]. Styrene-acrylic polymers, used extensively in water-based inks, have the potential to associate with pigment structures through a plurality of bonding mechanisms - hydrogen bonding, as well as, polar, electrostatic and dispersive interactions. Typically formulated under alkaline conditions with

ammonia, the acrylic side groups would essentially deprotonated, negatively charged and opposed by an ammonium counterion. The amphoteric nature of DMQA tends more toward Lewis base[13] in character, and therefore, would facilitate acid-base interactions with the resin. This carboxylate group is known to chemisorb onto a variety of substrate surfaces including the high surface area pigment particles[11-14]. Styrene-acrylic co-polymers would also possess a substantial, albeit uncoordinated, permanent dipole moments[15]. Lastly, the styrene subgroup would allow for a variety of dispersive interactions including π-π and van der Waals interactions[16]. In addition to pigment-resin interactions, resin-resin interactions are also likely to contribute to the formation of a supramolecular network resulting in unstable ink rheology. This theoretical study is part of a larger research program to resolve the operative association mechanisms that give rise to unstable water-based ink formulations comprising these components.

2. Methods

2.1 C.I. pigment red 122 surface

A surface, composed of one molecular sheet of four 2,9-Dimethylquinacridone molecules, was constructed using x-ray crystallography data[4]. Model building was done using Hyperchem Build 3.0 for the Mac (Hypercube, Inc. USA). After model building the structure, the molecular complex was further geometry minimized with an Amber geometry optimization protocol using Polak-Ribiere conjugate gradient algorithm with a cut-off set to 0.02 kJ/mole. The resulting structure is shown in Figure 1. After the geometry was optimized and the hydrogen-bonding distances and angles were confirmed relative to the x-ray data, an MNDO/PM3 single point semi-empirical calculation was performed using the Hyperchem default settings for this calculation to obtain dipole moment and enthalpy of formation values. This DMQA complex was treated as a static surface, with their aromatic faces comprising the surface, in order to focus on the effect the resin system would have in and near the force field generated by this surface.

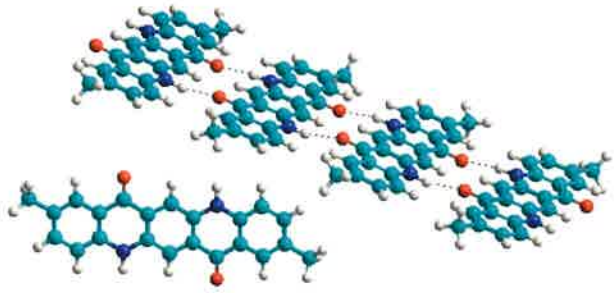


Figure 1: DMQA structure and surface model

2.2 Resin model systems

Two resin systems models were developed. A diacrylic model (DA) and a styrene-triacrylic (STA) model were built and optimized using the same procedure as described for DMQA. The DA and STA structures are shown in Figure 2. Dipole and enthalpy of formation calculated values were determined using the single point MNDO/PM3 method. Each resin was modeled and minimized with an ammonium counter ion with each ionized acrylic side group.

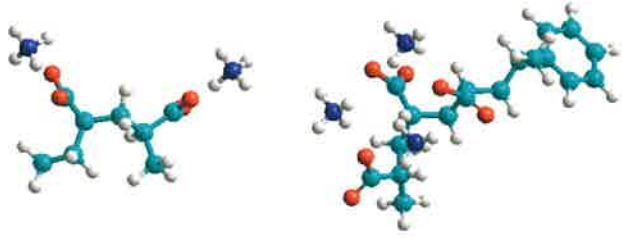


Figure 2: Diacrylic (left) and Styrene-triacrylic resin models with ammonium counter ions

2.3 Enthalpy of association

The enthalpy of association (ΔH_{assoc}) for complex formation between DA or STA and DMQA was calculated by taking the difference between the heats of formation (ΔH_f) calculated for the complex minus the sum of the heats of formation calculated for each molecular system in isolation as shown in Equation 1.

$$\Delta H_{assoc} = \Delta H_f(Complex) - (\Delta Hf(\text{Resin}) + \Delta Hf(DMQA)) \quad (1)$$

2.4 Complex formation model and geometry analysis

A complex model between each resin system and the DMQA surface were prepared by merging the two geometry-optimized files. The resin system was then translated over the center of the DMQA surface and displaced a distance of about 10 angstroms. A Rotation ΔH_{assoc} energy map was generated by manually rotating the resin system by approximately 20 - 30 degree increments over a full 360 degrees within the plane of the DMQA surface. The DA/STA dipole moment was aligned with the plane of the DMQA surface through every rotation angle. With each step, a MNDO/PM3 single point calculation for the ΔH_f complex value and dipole moment per position were obtained. The motion angle was defined as the angle between the short axis of the resin with the long axis of the DMQA surface. Zero degrees, therefore, would represent co-linear (charges aligned) dipole moment angles in the case of the DA resin system and anti-parallel (charges opposed) dipolar orientation with the STA system. The STA arrangement was made preferentially to emphasis the presentation of the phenyl ring rather than the dipole orientation. Likewise, a Tumble ΔH_{assoc} energy map was obtained by tumbling the resin system by 30 degree increments over 360 degrees at a distance of about 10 angstroms from the surface. Finally, an Approach ΔH_{assoc} energy map was obtained by manually moving the resin system, by approximately one angstrom steps, toward the DMQA surface using the Tumble and Rotation geometry that yielded the most favorable ΔH_{assoc} in each case. These three constrained motions were used to position the resin model in a conformation that would presumably be the most likely approach geometry and position presented to the DMQA surface. This procedure was also used to prevent trapping the complex geometry in a local energy minimum that might not directly reflect the experimental condition. Once in the starting geometry prepared by the optimized values obtained by the three energy maps, the resin system alone was allow to undergo an unconstrained Amber geometry optimization in the presence of the constrained DMQA force field. The ΔH_{assoc} for the new optimized complex was then calculated using the MNDO/PM3 method. Hydrogen bond positions were recalculated, and a map showing total charge density was obtained.

3. Results and discussion

3.1 ΔH_{assoc} of DMQA, DA and STA

In order to calculate the ΔH_{assoc}, the heats of formation of DMQA surface and each of the resin models were required. Table I illustrates the ΔH_f and permanent dipole moment values obtained for the optimized geometry of each system. As expected, DMQA has an exceptionally weak permanent dipole moment relative to the charged resin systems[6,16]. From this data, dipole-dipole interactions would appear not to play a major role in the complex formation.

Table I: ΔH_f and calculated dipole moment of DMAQ, DA and STA

Molecular System	ΔH_f (kJ/mole)	Dipole Moment (D)
DMQA Surface	+3.43	0.039
Diacrylic Resin (DA)	-803.55	8.09
Styrene-Triacrylic Resin (STA)	-891.56	11.0

3.2 Rotation, tumble and approach ΔH_{assoc} maps for the DMQA:DA complex

A DMQA:DA complex was modeled as described. The Tumble ΔH_{assoc} map was constant through all tumble angles (data not shown). A 10 angstrom Rotation ΔH_{assoc} map indicated a very slight - ΔH_{assoc}, indicative of favorable complex formation, at an angle of approximately 75^0 (data not shown). This angle (also equal to the

DA permanent dipole moment angle) was almost perpendicular to the DMQA surface dipole moment. An Approach ΔH_{assoc} map was then generated with perpendicularly oriented dipole moments (Figure 3). The force field of the two molecular systems begins to interact at about five angstroms with an increasingly positive ΔH_{assoc}. At no point along the approach axis did the ΔH_{assoc} dip below zero.

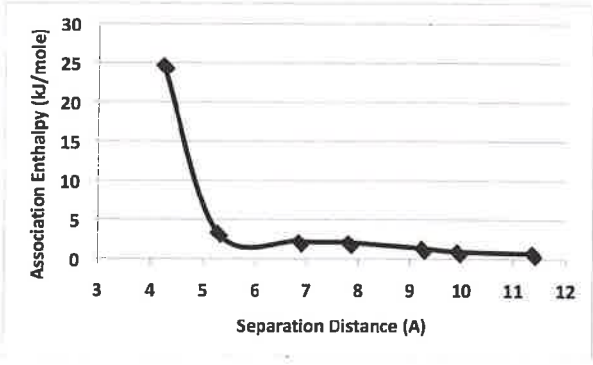


Figure 3:
DMQA:DA approach ΔH_{assoc} map

Another Rotation ΔH_{assoc} map was generated at a separation distance of 4.66 angstroms. As shown in Figure 4, a relatively strong associative complex is formed with at an angle of about 250^0. If dipolar interactions were going to play a role, a ΔH_{assoc} minimum would occur at 180^0 and a maximum at zero degrees. Neither result was obtained. Clearly, another type of attractive interaction was occurring at about 250^0.

Using the combination of the constrained motion ΔH_{assoc} energy maps, the complex geometry that was used for the starting point of an unconstrained resin system geometry optimization will be a DA molecule 4.66 angstroms from the DMQA surface at a rotation angle of 250^0 (dipole moments misaligned by about 70^0) from the surface long axis as shown in Figure 5.

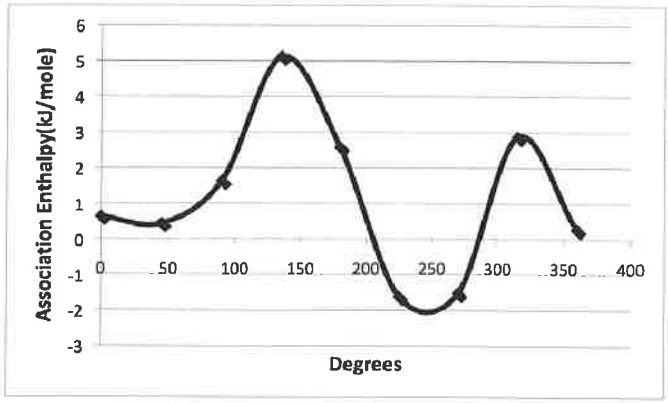


Figure 4:
DMQA:DA rotation ΔH_{assoc} map

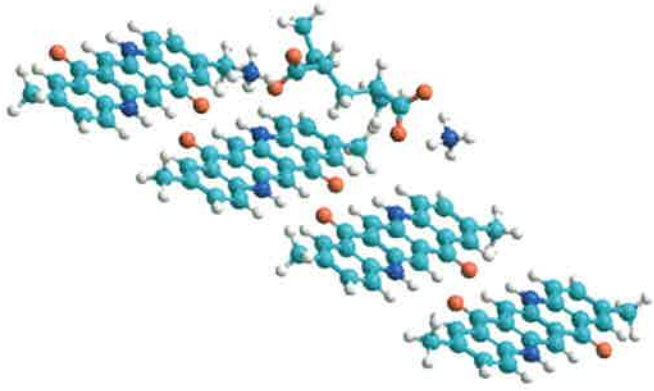


Figure 5: DMQA:DA complex prior to unconstrained geometry optimization in the presence of the DMQA surface

3.3 Rotation and approach ΔH_{assoc} maps for the DMQA:STA complex

The influence the styrene subunit would have on complex formation was evaluated by building a styrene-triacrylic (STA) resin model (see Figure 2, Right). Molecules designed for applications as dispersants (HLB dispersants) similarly have polar and non-polar functionalities. The question would then focus on whether the styrene-acrylic resin system performs more like a dispersant or more like an ink vehicle in the presence of DMQA.

As with the DA system, a DMQA:STA complex was merged using the same DMQA surface used for the DMQA:DA computations. The STA position, placed about 10 angstroms above the DMQA plane, was adjusted so that the styrene subgroup would point towards the DMQA surface, and that the calculated STA dipole moment would process co-linearly along the plane of the DMQA surface. The starting STA geometry, in this case, was arranged so that zero degrees corresponded with anti-parallel dipole moment alignment with the DMQA surface. Preference was given to the phenyl ring presentation to the DMQA surface.

The Approach ΔH_{assoc} map revealed an attractive potential, and therefore favorable association, at a very close approach distance between the STA phenyl ring and the DMQA surface ring system (Figure 6). This attraction, between phenyl rings, would be expected for a π–π interaction. With anti-parallel dipole alignment, this attraction could also be the result of dipole-dipole interactions. The complex geometry at three angstroms was not favorable for any hydrogen bonding interaction between the complex.

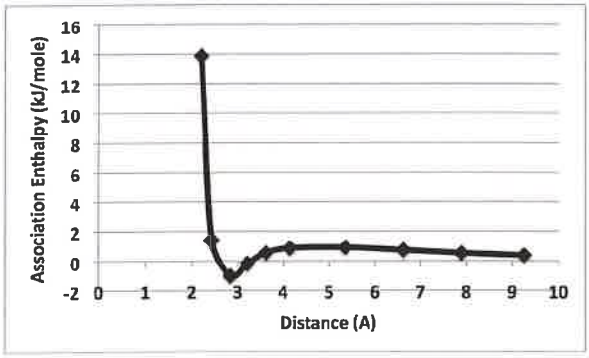


Figure 6:
DMQA:STA approach ΔH_{assoc} map

The Rotation ΔH_{assoc} map was generated by placing STA about 3.2 A above the DMQA surface. This was the distance where an attractive association was being calculated for the complex. A similar result shown for the DMQA:DA complex was found for DMQA:STA; that is, the strongest attraction, most negative ΔH_{assoc}, was found for a complex geometry were the dipole moments are arranged in what would appear the be the most unfavorable, charges matched, orientation (see Figure 7).

As with both complexes, the optimum association geometry was one whereby the dipole moments are charge-matched and offset by about 20 - 30^0. It would appear that dipolar interactions are not driving a complex formation between either of these model resin systems.

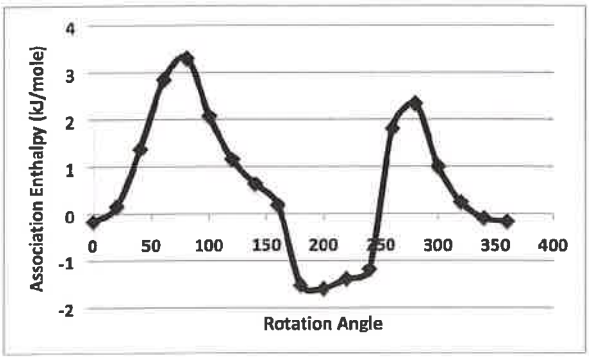


Figure 7:
DMQA:STA rotation ΔH_{assoc} map

As shown in Figure 8, the complex geometry exhibiting the strongest association in the constrained approach and rotation motions, appears to favor a T-type π - π interactions between phenyl rings and π - π interactions between a STA carboxyl group and the N-H group on the DMQA surface.

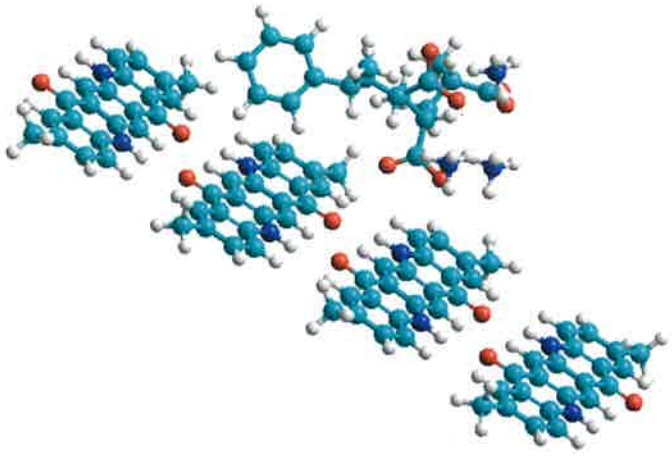


Figure 8:
DMQA:STA complex prior to unconstrained geometry optimization in the presence of the DMQA surface

3.4 Unconstrained geometry optimization for the DMQA:DA complex

Using the geometry illustrated in Figure 5, the DA resin system was allowed to freely rearrange its position and geometry in the presence of the static DMQA surface. Using an Amber geometry minimization protocol, the energetically preferred conformation was not that different than the starting point geometry (see Figure 9). The preferred orientation suggests that dipolar or hydrogen bonding associations are not dominant, but dispersive interactions appeared to be searched and found by the DA system. This association, however, seems to come at an energy cost as the ΔH_f for the new complex was found to be almost 200 kJ/mole more positive than the starting configuration.

Since a weakly dispersive interaction seemed to be present in this complex, an evaluation of the total charge density overlap was conducted. As shown in Figure 10, there was minimal contact between the DA and DMQA surface. Contact seems to be facilitated only through weakly associated π - π interactions between the carboxyl π bond and the nitrogen π bonds on the DMQA surface.

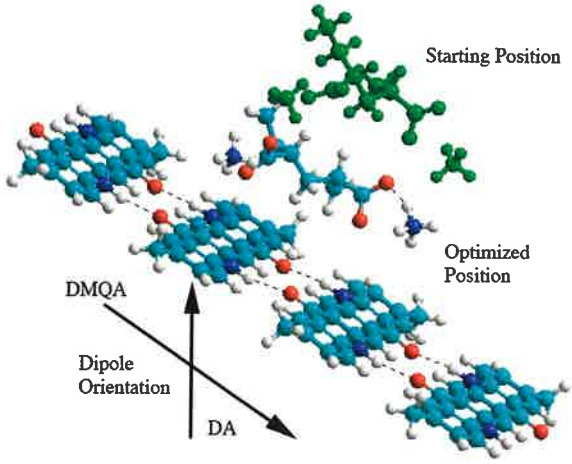


Figure 9:
DMQA:DA optimized geometry

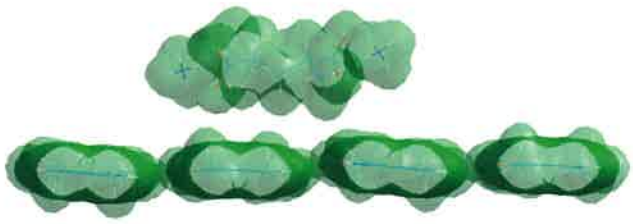


Figure 10:
Charge density overlap in the DMQA:DA complex

3.5 Unconstrained geometry optimization for the DMQA:STA complex

Using the geometry illustrated in Figure 8 as a starting point, the STA resin model was allowed to freely find an energy minimum conformation. The result was strikingly different that that found for DMQA:DA (see Figure 11). The complexation pathway could be visualized during the Amber geometry minimization. The STA molecule made a substantially closer approach to the DMQA surface resulting in two very interesting dynamic processes. One, the ammonium counterions were rejected by the STA carboxylate groups in favor of an apparent π - π interaction with the C = O π bond of the DMQA surface (Figure 12). There was, secondly, an improved and significant charge density overlap between phenyl rings of the two systems in an apparent T-type π - π interaction. Approximately four new charge density overlapping contact points were formed during the complexation reaction (Figure 12). The final ΔH_f for the complex was also about 22 kJ/mole more negative, a favorable association value, than the starting heat of formation.

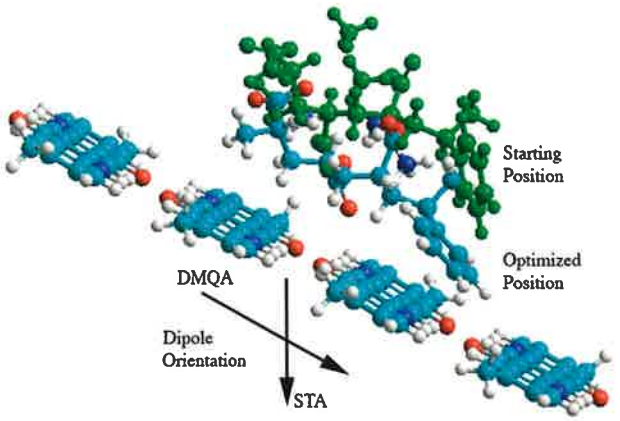


Figure 11:
DMQA:STA optimized geometry



Figure 12:
Charge density overlap in the DMQA:STA complex

4. Conclusion

We are investigating the mechanism of water-based printing ink bodying with time on the molecular level. Our earlier experimental results indicated that the magenta bodying reaction was occurring from pigment-resin and resin-resin interactions on a relatively fast timescale. Using an MNDO/PM3 computational approach, the molecular models indicate that the presence of the styrene side group on the resin chain facilitates strong π - π dispersive interactions between the resin and DMQA planar surface. In the absence of the styrene subunit, the charged, and highly polar, acrylic portion of the styrene-acrylic polymer interacts rather poorly with the same surface. Overlap between the charge densities of the DA carboxyl side group with the π-network of the DMQA surface was found to be very weak. The association energy becomes increasingly positive as the carboxyl groups are presented to the DMQA surface. With a very low DMQA permanent dipole moment, assistance from dipole-dipole interactions appeared to be non-existent. Although a water solvation shell was not included in this initial study, hydrogen bonding did not seem to contribute to either DA or STA complex formation. Perhaps with a water molecule as a bridge, hydrogen bonding may be possible. This investigation will be reserved for future work. DMQA pigment particles would also have a

crystal face surface (not the face surface analyzed in this work) that would be replete with intrinsic hydrogen bonding sites. Probing this surface will also be the subject of future work.

The enhanced association strength between styrene-acrylic co-polymer with the DMQA aromatic face was found to be primarily due to strong π - π interactions between the phenyl rings of both systems. Presumably once established, the phenyl "anchor" would promote further π-bonding between the resin carboxylate group and the DMQA π network driving the complexation reaction. These dispersive interactions are also seen in other pigment-resin systems, such as with other members of the quinacridone pigment family[17]. In summary, dispersive interactions theoretically drive the formation of stable complexes between the aromatic surface face of a DMQA pigment particle and a styrene-acrylic resin system. The interaction appears to follow a similar reaction path that would be found for similarly designed HLB dispersants. Further theoretical and experimental work will be conducted to confirm the identity of these DMQA:Styrene-Acrylic resin complexes in ink systems.

References

1. Pieruccini, S. and Williams, S. (2007), *Pigment-Resin Aggregation Effects in Water-based Gravure Inks*, Adv. in Printing and Media Technology, 34, pp 93 - 99
2. Stewart, J. (1989), *Optimization of Parameters for Semiempirical Methods I. Methods*, J. Comp. Chem., 10:2, pp. 209 - 220
3. Stewart, J. (1989), *Optimization of Parameters for Semiempirical Methods II.* Applications, J. Comp. Chem., 10:2, pp. 221 - 264
4. Mizuguchi, J., Senju, T. and Sakai, M. (2002), *Crystal Structure of 5,12-dihydro-2,9-dimethylquino[2,3-b]acridine-7,14-dione, at 123K*, Z. Kristallogr. NCS, 217, pp 525 - 526
5. Mizuguchi, J. and Senju, T. (2003), *Color Generation Mechanism of Quinacridone Derivatives as Viewed from Intermolecular Hydrogen Bond, IS&T NIP19 International Conference on Digital Printing Technologies*, pp 678 - 682
6. Mizuguchi, J. and Senju, T. (2006), *Solution and Solid-State Spectra of Quinacridone Derivatives as Viewed from Intermolecular Hydrogen Bond*, J. Phys. Chem. B, pp 19154 - 19161
7. Senju, T., Sakai, M. and Mizuguchi, J. (2007), *Cohesion of g-Quinacridone and 2,9-Dimethylquinacridone in the Solid State, Dye and Pigments*, 75, pp 449 - 453
8. De Feyter, S., Gesquiere, A., De Schryver, F., Keller, U. and Mullen, K. (2002), *Aggregation Properties of Soluble Quinacridones in Two and Three Dimensions*, Chem. Mater., 14, pp. 989 - 997
9. Kissa, E. (1999), Dispersion: Characterization, Testing and Measurement. CRC Press, 1st Ed.
10. Daescu, C. (1998), *Dispersability of Organic Pigments, Dyes and Pigments*, 38:1-3, pp 173 - 180
11. Coast, R., Pikus, M., Henriksen, P. and Nitowski, G. (1996), *Vibrational Spectroscopic Observation of Acrylic Acid Coabsorbed in Dissociated and Molecular Forms on Oxidized Aluminum*. J. Phys. Chem., 100:37, pp 15011 - 15014
12. Kirwan, L., Fawell P., van Bronswijk, W. (2004), *An in Situ FTIR-ATR Study of Polyacrylate Absorbed onto Hematite at High pH and High Ionic Strength*. Langmuir, pp 4093 - 4100
13. Fagelman, K. and Gunthrie, J. (2005) Preferential Interactions in Pigmented, Polymer Blends - CI Pigment Blue 15:4 and CI Pigment Red 122 - as Used in a Poly(carbonate)-poly(butylene terephthalate) Polymer Blend. J. of Chromatog. A, 1095, pp 145 - 155
14. Shao-Hai, F. and Kuan-Jun, F. (2007) *Properties of Waterborne Nanoscale Pigment Red 122 Dispersion Prepared by Phase Separation Method.* J. Appl. Polymer. Sci., 108, pp 3968 - 3972
15. Riande, E. and Guzman, J. (1996) *Synthesis and Polarity of Acrylic Polymers with Long Hydrophilic Side Groups*. Macromolecules, 29, pp 1728 - 1733
16. Ye, K. et. al. (2005) *Supramolecular Structures and Assembly and Luminescent Properties of Quinacridone Derivatives*. J. Phys. Chem. B, 109, pp. 8008 - 8016
17. Nsib, F., Ayed, N. and Chevalier, Y. (2007) *Selection of Dispersants for the Dispersion of CI Pigment violet 23 in Organic Medium*. Dyes and Pigments, 74, pp. 133 - 140

Toner spreading during the fixing stage

Elina Hakola[1], Pirkko Oittinen[2], Jorma Koskinen[1], Ulla Forsström[1]

[1] Oy Keskuslaboratorio - Centrallaboratorium Ab (KCL)
P.O.Box 70, FI-02151 Espoo, Finland
E-mail: Elina.Hakola@kcl.fi

[2] Helsinki University of Technology (TKK)
P.O.Box 5500, 02015 TKK, Finland

Abstract

Toner spreading is studied using a fixing simulator where the toner layer is fixed by means of both heat and pressure. The fixing temperature and pressure of the instrument can be individually adjusted. Toner starts to spread as soon as the toner particles have coalesced. The initial spreading is very fast after which the spreading rate slows down. Finally, an equilibrium state is achieved. The increase in the fixing pressure accelerates the spreading of toner since toner is pushed more effectively against the paper and squeezed. This leads to better wetting and spreading. However, the penetration of toner into the pores of the substrate prevents the spreading of toner to some extent. A low viscosity enables faster and easier spreading but it can also accelerate toner penetration. In addition, thick toner layers and the use of polyester resins increase the amount of spreading.

Keywords

Electrophotography, toner fixing, toner spreading

1. Introduction

In electrophotography, toner is permanently fixed onto paper usually by means of heat and pressure [Leroy et al., 2002). The fixing stage consists of several steps, such as coalescence, wetting, spreading, penetration, and solidification. [Hwang, 2000; Lee, 1975; Sipi, 2002; Vernhes et al., 2006] As the toner particles are heated above their glass transition temperature, they start to soften and coalesce forming a uniform layer. This occurs typically at 60 - 80°C. After this, the toner wets the paper and spreads on it. Toner also penetrates into the paper pores to some extent. As the toner layer exits the fixing stage, its temperature drops below the glass transition temperature, resulting in a solidified and permanently attached film on the paper.

Pettersson and Fogden [2005] have studied the spreading of individual toner particles on glass substrates in a heating cell. The toner particles do not spread until their temperature rises above 80°C, such that polymers are softened. With increasing temperature, the diameter of a toner particle starts to increase linearly, with increasing temperature. This is caused by the decrease of the toner viscosity at elevated temperatures. The spreading of the toner slows down at some point, after which the diameter of a toner particle does not change anymore. In addition to viscosity, the surface energy of the substrate has been noticed to affect the spreading behaviour. On high-energy substrates, toner spreads rapidly and Vernhes et al.[2006] have showed further that similar spreading behaviour applies for toner layers as well.

Despite these advances, the spreading dynamics of a toner layer has not been completely studied. In previous reports [Pettersson and Fogden, 2005; Vernhes et al., 2006], the spreading analyses have been done without applying pressure on heated toner particles. In order to take the pressure effects into account and perform the studies under realistic conditions as well as use papers as printing substrates, we have analyzed the spreading dynamics of the toner layer with a fixing simulator, developed in this study. This instrument simulates nip fixing by applying both pressure and temperature. Since toner spreading is also a precondition for good toner adhesion, a proper understanding of toner spreading is needed. The purpose of this study is to determine the spreading behaviour of toner during fixing. Furthermore, the aim is to analyze the effect of the fixing conditions, substrate type, and toner properties on the spreading.

2. Methods

The toner spreading during the nip-fixing stage was studied in a fixing simulator illustrated in Figure 1. In this configuration, the nip is formed when a piston is pressed against a 6-mm thick glass plate with the help of pressurized air. The nip pressure can be adjusted by changing the air pressure. Both the glass plate and the piston head are individually and controllably heated to the desired fixing temperature: the glass plate by blowing hot air on its surface and the piston electrically by resistive wires inside the piston head. The fixing stage is recorded with a CCD camera at high speed from above through the glass plate.

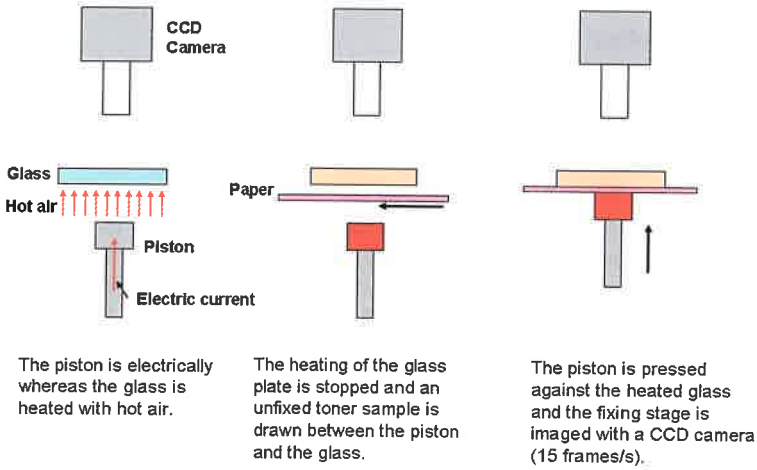


Figure 1: Operating principle of the fixing simulator

Unfixed samples were printed with KCL Duplo, which is an electrophotographic printer designed for research purposes. The paper path of the printer is planar. The papers used in this study were a standard copy paper (80 g/m^2) and a commercial coated paper for digital printing (130 g/m^2). Printing was done with melt-ground Xerox DC40 toner and chemical Xerox EA toner with properties presented in Table I. The unfixed samples were fixed in the simulator under various fixing conditions.

Table I: Properties of the Xerox DC40 toner and the Xerox EA toner

Property	Xerox DC40	Xerox EA
Resin type	polyester	polystyrene-acrylate
Glass transition temperature (T_g)	78°C	71°C
Average particle size	9 µm	6 µm
Viscosity	210 Pa·s at 130°C 50 Pa·s at 150°C	225 Pa·s at 130°C 80 Pa·s at 150°C
Manufacturing method	melt-grinding	chemical

The spreading of the toner during heating was studied by steadily raising the piston temperature from 80°C to 140°C and simultaneously capturing the evolution of the dot area. The nip pressures used were 0.2, 0.6 and 1 bar. The area of the printed dots was then analyzed with ImageJ image analysis software for images captured every 2.4 seconds. The spreading percentage was calculated as a change in the area of the dots.

The spreading behaviour of toners was studied with the simulator of Figure 1. The temperature of the piston was kept at 130°C while the glass was heated to temperatures of 130, 145 and 160°C. The nip pressures were 0.2, 0.6 and 1 bar. The dot area was determined with ImageJ for every image captured during the first six seconds of fixing.

3. Results

The toner layer starts to spread as soon as the temperature of approximately 110°C is reached (Figure 2). This delayed spreading results probably from the coalescence of the toner particles to form a uniform layer. After the layer has been formed, toner starts to spread rapidly and nearly linearly as a function of temperature and

time. The spreading of the chemical toner Xerox EA could not be analyzed, since it had already spread to some extent before the image capturing begun. This is likely due to its lower glass transition temperature (Table I), which causes the spreading to start earlier.

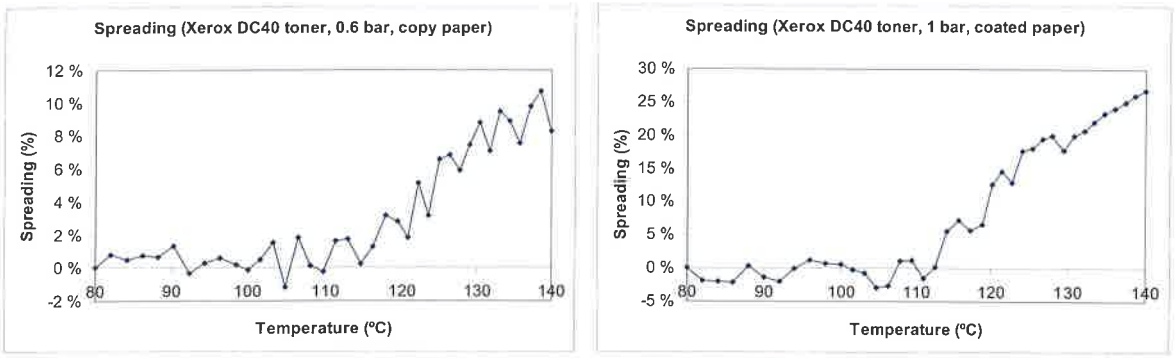


Figure 2: Spreading behaviour of the toner Xerox DC40 during heating. The average size of dots was approximately 0.1 mm^2 prior to fixing

Figure 3 illustrates the spreading behaviour of toner during nip fixing. Both of the toners behaved similarly at different fixing conditions and on different papers and they eagerly spread on the paper surface during fixing. The initial spreading is fast after which the spreading rate slows down. Finally, an equilibrium state is reached. This state is presumably determined by the surface energy of the substrate, viscosity of the toner, and nip pressure. The amount of spreading between successive test points cannot be directly determined, since the camera system used in these experiments was quite slow. Therefore, toner spread somewhat before the first image was captured.

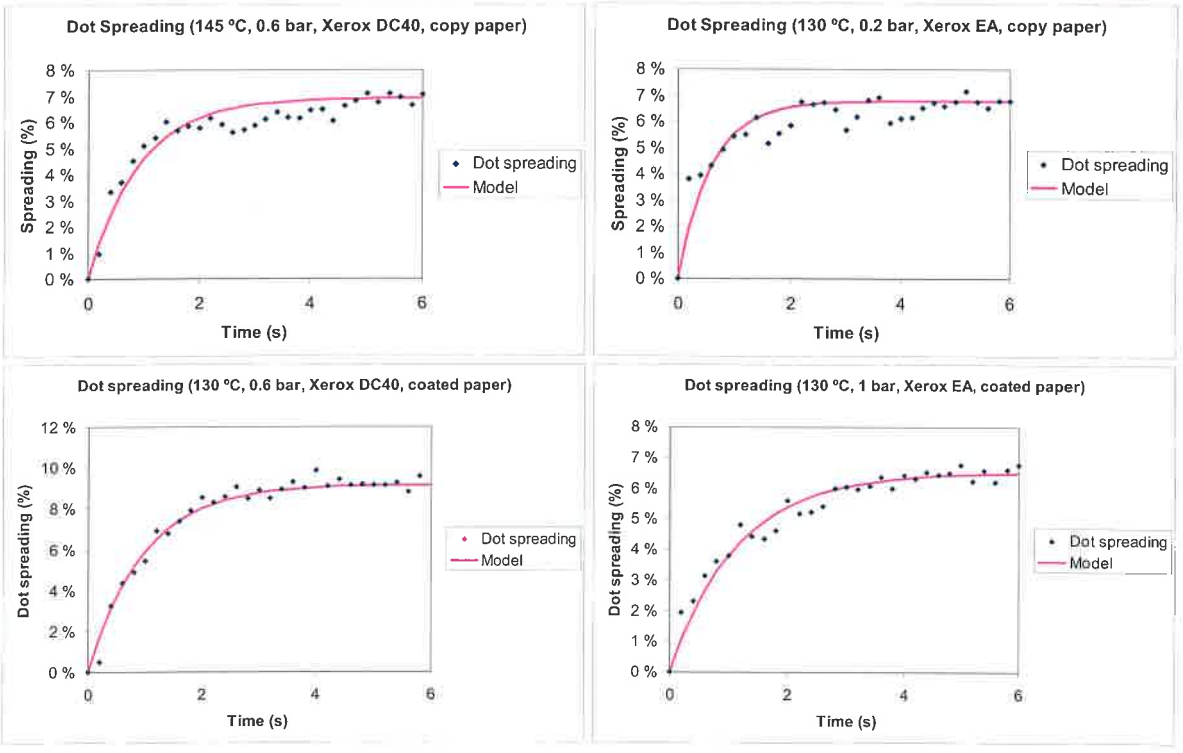


Figure 3: Spreading behaviour of melt-ground Xerox DC40 (left) and chemical Xerox EA (right) toner during their fixing stage on copy paper (top) and coated paper (bottom)

Assuming that the spreading rate is directly proportional to the deviation of the dot area from the final dot area, the spreading behaviour of toner is obtained from a first-order differential equation, which describes the change in the dot area A as a function of time t:

$$\frac{dA}{dt} = a(A_S - A), \tag{1}$$

where a is a spreading-rate constant determined by fixing conditions and toner properties and A_S is the final area of the dot (equilibrium area). The model explains the obtained results remarkably well since the coefficients of determinations are rather large (Table II). This can also be seen in Figure 3.

Table II: Minimum, maximum, and average coefficients of determination of the spreading model. The effect of the paper and toner type are also shown

Toner	Paper	Min R^2	Max R^2	Average R^2
Xerox DC40	Copy	72.5%	94.8%	88.2%
	Coated	68.5%	97.9%	87.8%
Xerox EA	Copy	60.4%	93.9%	79.1%
	Coated	80.2%	97.8%	93.4%

The traditional toner spreads more than the chemical toner due to differences in viscosity, resin type, and toner layer thickness. For example, the viscosity of the Xerox DC40 toner is 50 Pa·s at 150°C whereas the viscosity of the Xerox EA toner is 80 Pa·s. The spreading of the toners as a function of the fixing pressure is shown in Figure 4. The results show that the lower viscosity of the traditional toner compared to that of the chemical toner promotes spreading. In addition, the chemical toner layers are typically significantly thinner than traditional toner layers because of their smaller particle size [Hwang, 2000; Pettersson and Fogden, 2005; Sipi, 2002; Vernhes et al., 2006]. As a result, thinner layers do not spread as much as thick ones.

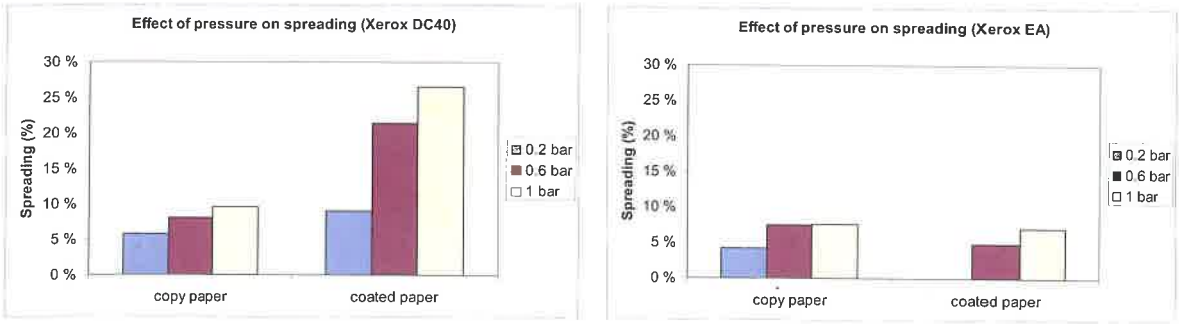


Figure 4: Spreading of toner as a function of fixing pressure on different papers. It should be noted that the chemical toner (Xerox EA) did not spread at all on the coated paper when the fixing pressure was 0.2 bar

Figure 4 shows that an increase in the nip pressure accelerates toner spreading. As the pressure increases, toner is pushed more effectively against the paper, thus squeezing it and making it flow more along the paper surface. Toner spreads better on coated papers since the more closed surface of these papers prevents the penetration of the toner. In the case of uncoated papers, spreading is prevented by deep and large irregularities of the paper surface as well as penetration of the toner into the paper pores. In the case of chemical toners, the paper type seems not to affect spreading. This can be due to the fact that spreading already takes place when the image capturing is started or that the thin toner layer spreads only slightly.

From Figure 4 one also notices that the toner type has a significant influence on the spreading coverage, particularly when the paper is coated. Traditional toner can spread more than chemical toner due to its lower viscosity and polyester resin (Table I). On copy papers, there is only a slight difference in the spreading between the two toner types. This results from the toner penetration which prevents spreading.

4. Conclusion

In this article, the melt-ground toner layer starts to spread as soon as the temperature of approximately 110°C is reached. This delayed spreading results probably from the coalescence of toner particles into a uniform layer and only after this step the newly formed layer starts to spread rapidly along the paper surface. The

spreading rate slows down after the initial fast spreading of the toner. Finally, an equilibrium state is achieved, which is believed to be determined by the surface energy of the substrate, the viscosity of the toner, and the fixing pressure. The increase in the fixing pressure accelerates the spreading of toner since toner is pushed more effectively against the paper and squeezed. This leads to better wetting and spreading. Toners spread better on coated papers than on copy papers due to their closed structure. On copy papers, the penetration of toner prevents the spreading of toner to some extent.

The spreading rate depends on the resin, viscosity, and thickness of the toner layer. Low viscosity and the use of polyester resin enables faster and easier spreading. On the other hand, they can also accelerate toner penetration into paper pores. In addition, thick toner layers are able to spread more than thin layers. Therefore, chemical toner spreads significantly less than melt-ground toner.

Toner spreading is related to toner adhesion. The more the toner wets the paper and spreads on it, the higher is the probability of good adhesion. In addition, spreading makes the printed areas uniform as the toner particles spread into each other. The results of this study are significant since they show the basic dynamics of the spreading of toner. In addition, the effect of the fixing pressure on the spreading is shown. These results may help in designing the fixing process to be more energy-efficient and they also give important data for the toner manufacturers. In the future, a more detailed analysis of the effects of the substrate properties on the spreading of the toner will be done. In addition, the influence of fixing conditions on the spreading will be studied further.

Acknowledgements

The authors wish to acknowledge the financial support of the Finnish Funding Agency for Technology and Innovation (TEKES) and the Finnish Foundation for Technology Promotion (TES). The authors also wish to thank the owner companies of KCL (M-real, Myllykoski, Stora Enso, UPM-Kymmene).

References

1. Anon., ImageJ - Image Processing and Analysis in Java website, http://rsb.info.nih.gov/ij/, accessed December 2007
2. Hwang, S. S., 2000, Toner penetration into paper at fusing, J. Imaging Sci. and Technol., Vol. 44, No. 1, pg. 26 - 30
3. Lee, L. H., 1975, Thermal fixing of electrophotographic images, Adhesion Science and Technology, Vol. 9B, pg. 831 - 852
4. Leroy, L., Morin, A., Gandini, A., 2002, Electrophotography: Effects of printer parameters on fusing quality, Proc. 11th Intl. Printing and Graphic Arts Conference (IPGAC)
5. Pettersson, T., Fogden, A., 2005, Spreading of individual toner particles studied in situ optical microscopy, J. Colloid Interface Sci., No. 287, pg. 249 - 260
6. Sipi, K., 2002, Toner-paper interactions induced by the fixing process in electrophotographic printing, Lic.Sc. Thesis, Helsinki University of Technology (TKK), Espoo, Finland, pg. 33
7. Vernhes, P., Rolland du Roscoat, S., Blayo, A., Bloch, J. F., Pineaux, B., 2006, Dynamic interactions between toner and paper in the nip of an electrophotographic printer, Proc. 33rd Intl. Research Conf. (Iarigai), pg. 17



Curing of UV ink and product safety

Merja Kariniemi, Anu Ilmonen, Eija Kenttä, Satu Sundqvist, Birgit Aurela

KCL, Oy Keskuslaboratorio - Centrallaboratorium Ab
PL 70, 02151 Espoo, Finland
e-mail: firstname.lastname@kcl.fi

Abstract

Two methods to measure the curing degree of UV inks were developed in this study. The surface curing method, based on ATR-IR, measured the curing only in a thin layer of the surface of the printed sample. The total curing method, based on NIR, measured the curing degree also from the ink that has penetrated deeper into the substrate. Studying the total curing degree is useful from the product safety aspect.

Based on the novel curing degree measurement techniques applied in this study, a concept for studying paper/board in combination with the ink system was established. The concept (including ink analyses, curing methods and product safety analyses) was applied to different substrates. Both offset and flexo trials were carried out at full-scale.

On the basis of this study, it became clear that the surface properties and structure of paper have a significant influence on the total curing degree obtained for the studied paper and ink systems. This result has not been evident in earlier studies on UV printing. The migration tests done to the printed samples seemed to correlate with total curing results, which now can be measured in a quantitative way.

Keywords

Curing, full scale printing, product safety, spectroscopy, UV inks

1. Introduction

The use of ultraviolet (UV) curable inks has increased rapidly in the past years and the trend is still the same. UV inks are used with conventional printing methods as well as with digital methods. Although originally the environmental friendly aspects were the major driving forces, the main reasons for growth are today operational, efficiency, and product quality benefits. This is mainly due to the development of inks: odor and migration levels have decreased, curing speeds have increased and they have improved with runnability and adhesion [Casatelli, 2007].

UV light triggers a polymerization reaction in the UV ink. Polymerization makes the ink layer dry, and the drying is called curing. When the printed substrate has passed the UV lamp, only the trigerred polymerization reactions go to the end and after that the curing stops. This holds true for free-radical inks whose market share is over 90% on UV curable inks. However, the research on this area has been concentrated on ink and ink ingredient properties as well as ink - lamp interactions. There has not been much research on UV ink - paper interactions and how the paper properties affect curing degree. In addition, a simple and quantitative method to measure curing degree of printed ink layer has been lacking. After all, the curing degree of the ink layer is a very important factor in UV printing: inadequate ink curing leads to poor adhesion and cohesion as well as migration and odor problems.

Especially in food package printing the high curing degree of the ink layer is important, because it is more a product safety issue than just a print quality problem. Before becoming a product safety issue, it can be an image issue. If any unwanted components are found in food, the sales of this brand will fall. For example, the careless manufacturing of packages did cause a situation where photoinitiator (ITX) was found from baby food and juices. This influenced the UV printing industry and opened the eyes for deeper safety considerations. GMP regulation 2023/2006/EC for food packaging industry was prepared and published to make sure that the manufacturing process for packages is safe.

2. Product safety aspects in UV printing

UV lamps produce the radiation power which is needed to cure the ink layer. Different lamp types produce different emission spectra. Matching the spectral distribution of the lamp to the sensitivity of photoinitiator blend used in the ink is very important. The pigments in the blue and violet colour range absorb light in the UV wave bands and are competing with photoinitiators for the photon energy.

The development of UV lamps has been rapid. The use of LED technology in UV curing was strongly present in the Drupa 2008 fair. If these lamps prove to work the way they should, the space and energy need of the lamps is reduced remarkably [Deutsher Drucker, 2008].

UV inks consist of monomers, oligomers, photoinitiators, additives, and pigments. The monomers and the oligomers are typically acrylated pre-polymers which are able to crosslink with each other on the influence of excited photoinitiators. They are responsible for the overall properties of ink and the cured ink layer. Photoinitiators trigger the polymerization reaction by passing the energy to the monomers and oligomers. Different photoinitiators absorb light at different wavelengths and for example pigment colour is one reason to select adequate photoinitiator to the ink.

The photoinitiator type devides inks to two categories: free radical and cationic inks. These inks differentiate by the curing mechanism. This study concentrates on free radical inks, because 90% of the commercial UV inks are based on free radicals. Figure 1 shows an example of a free radical curing mechanism. First the UV light generates a free radical in photoinitiator which can break the carbon-carbon double bond of acrylate monomer/oligomer and react with another carbon. This forms again a free radical, which breaks another carbon-carbon double bond, and the polymerization proceeds. The kinetics of the photopolymerization reactions does not only depend on the choice of the photoinitiator, but also on its concentration. Kinetics is also affected by various chemical and physical factors like composition, light intensity, wavelength, and temperature.

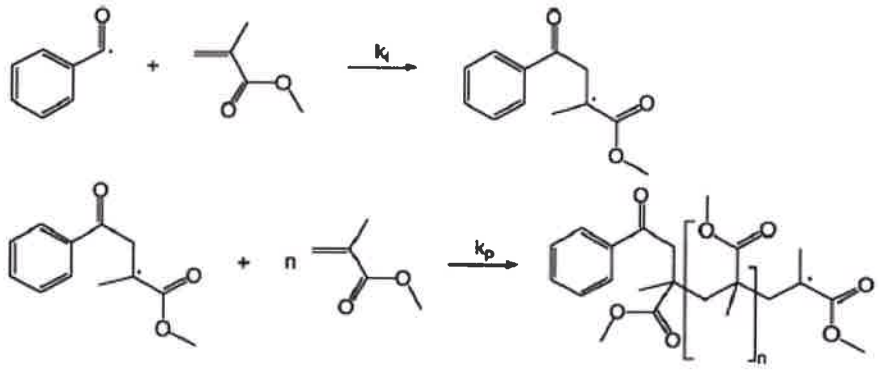


Figure 1:An example of polymerization due to free radical - mechanism [Silvares Adriano et al, 2006]

UV cured inks contain very low levels of VOCs (volatile organic compounds) because they are solvent free formulations. The low VOC producing inks become increasingly important to printing houses, offering a way to meet the current and pending environmental regulations to limit emissions and control air quality.

UV curable inks are also commonly used for food packaging. Testing of extractables is often performed on packaging to ensure that the ink and/or coating-borne migrants are well below thresholds. Migrants can cause off-flavor or be a regulatory concern [Yoo et al, 2004]. Recently, low-migration and low-odor UV inks have been developed to ensure product safety.

The printing quality demands in UV curing are fulfilled when the ink is considered as optimally cured. However, it cannot be assumed with absolute certainty that non-cured components of the UV ink do not migrate from the ink film to the surface or penetrate through the paper into food and thus present a potential health risk to the consumer [Anon, 2007] .Therefore from the safety point of view, there is also a need for an efficient and reliable method for the quantitative determination of the curing degree of printed papers and boards. Due to the lack of quantitative curing degree measurement method, the product safety issues could not have been systematically studied.

3. Materials and methods

The curing degree is the most important parameter, which largely determines all the other functional properties of the ink layer e.g. scratch and abrasion resistance, weather resistance, and the quantity of extractables. Therefore, one of the main objectives in the UV curing of the printing inks is to attain a high degree of curing both at the surface and in the bulk layer [Scherzer, 2002].

In general, two different alternatives for measurement of curing degree exist. Direct measurement of residual monomers and other ink components is possible by substance analysis with the gas chromatography (GC). In addition, the actual measurement of crosslinkage degree of a cured UV ink can be carried out by e.g. infrared (IR) spectroscopy [Anon, 2007].

During this study two quantitative methods to measure curing degree of the ink layer were developed and applied: surface and total curing methods. The surface curing degree measurement is based on attenuated total reflectance infrared (ATR-IR) spectroscopy, which measures only surface layer of 1 - 2 μm. The total curing degree measurement is based on near infrared (NIR) spectroscopy and it measures the whole ink layer, including the ink that has penetrated into the substrate.

3.1 Surface curing degree

The curing process of monomeric or oligomeric acrylates on the surface of printed sample was followed with ATR-IR analysis by calculating the decrease of $CH = CH_2$ groups. As a reference band, C-H absorption band of cyan pigment was used. The acrylate C = C/cyan pigment C-H ratio was calculated from printed and cured samples and compared to printed and uncured sample to determine the curing degree. The curing degree was calculated by the following equation:

$$\text{Curing degree (\%)} = (A_o - A_t) / A_o \times 100 \quad (1)$$

Where A_o is the band ratio of uncured printed sample and A_t is the band ratio after UV exposure.

IR spectra were collected by averaging 20 spectra at a resolution of 4 cm^{-1}. Five points were measured from one printed sample sheet, and typically two sheets of each trial point were analysed. The uncured ink layer was printed on a non-absorbing film in order to avoid any penetration of uncured monomers and oligomers into deeper layers of sample. Ink amount printed on the film was the same as printed on paper.

3.2 Total curing degree

The analysis of acrylates by NIR spectroscopy is based on the band of the first overtone of the C-H stretching vibration of the acrylic double bonds. Scherzer [Scherzer et al, 2006] has studied UV curing degree measurements by NIR. However, most of these applications have been performed on thick samples (about 1 - 6 mm). The investigations of thin coatings (e.g. printing inks) with a thickness of only a few micrometers are difficult because of weak absorption (due to relative low extinction co-efficients of acrylates) in the near-infrared region.

However, it was previously shown [Scherzer et al, 2004] that it is possible to obtain spectra of good quality from coatings with a thickness of some micrometers only, such as those in radiation curing processes, when the spectra are taken in reflection with an instrument with sufficient sensitivity.

NIR spectra were recorded right after printing and curing with UV light. A laboratory device for NIR reflection spectroscopy measurement was used. The spectra were taken at several points of each sample, and the resulting spectra were averaged before further processing. NIR measurements were made with the same ink amount for uncured layer. The curing degree was calculated using the equation (1).

3.3 Time dependency of the curing degree measurements

It has been stated that UV radiation curing proceeds seconds, minutes or even hours after the UV light has been switched off [Scherzer et al, 1999]. Obviously, the curing reaction started by the UV light exposure is completed after printing.

To test the post curing, the laboratory printed samples with target density of D1.45 were measured 10 minutes after printing and once again after one day. Printed samples were kept in dark at room temperature for 24 hours and then the curing degree was measured again with ATR-IR technique.

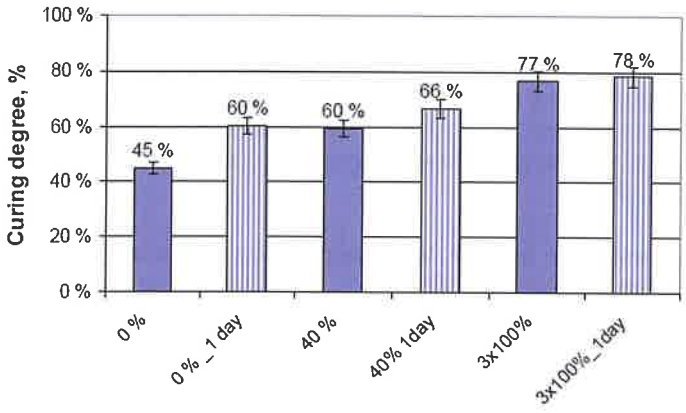


Figure 2: Surface curing degree measured with ATR-IR, of UV ink printed on reference paper, 10 minutes or one day after printing. Numbers under the columns refer to different UV radiation powers of the lamp where 0% is no curing and 100% full power of the lamp. In 3 x 100% the printed sample was exposed 3 times to the full power of the lamp

Results indicate that if the UV exposure is not high enough, the curing degree on paper surface increases during one day of sample storage in dark (Figure 2). Especially without any UV exposure, the amount of uncured acrylates has decreased strongly during one day. However, since the ATR-IR analysis detects acrylates only on the paper surface, the lower amount of uncured acrylates on paper surface may be due to either higher surface curing degree or penetration of uncured acrylates into deeper layers of paper. To clarify whether acrylates were surface cured or penetrated deeper into the paper, the same amount of ink was printed on a nonporous film with same UV power settings as in paper printing.

ATR-IR measurement 10 minutes and one day after printing on a nonporous film showed no differences in the surface curing degree. The samples were stored in dark. Even without any UV exposure the ink layer contains roughly the same amount of uncured acrylates after one day as directly after printing. This result indicates that there is no post curing after UV lamp exposure in the time period from 10 minutes to 1 day if the sample is kept in dark. As the printed paper samples showed a higher surface curing degree after one day on printed paper surface, this originates mainly from acrylate penetration into deeper parts of paper. ATR-IR measurement cannot detect the uncured particles that have penetrated into the paper due to the fact that it measures only the surface layer of the sample.

The same type of time dependency testing was done with the NIR measurement. There was a small change in the results during the two days of storage, but not as radical as seen with the surface cure measurement. The NIR measurement for total curing was selected to the paper and board samples to detect the amount of uncured compounds that can transfer to the food. To find out the curing degree difference of different papers, it is suggested that the NIR measurement should be carried out right after printing to detect the differences between the samples.

3.4 Product safety tests

GC-MS analysis (Gas Chromatograph with Mass Spectrometric detector) was used to identify the components in the UV ink. Gas chromatograph can separate compounds with small molecular size from each other and identify and quantify them by mass spectrometric detector. The inks are diluted into a solvent that is chosen by the ink components and the components to be detected. By the GC-MS analysis it was possible to find the photoinitiators and some monomers of the acrylates.

Migration tests were made on the printed samples. Migration tests were made according to EN 14338: Conditions for determination of migration from paper and board using polyphenylene oxide (TENAX) as a simulant.

3.5 Printing trials

The Substrates in this study were a commercial reference paper (130 g/m^2), porosity series papers (~80 g/m^2) and commercial paperboards (200 - 220 g/m^2). Paper properties are presented in Table I. The reference paper was a woodfree coated paper. It had quite similar properties as other papers except for the significantly lower specular gloss. The papers in the porosity series were coated at KCL's pilot coater to different porosity levels by changing the type and quantity of calcium carbonate pigment. Three commercial paperboards with slightly different coatings were also used.

Table I: Properties of the papers used in this study

Property	Method	Refe-rence paper	Poro-sity1	Poro-sity2	Poro-sity3	Board 1	Board 2	Board 3
Grammage [g/m^2]	EN ISO 536:1995 modif.	130	81	81	81	201	217	218
Roughness, PPS10, [um]	ISO 8791-4: 1992	1.15	1.13	1.02	0.97	0.81	1.00	1.10
Specular Gloss, md, Hunter 75, [%]	ISO 8254-1:1999	34	60	59	58	52	54	52
Air permeance, PPS20, [um/Pas]	internal		0,014	0,016	0,017			
Air permeance, Bendtsen [ml/min]	ISO 5636-3:1992	0.0				1.3	0.0	0.0

Sheet-fed offset printing trials were conducted at the Future Printing Center, Raisio, Finland. The porosity series, commercial boards and reference paper were printed with Ink2 and Ink3. Both total curing with NIR and surface curing with ATR-IR were determined from the samples. Process cyan was printed on two printing units and printing was performed as a wet-on-wet printing, meaning that there was no drying between the printing units. The two ink layers were dried with an interdeck dryer and an end-dryer consisting of three lamps.

Target print density in the offset printing for the reference paper was1.45 for both units. Thereafter as this print density was reached with reference paper, the printing ink feed and other adjustments were kept constant through the day with all other papers. As the ink feeding was kept constant, only the lamp power was adjusted from high to low power level. The high lamp power was 4 x 90%. The low lamp power was the drying power where the reference paper was tolerable dry. Based on printers rub-off test ("thumb test") the low lamp power was chosen to be 4 x 50%. These lamp power levels were used throughout the printing trials. The Ink3 - fountain solution emulsion was not stable during the trial. This gave too much variation to the results, so we will concentrate to the results from Ink2.

Web-flexo printing trials were performed at commercial print house in Finland. Three commercial boards were printed with Ink4, cyan. Only one ink layer with the target density of 1.75 was printed with an anilox roller transferring a high amount of ink. There were two interdeck dryers, first dryer after the printing unit and second after the subsequent unit. The lower lamp power was 2 x 40% and the higher 2 x 100%. With board 3 there was used also 4 different curing powers. Ink feed was adjusted with first board and kept constant during the trial.

Table II: Printing trial information with different printing methods, inks and substrates. x - combination tested (x) - combination tested, test unsuccessful ***x*** *- product safety tests preformed*

Printing Method	Ink	Ink analysis	Refe-rence paper	Poro-sity1	Poro-sity2	Poro-sity3	Board1	Board 2	Board 3
Laboratory	Ink1	x	x						
Laboratory	Ink2		x						
Laboratory	Ink3		x						
Offset	Ink2	x	**x**	x	x	x	**x**	**x**	**x**
Offset	Ink3	(x)	**x**		(x)	(x)	**x**	**x**	**x**
Flexo	Ink4	x					**x**	**x**	**x**
Flexo	Ink5	x							

4. Results

The results are divided into three parts. First the inks were analyzed to choose the right inks for the printing trials. Then the printed samples were measured to know how well they are cured and finally the product safety tests are performed to find out if the uncured ink components are a risk to safety. In addition to the results here several print quality measurements were made.

4.1 Inks

Inks used in this study were meant for use on food wrappers and packages. The inks were qualitatively analyzed. When the two offset inks were compared, the result was that Ink1 contained more photoinitiators than Ink2. This result meant that the amount of unreacted photoinitiators that may migrate was much higher with Ink1 than with Ink2, according to extraction-GC/MS analyses. According to manufacturers technical information of Ink2 it is a benzophenone free ink. However, according to ink analyses and MSDS (material safety data sheet), Ink2 contained benzophenone. In addition also ITX was detected from the ink even though it was not mentioned in MSDS.

Both of the flexo inks (Ink4 and Ink5) contained different amounts, but lots of monomeric acrylates and were in this way different from offset inks. Monomeric acrylates are used in flexo inks, because these decrease the viscosity of the ink, and are so needed as one effective compound in the ink of flexo printing.

All four analyzed inks had different photoinititor blends with different types of photinitiators. From Ink2 (offset) was found more different photoinitiators than from Ink1 (offset). The flexo inks did contain a smaller variety of photoinitiators than the offset inks did.

4.2 Effect of substrate on curing

Surface curing (based on ATR-IR) results were related in the offset trial more to UV dose and print density than to the paper properties. This is reasonable, since the method does not take into account the uncured components penetrated deeper into the paper. The portion of the ink that has penetrated deeper into the paper is more difficult to cure.

The total curing results for the offset printing (based on NIR) were clearly affected by paper properties (Figure 3). Overall, the ink layers on the surface of commercial board cured better than on the surface of porosity series paper. For board print density seemed to be the most critical parameter. The ink layer on the reference paper exhibited a significantly lower total curing degree than the ink layers on boards and even on porosity series. Figure 3 also shows that paper properties determined the total curing degree more than the UV lamp output.

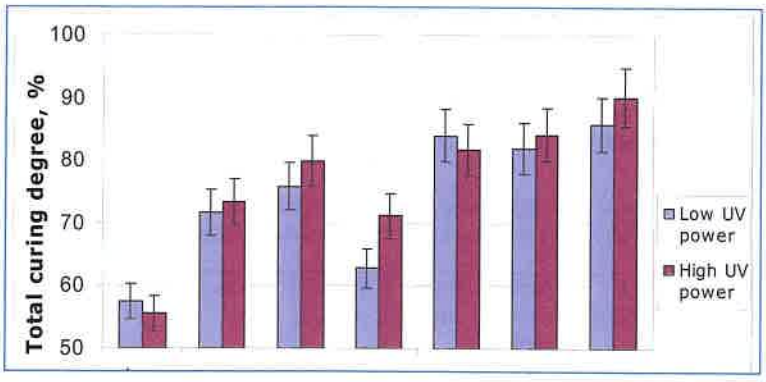


Figure 3: Total curing degree results for full-scale UV offset printings. First column is for reference paper, three following columns for porosity series papers and last three columns for commercial board.

In full-scale flexo printing only commercial boards were printed. The results for total curing degree varied little between the boards. The ink layer on board, with more open coating structure, exhibited a lower total

curing degree, with low UV curing power. When a high UV power was used the board with a more open structure gained the same total curing as other samples. This can be explained by the fact that flexo inks have low viscosities, allowing the ink to penetrate easily into the open coating structure, where it then needs more UV power to be cured.

4.3 Product safety

In the offset trial for commercial boards, migration of some photoinititaors exceeded the migration limits (specific migration limit of the substance, if available, or limit of 10 µg/kg in food). This was the case with even high curing degrees (> 90%). According to multivariate data analysis, these extraction results correlate strongly with total cure. The UV power had similar effect on migration as it had on extraction: the amount of unreacted migratable compounds decreased due to the increased UV power.

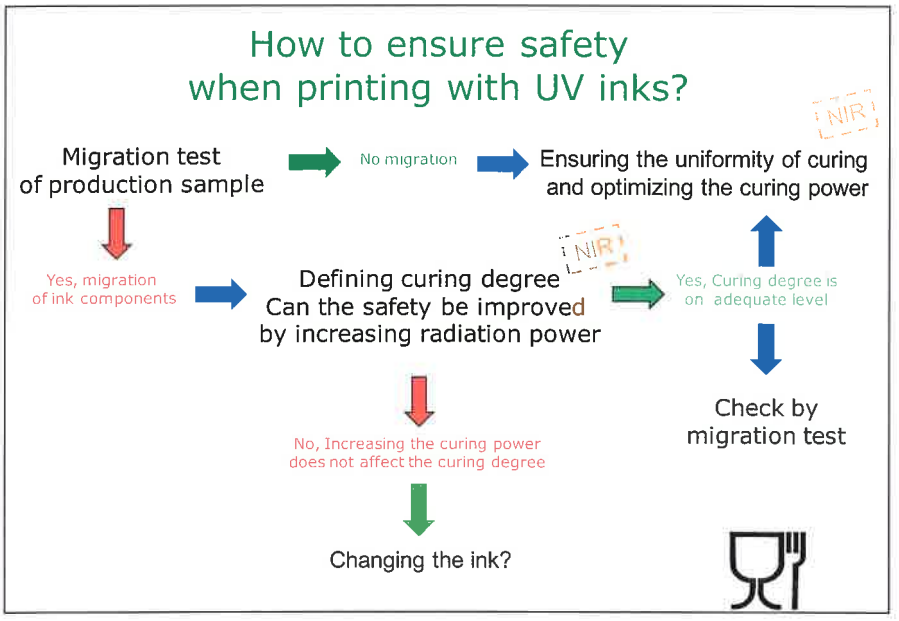
The flexo trial with the same commercial boards, but a different ink, also revealed a migration risk for some ink components. An observed migration risk is always an image question, although the health risk might still be far from causing general concern.

5. Discussion

The analysis of inks suggested that the inks can contain components that are not mentioned in the material safety datasheet or in the technical specifications of the inks. The total curing degree influencing the possible migration or set-off of unwanted components depends on the substrate.

It is hard to define why the different papers cured differently in these tests. The paper properties had a strong effect on the curing degree. To divide the paper properties to porosity, roughness, gloss and absorption properties in addition to the chemical properties of the paper did not give a single property that would have been dominant. The printing process itself had a strong influence to the attained curing degree. Lamp power, ink amount and the ink used all affected the results.

The previous studies have concentrated on printing ink - UV lamp compatibility, but this study showed that the substrate has to be included in the equation. By finding out the most suitable conditions for different combinations, it is possible to print UV inks in a safe and economical way. This optimization can be done with the following procedure (Figure 4). The same procedure can be applied to samples printed with different printing methods and for magazines, packages etc.



Figue 4: How to ensure safety when printing with UV inks. NIR measures the attained total curing degree

Now having a reliable measurement for the total curing degree, the study of UV printing will continue. The main focus will be the inkjet inks and their ink- paper interactions

6. Summary and conclusions

Based on novel curing degree measurement techniques applied in this study, a concept for studying paper/board, in combination with the ink system was established. The concept (including ink analyses, curing methods and product safety analyses) was applied for different substrates. Both offset and flexo trials were carried out in full-scale. Total curing and surface curing, describing different phenomena, were differentiated from each other. Total curing degree is useful from the product safety aspect and to optimise the amount of UV power for curing.

On the basis of this study, it became clear that the surface properties and structure of paper have a significant influence on the total curing degree obtained for the studied paper and ink systems. This result has not been evident in earlier studies on UV printing. Therefore, as the migration tests seemed to correlate with total curing results, which now can be measured in a quantitative way, it would be valuable to continue studying different paper + ink combinations and to find out the effect of paper on total curing. GMP Regulation 2023/2006/EC demands quality control measures for food industry to ensure safety. The measurement of total curing degree could be a suitable tool for UV printing.

Acknowledgements

The authors wish to thank the Contact Group of the KCL Project. This group consisted of representatives from the paper industry (UPM-Kymmene, M-real, Stora Enso and Myllykoski).

References

1. Anon. Possible test methods - drying or curing of UV inks, ESMA, available 1.10.2007 at www-form: URL:http://www.glassonline.com/infoserv/Glass_recycle_reuse/pdfESMA/uv_drying_uk.pdf/.
2. Casatelli, L. (2007) UV/EB Technology Continues to Grow. Ink Maker 3(85), 27 - 30 p-p
3. Deutscher Drucker Nr. 17/15. 5. 2008, p. 65
4. Scherzer, T. (2002), Depth profiling of the conversion during the photopolymerization of acrylates using real-time FTIR-ATR spectroscopy, Vibrational Spectroscopy, 29, 139 - 145 p-p
5. Scherzer, T., Decker, U.(1999), Real-time FTIR-ATR spectroscopy to study the kinetics of ultrafast photopolymerization reactions induced by monochromatic UV light, Vibrational Spectroscopy, 19, 385 - 398 p - p
6. Scherzer, T., Mehnert, R., Lucht, H. (2004), On-line monitoring of the acrylate conversion in UV photopolymerization by Near-Infrared reflection spectroscopy, Macromol. Symp., 205, 151 - 162 p - p
7. Scherzer, T., Müller, S., Mehnert, R., Volland A., Lucht, H. (2006), Process Control in UV curing: In-line monitoring of the acrylate conversion by Near-Infrared spectroscopy, JCT Coatings Tech., August, 30 - 37 p - p
8. Silvares Adriano, A. F. M., Nascimento, C. A. O., Bossmanna, E. S. H., Braun, A. M., (2006), Chemical Engineering and Processing 45, 1001 - 1010 p - p
9. Yoo, J. S., Pace, G. V., Khoo, B. K., Lech, J., Hartman, T. G. (2004), Mass spectrometry and gas chromatographic retention indices, Radtech report May, June, 60 - 68 p - p

In situ monitoring of the photo polymerization of UV curable acrylate coatings

Elena-Magdalena Casagrande[1,2], *Andreas Hörner*[2], *Achim Wixforth*[2]

manroland Duckmaschinen AG
Augsburg, Germany
E-mail: elena-magdalena.casagrande@manroland.com

[2] Chair for Experimental Physics I, University of Augsburg, Germany

Abstract

Employing a surface acoustic wave sensor and real time FTIR spectroscopy, we investigate the photo polymerization kinetics in UV curable multifunctional acrylate clear coating systems. Being sensitive to changes of the viscoelastic properties of the coating, the changes in the amplitude of the surface wave and the monomer conversion in the Acryl ate Systems during the irradiation time yields the polymerization rate and cure extent in real time. The onset of the polymerization was observed not to occur instantaneously after UV irradiation but rather after a certain time interval. The time delay between onset of the polymerization and the changes in the acoustic wave transmission parameters is attributed to the introduction of the crosslinking, leading to a gel state.

Keywords

Acoustic wave transmission, FTIR spectroscopy, photo polymerization

1. Introduction

As polymer coatings are utilized in virtually all industrial products, research in this area ranks among the most important braches of the chemical sciences.

Our homes, furniture, and automobiles all employ polymer coatings as protective layers. Producers of the most advanced optoelectronic devices have a significant interest in the development of uniformly thin, yet durable films. Photolithography, packaging of electronic components, labelling of devices, and cladding of high-speed fiber optics forming the backbone of a network all employ thin film coatings.

Among the several methods for preparation of polymer coatings, radiation curing is potentially one of the most effective. According to some market surveys, radiation curable inks are forecast to enjoy a ten percent yearly growth rate for the next decade or so. This growth is also due to a continuous improvement in printing technology. Recent developments in printing presses (sheet fed and web machines in term of high speed production and inking/dampening units) and drier equipment (nitrogen blanketing, cold lamps) have led to a significant increase in the number of applications in the graphic arts industry: boxes for cosmetics, food, tobacco, spirits, business forms, direct mail, lottery tickets, credit cards.

The formulation of UV curable printing clear coating systems depends on many variables. The common aim of all formulations, however, is a high quality product.

Therefore, it becomes a crucial point in all printing companies to monitor and control the polymerization processes, preferably in situ and under production conditions.

We have investigated the physical properties of multifunctional acrylate clear coating systems by means of a $LiNbO_3$ piezoelectric substrate on which we excite and propagate piezoactive surface acoustic waves (SAW). For our purpose, SAW sensors, particularly those operating in transmission mode, are very attractive for several reasons:

First, it is recognized that - at a fundamental level- these sensors interrogate, to a depth of several micrometers, all changes registries of material present on the piezoelectric substrate. Earlier conceptions that these devices

essentially act as mass detectors turns out to be too much simplified except under very special conditions. Moreover, we find that the viscoelasticity, and with that the photopolymerization can be monitored in real time with minimal interference to the material itself.

Secondly, multifunctional Acryl ate exhibits a variety of viscoelastic properties especially while passing from the liquid state to the solid state or through the "gelling" phase.

For a better understanding of those properties we have employed also other methods for the study of the mechanical, and in particular the viscoelastic properties of the Acryl ate systems. The chemical changes during the Photopolymerization process and the degree of cure is have been studied by real-time FTIR for comparison and as an independent method to calibrate our SAW senor signals.

2. Experimental section

The Acrylate clear coating systems are available commercially and used as received.

The curing behaviour of following monomers have been studied:

1. tripropylene glycol diacrylate (H_2C=CH-C(O)-$(OC_3H_6)_3$-OC(O)-CH=CH_2, TPGDA), 2
2. trimethylolpropane triacrylate (H_2C=CH-C(O)-$OCH_2)_3C$-C_2H_5; TMPTA;
3. DPDGA;

Photoinitiator: benzophenone and BDK.

Sample purity generally has not been taken into consideration for the analysis of crosslinking kinetics. To ensure a constant temperature during the experiment, a thermocouple and Peltier element has been connected to the sensor.

2.1 Measurement technique

A new apparatus incorporating a SAW sensor was constructed to measure the changes in the sample's SAW transmission properties during the curing by registering the changes in the phase and amplitude of the acoustic wave (Fig. 1).

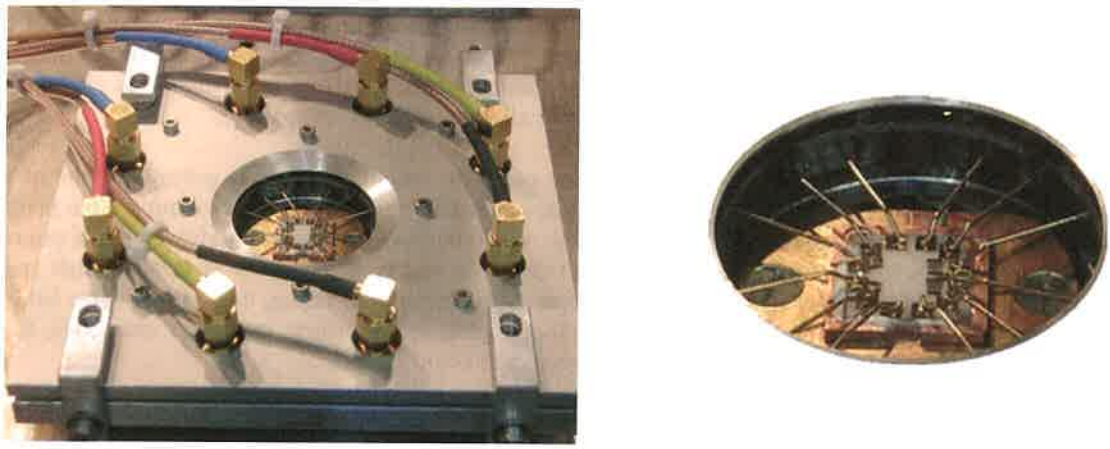


Figure 1: SAW Sensor; the surface is protected with a SiO2 layer. A thermocouple and a Peltier element are attached to the sensor

The whole setup is illuminated with a UV lamp to initiate the curing process. During illumination, the SAW propagation parameters are monitored.

The clear coating formulation is applied directly onto the $LiNbO_3$ substrate, the conversion rate and mechanical properties of which are well known. A high frequency electrical pulse (f = 82 MHz, P = -39.47 dB, Mag = 10 dB) is applied to one of the interdigital transducers, converting it into a SAW. After passing the acrylate sample, the SAW is picked up by a second transducer at which the transmitted signal can be analyzed in terms of amplitude and phase shift with respect to the incoming signal.

The sample is, contemporary, irradiated with a UV lamp at P = 118,8 mW/cm^2. Polymerization occurs when the monomer is irradiated. By choosing an appropriate range for the SAW power applied, even smallest changes in the cure of the Acryl ate systems can be monitored, employing a Spectrum analyzer or a Vector Network Analyzer.

Figures 2 and 3 shows the changes of the SAW amplitude data during the cure of an UV-curable sample. As the irradiation time increases, the photochemical reaction is initiated (causing a decreased ion mobility due to crosslinking) and competes with the exothermic temperature effect. This results in an amplitude increase due to the loss in damping from the liquid phase to the solid phase of the Acrylate.

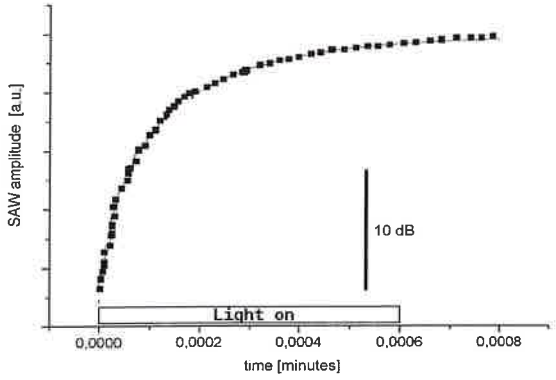


Figure 2:
Kinetics of the photo polymerization process for an Acrylate clear coating system as being detected by a SAW sensor. The polymerization process of the thin coating layer causes a change in the SAW amplitude of order 25 dB

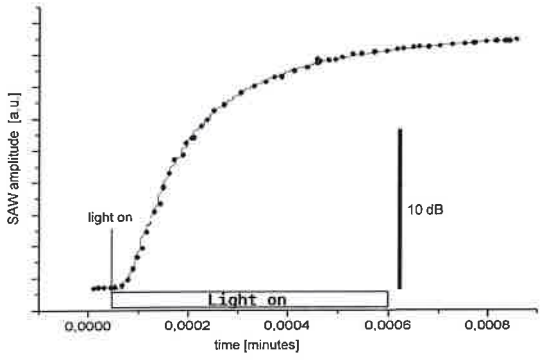


Figure 3:
Kinetics of the photo polymerization process for a different Acryl ate clear coating sample as being detected by a SAW sensor. The moment at which the curing light is switched on is marked in the figure

Shortly after the light is switched on, the SAW attenuation exhibits a rapid decrease, resulting an increase in amplitude as the reaction begins to dominate.

As the UV induced curing proceeds, the physical nature of the UV curable mixture changes from a Newtonian fluid into a gel and finally a glassy solid. Gelation corresponds to the point at which an infinite network is formed, while the vitrification is the point at which the chains become closely packed and there is insufficient volume for co-operative motion to occur.

At vitrification, the material changes from a rubber to a glass and reaction is effectively quenched for those reactions where intramolecular reactions are not important. We notice the same tendency between both curves representing respectively the amplitude and monomer conversion.

Typically, the samples were exposed to UV radiation for 3 min and then radiation was turned off.

We can see that after the UV source is turned off (beim 0,0006 min), polymerization continues, so the amplitude registred no decline, but continue at the same range. The "dark polymerization" has been found for multifunctional Acryl ate in both liquid and solid states.

For comparison, we have also used real time FTIR for monitoring the chemical changes in Acryl ate thin film. For the multifunctional monomers used, it is anticipated that a highly cross-linked system (gel) will develop. The relationship between functionality and elation point has been derived using a number of different approaches. The relative concentration of reacted and unreacted monomers is considered to be a function of time, dosage, or degree of conversion.

The degree of conversion was measured using a Bruker FTIR spectrometer. The carbon-carbon double bond stretching band at 1638 cm^{-1} was used as a measure of the acrylate concentration, and the aromatic ring breathing band at 1610 cm^{-1} was used as internal reference. The spectra were deconvoluted, the peak areas were obtained through integration, and the acrylate peak area was normalized by division by the area of the reference peak.

Comparison of the acrylate peak area in a monomer sample yielded the degree of conversion of acrylate groups after cure. All measurement were performed at ambient temperature.

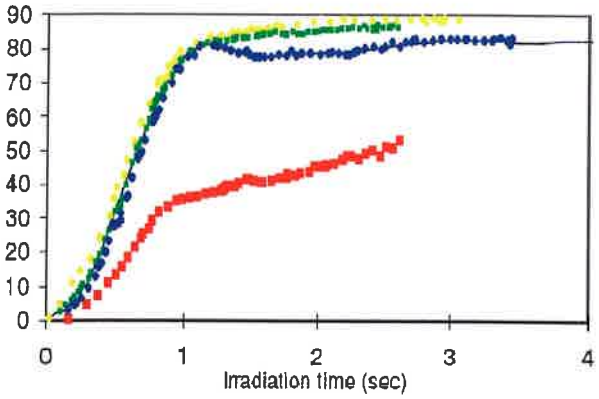


Figure 4:
Degree of conversion (100%) of 4 commercially available Acrylate clear coating systems

3. Conclusion

This study has outlined some of the applications that have benefit from the ability to perform real-time SAW sensor measurements on the photo polymerization process for UV curable coatings.

We have established a correlation between the two very efficient analytical methods: the real-Time FTIR and *In situ SAW*.

It clearly appears that the SAW analysis shows a very fast and easily manageable on-line process control of the UV curing process and should be useful in monitoring such UV ultra fast reaction commonly used in coatings, composites, adhesives and others industrial applications.

References

1. Hörner, A. L.: Untersuchung von Metall-Isolator Übergängen mit Oberflächenwellen, Dissertation, Fakultät für Physik der Universität Augsburg (2005)
2. Strobl, C. J., Rathgeber, A., Wixforth, A., Gauer, C., Scriba, J.: Planar microfluidic processors, IEEE Ultrasonics Symposium (2002)
3. Strobl, C. J., Schäflein, C., Beierlein, U., Ebbecke, J., Wixforth, A.: Carbon nanotube alignment by surface acoustic waves, Applied Physics Letters, 85, 8 (2004)
4. Strobl, C. J.: Mikro- und Nanofluidik auf piezoelektrischen Substraten, Dissertation, Fakultät für Physik der Ludwig-Maximilian Universität München (2005)
5. Stroock, A. D., Dertinger, S. K. W., Ajdari, A., Mezić, I., Stone, H. A., Whitesides, G. M.: Chaotic mixer for microchannels, Science, 295, 647 (2002)
6. Tabeling, P.: Introduction to Microfluidics, Oxford Press (2005)
7. Takanaga, I., Kushibiki, J.: A method of determining acoustical physical constants for piezoelectric materials by line-focus-beam acoustic microscopy, IEEE Transactions on Ultrasonics, Ferroelectrics, and Frequency Control, 49, 7 (2002)
8. Talkner, P.: Persönliche Mitteilung Prof. Dr. Peter Talkner, Universität Augsburg (2006)
9. Tomeno, I., Matsumura, S., edited by K. K Wong: Dielectric constants of LiNbO3, in: Properties of Lithium niobate, EMIS No. 28, INSPEC (2002)
10. van den Heuvel, A. P.: Use of rotated electrodes for amplitude weighting in interdigital surface-wave transducers, Applied Physics Letters

Considerations for thermally engineered coated printing papers: focus on electrophotography

Philip Gerstner[1], *Patrick A. C. Gane*[2]

[1] Helsinki University of Technology
Faculty of Chemistry and Materials Science, Department of Forest Products Technology
Vuorimiehentie 1A, P.O. Box 6300, 02150 Espoo, Finland
E-mail: firstname.lastname@tkk.fi

[2] Gane is also Head of Research and Development
Omya Development AG,
CH-4665 Oftringen, Switzerland

Abstract

For the printing of coated papers, the coating layer fulfils a specific role as the image receiving interface. Its physical properties are vital for quality and efficiency of the printing process. This work takes the thermal properties of the coating layer into consideration as heat is applied to its surface, and illustrates its role in respect to toner adhesion as a print quality parameter in the electrophotography process. Pigment tablets are used to provide experimental values of thermal diffusivity and conductivity. Three types of coating pigments are studied: ground calcium carbonate, both very fine and coarse grades (vfGCC, cGCC), a very porous and bulky modified calcium carbonate (MCC) and talc. Temperature gradients within the coating and base sheet substrate, and fusing nip conditions, are studied adopting finite element simulation. Toner adhesion is measured by a tape test on laboratory coated paper samples. The simulation of the fusing nip clearly shows advantages of having a thermally insulating MCC coated substrate, in that the local, surface concentrated, temperature gradients are beneficial for the fusing process and the base paper is shielded, thus minimizing heat losses. Because of the strong influence of surface roughness on the printed sheets, and the high fusing temperature/degree provided by commercially applicable printers, no direct relation between the toner adhesion measurements and the thermal conductivity of the coating layer could be seen. However, it is recognized that a smooth and even printing surface, in combination with an insulating coating structure, could be used to lower the specific energy required to fuse toner, provided the surface structure continuity/packing density is sufficient.

Keywords

Electrophotography, thermal properties, toner adhesion, surface roughness, printability

1. Introduction

The ambition for higher print quality in all printing processes is continuing to set growing standards for the requirements of paper. In general, these emerging requirements aim to improve print quality, the printing process itself, and, foremost, its economy. For high quality prints the use of coated paper is generally required, placing the coating layer as the interface between printing process and base paper substrate. Increased knowledge of the properties of the coating layer is therefore necessary in order to cope with the development needs. Improved thermal response of paper is seen as important for a wide range of printing applications, including primarily electrophotography and heatset offset, the difference between these methods, in respect to heat transfer, being physical contact in the former and air impingement in the latter.

In the electrophotographic printing process small polymeric toner particles are thermally fused onto the substrate surface. The adhesion of toner is considered to be an important print quality parameter [Sipi, 2001]. Toner adhesion is based on complex, not yet fully clarified mechanisms. In general, the mechanisms can be split into mechanical adhesion, depending on the degree of surface structural intermingling, as well as chemical adhesion phenomena, such as adsorption. Both mechanisms depend on the melting characteristics of the toner and, therefore, on the thermal conditions in the fusing nip.

Gerstner *et al.* [2007a] introduced a lumped parameter model to calculate thermal conductivity of paper coatings, supported by comparison with experimental observation. However, such a model alone does not give any

information about the influence of the thermal conductivity on the printing process, as the materials involved in printing (ink, fountain solution, or toner, for example) are omitted. This study examines a range of carefully controlled paper coating structures from the perspective of their thermal properties, and analyses the effects on the thermal response in an electrophotographic fusing nip by modelling the nip conditions for the different coatings. As a print quality parameter, the resulting toner adhesion, applied in a commercial office printer, is measured and compared to the physical properties of the coatings.

2. Materials and methods

2.1 Materials

The coatings examined in this study are based on three different pigment systems. A ground calcium carbonate of very high fineness[1] (vfGCC) is compared in respect to thermal properties with data from a previous study [Gerstner *et al.*, 2008] of a coarser ground calcium carbonate[1] (cGCC), and then with a speciality modified calcium carbonate[2] (MCC), which forms a very porous, bulky structure (see Figure 1) and a talc[3] pigment coating. The binder used for all coatings was n-butyl acrylate styrene latex[4] (Table II) in dosages of 10, 15 and 12 pph, based on 100 parts by weight of pigment, respectively. The very same coating colour formulations were used in both a tablet forming process, for the measurement of thermal diffusivity, and in laboratory coating of sample sheets for the measurement of toner adhesion.

Table I: Summary of particle size data for the three pigments used

	cGCC	vfGCC	MCC*	Talc
Latex [pph]	0 to 25 Ref. /4/	10	15	12
PSD [w/w%]				
< 5 µm	93	100		82
< 2 µm	60	98		46
< 1 µm	40	90		
d_{50} (weight median) [µm]	1.6	0.4	5.1	2.4

* Particle size determined by SEM

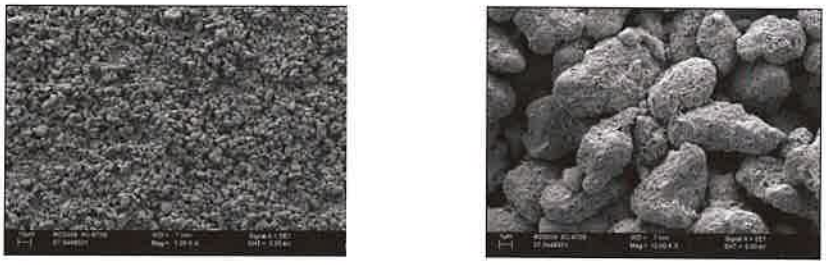


Figure 1: SEM images of modified calcium carbonate (MCC). Magnification 1 000 and 10 000 x.

Table II: Basic properties of the SA latex used in the experiments

	SA latex
MFFT*	< 1°C
Av. particle size	0.2 µm
Solids content	50 wt-%
Density	1 050 kgm^{-3}
pH	8
Viscosity	375 mPas

*Minimum film forming temperature

[1] Setacarb HG (vfGCC) and Hydrocarb 60 (cGCC) are registered trademarks of Omya AG
[2] MCC564, 5 µm, 64 m^2g^{-1}, Omya AG
[3] Finntalc C10, Mondo Minerals Oy
[4] Acronal S360D is a registered trademark of the BASF AG

The thermo physical properties of fibrous paper, used to describe the base paper, are taken from a study by Kartovaara *et al.* [1985]. They analysed the thermal diffusivity of different pulps at different refining degrees. For the copy grade sheet, used here as base paper, we chose values of chemical pulp at a refining degree of 22 °SR, which is in the typical range of copy papers. The properties of pigment binder and paper are assumed to be constant in the temperature range of our measurements and simulations. This is a simplification in practice considering that different moisture content can play a role especially for the properties of paper. We, however, neglect the role of moisture because all measurements were executed at the same ambient conditions.

The thermo physical properties of toner cannot be taken as constant, because the material goes through a phase change and, since the toner layer is the interface between coating and process, it is of main interest for the scope of this study. The basic properties of toner are taken from a study by Mitsuya *et al.* [1991]. Hartus [2001] describes three thermal stages in the fusing process of toner: at first an increasing temperature of the particles (warming), then a softening stage where toner particles begin to melt and cohere, and finally the actual melting stage. For softening and melting the consumption of energy is increased. This extra amount of required melting energy effectively increases the heat capacity of toner. We therefore add the melting energy measured by Hartus to the heat capacity of toner, i.e. 50 $Jkg^{-1}K^{-1}$ for the softening stage ($90°C < T < 120°C$) and an additional 200 $Jkg^{-1}K^{-1}$ for the melting stage above 120°C.

Table summarizes the thermo physical properties of the materials involved. The effective heat capacity of the coatings ($c_p = c_{eff}$) is calculated additively for the mass share of the two phases, pigment (c_{s1}) and binder (c_{s2}):

$$m_{tot} \cdot c_{eff} = m_{s1} \cdot c_{s1} + m_{s2} \cdot c_{s2} \tag{1.1}$$

The contribution of air in pores to the total heat capacity is neglected because of its very low mass and low specific heat capacity compared to the solid phases. With $m_{tot} = m_{s1} + m_{s2}$ and $m_{s2} = \beta m_{s1}$, the effective heat capacity of a tablet becomes:

$$c_{eff} = \frac{c_{s1} + \beta c_{s2}}{1 + \beta} \tag{1.2}$$

where β is the binder dosage in w/w% with respect to 100 w/w% pigment. For the individual phases, literature values of c_{s1} = 880 $Jkg^{-1}K^{-1}$ [Landolt-Börnstein, 1980b] and c_{s2} = 559.8 $Jkg^{-1}K^{-1}$ [Mark, 1996] are used for calcium carbonate (pigment) and n-butyl acrylate (binder), respectively. The measurement of the thermal diffusivity properties of the coatings is described in the following section.

Table III:. Thermo physical properties of toner, coatings and base paper as used in the calculations. [The thermal diffusivities of the coatings are measured from the tablet material]

	Thickness *d [μm]*	***Density*** *ρ [kgm^{-3}]*	***Heat Capacity*** *c_p [Jkg^{-1}K^{-1}]*	***Th. Cond.*** *k [Wm^{-1}K^{-1}]*	***Th. Diff.*** *D [m^{2}s^{-1}]*	***Ref.***
Toner*	16	1 115	1 255.00	0.120	0.85E-7	/9, 11, 12/
vfGCC	20	1 703	850.89	0.566	3.90E-7	/7, 9/
MCC	20	825	838.23	0.115	1.67E-7	/7, 9/
Talc	20	1 670	842.12	0.848	6.03E-7	/7, 9/
Paper	100	971	1 445.00	0.101	7.20E-8	/6/

* values for ambient temperature

2.2 Tablet forming and measurement of thermal diffusivity

For the measurement of thermal diffusivity, pigment-binder tablets of the coating colour formulations were formed. A constantly applied pressure of p = 20 bar was used to dewater the suspension mix (coating colour) through a membrane. After forming and decanting any remaining slurry, the tablets were removed and oven dried at 60°C, following the method of Ridgway *et al.* [2004]. In order to get a well-defined cylindrical tablet shape, all the tablets were ground after drying using a rotational grinder. The tablets were ground to thicknesses from approximately 9 mm to 14 mm depending on their initial size, determined by forming quality and pigment type. Their diameter varies from 38 mm to 40 mm. For subsequent calculations, their individual, carefully measured dimensions were used.

The thermal diffusivity measurement is based on a technique introduced by Gane *et al.* [2006] and further developed by Gerstner *et al.* [2007b, 2008]. The pigment tablets are subjected to a temperature step on one side while the temperature response on the other side is recorded. The measured temperature response, along with initial and boundary conditions, allows calculation of the tablet's thermal diffusivity by matching the numerical solution of the one dimensional heat diffusion equation to the measured topside temperature response. This is done by a self adaptive iteration of the parameters thermal diffusivity and heat loss. The numerical solution matching the experimental curve delivers the value for thermal diffusivity.

2.3 Toner adhesion and surface roughness

The measurement of toner adhesion was done on laser printed laboratory rod coated sheets using standard 80 gm^{-2} copy paper as a base. In order to have different roughness levels for comparison for each coating type, a set of sheets was calendered in a single nip laboratory calender at a temperature of 80°C, a load of 100 kNm^{-1} and a speed of 10 $mmin^{-1}$.

The sheets were printed with a test pattern on an HP LaserJet 5L. The test pattern consisted of areas to measure toner adhesion on full-tone black (100% black) printed surfaces and on grey tone (40% black) surfaces. The straightforward design of the printer furthermore permitted a thermocouple to be fed along with the printed sheet, thus recording the temperature time curve of the surface of the sheet (below the toner when present) in the fusing nip. The temperature data thus gathered are considered for mathematical simulations of the thermal transfer in the printing nip.

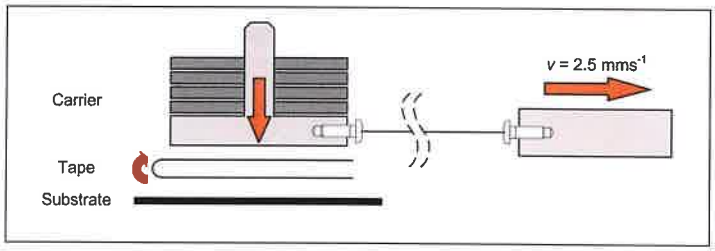


Figure 2: Adhesive tape test for the measurement of toner adhesion to substrate

Toner adhesion was measured by the change in optical print density after removal of an adhesive tape, contacted under pressure, from a printed surface. In order to ensure constant angle and speed of the tape removal, a device, as described in ASTM D 1894 (Standard test method for static and kinetic coefficients of friction of plastic film and sheeting), was used. The tape is attached to the printed surface, turned and attached to a carrier. The carrier pulls away the tape at constant speed, while applying constant pressure (Figure 2).

Toner adhesion ξ is calculated by the relative loss in optical print density:

$$\xi = \frac{D_2}{D_1} \cdot 100\,\% \qquad (2)$$

where D_1 is print density before attachment of the tape and D_2 is print density after tape removal.

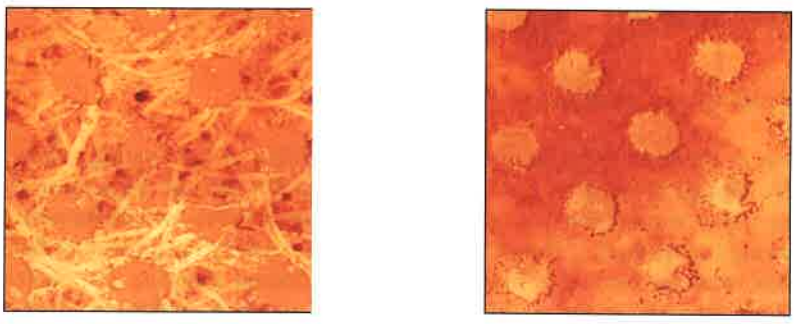


Figure 3: CLSM images of printed dots (40% black) on calendered base paper and calendered talc coated paper: the image width is 750 μm, the dot size approximately 120 μm

Surface roughness was measured with the Parker Print Surf method (ISO 8791-4) for both the calendered and uncalendered sheets. Additionally, the surface micro roughness was measured by confocal laser scanning microscopy (CLSM). The micro roughness is expressed as the root mean square deviation about the mean surface measured along a line of 40 µm length. The out of plane resolution was set to ca. 1 µm, the in plane resolution was ca. 1.6 µm. Figure 3 shows CLSM images of 40% black printed surfaces on a calendered uncoated base paper and a calendered talc coated sheet. The dot size of the print is approximately 120 µm.

2.4 Simulation of electrophotography fusing nip

In general, the main components of a fusing system are a heated metal roll (fusing roll), a polymer backing roll and the printing substrate. The substrate passes the nip formed by fusing and backing rolls. In order to focus on the thermal conditions in an electrophotography nip which lead to toner fusing, the nip is modelled in a simplified two dimensional version, using commercially available finite element software[5]. The model excludes effects of surface roughness or surface chemistry as these can be evaluated initially separately by comparison of deviation with experiment. For the simulation, instead of passing the substrate through the nip, the nip "moves" along the surface of the substrate with the printing speed v. The substrate itself can be described as a layered structure consisting of base paper, coating and toner. The model dimensions are given in Figure 4. The thermal transmission through each finite element in each layer is defined by:

$$\nabla \cdot (k \nabla T) = \rho c_p \frac{\partial T}{\partial t} \tag{3}$$

where: k is the thermal conductivity [$Wm^{-1}K^{-1}$]
T is the Temperature [K]
ρ is the density [kgm^{-3}]
c_p is the heat capacity at constant pressure [$Jkg^{-1}K^{-1}$]:
for toner: $c_p = f(T)$ allowing for melting, and
t is the time [s]

The toner layer thickness is based on the literature value of the toner material source (Mitsuya and Kumasaka, 1992], the coating layer and base paper thicknesses are approximate to those of the lab coated sheets. In order to investigate the thermal properties alone, these dimensions are kept constant during the simulation and for all three coating formulations, thus ignoring compression.

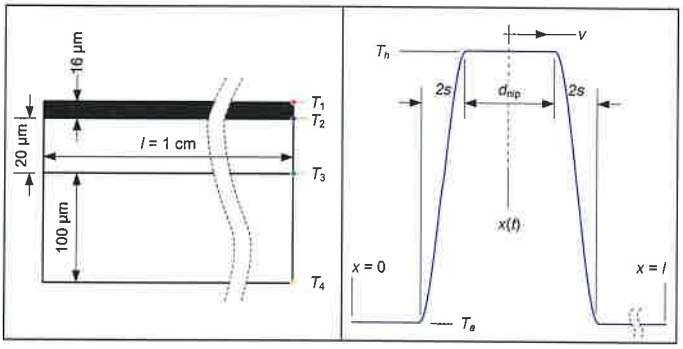


Figure 4: Left: layered structure of the model printing substrate. Right: temperature boundary condition for the fusing nip imposed on the surface of the toner layer: $T_1(x, t)$. The temperature step moves along the surface with the printing speed v

Because of the insulating behaviour of the polymer backing roll, and low temperature gradient in respect to the air boundary, there is a zero heat flow condition applied for the lower boundary of the substrate. The transient upper boundary condition of the substrate is imposed by the moving printing nip. The heating temperature in the nip is believed to be constant because of the comparatively large thermal mass of the metal (aluminium) fusing roll. Before the substrate enters the fusing nip, the surface is at ambient temperature T_a. However, because of the low thermal mass of the air layer adjacent to the upper boundary, it is not immediately obvious whether the ambient temperature can be imposed as a boundary condition right after the

[5] Comsol Multiphysics, Version 3.4, Copyright COMSOL AB

printing nip. In contrast to the lower boundary there is a much higher temperature gradient and it is unclear whether the air layer after the printing nip insulates the upper boundary. For this reason we look at alternative boundary conditions: (i) we impose a constant heat flow in the nip and a zero heat flow condition across the boundary before and after the nip - this configuration is shown on the left side of Figure 5 - (ii) we apply a boundary condition with a step in temperature (right side of Figure 5). Both figures are given for a time $t > 0$, so the nip has moved in the positive x direction. It can be seen that the step in the heat flow boundary condition causes a very asymmetrical temperature response for case (i). Because of the assumed insulating behaviour of the upper boundary, the temperature after the nip drops considerably slower. For the temperature step boundary condition (ii), on the right side of Figure 5, there is heat flow into the substrate ($q > 0$) in the nip area and heat flow out of the substrate right before and after the nip. This results in a more symmetrical response for the temperatures of the layers beneath the interface.

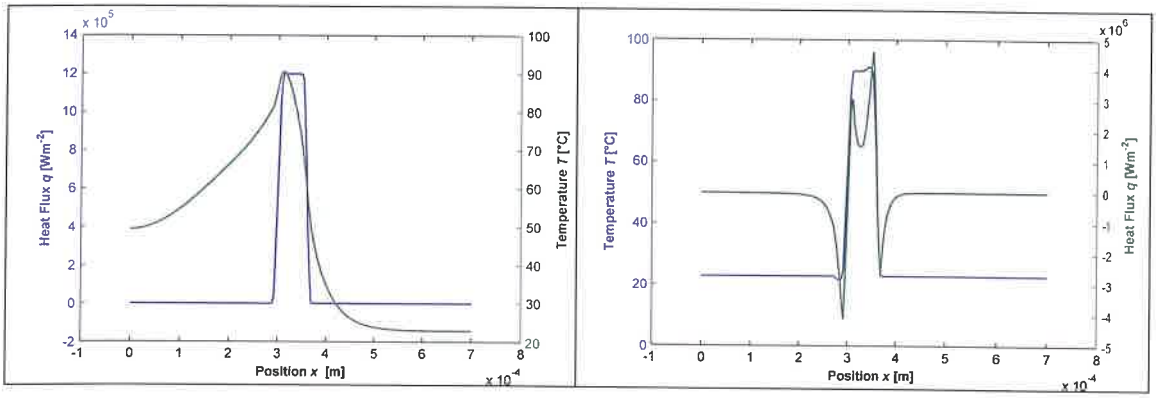


Figure 5: Left: upper boundary condition (i) for a step of z-directional applied heat flux in the fusing nip and the resulting temperature on top of the toner layer (T_1). Right: upper boundary condition (ii) for an imposed step of temperature (rising to T_1) in the fusing nip and the resulting z-directional heat flux through the top of the toner layer. [Positive heat flux indicates flux into the substrate]

The simulated temperature response beneath the toner layer (T_2 of Figure 4) can be compared with experimental results. A thermocouple was mounted at a fixed position of the surface of a coated sheet (in this case talc) and printed fully black. Figure 6 shows the experimental result of the thermocouple temperature measurement as a function of time and compares it to the temperature response for the simulation of printer NP-I (Table IV) using the temperature step boundary condition (ii). To remove absolute timescale differences, the relative time is used, based on the time when the temperature in the nip is at its maximum.

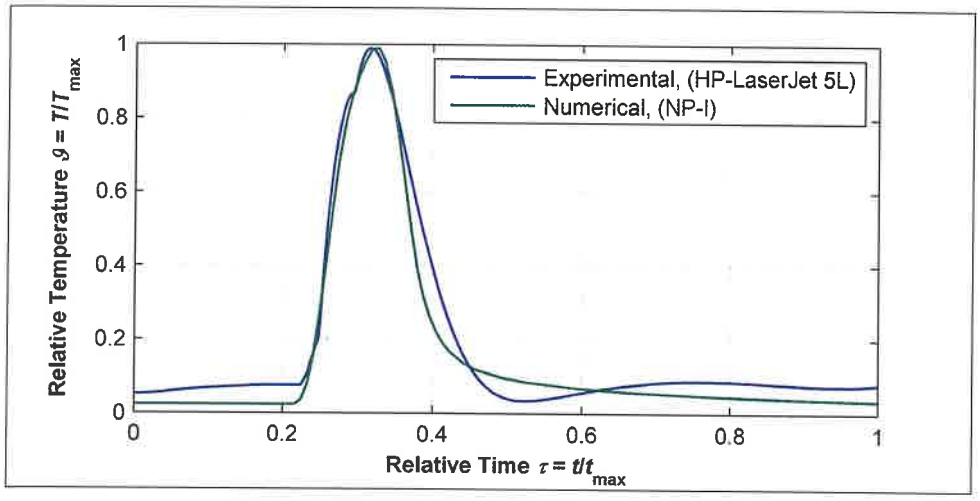


Figure 6: Experimentally measured temperature response beneath the toner layer (T_2) on a talc coated sheet in the printing nip of an HP LaserJet 5 in comparison with a numerically calculated temperature response beneath the toner layer (T_2) on a "talc coated sheet" in the simulated printing nip (NP-I) using boundary condition (ii). [To remove absolute timescale differences, the relative time t/t_{max} is used, where t_{max} is based on the time when the temperature in the nip is at its maximum T_{max}.]

Although the quantitative result depends on the printer parameters, i.e. printing speed, nip length and fusing temperature, it can be seen that the shape of the curves in Figure 6, expressed on a relative time base, agree remarkably well. Since any temperature response of the heat flow step boundary condition (i) would be much more asymmetric, we may confidently choose the temperature step boundary condition (ii) for all subsequent discussions and ignore heat flow retardation properties within the air boundary. The conditions imposed to the boundaries of the substrate are, therefore, a constant ambient temperature T_a and a defined step to the constant heating temperature T_h of the fusing roll in the nip (see Figure 4, right) for the upper boundary (equation 4.1), and a zero heat flow condition at the lower boundary (equation 4.2).

$$T_1(x,t) = \begin{cases} T_a, & \forall x \in \left(v \cdot t - \frac{d_{nip}}{2} \right) > x > \left(v \cdot t + \frac{d_{nip}}{2} \right) \\ T_h, & \forall x \in \left(v \cdot t - \frac{d_{nip}}{2} \right) < x < \left(v \cdot t + \frac{d_{nip}}{2} \right) \end{cases} \tag{4.1}$$

$$\frac{\partial T_4}{\partial z} = 0 \tag{4.2}$$

For the simulation, the temperature step in the upper boundary condition is smoothed by the factor $2s$ at both sides. This serves two purposes: at first, the finite element method requires a step of finite gradient (continuous first derivative) to avoid convergence problems. Secondly, the nip pressure is in practice lower at the outer parts of the nip, and therefore the contact resistance to the substrate is higher and the thermal transfer lower. The total effective nip length d_{eff} consists, therefore, of:

$$d_{eff} = 4s + d_{\text{nip}} \tag{5}$$

The value for d_{eff} was estimated to be 5 mm for a parabolic pressure distribution as described in a numerical example by Williams [1984]:

$$d_{eff} = \left(\frac{3hDF}{4EL} \right)^{\frac{1}{3}} \tag{6}$$

where: h, E is thickness and modulus of elasticity of the polymers, respectively,
D is diameter of both rolls (hard fusing roll and deformable backing roll) and
F/L is load per unit length.

The values for equation 6 were taken from a numerical example given in the reference. Due to the more compact construction types of current laser printers a smaller roll diameter of D = 2 cm was used here. A summary of the simulated "numeric printer" configurations studied is given in Table IV. NP-I resembles a current laser printer model. NP-II and -III are variations of this typical printer having lower specific fusing energy achieved by either reduced fusing temperature or by higher printing speed, respectively.

Table IV: Parameters of the "numeric printers" used to simulate the nip conditions

	NP-I	***NP-II***	***NP-III***
Fusing Temperature T_h	180°C	140°C	180°C
Ambient Temperature T_a	23°C	23°C	23°C
Printing Speed v	10 cms^{-1}	10 cms^{-1}	20 cms^{-1}
Effective Nip Length d_{eff}	5 mm	5 mm	5 mm
Nip residence time t_{res}	50 ms	50 ms	25 ms
Spec. Fusing Energy Q^*	10.17 kJm^{-2}	7.48 kJm^{-2}	7.35 kJm^{-2}

* calculated from the net heat flux into an MCC coated substrate

3. Results and discussion

3.1 Thermal diffusivity of the coatings

Figure 7 shows the measured thermal diffusivities of the three coating formulations along with data from the coarser ground calcium carbonate (cGCC) at different binder concentrations. It can be seen that, despite its high fineness, the vfGCC coating has very similar thermal diffusivity to the cGCC at the same binder concentration. However, the talc coating shows a notably higher thermal diffusivity, which can be accounted for by the higher inherent thermal conductivity of the talc. A literature value for talc is k_{talc} = 3.1 $Wm^{-1}K^{-1}$ compared to calcium carbonate k_{CaCO3} = 2.0 $Wm^{-1}K^{-1}$ [Landolt-Börnstein, 1980b].

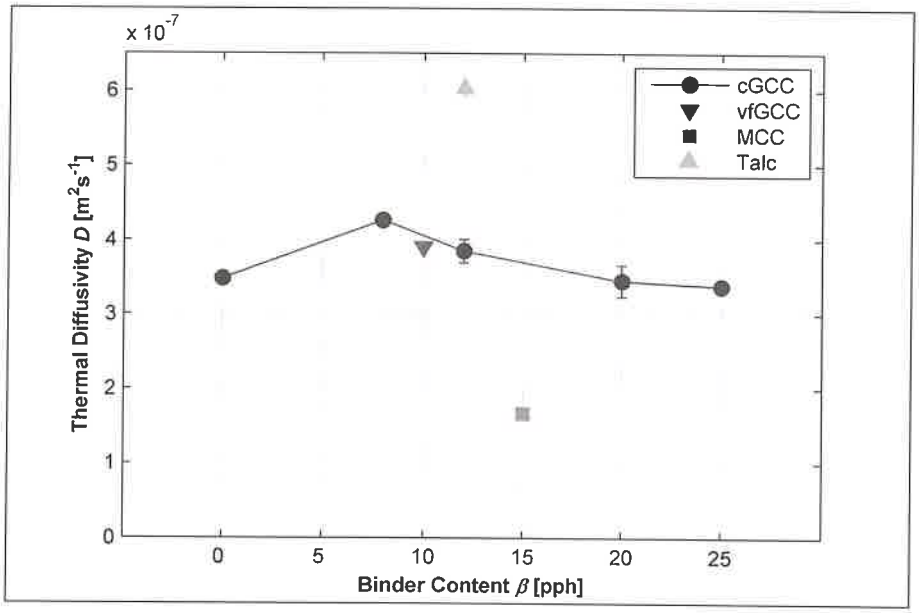


Figure 7: Thermal diffusivity as a function of binder content for the vfGCC, modified calcium carbonate (MCC) and talc. For comparison, diffusivity of a coarser GCC (cGCC) pigment from a previous study [Gerstner et al., 2008] is given

The modified calcium carbonate shows a very low thermal diffusivity, but in addition it should be noted that its density is roughly half that of the vfGCC. However, by taking the corresponding heat capacity of these materials (compare Table III) it results in a substantially smaller thermal conductivity for the MCC. It is remarkable that the structural properties of two particle systems, having particles of the same inherent solid phase thermal conductivity can lead to a difference in structural thermal conductivity, in this case, by a factor of five.

3.2 Toner adhesion

Figure 8 shows the results of the tape test for toner adhesion. First of all it should be noted that a commercial laser printer was used and these are normally designed to work on a great number of different paper substrates, and thus apply high fusing temperatures and run sufficiently slowly to ensure toner adhesion. The 95% confidence intervals are narrow enough, however, to discuss differences in toner adhesion. It should also be added that a large part of the variation in the toner adhesion measurement does not come from a variation in toner adhesion itself but from the originally high variation in print density related to uneven printing properties in the experimental setup of the printer used. In general we see on the left side of Figure 8 that calendering improves toner adhesion on all the given papers, regardless of whether it is on grey or black printed areas. However, the extent of the improvement varies significantly. The biggest improvement due to calendering is observed for the MCC coated sheets. Toner adhesion on black printed areas of calendered sheets is very good for all grades, but is distinctly lower on grey printed areas. On the uncalendered grades, toner adhesion on black areas varies more, but is also higher than on grey areas of the corresponding grade. Again the MCC grade shows a large difference, but even more striking is the uncoated base paper.

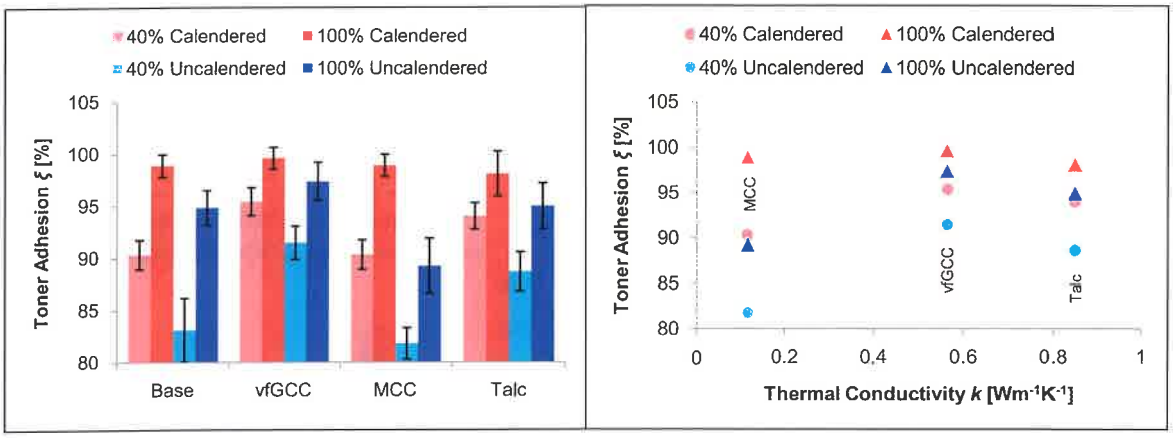


Figure 8: Left: toner adhesion and 95% confidence intervals for base paper and laboratory coated sheets. Toner adhesion was measured on 40% black printed areas as well as fully black printed areas for calendered and uncalendered sheets. Right: toner adhesion on the coated sheets plotted against thermal conductivity of the coating layer calculated from the diffusivity measurement of the tablet material

The lowest values for toner adhesion are observed on the grey areas of uncalendered MCC sheets. Figure 9 shows a magnified surface image of this sample. The left side displays the surface before and the right side after the tape test. This figure is used as an example to identify three basic phenomena of toner adhesion failure.

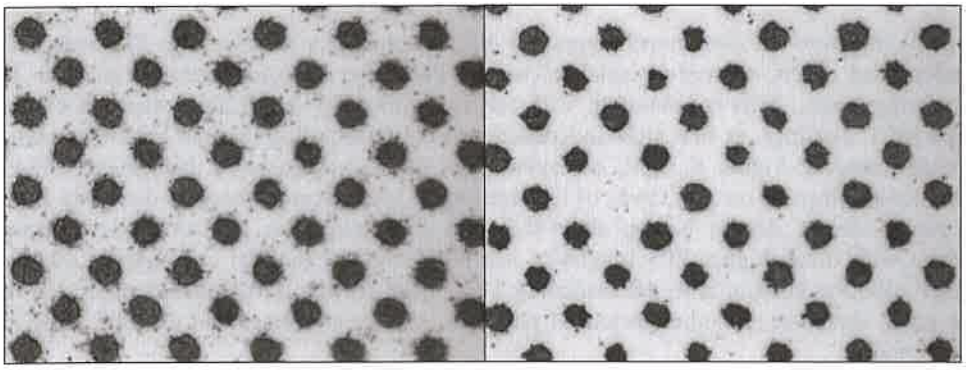


Figure 9: Surface image of a 40% black printed area on uncalendered MCC coated paper before and after the tape test, respectively. The dot size before the tape test is ca. 120 µm

At first it can be seen that the interspersed toner "dust" in between the dots is almost completely removed by the tape. The second effect is a reduced dot size or partially broken dots. Thirdly, there are even a few missing dots. These phenomena explain to some extent the generally lower toner adhesion on grey areas. On an evenly black printed area the working surface for the tape is greater per unit force, in contrast to a grey area where the dots provide additional possibilities for the tape to pull out toner. This also explains the consistently high toner adhesion on black for all the calendered papers. The full-tone printed area is a more even layer, and thus any toner pulled out by the tape is more likely to have to overcome cohesive failure in the toner layer before manifesting low toner adhesion to the substrate.

The right side of Figure 8 shows the toner adhesion versus thermal conductivity. Although in the medium range of thermal conductivity, the vfGCC coated sheets show generally better toner adhesion. So, before we can draw any conclusions in relation to thermal properties in practice, we need to consider what we mean by surface roughness more closely.

3.3 Effects of substrate roughness and packing density

Surface roughness is considered to be an important parameter for toner adhesion [Sipi, 2001], and so it is necessary here to decouple its effect from that of other surface phenomena, such as thermal conductivity and

surface chemistry. The uncalendered substrates indeed show greater toner adhesion failure even on black printed areas. Surface roughness measured by PPS is given on the left side of Figure 10. For calendered sheets we see, as discussed before, that toner adhesion on black areas is good even though the PPS roughness varies. The fusing is apparently quite complete and the closed black surface doesn't allow the tape to pick out toner to the extent that would lead to a measurable print density loss. On grey areas, toner adhesion varies more.

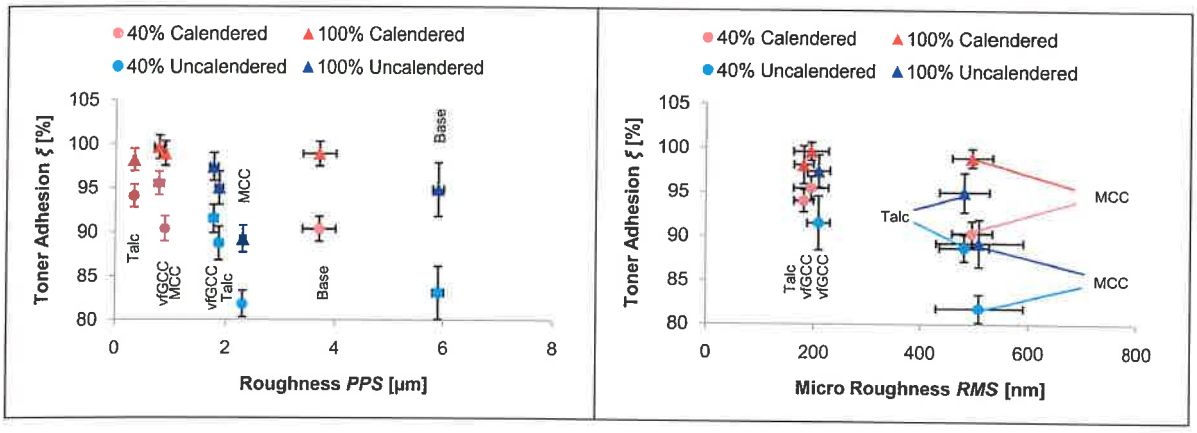


Figure 10: Left: toner adhesion as a function of PPS roughness including 95% confidence intervals. Right: toner adhesion of calendered coated sheets as a function of RMS micro roughness measured by CLSM including 95% confidence intervals

Figure 10 (left) indicates no clear trend across the different surfaces in respect to PPS roughness. For the coated uncalendered sheets, viewed in isolation, we see that toner adhesion increases more or less linearly with surface smoothness. This is consistent with earlier findings by Sipi [2001] and can explain why the uncalendered MCC coatings, at first sight independent of their insulating thermal behaviour, result in lower toner adhesion (compare Figure 8, right, and subsequent thermal discussion). Nonetheless, Figure 10 also indicates that toner adhesion on grey areas of the calendered MCC coated sheets is distinctly lower than that of vfGCC coated sheets, despite having about the same PPS roughness, and even more importantly, the uncoated sheet with much higher PPS roughness and similarly low thermal conductivity (Table) displays superior toner adhesion compared to the insulating MCC even for the uncalendered surface in the full tone area. There must, therefore, be other factors at play than surface roughness on the PPS scale and average thermal conductivity.

The right side of Figure 10 shows that because of the very porous structure of the MCC coating, its surface retains a significantly higher micro roughness after calendering compared to vfGCC, as seen in the CLSM. We see, therefore, that micro roughness, even at high levels does not define the toner adhesion per se. This is logical since it is much finer in scale than both the printed dot (120 000 nm) and the toner agglomerate particle size itself (~15 000 nm). The main difference between uncalendered and calendered surface is then the density of the sheet, and thus its micro structural effects on electrical charge and its related thermal conductivity, as predicted by Maxwell [1873].

It is so derived, therefore, that there is a critical coating density, or better described as surface continuity, independent directly of surface micro roughness, required for good toner adhesion, below which the dielectric and thermal conductive components of the coating are too low.

3.4 Effects of thermal properties of the coating layer

The two dimensional finite element simulation of a fusing nip can be used to discuss the effects of the thermal properties of the coating layer on the dynamic temperature conditions in the fusing nip. As described in the introduction of the method, merely the thermal properties of the coating layer are changed in this simulation. All dimensions, as well as the material properties of toner and base paper are kept constant, as previously described. Figure 11 shows the temperature-time responses at the given position x = 5 mm (middle of the simulated substrate length) for the printer configuration NP-I. The left side shows the temperatures between toner and coating layer, the right side the temperatures between coating and base paper.

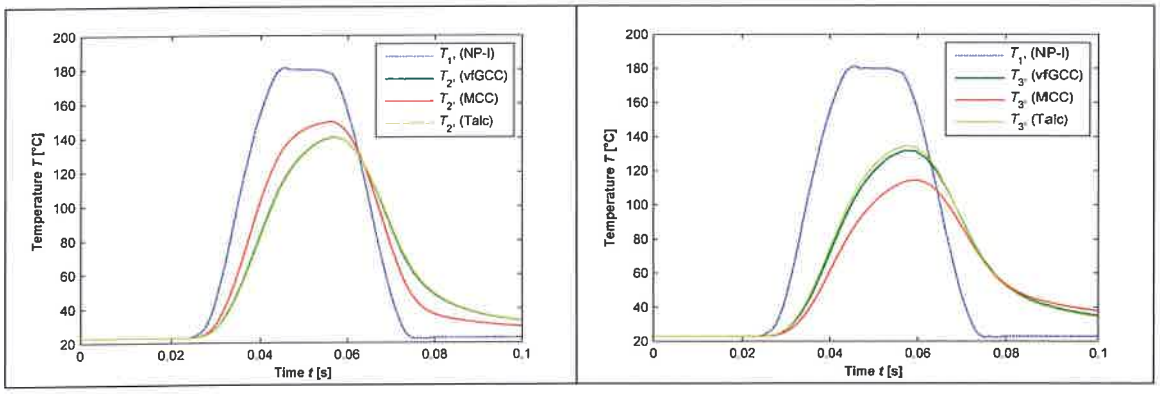


Figure 11: Left: temperature-time responses beneath the toner layer (T_2). Right: temperature-time responses beneath the coating layer (T_3). Both figures are given for the position x = 5 mm on the substrate for the printer configuration NP-I

It can be observed that, despite their different thermal diffusivity, both the vfGCC and the talc coating show very similar calculated temperature responses at both interfaces. However, the MCC coating displays different behaviour. The temperature T_2 rises notably faster at the interface between toner and coating on the MCC coated surface, whereas at the base paper-coating interface the temperature T_3 is affected much slower. Therefore, the MCC layer, with its rather low thermal conductivity, acts as a thermal insulator in front of the base paper, but, also, importantly provides a rapid surface temperature rise and a higher maximum temperature in contact with the toner. From the viewpoint of energy efficiency, the shielding properties of the MCC layer can be seen as an advantage. At a given time in the printing nip, the heat does not penetrate so deeply into the substrate structure; the energy remains more at the interface of toner and coating. As a consequence, the surface temperature rises quicker, which provides potential for improvement in either printing speed or optimisation of the heating temperature of the fuser roll. Both of which are important factors for the print economy.

Given the criterion above, regarding the requirement of sufficient surface continuity in relation to pigment packing density, the insulation effect, though positive, should be achieved by limiting pigment particle size or by compressing the layer sufficiently to achieve the required packing density. Alternatively, a dense thin top layer, of sufficient thermal conductivity, could be additionally employed.

3.5 Comparison of printer configurations

To illustrate the energy saving potential of insulating coatings, Figure 12 shows the temperature responses for two proposed model "improved" printers NP-II and NP-III on an MCC coated substrate (left) and on a vfGCC coated substrate (right). As discussed earlier, a talc coated substrate would show very similar behaviour as the vfGCC coated one does. Especially for the printer NP-III (higher printing speed) the benefits of the thermally insulating MCC coating can be seen. The temperature at the interface of toner and coating layer (T_2) rises quite quickly up to 140°C. Therefore, the temperature of the entire toner layer is higher than this, allowing the toner to melt readily. At the same time, the temperature at the base paper interface (T_3) never goes above 100°C. This prevents unnecessary energy losses into the base paper and in addition it might also help to avoid curl induced by an uneven moisture profile, which can be a result if parts of the base paper temperature rise above the vaporisation point of water. On the right side of Figure 12 we see that, because the vfGCC coating structure is less insulating, the temperature gradient within the coating is quite small compared to the MCC coating. It is also small compared to the temperature gradient in the toner layer. Therefore, both the beneficial effects, as discussed for the MCC, are reduced for the finer denser product (vfGCC). The temperature, especially in the lower region of the toner layer, is lower, and part of the base paper temperature rises above 100°C.

The net heat flux into the substrate, and therefore the specific energy per unit area depends not only on the printer configuration, but also on the thermal properties and the resulting temperature gradient of the substrate. Table gave the specific energies for the printer configurations exemplified on the MCC coated substrate. It was seen that the specific energy is very similar for both NP-II (7.48 kJm^{-2}) and NP-III (7.35 kJm^{-2}). Calculations for the same printer configurations on the vfGCC coated substrate reveal that the energy amount penetrating into

the structure is higher than in the MCC case, i.e. 9.72 kJm^{-2} and 9.55 kJm^{-2} for NP-II and NP-III, respectively. This further illustrates that, if the coating is more conducting, then not only is the temperature gradient within the substrate less favorable for the process of fusing but also the consumed energy is higher. As a result, an insulating coating layer can therefore help to concentrate the energy at the place where it is more beneficial for both the process and the substrate, provided, as stressed above, the surface thermal continuity (coating linear density level) is guaranteed.

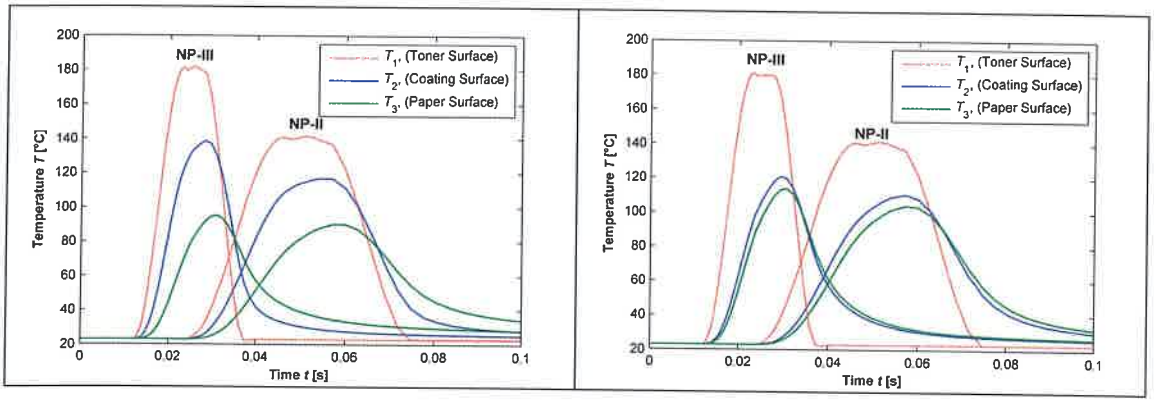


Figure 12: Temperature-time responses on MCC (left) and on vfGCC (right) coated substrate for the printer with reduced fusing temperature NP-II and the faster printer NP-III

4. Conclusions

In this work, the thermal diffusivity of three different mineral pigment paper coating formulations was measured using tablet-making techniques. Their thermal conductivities were then calculated using literature data of the involved materials. By using the thermal properties of toner, the measured coating formulations and base paper, it was possible to simulate the transient temperature responses upon, within and below the coating layer of the respective coated papers in an electrophotography fusing nip. The simulation showed that the insulating behaviour of the coating layer of a high volume modified calcium carbonate causes a faster temperature response and a higher average temperature on top of the coating layer, while the temperature below the coating rises slower. For toner fusing, this seems to be a desirable behaviour because the thermal energy concentrates on top of the coating where it is required for the fusing process and, at the same time, the base paper is shielded. However, it was shown that the micro roughness on both the calendered and uncalendered surfaces of a coated paper having a special insulating coating layer, containing highly porous modified calcium carbonate (MCC), was similar and significantly higher than the other coated surfaces. Nonetheless, toner adhesion in full tone areas on the calendered surface was equally good. For good toner adhesion, a smooth and even surface is a known prerequisite, but this work shows newly that a surface continuity or sufficient packing density is also required, such that an optimal coating for an electrophotography printing paper should have both a thermally insulating coating layer and sufficient coating pigment packing density. This latter effect can be related to pigment particle size. Calendering the low density insulating MCC coating, having a particle size weight median at least twice that of the other tested pigments, was shown to suffice in providing the required packing density for good toner adhesion in the full tone areas, but less so in the half tone areas. Additionally, an ultra thin thermally conducting layer could, in principle, be applied on top of such a highly porous insulating layer to provide sufficient lateral thermal continuity for improved half tone area adhesion. Further studies on toner adhesion are required in order to define the limits on packing density in relation to lateral continuity of conductivity at the coating surface more thoroughly.

Acknowledgements

Grateful thanks are given to Omya Development AG for its continuing financial support of this work. A particular thanks also to Dr. Cathy J. Ridgway, Senior Scientist at Omya's R&D Laboratories, Oftringen, Switzerland, for her expertise and support in assisting in the sample preparation. Thanks also to Timo Hartus at TKK for his assistance in the print testing.

References

1. *Gane, P. A. C., Ridgway, C. J., Schölkopf, J., Bousfield, D. W.,* (2006), Heat Transfer through Calcium Carbonate-based Coating Structures: Observation and Model for a Thermal Fusing Process, Paper presented at the International Printing and Graphic Arts Conference, Cincinnati, Tappi Press
2. *Gerstner, P., Paltakari, J., Gane, P.A.C.,* (2007a), A Lumped Parameter Model for Thermal Conductivity of Paper Coatings, Advances in Printing and Media Technology, Vol. XXXIV, Acta Graphica Publishers, Zagreb, pp. 115 - 121
3. *Gerstner, P.,* (2007b), Heat Transfer Through Paper Coatings, M.Sc. Thesis, Helsinki University of Technology, Espoo, Finland
4. *Gerstner, P., Paltakari, J., Gane, P. A. C.,* (2008), Measurement and Modelling of Heat Transfer in Paper Coating Structures, Proceedings of the 10th TAPPI Advanced Coating Fundamentals Symposium, Montréal, Canada, pp. 300 - 314
5. *Hartus, T.,* (2001), Adhesion of Electrophotographic Toner on Paper, Graphic Arts in Finland, 30, 3, pp. 14 - 19
6. *Kartovaara, I., Rajala, R., Luukkala, M., Sipi, K.,* (1985), Conduction of Heat in Paper, Paper Making Raw Materials, Trans. 8th Fundamental Research Symposium, Oxford, Mechanical Engineering Publications Ltd, London, pp. 381 - 412
7. *Landolt-Börnstein,* (1980a), Zahlenwerte und Funktionen, Band IV Technik, 4. Wärmetechnik a, 6. Auflage, Heidelberg, 1980
8. *Landolt-Börnstein,* (1980b), Zahlenwerte und Funktionen, Band IV Technik, 4. Wärmetechnik b, 6. Auflage, Heidelberg, 1980
9. *Mark, J. E.,* (1996), Physical Properties of Polymers Handbook, American Institute of Physics, Woodbury, New York
10. *Maxwell, J. C.,* (1873), A Treatise on Electricity and Magnetism, Clarendon Press, Oxford, p. 365
11. *Mitsuya, T., Kumasaka, T., Fujiwara, S.,* (1991), Study of Toner Melting Conditions during Flash Fusing, Optical Engineering, 30, 1, pp. 111 - 116
12. *Mitsuya, T., Kumasaka, T.,* (1992), Heat Transfer and Toner Melting in an Electrophotographic System, Journal of Imaging Science and Technology, 36, 1, pp. 88 - 92
13. *Ridgway, C. J., Gane, P. A. C. and Schoelkopf, J.,* (2004), Modified Calcium Carbonate Coatings With Rapid Absorption and Extensive Liquid Uptake Capacity, Colloids and Surfaces A, 236(1-3), pp. 91 - 102
14. *Sipi, K. M.,* (2001), Toner Layer Structure and Toner Adhesion on Coated Paper, NIP17: international conference on digital printing technologies, Fort Lauderdale, FL, USA, 30 Sept.-5 Oct. 2001, pp 145 - 150
15. *Williams, E. M.* , (1984), The Physics and Technology of Xerographic Processes, New York, p. 256



Highly accurate material characterization of paper for the simulation of printing processes

Thomas Kaulitz, Edgar Dörsam

Technische Universität Darmstadt, Institute for Printing Science and Technology
Magdalenenstraße 2, 64289 Darmstadt, Germany
E-mail: kaulitz@idd.tu-darmstadt.de

Abstract

Precise and reproducible measurements from characterization of material are the basis of a good simulation of the printing process. Paper has not yet been properly analyzed in engineering terms in this regard. It is known that paper displays an orthotropic material behavior in the three primary directions MD, CD and ZD. The existing measurement data found in the literature cannot be designated as confirmed. Only the uniaxial tensile tests in the MD and CD direction are completed.

Moreover, there is unclarity of the relationship between tensile and compressive loads in the material.

This article is limited to the characterization of paper in the MD direction. It shows that the material behavior of paper is not identical under a tensile and compressive load. Measurement techniques and a classification system are proposed for generating reproducible and highly precise measurement results. The need for such investigations is illustrated by a practical example: The determination of the conveying speed of a roll with a paper web looped around.

Keywords

Experimental, force-deformation behavior MD, paper

1. Introduction

The computer simulation of printing processes is gaining in importance for the development of new printers and printing processes. On the one hand, the simulation technique saves valuable time in development, on the other it permits a better analytical understanding of the actual processes. Besides the software and the simulation, the quality of the material parameters is of decisive importance for the quality of the achieved results.

Paper as a material of the printing process has been very inadequately characterized by measurement technologies for computer simulations. Here by the organic constituents and the complex structure of paper represent the greatest challenge.

Because of its geometric structure, paper may be regarded as a 3-dimensional network of fibers. In these the cellulose and/or lignin fibers, usually of vegetable origin, as well as the additives and accessory materials used for refining purposes are arranged irregularly. Due to this nonuniformity of structure of a paper sheet a strongly pronounced force-deformation behavior is developed in three directions. These three main directions are: The travel direction of the machine (MD direction), the cross direction (the direction transversely to the travel direction of the machine (CD direction)) and the direction of the thickness is named (ZD direction).

In the literature extremely different measurement-technical solutions are found for the experimental determination of this force-deformation behavior which depend on the type of load and the direction of the load. The geometric dimensions and the highly nonlinear force-deformation behavior of paper make it possible to determine the force-deformation curves for the individual load directions only under high measurement-technical expenses.

Conflicting results are obtained especially in the experimental analysis of the load when it changes from the pulling direction to the pushing direction. Studies have shown a region of unsteadiness that cannot be explained by existing mechanical knowledge. Only tensile tests have been performed frequently. Assuming the material behaving under compressive loads, the results of the tensile tests are extrapolated to the origin.

In the experimental studies published on the compression behavior, the investigation is largely confined to determining the failure values, i.e. no relationship between stress and strain is pictured. In the studies where the stress-strain behavior was investigated more closely, stress-strain curves and zones of unsteadiness are shown that cannot be explained by current knowledge in the field of material mechanics.

Absent or mutually strongly deviating national and international standards have had the result that the force-deformation curves determined in the literature are not comparable or can not be considered to be confirmed.

Literature researches show no comprehensive investigation of the force-deformation behavior which has been performed. Table I gives an overview of the published studies on this subject, which will be referred to in this article.

Table I: Literature research for the material characterization of paper

research results force-deformation behavior author	MD - tensile	MD - compression	CD - tensile	CD - compression	year of publication
unidimensional tests					
Göttsching					1970-71 /1/2/
Brecht					1963 /3/
Paetow et. Al.					1989-1991 /4/5/
Rauhut					1991 /6/
Oltrogge					1992 /7/
Haraldsson					1994 /8/
Westerlind					1991 /9/
Höke					1983-1985 /10/11/
Knoll					2001 /12/
Golz					2002, 2003 /13/14/
multidimensional tests					
Fellers et. Al.					1981, 1983 /15/16/
Gunderson					1983 /17/
Paetow					1991 /5/
Tryding					1994 /18/
Xia					2002 /19/
Hammelmann					2004 /20/
Wolf					2005 /21/]

The primary goal of this research project at the Institute for Printing Science and Technology is to expand the knowledge base on the force-deformation behavior of paper and make it usable for simulations in the future. In order to illustrate better the necessity of this research project and to give the rather abstract studies a relationship to practice the following example will be provided concurrently.

A continuous paper web is looped around a roll (Fig. 1). The roll will be of zero mass ($m = 0$) and considered to be non-frictional ($\mu = 0$) to keep the example as simple as possible. The circumferential/peripheral velocity v_0 of the roll is known.

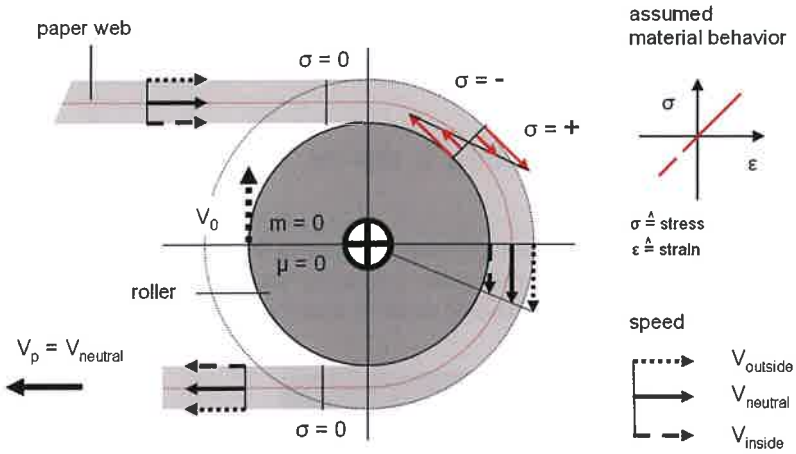


Figure 1: Example of a roll with paper looped around

In practice the question frequently arises: at what speed is the paper moving if the peripheral velocity of the roll is known? This apparently simple problem is not at all as trivial as it first appears; it is also very closely related to the material behavior of paper.

As an approach to a solution, the kinematic functions of a looped-around roll can be utilized. The paper web is forced from its rectilinear path onto a circular path around the roll.

At this time the material of the paper experiences a bending stress with a compressive stress on the inner web and a tensile stress on the outer web. At the transition between these two states of stress the stress is zero. This zone is called the neutral fiber in mechanics. On the assumption of identical material behavior under tensile and compressive stress, the neutral fiber is in the center of the paper web.

The neutral fiber designates that fiber on the paper web that is not subjected to stretching due to the looping. Or expressed in different terms, the points on the neutral fiber have the same velocity everywhere.

Based on these kinematic functions, by using the radius on which the neutral fiber is located, the velocity of the paper web can be determined.

This example is based on the assumption that the paper web behaves the same under tensile and compressive loads. There will be different results if the assumption I not like this. According to the experimental studies and their results, at the end of this article this problem will be discussed again and the results will be extrapolate obtained to the example.

2. Methods

Within the scope of this report, the force-deformation behavior of paper under standard uniaxial loads is determined for three different varieties of paper and cardboard.

The papers analyzed belong to the main groups of printing and newsprint/office and administrative papers. Table II shows the varieties of paper selected.

Table II: Selected paper varieties

Identification	Description	Grammage
M-real, Tauro	Classic offset-paper, uncoated paper, matt finish, woodfree paper	100 g/m^2
Myllykoski, Inapa Bavaria	Art paper, two-side coated paper, glossy, finely woody	135 g/m^2
Scheufelen, Phoenix Imperial II/II APCO	Natural white art paper, two-side coated paper, glossy, woodfree paper	150 g/m^2

To eliminate the effect of weather conditions of the environment on the mechanical force-deformation behavior the experimental studies were performed under standardized climatic conditions. The climate is specified in DIN 50014 and prescribe a range of 23 ± 0.5°C for the temperature and a range of 50 ± 1.5% for the relative humidity.

The samples were preliminarily treated according to DIN EN 20187 in order to assure an equal moisture content in the various items delivered.

To assure a representative average for the results being determined the samples were taken from the delivered items with consideration of DIN EN ISO 186. After collecting the samples the dimensions of the samples were subjected to an additional test for dimensional stability and not existing defects.

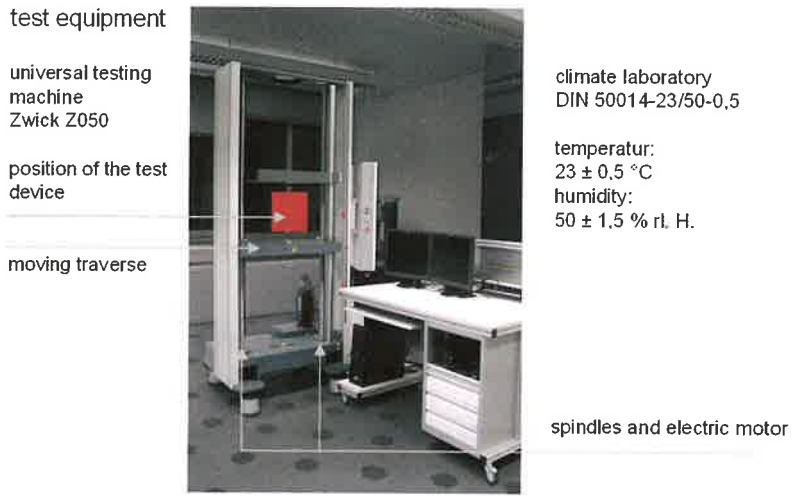


Figure 2: Zwick Z050 universal testing machine in the climate-controlled laboratory

A universal testing machine by the Zwick Co., type Z050 (Fig. 2) was used for the experimental studies. The main components of this test machine are two spindles driven by an electric motor driving a traverse vertically. When the traverse is driven, covered the path is plotted by using a glass measuring rod directly on the sample with a resolution of 50 nm. A dynamometer is situated in the center of the traverse to register forces of up to 1 kN. According to the manufacturer's data the resolution of the dynamometer is ± 0.2% of the indicated measured values. There are recesses for installing the sample holders on the dynamometer and on the baseplate of the testing machine.

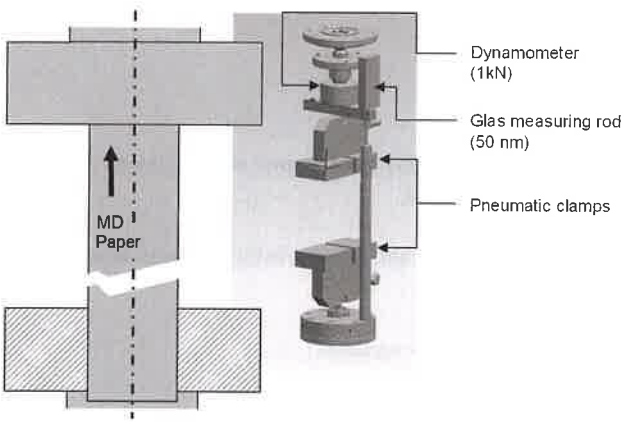


Figure 3: Sample holder 1 for tensile tests in the MD direction

The actual core of the experimental studies are the two positioned sample holders. The two sample holders for studying the loads in the MD direction are designed essentially for use in the measurement procedures described in the standards DIN ISO 1924-1 and - 2 and DIN 53134. They were optimized only by making minor modifications.

Sample holder 1 for tensile tests in the MD direction (DIN ISO 1924-1 and -2)

The sample is pneumatically clamped with clamping jaws in the sample holder in the ZD direction. The length between the sample holders is 180 mm and the width of the sample is 30 mm. Additional holders assure that the sample is mounted vertically in the center.

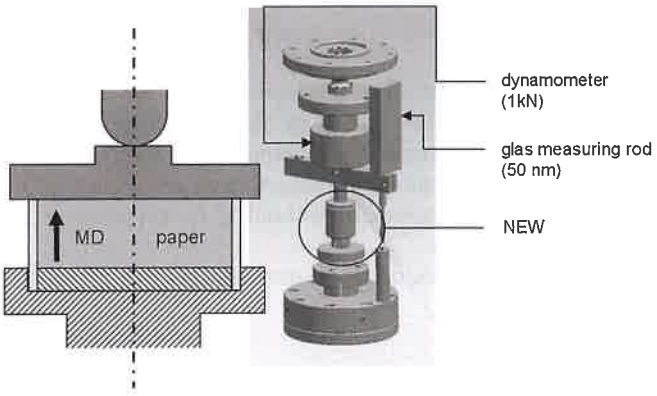
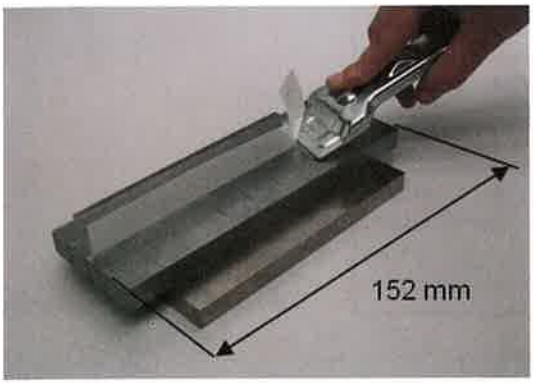


Figure 4: Sample holder 2 for compression tests in the MD direction

Sample holder 2 for pressure test in the MD direction (DIN ISO 53134)

The sample holder is known by the name ring crush test. The exactly cut-to-size sample with the dimensions 152 x 12.7 mm is inserted in a depression of circular shape in the lower sample holder. The counterpiece a floating-mounted plate presses on the upper edge of the strip. The preparation of the sample is an important detail in this case. The samples can only be prepared at high expenses. For this purpose we developed our own blank cutting device at the Institut for Printing Machines and Printing Processes.



new trimming system

Figure 5:
Plane-parallel plates for the blank

The core of the newly developed blank cutter are two plane-parallel plates (Fig. 5) displaying parallelism of ± 1 µm over a length of 152 mm. The sample is clamped between these plates and cut with a very sharp blade. The cut in this case runs rotated by 90 against the alignment of the otherwise conventional blank cutter.

This material characterization is performed by monotonic, force-controlled tests. In preliminary tests it was determined that even at the shortest loading times of the paper it is possible to measure viscous elongation degrees. In order to achieve comparable results identical elongation rates are assumed for the loading and unloading. The elongation rate corresponds to the speed of the traverse divided by the distance between the clamps.

3. Results

The studies of the normal loads in primary direction are qualitatively summarized in the following. Figure 6 shows the measurement data obtained for material characterization.

Under uniaxial normal loads, all curves of stresses and the corresponding elongations/strains have a nonlinear relationship. All tensile loads display a degressive curve. A degressive curve may also be recognized for the compression loads in the MD direction.

The viscoelastic properties of paper are recognizable. The recommendations given in a series of scientific works assuming the material behavior of paper as purely linear up to an elongation of 0.2 %, are acceptable. The ratio of the calculation effort to the accuracy of the results is a good compromise in this case.

The transition from tension to pressure loads upon the switching of the load is clearly recognizable. This shows that the force-deformation behavior of paper in the MD direction differs under a tensile and compression load. While maintaining the above-noted maximal elongation of 0.2 % two moduli of elasticity can be determined; one for tensile stress and one for compressive stress.
Occurring errors in other measurements are presumably caused by the preparation of the samples.

If these results are extrapolated to the example of the looped-around rolls provided in parallel is showing in the following figure (Fig. 7).

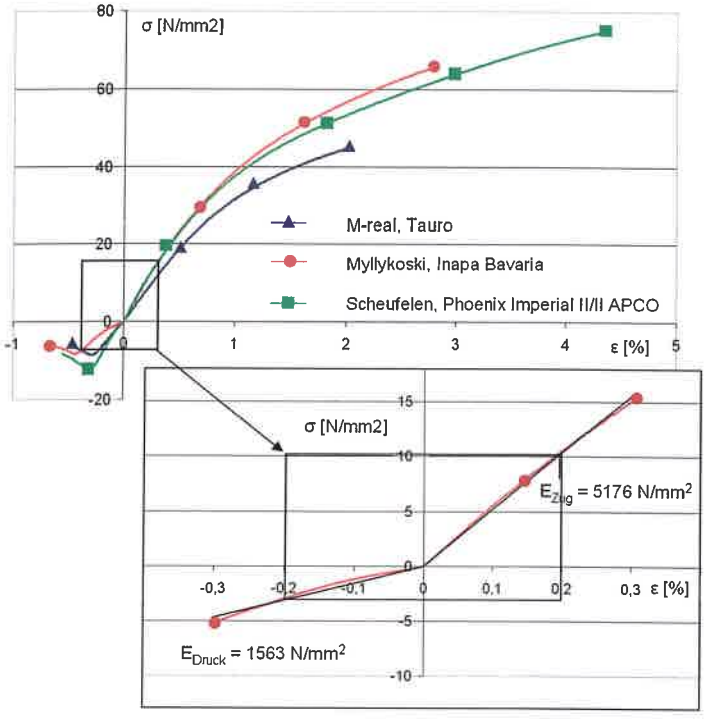


Figure 6:
Results of the material characterization

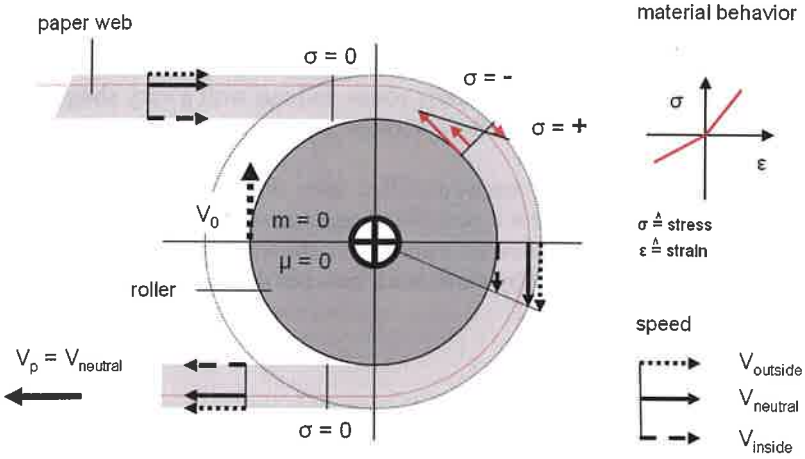


Figure 7:
Example of a roll with paper web looped around

The material behavior important for the conveying behavior has been characterized to the extent that the pronouncements regarding conveying speed of the paper web can be stipulated with high precision.

Due to the variable force-deformation behavior under tensile and compressive loads, the neutral fiber is shifted out of the center to the outer marginal zone of the paper web. In contrast to the generally accepted assumption, this causes a higher resultant speed for the paper web for the same tensile and compressive behavior.

This phenomenon is erroneously called "slip" in the literature and in everyday usage. However, this has nothing to do with the definition of slip. A purely kinematic problem is involved that depends exclusively on the material behavior of the paper web.

4. Outlook

The studies in general are not concluded. The shearing loads and the loads in several axes must also be analyzed, especially the combination of normal and shearing loads. Testing devices required for these tests are already developed.

The results acquired with material-mechanical modelling techniques can also be described physically. These physical descriptions can then be embedded into the existing simulations.

References

1. Göttsching, L.: Das Festigkeitsverhalten von Papier unter statischer und dynamischer Beanspruchung, Teil 1 Paperi ja puu, no. 7, pp. 535-542, no. 10, pp. 655 - 669, no. 11,pp. 781-794 ,1970
2. Göttsching, L.: Das Festigkeitsverhalten von Papier unter statischer und dynamischer Beanspruchung, Teil 4 Paperi ja puu, no. 1, pp. 27 - 36, 1971
3. Brecht, W.: Über neue Messungen zur Kompressibilität von Papieren Das Papier 17, no. 10a, pp. 626 - 634, 1963
4. Göttsching, L.; Paetow,R.: Das Papier als berechenbarer Werkstoff Das Papier 43, no. 6, pp. 229 - 236, 1990
5. Göttsching, L.; Paetow, R.: Über das Spannungs-Verformungs-Verhalten von Papier Dissertation, Technische Hochschule Darmstadt, 1991
6. Rauhut, M.: Dehnungseigenschaften von Papier Diplomarbeit, Technische Hochschule Darmstadtn1991
7. Oltrogge, K. P.: Entwicklung einer neuen Messmethode zur Bestimmung des Stauchverhaltens von Papier und Karton in X- und Y-Richtung Diplomarbeit, Technische Hochschule Darmstadt, 1992
8. Haraldsson, T.; Fellers, C.; Kolseth, P.: A Method for Measuring the Creep and Stress-Strain Properties of Paperboard in Compression Journal of Pulp and Paper Science 20, no. 1, pp. J14-J20, 1994
9. Westerlind, B. S.; Leif, A. C.: Compressive Response of Corrugated Board Proceedings of the International Paper Physics Conference, pp. 641 - 645, 1991
10. Göttsching, L.; Höke, U.: Stauchprüfungen von Wellpappenrohpapieren und ihr Bezug zu Wellpappen- und Schachteleigenschaften Das Papier 37, no. 10a, pp. V67 - V76 1983
11. Göttsching, L.; Höke, U.: Stauchfestigkeit von Papier, Wellpappen und Schachteln Das Papier 39, no. 10a, pp. V65 - V73 1985
12. Knoll, P.: Experimentelle Ermittlung der Werkstoffeigenschaften von Papier Diplomarbeit, Ruhr-Universität Bochum, 2001
13. Golz, J.: Experimentelle Analyse der Biegesteifigkeitsverluste von Karton Studienarbeit, Ruhr-Universität Bochum, 2002
14. Golz, J.: Theoretische und experimentelle Analyse des Kraft-Verformungs-Verhaltens von Papier Diplomarbeit, Ruhr-Universität Bochum, 2003
15. Fellers, C.; Westerlind, B.; Ruvo, A.: Aninvestigation of the biaxial failure envelope of paper Proceedings of 7th Fundamental Research Symposium, pp.527 - 556, 1981
16. Fellers, C.: Paper properties in compression In: Handbook of Physikal and Mechanical Testing of Paper and Paperboard, Marcel Dekker Inc., New York, 1983
17. Gunderson, D. E., Rowlands, R. E.: Determining paperboard strength - Biaxial Tension, Compression and Shear Tappi Proceedings, Paper Physics Conference, pp. 253 - 263, 1983
18. Tyring, J.: A Modification of the Tsai-Wu failure criterion fort he biaxial strength of paper Tappi Journal, no. 8, pp. 132 - 143, 1994

19. Xia, Q. S.; Boyce, M. C.; Parks, D. M.: Mechanics of inelastic deformation and delamination in paperboard, A constitutive model fort he anisotropic elastic-plastic deformation of paper and paperboard International Journal of Solids and Structures 39, pp. 4053 - 4071, ISSN 0020-7683, 2002
20. Hammelmann, R.: Experimentelle Untersuchung des Versagenverhaltens von Papier unter mehrachsiger Beanspruchung Studienarbeit, Ruhr-Universität Bochum, 2003
21. Wolf, E.: Theoretische und experimentelle Grundlagenuntersuchungen zum Scherschneiden von Papier Dissertation, Ruhr-Universität Bochum, 2005
22. DIN 50014
23. DIN EN 20187
24. DIN EN ISO 186
25. DIN ISO 1924-1 and - 2
26. DIN 53134



3

Special printing

Colour control with dual separation for daylight and daylight/infrared light

Ivana Žiljak[1], *Jana Žiljak Vujić*[2], *Klaudio Pap*[1]

[1] Faculty of Graphic Arts
Getaldićeva 2, 10000 Zagreb, Croatia
E-mail: ivana.ziljak@vip.hr

[2] Polytechnic of Informatics and Design
Vrbik 8, 10000 Zagreb, Croatia

Abstract

Security graphics is an area that requires research and continuous development. The goal is to obtain top-quality security through design, individualization and innovations in graphic technology. In practice up to date security graphics have developed by applying special toners or extreme printing techniques reserved only for security printing, as for instance Infrared toners, UV toners, intaglio printing, steel die printing, security paper, kinegram. Designers usually remain in the area of graphics that are visible in daylight. Securities experts perform additional mixing of colors that alter under UV light. Knowledge on the printing colors IR system is a new area in the printing business. The area of software designing has been opened, purpose designing and coded graphic product security. Studying the characteristics of many colors in IR radiation has started programming of security graphics in a new way. Collaborators in this assignment have developed algorithms of dual separation in the visible RGB system for graphic prepress of spot and process toners using information on light response in the IR area.

Keywords

Colour control, daylight, dual separation, infrared, security graphics

1. Introduction

Printing toners have been designed to reach top quality of color reproduction in the visible area, i.e. from 400 to 700 nm. Many printing toners respond in other areas as well; of lower wave lengths from 100 to 400 nm that is the area of UV wave lengths and higher wave lengths from 700 to 1000 nm which is the IR color area. The subject of our research work are toner characteristics that would respond in other areas as well; - the ones not visible to the human eye, but can be studied by scanning under UV or infrared wave lengths. We can use such toners in places where we want to hide information that is on the print, - carried by the colors. Furthermore, in places where we want to be certain about the print's authenticity, because only the targeted toner design must be identical to the toner that will subsequently be checked in respect to authenticity.

Each toner is observed as the possible one in applying graphic product security or as the beginning of producing a new individual design in the general area of document and securities safety. This study is on color altering depending on the source of light from 254 to 1000 nm and the angle of observing the print. This may be used in proving the authenticity of the print, paper and color. Our approach to security graphics is by using specific characteristics that come out of the possibility of programming for digital printing: print individuality, color mixing programming, multi-layer toner covering, and controlled separation of colors for printing, simultaneous double-side printing.

It is shown that by programming graphic element structure a better quality security may be obtained by applying conventional toners if more is known about their structure. Prior to that there is the analysis of each color and its behavior in the invisible specter part.

2. Research methods

Research work in respect to the characteristics of printing process toners in infrared light has made it possible to determine the translation relations for the same color tone in two areas: the print visible only to the human eye - DL, and the print we se in daylight and under infrared light - DL/IR. The "dual separation" algorithm makes it possible to program part of the print that will appear under IR radiation and will not disturb color tone perception of not a single image element seen in daylight.

The color tone determined by the RGB, HSB and Lab systems may be determined through:

1. $C_0\ M_0\ Y_0\ K_0$ values visible to the human eye (convetional GCR, UCA, UCR method).
2. $C_{-1}\ M_{-1}\ Y_{-1}\ K_{-1}$ values visible to the human eye but invisible in IR wavelengths.
3. $C_1\ M_1\ Y_1\ K_1$ visible to the human eye and visible in IR wavelengths that is more widely seen in wavelengths of the visible specter part as well as the IR wavelengths may be joined with the same color tone.

Visibility under IR light is obtained by adding more of the black component. Color tone maintenance is obtained by decreasing the CMY component value. Each color tone has it own relations in respect to certain CMY values decrease. The $C_m\ M_m\ Y_m\ K_m$ maximum possible response in the IR area is determined for every color tone. The dual separation program uses two images: A and B. The first image is the one we see in its integrity in the visible specter part. The second image is the sample that has the role of a mask. The CMYK separation is controlled on basis of the sample in order to achieve the first image's appearance and rejection in the IR area (Figure 1).

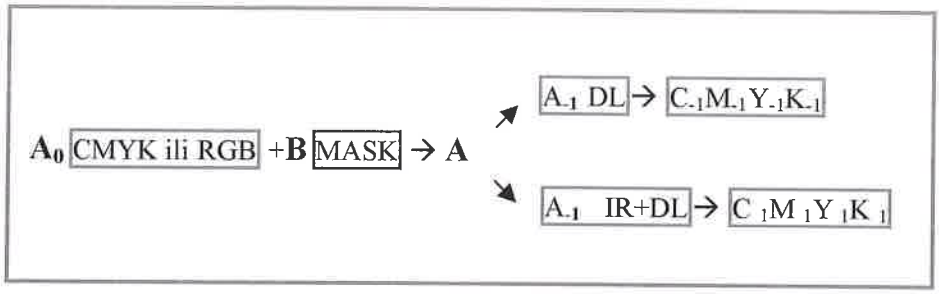


Figure 1: Controlled CMYK separation on basis of the sample for IR effect

CMYK values of each individual pixel of the A_0 image will be separated in A_1(DL/IR) or A_{-1}(DL) depending on the value of the identically positioned pixel in image B. B is the filter determining how certain pixels will respond in the IR area.

The covering capacity of image elements in the Figure 2 is most often equal to null or equal to maximum covering capacity. Each covering capacity value that falls into the space between the two extremes enables contouring of visibility control in the IR specter. Each color tone has its own values of the S angle for CMY components depending on the K component increase. The S_C, S_M and S_Y gradient of each component depends on the $C_0\ M_0\ Y_0$ values that generate the observed color. This paper contains a matrix of gradient coefficients with three independent variables fro each color. Parameter values are determined by linear regression and on basis of print measuring. The once set gradient parameters for a printing technique under observation and the corresponding process colors are the basis for unlimited application of IR control in color images by using only process toners.

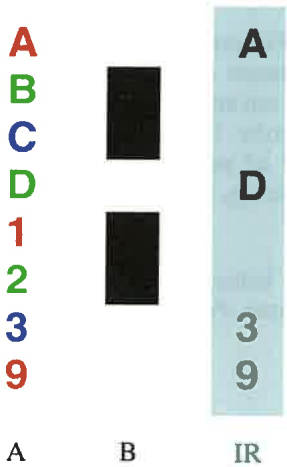


Figure 2:
A:Original; B: Mask; IR:Infrared

Research work has shown that it is possible (taking into consideration acceptable tolerances) to determine mutual relations for a wide specter of coloring (Figure 3) [Žiljak I., Pap K., Žiljak-Vujić J. , 2008-2]. The decrease coefficient and the decrease function of each CMY color is determined by the presence of all four colors.

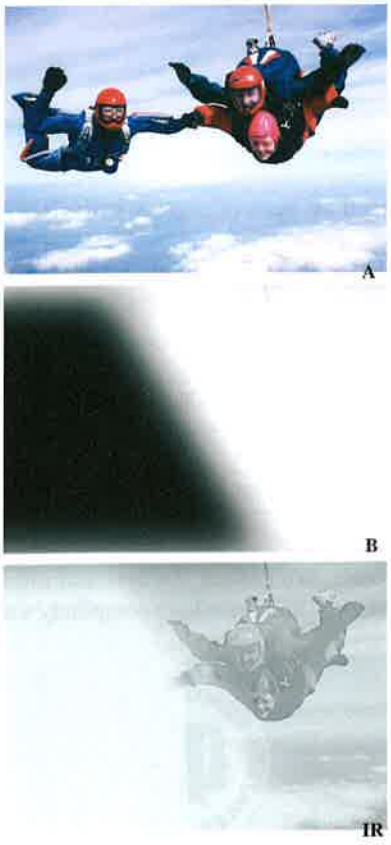


Figure 3:
A:Original, B: Mask, IR:Infrared

Relations behave well within the allowed limits. The first limit is determined by the value null on the black component. The second limit is determined by the moment when one of the CMY components drops to the value of null. That point may be even lower or higher than the value determined on basis of the minimum of a C_0 M_0 Y_0 value, and in cases when the black component equals to null.

Usually the first image is the one we see fully in the visible specter part and the second image is the pattern that has the role of a mask for IR effect [Žiljak I., Pap K., Žiljak-Vujić J., 2007].

3. Results

The novelty in this paper is introducing the "dual separation" algorithm for conventional process toners visible only under daylight (DL) or in the wider areas: DL and IR areas.

The overall solution for the "IR progress" model that would be accepted for a wide range of colors is based on the following relations:

$$K_2 = K_1 - g * K_1^2 \tag{1}$$

where K_1 is the minimum value in CMY tones with the value K = 0. This relation is improvement of decreasing the maximum GCR separation values that is in fact not necessary with tones that have high values in CMY minimums. The parameter g value is from 0.3 to 0.34.

General CMYK transformations are given in the following relations:

$$\begin{aligned} C &= C_0 - (K_2 * Sc) \\ M &= M_0 - (K_2 * Sm) \\ Y &= Y_0 - (K_2 * Sy) \\ K &= K_2 \end{aligned} \tag{2}$$

Where:

$$S_c = a_c C + b_c M + c_c Y + d_c$$
$$S_m = a_m C + b_m M + c_m Y + d_m \quad (3)$$
$$S_y = a_y C + b_y M + c_y Y + d_y$$

Parameters, *a, b, c* and *d* are the results of measuring and determined on basis of regress analysis with values in Table I.

Table I: Parameters, a, b, c and d from regress analysis

	a (at cyan)	b (at magenta)	c (at yellow)	d
S_c	- 0,007116	0,00141	0,000223616	0,899828
S_m	0,002107	- 0,007018	0,003217556	0,586924
S_y	0,004514	0,004109	- 0,006560989	0,488044

On Figure 4 is presented implementation of IR effect on one certificate. We can see daylight and infrared view of this document. Infrared view displays words "fotosoft infrared security" and main logo complitely vanishes.



Figure 4: Daylight and infrared view of a certificate

4. Discussion

The double separation method "Infared Controle" means separation as example of the two neighbouring pixels with two different algorhytms. The first pixel will not include black colour and so it will not be visible in the infrared light. The second pixel will be separated with the maximal black colour and it will be visible in the IR light. If we consider that the both pixels have the same colour tone (the same value in RGB, HSB, Lab) i.e. they have to give the same expression of colour in the daylight, it is obvious that the issue is very sensitive. The realization of the such separation depends on print technology, colours and the paper type.

In this paper we present relationships for the converting CMY K = 0 in CMYK where K is bigger then 0 for the experiments applied on the Xeikon. The attempt was made to define the general relationship which

includes the whole range of colour tones. By this mode, the separation could be done concerning the continous flow of the black colour, depending on the picture which is given the name "mask". As an example the two tones of colour, which differ in a bigger extent concerning the separation with continous increasing of the black component, are presented in Figure 5 and Figure 6. Before each graph are presented systems of equations Eq. 4 and Eq. 5.

$$C = -0{,}00745\ K^2 - 0{,}3100\ K + 40$$
$$M = -0{,}00568\ K^2 - 0{,}2890\ K + 55 \qquad (4)$$
$$Y = -0{,}00296\ K^2 - 0{,}28911\ K + 75$$

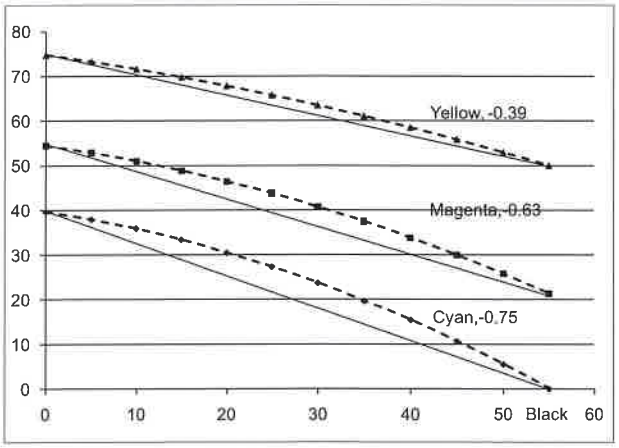


Figure 5: Graph of the color tone CMY: 40%, 55%, 75% with K range [0,55]

The double separation is a very sensitive issue. The conventional separation uses GCR, UCA and UCR methods equally on the whole picture. Until now we have accepted with conformism the quality of printed material. The persons included in this process are: reprophotographer, photographer, graphic artist, editor and the designer. They accepted the responsibility for the first print with the considerable tolerance. The double IR separation consists of the two different methods applied for the each pixel in the different way on the same print; the maximal precision is must have. Human eyes notice even minimal mistake of the non-equal tones on the same picture; these tones were equal in the RGB. For these reasons a lot of work has to be done on the adjusting of the parameters of the double separation, concerning the printing technique on which such protection is applied. Much simplier solutions consist of vector's graphic or application in the typography, with the goal to hide the information.

$$C = -0{,}00152\ K^2 - 0{,}172\ K + 80$$
$$M = -0{,}00136\ K^2 - 0{,}0235\ K + 95 \qquad (5)$$
$$Y = -0{,}00909\ K^2 - 0{,}679\ K + 50$$

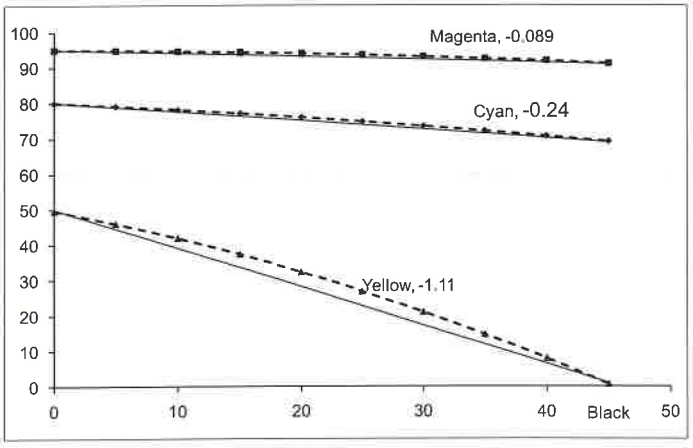


Figure 6:
Graph of the color tone CMY: 80%, 95%, 50% with K range [0,45]

The IR effect has multiple applications. The goal can be set to introduce the original methods of the protection of the graphic products in all printing areas. After printing, the graphic is protected and only the author of applied double separation (designer, editor) can establish the presence of the IR effect. We do believe that no method exists which could decode this continous presence of the IR protection. By scaning, photographing, photocopying or some other decodeing methods is impossible to establish which pixel separated under particular conditions. RGB scaning possesses no posibility of the differing the internal structure of the dosageing of the K component which is responsible for the IR light. We kindly warn the reader of this text that the print in this publication was made by the conventional reproducing and it has no built-in programmed IR effect. Many examples can be obtained by post contacting the authors of this paper.

Application in a multicolor image (a portrait, for instance) makes it possible to incorporate a piece of information visible under IR light which has been derived with the help of a software source, for instance: initials, numeration, drawing and logotype from the database, with stochastic choice with a planned initiator (seed) (Žiljak I., Pap K., Žiljak-Vujić J.,2008-1). Printing with digital techniques expanded the complexity of experimentally produced securities protection and nn a certain sense this made way for a new approach to expanding the topic of preventing counterfeit production (Žiljak I., 2008).

5. Conclusion

The conventional transformation of the RGB system transition into CMYK is carried out according to set GCR, UCA and GCR separation models. A chosen algorithm is set for all image parts, all pixels. The chosen algorithm will show the print in the IR area to a lesser or greater extent. Our research work determines and sets the separation method to control the appearance in the IR area according to the programmed task. This method (let us name it as the *Infra Red Control-IRC*) has two different images at the entrance: color image A and Gray scale image B. Each pixel of image A will have CMYK values depending on the blackening of the pixels in the same position on image B. Certain parts of image A, more precisely "pixels in image A", will respond in the IR area in a proportional value to the blackening value in image B, taking into account also the covering capacity CMYK value of the same pixel in image A. Image B may be defined as "the mask" for the appearance of part of the image in the infrared area regardless of the color tones. In this manner simulation of IR colors is obtained in the whole color system all in the same image. The IRC method begins with image A in the following states: RGB, or CMYK or HSB. The general mathematical model is described with the equation system, the parameters of which are set on basis of measuring prints from digital print.

References

1. Žiljak I. (2008): *Designing for the Infrared Security Printing Area, Tiskarstvo08, Zagreb, Croatia, ISBN 978-953-7064-08-2*
2. Žiljak I., Pap K., Žiljak-Vujić J. (2008-1): *Alternative Infrared Solutions for Security Graphics with Digital Print, 8th International Conference on Security Printing & Alternative Solutions, Ljubljana, Slovenia*
3. Žiljak I., Pap K., Žiljak-Vujić J. (2008-2): *Infraredesign, Scientific Book, Fotosoft, Zagreb, Croatia, ISBN 978-953-7064-09-9*
4. Žiljak I., Pap K., Žiljak-Vujić J. (2007): *Design of security graphics with infrared colours, 39 th Conference of the International Circle of Educational Institutes for Graphic Arts, Technology and Management, Lausanne, Switzerland*

Gravure printing of enzymes and phages

Tarik Jabrane[1], *Jawad Jeaidi*[1,2], *Martin Dubé*[1], *Patrice J. Mangin*[1]

[1] Centre Intégré en Pâtes et Papiers (CIPP), Université du Québec à Trois-Rivières
3351 boul. Des Forges, C.P. 500 Trois-Rivières, Québec, Canada G9A 5H7
E-mail: Martin.Dube@cipp.ca

[2] PAGORA
461 Rue de la papeterie, BP 65, 38402 Saint-Martin d'Hères, France

Abstract

Detection and disabling of biological pathogens such as bacteria and viruses is of great importance to control diseases apparition and to insure the environmental integrity of air, water or food. Due to their flexibility, low cost and ease of fabrication, papers and non-wovens are ideal substrates to support bio-chemical sensors.

In this work, we show that a hydrogen peroxide bio-sensor can be made by gravure printing of horseradish peroxidase enzyme on paper. In particular, we discuss the effect of shear rates on the biological functionalities of the enzyme and show that shear is not large enough to impair large scale industrial printing of this particular enzyme. We also show that phages, viruses that can infect and destroy E. Coli bacteria can effectively be printed on paper.

Keywords

Bioactive paper, gravure, printed functionality

1. Introduction

Complex bio-molecules such as enzymes and proteins can now be directly printed on a support (either rigid or flexible) for applications as diverse as protein analysis [Roda, 2000], DNA sampling [Okamoto, 2000], neural science [Sanjana, 2004] or even tissue engineering [Boland, 2006]. The development of reliable printing techniques based on ink-jet technologies [Di Risio, 2007], microcontact printing [Renault, 2003] or soft lithography (pad printing [Thibault, 2007] has opened extremely rich possibilities for research and already several products are commercialized.

These methods are however relatively slow in terms of production. In some cases, such as epidemic outburst, it may be desirable to have the means to detect and disable biological pathogens on a short time period and to dispose of large quantities of sensors or filters. High-speed printing techniques such as offset, gravure or flexography may then become extremely useful. Furthermore, bio-printing on paper substrates offer several advantages, including their flexibility, low cost, ease of fabrication and recycling properties. However, a major point to be clarified is whether or not fragile biological molecules can sustain the high shear stresses and pressures of the printing process.

In this work, we describe how an enzyme (Horseradish peroxidase) and a T4 phage (a virus that infects *E. Coli* bacteria and makes it harmless) can be printed on a coated paper while retaining their biological functionalities. We first describe in Section 2 the detailed bio-mechanisms and possible commercial applications involving the horseradish peroxidase enzyme (HRP) and the T4 bacteriophage. We also discuss in this section the shear stresses that can be expected in a printing press, as well as the expected response of these molecules under the printing nip. Section 3 details the materials and method used to print and assess the biological efficiency of printing with the results described in Section 4. The main point of the paper is that T4 phages as well as the HRP enzyme can be efficiently printed at high speed on paper, thus opening the way for potential applications.

This work is carried within the Sentinel Network (www.bioactivepaper.ca), a broad collaboration of Canadian universities, research centres and industrial partners which aims to develop the biological potentialities associated with paper, whether as filter papers, bio-sensors or virus deactivators.

2. Bio-products and shear stress

2.1 Horseradish peroxidase (HRP) enzyme

Enzymes are essentially proteins which can act as catalyst in several chemical reactions [Fernandes, 2005; Lei, 2005; Nestorson, 2007; Voss, 2007; Di Risio, 2007]. The specific horseradish peroxidase enzyme (HRP) can be extracted in large quantities at low cost from horseradish root and is commonly used in molecular biology applications, most particularly through its capacity to oxidize (i.e., cause an electron transfer) a large variety of molecules. The HRP enzyme has molecular weight of 44 kDa and a physical volume of about 125 nm^3. The enzyme is fairly stable for temperatures up to 60°C and has optimal activity in an aqueous solution with pH of 6.9.

Role as a peroxide biosensor: In the present work, HRP enzyme is used as a catalyst for the oxidation of 2,2'-Azino-bis 3-ethylbenzthiazoline-6-sulfonic acid (ABTS, A1888, Sigma) by hydrogen peroxide (H_20_2). ABTS is a chromogen (organic colorant) which acquires a green tint in its oxidized form. Combined with colorimetric detection, the HRP-ABTS complex can thus be effectively used as a biosensor for hydrogen peroxide, as described in Fig. 1.

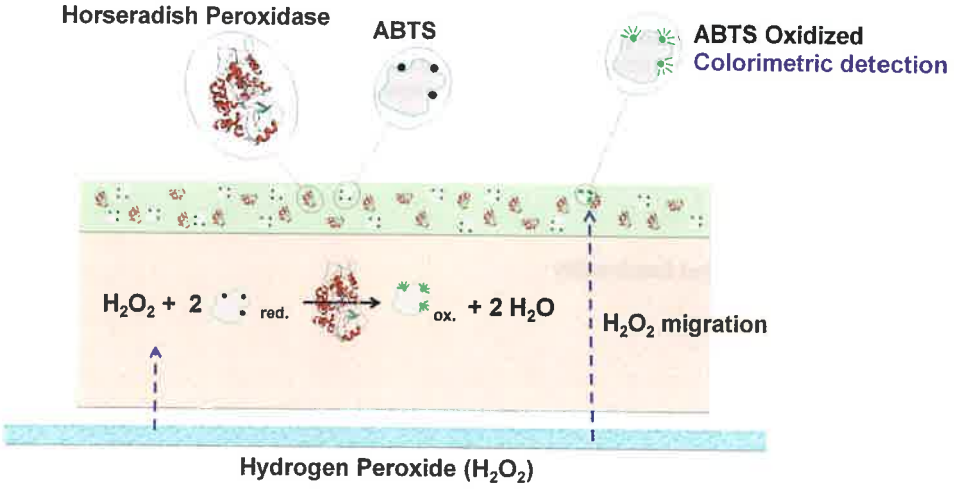


Figure 1: Schematic representation of the hydrogen peroxide bio-sensor. A bio-ink containing the HRP enzyme and the ABTS organic colorant is first printed on a lightweight coated paper. The role of the enzyme is to catalyze ABTS oxidation by H_20_2. Oxidized ABTS becomes green and the resulting change in colour is measured through colorimetry

The sensitive and accurate detection of hydrogen peroxide (H_2O_2) has several uses in pharmaceutical, clinical and industrial settings. For example, in the food science field, hydrogen peroxide can be used to monitor the state of oxidation of a given product [Laurienzo, 2001]. Furthermore, since hydrogen peroxide can also be used to prevent food decay, it is imperative to properly control its dosage. Several techniques have been proposed for the detection of H_2O_2 using HRP (eg., incorporation on polyaniline [Fernandes, 2005], in Au-nanoarrays [Lei, 2005] or in nanoparticles [Voss, 2007]). These techniques can however involve high costs and are time consuming. Within the spirit of the Sentinel Network, it then becomes interesting to explore HRP immobilization on a substrate using high-speed printing techniques. It is not our goal to design a sensitive peroxide bio-sensor, but rather to explore the feasibility of large scale printing of bio-molecules. A secondary goal of the study is to explore the effect of shear stresses on the bio-molecules.

2.2 T4 Bacteriophage

Bacteriophages, also simply called phages, are viruses that infect and destroy bacteria [Mandeville, 2003]. Some phages, such as T4 phages, are lytic, meaning that they can bind to a bacterium, destroy it and replicate themselves. We focus on the so-called T4-phage, which infect *E. Coli* bacteria, in particular the *E. Coli O157:H7* stain [Oda, 2004], the cause severe damage to the lining of the intestine, often resulting in death for small children. Furthermore, these bacteria can easily contaminate ground beef, raw milk and chicken as well as water [McMeekin, 2003]. There is thus an obvious potential for phages in water or food decontamination.

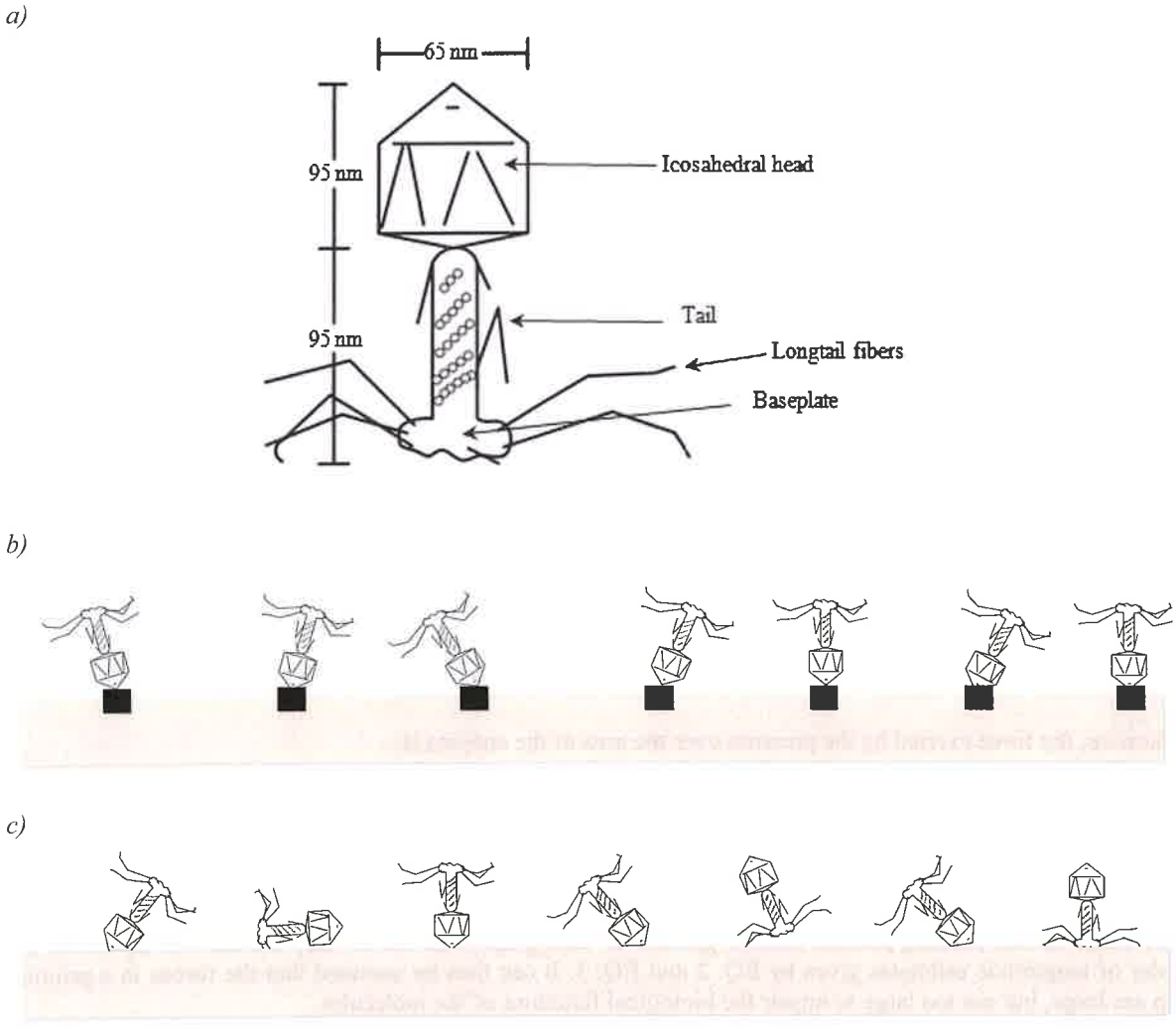


Figure 2: Schematic representation of phages and their use. The T4 phage, represented in a) is composed of an anionic head and a tail terminated by long fibres. To infect and destroy bacteria, the tail of the phage must be in contact with bacteria. Two strategies to attach the phages to a substrate are possible. In b), the phages are modified such that their head is strongly bound to the substrate, with the tails in the correct position. In c), a large number of phages are simply put in contact with the substrate with random orientation such that only a fraction is correctly positioned

Physically, T4 phages can be represented as an oblong molecule, with about 200 nm in height for 20 nm in diameter. In comparison, bacteria have a typical scale of the order of the micron. Phages are composed of a negatively charged "head" and a "tail" that binds to the bacteria. It is thus important that the head be attached to the substrate while the tail can be accessed freely. The *E. Coli* infection mechanism by T4 virus takes approximately 30 minutes at 37°C. It begins with the adsorption of the phage, and penetration of its genetic material inside the *E. Coli*. Once the genetic material is inside, there is generation of new phages *inside the bacterium* until it bursts open (being effectively killed). The newly produced phages are then free to infect other bacteria.

There are several techniques to immobilize phages on a substrate. The simplest one is physical adsorption, although it results in very weak adhesion and efficiency [Su, 2007]. On the other hand, phages can be modified such that they are bound covalently on a substrate [Gervais, 2007] or directly on cellulose through "Cellulose Binding Domains" [Ong, 1989]. These procedures give very efficient bio-sensors but are again quite slow and involved. With the goal of cheap and mass production, it is interesting to first simply print phages on paper and to observe the efficiency of the process. It is clear that not all phages will be in an optimal position to infect bacteria. However, due to the large numbers of phages being deposited, some will be in the correct position. Since phages are relatively cheap, this may represent only a minor concern for future applications.

2.3 Shear stress and bio-molecules

A first impression of bio-molecules such as enzymes and phages is that these are very fragile systems which cannot resist the pressure and stress exerted in modern high-speed presses. There are unfortunately very few studies on the mechanical resistance of such molecules. Some order of magnitude estimates can nevertheless be calculated.

Shear stress in the nip: The pressures P exerted in a printing are usually in the order $P \approx 1$ MPa [Kipphan, 2001] while the shear stresses tensor σ_{ij} depend on the shear rate $\dot{\gamma}_{ij}$ and the ink viscosity η as

$$\sigma_{ij} = \eta(\dot{\gamma})\dot{\gamma}_{ij} \tag{1}$$

where the shear rate $\dot{\gamma}_{ij} = (\partial v_i/\partial x_j + \partial v_j/\partial x_i)$ depends on the fluid velocity gradients. The rheology of the fluid is included with the shear rate dependence of the viscosity. However, for the sake of simple numerical estimates, the fluid will be considered as Newtonian. In simple nip transfer as in roll coating, the shear rate can be simply estimated as $\dot{\gamma} \approx U_0 / d$ [Coyle, 1986] where U_0 is the web velocity and d is the inter-nip engagement. For a web speed $U_0 = 1$ m/sec and d=1 μm, the shear rate $\dot{\gamma} = 10^6 \text{sec}^{-1}$, which, for water as a solvent, translate to a stress $\sigma = 1$ kPa. However, this is only a stress, i.e., a force per unit area. For a typical length scale of 10 nm, the force exerted on the bio-molecule is thus:

$$f_\sigma = \sigma R_0^2 \approx 10^{-13}\ \text{N} = 0.1\,\text{pN}. \tag{2}$$

Likewise, the force exerted by the pressure over the area of the enzyme is:

$$f_P = PR_0^2 \approx 10^{-10}\ \text{N} = 100\,\text{pN}. \tag{3}$$

These are of course very small forces but their range is comparable to the typical forces needed to break chemical bonds in complex molecules [Simson, 1999]. It is difficult to estimates properly the shear rates that take place in real printing process such as gravure or flexography. However, they should still be within the order of magnitude estimates given by EQ. 2 and EQ. 3. It can thus be assumed that the forces in a printing nip are large, but not too large to impair the biological functions of the molecules.

Ideal polymer approximation: Even though enzymes are more complex, they are essentially formed of organic chains akin to polymers. Dilute solutions of ideal polymers are essentially characterized by their radius R_0 and the viscosity η of the solvent. The force f(r) needed to stretch the polymer by a distance r is readily calculated as [de Gennes, 1979]:

$$f(r) \approx 3\frac{k_B T}{R_0^2} r \tag{4}$$

where T is the temperature and $k_B = 1.38\ 10^{-23}$ J/k is the Boltzmann constant. Concentrating on HRP enzyme in water, the radius $R_0 \approx 5$ nm for a solvent viscosity $\eta = 10^{-3}$ Pa·sec. The force needed to stretch the polymer by a distance R_0 is thus $f(R_0) \approx 5$ pN, which is in the range of forces exerted by the printing press. Likewise, the relaxation time (the time needed to return to the equilibrium shape) of an ideal polymer chain is [de Gennes, 1979]:

$$\tau \approx \frac{\eta R_0^3}{k_B T} \tag{5}$$

For the same parameters as in the force calculation, the relaxation time $\tau \approx 0.1$ μsec. When this is compared to the shear rates, the product $\dot{\gamma}\tau \approx 0.1$ which means that the nip only exert a small perturbation [de Gennes, 1979] on the bio-molecules, probably not sufficient to impair their biological functions. The effects of shear stress on the HRP enzyme will be explored by printing with ink having several viscosities as well as printing at several speeds. Those results are discussed in more details in Section 4.1.

3. Materials and methods

3.1 Printing system and paper

Bio-inks composed of HRP enzyme, ABTS and T4 Phages were printed onto 50 × 300 mm paper samples using a IGT Global Standard Tester 2 printability tester with gravure printing method at velocities ranging from 0.2 to 4 m/s and printing pneumatic force from 100 N to 1000 N. A doctoring system was used for metering the ink before its transfer to paper. The IGT gravure disc 402.151.412 with 40 l/cm, screen angle of 53° and 4 engravings (cell depths of 65 μm, 70 μm, 75 μm and 80 μm, corresponding respectively to cell volumes of 14 ml/m^2, 17 ml/m^2, 20 ml/m^2 and 25 ml/m^2) was used. Printing was done in conditioned atmosphere, 50% relative humidity and 23 °C according to the TAPPI standard T 402 sp-03. A lightweight coated paper (basis weight 60 g/m^2) provided by Centre International de Couchage (CIC, Trois-Rivières, Québec) was used for print trials. The coating consisted of a mixture of clay and calcium carbonate.

3.2 Ink formulation

3.2.1 Viscosity Modifier: Carboxy Methyl Cellulose (CMC) purchased from Sigma was used as viscosity modifier. The CMC average molecular weight was estimated to be 66 kg/mol from viscosity measurements [Lehtinen, 2000]. The rheogical properties of the CMC solutions were measured with a STRESSTECH laboratory shear rheometer. As a function of shear rate, CMC solutions are found to be shear-thinning. CMC is water soluble, very robust against shear and is often used as coating binder [Lehtinen, 2000].

3.2.2 Colorant: In order to asses ink transfer, 10 μl of food color-dye (Water, Propylene Glycol, Colour, Propylparaben) purchased from McCORMICK (Canada) was mixed to 1 ml of water and a certain amount of CMC for viscosity control.

3.2.3 HRP Enzyme + ABTS: Horseradish peroxidase (EC 1.11.1.7, type VI, highly stabilized, 200 - 300 U/mg) was purchased from Sigma (Oakville, ON, Canada). Solutions of enzyme having an activity of 254 U/ml (pyrogallol units) and solutions of ABTS 18.2 mM, were prepared using a 40 mM Potassium Phosphate buffer (pH 6.8) containing Carboxy Methyl Cellulose (CMC) as viscosity modifier.

3.2.4 T4 Phages: Original phages solution with four different concentrations of 10^7, 10^5, 10^4 and 10^2 phages/ml where obtained from the biology laboratory of the Université du Québec à Trois-Rivières (UQTR, Trois-Rivières, Québec). For each concentration, 2 ml of bio-ink was composed of 1ml of T4 phage solution and 1ml of Carboxy Methyl Cellulose solution (4% concentration), yielding a viscosity of 50 mPa·sec.

3.3 Assessment of biological efficiency

After printing, the biological efficiency of the transfer was evaluated as follows:

3.3.1 HRP Enzyme with ABTS

The role of the HRP enzyme is to catalyze a reaction between the ABTS chromogen and hydrogen peroxide. After printing and two hours drying at conditioned atmosphere, the backside of the printed paper samples was kept in contact with solutions of H_2O_2 of 10 mmol/l concentration for 20 seconds. Samples were then measured with a Technidyne Color Touch spectrophotometer. The CIE L*a*b* color system [Kipphan, 2001] was used and color changes were quantified with the ΔE value:

$$\Delta E^2 = \left(\Delta a^*\right)^2 + \left(\Delta b^*\right)^2 + \left(\Delta L^*\right)^2 \quad (6)$$

Normally, a colour difference ΔE superior to three can be distinguished by the human eye.

3.3.2 T4 Phages

E. Coli infection and destruction by the phages was qualitatively assessed by a culture method [McMeekin, 2003]. An *E. Coli* culture composed of 1 colony of *E. Coli B*, 4ml of nutrient media is let to rest for 24 hours in order to allow sufficient growth of the bacteria. After this step, an agar gel is prepared by boiling of top agar (composed of 1 liter water + 10g Tryptone + 8g NaCl + 5g of agar (0.5%)) and letting it equilibrate at

52°C for 2h. 5 ml of the top agar gel is then mixed with 100 µl of the previously prepared *E. Coli* solution and placed on standard agar plates. Printed sample with T4-phage bio-ink are then placed on top of each agar plate and incubated at 37°C overnight.

The top agar + *E. Coli* preparation is turbid but, if *E. Coli* is destroyed, it becomes transparent. *T4 phages efficiency can thus be qualitatively assessed by observing whether or not transparent rings become apparent around the paper samples.*

4. Results and discussion

4.1 HRP with ABTS printing

Printing of HRP + ABTS solutions described in Section 3 was performed on paper samples with the IGT laboratory press at several velocities and pressure. In this Section, we only consider the gravure cell with volume of 20 ml/m^2. The biological efficiency of the transfer was then evaluated by a measure of the color difference (cf., EQ. 6) of the paper before and after the oxidation reaction with hydrogen peroxide. An essential point is that the efficiency of the transfer depends simultaneously on the amount of bio-ink transferred and the damage which may be caused to the HRP+ABTS complex by the shear stresses experienced during the transfer.

To estimate this effect, printing with a simple dye colorant was also performed for the same parameters as the bio-ink. It is assumed that the ΔE value of the dye depends only on ink transfer. A comparison of the trends in ΔE for both colorant and bio-ink can thus give information on the physical (shear) as well as possible chemical effect of CMC [Di Risio, 2007] on the enzyme and oxidation reaction.

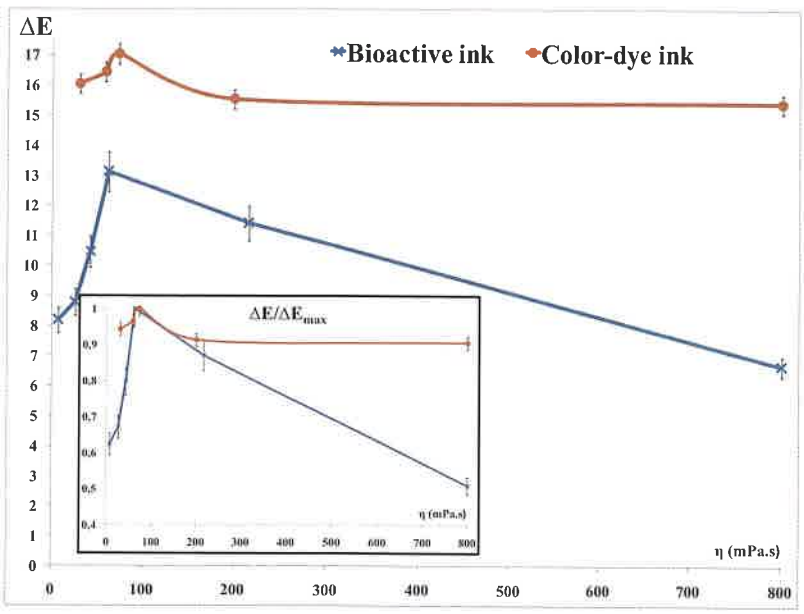


Figure 3: Color difference of the printed paper with colorant and bio-ink containing the HRP+ABTS complex (after oxidation with H_2O_2). The printing speed was set to 0.6 m/sec and the force to 500 N. The main figure shows the ΔE for both the colorant and bio-ink. In inset, the data are scaled with their respective maxima (ΔE_{max} = 17 for the colorant and ΔE_{max} = 13 for the bio-ink) in order to facilitate comparisons. The marked decay of the bio-ink ΔE indicates loss of biological efficiency with increasing viscosity

Figure 3 first shows the effect of viscosity on the ΔE of both colorant and bio-ink. The results are normalized with respect to the maximal value of ΔE in both cases in order to allow comparison. It is important to notice that ΔE_{max} = 13 for the bio-ink, meaning that the color change caused by oxidation is easily discernable to the human eye. It is first seen that ΔE for the colorant is essentially constant for all viscosities implying that ink transfer is roughly constant for this range of viscosity. On the other hand, after an initial peak, the ΔE of the bio-ink decreases steadily with increasing viscosities. This may be an effect of increasing shear stresses, as

described by EQ. (2.1), but it may also be due a chemical effect of the CMC tending to impair the ABTS oxidation [Di Risio, 2007]. This effect would then be more pronounced as CMC concentration is increased.

This question is further discussed in Fig. 4, which compares the ΔE values of the dye and bio-ink for a constant viscosity (i.e., at constant CMC concentration) but at different printing speeds. Once again, ink transfer is roughly constant, as indicated by the ΔE-value of the dye. However, the ΔE value resulting from HRP printing followed by ABTS oxidation is smaller at higher printing speeds. This result can clearly be associated to an increase of the shear stresses at higher velocities.

4.1.1 Storage degradation:

From a commercial application point of view, it is interesting to study the effect of storing the printed HRP+ABTS complex before use as H_2O_2 sensor. Figure 5 shows the effect of different storage conditions. Printed samples are left to rest in broad daylight and in darkness at 23°C and 50 % RH as well as in darkness at a temperature of 5°C. After oxidation, a visually observable value of ΔE is measured for all storage conditions for up to 8 days, with storage in daylight having the most severe degradation effect. A slight effect of temperature, most probably due to modified reaction kinematics, is also observed.

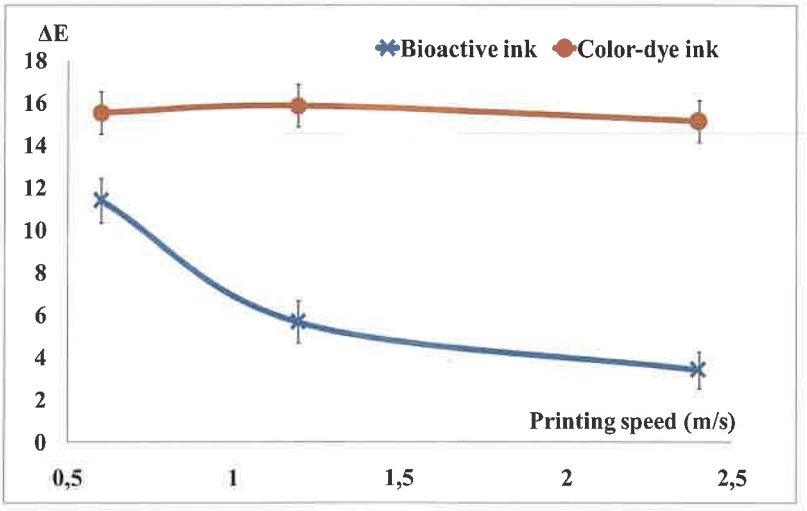


Figure 4: Biological efficiency of enzyme printing with respect to press velocity (the force is set to 500 N). The relatively constant curve for the dye indicates a constant ink transfer. The decrease in ΔE seen for the bio-ink can thus be attributed to an increase in the shear. The lines are guide to the eyes only

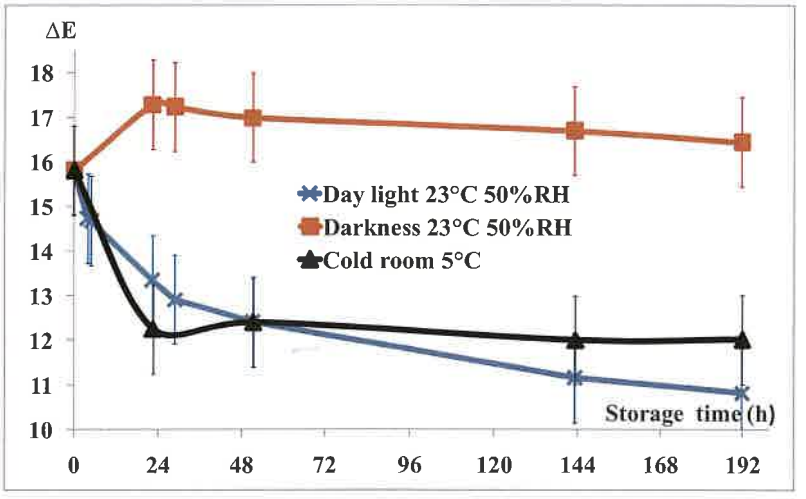


Figure 5: Effect of storage conditions on biological efficiency. The printed samples are stored by three different means and analysed as a function of time. The lines are guides to the eye only

4.2 Phage printing

Printing of a bio-ink containing the four concentrations of T4-Phages were done of LWC paper with the IGT laboratory press at a velocity of 1 m/sec and pneumatic force of 600 N. After printing, paper samples were immediately put upon the *E. Coli* bacteria and left overnight at 37°C. Figure 4.4 displays photographs of the visual appearance of the immersed samples obtained on the next day. A transparent ring (indicative of *E. Coli* destruction) around the samples is clearly visible for the largest phage concentration (10^7 phages/ml) while it is only slightly visible for a concentration of 10^5 phages/ml. At the lowest concentrations, no *E. Coli* destruction is observed. Those qualitative results nevertheless show that it is possible to print a bio-ink containing phages at high speed such that some biological activity is maintained.

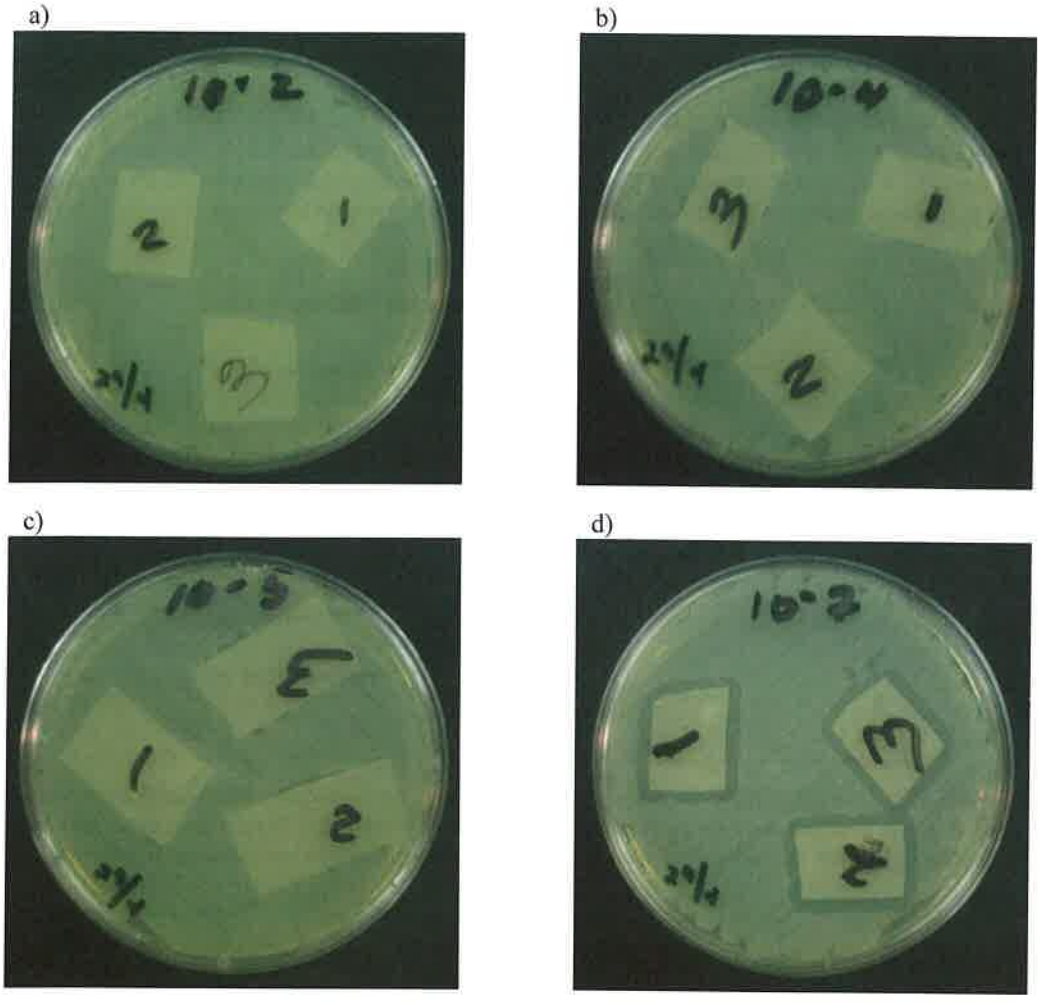


Figure 4.4: Visual evaluation of bacteria destruction by the T4 Phages printed on paper. The insets a) to d) correspond respectively to bio-ink containing 10^2, 10^4, 10^5 and 10^7 phages/ml. The labels 1 to 3 on the paper samples respectively correspond to gravure cell volumes of 25 ml/m^2, 20 ml/m^2 and 17 ml/m^2. The clear ring around the paper samples in inset d) indicates E. Coli destruction. The volume of the gravure cell does not seem to affect significantly the results

5. Conclusion

In conclusion, we have shown that two complex bio-molecules, HRP enzyme and T4-Phage can be printed on paper with high-speed techniques without incurring a severe detrimental loss of biological activity. Detrimental effect of shear stresses (about 50 % loss in ΔE) is observed for the HRP enzyme as well as possibly also for the phages (since only the bio-ink with the largest phage concentration shows destruction of *E. Coli* bacteria). Although the process could still be optimised with respect to efficiency and sensitivity, our results indicate that large-scale production of bioactive paper is indeed possible. Future research will focus on the effect of bio-ink composition (bio-molecules, binders, viscosity modifiers...) and on the complex interactions between the printing process, bio-ink and paper.

Acknowledgements

The authors gratefully acknowledge the financial support of the NSERC Bioactive Paper Network (Sentinel). S. Di Risio (U. Toronto) L. Brovko and H. Anany (U. Guelph) as well as R. Voss (U. McMaster) are thanked for their valuable inputs and comments. We thank most particularly Micheline Ménard-Boulianne (Biochemistry, UQTR) for her help in laboratory experiments.

References

1. Boland, T., Xu, B., Damon X. (2006) Application of inkjet printing to tissue engineering, *Biotechnol J* **1** (9), 910 - 917
2. Coyle, D. J., Scriven, L.E., Macosko, C.W. (1986) Film Splitting Flows in Forward Roll Coating. J. Fluid Mech. **171**, 183 - 207
3. de Gennes, P.-G. (1979) Scaling Concepts in Polymer Physics (Cornell University Press)
4. Fernandes, K F., Lima, C. S., Lopes, F. M., Collins, C. H. (2005) Hydrogen peroxide detection system consisting of chemically immobilised peroxidase and spectrometer. Process Biochemistry **40** (11), 3441 - 3445
5. Gervais, L., Gel, M., Allain, B., Tolba, M., Brovko, L., Zourob, M., Mandeville, R., Griffiths, M., Evoy, S. (2007) Immobilization of biotinylated bacteriophages on biosensor surfaces. Sensors and Actuators B **125** (2), 615 - 621
6. Kipphan, H. (2001) Handbook of Print Media (Springer)
7. Laurienzo, P., Malinconico, M., Volpe, M. G., Luongo, D., Ranieri, V., Scoponi, M. (2001) Compatibilized Ny6-based blends as innovative packaging materials: determination of some important properties relevant to food contact application. Packaging Technology and Science **14** (3), 243 - 251
8. Lehtinen, E. ed. (2000) Pigment Coating and Surface Sizing of Paper (Fapet Oy).
9. Lei, C. X., Long L. P., Cao Z. L. (2005) An H_2O_2 Biosensor Based on Immobilization of Horseradish Peroxidase Labeled Nano-Au in Silica Sol-Gel/Alginate Composite Film. Analytical Letters **38** (11), 1721 - 1734
10. Mandeville, R., Grifftith, M., Goodridge, L. *et al.* (2003) Diagnostic and Therapeutic applications of Lytic Phages. Analytical Lett. **36** (15), 3241 - 3259
11. McMeekin, T. A (2003) Detecting Pathogens in Food. (Woodhead Publishing)
12. Nestorson, A., Neoh, K. G., Kang, E. T., Jarnstrom, L., and Leufven, A. (2007) Enzyme immobilisation in Latex Dispersion Coatings for Active Food Packaging. Packaging Technology and Science **21**(4), 193 - 205
13. Oda, M., Masamoto, M., Unno, H., Tanji, Y. (2004) Rapid Detection of Escherichia coli O157:H7 by Using Green Fluorescent Protein-Labeled PP01 Bacteriophage. Appl. Environ. Microbiol. **70**, 527 - 534
14. Okamoto, T., Suzuki T., Yamamoto N. (2000) Microarray fabrication with covalent attachment of DNA using bubble jet technology. Nat. Biotechnol. **18**, 438 - 441
15. Ong, E., Gilkes, N.R., Antony, R., Warren, J., Miller, R. C., Kilburn, D.G. (1989) Enzyme immobilization using the Cellulose-Binding Domain of *a Cellulomonas Fimi* Exoglucanase. Bio/Technology **7**, 604 - 607
16. Renault, j.P., Bernard, A., Bietsch, A., Michel, B., Bosshard, H. R., *et al.* (2003) Fabricating arrays of single protein molecules on glass using microcontact printing, J Phys Chem B **107** (3), 703 - 717
17. Roda, A., Guardigli, M., Russo, C., Pasini, P., Baraldini, M. (2000) Protein microdeposition using a conventional ink-jet printer. Biotechniques **28**, 492 - 496
18. Sanjana N. E., S. B. Fuller S. B. (2004) A fast flexible ink-jet printing method for patterning dissociated neurons in culture, J Neurosci Methods **136** (2), 151 - 163
19. Simson, D. A., Strigl M.,Hohenadl, M., and Merkel M. (1999) Statistical Breakage of Single Protein A-IgG Bonds Reveals Crossover from Spontaneous to Force-Induced Bond Dissociation. Phys. Rev. Lett 83, 652 - 655
20. Su, S., Razvan, N., Flilipe, D. M., Li, Y., Pelton, R. H. (2007) Adsorption and Covalent Coupling of ATP-Binding DNA Aptamers onto Cellulose. Langmuir **23** (3) 1300 - 1302

21. Thibault, C. (2007) Impression de biomolécules par lithographie douce: application pour les biopuces, de l'échelle micrométrique à nanométrique. Thesis, Université de Toulouse

22. Voss, R., Brook, M.A., Thompson, J., Chen, Y., Pelton, R.H., Brennan, D. (2007) Non-destructive horseradish peroxidase immobilization in porous silica nanoparticles. J. Mater. Chem. **17**, 4854

23. Di Risio, S., Yan, N. (2007) Piezoelectric ink-jet printing of horseradish peroxidase: Effect of ink viscosity modifiers on activity. Macromolecular Rapid Communications, 28, 1934 - 1940

Rotogravure for printed electronics

Alexandra Pekarovicova, Erika Hrehorova, Paul D. Fleming, Marian Rebros, Margaret K. Joyce

Center for Ink and Printability Research
Department of Paper Engineering, Chemical Engineering and Imaging, Western Michigan University
Kalamazoo, MI 49008, USA
E-mail: a.pekarovicova@wmich.edu

Abstract

A flexo press unit was modified to print in a gravure offset configuration, direct gravure equipped with metering roll, and in a direct gravure with an enclosed doctor blade mode. Rotogravure test forms were prepared by laser ablation and chemical etching. Different features such as lines, gaps and source and drain electrodes were engraved at different angles to the print direction. Graphic ink and conductive nanosilver and silver flake water based inks were used for printing. Results showed that offset gravure did not produce missing areas/missing dots, however, printed lines had much higher gains than those printed by direct gravure. Direct gravure with metering roll causes premature solvent evaporation resulting in missing areas in fine features printed on paper substrates. Direct gravure printing with an enclosed doctor blade produced the most consistent results.

Keywords

Direct gravure, fine features, printed electronics, print fidelity, offset gravure

1. Introduction

The top five major opportunities for printed electronics, representing about 79% of market share in next five years are: radio-frequency identification (RFID), displays, photovoltaics, signage, and backplane technologies [Gasman, 2008]. The printing of necessary functional layers for RFID, solar cells, displays, or sensors and disposable electronics is possible by rotogravure. Gravure can print at high production speeds and at the same time produce consistent print quality at higher resolutions than possible with other printing methods using a master image carrier. A gravure press can be employed for the roll to roll fabrication of printed electronics, which is a very fast and inexpensive fabrication method, especially for application on flexible substrates. Newer rotogravure presses are capable of achieving layer to layer registrations of 35 - 50 μm [Passarelli, 2007], depending on substrate type. Registration needs to be tightened for printed electronics, especially when it is aimed to print integrated circuits, where precise overprinting of materials is critical for circuit performance.

In the past several decades, rotogravure used mostly electromechanical engraving, which produced characteristic ragged, serrated edges and offered resolutions slightly above 200 lpi. The diamond stylus geometry used in this engraving method produced predetermined cell shape and depth. Current systems, such as Ultimate from Aabach [Anon 1, 2008] allow for electromechanical engraving of halftone dots and line features at the same time, creating fine detail without serrated edges at resolutions of 350 lpi. Many improvements have been made in this aspect by using laser technologies, which offers much higher resolutions than normally possible with electromechanical engraving. Cellaxy, with a multi-kilowatt high power laser from Hell Gravure Systems, is direct laser engraving into copper surfaces at resolutions of 2540 lpi [Anon 2, 2006]. Digilas's 3D laser engraving, with fiber laser technology from Daetwyler, is able to obtain resolutions of 5080 dpi, with positioning precision of laser head of 1 μm [Anon 3, 2008], and engraving the smallest features of 5 μm size [Serenius, 2008]. Indirect laser engraving, involving laser ablation of a protective mask on a copper surface, followed by a closely monitored chemical etching of the copper layer, improved the smoothness and straightness of the lines and gaps. With indirect laser, detail can be imaged at a focus point diameter of 20 μm to produce a resolution of 2540 dpi, or with a 10 μm laser beam a 5080 dpi resolution is possible [Anon 4, 2008]. Chemical etching offers not only improved edge definition, but enables cell depths to be varied, which is not possible with electromechanical engraving.

In order to decrease the cost of RFID tags to allow for item level tagging, it is necessary to change the existing processes of RFID production. Until recently, only 10% of RFID tag antennae were printed, typically using silver based inks [Ramsey et al., 2000; James, 2003; Oguchi, 2003; Rebros, 2008]. These materials may be

screen-printed, flexo or gravure printed, or digitally printed on a variety of substrates, ranging from polyester, polycarbonate, polyimide, PVC, paper and glass. Most silver-based materials are based on special "leafing" silver flakes [Mohanty, 2004], which are designed to float to the surface during drying to promote high surface conductivity. The silver-based flake inks are well suited for printing RFID antennae [Woloznicki, 2002; Rigney, 2004] and circuit interconnects, but they are not suitable for printing the finer contact electrodes found in integrated circuit (IC) components, due to the large size of silver flakes. This, however, can be overcome by employing silver nanoparticles [James, 2003; Oguchi, 2003], gold nanoparticles [Ko, 2007], or indium tin oxide nanoparticles [Puetz, 2008]. Furthermore, printed ICs require semiconducting materials to replace silicon-based semiconductors. Optimal performance of the ICs can be obtained if materials with a wide range of band gaps and conduction mechanisms (e.g. p or n) are available.

Besides the metal filled conductive materials, solution processable conductive and semiconductive polymers are already leading to low cost sensors and inexpensive, disposable electronics. The majority of work to date has focused on two conducting polymers, polyaniline (PANI) and poly (3, 4 ethylenedioxythiophene)-poly (styrenesulfonate) (PEDOT: PSS) [Hrehorova et al, 2006; Hrehorova et al, 2007; Groenendaal, 2000]. PEDOT: PSS based inks have been used to print conductive layers [Groenendaal, 2000; Groenendaal, 2005]. This conductive polymer is commercially available as a water-soluble polyelectrolyte system, with good film-forming properties, high visible light transmittance, and excellent stability [Kirchmeyer, 2005]. Some applications of PEDOT: PSS include antistatic coatings, conductive layers in organic light emitting diodes (OLEDs), capacitors and thin film transistors [Asizawa, 2005].

At Western Michigan University, rotogravure printing was used to print RFID antennae, using solvent based and water based silver conductive inks on multiple paper and paperboard substrates. Surface properties of substrates were thoroughly characterized (surface roughness, topography, porosity, wetting properties, surface energy). The Alien Technology ultra high frequency (UHF) RFID tag "squiggle" (2nd generation) antenna design was printed. Performance of printed antennae has been tested and reported [Rebros, 2008]. Printed conductive line width, length [Hrehorova, 2008], along with resistance measurements enabled calculation of sheet resistivity of different combinations of ink, paper and print conditions. Antenna performance has been extensively characterized in WMU's RFID testing laboratory [Rebros et al., 2008; Fleming et al, 2007; Pekarovicova et al, 2007]. Further necessary steps include gravure trials focused on printing functional layers and elements of integrated circuits. For this, it was necessary to find the best inking and transfer configuration for the gravure print unit, along with studying of the fidelity of printed fine features under these varying conditions.

2. Experimental

Indirect laser engraving was done by laser ablation of a mask followed by chemical etching. For the trial, 200 and 300 lpi resolutions were employed with cell depths of 20 and 30 μm, respectively. The engraved image contained various features, comprising of lines in various angles to the print direction, lines and gaps of different widths, source and drain electrodes for printed transistors, as well as graphic features like tone steps to be able to check for ink transfer in the print and cross print direction. The design of the engraved features is shown in the Figure 1.

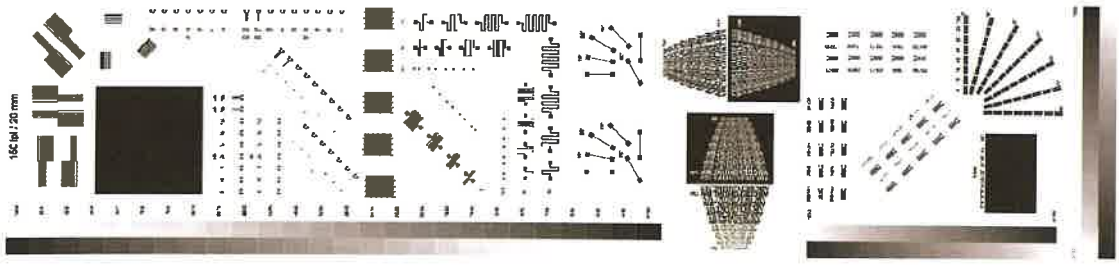


Figure 1: Design of cylinder engraving

A cyan solvent based graphic ink was used for the initial gravure press runs to set the press conditions for each configuration. For direct gravure with open pan and offset gravure settings, the graphic ink was slowed down with proprietary resin system and slower solvent to reduce ink drying before reaching the substrate. Two different viscosities, 25cP and 35cP were used. Nanoparticle silver gravure ink (Inktec Co., Korea) and water based silver flake ink were employed for conductive ink printing. As substrates, commercial biaxially

oriented polypropylene (BOPP) was used for printing with graphic inks. For conductive inks, a commercial label paper (Label paper 1) and 2 μm polyethylene terephthalate (PET) film were employed. Label paper 1 was coated in WMU laboratories at three different conditions in order to reduce roughness and to tailor other desirable properties. These substrates are denominated as Coat 1, Coat 2 and Coat 3. A flexographic label press, based on Comco's C2 platform was modified to operate in gravure mode. Offset gravure with open pan, direct gravure with open pan and direct gravure with enclosed doctor blade chamber with varying impression pressures were studied. In the offset mode, two nip pressures were varied; the nip between the gravure cylinder and offset blanket cylinder, and the nip between the blanket cylinder and impression roller.

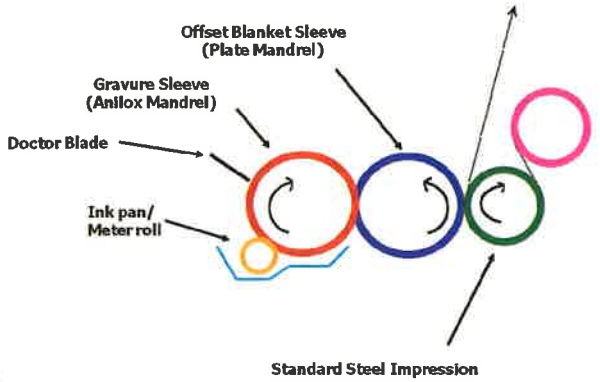
An atomic force microscope (AFM) Autoprobe CP (Thermomicroscopes, USA), with Proscan version 1.3 software operating in tapping mode was employed for microroughness evaluation of coated papers. The root mean square (RMS) roughness was calculated as a deviation of the surface heights from the mean surface plane. Line width, line raggedness, gap quality and line geometry, as well as directionality of printed lines, were examined using image analysis ImageXpert, KDY Inc. [Kipman, 2001] equipped with motion table for positioning of samples, two calibrated cameras and image analysis software (IX 10.0b63).

3. Results and discussion

In order to optimize the press printing condition, three different gravure print configurations were tested: offset gravure (Figure 2A), direct gravure with open pan and inking roll (Figure 2B), and direct gravure with enclosed doctor blade chamber (Figure 2C). A metering inking roll was used for offset and direct gravure with open pan in order to force the ink to the gravure cells, because the engraved cylinder was too large to fit into the ink fountain to be inked. This set up is different from what is typical for gravure process, where the cylinder is immersed in the inking pan. A metering roll is more common to the flexographic process. Unfortunately this unusual configuration resulted in the ink prematurely evaporating, requiring the ink viscosity to be adjusted approximately every 15 minutes by adding an appropriate amount of solvent. So, it was not possible to determine the actual viscosity of the ink, or maintain it at a constant level. The increase in ink viscosity reduced the amount of ink transferred from the engraved cells resulting in missing dots. It also limited the amount of spreading, and caused poor coverage on the substrates, especially in the phase of printing with conductive inks.

Since the Comco press platform was not equipped with electrostatic assist, offset gravure was employed and expected to transfer all of the ink, thus preventing missing dots/print area problems. As expected, all the dots were transferred during offset gravure, compared to some missing dots being present with the direct gravure with enclosed doctor blade (EDB) configuration (Figure 3). The results showed the direct gravure with EDB as having far superior dot fidelity.

However, offset gravure produced distorted dots, having at some conditions star shape rather than circular, which might be attributed to multiple ink splits, as well as to offset blanket distortion at high impression pressures. Dot roundness in offset gravure was in the range of 0.77 - 0.81 compared to direct gravure with open pan 0.82 - 0.84 and direct gravure with EDB 0.84 - 0.86.Considering that perfectly round dots have a roundness of 1; the direct gravure with EDB printed the best dots.



A

Continued on page 292

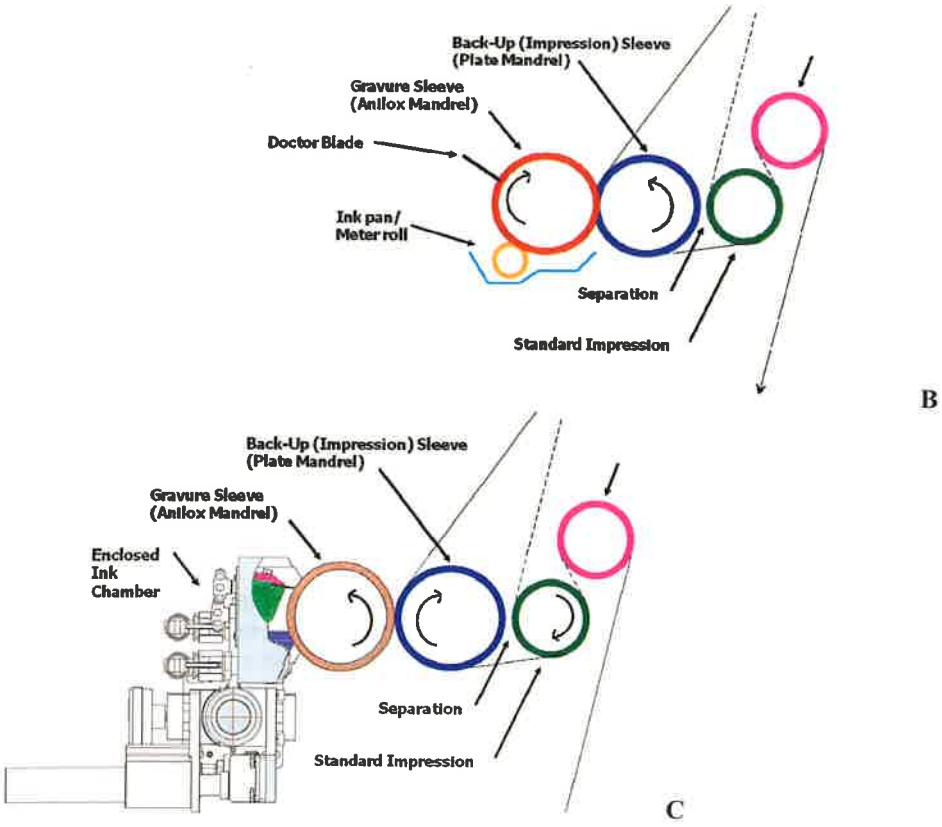


Figure 2: Offset gravure with open fountain (A), direct gravure with open fountain (B), direct gravure with enclosed doctor blade system (C)

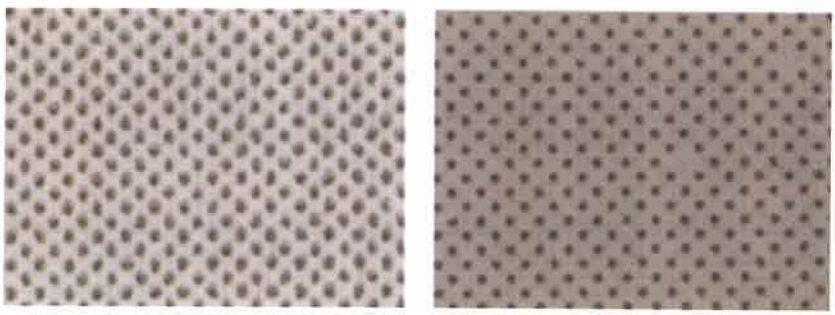


Figure 3: Comparison of halftone dot printing with offset gravure (left) and direct gravure with EDB (right) at their best print conditions

Line of 40 μm nominal width, printed in machine direction, was measured for all three press configurations. From all of those three settings, direct gravure produced the best fidelity of line width (Figure 4), and offset gravure produced the worst. In the case of offset gravure, the best line reproduction was accomplished with the smallest impression pressure for both nips (condition 0, 0). Width gain increased with increasing pressure at the second nip (condition 0, 2), where transfer occurred between the offset blanket to the substrate. Increased pressure at the first nip (1, 0) similarly worsened the situation, and resulted in a higher widening effect (2, 0), and line width increase to 97 ± 6μm. Also, second nip pressure had more pronounced effect on line widening than first nip pressure. The highest impression pressure at both nips created more than a 100 % gain, resulting in a 98 ± 8μm line width. This is quite understandable, because higher pressure on an offset blanket produces more distortion. Thus, for offset gravure, higher blanket hardness or lower impression pressures are needed to maintain the fidelity of printed features. Direct gravure with enclosed doctor blade chamber printed with the highest fidelity, and here higher impression pressure resulted in better reproduction (62 ± 4 μm) of line width. Excessive solvent evaporation occurred in the direct gravure configuration with open pan, leading to unstable viscosity, thus inconsistent print results.

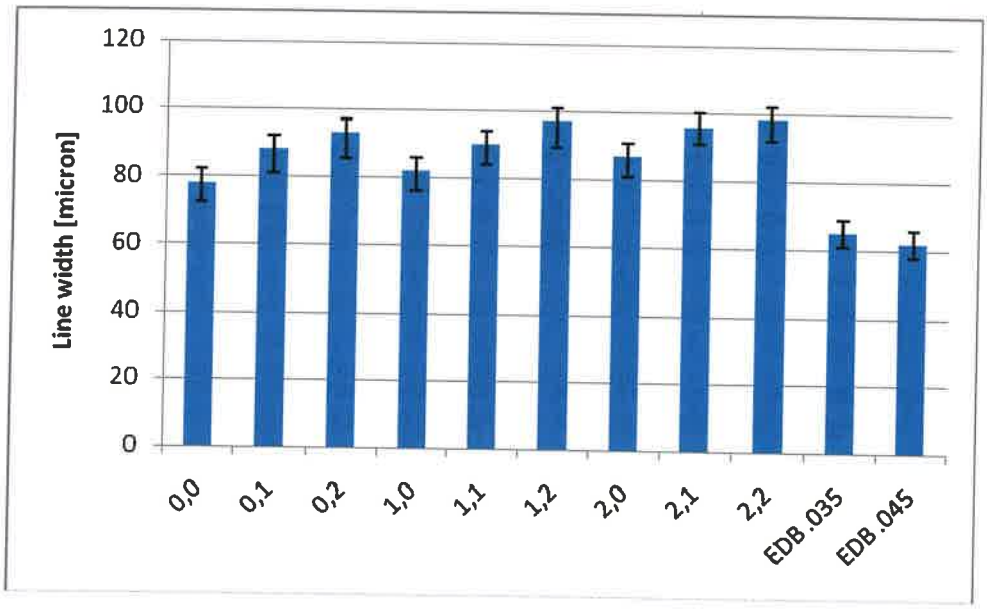


Figure 4: Measured width of nominal 40 μm line in print direction printed with offset gravure and direct gravure with EDB. Gravure offset conditions from 0,0 to 2,2 indicate increasing impression pressure for nip between gravure cylinder and offset blanket (first number) and nip between offset blanket and impression roller (second number). EDB 0.035 and 0.045 mean increasing impression pressure

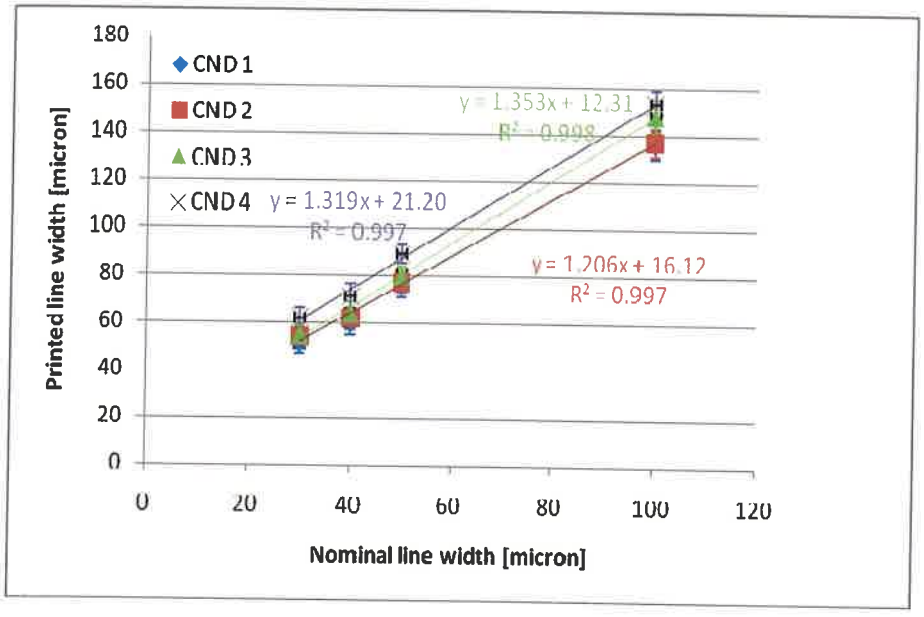


Figure 5: Nominal versus printed line width for direct gravure with enclosed DB in print direction: CND 1-printed with 35cP graphic ink and higher impression pressure; CND 2- 35cP second ink with lower impression pressure; CND 3-25cP ink and higher impression pressure; CND 4 -25cPink with lower impression pressure

Further detail on line reproductions with the EDB is shown in Figure 5. The fidelity of the lines can be improved with the modification of the ink viscosity. Higher ink viscosity and higher impression pressure resulted in the best line width reproduction of 50.7 ± 4μm width for the 30 μm nominal line (CND 1), compared to the worst conditions (CND 4), resulting in 62 ± 4μm width for the same line.

Lines rotated 90° to print direction gave worse reproducibility than those in the print direction (Figure 6). Lines of a 30 μm nominal width resulted in a 61 ± 4μm printed width for the best conditions (higher viscosity, higher impression), and 75 ± 6 μm width printed for the worst conditions (lower impression, lower viscosity).

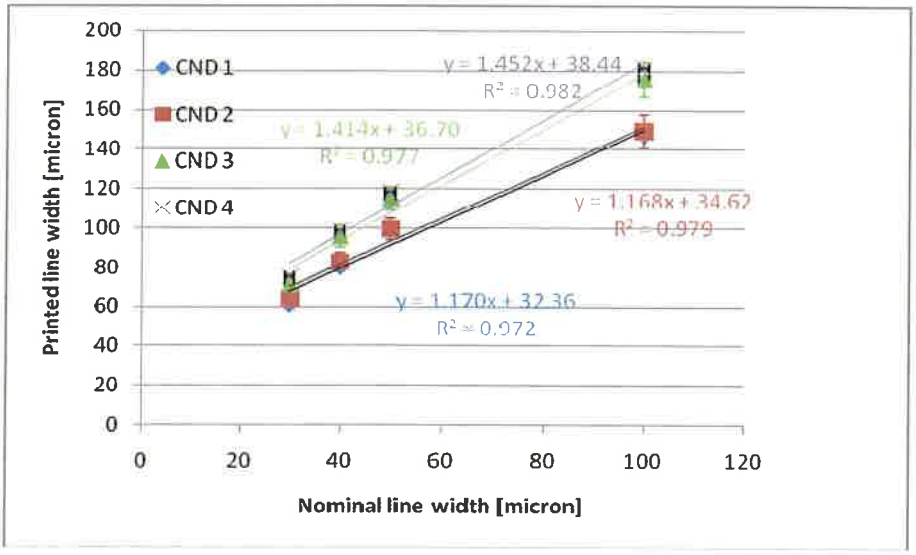


Figure 6: Nominal versus printed line width for direct gravure with enclosed DB in cross-print direction: CND 1-printed with 35cP graphic ink, and higher impression pressure; CND 2- 35cP ink with lower impression pressure; CND 3-25cP ink, higher impression pressure; CND 4 -25cP ink with lower impression pressure

Table I: Gaps in print and cross print direction printed by direct gravure with enclosed DB. [Conditions (CND) explained above, PD- print direction, CPD- cross print direction, ND-not detectable gap]

Print direction	**PD**			
Nominal width	CND 1	CND 2	CND 3	CND 4
40 μm	22.8 ± 3	23.2 ± 3	ND	ND
50 μm	32.6 ± 4	32 ± 4	24.2 ± 3	ND
100 μm	77.6 ± 6	77.6 ± 5.8	59.8 ± 8	56.7 ± 6.6
150 μm	126.6 ± 5	124 ± 5.4	109.4 ± 7	106.3 ± 6.8
Print direction	**CPD**			
Nominal width	CND 1	CND 2	CND 3	CND 4
40 μm	ND	ND	ND	ND
50 μm	30.8 ± 9	30.1 ± 8.4	ND	ND
100 μm	50.8 ± 9	50.2 ± 9.2	28.8 ± 6.6	29.6 ± 7.4
150 μm	101.8 ± 8	104.3 ± 7.6	75.2 ± 7	80 ± 7

All gaps reproduced better in the print direction than inthe cross print direction (Table I). Ink viscosity affected the print resultsmuch more than impression pressure. As expected, a higher viscosity resulted in less spreading, thus better gap reproduction (CND 1 and CND 2).

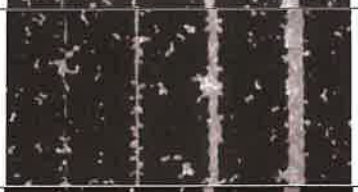
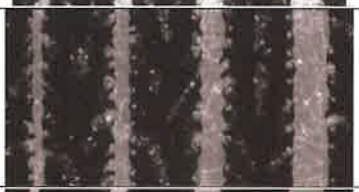
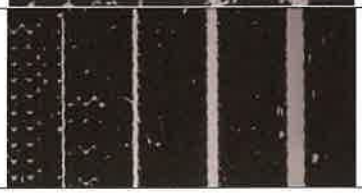
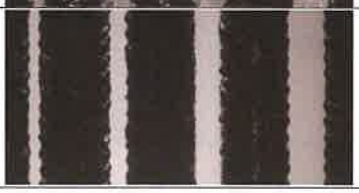
A further step was to evaluate printability of the conductive inks for the printing of fine features. The direct gravure with open pan configuration was selected for these experiments because it provided the opportunity to modify the inking system to ink only 1/3 of the cylinder. This modification represented a remarkable savings in silver ink costs. A solvent based nanosilver ink and water based silver flake ink were employed. Our previous work demonstrated that gravure is capable of printing antennae on paper substrates, which work in the UHF range [Rebros, 2008]. It was found that sheet resistivity and impedance depend, among other things, on the smoothness of the substrate. When printing fine lines and small features for field effect transistors, roughness of the substrate, along with the roughness of functional layer, and its integrity, are very important issues. In previous work, Label paper 1 was the best performing substrate among 4 studied paper substrates for conductive ink printing, with 1.24 ± 0.06μm Emveco roughness. PET, which is popular flexible packaging grade plastic film, had 0.2 μm roughness. Similarly, microroughness of PET as measured by atomic force microscopy (0.010 μm) is much lower than that of Label paper 1 with RMS of 0.043 μm (Table II). To

increases the smoothness of Label paper 1, it was further treated with different proprietary non-pigmented coatings. The surfaces of best samples (Coat 1, Coat 2 and Coat 3) approached or slightly surpassed the microroughness of the PET. However, Coat 1 and Coat 2 developed mircocracks in then nanosilver ink film; therefore they were not considered for further studies. The first measurable gap printed with nanosilver ink was the nominal 40 μm gap, although some bridging across the gap was evident (Table IIIA). The most uniform gap was formed on the PET substrate (19 ± 2μm). Additional three gaps with higher specified width (50, 100, 150 μm) were considered for measurements.

Table II: Substrates used in direct gravure open pan trials with conductive inks

Substrate	Surface Energy [mN/m]	RMS AFM [μm]	Emveco [μm]
Label paper 1	49.30	0.043	1.24
PET	43.80	0.010	0.44
Coat 1	47.70	0.011	0.81
Coat 2	43.39	0.004	1.43
Coat 3	30.66	0.011	1.15

Table III: Printed gaps with nanosilver ink (A) and water based flake ink (B)

Substrate	Specified gap width / μm							
	A				B			
	40	50	100	150	100	150	200	300
Label paper 1								
Coat 3								
PET								

In the case of the WB ink, only the gaps with specified widths of 100, 150, 200 and 300 μm were measured (Table IIIB), because the gaps narrower than 50 μm were completely filled in. Compared to PET substrate, poor ink film integrity and ink coverage were achieved with both inks on Label paper 1 and Coat 3 (Table III). Moreover, the edges of the gaps were very ragged. Better coverage was found for the samples printed with WB ink than nanosilver ink, but the edge definition was still not uniform enough. The first measurable gap for the WB ink was for 100 μm compared to 40 μm nominal gap printed with nanosilver ink. In the case of the nanosilver ink, the highest decrease in gap width was measured for substrate Coat 3 and the lowest for PET indicating lower spreading. For the WB ink, the narrowest gaps were measured for Label paper 1 and the widest for PET. The reason for poor coverage of nanosilver ink is probably due to very slow press speed, which was necessary to assure sufficient drying of printed ink film. However, the PET coverage was fairly good. Also, the configuration used for printing with nanosilver ink was direct gravure with open pan equipped with metering roll to ink the gravure cylinder. At this slow speed, the isopropyl alcohol had an opportunity to evaporate from the ink, which resulted in poor ink transfer and lower spreading on the substrate, but for the same reason exhibited narrower gap printability, than achieved with the WB silver ink. Fine lines printed on Label paper 1 with nanosilver ink showed very poor printability and line widths were non-measurable (Table IVA), because of poor ink film integrity and coverage. Slightly better results were obtained for Coat 3.

However, lines were disconnected in many places, which is unacceptable for the material intended to conduct. For both substrates, the same specified width lines printed with the WB ink (Table IVB) had better integrity than the ones printed with nanosilver ink, but the edge definition was not uniform enough. As obvious from Table III and IV, ink film coverage was not perfect. Conductive area coverage is an important parameter for electrical properties evaluation, and it was measured using an ImageXpert image analysis system as a proportion between bright pixels (non covered areas of substrate) and dark pixels (covered areas with ink). The best coverage was recorded for the PET substrate 98.3% for both inks, (Figure 7). In terms of inks, the samples printed with the nanosilver ink did not show as good coverage (84 - 88%) as the samples printed with the WB ink (95 - 90%) for Label paper 1 and Coat 3, respectively.

The lowest sheet resistivity was found for the PET substrate printed with nanosilver ink reaching 0.144 Ohm/sq (Figure 7), followed by Label paper 1 printed with WB ink (0.386 Ohm/sq). Coat 3 produced the worst sheet resistivity with both inks (0.616 and 0.642 Ohm/sq) nanosilver and WB, respectively. Thus, nanosilver ink proved to exhibit better conductivity than WB ink. Also, ink films printed with nanosilver were smoother than films printed with WB silver flake ink (data not shown), which is important for circuitry printing.

Table IV: Lines printed with nanosilver ink (A) and water based ink (B)

Substrates	Specified line width / μm							
	A				B			
	40	50	100	150	100	150	200	300
Label paper 1								
Coat 3								
PET								

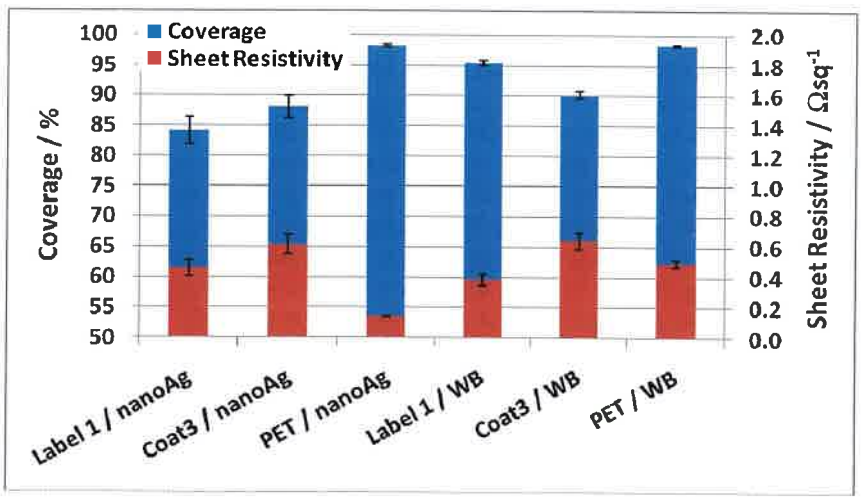


Figure 7: Ink coverage printed with nanosilver and silver flake WB inks and corresponding sheet resistivity

4. Conclusions

Offset gravure, direct gravure with open pan and direct gravure with enclosed doctor blade chamber were used for printing single elements for circuitry. Offset gravure did not produce missing dots or missing areas, but produced excessive gain on printed lines (more than 100% line width gain). Direct gravure with EDB produced the most consistent results. Elements printed with direct gravure and open pan with conductive nanosilver and water based silver flake ink showed the best printability on PET substrate. Nanosilver ink did not achieve as good of coverage as the water based silver ink, but reached the lowest resistivity on all substrates.

Acknowledgement

Authors are grateful to Kevin Manes and David Kuhn from Mark Andy for gravure printing of the samples in their facilities. This work was supported in part by the Michigan Economic Development Corporation in the framework of Michigan 21 Century Jobs fund.

References

1. Anonymous 1: The Ultimate Innovation from AABACH Graphic Systems, http://www.aabach.com/ Accessed June 2008
2. Anonymous2:http://www.hell-gravure-systems.com/topics/etopics/archive/en/hell_etopics_en_2006_09_05.pdf, Accessed June 2008
3. Anonymous 3: Laser Precision for Gravure and Flexo, http://www.daetwyler.com/user_content/editor/files/Fact_sheets_digilas_en/4p_dig_eng_eu.pdf; Accessed June 2008
4. Anonymous4: http://www.daetwyler.com/en/produkte/engraving/digilas.html?SID=650819c683133060ff5b0b4e9b6738c0;Accessed June 2008.
5. Ashizawa, S., Horikawa, R., Okuzaki, H., (2005) Effect of Solvent on Carrier Transport in Poly (3, 4-ethylenedioxithiophene)/poly (4-styrenesulfonate), Synthetic Metals, 153, p. 5 - 8
6. Fleming III P.D., Bazuin B., Rebros M., Hrehorova E., Joyce M. K., Pekarovicova A. and Bliznyuk V.: (2007) Printed Electronics at Western Michigan University, 07 AIChE Annual Meeting, Salt Lake City, UT
7. Gasman L.: (2008) Flexible Electronics: Capacity and Investment Forecast, USDC Flexible Display Conference, Phoenix, AZ, January 21 - 24
8. Groenendaal, L., Jonas, F., Freitag, D., Pielartzik, H., Reynolds, J. R. (2000) Poly (3, 4-ethylenedioxythiophene) and Its Derivatives: Past, Present, and Future, Adv. Mater., 12, 7, p. 481 - 494
9. Groenendaal, L.; (2005) Conductive Polymers, in: G. P. Crawford (Ed.) Flexible Flat Panel Displays, Willey-SID Series in Display Technology, Chichester, p. 135
10. Hrehorova E., Pekarovicova A. and Fleming P. D.: (2006) Gravure Printability of Conductive Polymer Inks, *Proceedings of IS&T Digital Fabrication 2006*, Denver
11. Hrehorova E., Pekarovicova A., Fleming P. D.: (2008) Evaluation of Gravure Printing for Printed Electronics, Proceedings TAGA 2008, San Francisco, In press
12. Hrehorova, E., Rebros, M., Pekarovicova, A., Fleming, P. D., Bliznyuk, V. N.:(2007) Characterization of Conductive Polymer Inks based on PEDOT: PSS, Proc. of TAGA 59th Annual Technical Conference, Pittsburgh, PA
13. Hrehorova E., Pekarovicova A., Bliznyuk V. N. and Fleming P. D.:(2007) Polymeric Materials for Printed Electronics and Their Interactions with Paper Substrates, *Proceedings of IS&T Digital Fabrication 2007*, Anchorage
14. James M. R.: (2003) Manufacturing Printed Circuit Boards Using Ink Jet Technology, Proceedings of NIP19, International Conference on Digital Printing, Society of Imaging Science and Technology, New Orleans, p. 651
15. Kipman Y: (2001) DPP2001: Int. Conference on Digital Production Printing and Industrial Applications, 373
16. Kirchmeyer, S., Reuter K.: (2005) Scientific importance, properties and growing applications of poly (3, 4-ethylenedioxythiophene), J. Mater. Chem., 15, p. 2077 - 2088
17. Ko S. H., Chung J., Pan H., Grigoropoulos C. P, Poulikakos D.: (2007) Fabrication of multilayer passive and active electric components on polymer using inkjet printing and low temperature laser processing, Sensors and Actuators A 134, 161 - 168
18. Mohanty R.:(2004) Silver Migration in Polymer Thick Film, SGIA Journal, 8, 41 - 45

19. Oguchi T, Suganami K., Nanke T., and Kobayashi T.: (2003) Formation of Precise Electrically Conductive Pattern Using Metal Colloid I-J Ink", Proceedings of NIP19, International Conference on Digital Printing, Society of Imaging Science and Technology, New Orleans, p. 656
20. Passarelli F.: (2008) Gravure Press Register, Bobst Group, Personal communication.
21. Pekarovicova A., Hrehorova E., Joyce M. K., Fleming III P. D., Rebros M., Bliznyuk V. and Bazuin B.: (2007) Flexo and Gravure Printing of RFID Tags, (Invited lecture), Nanoengineered Inks and Pigments, PIRA Intertech, Philadelphia, PA
22. Puetz J., Aegerter M. A.: (2008) Direct Gravure Printing of Indium Tin Oxide Nanoparticle Patterns on Polymer Foils, Thin Solid Films, 516, 4495 - 4501
23. Ramsey, B., Harrison, D., Lochun, D., Evans, P., Harrey P.: (2000). Handbook of conductive lithographic films, Serenius E.: Personal communication, Daetwyler, June 2008
24. Surrey: Brunel University, ISBN: 0-9538356-0-X, downloaded from http://dea.brunel.ac.uk/cleaner/Electronics_Projects/Handbook_1.htm
25. Rigney J.: (2004) Materials and Processes for High Speed Printing for Electronic Components", Proceedings of the IS&T NIP20: International Conference on Digital Printing Technologies, Salt Lake City, pp. 275 - 278
26. Rebros M., Hrehorova E., Bazuin B., Joyce M., Fleming P. D., Pekarovicova A.: (2008) Rotogravure Printed UHFRFID Antennae Directly on Packaging Material, Proceedings TAGA 2008, San Francisco, In press
27. Woznicki, T.: (2002), Pads-Only Plating and Conductive Inks, The Flex Circuit News [On Line], Available: http://www.flexdude.com/Back_Issues/FCN1-02A.PDF, Accessed November 2007

The impact of conductive carbon properties on print performance

E. H. Jewell, T. C. Claypole, S. R. Roberts, D. C. Bould

Welsh Centre for Printing and Coating
School of Engineering, University of Wales Swansea
Singleton Park, Swansea SA2 8PP, UK
E-mail: e.jewell@swan.ac.uk

Abstract

Carbon graphite inks are often used in the thick film screen printing electronics industry for depositing conducting and controlled resistance features within circuits. Although it provides lower conductivity than silver, its relative cost and toxicity makes it an attractive proposition. Where the highest possible conductivity is required the material formulator and printer are faced with the challenge providing with maximum carbon content while remaining within the range of printable rheologies of the process.

The aim of the study was to examine the relationship between the rheology of the materials and the printed feature characteristics. Inks between 38% and 43% carbon were measured using shear and extensional rheometers and their print characteristics were measured. Increasing the print speed resulted in a narrower, taller line while increasing carbon content increases the line height and reduces the line width. For the formulation tested, the ink reaches a maximum transfer at around 42%, whereupon there is a reduction in printed material. This behaviour can be explained by a plug flow phenomenum of the ink through the screen. No clear direct correlation between the rheological measurements and print characteristics could be obtained. Recommendations are made for larger data sets and more advanced statistical models of the process.

Keywords

Carbon ink, printed electronics

1. Introduction

The basic building blocks of any printed electronics are the conductive elements which carry current around a circuit. The circuit tracks are produced by an ink which commonly consist of conductive particles within a binder which holds the particles to each other and binds the cured ink to the substrate. The conductive particle of choice is silver due to its low resistivity and inertness (copper has a higher conductivity, but rapidly oxidises to a non conductive copper oxide). However, for applications such as disposable sensors for packaging and healthcare, the cost of silver becomes prohibitive, particularly as silver commodity prices increase rapidly. For packaging, there is the additional issue of recycling silver sensors which are introduced into the waste stream as part of the packaging.

Another material which is suitable as a conductive particle within the ink is carbon graphite. This possesses lower conductivity, typically at least 2 orders of magnitude lower than silver, but is considerably cheaper and more environmentally friendly. Thus, while its electrical properties are far from ideal, carbon offers other significant advantages in terms of cost and the environment. For example, where there is "use once and dispose" (such as blood glucose sensor manufacture) there is a demand for high volume production with a low cost conductive element. There are a number of issues which became apparent when formulating carbon conductive inks. Increasing the proportion of conductive element in the ink improves conductivity, but can push the material properties beyond the operational window of the application process. The formulator is then facing the dilemma of increasing carbon content in order to improve conductivity while maintaining a rheology which is compatible with the printing process.

The aim of the study was to establish the relationship between the ink formulation (predominantly the carbon content), the rheology of the material and its subsequent effect on printability and electrical properties. This initially examined screen printing as the process of choice for thick film deposition. Before describing the work carried out in this study, the paper first examines the literature on carbon ink rheology and its subsequent effect on ink transfer. Fundamental to this is the understanding of the ink transfer process.

2. Literature

The review first examines the literature in the fields of rheology and process parametrics of thick film screen printing of lines. This is followed by a review of the mechanisms of screen printing ink transfer, as this understanding forms the basis of any rheology - print quality relationship developed within the study.

Pan et al [1999] report the findings of an experiment into the effects of print speed, squeegee hardness, squeegee pressure and snap-off distance. Using a Ag (Silver)/ Pd (Palladium) paste they found that the lower the print speed the better in terms of reproducing a geometrically consistent fine line.

Hoornstra et al [1998] document an experiment performed using seven silver pastes, which were analysed in terms of easy print and slumping (loss of fine line quality). The paper states that it is difficult to simulate the "printing behaviour" of inks using basic rotational viscometry. Oscillation rheometry was employed to mimic the shear conditions in the screen printing process. Higher printing speeds resulted the line width while being produced while increasing the line height. No firm correlations between the printing characteristics and the rheological properties were found although it summarises that low viscosity fluids are conducive to easy printing yet exhibit significant slumping while higher viscosity fluids are difficult to print but exhibit good line quality. Ročak et al [1995] also conclude that increasing the print speed increases the paste film height.

The rheology and use of carbon as a conductive material is not widely reported, although some studies have been carried out which have sought to examine the relationship between rheology and print quality. Trappe and Weitz [2000] specifically examined the rheological behaviour of varying concentrations of carbon black particles and dispersant within a screen printing ink. There was a tendency for the carbon particles (30 nm mean diameter) to flocculate and form a large loose interconnected network of 0.5 mm clusters when no dispersant was present in the formulation. The authors consider the particle volume fraction (f) the strength of the inter-particle interaction (U) and postulate that these are good indicators of the material storage and loss modulii. The authors present a model that scales the behaviour of the modulii onto a single master curve, by combining the elasticity of a solid network formed by the particles and the viscosity of the suspending fluid. Amari et al [1997] also propose the production of highly flocculated networks within the ink which dictate visco-elastic properties.

Hunge et al [2008] examined a range of particulate screen printing inks and measured their rheology through shear ramp curves and oscillatory rheometery. All inks exhibited pseudoplastic properties and the polarity of the solvents altered the rheology as a result of particle - particle interactions. Little was correlated between the rheology with the inks' printing performance.

In examining the fundamentals of the ink transfer mechanism in screen printing, a number of authors have suggested a transfer mechanism based on the development of hydrodynamic pressure at the squeegee tip which pushes the ink into the substrate, Reimer [1988], Huner [1994]. They postulate that this push force is plays the dominat role in ink transfer. Factors such as material elasticity, mesh tension and snap speed between the substrate and screen are ignored by this mechanism, although these are known to have an effect, Jewell et al [2003].

Others, primarily working in the solder paste printing industry, have promoted a "pull" theory where transfer occurs as the adhesion between ink and substrate overcomes the cohesive nature of the material, Messerschmitt [1982]. Numerical models developed by Abbot et al [2000] predict the effect of some printing parameters, but others' effects are contradictory to those seen experimentally; e.g. the model predicts a lower film thickness with increasing speed which is opposite to the findings of Hoornstra et al [1998], Ročak et al [1995] and Jewell et al [2003]. Material elasticity is ignored by this model and in heavily particulate laden systems, this assumption is clearly invalid.

The literature has highlighted that no simple correlations exist between the ink rheology (however measured) and the quality and quantity of the ink deposit. The literature also shows that there is no universal agreed scientific explanation or model of the ink transfer mechanism which considers the main physical characteristics of the ink.

Without a clear theoretical understanding of the ink transfer mechanism, then a process model for rheology - print characteristics needs to be statistically based.

3. Method

A range of carbon inks were formulated with varying conductive carbon content from 38% to 43% by mass. Non flocculated systems which could successfully be printed could not be achieved beyond the 43% upper limit, while the lower limit is derived from the conductivity requirements of the print. The inks were printed on a DEK screen printing machine and consisted of a 75 mm x 75 mm image containing a solid area lines of various thickness printed parallel, perpendicular and at a 45° angle to the squeegee direction. In order to simulate the effect of shear rate, the press speed was run at low (50 mm/s) and high (100 mm/s) speeds. One polyester mesh and 1 stainless steel mesh were printed, Table I. These were chosen as their mesh ruling properties were close (thus allowing similar detail definition) and lie in the middle of the mesh ruling range recommended for the ink. All samples were printed to a polyester substrate and were cured for 30 minutes at 90°C in an oven.

Table I: Meshes used in the study

Mesh material	Mesh ruling (/cm)	Thread diameter (μm)
Polyester	77	48
Stainless steel	78	40

The shear rheological properties of the inks were measured using an A-RES parallel plate rheometer capable of shear ramp and full viscoelastic characterisation. The extensional properties of the inks were measured using a custom built extensional viscometer operating in a CABER mode. A sample of material is placed between two anvils and the plates are separated at an "instantaneous" speed. The separation causes extension in the sample and by analyzing the evolution of the 2 dimensional sample profile with time using a high speed CCD camera, it is possible extract the extensional viscosity over a wide range of extensional strain rates from

$$\mu_{ext} = \frac{\sigma}{-2.\frac{\partial R}{\partial t}} \qquad (1)$$

Where σ is the surface tension and R/t is the rate of change of the mid filament diameter. This requires measurement of the rate of change of mid filament diameter and surface tension. Further details of the apparatus and the analysis method used can be found in Degenello et al [2007].

The electrical properties of the cured prints were measured by 4 point probes driven by an Agilent 5262A source - measure unit. Samples were subjected to a -10mA to +10 mA current sweep. To minimize errors associated with the probe tips indenting the relatively soft printed ink each sample was measured 5 times. The physical topology of the lines was measured using a Veeco NT2000 white light interferrometer, [Veeco 1998], which obtains a topographic surface map allowing line width, height and cross sectional area to be calculated via external custom written software.

3. Results

The effect of the changing formulation on the rheological properties of the ink is first presented. This is followed by an examination of the effect of formulation and process settings on the ink deposit characteristics.

3.1 Material properties

Simple flow curve measurements show that increasing the carbon proportion of the ink increases the viscosity of the material, Figure 1. This is expected, and there is a near linear relationship between the proportion of carbon and the viscosity at a given shear rate.

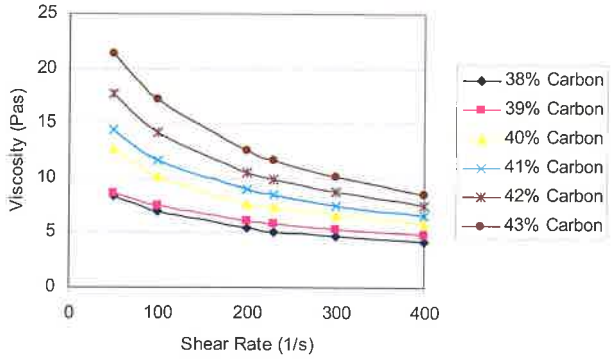


Figure : Flow curves for the carbon ink formulations examined in the study

The elastic component of the ink increases as the carbon proportion increases and all inks exhibit a linear visco elastic range until about 0.1 s^{-1} (measurements taken at 1 Hz) which is followed by a reduction in elastic component, Figure 2. There is an anomaly regarding the 39% ink whose elastic is less than that of the 38% ink. This feature remained throughout the rheological analysis and its cause is not immediately apparent. Increasing the carbon proportion resulted in an earlier reduction in the elastic component of the ink. The viscous component of the materials remains relatively consistent before reducing slightly at around 0.1 - 1 s^{-1}.

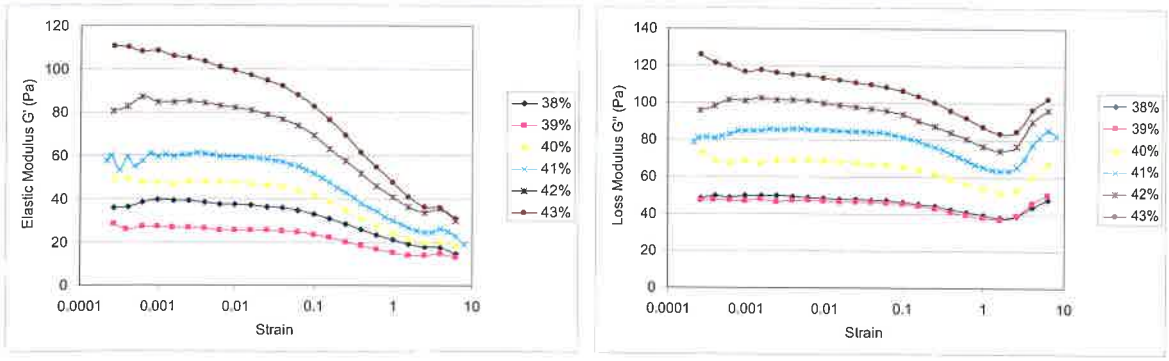


Figure 2: Elastic and viscous modulii for the carbon ink formulations

The extensional tests of the fluid show that the material is Newtonian in extension, Figure 3. The extensional viscosity shows a stepwise increase as the carbon content is increased.

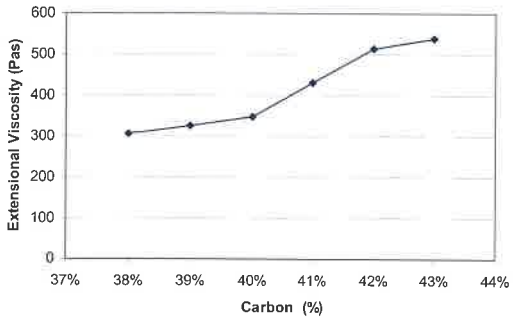


Figure 3: The extensional viscosity for the carbon ink formulations

The extensional Newtonian nature of the materials was not expected, but is observable as the gradient of the mid filament diameter / time plots over the initial period of extension, Figure 4. Some digitization of the mid point diameter measurement associated with the finite number of camera pixels can be seen in the multiple diameter measurements at a given time.

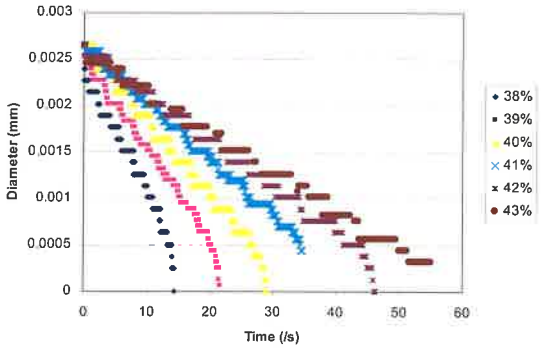


Figure 4: The mid filament diameter - time for the carbon ink formulations during the CABER test

3.2 Print quality

The results for a single printed line (0.5 mm wide) feature printed with the one polyester mesh (77 threads /cm) at the high and low print speeds are presented, as these are representative of the findings with other mesh. Increasing the carbon content produces a narrower higher line (Figure 5a) whose thickness is higher, Figure 5(b). The line width remains more or less contact up to 41% carbon and then reduces from 41%. Figure 5(b) also illustrates that the speed has a reasonable effect on the printed line height. The height reaches a maximum at around 41% and reduces as the quantity of carbon is further increased. It is postulated that this phenomena is associated with the reduction of ink slump which occurs during the printing process.

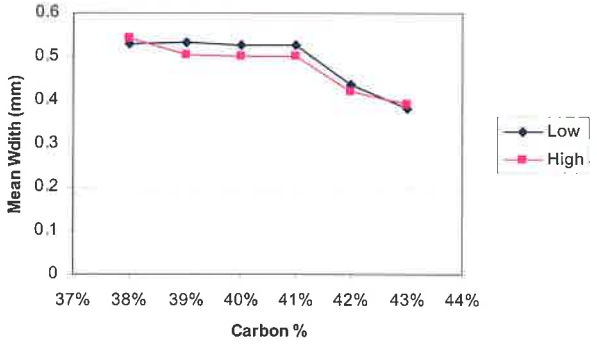


Figure5 (a): The effect of carbon content on the printed line width

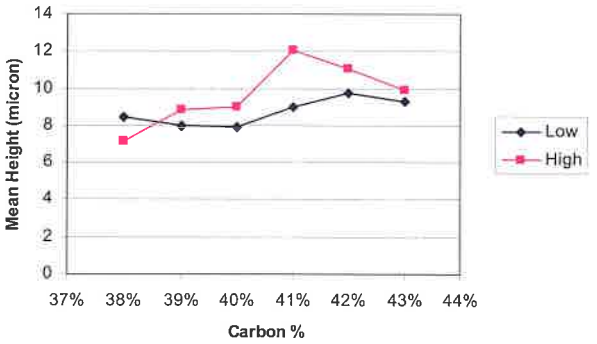


Figure 5 (b): The effect of carbon content on the printed line height

By integrating the cross section of the line it is possible to show that the net result of the changes in print height and width is to maintain the line cross sectional area (the available area for current flow) until about 42%, *Figure 6*.

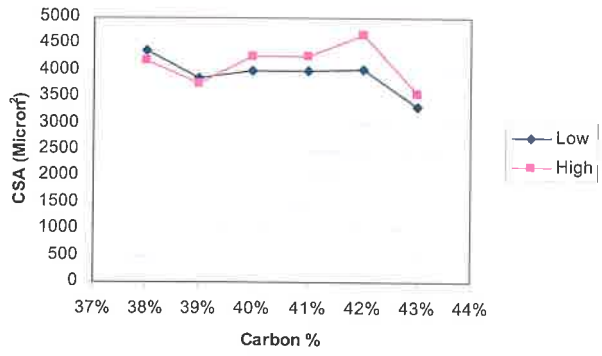


Figure 6: The effect of carbon content on the printed line cross sectional area

The net effect of the conductive carbon proportion on the conductivity of the line is to reduce the overall resistance which is a minimum at 43% at low speed and a minimum of 41% at high speed, Figure 7.

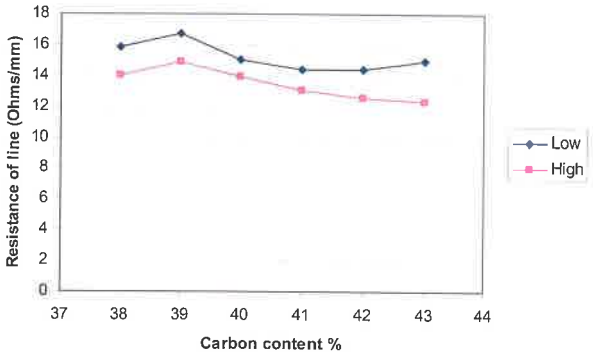


Figure 7: The effect of carbon content on the printed line resistance

4. Discussion

The primary goal of the research was to examine where a correlation could be drawn between the rheological measurements which can be carried out off the press and the printing behaviour of the ink on the press. Whenever such statistical correlations are drawn, care should be taken given the effective sample size of 6 inks at a given printing condition used in the study. Also, with such a limited dataset, there can be a tendency to over fit the data by using too high an order of polynomial. For this reason a simple linear correlation was used to examine the print quality - material property relationship. This has the added advantage of providing a more readily usable tool for the ink formulator. The inclusion of the other printing conditions (speed and mesh type) to increase the sample size produces unnecessary noise as their effect is at least as significant as the effect of ink formulation. It is also relevant to consider that any correlation should have as the basis is the physical science and not simply in statistical space where any parameter can be correlated to any other parameter. The correlation between the print height and a selection of rheometric characteristics show that no that there is no clear significant correlation (maximum R^2 of 0.79) between the print height and the rheological characteristics of the ink. The correlation are of a poorer quality for the higher speed prints.

Other tables were obtained for the correlation between the rheological properties and the printed cross sectional area and line width, but no significant correlations were apparent. Similarly other representative values of shear rate and G', G'' did not show significant correlation. The quality of the correlations can in part be linked to experimental variations, but it is likely that the assumption that a single point in a rheological measurement can be directly linked to an ink's printability is the most likely cause. The complexity of the materials and the likely multi shear rate and extension rate processes which occur during ink deposition makes a direct correlation with a single measurable parameter unlikely. If such a rheology - print quality model were to be produced, then it is likely that a larger dataset and more advanced statistical model (e.g. based on Neural

Networks or dimensionless analysis) would have to be developed. This could be developed from process QA measurements.

Table II: Linear correlation (R^2) coefficients between carbon content and print height

	Low speed Print height	High speed Print Height
Ext Viscosity (Pas)	0.789	0.469
Shear Viscosity at $50s^{-1}$	0.626	0.376
G' at 0.1 s^{-1}	0.730	0.310
G" at 0.1 s^{-1}	0.689	0.485
G' at 0.01 s^{-1}	0.727	0.299
G" at 0.01 s^{-1}	0.695	0.467

The study has however shown that the combined measurement of the rheology and ink deposit has allowed an understanding of the ink transfer mechanism in screen printing. The increase in height and reduction in line width with the higher viscosity materials tends to suggest that there is evidence of plug flow through the screen where a high shear lubricating layer is formed at the surface of the mesh and a coherent central solid material is transferred as it is placed in contact with the surface. This low shear high viscosity material is then removed from the screen as the screen lifts from the surface. This is corroborated by Hoornstra et al [1998] and Pan et al [1998].

The effect of the speed on the resistance and ink deposit can be greater than that of the carbon proportion in the formulation. This highlights the need for consistent methods for evaluating the inks' printing performance and suggests that there is considerable scope for the printer to alter the print quality at the production stage. The experimental set up and results were focused on lines greater than 100 micron in width (in order that they could be printed on each mesh). With a finer mesh, there is scope for reducing the printed line width to approximately 50 micron and it is likely that the relationship between rheology and print quality will be more critical as feature sizes decrease.

Although this study has examined the role of carbon content, the results are also likely to be applicable to other inks with a high particulate loading such as those using precious metals or ceramics. Also, preliminary studies have shown that the inks used in this study can be printed (with some specified rheological adjustment) by flexography using bench top printers with a coarse (300 lpi) anilox. It is intended that this study be used to examine the relationship between ink rheology and flexographic ink deposition which is more likely to be the process for mass producing basic electrical circuits on packaging. This work could also be extended to graphic inks to examine the relationship between rheology and halftone dot structure in order to develop a better understanding of the process and the relationship between rheology and tone gain.

5. Conclusions and recommendations

An experimental study investigating the effect of carbon content on the rheology and print characteristics has been carried out.

1. The quantity of carbon in the formulation, alters its rheology and has a subsequent impact on the geometry and topology of the printed feature.
2. Increasing carbon content increases line ink height while reducing line width. For the formulation tested, the ink reaches a maximum transfer at around 42%, whereupon there is a reduction in printed material.
3. No direct simple correlation could be found between a single measure bale rheological characteristic and the print quality characteristics.
4. The study has highlighted the main limitations of the current understanding of the screen printing ink transfer process.

Further work should examine

1. Improving any correlation through a larger test sample and improving the statistical correlation methods.

2. The relationship between the ink concentration for finer lines using a higher mesh rulings should be investigated.
3. A similar study should be carried out for flexography, where carbon inks are likely to be used for smart packaging.

References

1. Abbott S. J., Gaskell P. H., Kapur N. "A new model for the screen printing process - from theory to practical insight". 2nd International Symposium on Printing & Coating Technology, 2000
2. Amari T., Uesugi K., Suzuki H., "Viscoelastic Properties of Carbon Black Suspension as a Flocculated Percolation System". Progress in Organic Coatings 31 (1997) pp 171 - 178
3. Deganello D., Lubansky A. and Claypole T. C. - "Measuring extensional characteristics of printing inks", Proceedings of IARIGAI 2007
4. Hoornstra J., Weeber A. W., de Moor H. H. C., Sinke W. C. "The Importance of Paste Rheology in Improving Fine Line, Thick Film Screen Printing of Front Side Metallization" Netherlands Energy Research Foundation, 1998
5. Hung-Wen Lina, Chang-Pin Changb, Wen-Hwa Hwub, Ming-Der Gerb, -"The rheological behaviours of screen-printing pastes", Journal of Materials Processing Technology 1 9 7 (2008) 284 - 291
6. Huner B. "A Stokes Flow Analysis of the Screen Printing Process". The International Journal of Microcircuits & Electronic Packaging, Volume 17, Number 1, 1994, pp 21 - 25
7. Jewell E. H, Claypole T. C. and Gethin D. T. - "The impact of ink rheology on the image transfer mechanism in screen printing", Institute of Non Newtonian fluid mechanics, UK Institute of Non Newtonian fluids Conference on rheometry, Miskin manor April 2003
8. Messerschmitt E. "Rheological Considerations for Screen Printing Inks." Screen Printing. September 1982
9. Pan J., Tonkay G. L., Quintero A. "Screen Printing Process Design of Experiments for Fine Line Printing of Thick Film Ceramic Substrates" Department of Industrial and Manufacturing Systems Engineering, Lehigh University. October 1999
10. Riemer D. E. "Analytical Engineering Model of the Screen Printing Process: Part 1." Solid State Technology, August 1988, pp 107 - 111
11. Ročak D., Stopar V., Plut J. F., "Solder Paste for Fine Line Printing in Hybrid Microelectronics" Microelectronics Journal, 26 (1995) pp 441 - 447
12. Trappe V., Weitz D. A., "Scaling of the Viscoelasticity of Weakly Attractive Particles" Department of Physics and DEAS, Harvard University. March 2000
13. Veeco 1998 "WYKO surface profilers technical reference manual", Veeco Process Metrology

Security printing for product packaging in industrial printing applications

Slavtcho Bonev, Bernhard Wirnitzer

Institute of Digital Signal Processing/Mannheim University of Applied Sciences
Paul-Wittsack-Str. 10, D-68163 Mannheim, Germany
E-mail: s.bonev@hs-mannheim.de

Abstract

A new anti-counterfeiting technique combines the advantages of (i) a high-density halftone printed data storage and (ii) an unique signature caused by the physical interaction between printing medium (ink, toner) and substrate (paper, film). The high density data storage comprises a 2D-code (matrix code composed of code symbols), which can store several hundred bytes of binary data, and can be applied to protect products and packaging against counterfeiting and for track-and-trace applications. The unique signature (fingerprint) is extracted by measuring the code symbol irregularities. This innovative method is for the first time applied to offset printing and EER (equal error rate) better than 10-30 is achieved using a printed area of 5.1 x 5.1 mm. A quantitative comparison between the results of offset and laser printing is given.

Keywords

Anti-counterfeiting, brand protection, high-density 2D matrix code, low-cost security printing, printer signature, product packaging

1. Introduction

Security printing and anti-counterfeit packaging uses a combination of overt and covert security layers such as special coatings, inks or printing techniques, holograms, de-metallization, micro text, numbering, bar-codes, track and trace and tamper evident materials. The state of art in this field is described for example in [Ren, 2006]. Most of the current solutions are cost-intensive, the authentication cannot be realized by the consumer and the appearance of counterfeits often is only a question of time.

To overcome these drawbacks, more than two decades ago, fingerprinting techniques were suggested and successfully tested in several applications [Gol, 1981]. The main idea of fingerprinting is, to use the stochastic nature of materials or manufacturing processes for individualization and recognition of the originals. Fingerprinting, however, has been never used widely as it appeared to be sensitive if the protected product is slightly damaged or if the measuring devices are distorted. Recently these techniques were reinvented in a special modification using laser illumination [Buc, 2005].

In the mean time new watermarking and stochastic printing techniques have been developed [Pro, 2008]. These are based on visible or invisible secret patterns. At least in some spatial frequency components these patterns carry secret information which in some way is damaged if the print is copied. Since standard inks and packaging materials are used, effective and low-cost protection for mass products against counterfeiting gradually seems to become feasible. In the last years most these systems were improved by adding printed data storage, especially by using the well-known DataMatrix code, and PKS (public key cryptography). All these methods have in common, that they rely on the fact that the printed pattern remains secret - an assumption which is very critical in security printing applications.

In this paper the *EpiCode* technology suggested in [Wir, 2003, Wal, 2007] is experimentally verified and evaluated quantitatively for the first time. A high-density 2D matrix code is printed and its signature, caused by the physical interaction between printing medium (ink, toner) and substrate (paper), is extracted.

This high-density 2D matrix code (DataGrid) can carry encrypted information about the product protected. In addition a stochastic code (EpiCode) is extracted from each printed 2D matrix code and is used to identify each item. It is shown, that the EpiCode is very robust even if the protected package or print is damaged or if the detector devices are distorted in some way or another.

2. Methods, EpiCode and DataGrid

Whenever a 2D matrix code is printed onto a substrate, an individual stochastic code is generated during the production process [Wir, 2005]. As shown schematically in Figure 1, this so called EpiCode hovers above the digital data stored in the 2D matrix code. The EpiCode depends on a number of factors, e.g. paper roughness [Xur, 2005], toner granularity [Mal, 2004] or ink properties, printing process characteristics [Ali, 2003] and many more. For anti-counterfeiting applications the physical details of these effects have an influence on the security achieved. A good interaction between medium (ink or toner) and the substrate (paper, film) will generate an EpiCode of good quality. In order to enhance the EpiCode-effect, the investigations in this paper are based on a special 2D matrix code, the so called DataGrid [Wir, 2005].

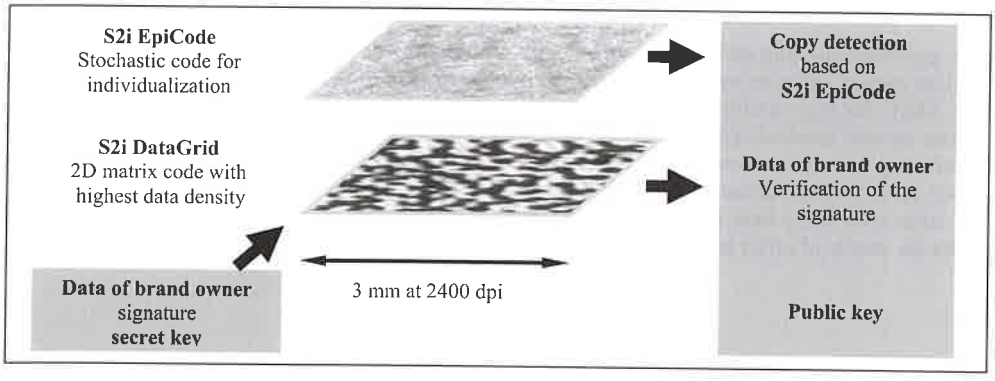


Figure 1: Security concept based on DataGrid und EpiCode

DataGrid (Figure 2) is composed of raster cells which are formed by 6 x 6-dots. In each raster cell, one of eight different symbols is printed in order to store three bits of digital information. The symbol structure has been optimized for security applications, high data density, poor print quality and low-end scanner optics.

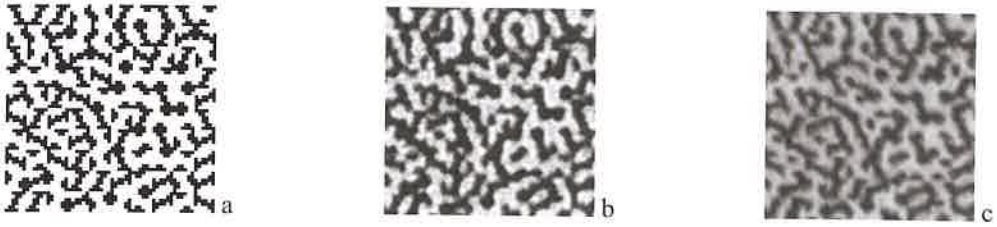


Figure 2: Examples of an original (a) and the printed (b-laser, c-offset) data storage DataGrid

The steps for anti-counterfeiting applications are:

i) Coding data in a 2D matrix code and printing the matrix code,
ii) Capture the image of the printed code, decode it and extract the EpiCode.

In the coding step PKS (public key cryptography) can be used. In this way only the owner of the secret key can generate the data for the matrix code, but all owners of the public key may read this data. In the second step the matrix code is decoded and the EpiCode is extracted. The investigations presented in this paper are based on software offered by Epyxs Inc. [Epy, 2008]. The software decoder processes a scanned image of a DataGrid and delivers two vectors - an (error corrected) data vector and a binary EpiCode vector $\underline{\mathbf{e}} = [e_1, e_2,...e_N]$, which contains the signature of the printed code.

A quantitative measure is needed to compare different printing technologies and substrates. Using standard methods for biometrical systems analysis [Gar, 2006, Dau, 2006], the false acceptance rate (FAR), false rejection rate (FRR) and receiver operating characteristics (ROC) based on cross-correlation coefficients $\mathbf{c}$ of EpiCode vectors $\underline{\mathbf{e}}$ and reference vectors $\underline{\mathbf{r}}$ are calculated. The correlation coefficient of the vectors $\underline{\mathbf{e}}_i$ and $\underline{\mathbf{r}}_j$ is

$$c_{ij} = \frac{2 \cdot \sum_{k=1}^{N} NXOR(e_i(k), r_j(k))}{N} - 1$$, where NXOR is the negated XOR operator.

In case of an original print, the captured EpiCode $\underline{e}_i$ of print number i will be highly correlated to the reference vector $\underline{r}_i$ of print number i stored in a database and the correlation with all other prints i!=j in the data base will be low. In the experiments, correlation coefficients are evaluated and depicted in a histogram. Gaussian distributions are fitted to the measurements and FAR and FRR are calculated for defined thresholds of discrimination. Finally, the EER achieved is presented in a ROC diagram.

3. Experimental results

In Figure 3 the experimental concept is presented. A single test chart of DataGrids was created. Each column contained the same DataGrid and adjacent columns carried different DataGrids. The test chart was multiple printed on a *PAPERONE Copier* paper using laser and on *FASSON* adhesive data sheet using offset printing and eight sheets were selected. Then, reference and authentication scans were performed on each set of sheets to create enrolment and authentication sets [Gar, 2006]. For further details see Table I.

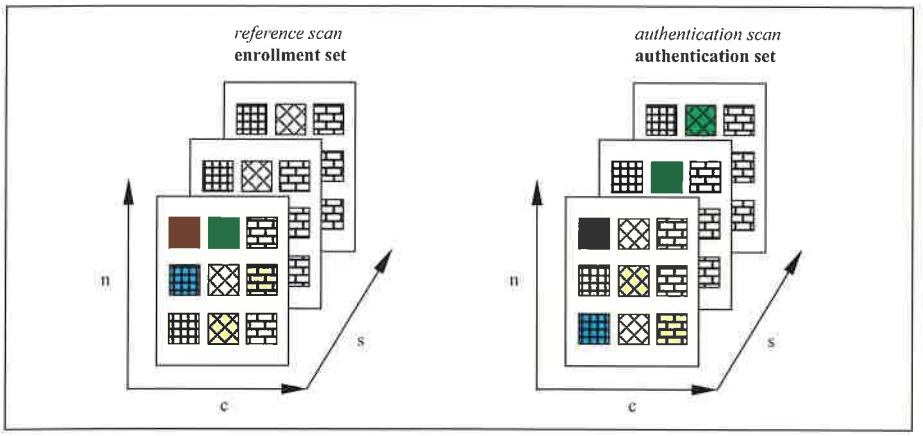


Figure 3: Experimental concept: n - matrix code number (N=13), c - matrix code info (C=10), s - sheet number (S=8)

Table I: Experimental data

Nr	Printing devices: device type	Printing resolution	DataGrid size symbols/mm	Scanning devices: flatbed scanners	Scanning resolution	Scan type
1	HP laserjet 2420	600 dpi	40 x 40 symbols	HP scanjet 8200	1200 dpi	reference
2	laser printer		10.2 x 10.2 mm	Canon LiDE 70	1200 dpi	authentic.
3	Roland 200	1200 dpi	40 x 40 symbols	HP scanjet 8200	2400 dpi	reference
4	offset printer		5.1 x 5.1 mm	HP scanjet 8200	2400 dpi	authentic.

The results of the laser and offset print experiments are presented in Figure 4.

The distributions on the right side illustrate the correlation between *originals*, i.e. comparisons between different scans of the same print. The mean values of the correlation coefficients are 0.551 (laser) and 0.666 (offset). As expected, the correlation coefficient for comparisons of originals is not 1.000, due to the influence of noise and distortions in the scanning process.

The distributions in the middle left of the graphics illustrate the correlations between *different* prints of the *same* DataGrid at *different positions* on the test sheet, i.e. the same column in all sheets. The mean values of the correlation coefficients are 0.133 (laser) and 0.104 (offset). Compared to the correlation values of the originals these low correlation values impressively confirm that each printed item has its individual characteristics. The calculated FAR and FRR at a threshold of 0.4 show, that there is an overwhelming amount of discriminatory information in the signatures [Pan, 2002].

The distributions in the middle right of the graphics illustrate the correlation between *different* prints of the *same* Datagrid at the *same position* on the test sheet. The mean values of the correlation coefficients are 0.142

(laser) and 0.295 (offset). The mean value measured for laser printing shows no significant difference to its corresponding value above. The mean value for offset printing is significantly different from its corresponding value and forms a separate distribution, which is a good indication for an individual signature of the printing plate. This signature is generated during the exposure of the printing plate.

Finally, the distributions on the left side illustrate that there is no correlation between the signatures of different DataGrids.

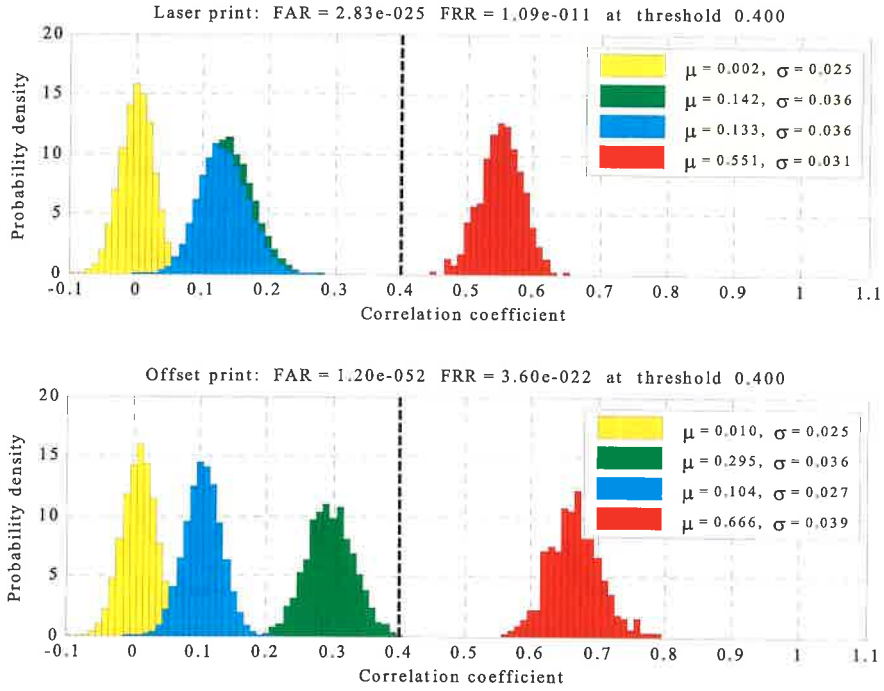


Figure 4: Results for laser and offset printing. The EpiCode (individual print signature) is a binary vector with 1600 elements

The receiver operator characteristic (ROC) in Figure 5 represents the trade of FRR and FAR [Gar, 2006]. A threshold is swept across the range of calculated results. At each step the values of FRR and FAR are recorded. Plotting the values creates an ROC curve, which is used to estimate the equal error rates (ERR). The EER is the location on a ROC curve where the false acceptance rate and false rejection rate are equal [Nst, 2006]. In general, the lower the equal error rate value, the higher the accuracy of the biometric system. For laser printing at 600 dpi an ERR of 10^{-18} and for offset printing at 1200 dpi an ERR of 10^{-33} were achieved.

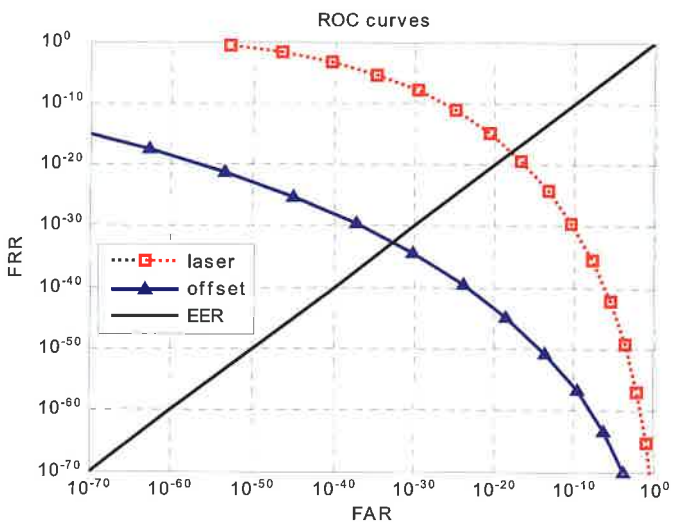


Figure 5: Prediction of FAR, FRR and EER for laser and offset printing from measurement results

4. Discussion

We have demonstrated a reliable measurement of the individual print signature called EpiCode of a printed DataGrid matrix code. It is verified, that this halftone pattern can be used for identification purposes and that conventional offset printing is suitable for security printing applications. In particular, the individual signature of the printing plate was reliably detected. It is proposed to use this feature for security applications.

The experimental results impressively demonstrate the following quantitative features of the technique:

- In the case of 600 dpi laser printing an area of 10.2 x 10.2 mm is necessary to achieve an EER of 10^{-18}.
- For 1200 dpi offset printing the results are even better: 5.1 x 5.1 mm are needed for an EER of 10^{-33}.
- Partial distortion of the DataGrids is not critical because of the 66 % redundancy is used for error correction.

The principal difference of the presented anti-counterfeiting technique compared to other recognition methods is that the fingerprint is clearly related (adherent) to the binary information of the matrix code. As a consequence, distortions in the EpiCode or in the reading device can easily be detected and eliminated. Certainly, in this case the EER will decrease but the EER achieved are far beyond the security needed in most of the practical applications (remember that the world population is lower than 10^{10}).

5. Conclusions and future work

Though the system was already applied for counterfeit protection of packages and adhesive labels in a pilot application (Figure 6), "EpiCoding" is only at the beginning. Investigations are necessary for different combinations of the printing medium (ink, toner) and the substrate (paper, film, metal etc.). Further scan devices and printing processes are to be considered, as well as their influence on the recognition performance and the integration into printing and packing machinery.

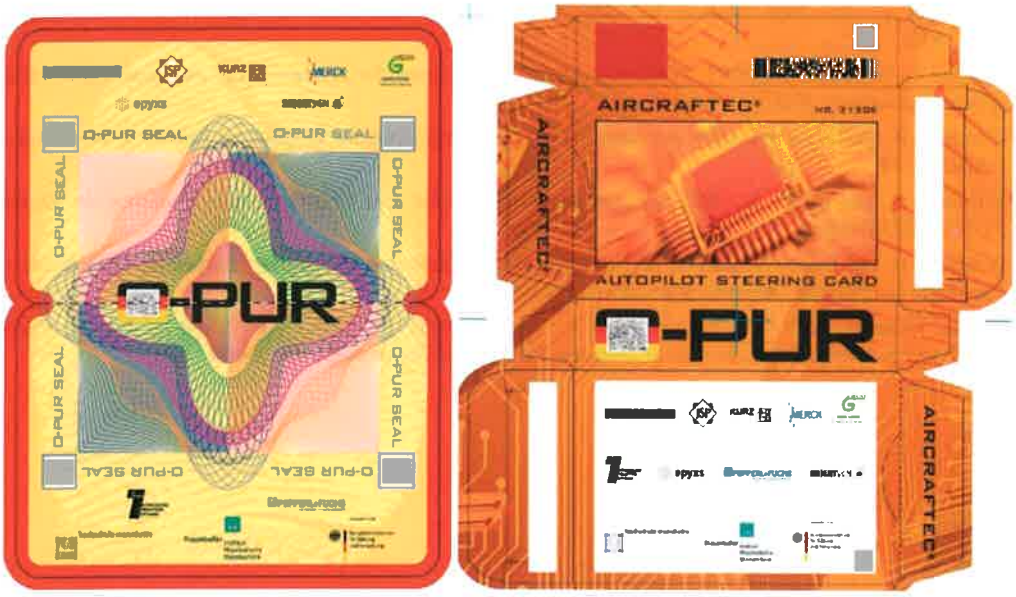


Figure 6: Adhesive label with several security elements (left). The EpiCode is extracted from 4 DataGrids in the corners. Counterfeit protected package with 2 integrated Datagrids (right)

Acknowledgments

We gratefully acknowledge the financial support by the BMBF of the Federal Republic of Germany (FKZ 02PU1150, OPUR project, www.opure-secure.de). The results presented would not have been possible without the stimulating discussions together with Thomas Walther and without the printing test supported by MAN Roland Printing Machines AG.

References

1. Buchanan J. D. R., Cowburn R. P., Jausovec A. V., Petit D., Seem P., Xiong G., Atkinson D., Fenton K., Allwood D. A. and Bryan M. T., 2005, *Fingerprinting documents and packaging, Nature, 436, 1234 - 1235*
2. Chiang P.-J., Ali G. N., Mikkilineni A. K., Delp E. J., Allebach J. P. and Chiu G. T., 2006, *Extrinsic signatures embedding and detection for information hiding and secure printing in electrophotography, American Control Conference*
3. Daugman J., 2006, *Probing the Uniqueness and Randomness of IrisCodes: Results From 200 Billion Iris Pair Comparisons, IEEE Proceedings, 94, 11, pp. 1927 - 1935*
4. Epyxs Inc., 2008, *www.epyxs.com*
5. Garris M. D., Tabassi E. and Wilson C. L., 2006, *NIST Fingerprint Evaluations and Development, IEEE Proceedings, 94, 11, 1915 - 1926*
6. Goldman R. N., 1981, *Non-counterfeitable document system, US4423415,* 1985, *System of issuing secure documents of various denominations, US4675669*
7. Goldmann G., 2006, *Digital Printing: Techniques and Printing Technologies of OCE Printing Systems GmbH, ISBN 3-00-001019-X, 328 - 333*
8. Malvern Instruments Ltd., 2004, *Toner particle size and shape analysis, http://www.malvern.com/LabEng/industry/toners/shape.htm*
9. NSTC Subcommittee on Biometrics, 2006, *Biometrics Glossary, http://www.biometricscatalog.org/biometrics/glossarydec2005.pdf*
10. Pankanti S., Prabhakar S. and Jain A. K., 2002, *On the individuality of fingerprints, IEEE Transactions on Pattern Analysis and Machine Intelligence, 24, 8, 1010 - 1025*
11. Product information, 2008

    http://www.alpvision.com/cgoverview.html
    http://www.linoprint.de/de/Anwendungen/Seiten/Linoprotect.aspx
    http://www.thomson.net/GlobalEnglish/Solutions/content-tracking-security/packaged-media/Pages/default.aspx
    http://www.epyxs.com/cms/servlet/Query?node=58&language=2
12. Renesse R. L. van, 2006, *Optical Security and Counterfeit Deterrence Techniques VI, Proceedings of SPIE, 6075*
13. Walther T., Wirnitzer B., 2007, *Apparatus method and process for the stochastic marking and tracking of printed products, WO2008/049550*
14. Wirnitzer B., 2003, *Datenträger mit Kopierschutz und Verfahren zur Kodierung solcher Datenstreifen, DE10345669*
15. Wirnitzer B. and Bonev S., 2005, *Rasterdruckdatenspeicher und Verfahren zum Codieren der Daten, PCT/EP2005/008097*
16. Wirnitzer B. and Bonev S., 2005, *Fälschungsgeschützte Datenspeicherung in gedruckten Rasterbildern, Fachhefte Graphische Industrie (Bern/Switzerland)*
17. Xu R., Fleming III P. D., Pekarovicova A. and Bliznyuk V., 2005, *The Effect of Ink Jet Paper Roughness on Print Gloss, Journal of Imaging Science and Technology, 49, 6, 660 - 666*

Integration of screen-printed antennas in plastic body parts using in-mould technology

Ingmar Petersen[1], *Gunter Hübner*[1], *Markus Pfletschinger*[2]

[1] Hochschule der Medien (HdM), Institute for Applied Research (IAF)
Nobelstraße 10, 70569 Stuttgart, Germany
E-mail: huebner@hdm-stuttgart.de

[2] Hirschmann Car Communication GmbH, Antenna R&D
Stuttgarter Straße 45 - 51, 72654 Neckartenzlingen

Abstract

Antenna structures are produced via screen printing onto a film substrate and afterwards permanently integrated in plastic body parts of the automotives using the in-mould technology. Trials were carried out with thermoset materials like SMC (fibre-reinforced polyester) and PUR-LFI (polyurethane long-fibre injection) and with thermoplastic material like ABS (Acrylonitrile butadiene styrene). To achieve perfect integration (material combinations) different film substrates were used. Finally a comparison of the electrical performance of an integrated antenna to a state-of the-art solution is drawn.

Keywords

Antenna, in-mould, polymeric thick film, screen printing

1. Introduction

Due to the increasing amount of requested telecommunication services and functions such as radio, television, mobile phone etc. more and more antennas are necessary [1]. The present paper reports of a new technology to integrate antennas in the surface of different types of plastic materials of the automotive industry and latest results of the R&D work. Integrated antennas can be used where the body parts of the vehicle are not made of conductive material. Every antenna must be custom-made as the complete vehicle has got influence on the antenna performance.

Concerning the integration of antennas, screen-printed structures upon the rear window are state of the art [1]. Unfortunately, the realisable antenna layouts are very limited in this case because it influences the outside appearance of the vehicle very much.

The goal of this work is to develop an alternative technology which enables the integration in plastic body parts of the automotive industry to increase the degree of freedom in case of the feasible antenna layouts and furthermore to gain performance. Fortunately, the amount of plastic parts in the automotive industry is increasing [2] what enhances the possible implantation spaces, see Fig. 1. Especially vehicles without a rear window like convertibles and commercial vehicles offer great opportunities for this new technology.

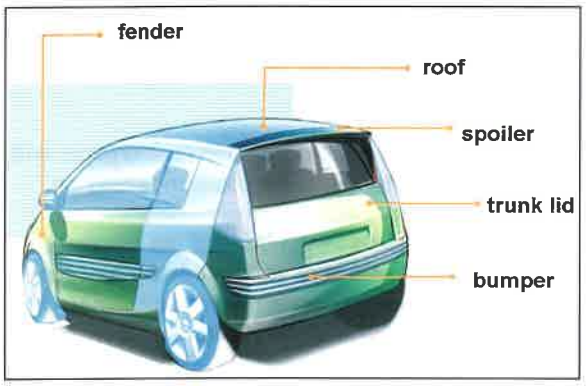


Figure 1:
Possible implantation spaces in vehicles

In-mould processes for "graphical" products could be termed as state of the art. They are well known in the packaging as well as in the automotive industry. Especially housings, facings and decoration are manufactured using this technology [5]. The challenge of the project is to expanse this technology for the production of functional products e.g. an antenna.

2. Methods

The core of this technology - the conductive structure - is realized via screen printing with various polymeric thick film pastes (PTF) on different substrates. The implantation of screen printed antennas made of silver-filled PTFs is well-known from RFID applications (13.56 MHz or 869 MHz) [3]. The suitability of PTF pastes for conventional FM-radio frequencies like 100 MHz was examined by us previously [4] using method of moments for electromagnetic modelling. Since a printed line usually has a different width than a rod (monopole) the influence of the line width and its conductivity was investigated. A typical result is depicted in Fig. 2 and shows that the performance of the printed structure above 4 mm line width comes rather close to the reference.

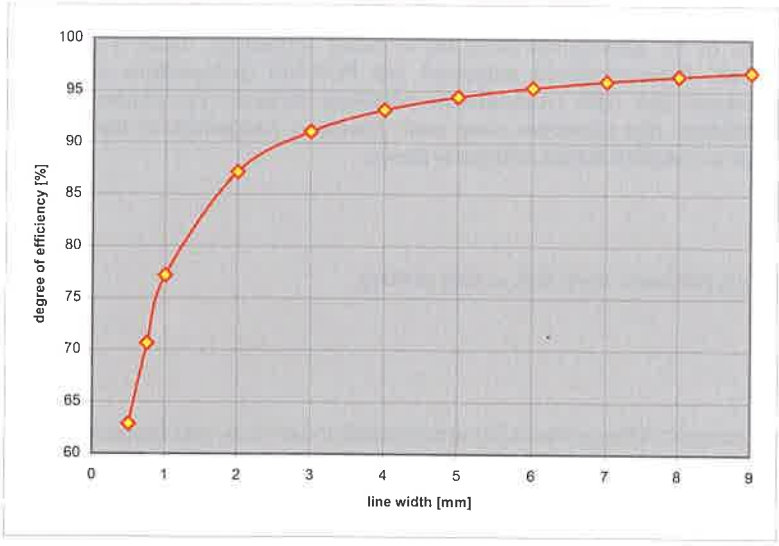


Figure 2: Simulation of the influence of conductivity and line width on the degree of efficiency - related to monopole 750 mm, 100 MHz, 30 mOhm/sq./15 µm - [4]

The PTF market offers a wide range of different silver-filled polymeric thick film materials where the type of binder, the silver content and the silver grain geometry vary. We decided to use thermoplastic binder PTF solely to keep the printed layer as flexible as possible. Thermoset based materials are mainly used for rigid substrates. After the screen printing the solvent (solvent blends) has to be evaporated. For complete evaporation the required temperature typically lies about 130°C simultaneously increasing the contact pressure of the silver grains and thus the conductivity.

A very important plastic body part material is SMC. Its use offers a wide range of advantages like weight saving, design flexibility, dent resistance, dimensional stability, corrosion resistance, low transmission losses and recyclability. For the integration process the antenna was printed on a special resin impregnated paper whose nominal processing temperature is 145 - 170°C. This fits perfectly to the drying temperature of the PTF (130°C), when a mould temperature of 150°C is chosen.

After positioning the SMC material in the opened mould (Fig. 3 left hand side) the resin impregnated paper with its printed antenna on top of it. The printed face shows into mould direction to enable the connection later on.

Due to high pressure and temperature during the compression process we observed an increase of conductivity of the antenna structures which is very welcome. A circuit of 4 mm width and 100 mm length showed a dc resistance of 0.35 Ohm before and 0.15 Ohm after the moulding process. Surface roughness (Sq) of the printed circuit changed from 10 µm to 1 µm. The images Fig. 5 and 6 were taken with an optical surface analysis and 3D measurement device.



Figure 3: Positioning of SMC material(left) and closed mould (right)

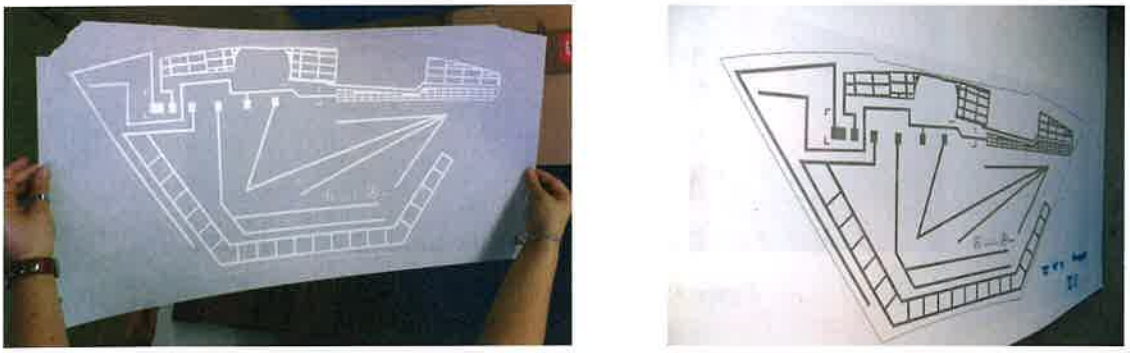


Figure 4: Printed antenna on resin impregnated paper (left) and SMC part with integrated antenna (right)

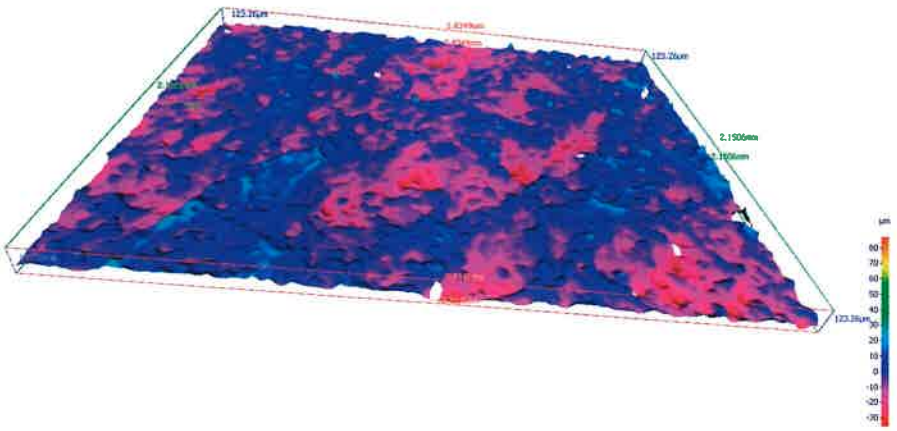


Figure 5: Surface roughness of circuit before SMC moulding process

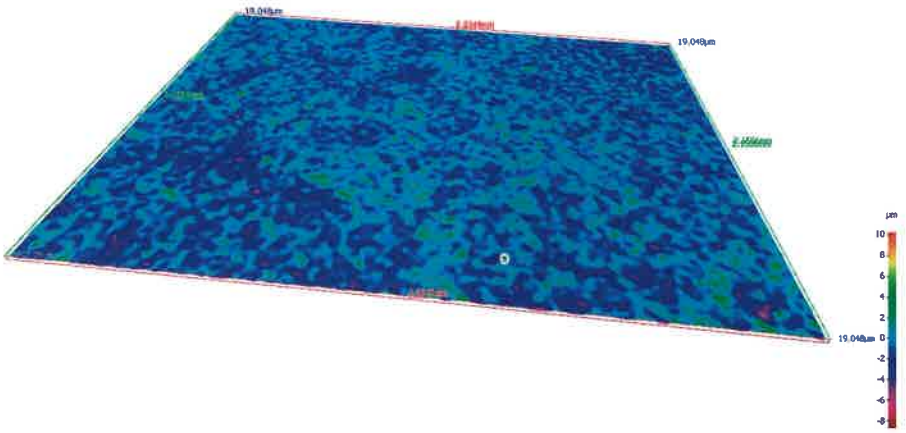


Figure 6: Surface roughness of circuit after SMC moulding process

Due to the harsh temperature treatment during the in-mould process the material combination needs to be adapted carefully. The thermal behaviour of the material has got a major influence on the result in every matter [6, 7]. For PUR over-moulding (process shown in Fig. 7) a lot of different substrates materials had to be tested, too. After processing the material still has to be error free and must not show damages like cracks (Fig. 8).

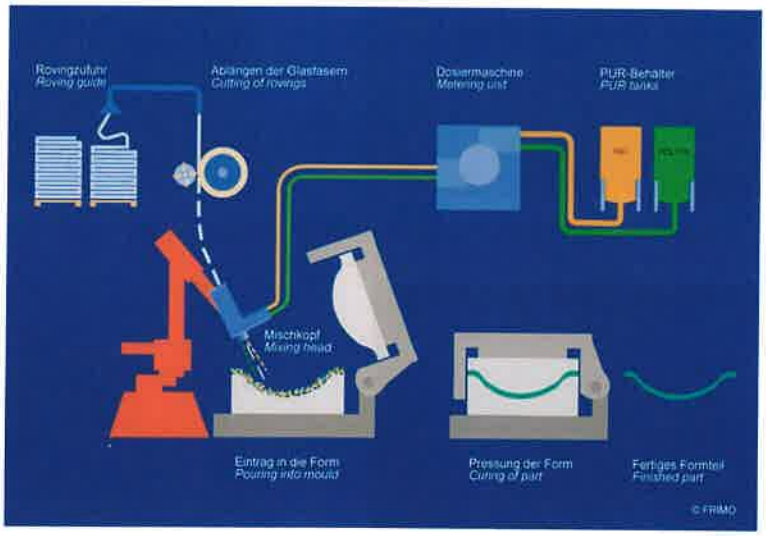


Figure 7: Principle of PUR-LFI process

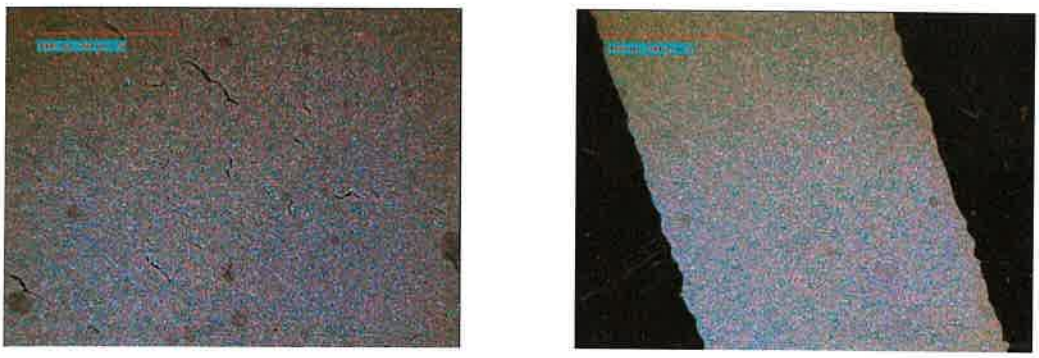


Figure 8: Inappropriate cracks (left) and suitable thermal material combination (right) for PUR

The mechanical requirements such as durability are also quite demanding. In order to connect the antenna to an amplifier in the final assembling process mechanical contacts have to be attached to the surface. Therefore a sufficient wear resistance, adhesion and cohesion are absolutely necessary. The scotch tape peel test with cross hatch cut (Fig. 9) revealed poor and very good candidates.



Figure 9:
Scotch tape peel test (cross hatch cut) with PUR test sample

The connection of the antenna structures can be realised by springs. This technology is known as "on-glass" solution which is common to rear window antennas [1]. A special frame is glued upon the surface in which the amplifier is clipped (Fig. 10). Its springs are directly connected to the surface of the printed circuit. It shall be understood that this solution is mostly suitable for planar surfaces.

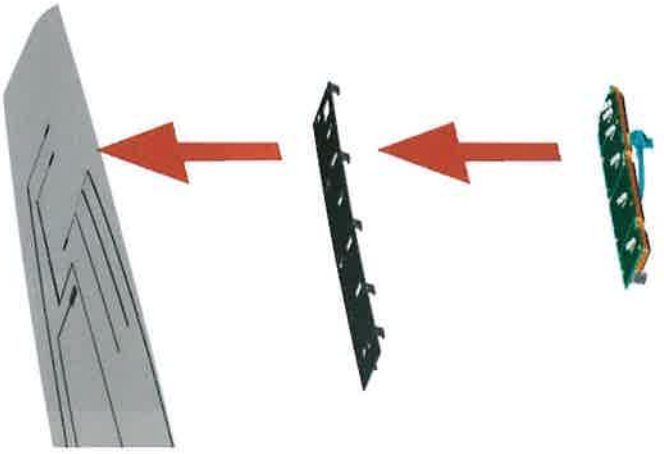


Figure 10: Connection of amplifier using "on-glass" technology

Finally prototyping was carried out with thermoplastic ABS. The current serial production for this car is a copper wire in the bumper (Fig. 11 left hand side) which should be replaced. The geometry of the body part is three-dimensional which makes in-mould processing more complex. First of all, an antenna layout for the available space was designed as shown in Fig. 11 right hand side.

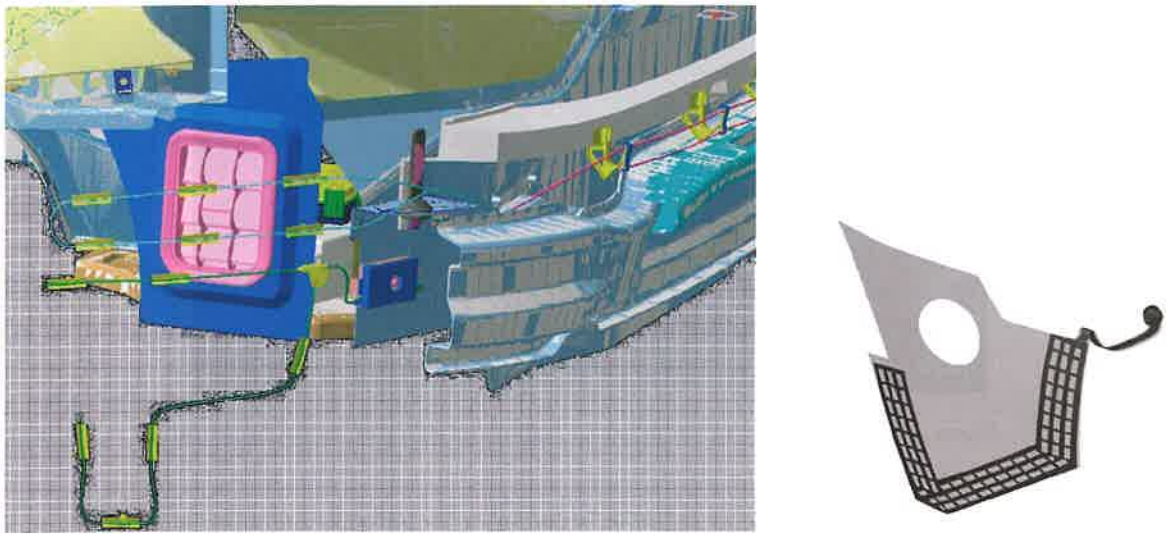


Figure 11: Current serial antenna with copper wire and replacement idea

We observed very good results with over-moulded ABS and PMMA substrates. Unfortunately these substrates are not stable up to 130°C which caused problems during the drying process of the printed circuits. Therefore we had to decrease the drying temperature and to increase drying time. The mould temperature is 50°C and the injection temperature 250°C. Injection pressure was 120 bar.

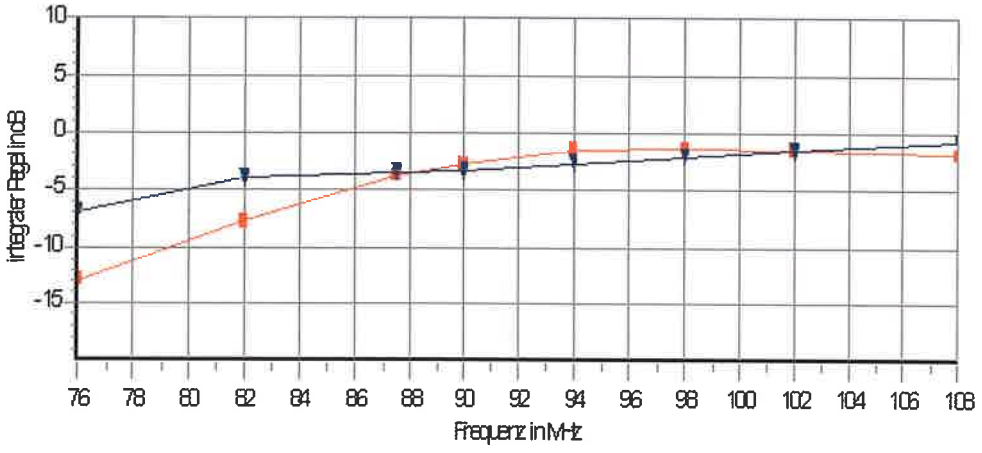
To compare the over-moulded integrated antenna to the copper wire solution it was connected with a screw-push button (Fig. 13) to a network analyser and the frequency response was measured. The measurements show better performance of the printed antenna than the copper wire (Fig. 14). Because of the printed layout and its line width the antenna has a more broadband characteristic.



Figure 12: Inserted antenna film in ABS injection mould and moulded part



Figure 13: Measurement setup for frequency response of ABS over-moulded antenna



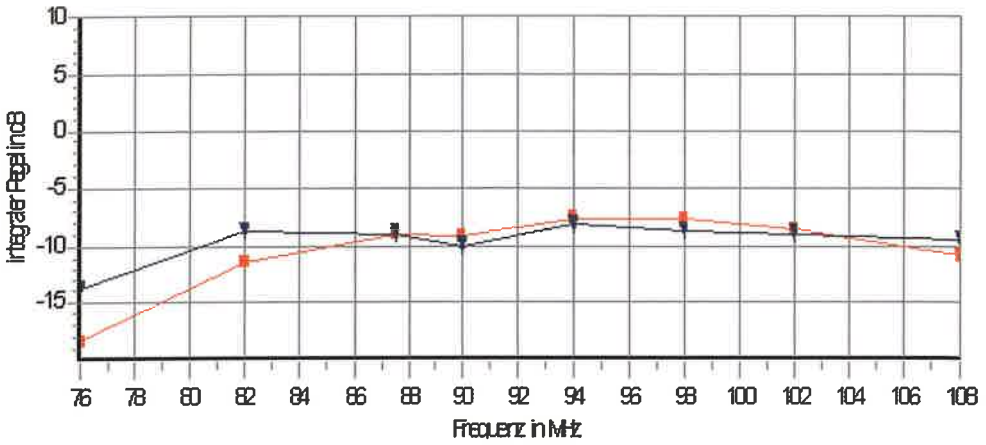


Figure 14: Frequency response of horizontal (top) and vertical polarisation (below)

3. Discussion

Although it seems that the screen printing process is very well known every new application like this integrated antenna technology requires a lot of optimisation work until a series production can be successfully run.

The mesh, the stencil technique and all the other parameters of the printing process have to be carefully adapted to the ink properties. Since the silver ink is very expensive during the print process waste must be minimized. The development at the research institute ends with a manufacturing recommendation and the hand over to a commercial print shop.

Further during this work several techniques beyond the pure printing technology had to be investigated. In order to develop competitive or even better products than the state-of- the- art a lot of effort had to be put in plastic material research and electric testing. The variety of materials and possible applications in the automotive industry is very high. Thus, although the first integrated antennas have gone to series production, now the development is still ongoing and more material combinations and more complex designs must be tested.

A very helpful circumstance and success factor lies in the increase of the conductivity of the antenna structure due to the applied pressure during the moulding process. It is not possible to yield such results by pure thermal treatment.

4. Conclusion

It could be demonstrated that for various types of thermoplastic or thermoset material a special material combination of film and conductive polymeric thick film paste is suitable to be over-moulded seamless. Even difficult mould geometries resulted in well functioning parts as the chosen film substrate and PTF were well adapted to the injected plastic material.

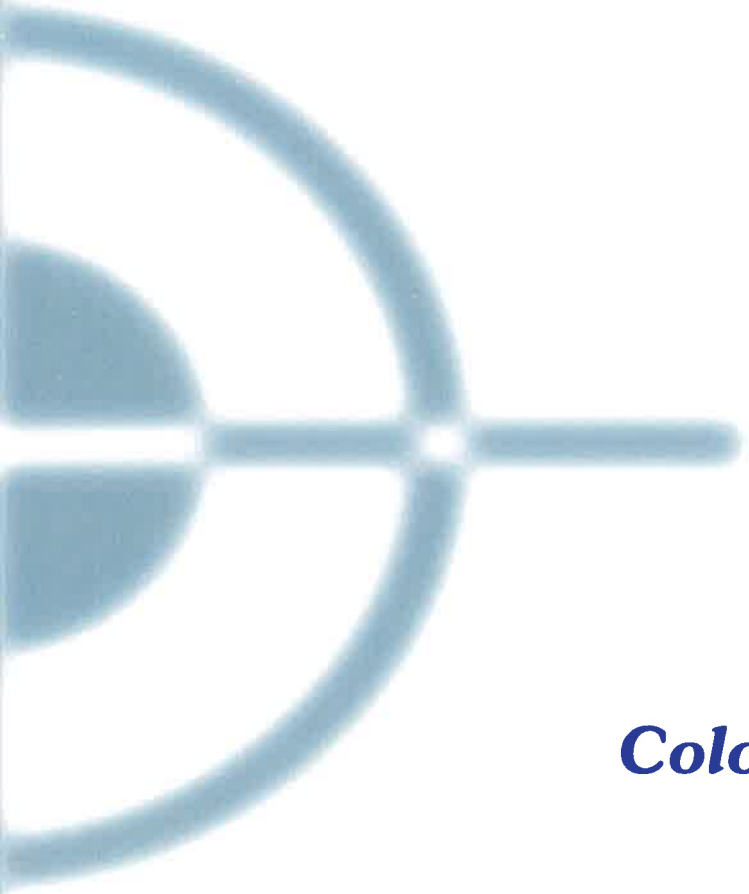
Acknowledgement

This work was supported and funded by Hirschmann Car Communication, Germany.

References

1. Gottwald, G. - Moderne Antennensysteme - Moderne Industrie, Landsberg 2003
2. VKE e.V. - Kunststoff im Automobil - Frankfurt/Main 2002
3. Koptioug, A., Jonsson P., Olsson T., Sidén J. - On the behaviour of printed RFID tag antennas, using conductive paint. - Sweden 2003 url: http://www.sensiblesolutions.se/articles/antenn 03-on the behavior.pdf

4. Petersen, I. - Printing conducting aerials - Stuttgart 2007 - presented at Technical Research Conference - WCPC, Swansea
5. Bayer AG - New applications and practical examples involving in-mould decoration. - ATI 7007 - Leverkusen 1998 url: https://pc-films.de/pc-films/emea/en/docguard/A7007.pdf?docId=1850
6. Saechtling, H. - Kunststoff Taschenbuch - .Hanser Verlag, München 1986
7. 3D-MID e.V. - 3D-MID Technologie - Hanser Verlag, München 2004



4

Color reproduction and quality

High definition halftone printing - HDHP: background, current status and challenges of the adaptive screening developments

Yuri V. Kuznetsov

North-West Institute of Printing of the St. Petersburg
State University of Technology and Design
Dzambula lane 13, 191180 St. Petersburg, Russia
E-mail: yurivk@mail.ru

Abstract

Along with the short overview of modern digital screening approaches the paper discusses and presents:
- basic principles of patented HDHP technique;
- HDHP method of an image files adaptive processing;
- specific, advantages and promotion issues of its practical application;
- concept of the further development of this approach potential in direction of the quantization scale spatial dispersion which is adaptive to the arbitrary contour of an image.

The samples of test images and microphotographs of fragments of illustrative print jobs using the HDHP technology are also presented.

Keywords

Fine detail, resolution, screening, sharpness, tone rendition

1. Introduction

The issues of tone (color) rendition and of fine detail or contour accuracy are used to be to certain extent independently concerned in the imaging science. Screening comprises, however, the unique kind of an image transformation which enables the conflict in providing both tonal and spatial resolution. The trade off is solved in reproduction practice on behalf of the first of these requirements, i.e. by keeping the tone range constant (between 3-5 and 95-97 percent) for all the variety of screen frequencies [1, 2].

At this condition, the screen ruling value depends on the absolute minimal size of a halftone dot which is steadily available for given type of a job, i.e. for the particular kind of print stock, ink, plate, equipment, etc. Providing this size over the print sheet within a run comprises therefore the basic criteria of optimal adjustments within the substrate-plate-ink system for the halftone printing. It's worthwhile to note, that the ink solid densities, used in wide practice to indicate the match to some standard printing conditions, are just the secondary factors found in press optimal adjustment evaluations.

To provide both as much as possible amount of grey steps within the mentioned tone range and visual uniformity of an image vast stationary areas the optimal geometry of a screen and halftone dot, as well as the way of dot form variation along a grey scale were empirically found during over a century of the autotypie printing practice. However, the number of lately suggested digital screening techniques, being aimed to achieve a certain novel image quality, failed to be practical because of ignoring said industry approved experiences.

The non-periodic or screenless photomechanic halftones, provided, for example, in collotype printing of the past, were renewed by digital screening techniques of last decades under the new names of FM, dither, stochastic, error diffusion, etc. In spite of providing the greater spatial frequency response, as compared to periodic screening, these non-periodic halftones have found, meanwhile, very limited industrial application because they don't take into account the practically approved priority of above mentioned tone rendition and printability requirements. The use of minimal available dot and non-inked area over the whole tone range makes such a screen very sensitive to the smallest non-stability of a printing system. (This statement can be easily approved on any printer by outputting the page comprised of the minimal printer dots located in chessboard order, i.e. corresponding to 50% ink coverage.)

Recently, the concept of dots amount variation was, nevertheless, partially implemented in the so called hybrid halftones where the number of dots is randomly decreased to somehow expand in highlights the range of gradation reproduced by the basic periodic screen. However, such a solution still stays within the approach of the auxiliary screen frequency variation used in photomechanic Respi screens of 60ies or for digital screening of K-separation in Hell Chromograph 300 of 70ies. In terms of the adaptive screening techniques this way of modifying a halftoning algorithm over an image area can be related to the **tone dependent** one. At the same early period of electronic screening developments the other, **tone gradient dependent** approach was suggested for more effective, optimal use of an imaging system resources and withdrawing the eternal conflict of simultaneous providing both tonal and spatial resolution of a halftone image [3].

Unlike the other imaging systems the specific process of graphic industry is to transform the continuous tone original to a bi-level print comprised of the plurality of small inked and blank elements. As far as the resulting amount of ink transferred to a print and, hence, the basic quality issues of the latter such as color, definition, tone rendition, sharpness, etc. are fundamentally dependent on these elements area, form and geometry of placement the screening has always comprised the actual, cornerstone R&D issue of illustrative printing.

With taking into account such, clear to any printer, facts, not only the RIP vendors but, as well, the producers of a lot of just related printing equipment and consumables have to permanently suggest some novel, their own ways of a halftone dot formation and positioning to accentuate thereby their standing on a proper level of innovation as a moving marketing forth. As result, many dozens of currently available, announced or upcoming, patented and trade marked screening techniques are currently pretending on their approbation and practical use.

In such situation the demand arises for correct, quantitative comparison of various screening techniques efficiency with the other important factors involved to the process being, if possible, kept the same [4]. However, the screening developments, estimations and implementations are accompanied today by the number of certain misconceptions and illusions. Along with the importance and due to the interest to this problem the great amount of "halftoning myths" has appeared, which are shared not only by the practitioners, but, as well, by many educators and researchers. The whole list of such myths can be completed by the analogy with "color myths", commented by Giorgiani and Madden in their book [5]. So, it looks worthwhile to comment, forehand the further discussion, some popular myths concerned of screening.

2. Halftoning myths

Myth: *In "Hi-Fi" printing the use of non-periodic halftone eliminates the problem of additional fifth (green), sixth (orange) and seventh (violet) inks to share screen angles with the process CMY inks to avoid moiré.*

Reality: With periodic screening the halftones of these additional colors are successfully printed at the angles of corresponding complementary process colors. With taking into account the color gamut expanding as the main goal of "Hi-Fi" printing, the appearing of moiré just indicates the usefulness of an additional ink because of non-complete withdrawal in prepress of the corresponding opposite process color for given image area.

Myth: *The sharper is the halftone dot on a film the sharper is the halftone image on a print.*

Reality: Sharpness of dot on a film defines the stability of its area (tone value) transfer to a plate within the tolerances of given plate making process and therefore effects on tone value reproduced on a print.

Myth: *The number of "grey levels" reproduced on a print comprises the square of the printer resolution and screen ruling ratio (plus yet one else level provided by the non-inked substrate).*

Reality: This number comprises just the formally available amount of reflectance factors proportional to the light intensities coming to the viewer from a print. However, the customer needs not "arithmetical" but perceptible grey level which is expressed by the optical density or CIE Lab lightness. So, the logarithmic or cubic root non-linier transformation should complete this kind of calculation to make it theoretically representative or practically useful.

Myth: *The frequency response of vision at reading distance is limited by about 150 lines per inch. That's why the halftone frequency of 150 Lpi is appropriate for the most of print jobs.*

Reality: The theory teaches that the sampling frequency should be at least twice higher of the input data frequency which is intended to be transmitted or reproduced. So, the screen rulings up to 300 Lpi are desired

to make prints more informative for a viewer. Such rulings, to the pity, aren't available in the wide practice due to the limitations inherent to printing process.

Myth: *The image fine detail distortion by the halftone dots can be eliminated (compensated) previous to screening stage with the use of some high frequency corrections (USM or sharpening filters) in the image processing software application.*
Reality: The input image digital file is once again encoded in screening. This involves the inherent to image encoding procedures of spatial sampling (predominantly with screen ruling frequency) and quantization (by the halftone dots alphabet). So, the correction of such kind of distortion should be provided somewhere within this second encoding process.

However, the most persistent and widespread in last 15 years is the illusion of the so-called "stochastic" or "FM" screening. Its generalized formulation sounds approximately like that *"the golden age of illustrative printing will start when some great algorithm will be practically implemented to break a continuous tone into irregularly-spaced tiny dots of the same size".*

Reality: Halftone dots can be "spaced" just in the highlights. Starting from quartertones they inevitably touch each other forming the larger dots whose shape is far from the best printable one. The use of a "tiny dot" over the whole grey scale makes the screening system non-stable, i.e. extremely sensitive to the slightest deviation of printing conditions.

3. Tone gradient dependent modification of the screening procedure

As far as the spatial dispersion of an image tone measure is inherent in any screening procedure, the digital halftoning accomplishes the distribution of an input image pixel quantization scale among the number of adjacent micro locations (microdots) of an output image [6]. That requires at least the order of magnitude excess of a printer resolution in relation to the screen ruling or target definition of a halftone print. At the same time, said excess comprises the real reserve for a printed image quality improvement. The additional facility is concealed in the way of an image data encoding in graphic technology. This way is nowadays far from the optimal one because any pixel of an input image is assigned in the output bit map by 256 levels for each of process colors of CMYK file. Comprising the procedure of modifying the image code the digital screening of today formally pretends to reproduce (to transmit through the printing channel) any detail of an image and, for example, the quarter of millimeter thick line in as much as 16 million colors (256^3). The local image area content or the fact that the eye can scarcely tell if such a line is somewhat darker or lighter, and is it green, cyan or grey aren't taken into account. Such luxury of an image data interpretation isn't available for the most of other imaging techniques or image data processing systems where the necessary conformity between the properties of an output data and abilities of an end user has to be provided.

That's why the fundamental objective of image optimal encoding in screening process is to shorten the gap between the printing process resolution and the halftone image definition by more effective use of the imaging system resources. This can be done by introducing in this process the elements of artificial intellect taken, by analogy, from the work of a manual engraver who uses to combine over an image area the continuous tone (CT) and line work (LW). That allows him to reproduce the stationary areas and fine details of an image with correspondingly as much as possible tone levels and geometric accuracy.

In **tone gradient dependent** screening procedure the image nature is evaluated in the closest vicinity of a processed pixel by the differential operator to form the parameter controlling the highly dynamic, over a picture area, readjustment of the screening algorithm [7]. The first examples of such control were comprised in the halftone dots or their parts displacement toward the darker side of a contour to eliminate its stepwise serration introduced by screening (analogue electronic halftones of PDI scanner of 70ies [8] and their digital version [9]). Modifying the form of dots (their elongation matching direction of a contour) was also suggested [10].

Similar to optimal encoding techniques used in color TV and image data compression applications our later solutions explore within this approach the specific of decrease of HVS sensitivity to tone and color variation with reducing the image detail angular dimension. According to the equation

$$S = (1 - q)\, S_1 + q\, S_2 \qquad (1)$$

the input tone value S is divided on two parts S_1 and S_2 in proportion depending on the local image area content characterized by the busyness factor q.

The first part S_1 of an input tone value S controls the any kind of a basic, practically approved screening algorithm providing the appropriate halftone printability and tone rendition for the stationary, low spatial frequency image area. The other one S_2 relates to the fine detail and controls the auxiliary screen functions of shorter quantization scale, as compared to that of a basic function, but having the higher spatial frequency.

In our developments of beginning of 70ies [7], these auxiliary functions generated on detail boundaries the sequence of square root of two higher frequency screens. However, the very first experiments have shown that the abrupt changing of dots structure along the contour of gradually fading contrast is distinct for the viewer. To get rid of the stepwise, hence noisy changing of a halftone image structure there was proposed to seamlessly blend with each other the auxiliary screens and basic screen on the basis of above equation [11, 12].

This approach, recently again patented by HP [13], was further developed in our later implementations with the use of a set auxiliary functions having the constant, twice higher frequency than basic function but providing the halftone dots (tiles) of different form (Fig. 1).

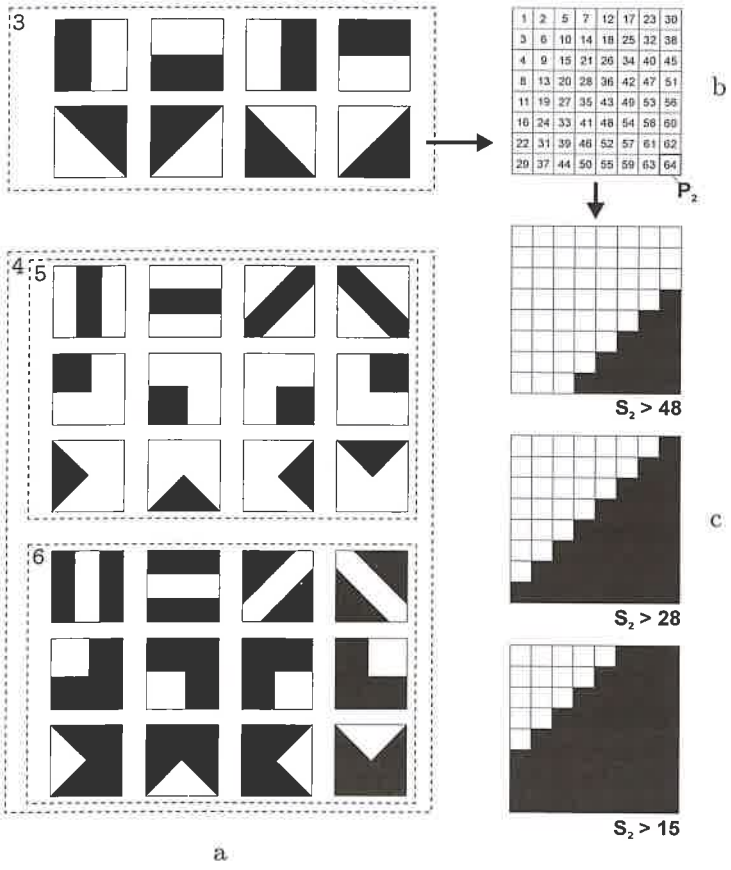


Figure 1: The exemplary geometries (a) of tiles with their first plurality 3 and second plurality 4 subdivided onto the subsets 5 and 6; the auxiliary screen function (b) for one of these geometries; the tiles (c) produced with the use of this function in accordance with the three exemplary tone values S_2

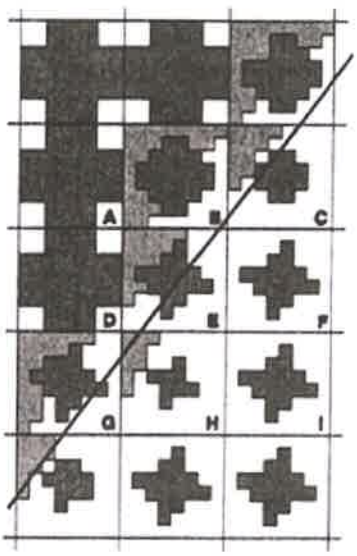


Figure 2: The mixture of tiles and halftone dots reproducing the contour of intermediate contrast separating on an original the areas of 75% and 25% tone value

Pattern recognition technique is used in the closest vicinity of processed input pixel for the proper function identification within a set. As result, the tile precisely matching this or other detail/contour geometry is produced [14]. Each non-stationary input image area is presented on a print by a mixture of these tiles and parts of conventional halftone dots in proportion defined by the busyness factor q. This mixture is illustrated by Fig. 2 for the contour of intermediate contrast separating on an original the areas of 75% and 25% tone value, i.e. having, for example, q = 0,5.

The share of tiles increases with higher q values for detail of greater contrast resulting in more precise match the detail geometry as shown on Fig. 3d.

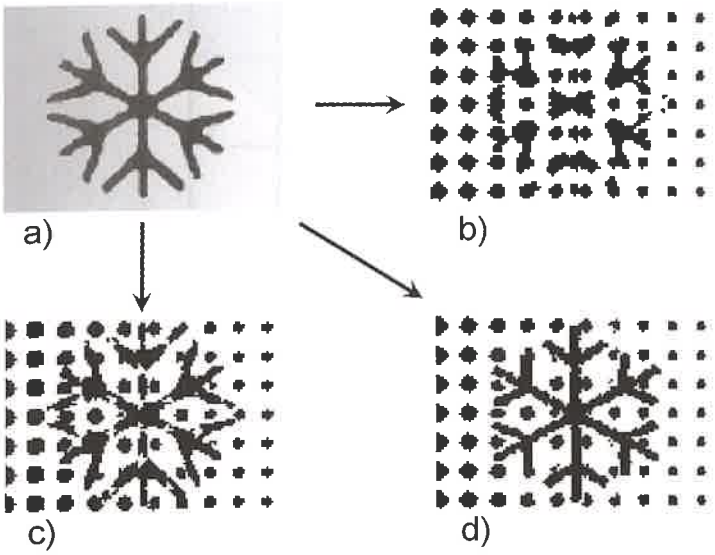


Figure 3:
The fine detail (a) of CT original and its halftone copies provided by the conventional method without (b) and with (c) the use of USM; by the adaptive screening (d) at screening factor of 2.0

In conventional screening, as well as in the most of imaging techniques the sharpness (accuracy of detail boundary reproduction) and definition (the potential amount of minimal details to be reproduced on an image) are in rigid connection. However, the adaptive approach allows, with use of tiles produced by the auxiliary screen functions, for more effective control of detail boundary reproduction.

The use of tiles of different geometry is far from being uniform as illustrated by the exemplary histogram on figure 4. The greatest demand has place for the tiles of their first plurality 3 indicated on figure 1, i.e. corresponding to a single tone transition within an input image sampling area.

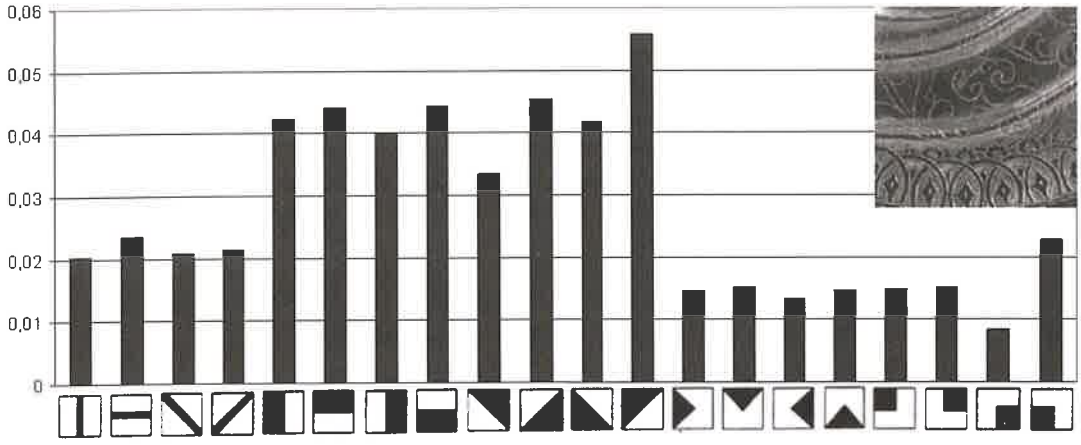


Figure 4: Exemplary histogram of the use of tiles of different geometry

As it became clear from further experiments, the issues of seamless blending of different dot structures can be concerned in different way also for the boundary and the thin line, i.e. for the single and the double tone jump, the latter relating to the line which is thinner of an input pixel area. The constrained prevailing of an auxiliary function tiles over a dots of basic screen isn't caught here by the eye. That allows for reproducing such line by the ink solid instead of the mix of tiles and scattered conventional dots. From the other hand, the gradual contrast fading along such a line can be quite satisfactorily compensated by just the reducing of a line width. The 100 microns thick grey line doesn't need screening at all and can be printed by solid at, for example, half of an original width to simulate its grayness (Fig. 5).

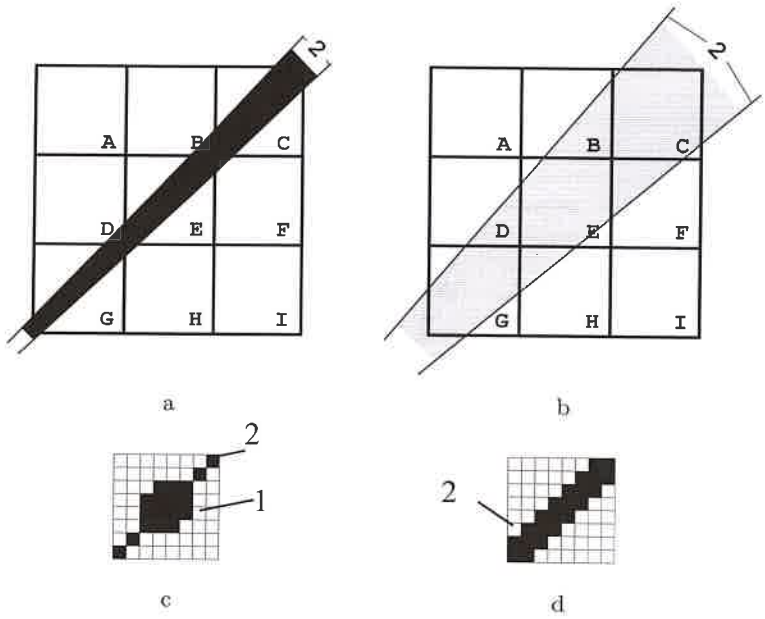


Figure 5: Thin black line (a) and thicker grey line (b) producing the same reflectance value due to its averaging over a sampling area at the stage of CT original encoding; halftone copies of these lines for area E according to the previous (c) and current (d) HDHP versions; 1 - microdots set dark according to the basic screen function; 2 - microdots belonging to the tile of an auxiliary halftone alphabet

With taking into account these issues the set of auxiliary screen functions was divided in two groups with subdividing the second of them on two subsets, as indicated on figure 1. It allowes for the selective use of tiles of different geometry and polarity [15]. As result, the standing alone thin lines are reproduced by our latest version of adaptive technology with the complete use of printing process resolution, as it shown on Figure 5d.

4. HDHP testing

The described above selective distribution of the imaging system resources over a picture with taking into account its local area content allows for mutual exchange of printing system facilities in relation of tone/color rendition and contour/fine detail graphic accuracy, i.e. with tonal and spatial resolutions of this system adaptively replacing each other. This new way to form and place the halftone dots on illustration was realized as the computer program. Meanwhile, the absence of iterative procedures in algorithm facilitates its implementation in a RIP or in a hardware halftone dot generator. The technology was named High Definition Halftone Printing (HDHP) and tested in lithography, flexography, silkography.

The results of experimental printing of tests and realistic images as well as of the commercial jobs with the use of adaptive screening image files vividly show the following advantages:

- ◊ twice higher definition at any screen ruling used for the stationary image area;
- ◊ reproduction of black or white lines thinner than half of a screen mesh by the ink solid or clean paper instead of the scattered or, so called, partial dots in any other kind of halftoning;
- ◊ higher appearance of contrast and color gamut accompanying the increase in the image sharpness and definition;
- ◊ providing these significant quality improvements with the use of a standard volume of an input image data and without any additional requirements to ink, plate, paper or their interaction in printing equipment.

These advantages were confirmed by the number of commented below printing experiments.

Over a dozen pictures of different image content were printed on same sheet in about 1000 copies at conventional printing conditions on production sheet fed offset press Rapida 130. The pictures were positioned in side by side pairs allowing for comparison of quality provided by Scitex Class Screening 175

Lpi and HDHP. As far as the latter used as its basic function the screen of the former the stationary image area in each pair was characterized by exactly the same tone and color which provided the correct conditions for comparison in relation of print sharpness and definition. As the digital microphotographs on Fig. 6 show, the quality improvement with the use of HDHP is more evident for pictures containing the greater amount of fine detail and textures and, as well, for gravures.

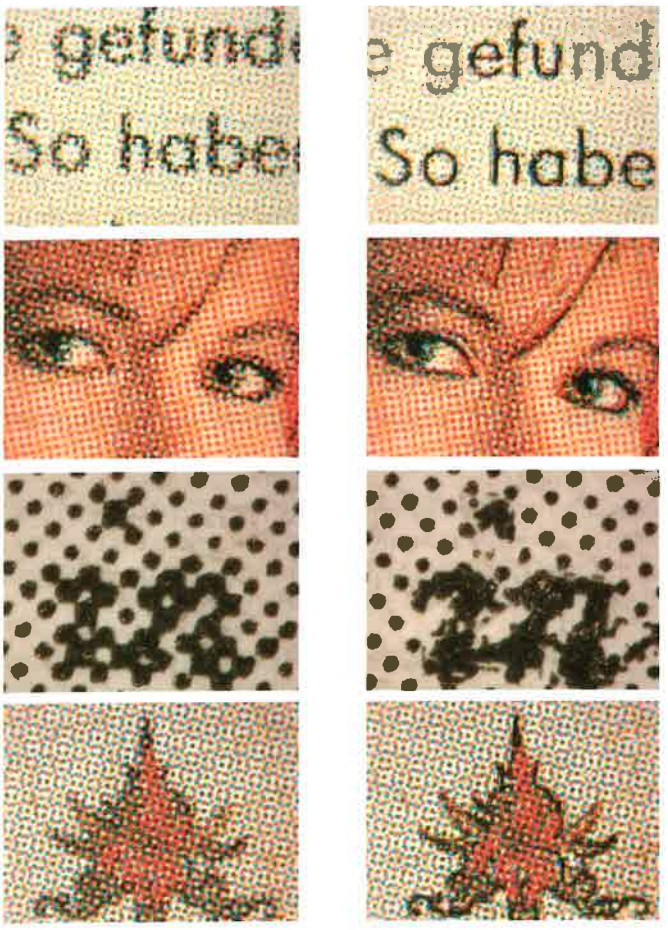


Figure 6:
Fragmentary microphotographs of 4-color halftone prints produced at 175 Lpi and screening factor of 2.0 with the use of Scitex Class Screening (left) and HDHP (right)

Another test run was performed to compare the HDHP of 175 Lpi with the Agfa ABS (175 Lpi) and Agfa Sublima (210 Lpi, 240 Lpi) technologies. Microphotographs on Fig. 7 vividly illustrate the higher sharpness and resolution of HDHP of 175 Lpi than that of the intended for the same purpose hybrid screening Sublima of as much as 240 Lpi.

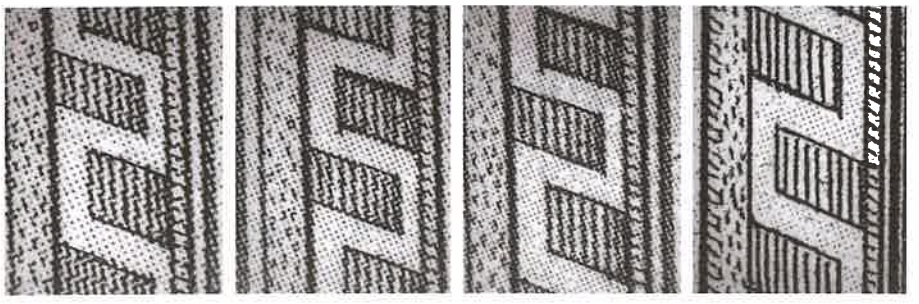


Figure 7: Fragmentary microphotographs of halftone prints produced at screening factor of 2.0 with the use of Agfa ABS (175 Lpi), Agfa Sublima (210 Lpi, 240 Lpi) and HDHP (175 Lpi) - from left to right

The same advantages of novel technology were also approved in screen printing tests in various combinations of halftone rulings of 85 Lpi and 100 Lpi with screen grids of 240 and 300 wires per inch for different kind of papers and boards.

The flexography test has shown the especially high, may be, too much increase of sharpness which can be explained by the use of tiles whose sizes in detail boundary area are less than minimal highlight dots predetermined for this kind of halftone printing. However, such an excess can be easily compensated by corresponding HDHP program adjustments.

5. HDHP use in graphic technology environment and direction of further adaptive screening developments

At our first attempts of practical using of adaptive halftoning the basic screen function was created within the program to simulate some kind of dot form and placement by a professional RIP and thereby to somehow preserve the color and tone rendition which the customer used for given kind of his job. With the use of such basic and auxiliary screen functions of Fig. 1 the bitmaps for stationary and non-stationary areas of an image were produced. The combined bitmap of a whole halftone was then output from the program, inserted to the page and processed by the RIP as a line work (LW). This approach was further abandoned because of the following reasons:

- ◊ the difficulty of emulating the screen functions for all the variety of halftones of different RIPs;
- ◊ the much greater volume of LW file as compared with the CT TIFF;
- ◊ some difference of tone and color in adaptively screened images due to approximate emulation of dots form and area.

That's why the latest version of HDHP program creates the modified, according to the adaptive algorithm, CT file (byte map) for the stationary image area and the LW mask (bitmap) of tiles comprising the contours and thin lines the both maps being then combined in EPS TIFF. After EPS file interpretation the RIP creates a halftone bitmap for CT component and combines it in overprint mode with the LW mask (Fig. 8).

This way of operating allows for exactly the same tone and color rendition as of those reproduced through a RIP or customer profiles and the use of any available in a RIP screening procedures for the stationary image area. Moreover, the parts processed in the HDHP mode and in some conventional manner can be seamlessly combined in any area of the same image. By these means the facility of absolutely correct visual comparison of reproduction quality for HDHP and other screening techniques is created.

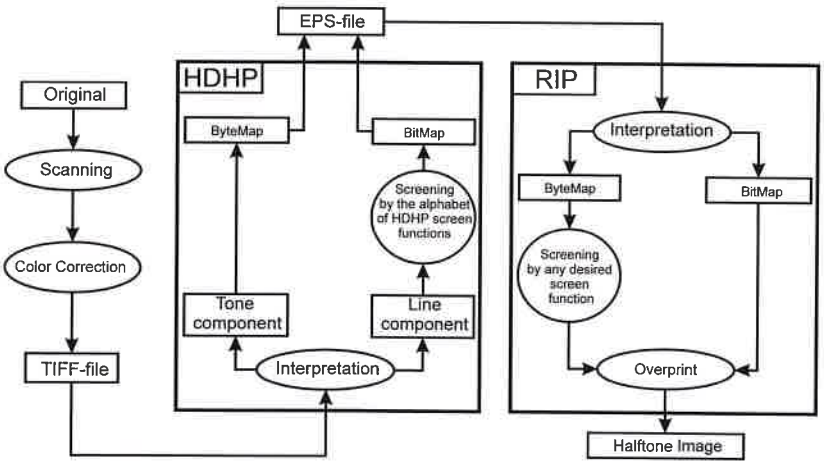


Figure 8: The current version of HDHP workflow

With the on-line use of this HDHP version the films were output and the number of art books was produced in serial four color production runs without any additional adjustments of printing conditions or requirements to printing consumables. Some color images seamlessly combining two screening techniques were also published in graphic technical magazines.

Relying on the standard volume of an input image data at the, so called, screening factor (SF) of 2, 0, i.e. on the coarse-scan/fine-print mode [16] the HDHP provides the accuracy of stand alone narrow lines at the level

of printer resolution, which is, as was mentioned above, about ten times higher of screen ruling. However, the halftone definition or the ability to discern bar pattern or texture is increased just twice. From one hand, this limit has place due to the lack of higher frequency data in an image encoded at SF of 2.0 and by the use of an auxiliary function of just twice higher frequency than that of the basic one.

For more complete use of this reserve the fine scan/fine print mode with about hundred times larger input image file is required. With taking into account the constant increase of data storage facilities, computation/transmitting speeds and in view of permanently growing requirements to print image quality the processing of files of such volume doesn't look nowadays as a problem in contrast to the times of the beginning of adaptive screening research.

Instead of operating with the predominantly given in HDHP set of a finite sized weight matrixes, one of the ways to effectively use the "excessive" input image data is comprised in spatial dispersion of the tone measure quantization scale this dispersion being adaptive to the arbitrary contour [17]. As result of dispersion the auxiliary screen function is on-fly produced on the basis of the signal of contour "trace or path". This signal is created by the differential operator dealing with the high resolution input data and that's why it is completely representative for the image high spatial frequency content. With such a signal being formed the input data can be lossless down sampled at over 100 compression factor. So, the combination of down sampled byte map and of bitmap of contour trace signal may comprise the basis for the file format to be effectively used in fine-scan/fine-print way of an image reproduction.

6. Conclusions

The results of research and industrial approbation allow foresee the HDHP as the "by default" prepress image processing function, i.e. as the wide spread norm in graphic technology of the nearest future. There is useful to differentiate the way of processing the single and double sharp tone transitions in tone gradient dependent adaptive screening.

In fine-scan/fine-print way of an image processing it's purposeful to provide screening with the use of a weight function created by the tone measure spatial dispersion which is adaptive to the arbitrary contour.

References

1. ISO 12647-1: Graphic technology - Process control for manufacture of half-tone colour separations, proofs and production prints
2. Kuznetsov, Y. Does some philosophy still exist for the halftone frequency selection? NIP 15 Conf. Proc., IS&T, pp. 362 - 365
3. Kuznetsov Y., Uzilevski V. Electronic Screening in Graphic Arts. "Kniga", Moscow, 1976 (in Russian)
4. Kuznetsov, Y. Screening Technique Modification and Its Effect on the Halftone Print Quality. In Recent Progress in Digital Halftoning II, IS&T, pp. 358 - 362
5. Giorgiani, E., Madden T., Digital Color Management. Addison-Wesley, 1998
6. Schadenko A., Kuznetsov Y., Halftoning Methods: Background of Classification, Printability, Print Quality. "Printing Technology SPb'06" Conf. Proc., pp. 194 - 198
7. Kuznetsov Y., Kogan E., Nishnianidze G., Schadenko A., SU patent 832771
8. Electronic Dot Generation. British Printer, August 1974, pp. 38 - 39
9. Ershov G. et al. US patent 5229867
10. Hammerin M, Kruse B., Adaptive Screening. In Recent Progress in Digital Halftoning, IS&T, 1994, pp. 91 - 94
11. Kuznetsov Y., Kogan A., Nishnianidze G., SU patent 1246408
12. Kuznetsov Y., Nishnianidze G., SU patent 1288934
13. Lin Q., Bradburn B., Hofmann B., EP 0946049
14. Kuznetsov, Y. US patent 5822086
15. Kuznetsov, Y., Volneikin, P., Int. pat. publication WO 2007/053062 A1 (PCT/RU2006/000565)
16. Wong, K., Method of coarse-scan/fine-print character reproduction with compression. US patent 4150400
17. Kuznetsov, Y., Schadenko, A., Int. pat. publication WO 2007/018448 A1 (PCT/RU2006/000332)



Finding optimum screen combinations for flexible hybrid screening technologies in flexography lithography

Yung-Cheng Hsieh, Hui-Wen Cheng

Department of Graphic Communication Arts, National Taiwan University of Arts
59, Section 1, Ta-Kuang Rd., Pan-Chiao City
Taipei County, Taiwan R.O.C.
E-mail: t0308@mail.ntua.edu.tw

Abstract

This study investigates the use of AM/FM hybrid screening in conjunction with computer to plate (CTP) technology in order to obtain an optimum hybrid screening combination for the flexography printing process. The study employs the true experimental method to design 11 different hybrid (FM-AM-FM) screening combinations in accordance with Kodak/Creo's Maxtone hybrid screening technology. Hybrid screening and CTP technologies were used in flexography to print a specially-designed test form on PVC substrate. Differences in print attributes between PVC substrates printed via the 11 hybrid screening combinations were measured, and statistical analyses were used to identify a combination with an optimal FM-AM-FM tone percentage. It is hoped that the results of this study can help flexography printers to better understand the characteristics of various screening techniques, allowing them to improve printing quality and achieve the highest customer satisfaction. The best hybrid screening combination of FM-AM-FM (highlight-midtone-shadow) found in this study is provided to printers as a reference enabling them to improve production effectiveness and quality, while reducing printing costs and waste, enabling the quality of flexography in Taiwan to progress.

Keywords

AM screening, flexography, FM screening, hybrid screening, print attributes

1. Introduction

The printing industry commonly uses the conventional amplitude-modulated (AM) screening process. The principle of AM screening is that the distance between dots is fixed, and dot size is changed to simulate continuous tones. However, factors such as fixed screen angle, screen ruling, and screen shape may cause depiction of the lighter and darker parts of the image to be inadequate. The frequency-modulated (FM) screening method was developed to remedy this problem. Dots are identical in size in FM screening. Randomly-distributed dots with identical size form an image in FM screening, and the density of the dots expresses depth of tone. The problem of dot expansion is severe in FM screening, however, and AM dots are better able to reproduce the original image than FM dots in areas with intermediate tones [Blondal, 2003]. AM/FM hybrid screening was later developed in order to combine the advantages of AM and FM screening. By adopting the strengths of different screening techniques, this method achieves optimal printing quality, and it forms the main basis for this study.

2. Research motivation and purposes

Similar to FM screening, the hybrid screening technology (Kodak/Creo Maxtone) used in this research employs a random distribution of dots. This technique offers a wide range of brightness levels and color tones, and renders bright and dark details. It is thus expected to improve inadequate rendering of highlight areas and details in conventional flexography. In addition, Maxtone allows the user to set an AM and FM switching point percentage according to need. This is to say that the user choose to switch from one screening technique (AM or FM) to another screening technique (AM or FM) when the dot density reaches a certain percentage value [Flexo CtP Developments Announced by Creo, 2003].

The chief goal of this study was to determine the optimal hybrid screening combination on the basis of printing quality after using flexography to perform printing with different hybrid screening combination on PVC. The research framework to describe the purpose and process of the research is listed in Figure 1.

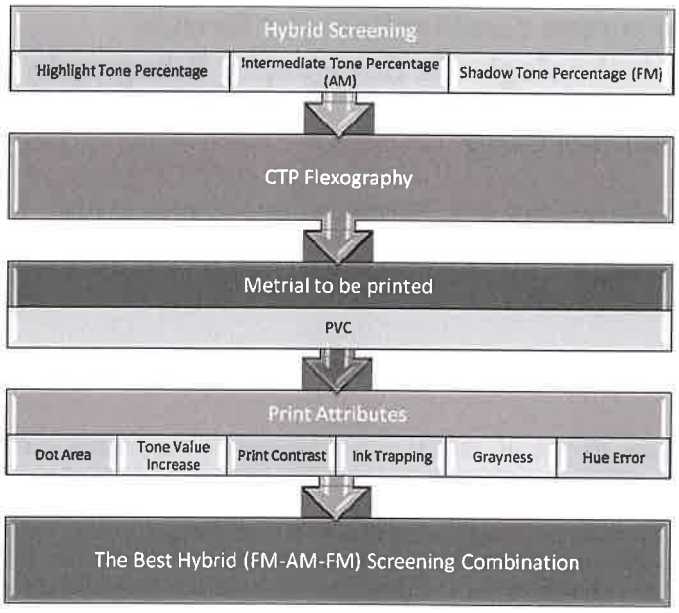


Figure 1: Research framework

3. Research hypotheses

This study sought to find the best hybrid (FM-AM-FM) screening combination as a reference for flexography on PVC. Based on the foregoing research motivation, the study made and attempted to verify the following hypotheses.

Hypotheses

Ho: When the same test form is printed on the same flexography press, and measured using the same instruments, there will be no significant difference in the print attributes (tone value increase, print contrast, ink trapping, hue error, grayness) of different screen dot combinations printed on PVC, implying:

$$\text{Ho: } \mu_PA.i = \mu_PA.j \quad (1)$$

(where μ is the mean value of the measured print attribute, PA is the print attribute, i is one of the 11 different screening combinations, and j is one of the 11 different screening combinations; $i \neq j$).

Ha: When the same text form is printed on the same flexography press, and measured using the same instruments, there will be significant difference in the print attributes of at least a pair of different screen dot combinations printed on PVC, implying:

$$\text{Ha: } \mu_PA.i \neq \mu_PA.j \quad (2)$$

4. Dependent and independent variables

This study employed the true experimental method in order to determine an optimal FM-AM-FM tone percentage combination using hybrid screening technology. The experimental design employed experimental confirmation to investigate differences in the print attributes of flexographic printing on PVC using different screening techniques.

Dependent variables

(1) Tone value increase
(2) Print contrast
(3) Ink trapping
(4) Hue error
(5) Grayness

Independent variable

FM-AM-FM hybrid screening combinations.

5. Measurement instruments and research methods

The print attributes on the PVC were measured using a GretagMacbeth Eye-One iO reflective spectrophotometer. This instrument can automatically measure and display color density data read from a test form. In this experiment it was chiefly used to measure K, C, M, Y at 5%, 10%, 15%, 20%, 25%, 30%, 40%, 50%, 60%, 70%, 75%, 80%, 85%, 90%, 95%, 100% dot area percentage/density, and RGB density. A total of twelve press runs were conducted, where the first run served as the pilot test to familiarize the press crew with the required press setting, conditions, and substrate. Each press run was required to print 1000 PVCs after the press was determined to be ready for the actual experiment.

The printed PVCs were then systematically randomly selected to be measured. The GretagMacbeth Eye-One iO was used to measure the solid ink density, highlight area, shadow area, and ordinary tone densities of K, C, M, Y color, plus RGB densities. The densities were used as reference values. Microsoft Office Excel 2007 applied printability formulas and calculated print attributes such as tone value, tone value increase, print contrast percentage, ink trapping percentage, hue error, and grayness. The measured data was recorded and organized so as to facilitate subsequent analysis.

After the measured data was recorded and compiled, statistical software was used to perform various types of analysis and hypothesis testing, and derive the print attributes when different screening techniques were used. The statistical analysis methods used in this study consisted of descriptive statistics and one-way ANOVA.

6. Experimental procedures

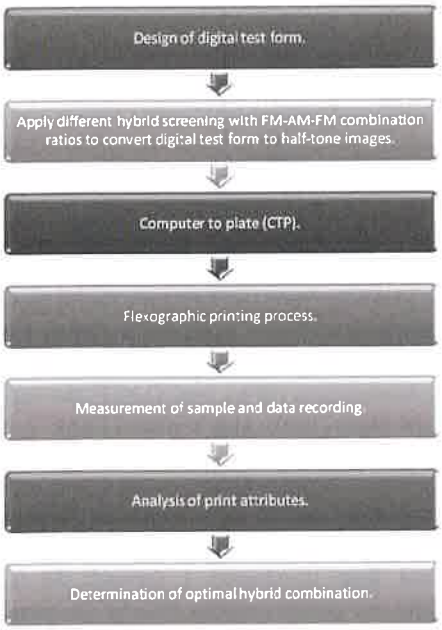


Figure 2:
Experimental process flowchart

The electronic test forms used in this study were generally adapted from the Digital Test Form 5.0 of the Graphic Arts Technical Foundation (GATF), and were used to establish color quality specifications and perform attribute analysis. The ECI2002R test form (patches are randomly arranged) was the main basis for measurements. The test forms used by the experiment were 28 x 45 cm in size.

This study employed FM dots for highlight areas and shadow areas (taken as a% and c% respectively) and AM dots for intermediate areas (taken as b%). Since the theoretical gray scale was 0% - 100% from the brightest to the darkest areas, $a + b + c = 100$. The area occupied by intermediate tone AM dots is set as b%, as shown in Figure 3.

Because the naked eye cannot easily distinguish tone differences of less than 5% in ordinary printed items, this study used a 5% interval. Eleven hybrid screening combination ratios were used in the printing process. For instance, when $b = 90$, then $a + c = 100 - b = 10$, as shown in Table I.

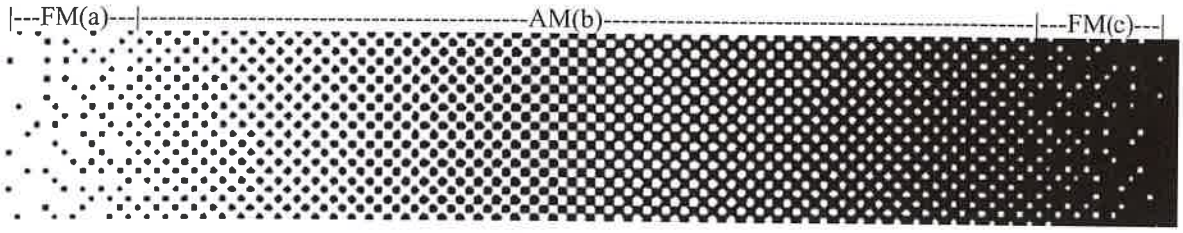


Figure 3: Hybrid AM/FM screening combinations

Table I: Hybrid screening combination ratios employed in this study

Combination	a+b+c=100		
	a	b	c
1	5	80	15
2	5	85	10
3	5	90	5
4	10	70	20
5	10	75	15
6	10	80	10
7	10	85	5
8	15	70	15
9	15	75	10
10	15	80	5
11	20	70	10
	Total of 11 combinations		

The completed electronics test form was printed out via flexography. The output plates were four color (C, M, Y, K) CTP plates with 175 lpi in terms of resolution. During printing, because Taiwan's flexographic industry complies with the GRACoL (General Requirements for Applications in Commercial Offset Lithography) printing condition and operating environment requirements jointly established by the US Graphic Communications Association (GCA), International Prepress Association (IPA), and GATF, the standard solid plate density value was set for K plate (1.70), C plate (1.40), M plate (1.50), and Y plate (1.05).

The experiment used systematic random sampling to select printed samples from among 100 printed PVCs in each printing run. Due to the possibility of uneven ink distribution due to an increase or decrease in roller pressure at the beginning or end of each printing run, only 40 samples were accepted after removing the ten samples at the beginning and end. The 80 samples were then numbered 1 through 80 to the final measurement. Because the interval was established by dividing the parent number (80) by the sample number (40), the study selected one sample from each two units and used simple random sampling to select one number between one and 80. This number was used as the starting point. One sample was afterwards taken from each two units. A GretagMacbeth Eye-One iO reflective spectrophotometer was used to measure solid plate, highlight area, shadow area, ordinary tone density, and R, G, B density data in K, C, M, Y color areas. Various print attributes, including tone value, tone value increase, print contrast percentage, ink trapping percentage, hue error, grayness, and color gamut were calculated. The resulting data was compared and analyzed using statistical software to obtain the optimal screening combination.

7. Descriptive statistics

Descriptive statistics concerning dot area, tone value increase, ink trapping, print contrast, hue error, and grayness of samples in each group gave provided an understanding of print attributes and quality. Table II contains descriptive statistics for all 11 hybrid screening combinations. For the sake of simplicity, the data in this table is rounded to the second decimal place.

Table II: Descriptive statistics for 11 flexographic PVC hybrid screening combinations

Combination		5-80-15	5-85-10	5-90-5	10-70-20	10-75-15	10-80-10
Ink trapping (%)	R(MY)	85.90	88.24	83.82	87.844	93.17	94.44
	G(CY)	100.99	104.05	94.80	99.591	109.31	111.09
	B(CM)	87.36	88.56	88.50	87.401	87.78	87.91
Print contrast (%)	C	44.46	45.42	46.55	48.38	46.93	45.67
	M	46.67	46.53	49.53	46.27	49.56	44.31
	Y	47.60	46.57	47.90	46.29	47.66	44.39
	K	47.22	45.11	44.71	45.82	45.36	45.03
Hue error	C	10.94	10.53	10.76	11.74	10.73	10.79
	M	46.01	45.07	45.16	45.28	45.38	45.16
	Y	2.71	2.67	2.58	2.46	2.21	2.74
Grayness	C	14.81	14.39	14.63	15.17	14.78	14.54
	M	7.18	6.89	6.91	6.99	6.98	6.93
	Y	0.74	0.68	0.71	0.71	0.71	0.74
50% TVI	C	16.19	18.76	15.68	13.38	14.67	14.64
	M	18.67	21.82	19.71	17.92	18.33	17.11
	Y	11.72	18.79	14.30	12.85	14.77	13.43
	K	17.24	20.92	19.09	17.62	19.64	19.06

Combination		10-85-5	15-70-15	15-75-10	15-80-5	20-70-10
Ink trapping (%)	R(MY)	88.88	86.69	89.57	87.97	91.60
	G(CY)	101.16	98.96	103.76	104.67	104.84
	B(CM)	88.92	86.26	89.14	86.06	90.49
Print contrast (%)	C	45.76	44.83	46.63	43.24	43.92
	M	39.43	44.16	47.36	40.92	42.88
	Y	47.03	45.90	46.87	45.70	46.74
	K	44.98	44.42	43.97	45.80	45.88
Hue error	C	10.55	8.40	10.80	8.06	10.60
	M	43.92	46.20	45.16	45.05	45.51
	Y	2.17	3.06	2.54	2.86	2.48
Grayness	C	14.45	16.56	14.70	16.15	14.58
	M	6.76	9.35	6.98	9.08	7.04
	Y	0.69	2.01	0.71	2.10	0.71
50% TVI	C	17.88	15.69	17.45	15.47	18.00
	M	27.43	17.85	20.80	23.11	20.56
	Y	16.61	14.50	16.54	16.50	14.56
	K	19.02	16.89	22.22	17.02	18.96

8. Testing of hypotheses

Analysis of the K, C, M, Y 50% tone value increase of the screening combinations showed that when the same test form is printed on the same flexography press, and measured using the same instruments, there was a significant difference in 50% tone value increase in at least one group of different dot combinations (see Table III); significant difference in R, G, B ink trapping in at least one group of combinations (see Table IV); significant difference in C, M, Y, K print contrast in at least one group of combinations (see Table V); significant difference in C, M, Y hue error in at least one group of combinations (see Table VI); and significant difference in C, M, Y grayness in at least one group of combinations (see Table VII). The smaller the ordinal number, the

better the print quality is. Combinations with the same ordinal number have identical average within a 95% confidence. The data sets were then named after their order number. For the sake of simplicity, the data in all the table was rounded to the second decimal place. The color process forms then indicated the optimal combination. Graphical analysis showed that none of the combination numbers departed far from a normal distribution curve, allowing the data tolerance to be calculated using a 95% confidence interval.

Table III summarizes the 50% tone value increase of the 11 flexographic PVC screening combinations. Tone value increase is caused by dot expansion during printing, and is due to both physical and optical factors. A smaller tone value increase is better.

Table III:. Summary of 50% tone value increase of the 11 screening combinations expressed by a 95% confidence interval

Screening combination	K50%	Order	C50%	Order	M50%	Order	Y50%	Order	Overall order
5-80-15(A)	17.24±0.34	3	16.19±0.25	7	18.67±0.58	5	11.72±0.40	1	16
5-85-10(B)	20.92±0.20	10	18.76±0.30	11	21.81±0.46	9	18.79±0.31	11	41
5-90-5(C)	19.09±0.14	5	15.68±0.16	4	19.71±0.56	6	14.30±0.28	4	19
10-70-20(D)	17.62±0.18	4	13.38±0.18	1	17.92±0.56	2	12.85±0.23	2	9
10-75-15(E)	19.64±0.21	9	14.67±0.14	2	18.33±0.42	2	14.77±0.28	4	17
10-80-10(F)	19.06±0.19	5	14.64±0.16	2	17.11±0.36	1	13.43±0.31	3	11
10-85-5(G)	19.02±0.28	5	17.88±0.26	9	27.44±0.37	11	16.61±0.31	8	33
15-70-15(H)	16.89±0.22	1	15.69±0.19	4	17.85±0.38	2	14.50±0.26	4	11
15-75-10(I)	22.22±0.15	11	17.46±0.17	8	20.80±0.44	7	16.55±0.25	8	34
15-80-5(J)	17.02±0.21	1	15.47±0.22	4	23.11±0.33	10	16.50±0.25	8	23
20-70-10(K)	18.96±0.19	5	18.00±0.18	9	20.56±0.37	7	14.56±0.19	4	25

Table IV summarizes the mean R, G, B ink trapping values of the 11 screening combinations. Ink trapping represents the RGB color rendering ability after CMY trichrome solid plate overlays. Greater ink trapping is better. The largest value in the table is thus ranked 1, and represents the best result.

Table IV: Mean ink trapping values of the 11 flexographic PVC screening combinations expressed by a 95% confidence interval

Screening combination	R (MY)	Order	G (YC)	Order	B (CM)	Order	Overall order
5-80-15(A)	0.86±0.01	9	1.01±0.01	7	0.87±0.01	6	22
5-85-10(B)	0.88±0.01	4	1.04±0.01	3	0.89±0.01	2	9
5-90-5(C)	0.84±0.01	11	0.95±0.01	11	0.89±0.01	2	24
10-70-20(D)	0.88±0.01	4	1.00±0.01	9	0.87±0.01	6	19
10-75-15(E)	0.93±0.01	1	1.09±0.01	2	0.88±0.01	6	9
10-80-10(F)	0.94±0.01	1	1.11±0.01	1	0.88±0.01	6	8
10-85-5(G)	0.89±0.01	4	1.01±0.01	7	0.89±0.01	2	13
15-70-15(H)	0.87±0.01	9	0.99±0.01	10	0.86±0.01	10	29
15-75-10(I)	0.90±0.01	4	1.04±0.01	6	0.89±0.01	2	12
15-80-5(J)	0.88±0.01	4	1.05±0.01	3	0.86±0.01	10	17
20-70-10(K)	0.92±0.01	3	1.05±0.01	3	0.91±0.01	1	7

Table V summarizes the mean K, C, M, Y print contrast values of the 11 combinations. Print contrast is the ability to render tones in shadow areas. A higher print contrast is better, as long as the value is not excessively high. The largest value in the table is thus ranked 1, and represents the best result.

Table VI summarizes the mean C, M, Y hue error values of the 11 screening combinations. Hue error represents error in the application of the three colored inks. A smaller hue error is better. The smallest value in the table is thus ranked 1, and represents the best result.

Table V: Mean K, C, M, Y print contrast values of the 11 flexographic PVC screening combinations expressed by a 95% confidence interval

Screening combination	K	Order	C	Order	M	Order	Y	Order	Overall order
5-80-15(A)	47.22±0.25	1	44.46±0.27	8	46.67±0.24	4	47.60±0.38	1	14
5-85-10(B)	45.10±0.21	5	45.42±0.57	5	46.53±0.48	4	46.57±0.36	4	18
5-90-5(C)	44.71±0.21	5	46.56±0.24	2	49.53±0.30	1	47.90±0.36	1	9
10-70-20(D)	45.82±0.44	2	48.38±0.35	1	46.27±0.27	4	46.29±0.44	4	11
10-75-15(E)	45.36±0.29	5	46.93±0.22	2	49.56±0.22	1	47.66±0.27	1	9
10-80-10(F)	45.03±0.31	5	45.67±0.22	5	44.31±0.30	7	44.39±0.81	11	28
10-85-5(G)	44.98±0.28	5	45.76±0.21	5	39.44±0.25	11	47.03±0.29	4	25
15-70-15(H)	44.41±0.38	10	44.83±0.23	8	44.16±0.30	7	45.90±0.28	4	29
15-75-10(I)	43.97±0.24	11	46.63±0.30	2	47.36±0.37	3	46.87±0.26	4	20
15-80-5(J)	45.80±0.25	2	43.24±0.60	10	40.92±0.27	10	45.70±0.31	4	26
20-70-10(K)	45.88±0.16	2	43.92±0.22	11	42.88±0.24	9	46.74±0.28	4	26

Table VI: Mean C, M, Y hue error values of the 11 flexographic PVC screening combinations expressed by a 95% confidence interval

Screening combination	Cyan (C)	Order	Magenta (M)	Order	Yellow (Y)	Order	Overall order
5-80-15(A)	0.11±0.00	3	0.46±0.00	10	0.03±0.00	3	16
5-85-10(B)	0.11±0.01	3	0.45±0.00	2	0.03±0.00	3	8
5-90-5(C)	0.11±0.00	3	0.45±0.00	2	0.03±0.01	3	8
10-70-20(D)	0.12±0.00	11	0.45±0.00	2	0.02±0.01	3	16
10-75-15(E)	0.11±0.00	3	0.45±0.00	2	0.02±0.00	1	6
10-80-10(F)	0.11±0.00	3	0.45±0.00	2	0.03±0.00	3	8
10-85-5(G)	0.11±0.00	3	0.44±0.00	1	0.02±0.00	1	5
15-70-15(H)	0.08±0.00	2	0.46±0.00	10	0.03±0.00	11	23
15-75-10(I)	0.11±0.00	3	0.45±0.00	2	0.03±0.01	3	8
15-80-5(J)	0.08±0.00	1	0.45±0.00	2	0.03±0.00	3	6
20-70-10(K)	0.11±0.00	3	0.46±0.01	2	0.02±0.01	3	8

Table VII summarizes the mean C, M, Y grayness values for the 11 flexographic PVC screening combinations. The smaller the grayness value, the more the three color C, M, Y inks approach gray when mixed at a 50% tone level. The smallest value in the table is thus ranked 1, and represents the best result.

Table VII: Mean C, M, Y grayness values of the 11 flexographic PVC screening combinations expressed by a 95% confidence interval

Screening combination	Cyan (C)	Order	Magenta (M)	Order	Yellow (Y)	Order	Overall order
5-80-15(A)	0.15±0.00	1	0.07±0.00	9	0.01±0.00	1	11
5-85-10(B)	0.14±0.00	1	0.07±0.00	2	0.01±0.00	1	4
5-90-5(C)	0.15±0.00	1	0.07±0.00	2	0.01±0.00	1	4
10-70-20(D)	0.15±0.00	9	0.07±0.00	2	0.01±0.00	1	12
10-75-15(E)	0.15±0.00	1	0.07±0.00	2	0.01±0.00	1	4
10-80-10(F)	0.15±0.00	1	0.07±0.00	2	0.01±0.00	1	4
10-85-5(G)	0.15±0.01	1	0.07±0.00	1	0.01±0.00	1	3
15-70-15(H)	0.17±0.01	11	0.09±0.01	11	0.02±0.00	10	32
15-75-10(I)	0.15±0.00	1	0.07±0.00	2	0.01±0.00	1	4
15-80-5(J)	0.16±0.00	10	0.09±0.00	10	0.02±0.00	10	30
20-70-10(K)	0.15±0.00	1	0.07±0.00	2	0.01±0.00	1	4

9. Finding the optimal screening combination ratio

This study constructed 11 hybrid screening combinations, and measured attributes relevant to printing quality (dot area, tone value increase, ink trapping, print contrast, hue error, grayness) on PVCs printed using these

combinations. The print attributes of different hybrid screening combinations were then compared with each other in order to find the optimal screening combination in terms of 50% tone value increase, ink trapping, print contrast, hue error, and grayness, and thereby find the optimal hybrid screening combination. According to the print attribute scores in Table III, hybrid screening combination 10-75-15 is optimal (and has the lowest score) in terms of all print attributes. This study therefore determined that 10-75-15 is the optimal screening combination. The order of print attributes from the most to the least desirable was E >F >C >D >K >I >G =A >B > J >H), (see Table VIII).

Table VIII: Overall print attribute scores of the 11 flexographic PVC screening combinations

Screening combination	Tone value increase	Ink trapping	Print contrast	Hue error	Grayness	Overall order
5-80-15(A)	16	22	14	16	11	79
5-85-10(B)	41	9	18	8	4	80
5-90-5(C)	19	24	9	8	4	64
10-70-20(D)	9	19	11	16	12	67
10-75-15(E)	17	9	9	6	4	□45
10-80-10(F)	11	8	28	8	4	□59
10-85-5(G)	33	13	25	5	3	79
15-70-15(H)	11	29	29	23	32	*124
15-75-10(I)	34	12	20	8	4	78
15-80-5(J)	23	17	26	6	30	*92
20-70-10(K)	25	7	26	8	4	70

According to the results of this study, when FM dots are used for a tone range of 0% - 10% in the highlight region, AM dots are used for a tone range of 10% - 75% in the intermediate region, and FM dots are used for a tone range of 75% - 100% in the shadow region, which is to say that the hybrid screening combination was 10-75-15 (FM-AM-FM), this combination yielded optimal printing quality when printing on PVC using flexography. The performance of this combination was particularly good for the attribute of print contrast. It is therefore recommended that industry and researchers take 10-75-15 or 10-80-10 as optimal hybrid screening combinations. In contrast, the hybrid screening combinations of 15-70-15 and 15-80-5 are least appropriate for flexographic printing on PVC.

In this time of increasing emphasis on printing quality, industry cannot ignore the need to improve product quality while maintaining a high level of printing efficiency. This study proposed a hybrid screening combination yielding optimal results in flexographic printing on PVC using the CTP process. It is expected that printing firms can adopt this combination in order to improve working efficiency, printing quality, and customer satisfaction.

Due to limited manpower, financial resources, and time, this study only conducted experiment using the material PVC. Future researchers may be able to perform the same type of research using other materials, such as coated and non-coated coated paper, etc., in order to perform cross-comparisons of the use hybrid screening in printing on different materials, and thereby obtain systematic printing specifications.

Acknowledgement

Sincere appreciation is expressed to the National Science Council of Taiwan who financed this research.

References

1. Chuck Surprise, (2003), *Flexo CtP Developments Announced by Creo.* Retrieved October 13, 2003, from http: http://www.printondemand.com/MT/archives/001522.html
2. QMS, Inc., (1996), *Color Reproduction.* Retrieved November 26, 2005, from http://www.tu-harburg.de/rzt/tuinfo/periph/drucker/Color_Reproduktion
3. Dan Blondal, (2003), *The Lithographic Impact of Microdot Halftone Screening. TAGA Proceedings 2003, p. 608*
4. General Requirements for Applications in Commercial Offset Lithography, (2007). *Guidelines & Specifications*

Implementation of global and local thresholding algorithms in image segmentation of coloured prints

Miha Lazar, Aleš Hladnik

Faculty of Natural Sciences and Engineering, University of Ljubljana
Snežniška 5, SI-1000 Ljubljana
E-mail: ales.hladnik@ntf.uni-lj.si

Abstract

Segmentation of a digital image whose histogram does not allow for clear and easy differentiation between the features of interest and the background pixels, requires the use of an advanced thresholding algorithm. In our study two local, i.e. adaptive, thresholding procedures with various sizes of small picture regions (windows) were implemented on an image of a lab handsheet made of repulped coloured prints in order to accurately identify the location and the number of residual toner particles. One of the applied algorithms was based on the information maximization of the thresholded image while the other was a modified Niblack's method. Results of the study suggest that the latter method outperforms the former one when using a large window size. Information maximization algorithm typically fails to detect some lighter and coloured areas of objects of interest.

Keywords

Algorithms, image binarization, image processing, local thresholding

1. Introduction

Segmentation of a digital image into two regions - one containing objects of interest and the other consisting of background pixels - is a crucial step in various image processing applications. In pulp and paper research, to evaluate performance of a printed paper recycling process (e.g. flotation deinking), it is necessary first to separate ink particles and other impurities from the unprinted areas, i.e. paper itself. This process, known as thresholding can be described as follows [Young *et al.*, 2008]:

$$\begin{aligned} &\text{If } a[m,n] < \theta && a[m,n] = object = 1 \\ &\text{Else} && a[m,n] = background = 0 \end{aligned} \qquad (1)$$

where parameter θ normally denotes brightness threshold applied to the image $a[m,n]$. Here we are interested in dark objects on a light background.

Digital images of a printed paper surface are typically acquired with a flat-bed scanner and are usually 8-bit monochrome images having 256 different grey levels ranging from 0 (black, particles and other impurities) to 255 (white, paper). For images that exhibit a pronounced bimodal grey level distribution - one peak represents grey levels of ink and dirt particles, and the other of the unprinted background pixels - setting the right threshold does not present a problem: it is located at the local minimum between both peaks [Antoine *et al.*, 2001]. Often, however, difference between the ink peak and the paper peak is not well-defined and the image histogram is characterized by an unimodal, rather than a bimodal curve shape. This happens, for instance, when there is a low contrast between an ink (e.g. yellow) and the paper. Here instead of simply setting one global threshold for the total image, a more sophisticated algorithm has to be implemented. One possibility is the use of a local (adaptive, dynamic) thresholding method where the threshold changes dynamically over the image, i.e. its values are computed locally for small region windows.

Objective of our research was to evaluate applicability of the two more advanced algorithms for digital image segmentation: an approach based on the digital image information maximization and an adaptive, locally-based thresholding technique, as described below.

2. Methods

In our study we investigated a 2.1 x 2.1 cm 32-bit RGB colour picture (Figure 1, left) of a laboratory handsheet made of repulped prints scanned at 300 dpi. Paper was originally printed on a digital offset printing machine Indigo E-Print 1000+ at 600V printing drum voltage so the handsheet contained coloured ink (toner) particles of various sizes and shapes. Relatively large areas of the residual particles are typical of this printing technique; their elimination in paper recycling process using conventional flotation deinking procedure has proven to be an extremely difficult task [Hladnik *et al.*, 2006].

To compare various thresholding algorithms implemented in our study and to monitor the effect of image type, we examined another digital image that was produced by scanning part of a black-and-white text document using uneven light illumination (Figure 1, right). Our goal in this example was to obtain a well thresholded, readable text inspite of the present top-right to bottom-left decrease in background brightness.

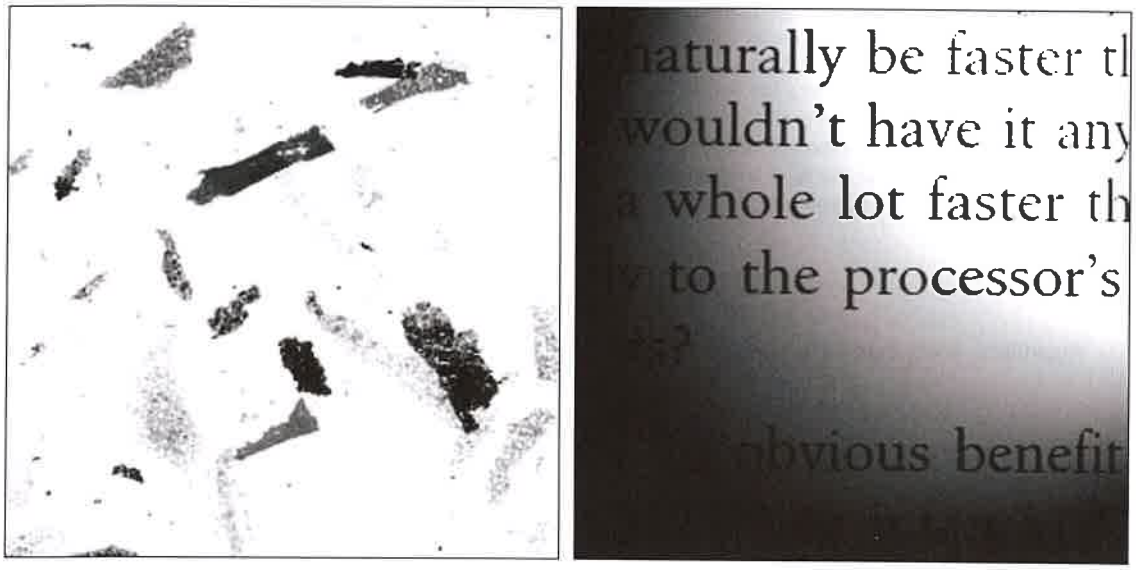


Figure 1: Images examined in the study: lab handsheet made of repulped print (left) and text document with illumination gradient (right)

Two thresholding techniques for image segmentation were applied. First one is the so called information maximization (IM) algorithm [Kapur *et al.*, 1985] where the threshold t_{max} maximizes the information of the thresholded image according to the formula:

$$t_{\max} = \arg \underset{t \in G_N}{Max} \{H_0(t) + H_1(t)\} \tag{2}$$

where H_0 and H_1 are defined as follows:

$$H_o(t) = \sum_{i=0}^{t} \frac{P_i}{P_{sum}(t)} \cdot \log \frac{P_i}{P_{sum}(t)} \text{ and } H_1(t) = \sum_{i=t+1}^{N-1} \frac{P_i}{1 - P_{sum}(t)} \cdot \log \frac{P_i}{1 - P_{sum}(t)} \tag{3}$$

P_i is related to the probability distribution of the relative frequencies P as described in the original article [Kapur *et al.*, 1985]. This procedure can also be used for determination of a threshold within a smaller picture region - window (local IM). Here a window of a chosen size moves from pixel to pixel in the image so that for each of them an optimum threshold value for its nearest neighbourhood can be obtained.

The second applied method was a modified local, i.e. adaptive thresholding algorithm that was originally developed by Niblack [Niblack, 1986]. He suggested to compute the threshold from the data on local mean and local standard deviation over a certain region - n x n window size (WS) - around each pixel location. The local threshold T at a pixel (i, j) is calculated as:

$$T(i, j) = m(i, j) + k \cdot v(i, j) \tag{4}$$

where $m(i, j)$ and $v(i, j)$ are the local sample mean and variance, respectively. Parameter k controls the effect of standard deviation due to objects features and while it can be a constant value for segmentation of, for example, document images, for grey level images having a lot of variations in grey levels it should vary according to their grey level distributions. Therefore Rais [Rais *et al.*, 2004] proposed the following formula for calculating the value of the weight k:

$$k = -0.3 \cdot \frac{(m_g(i,j) \cdot \sigma_g(i,j) - m_l(i,j) \cdot \sigma_l(i,j)}{\max((m_g(i,j) \cdot \sigma_g(i,j), m_l(i,j) \cdot \sigma_l(i,j))} \tag{5}$$

where σ_g (i, j) is the global standard deviation of the total image and σ_l (i, j) is the local standard deviation calculated for each window.

The above described algorithms were implemented on a personal computer using the MATLAB® software package.

Description of our work is presented in Figure 2. First, the original RGB image (Figure 1, left) was converted into an 8-bit greyscale (GS) one according to the following weighted formula:

$$Grey = 0.299 \cdot Red + 0.587 \cdot Green + 0.114 \cdot Blue \tag{6}$$

This GS image was binarized using both global IM as well as local Rais' thresholding (RT) algorithm. In the latter one, we experimented with various WSs ranging from 31 to 251 pixels. Alternatively, we performed CMYK split of the original image to produce separate C, M, Y and K 8-bit images, on which both thresholding techniques as with the GS image were applied. The four acquired thresholded C, M, Y and K images were in the end combined into a composite CMYK binary image.

Finally, as it is possible to vary WS also in the case of the IM algorithm, we tested a number of WSs - on GS as well as on CMYK-split images (dotted rectangles in Figure 2) - to see how altering this parameter affects thresholding efficiency and, consequently, detection of coloured pixels found in the original image.

The initial text document picture (Figure 1, right) was already acquired as an 8-bit GS image, so here only left part of the scheme was performed, i.e. without CMYK split images.

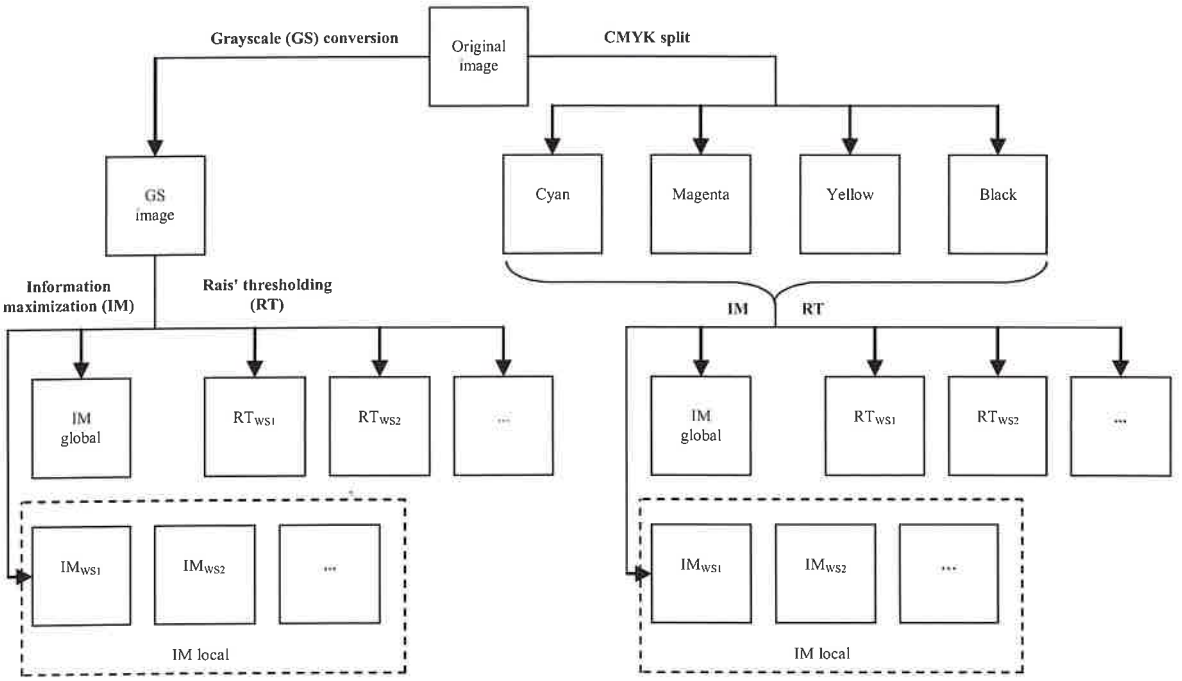


Figure 2: Scheme of experimental work

3. Results and discussion

RT and IM thresholded, i.e. binary, images of the text document image using various WSs are shown in Figures 3 and 4, respectively, while the corresponding results for the repulped print handsheet image are displayed in Figures 5 to 8.

Several researchers reported that the local thresholding techniques were particularly successful in binarizing document images [Rais *et al.*, 2004]. Our experiments with the text image (Figure 1, right) confirmed these claims. When RT algorithm with a small WS - e.g. 31 pixels - was used (Figure 3), uneven background illumination was removed to a large extent. With increasingly bigger WSs, however, more and more letters in the bottom-left part of the image merged with the dark background present in the original picture and were therefore unreadable. With the other applied algorithm - IM - the observed effect of WS was quite the opposite (Figure 4): here best results were obtained with larger WSs. As demonstrated in the right-most picture, global IM thresholding proved ineffective in properly segmenting the image.

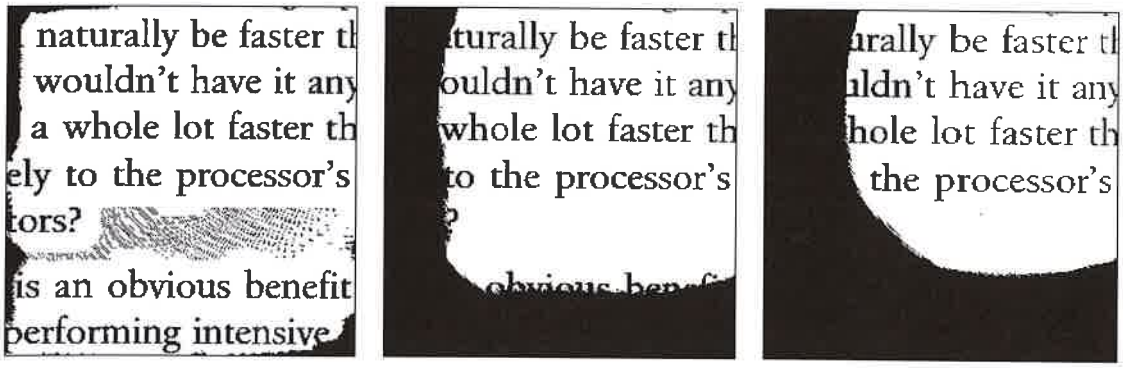


Figure 3: Text document image results: binary images obtained With RT algorithm using various WS: 31 (left), 141(middle) and 251 (right) pixels

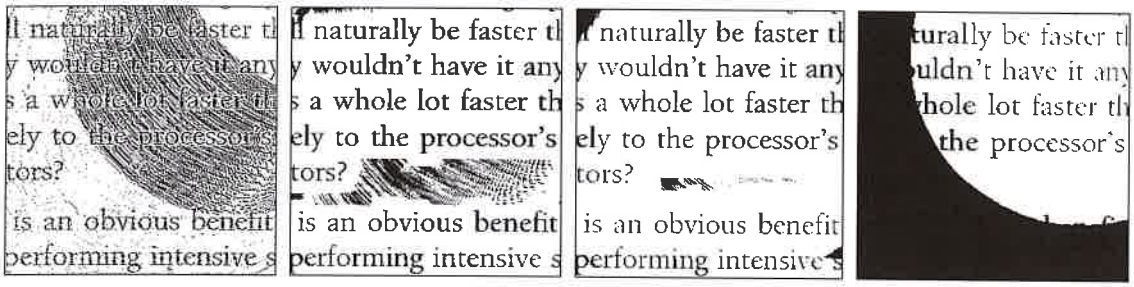


Figure 4: Text document image results: binary images obtained with IM algorithm using various WS: 3 (left), 25, 57 pixels and IM global (right)

Interpretation of results obtained with implementing the two above mentioned thresholding techniques on the repulped print handsheet picture (Figure 1, left) was, as could be expected, not as straightforward as with the text document picture. Partial overlapping of toner particles of various colours, presence of small objects belonging to paper, i.e. background, and not to particles of our interest; these and other peculiarities made successful segmentation of the original image more difficult and also called for final human judgement regarding the applicability of the particular algorithm.

RT algorithm applied on GS image (Figure 5) and using small WS (e.g. 31 pixels) generated many artifacts, i.e. particles not present in the original picture. Increasing the WS lead to progressively better results and with WS = 251, i.e, when the window size equaled the image size (250 pixels), the detection of the majority of features of interest was very good. In other words, although RT is a local thresholding method, smaller WSs did not produce satisfactory results. RT is an extremely locally sensitive algorithm, so it detects even the slightest differences in GS values, i.e. intensity variations in digital images.

When using IM thresholding technique on GS image (Figure 6), smallest WS again resulted in generating spurious particle pixels while with larger WS the situation improved siginficantly in this respect, although the

total number of successfully recognized and binarized object pixels was too low. On the other hand, with small WS (e.g. 14 or 25 pixels) the algorithm was successful in recognizing certain coloured residual particles (e.g. yellow) that remained undetected when using bigger WS. It therefore seems that certain trade-off in terms of WS is necessary, i.e. WS optimum should be somewhere between 14 and 57 pixels. Global IM (right-most image) exhibits further - too pronounced - reduction in the number of recognized toner particles.

As depicted in Figure 2, the original picture was also split into four separate C, M, Y and K channels and thresholded separately in an attempt to properly binarize and detect coloured image areas, i.e. toner particles. After performing the RT or IM thresholding, the resulting images were again combined into a composite CMYK image. With RT thresholding (Figure 7) detection of coloured (yellow) and brighter particles was, as expected, very good. Excellent performance was again demonstrated when choosing the biggest possible WS, i.e. 251 pixels (right-most image). Similar discussion applies as in the case of combination GS image-RT procedure (see above).



Figure 5: Repulped print handsheet GS image results: binary images obtained with RT algorithm using various WS: 31 (left), 141 (middle) and 251 (right) pixels

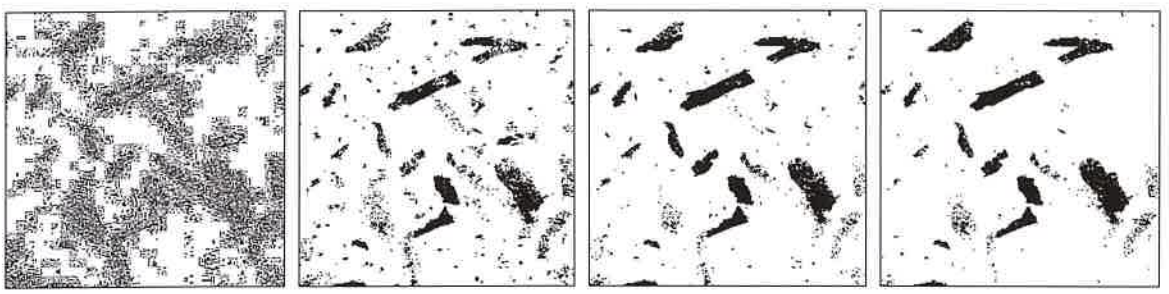


Figure 6: Repulped print handsheet GS image results: binary images obtained with IM algorithm using various WS: 3 (left), 25, 57 pixels and IM global (right)



Figure 7: Repulped print handsheet CMYK split image results: binary images obtained with RT algorithm using various WS: 31 (left), 141 (middle) and 251 (right) pixels

Performance of IM thresholding on CMYK split image (Figure 8) was similar, i.e. less than optimum, to that on GS image (Figure 6). The difference is that in the case of CMYK separation of channels the resulting binary images contained, at least to some degree, pixels of yellow toner particles that were present in the original picture.

It can be summarized that when comparing the original, repulped print handsheet image with the thresholded, binary images, the most complete and accurate detection of coloured features - toner particles - provides RT technique with a very large WS (251 pixels) applied either on the CMYK split or GS image. IM algorithm is less appropriate as it fails to detect some lighter and coloured areas of objects of interest, although its performance on CMYK split image is still acceptable.

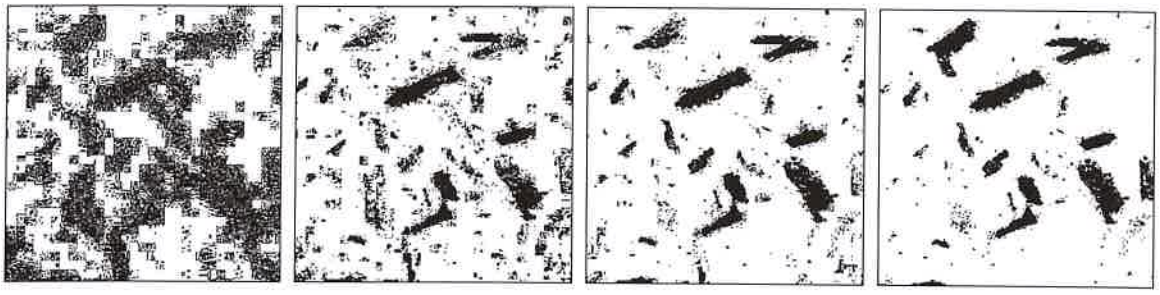


Figure 8: Repulped print handsheet CMYK split image results: binary images obtained with IM algorithm using various WS: 3 (left), 25, 57 pixels and IM global (right)

4. Conclusions

It is a well-known fact that the same thresholding method can be successfully implemented in one application, but may not work well for another one. As the results of our study indicate, adaptive, i.e. local thresholding techniques proved to be a promising way to accurately segment a digital image such as printed paper prints into two regions: one containing toner or ink particles together with other impurities and the other consisting of background - paper - pixels. In the future we will, apart from testing and studying other thresholding procedures, focus on further optimization and automation of the presented methods, for instance in terms of speed so that a larger picture area can be analyzed in a shorter time period.

Acknowledgement

The authors would like to thank Prof. Dr. Zdenka Bolanča from the Faculty of Graphic Arts, University of Zagreb, for providing digital sample images that were used in the study.

References

1. Antoine C., Lloyd M. D., Antoine J.: A robust thresholding algorithm for halftone dots. *Journal of Pulp and Paper Science*, Vol. 27, No. 8, 2001. P. 268 - 272
2. Hladnik A., Bolanča-Mirković I., Bolanča Z.: Characteristics of recycled fibres from digital prints using solid and liquid toner. *Prooceedings of 2nd International Symposium on Novelties in Graphics, Ljubljana, Slovenia, June 2006*
3. Kapur J. N., Sahoo P. K., Wong A. K. C.: A new method for grey level picture thresholding using the entropy of the histogram. *Computer Vision, Graphics and Image Processing*, Vol. 4, 1985. P. 274 - 285
4. Niblack W.: An introduction to digital image processing. Englewood Cliffs, N. J.: Prentice Hall, 1986. P. 115 - 116
5. Rais N. B., Hanif M. S., Taj I. A.: Adaptive thresholding technique for document image analysis. INMIC 2004. P. 61 - 66
6. Young I. T., Gerbrands J. J., van Vliet L. J: Image processing fundamentals - Segmentation: Thresholding. WEB: http://www.ph.tn.tudelft.nl/Courses/FIP/noframes/fip-Segmenta.html

Method of objective evaluation the fine detail distortion in process of screening

Yuri V. Kuznetsov, Denis E. Zheludev

North-West Institute of Printing of the St. Petersburg
State University of Technology and Design
Dzambula lane 13, 191180 St. Petersburg, Russia
E-mail: yurivk@mail.ru

Abstract

For objective quantitative measurement of the image fine detail distortion involved by screening the Screening Distortion Factor (SDF) is proposed. It comprises the norm of an error evaluated by superimposing of the original and halftoned resolution pattern bitmaps and counting the normalized sum of microdots, which changed their polarity (from black to white and from white to black) as result of screening. The losses in an image high spatial frequency component are illustrated by plotting the SDF curves via line test pattern frequency for variety of such screening process parameters as screen ruling, screening factor, screen and dot geometry, screening algorithm, etc.

Keywords

Distortion, halftone, MTF, screening

1. Introduction

Unlike the other imaging systems the specific process of graphic industry is to transform the continuous tone original to a bi-level print comprised of the plurality of small inked and blank elements. As far as the resulting amount of ink transferred to a print and, hence, the basic quality issues of the latter such as color, definition, tone rendition, sharpness, etc. are fundamentally dependent on these elements area, form and geometry of placement the screening has always comprised the actual, cornerstone R&D issue of illustrative printing. As result, many dozens of currently available, announced or upcoming, patented and trade marked screening techniques are currently pretending on their approbation and practical use.

In such situation the demand arises for correct, quantitative comparison of various screening techniques efficiency with the other important factors involved to the process being, if possible, kept the same [1]. The generalized approach to the halftone print quality evaluation was formulated in [2] on the basis of comparing not the original and its halftone copy themselves but the image metaphors of the both produced by the HVS model. So, this approach embraces the whole great number of halftone print quality parameters which can be subdivided on two groups. Parameters, related to the first of them, characterize the reproduced color, contrast or tone range, the number and distribution of the grey levels within the latter, the uniformity of vast image areas, etc. Along with the visual estimation, these quality indices of reproduction can be objectively and separately measured by colorimeter and densitometer with the use of corresponding test wedges, which results, for example, in plotting of the so called TCRs (Tone Reproduction Curves), color gamuts, tone deviation distributions, etc.

Given research is, however, related to the parameters of the second group which are responsible for reproduction of the high spatial frequency content of an image, i.e. for its sharpness, definition and accuracy of fine detail reproduction. The evaluation of this kind of parameters is actual for graphic digital screening techniques, which were especially modified for such parameters improvement.

The Modulation Transfer Function (MTF) is commonly used to model the frequency response of an imaging system [2, 3]. Micro photometric measuring of profiles or contrasts across the lines and gaps of the reproduced variable spatial frequency bar pattern can be applied, for example in photography, to verify the correlation of a modeled MTF to an experimental results. However, this micro photometric method isn't efficient to estimate the halftone reproduction of such a pattern because the micro structure of the latter stays bi-level, i.e. similar to the structure of an original test image. The only difference is in that instead, for

example, of solid lines and clean gaps of a test target the structure of its halftoned version comprises the scattered halftone dots or just parts thereof filling both the lines and gaps of a pattern in the manner dependant on specific of a screening method used in reproduction (Fig. 1).

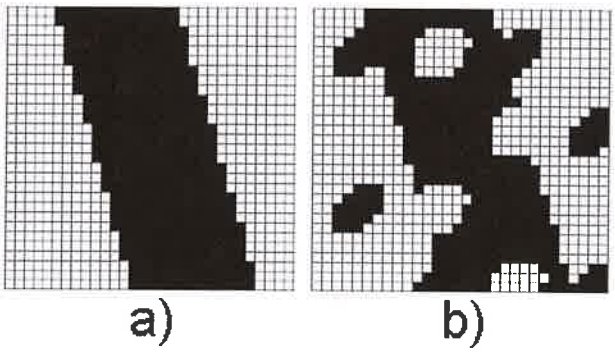


Figure 1: The bit maps of enlarged fragment of resolution test pattern (a) and its halftone reproduction (b)

Therefore, the facility of certain screening technology to preserve the sharpness and definition of an original continuous image is mostly judged by the visual evaluation of resolution test patterns. Such practice doesn't make possible the objective comparison of various screening techniques efficiency in relation of these important image quality issues because of the difficulty of providing the multiple of other imaging conditions exactly the same. The enlarged halftone reproductions of graphic elements (letters) of continuous tone original are presented on figure 2. They were produced at different screening conditions, such as the volume of an input data (screening factor - SF), the use of USM and halftone dots or their parts displacement in direction of a detail boundary. The difference in graphic accuracy of these elements is evident.

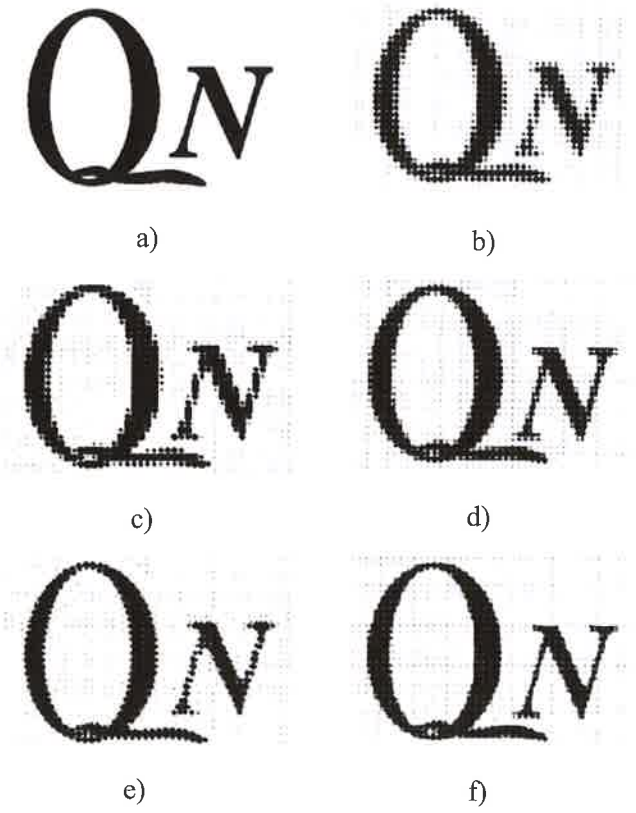


Figure 2: Enlarged halftone reproductions of graphic elements of continuous tone original produced at different screening conditions

So, the need exist in a quantitative method allowing for evaluation of effect of various imaging parameters (volume of a scanned/input image data, printer resolution, type of printing, etc.) and of various screening settings (screen and dot geometry, screen ruling and angle, screening algorithm, etc.) on halftone picture quality at different spatial frequencies and contrasts, as well as, along the whole chain of reproduction stages.

2. Method and measurement procedures

We have measured the norm of an error to quantitatively estimate the fine detail distortion involved by screening. This norm is evaluated by superimposing of the original and halftone pattern bitmaps and counting some normalized sum of the microdots, which changed their polarity (from black to white and from white to black) as result of screening. With the use of such a norm the Screening Distortion Factor (SDF) can be calculated according to the equation

$$\mathrm{SDF} = 1 - 0{,}5 \cdot \left(\frac{\sum_{i=1}^{M} \sum_{j=1}^{N} \left| A_{ij} - B_{ij} \right|}{\sum_{i=1}^{M} \sum_{j=1}^{N} A_{ij}} \right), \qquad (1)$$

where $A_{i,j}$ and $B_{i,j}$ are correspondingly the bi-level values in A and B matrixes of an original and screened patterns, while M and N denoting the number of lines and columns in a matrix.

In this approach the initial test with resolution pattern of full or intermediate contrast is concerned as a detail of continuous tone original to be reproduced with the use of screening. So, the method of such test processing comprises, as is shown on figure 3, the following steps:

- formation the high resolution bitmap of a test resolution pattern (Fig. 3a);
- emulating the capturing and encoding of this test by a scanner at the predetermined screening factor and contrast settings with providing the multilevel CT (byte-map) image file (Fig. 3b);
- creating the PostScript file at predetermined settings of tone value percent for white and black levels (Fig. 3c);
- screening the PostScript image file in a RIP or some custom software with providing the halftone bitmap (Fig. 3d);
- superimposing the initial and final bitmaps to calculate the SDF according to above equation (Fig. 3e).

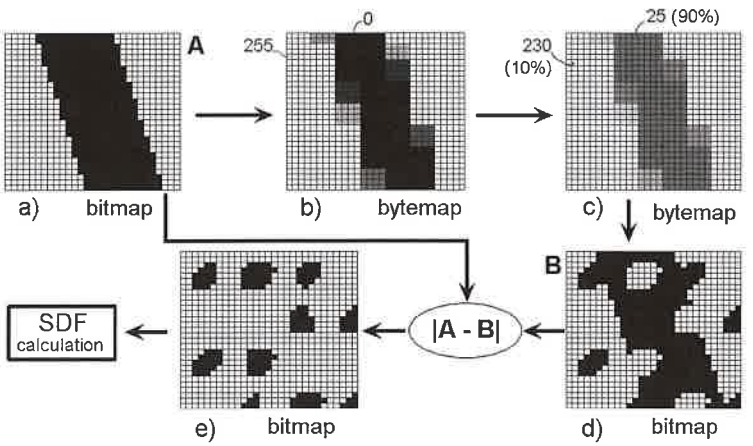


Figure 3:The sequence of resolution test pattern processing steps for SDF calculation

The predetermined quantization levels of 8-bit code emulating some contrast of an original pattern or taking into account certain artistic considerations are assigned to b/w levels of an input image at the first step (Fig. 3b). Nevertheless, if even the extreme values of, for example 0 or 255 are used for "black" and "white" of pattern, as indicates on the same figure, the intermediate values appear in encoded image version due to the aperture distortion of scanning or, in the other words, due to the averaging the tone value over an image

sampling area at detail boundaries. Such important variable of halftoning procedure as the sampling of screening factor (SF) comprising the ratio of image scanning and screening frequencies is also set at this step.

When the picture is further prepared for printing the other codes should be assigned to black and white corresponding to minimal and maximal, for example, 10% and 90% halftone dot area appropriate to the technology being used for given kind of a print job (Fig. 3c).

The use at the last of these steps of a bit map produced by screening program undermines the SDF evaluation in relation to some idealistic image copy. However, the superimposing a high resolution scanned bit map of a halftone transparency, plate or print may also be used here allowing for evaluating the share of distortion added by the corresponding further stage of printing technology.

The graphs of such a factor, plotted along the pattern ruling values, should comprise some equivalent of MTFs and allow for comparing the various screening methods efficiency in relation of the reproduction of high spatial frequency content of an image.

For testing this method working ability the MATLAB facilities [4] were used to create resolution test patterns at 3600 dpi, process them with analytically defined (Fig. 4) weight function, calculate and plot the SDF curves. Test image scanning and encoding were emulated in Photoshop.

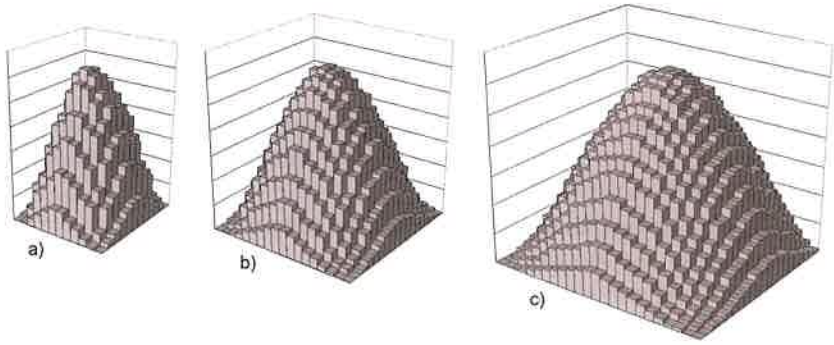


Figure 4: Examples of "screen hills" produced with the use of analytically defined (by analogy with [5]) screen function for three halftone frequencies

3. Testing and preliminary discussion of the method

The first graphs produced by the above described method (Fig. 5) allowed for some discussion of proposed Screening Distortion Factor representativeness.

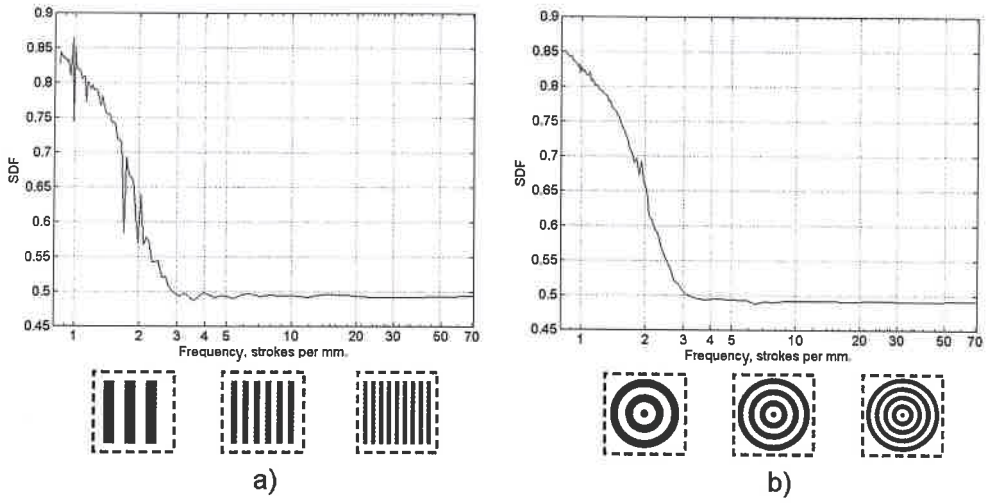


Figure 5: Screening Distortion Factor (SDF) plotted along the resolution test pattern frequencies for two geometries of a pattern: parallel (a) concentric and lines (b)

The SDF value equal to 1.0 relates to the opposite case of facsimile reproduction when all the input pixels remained unchanged. Such situation takes place for an input test of full contrast scanned at as high resolution as that of the printer and assigning to its white and black levels correspondingly of the 0% halftone dot and ink solid. The screening process has no place in this case, the halftone dot generator works as a simple Boolean repeater and SDF curve comes on a graph parallel to abscissa as shown on figure 9.

Zero value of SDF corresponds, according its formula, some virtual, theoretical presentation of an original by its negative (Fig. 6c) as result of screening by reversing the sign of all the bits of an input test.

The SDF value of 0.5 corresponds to the case in which the half of bits of both dark and light lines of an input test-pattern c has changed polarity as result of screening, as, for example, shown on figure 6b. The lines of an input pattern vanish at this SDF value, the resulting microdot structure appearing the uniform grey field. Small fluctuation of SDF curve near this value can be explained by some deviation from 50/50 relationship of black and white within resolution pattern patches of different frequencies. So, all the SDF values lower than 0.5 can be considered non-representative.

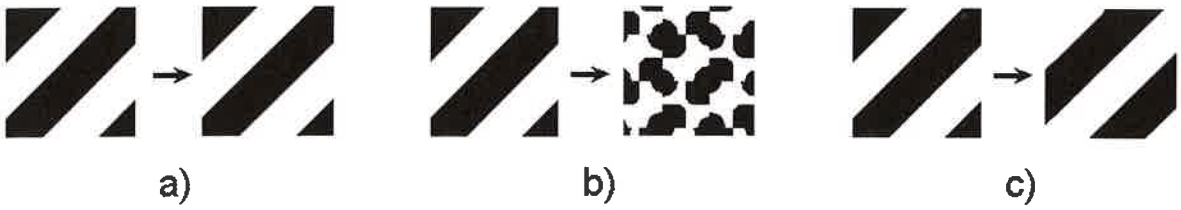


Figure 6: Examples of halftone copies of the input test pattern (a) for SDF values of 1.0 (a), 0.5 (b) and 0.0 (c)

It should be noted that the SDF level of 0.5 doesn't completely correlate with visual estimation of resolution pattern halftone copy because of aliasing which arises at some lower frequency of an input pattern than that corresponding to SDF = 0.5. Such aliasing appears due to the interference between pattern and screen frequencies. The peak on lower curve of figure 6 demonstrates the result of such interference at about 28 lines per mm ($20 \cdot \sqrt{2}$) of an input line pattern when the 20 l/cm orthogonal screen is used at 45 degrees angle. The number of such peaks increases (Fig. 5a) when the lines of a pattern are vertical and the screen isn't turned. From the other hand, the use of the pattern comprised of circular lines, as the graph on figure 5b shows, gives estimations which are less disturbed by the interference due to some compensation of its effect on calculated SDF value. Anyway, the SDF graphs properly reflect the visually perceived definition at the level which is somewhat higher of 0.5. Nevertheless, the plots coming down to 0.5 SDF level may be advised to be used as far as more extended graphs express the certain trends in the other factors influence on the fine detail distortion. Such different trends can be seen on graphs presented on figures 7 - 10 and calculated for the number of variables.

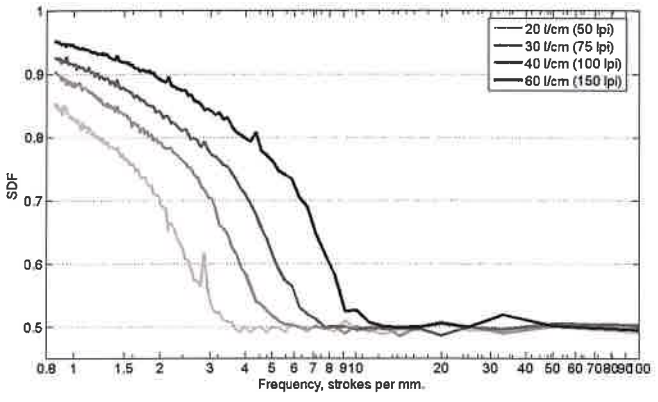


Figure 7: SDF plotted for different screen ruling at SF of 2.0

Figure 6 shows the screening distortion at different screen rulings at fixed SF of 2.0 and full contrast of an input test while figures 8 and 9 are plotted correspondingly for variable test contrast and screening factor. The curves on each of these figures are located differently in relation to each other, i.e. coming somehow parallel

or converging at highest frequencies. At the same time, the combination of four of these graphs on figure 9 allows to see how the effect of lower screening factor may be compensating by the increase of screen frequency and vice versa. The graph plotted for SF = 2.0 and screen ruling of 20 lines/cm comes there closely to the graph plotted for twice less SF = 1.0 but twice higher screen ruling of 40 lines/cm.

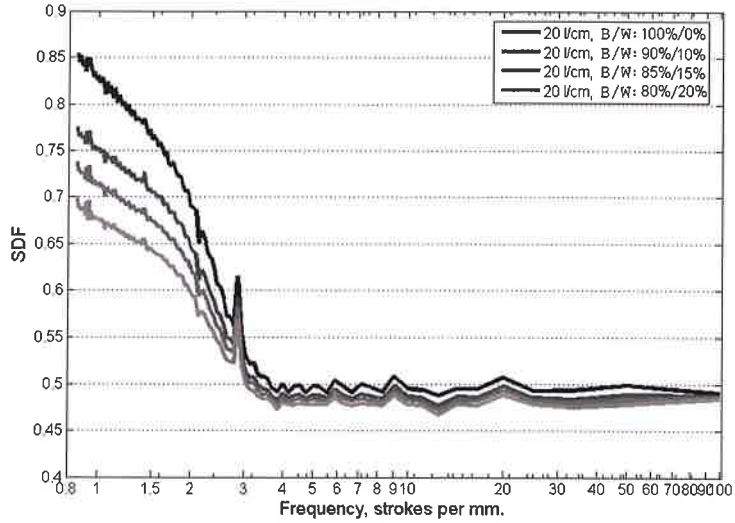


Figure 8:
SDF plotted for different contrasts of the input test at screen ruling of 20 lines/cm and SF of 2.0

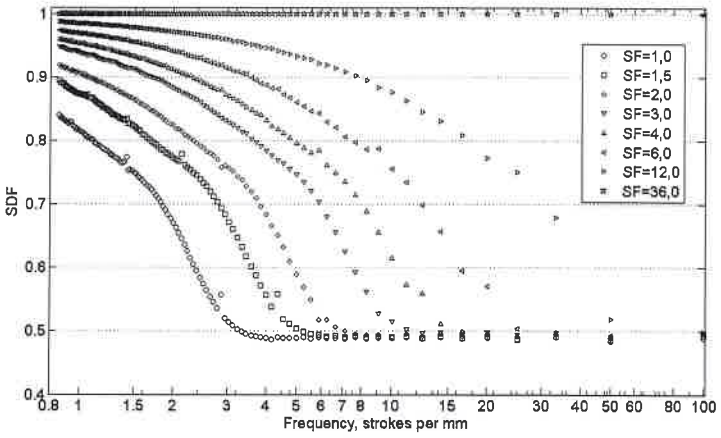


Figure 9:
SDF plotted for different SF at full contrast of the input test and screen ruling of 40 lines/cm

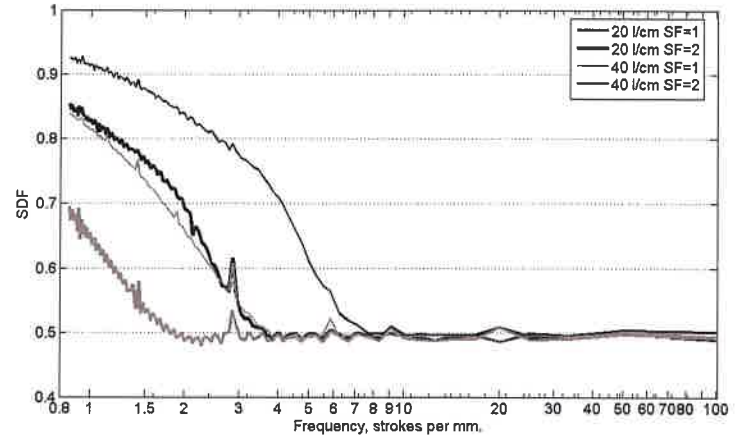


Figure 10:
The location of two middle graph illustrates some reciprocity effect of screen ruling and screening factor

Along with the idealistic, bitmap presentation of a screened pattern according to above listed steps the method allows for independent and comparative quantitative estimation of the additional share of low pass image

frequency filtration introduced in computer-to-film and computer-to-plate techniques at various output resolutions as well as with the use of various types of plates in conventional plate making. Being applied to silk printing it makes possible the objective evaluation of the effect of various silk screen parameters on sharpness and definition of the halftone image. The same kind of investigation can be related to the similar effects of anilox roller parameters in flexography. At last, the method stays helpful to practically evaluate the halftoning facilities of those digital printing devices where the screened bitmaps aren't available and the method of screening is unknown due to the closed architecture of such devices. There issues may comprise the objective for further research in this direction along with the development of some integral screening quality criteria based on SDF curves.

4. Conclusions

The need exist in a quantitative method allowing for evaluation of effect of various imaging parameters and screening settings on halftone picture quality at different spatial frequencies and contrasts of an input image, as well as, along the whole chain of reproduction stages.

The traditional methods of reproduction quality estimation for the high spatial frequency image content incompetently satisfy these purposes due to bi-level nature of halftone prints.

The use of proposed SDF criteria allows for plotting frequency response curves illustrating the effect of various factors inherent in different screening techniques.

Besides of these factors the specific effects of the further printing technology stages on fine detail reproduction quality can be estimated and analyzed.

References

1. Kuznetsov, Y., Screening Technique Modification and Its Effect on the Halftone Print Quality. In Recent Progress in Digital Halftoning II, IS&T, p. 358-362.
2. Kruse, B., Nilsson, F.,Objective quality measures of halftoned prints. In Resent progress in digital halftoning II, IS&T, 1999, p. 353-357.
3. Andreev, Y., Makeeva, T., Modulation transfer function for printing imaging systems estimation. Polygraphy, №4, 2007
4. Gonsales, R. C., Woods, R. E., Eddings, S. L., Digital image processing using MATLAB. Pearson Education, Inc., 2004. - 616 p.
5. Yamazaki T., et al. Generating screened half-tone images. Patent GB2133948 from 27.12.1982.



Colour management - differences arising between analogue and digital photo colour reproduction chains

Kristiina Saukkoriipi, Päivi Miettinen

Future Printing Center Oy
Kerrolankatu 2, FIN-21200 Raisio, Finland
E-mail: paivi.miettinen@fpc.fi

Abstract

This paper describes a research project studying colour rendition in each phase of the production chains from studio photographers to the printing house. Differences in colour adjustments of digital and film photos have been measured using standard colour checker charts and laboratory equipment. The typical results of these measurements are presented and discussed in this paper. The measurements and visual evaluation pinpointed the need for a colour chart with smooth colour transitions.

Keywords

Colour management, digital camera, film camera, printed image quality, printing process

1. Introduction

It is known that digital picture source files, which have been taken of the same target, come through the printing process with differing hue and colour depending on the photographer, camera, reproduction and printing press. These problems have been identified by photographers, prepress editors, printing houses, paper makers and end product customers alike. Photos, once printed, tend to have light hues, which look too flat to be natural, and the colours of the shadows, especially at boundaries, are not smooth. This causes the loss of the desired natural three-dimensional impression of roundness. Skin tones, for example, suffer strongly and may look unnatural. The colours of fabric tend not to render correctly in the printed pictures. Generally, the colours of the picture do not look like the colours of the original target and there are problems also in the rendering of details. These issues are generally recognised to affect across the printing and publishing industry, and form the subject of this paper.

Economics of publishing can be severely negatively impacted by a lack of control of the phenomenon. At worst the failure to reproduce realistically to the satisfaction of the publisher do not become evident until the final stages when the photos are being printed in the printing machine. Once this stage is reached, it is virtually impossible to apply further correction anymore. In reclamation conflicts it is frequently impossible to find out in which phase of the production chain the fault has emerged. In addition, the plethora of different proofing methods has each its impact on colour process control. Differences in colour and hue rendering of various monitors, for example, used in different phases of the process cause individual variations in digital photo colour management. It is often reported that these difficulties didn't exits in film image printing, and today forms a common hypothesis. In film image process it was assumed to be easier to locate retrospectively the places where the error emerged. We attempt to identify the differences and trouble points by comparing digital and film photo colour reproduction chains, and examine how they are effecting the final offset printed photo quality.

The main focus was to study how film and digital image differ in rendering shadows smoothly and in rendering the skin tones and the shadows of the facial colours. This study is focused on studio photography.

2. Methodology

The objectives of this project are to find and define methods that will allow us to print digital images better and more controlled than before.

To begin, three different workflows were compared, and their effects on the quality of a printed photo were studied. Initially, identifying precisely where the biggest problems in the reproduction chain occur was undertaken. This was done within three different commercial photo reproduction chains. To highlight the reproduction difficulties, the main subjects in the photos were chosen to include human beings, the objective being to study the way skin tone and shadows were rendered. All the changes were constituted by the actions applied through change of professional photographer and reproduction processor, respectively. Photographers took photos in studios, working in the same way as they normally do. The pictures of the same target were recorded both by a professional digital camera and by an analogue camera with conventional film. The cameras from Mamiya, Sinar and Canon were used. Reproduction professionals and photographers processed the photos and scanned the films. After the processing of the photos the proofs were taken. The way photographer or reproduction professional worked was not interfered. The aim was to take the pictures and process them the best way. All the images were processed with Photoshop. The workflow diagram of the three different reproduction chains is in the Appendix 1. The photos that were taken in chains are represented in Figure 1. The camera settings, taken from Photoshop image metadata or from interview of the reproduction processor are in Appendix 1 - 2 Table I-II.

The printer in every chain was the same. All the printings were done by a sheetfed offset printing machine. The printing was done according to ISO 12647-2 standard and proofing according to ISO 12647-7 standard. Two different papers of the paper type 2 (ISO 12647-2) were used. The papers were commercial coated fine papers with grammage of 115 g/m². To locate problems in workflow chains they were divided in to three parts:

- differences in the original film photo and digital photo;
- impact of the image processing;
- impact of the printing and proofing.

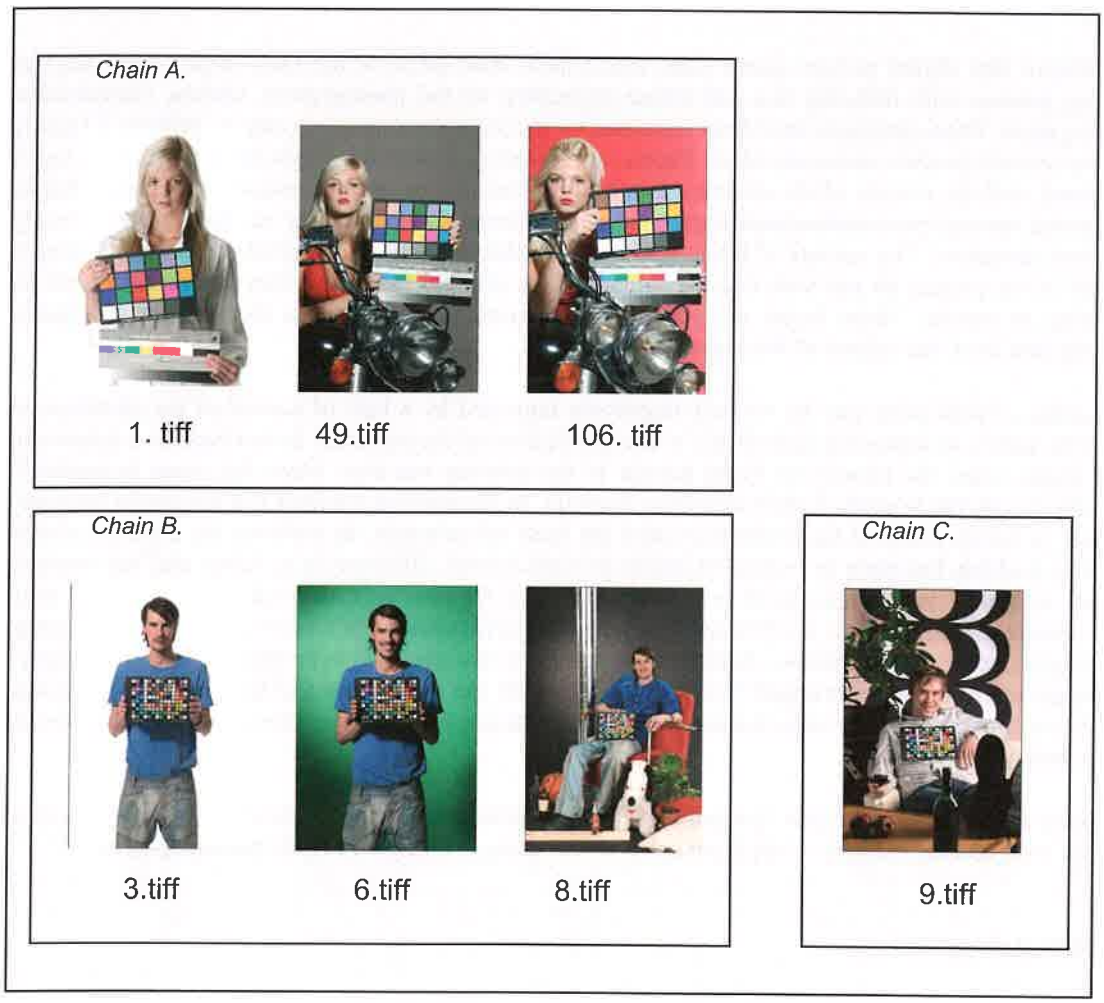


Figure 1: Reproduction chains with digital photos

Two Gretag Macbeth ColorCheckers (checkerboard array of 24 and colour checker for digital camera DC) were used in evaluating how different work phases influenced the original colours of the target and how smoothly the shadows were rendered. L*a*b* values of the targets were measured and chroma (ΔC, ΔE_{ab}*, ΔL*, Δ a*b* and hue angle (Δh) were measured, in order to define how different work phases effected the photo. Smoothness of the shadows was studied on how the grey areas of the target were rendered (L*, ΔE* and ΔC*) by comparing to the values in the original chart. The main aim was to study the smoothness of the shadows. Skin tones were studied from the skin coloured squares of the chart. Values were measured according to ISO 12647 - standard. Visual evaluations of the printed photos were also made.

3. Results

3.1 Differences in the original film and digital photo grey values

Shadow rendering was measured from the grey squares. When the original and film and digital photo were compared, it was discovered that lightness (L*) of the film was much closer to the original values of the chart. Digital photo had much bigger growth in lightness in the middle or light middle tones. This can be seen in Figures 2 and 3, which are the results from chains A and C.

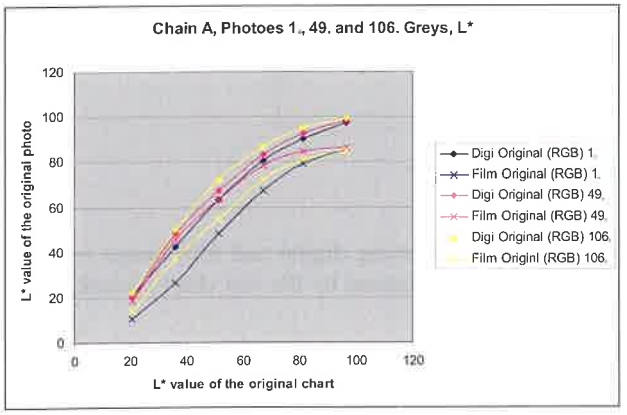


Figure 2:
*Chain A, Photos 1., 49. and 106, Greys, L**

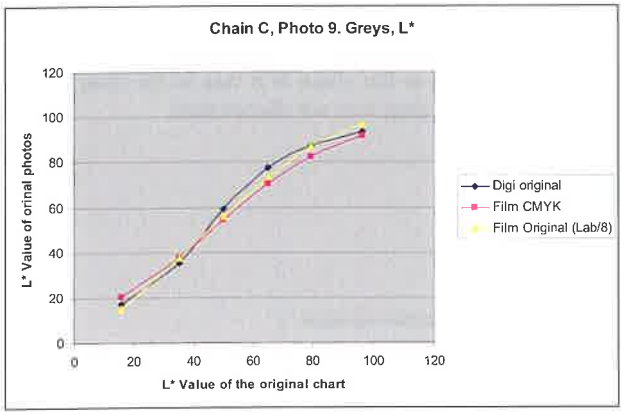


Figure 3:
*Chain C, Photo 9, Greys, L**

In the Chain B two professional digital cameras were compared. There were some differences in lightness between the photos taken with the two cameras. The amount of difference varied between the digital images. The images taken with Canon seemed to be a bit lighter in light middle tones. The two images (6 and 8) taken with Sinar had lightness deviations in the middle tones.

3.2 The effect of image processing

3.2.1 Lightness

In chain A in the film image processing the aim seems to be to get the overall grey values lightness (L*) to match the original chart values. As a result, the middle grey values match quite well with the original values

but the light and dark end values are darker than the original chart values. With the digital photo the image processed values did not match the original chart values. The middle tones were the same as before processing. Light end values were darkened, and dark end values were lightened.

In the Chain B lightness of the light middle tones was increased even though the lightness of these fields already was differing most from the original values. In addition, the inaccuracy in the two Sinar photos was corrected. This is illustrated in Figure 4. The photos of the chain A and B with white background were also darkened at the dark end.

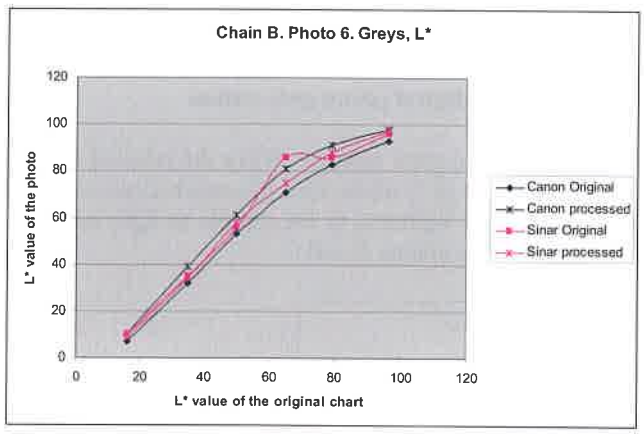


*Figure 4: Chain B, Photo 6, Greys, L**

In Chain C the lightness of the film was increased and after the processing digital and film image matched quite well. This was probably due to the fact that the images were processed by the test chart's black, white and grey squares.

3.2.2 Delta E and delta C

In squares of density 0.23, at the light end, there seems to be the smallest colour error value (ΔE*), where the greys hue is correct, in all of the chain A's photos (Figure 5). This was also the case with digital and film photos. Similar area was also in the Chain B photos 3 and 6, although in the chain B it was in the dark end of the grey area. In the third photo, photo 8, of Chain B similar low error area was not discovered.

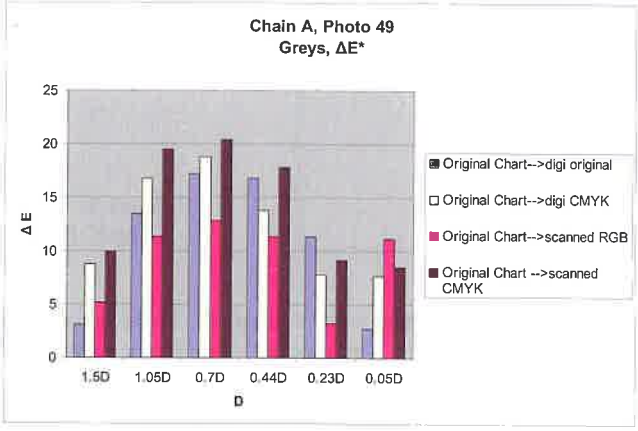


Figure 5: Chain A, Photo 49, Greys Δ E

In Chain A the chromatic values of the original film matched best to the original values of the chart. When processed the overall chromatic error raised but the deviation decreased. This was also the case in the digital image processing of the same chain.

In the Chain B, Sinar images matched well with the original chromatic values of the chart. In image processing they were left untouched or only the darkest value was rendered. With Canon images similar pattern in original values or processed values could not be found.

In chain C the processed film and original digital image chromatic values matched well with the original chart values. In the processed digital image the biggest chromatical error was in the light mid tones, but otherwise it matched well with the original tones.

Delta E error was biggest in the digital image mid tones and varied a lot depending on the area in the chart squares. In the processed film image delta E the variation was smaller.

3.3 Printing and proofing

In the proof taken from Chain A's images the grey values of film and digital images lightened so, that the proof had the biggest error compared to original chart values. The proof taken from the film lightened more than the one taken from the digital image. The form of the curve was still the same in the proofs.

In the chain B no proofs were taken, because they didn't normally take those in their reproduction chain.

In Chain C's CMYK images and the printed images matched quite well. Printed image was darker than the digitalised version of the same image. As a consequence of that, processed and printed images matched best to the original values of the chart. Film gave better rendition than digital image, which still had a bit too light mid tones.

3.4 Skin tones

The chart used in chain A's images were problematic in studying skin tones rendering. It had only a few skin tone squares. It was impossible to study how smoothly different skin tones were rendered and how well the roundness of human face were rendered. There were similar problems with the other chart too. Even if it had more skin coloured squares there it did not have smooth enough transition between skin colours. In the chain A the ability to render different colours were varied, depending of the colour and tone of the colour, between the original film and the digital image and processed ones.

In Chain C the original film had bigger colour error (delta E) and chroma error (delta C) but the smallest lightness error. In the processed images digital photo had the biggest errors in chroma and delta L. There were no significant errors in the hue angle. This in illustrated in Figure 6.

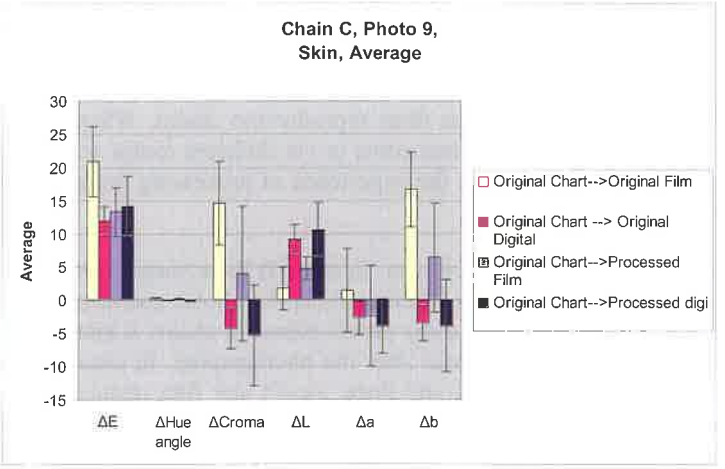


Figure 6: Chain C, Photo 9 average skin colours

In Chain B all the processed digital images from both cameras had huge chroma errors. Chroma errors were smaller in the unprocessed images. In image 3, with the white background, the photo taken with Sinar had a

big ΔE* error. Values in the Canon image were closer to original values with the exception of lightness, which was better in Sinar images. In photo 6 with the green background the Sinar had huge error in lightness. There were no significant errors in the hue angle in any of the chain B images.

In generally in all the chains image processing widened the colour gamut or all the colours were processed into some specific direction for example towards cyan. In all the chains errors were bigger in ΔC and only minor errors in Δh. Visually film was considered to be red and yellow and colours were softer than in digital image. In Chain A the digital image hair of the model looked grey and it looked more natural in the film.

4. Discussion

The findings allow us to state clearly that a standardised more controlled way of processing digital photos is needed. The biggest differences in the various process stages were observed, as expected, to be introduced before the printing. The printed photo and the CMYK image were shown to be matched quite closely.

Additionally, human error plays its role. There were several issues, for example, arising in the naming of the files at the different stages of the photos production. Also, some of the ways of working induce some of the problems. For example, nearly all of the photographers used laptops or some other non-calibrated display for checking the photo quality during the photographing. Clearly, therefore, the convenience of digital photography imaging is partially responsible for its variability.

Interestingly, between the different chains, the results differed markedly as to whether film or digital photo gave the better print rendition. This finding tends to undermine the hearsay that film is consistently better. Differences appeared to be stronger between different workflows, such as that the best result across the workflows was not dependent on the recording medium, but rather the combination of methodologies associated with both the recording of the image and its processing chain. Variation for the film image was identified as being related to problems in scanning the films. There was some lack of knowledge of the best scanning practise, for example, found in one of the workflow chains. The processor today has become more familiar with processing of digital images. As a result, the reliability of image reproduction associated with traditional film was lost in this study, and so the hypothesis that film provides the better rendition in principle could not be disproved. The findings, however, undoubtedly support the need for a better methodology for digital photos.

The importance of the first recording step in digital photography has been underlined in this work. For example, under-exposed digital pictures could not be improved sufficiently either in the image processing or during printing.

5. Conclusions

This paper describes our studies on how shadows and skin tones of the models rendered and on the differences between film and digital images in three reproduction chains. When choosing the chains, it was taken into account that photos to printing houses come in via different routes and the aim was to study three routes that differ from each others and where the experience of processing image was varied. The study was restricted into studio photography.

In preproduction the following differences were seen. In chain B there wasn't any reproduction professional to edit the photos, the photographer made all the adjustments in the photos and sent them straight to the printing house as he would normally do. He did not use any proofs either. In chains A and C the final processing of the images was made by a reproduction professional after the photographer. In chain B two digital images taken with different digital cameras were compared and there wasn't any film photo to compare with. The image reproduction chain was divided into three parts: differences in the original film and digital image, impact of the image processing and impact of the printing and proofing. When processing the photos the aim was to make the film and digital image as similar as possible and make the photos look as good as possible.

In digital image the lightness peak in light mid tones (50 - 80 %) and or the digital images were overall lighter than film photos. The difference remained even after the image processing. There were differences in between the three chains on how they processed the images. In chain A the preproduction professionals mainly adjusted

most of the films grey values to match the original values in the colour checker chart. This was done by darkening the overall lightness curve, so that most of the middle hues were correct even though the light and dark end of the curve might have been darker than the original chart values. The chromatic error of the grey values was adjusted to be near constant in all the different grey levels. In the digital images of chain A the darker end of the lightness curve were lightened and light end was darkened but the middle tones were left unattached.

In chain B images taken with two digital cameras were processed. The photographer increased the lightness in the middle hues which were of already lighter than the chart values and corrected the errors in lightness of the photos taken with the other camera. In chain A and B the images with white background the lightness of the dark end was darkened.

In chain C the reproduction professional adjusted the photos by the chart black, white and grey areas so that after the processing lightness of the digital photo and the film were almost the same. After the processing the film and digital image were left lighter than the original values of the chart.

The biggest problem in this study was to measure the differences in smoothness of the shadows which were visually seen between the film and digital image. The references, two colour checker charts, used in this study were too coarse to find out the subtle details in changes in colours. It was found out that the reference colour charts should have continuous and smooth colour fields from light to dark in different colours. This is important when measuring the digital image which visually seems to lack continuity in colours compared to film images.

Compared to film the digital images have the advantage of the possibility to add metadata in the image file. It could be used more to help image processing and to find out how the image was taken and processed in RAW image.

The next steps are to study in more detail what happens in the beginning of the process and to develop procedures for the beginning of the chain so that printed images would better fulfil the requirements of the end product customers. Special attention will be paid on rendering of memory colours and differences in the smoothness of the shadows between film and digital image. The ultimate goal is to provide the industry better methods throughout the chain. The research project still continues.

References

1. Breede, M., (1999) *Handbook of Graphic Arts Equations. GATFPress, 230 pages*
2. ISO 12647-2:2004, *Graphic tecnology - Process control for the production of half-tone colour separations, proof and production prints - Offset lithographic processes*
3. Uroz, J., Luo, R. and Morovic. J., (2002) *Perception of colour differences in large printed images. Colour Image Science, John Wiley & Sons Ltd.*

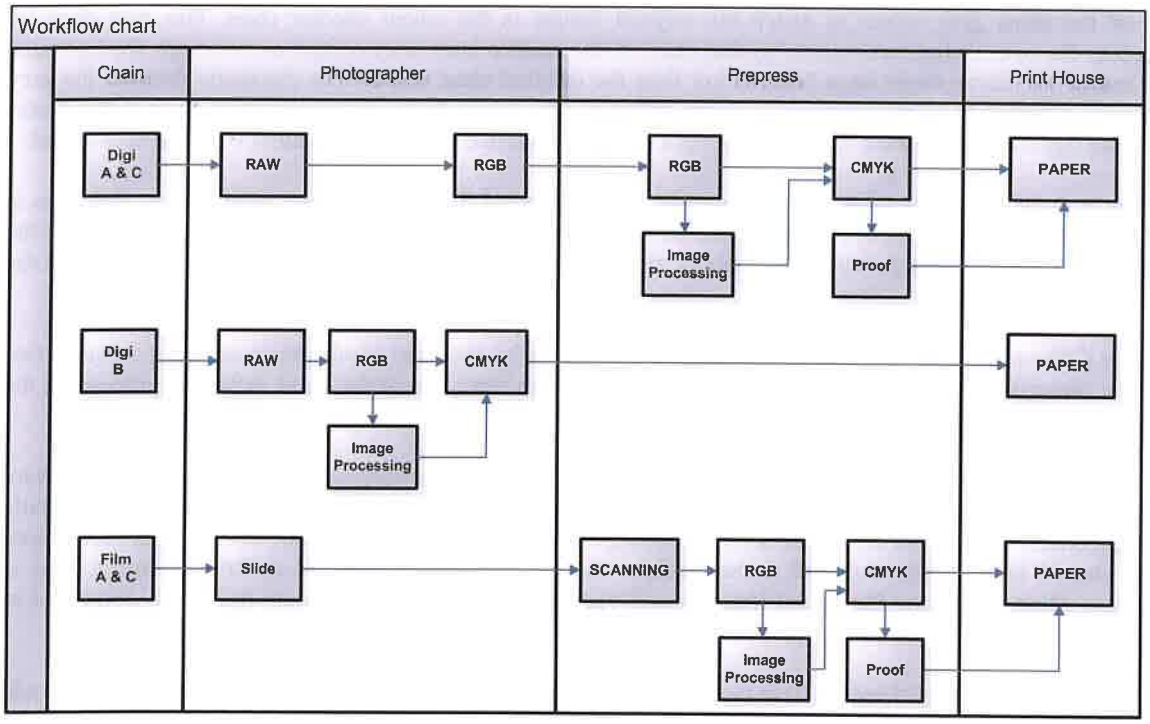


Figure 7: Workflow chart

Table I: Chain A film metadata

Scanning of the films (RGB)	**films 1, 49 and 106**
scanner (flatbed)	C550 Lanovia
input profile	C-55-T3-EKTACHROME.ICC
Bits per colour	16 bit
Magnification	835 % (194 x 293 mm)
Resolution	13.8/mm
Output Profile	ISO Coated.ICC
RGB → CMYK bits per color	8 bit

Table II: Chains A, B, C digital image,metadata

Image Chain	Chain A			Chain B			Chain C
Images Name (tif)	**1.**	**49.**	**106.**	**Canon 3.**	**Canon 6.**	**Canon 8.**	**Sinar 3. & 6. & 8**	**9.**
Camera	Canon EOS-1Ds			Canon EOS-1Ds Mark II			Sinar AG Sinarback eMotion 22	Canon EOS-1Ds Mark II
X,Y-resolution (inch)	350 x 350			300 x 300			300 x 300	300 x 300
Camera profile				ACR 2.4			Captureshop 5.4.2	ACR 2.4
Exposure	1/60	1/60	1/85	1/125				1/160
F-number	f/8	f/18	f/14	f/11	f/8	f/6.3		f/22
ISO speed ratings	100			50				100
Exposure values (Ev)	11,9	14,25	14,02	12,88	11,96	11,3		16,24
Focal Length in 35 mm film	160 mm	135 mm	155m	85 mm				85 mm
White balance	As Shot			As Shot			As Shot	As Shot
Temperature				5000				4550
Samples per Pixel	3 = [16][16][16]			3 = [8][8][8]			3 = [8][8][8]	4 = [8][8][8][8]
Contrast				25				
Brightness				50				
Tint				5				
Colorspace	AdobeRGB (1998)							
Output profile	ISO Coated .ICC							



Improved gamut boundary determination for colour gamut mapping

Arne M. Bakke, Ivar Farup, Jon Y. Hardeberg

The Norwegian Color Research Laboratory, Gjøvik University College
P.O. Box 191, N-2802 Gjøvik, Norway
E-mail: arne.magnus.bakke@hig.no

Abstract

We propose a new method for the computation of gamut boundaries, consisting of a combination of the segment maxima gamut boundary descriptor, the modified convex hull algorithm, and a sphere tessellation technique. This method gives a more uniform subdivision of the colour space into segments, and thus a more consistent level of detail over the gamut surface. First, the colour space is divided into segments around a centre point using the triangles from the tessellation algorithm. The measurement points are processed, and the point with the largest radius is found for each non-empty segment. The convex hull algorithm with a pre-processing step is then applied to these maxima points to generate the final gamut surface.

The method is tested on different input data, including data sets both with and without internal gamut points. Different numbers of segments are used, and the resulting gamut boundaries are compared with the gamuts constructed using the segment maxima method. A reference gamut is constructed for each device, and the average mismatch is calculated. Our method is shown to perform better than the segment maxima method, particularly for a higher number of segments.

Keywords

Convex hull, gamut boundary, segment maxima, sphere tessellation

1. Introduction and background

The colour gamut of a device is the range of colours that the device can reproduce. When an image is to be reproduced on another device, it is necessary to apply a gamut mapping algorithm (GMA) to compensate for the differences in their colour gamuts. These algorithms use gamut boundary descriptors (GBDs) to represent the extents of the colour gamuts. In order for the GMAs to give good results, it is important that the GBD is as accurate as possible. Any inaccuracies might result in the GMA failing to move all points to the inside of the destination gamut, or unnecessarily drastic gamut clipping.

Several methods exist that can be used to determine the boundary of a colour gamut with varying degree of success. Some algorithms take advantage of existing knowledge about the colorimetric behaviour of a device, and can only be used to compute gamut boundaries for a certain device type. By implementing a device model that is used to characterise the device, the theoretical boundaries of the gamuts are determined by the parameter limits used in the model, e.g., ink coverage.

1.1 GBDs based on device models

MacAdam introduced one of the earliest attempts to create an analytical approximation of a device gamut [MacAdam, 1935]. Later, the gamuts of printing systems were determined indirectly using the Kubelka-Munk (Engeldrum, 1986] equations. Meyer et al. [Meyer et al., 1993, Meyer and Robertson, 1997] showed how to use this approach. Alternatively, Mahy found the gamut of a multi-ink printing system using the Neugebauer equations [Neugebauer, 1937]. Inui made the assumption that there is a correspondence between colour space and the dye amount space [Inui, 1993], and used this to determine the gamut. Herzog used an analytical, mathematical approach to describe the colour gamut of a device, using deformed cubes referred to as gamulyts [Herzog, 1996, Herzog, 1998]. A set of distortion functions is defined, and used to fit the deformed cube to the colour gamut. By extending this model, it can also be used for devices with more than 3 colorants.

1.2 Point based methods

When no specific characterization model of the device can be assumed, it is necessary to utilize alternatives to the analytical models. Usually, measured or simulated data points from the device are used as input to these algorithms. By processing a set of points in a colour space without taking any structure into account, some of these algorithms can also be used to find the gamuts of images.

The colour gamut of a device with three colorants can be determined by assuming that the gamut boundary of a device is preserved between the device dependent and device independent colour spaces. By measuring colours that are part of the gamut boundary in the device dependent colour space, an estimate of the colour gamut can be found. Depending on the need for detail, planes [Stone et al., 1988] can be used to represent the boundary by connecting the theoretical extreme points. If better accuracy is required, Bolte [Bolte, 1992] suggested an approach where colours that form the basis of a regular structure in the device colour space are printed and measured. Assuming that the relative position of the points remains the same in the device independent colour space, a direct triangulation can be performed on the measured colours.

A possible complication of this method is that characteristics of the printing process and the colour space transformation can lead to the order of the triangle vertices being reversed, and internal points in the device colour space structure may end up outside the triangles that form the surface of the regular structure. This method can be further improved by checking for mirrored tetrahedra in the device independent colour space, and testing that there are no points on the outside of the surface structure [Hardeberg and Schmitt, 1997, Hardeberg, 2001]. Guyler [Guyler, 2007] has proposed an extension of the direct triangulation approach for data from CMYK printers, using Delaunay triangulation to find the surface triangles where the determination of the gamut in the device dependent colour space is made difficult by the use of the black colorant.

If the only available information about the device is a number of points in a device-independent colour space, which have been determined to be reproducible by the device, there are still algorithms that are capable of determining the gamut boundary. The convex hull is one of several algorithms that can be used to calculate a surface that approximately encloses the data points [Meyer et al., 1993, Meyer and Robertson, 1997]. Typically, the quickhull [Barber et al., 1996] algorithm is applied to the set of input points. Zhao used quickhull to determine the gamut boundaries of ICC profiles [Zhao, 2001]. One issue with this approach is that device gamut data generally do not constitute completely convex objects in CIELAB or related colour spaces.

Guyler [Guyler, 2001] converted the input points to the CIEXYZ colour space before using Qhull to compute the convex hull. The vertices of the surface could then be transformed to CIELAB, resulting in a gamut that more closely follows the concavities of the data. Guyler claims that the boundary of measurement data from a printer tend to be more convex in the CIEXYZ space, which results in a better approximation by using this approach. He also computes correction factors to compensate for the overestimation of gamut volume introduced by using the convex hull. An alternative to using CIEXYZ is to compute the convex hull in a linearised dye density space [Viggiano and Hoagland, 1998], assuming that the printing process does not distort the relationship between the points when performing the subsequent transformation to CIELAB.

Balasubramanian and Dalal extended the convex hull with a pre-processing step [Balasubramanian and Dalal, 1997] to better follow the concavities of the gamut. They suggested that the data points should be changed using a non-linear gamma function based on the distance from the colour to a centre point within the gamut, before the convex hull is calculated from the altered points. By varying the γ parameter from 1 to 0, the detail level of the gamut can be increased by making the object more concave. A γ value of 1 leaves the points unchanged before the convex hull is applied, while smaller parameter values make the pre-processed data more convex. With an optimal choice of γ, the final gamut boundary will closely follow the perceived surface of the data points [Bakke et al., 2006]. Figure 1 shows a gamut boundary computed using this method.

By dividing the colour space into cells based on the lightness and hue, a different method to find the gamut boundary can be defined [Braun and Fairchild, 1997, Reel and Penrod, 1999]. The colour with the largest chroma value is determined for each cell, and later used as vertices in a regular triangulation of this structure. Segment maxima [Morovic and Luo, 1997] is a similar method, which divides the colour space based on spherical coordinates. The colour that has the largest radius in its segment is found, and simulated points are calculated using interpolation for empty segments. This method can also be used to find the gamuts of colour images [Saito and Kotera, 2000, Saito and Kotera, 2004], substituting the mass centre for the colour space centre as the origin of the spherical coordinate system. The segment maxima method results in a gamut where

the surface is sampled more densely near the top and the bottom (Figure 2). Similarly, it is a well known fact that tessellation of a sphere by uniform subdivision of spherical coordinates results in a surface with highly varying size of surface triangles. Alternative solutions [Baumgardner and Frederickson, 1985] are often used when working with sphere approximations, such as when drawing a 3D sphere approximated by polygons.

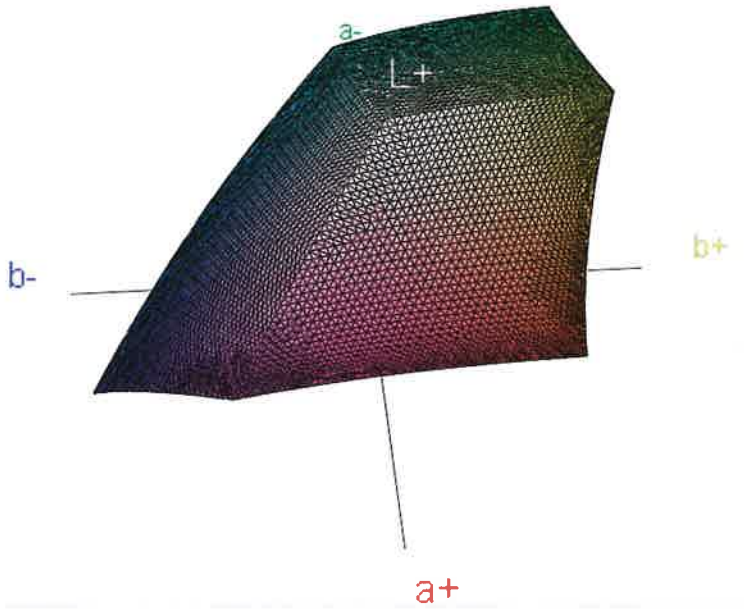


Figure 1: A gamut surface created using Balasubramanian and Dalal modified convex hull

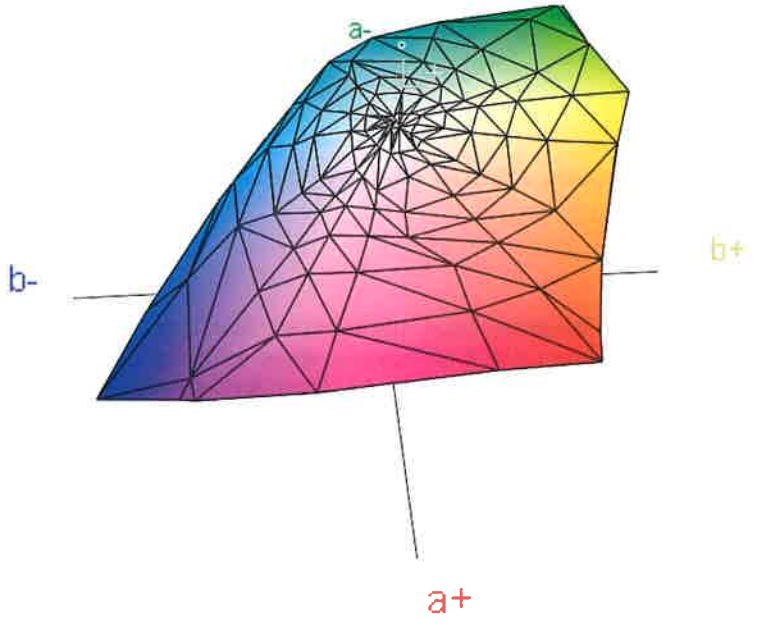


Figure 2: A gamut surface created using segment maxima. Note the smaller triangles near the white point

Edelsbrunner and Mücke introduced the concept of alpha shapes [Edelsbrunner and Mücke, 1994] as a solution to find a geometric representation of the volume and surface of a set of points. An alpha shape is constructed by first computing the 3D Delaunay triangulation of the input points. Then, a α-parameter is used to decide which tetrahedra, triangles, edges and points should remain a part of the shape. Varying the parameter, shapes from the convex hull to the set of individual points can be constructed. Cholewo and Love utilized alpha shapes to find the gamut of devices and images [Cholewo and Love, 1999]. They suggested that, for this application, the optimal gamut could be found by interactively changing the parameter value.

Giesen et al. [Giesen et al., 2005] proposed that what they called a discrete flow complex could be used to compute image gamuts. The colour space is divided into a grid, and for each grid point the distance to the nearest sample in the point data is calculated. This discrete distance map defines a flow direction for all positions in the colour space, and by traversing this structure the gamut of the image is determined.

2. Motivation

We have previously [Bakke et al., 2006] evaluated the performance of several gamut boundary determination algorithms on simulated device data. The Balasubramanian and Dalal modified convex hull algorithm was proven to perform well, particularly when 0.2 is used as the γ parameter value. However, the algorithm may result in a very large number of surface points, some of which form very small surface triangles. By combining existing methods for gamut determination with a more uniform segmentation algorithm, a good approximation of the gamut boundary can be found that uses a smaller number of surface points. The reduced surface complexity makes it possible to use less data to describe the gamut, which can be a factor when embedding gamut information in profiles or other files suitable for transfer and storage.

Perhaps more importantly, calculations of intersection points between the gamut surface and lines can be done in less time, improving the performance of gamut mapping algorithms. The segment maxima method provides a more compact gamut description, but its performance strongly depends on selecting a correct number of segments [Bakke et al., 2006], and generally gives a less accurate gamut boundary.

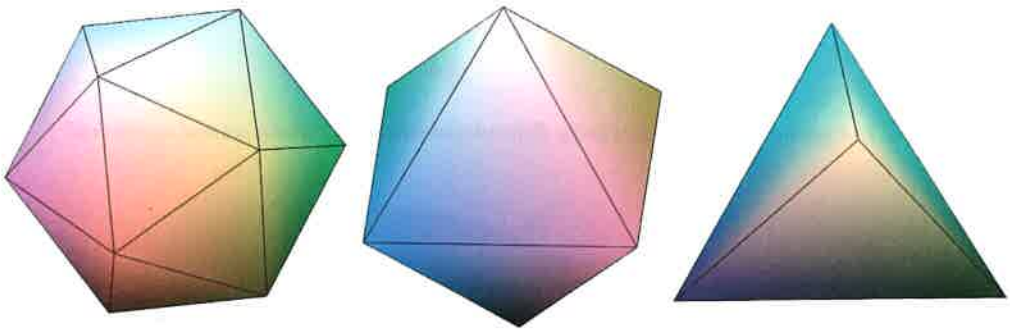


Figure 3: The geometric objects used as a basis for sphere tessellation: Icosaheron, octahedron and tetrahedron

3. Method

Our method computes the gamut boundary from any arbitrary selection of data points in CIELAB or a similarly structured colour space, given that a sufficiently dense sampling of the entire gamut volume has been performed. First, a triangle-based approximation of a sphere is computed using a well-known tessellation technique. A basic triangle-tessellated geometric object is generated as an initial sphere approximation, using a tetrahedron, octahedron or icosahedron (Figure 3). A subdivision of the surface triangles is performed as shown in Figure 4. Each triangle is subdivided into 4 smaller triangles recursively, until the desired number of triangles is achieved. The resulting vertices are then projected onto the surface of the sphere, giving a close approximation of a sphere with a more uniform triangle size than simple subdivision of spherical coordinates as used in segment maxima.

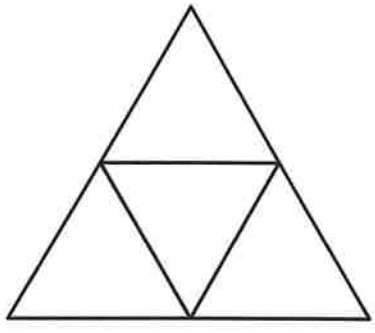


Figure 4:
The subdivision of a triangle

Upon construction of the tessellated sphere, a data structure is generated that includes the neighbourhood connectivity information for the triangles. Each surface triangle defines a segment around the centre of the colour space (alternatively the centre of the gamut), represented by the tetrahedron given by the 3 triangle vertices and the centre point. Figure 5 shows a surface triangle as solid lines, while the tetrahedron defined by the triangle and the centre point is illustrated using dashed lines. Each pair of vertices P_0, P_1, and P_2 defines an edge of the triangle. The tetrahedron is surrounded by three other tetrahedra, each sharing a different edge of the triangle.

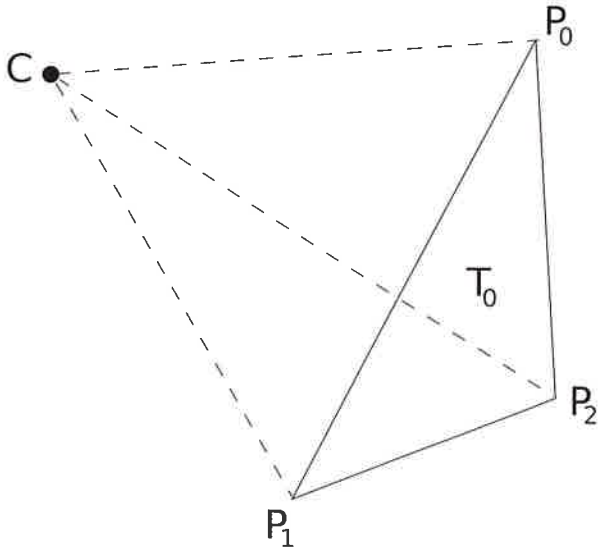


Figure 5: The surface triangle T_0 and the centre point C. The centre point and each pair of the triangle vertices define planes used to check whether a point is inside the segment

We then process the data points that belong to the gamut by finding the enclosing segment for each point. In order to determine which segment encloses each data point, a simple algorithm has been implemented. Start with an arbitrarily chosen segment, and evaluate the plane equation for the 3 planes defined by the centre point and each of the 3 edges of the segment surface triangle for the data point position. If any of these computations show that the point is on the outside of the segment, use the neighbouring segment on the other side of that plane as the basis for another iteration of this search. Since consecutive data points usually are in the same area of the colour space, especially for images, the segment that contains the previous data point should be used as the starting segment for the next point. This ensures that the number of segments that must be traversed to identify the location of the data points is low.

When the enclosing segment has been located for each point, the length of the radius from the centre point to the data point is calculated. Similarly to the segment maxima method, only the single maxima point per segment that has the largest radius from the centre point is kept for the next parts of the algorithm.

When all the input points have been processed, it is quite common to find that some of the segments do not contain any data points. The original segment maxima method solves this by creating artificial points from interpolation of surrounding maxima points. However, this interpolation phase can be quite slow when the number of segments is high. To avoid this operation, we suggest the use of the modified convex hull algorithm with $\gamma = 0.2$ on the maxima points from the non-empty segments to create the final surface triangles that constitute the gamut boundary.

4. Results and discussion

We have utilized the method previously described in [Bakke et al., 2006] to compare this gamut boundary determination method against the often-used segment maxima method. By establishing a reference gamut boundary using a device model, gamut boundaries found using these methods on different data sets from the device can be compared with the reference to compute a relative volume mismatch using a voxel technique. Results based on data from a total of 32 different data sets from 2 device gamuts are plotted in

Figure 6, where the average relative gamut mismatch of different segment numbers is shown. Our method performs well, especially as the number of segments increases. As the number of segments increases, the number of points preserved to the final surface calculation approaches the total number of points. Similarly, the performance approaches that of the Balasubramanian and Dalal modified convex hull used in the final stage of the method.

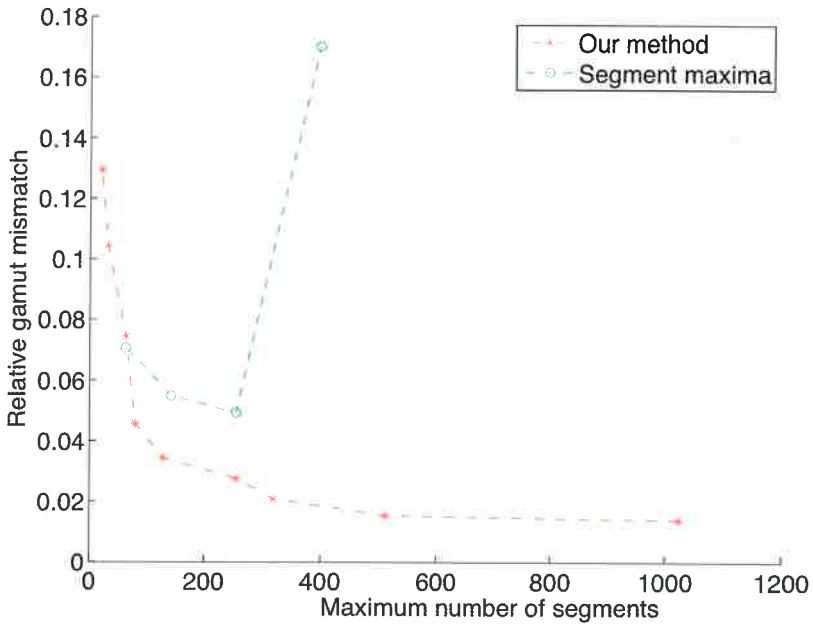


Figure 6: The average relative gamut mismatch of our method compared with segment maxima

The segment maxima method performs poorly with a high number of segments on generic data sets because internal points end up being added to the gamut surface. Due to the computational complexity of the interpolation method used by the reference segment maxima implementation when constructing points for empty segments, we did not use the segment maxima method with more than 400 segments. An example of the gamut boundaries computed using our method can be seen in Figure, based on the same input points as the previous two gamut boundaries in Figure 1 and Figure 2.

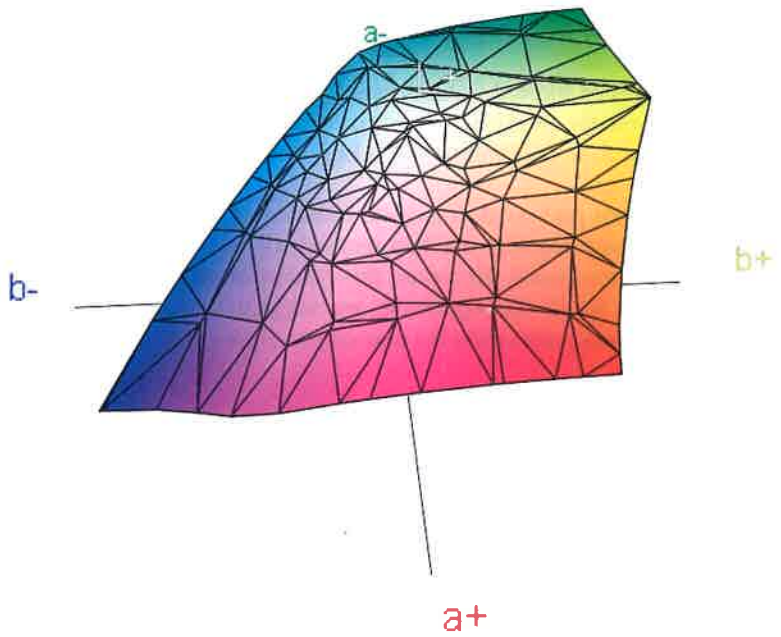


Figure 7: A gamut surface created using our method

5. Conclusions and future work

Our method can be used to find gamut boundaries with a specified maximum number of boundary points. We have compared the performance of this algorithm with the performance of segment maxima, and found that it is less sensitive to the number of segments used to approximate the gamut. This method leads to a reduced number of triangles compared to modified convex hull, making gamut intersection calculations faster. At the same time the performance approaches that of the modified convex hull.

We have looked at a method for reducing the number of input points used to generate the gamut surface. Alternatively, various mesh simplification algorithms [Cignoni et al., 1998] can be used to reduce the number of triangles in an existing surface structure. An interesting continuation of this work would be to compare our method to a surface generated using a combination of, e.g., modified convex hull, and a mesh simplification algorithm suitable for colour gamut surfaces.

References

1. Bakke, A. M.; Hardeberg, J. Y. and Farup, I. (2006). "Evaluation of Gamut Boundary Descriptors". In Proceedings of IS&T and SID's Fourteenth Color Imaging Conference, pages 50 - 55, Scottsdale, Arizona
2. Balasubramanian, R. and Dalal, E. (1997). "A method for quantifying the Color Gamut of an Output Device". In Color Imaging: Device-Independent Color, Color Hard Copy, and Graphic Arts II, volume 3018 of Proc. SPIE, San Jose, CA
3. Barber, C. B.; Dobkin, D. P. and Huhdanpaa, H. (1996). "The Quickhull Algorithm for Convex Hulls". ACM Transactions on Mathematical Software, 22(4), pp. 469 - 483
4. Baumgardner, J. R. and Frederickson, P. O. (1985). "Icosahedral Discretization of the Two-Sphere". SIAM Journal on Numerical Analysis, 22(6), pp. 1107 - 1115
5. Bolte, S. B. (1992). "A perspective on non-impact printing in color". In Color Hardcopy and Graphic Arts, volume 1670 of Proc. SPIE, pages 1 - 11
6. Braun, G. J. and Fairchild, M. D. (1997). "Techniques for Gamut Surface Definition and Visualization". In Proceedings of IS&T and SID's 5th Color Imaging Conference: Color Science, Systems and Applications, pages 147 - 152, Scottsdale, Arizona
7. Cholewo, T. J. and Love, S. (1999). "Gamut boundary determination using alpha-shapes". In Proceedings of IS&T and SID's 7th Color Imaging Conference: Color Science, Systems and Applications, pages 200 - 204
8. Cignoni, P.; Montani, C. and Scopigno, R. (1998). "A comparison of mesh simplification algorithms". Computers & Graphics, 22, pp. 37 - 54(18)
9. Edelsbrunner, H. and Mücke, E. P. (1994). "Three-Dimensional Alpha Shapes". ACM Transactions on Graphics, 13(1), pp. 43 - 72
10. Engeldrum, P. G. (1986). "Computing color Gamuts of Ink-jet Printing Systems". In SID Proceedings, volume 27, pages 25 - 30
11. Giesen, J.; Schubert, E.; Simon, K. and Zolliker, P. (2005). "Toward image-dependent gamut mapping: fast and accurate gamut boundary determination". In Color Imaging X: Processing Hardcopy, and Applications, pages 201 - 210, San Jose, CA, USA
12. Guyler, K. (2001). "Visualization of Expanded Printing Gamuts Using 3-Dimensional Convex Hulls". American Ink Maker, 79(9), pp. 36 - 56
13. Guyler, K. (2007). "Effects of Stochastic Screening on the Gamuts of Wide Gamut Printing Systems". www.iscc.org/ISCC2007/abstracts/T15IG1_Guylar.pdf
14. Hardeberg, J. Y. (2001). Acquisition and Reproduction of Color Images: Colorimetric and Multispectral Approaches. Dissertation.com, Parkland, Florida, USA
15. Hardeberg, J. Y. and Schmitt, F. (1997). "Color Printer Characterization Using a Computational Geometry Approach". In Proceedings of IS&T and SID's 5th Color Imaging Conference: Color Science, Systems and Applications, pages 96 - 99, Scottsdale, Arizona. Also in R. Buckley, ed., Recent Progress in Color Management and Communications, IS&T, pages 88 - 91, 1998
16. Herzog, P. G. (1996). "Analytical Color Gamut Representations". Journal of Imaging Science and Technology, 40, pp. 516 - 521
17. Herzog, P. G. (1998). "Specifying and visualizing colour gamut boundaries". In MacDonald, L. W. and Luo, M. R., editors, Colour Imaging: Vision and Technology. John Wiley & Sons Ltd.
18. Inui, M. (1993). "Fast Algorithm for Computing Color Gamuts". Color Research and Applications, 18(5), pp. 341 - 348

19. MacAdam, D. L. (1935). "Maximum visual efficiency of colored materials". J. Opt. Soc. Amer., 25, pp. 361 - 367
20. Mahy, M. (1997). "Calculation of Color Gamuts Based on the Neugebauer Model". Color Research and Application, 22, pp. 365 - 374
21. Meyer, G. W.; Peting, L. S. and Rakoczi, F. (1993). "A Color Gamut Visualization Tool". In Proceedings of IS&T and SID's Color Imaging Conference: Transforms and Transportability of Color, pages 197 - 201, Scottsdale, Arizona
22. Meyer, G. W. and Robertson, C. A. (1997). "A Data Flow Approach to Color Gamut Visualization". In Proceedings of IS&T and SID's 5th Color Imaging Conference: Color Science, Systems and Applications, pages 209 - 214, Scottsdale, Arizona
23. Morovic, J. and Luo, M. R. (1997). "Gamut Mapping Algorithms Based on Psychophysical Experiment". In Proceedings of IS&T and SID's 5th Color Imaging Conference: Color Science, Systems and Applications, pages 44 - 49, Scottsdale, Arizona
24. Neugebauer, H. E. J. (1937). "Die theoretischen Grundlagen des Mehrfarbenbuchdrucks". Zeitschrift f¨ur wissenschaftliche Photographie, Photophysik und Photochemie, 36(4), pp. 73 - 89
25. Reel, R. L. and Penrod, M. A. (1999). "Gamut Visualization Tools and Metrics". In Proceedings of IS&T and SID's 7th Color Imaging Conference: Color Science, Systems and Applications, pages 247 - 251, Scottsdale, Arizona
26. Saito, R. and Kotera, H. (2000). "Extraction of Image Gamut Surface and Calculations of its Volume.". In Color Imaging Conference, pages 330 - 334
27. Saito, R. and Kotera, H. (2004). "Imagedependent three-dimensional gamut mapping using gamut boundary descriptor". Journal of Electronic Imaging, 13(3), pp. 630 - 638
28. Stone, M. C.; Cowan, W. B. and Beatty, J. C. (1988). "Color gamut mapping and the printing of digital color images". ACM Transactions on Graphics, 7(4), pp. 249 - 292
29. Viggiano, J. A. S. and Hoagland, W. J. (1998). "Colorant Selection for Six-Color Lithographic Printing". In Proceedings of IS&T and SID's 6th Color Imaging Conference: Color Science, Systems and Applications, volume 6, pages 112 - 115, Scottsdale, Arizona
30. Zhao, X. (2001). "Implementing an ICC Printer Profile Visualization Software". Master's thesis, School of Printing Manamement and Sciences in the College of Imaging Arts and Sciences of the Rochester Institute of Technology

Predictability of spot color overprints

Robert Chung, Michael Riordan, Sri Prakhya

Rochester Institute of Technology, School of Print Media
69 Lomb Memorial Drive, Rochester, NY 14623, USA
emails: rycppr@rit.edu,

Abstract

Pre-media software packages, e.g., Adobe Illustrator, do amazing things. They give designers endless choices of how line, area, color, and transparency can interact with one another while providing the display that simulates printed results. Most prepress practitioners are thrilled with pre-media software when working with process colors. This research encountered a color management gap in pre-media software's ability to predict spot color overprint accurately between display and print. In order to understand the problem, this paper (1) describes the concepts of color portability and color predictability in the context of color management, (2) describes an experimental set-up whereby display and print are viewed under bright viewing surround, (3) conducts display-to-print comparison of process color patches, (4) conducts display-to-print comparison of spot color solids, and, finally, (5) conducts display-to-print comparison of spot color overprints. In doing so, this research points out why the display-to-print match works for process colors, and fails for spot color overprints. Like Genie out of the bottle, there is no turning back nor quick fix to reconcile the problem with predictability of spot color overprints in pre-media software for some time to come.

Keywords

Color management, overprint, portability, predictability, spot color

1. Introduction

Color portability is a key concept in ICC color management. Color portability between colors captured and colors displayed (or printed) is accomplished in an ICC-based pre-media software in two color conversions. As depicted in Figure 1, the first step is to translate color data captured into the RGB working space via the input device profile. The second step is to translate color data from the RGB working space into the monitor space (or CMYK printer space) via a monitor (or output) profile.

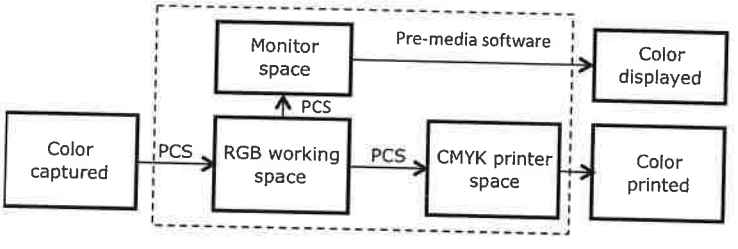


Figure 1: Color portability in color management workflow

There are two profiles used in a color conversion. The source profile provides the input-to-PCS (A-to-B) conversion, and the destination profile provides the PCS-to-output (B-to-A) conversion. A color conversion is also described as the A-to-B-to-A conversion. In a late device-binding workflow, pictorial color image data are converted and saved in the working space, such as Adobe RGB [1998]. Thus, the digital file can be rendered to any number of output devices with the appearance of the monitor display. Color rendering intent of pictorial color images is either *perceptual* or *relative colorimetric*.

In the context of pictorial color image reproduction, color portability means *WYSIWYG* or good color agreement between display and print as the result of correct pre-media settings. Why not an exact match between display and print? The reason is that color device is gamut-limited. In this case, monitor gamut is smaller than the working space, and printer gamut is smaller than monitor gamut.

1.1 Predictability of pictorial color images from display to print

Color predictability emphasizes the use of A-to-B-to-A color conversion to simulate printed color closely with a display. As shown in Figure 2, the source or *simulation profile* is the printer, and not the working space. Thus, color predictability is realized when (a) the display gamut is larger than that of the printer, and (b) the color rendering intent, used in the pre-media settings, is *absolute colorimetric*.

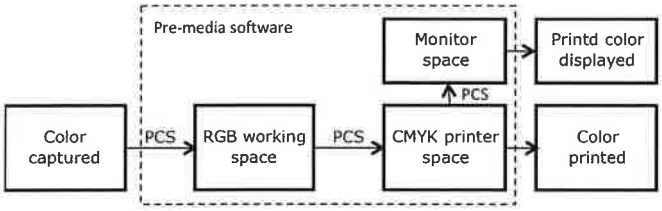


Figure 2: Color predictability in color management workflow

1.2 Spot color portability

Spot colors are colors that designers choose from a color swatch library, e.g., Pantone solid coated library, when creating artwork using pre-media software. There are many custom color libraries and each library contains more than 1,000 spot colors. The fact that in-gamut spot colors can be accurately displayed on the monitor is because there is a spot color-to-PCS conversion available and the pre-media software acts as the API to complete the color conversion for monitor display (Figure 3).

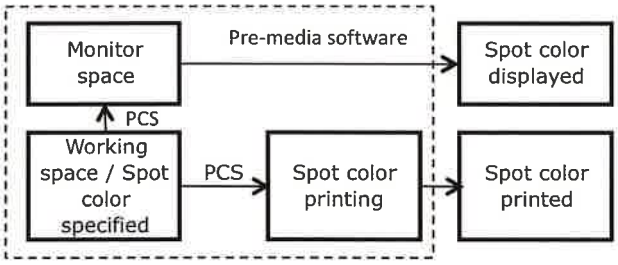


Figure 3. Spot color management workflow

There are two ways to reproduce spot colors in hardcopy. The first method is to print spot color alone as specially formulated ink on a printing press (Figure 3). In this case, these are high chromatic colors, e.g., Coca-Cola red, IBM blue, etc. The second method is to print spot colors as CMYK composites on a CMYK digital printer. There is a RIP-based look-up table that performs spot color -to-CMYK conversion prior to hard copy output. Due to gamut limitation of the digital printer, spot color accuracy is compromised (Pantone, 2008). In this research, hard copies from spot color printing using specially formulated ink serve as the reference.

1.3 Research questions on spot color predictability

When a spot color is specified in pre-media software by default, colors underneath the spot color are removed or knocked out from the digital file as if the ink is opaque. Due to the advent of pre-media software development, the rule of "printing spot color alone as an opaque ink" has been changed. Today, pre-media software, such as Adobe Creative Suite, allows spot colors to overprint on top of other colors with different blending and transparency effects. As a result, spot color overprint features offer many pre-media color choices to designers.

There are two research questions raised in this research. The first research question is, "What is the predictability of spot color solid between display and print?" The second research question is, "What is the predictability of spot color overprint between display and print?" If we can answer both questions with confidence, we will extend the understanding of color management from process color to spot color in the graphic arts industry.

2. Methodology

This research takes the following four experimental steps: (a) building a viewing platform to enable display-to-print comparison; (b) validating the predictability of process color between display and print; (c) testing the predictability of spot color solid between display and print; and (d) testing the predictability of spot color overprint between display and print. To elaborate, the first step is to set up an experimental condition for display and print comparison. The second step is to validate the experimental condition by means of psychometric analysis. The last two steps are to answer the research questions regarding spot color predictability.

2.1 Building a viewing platform to enable display-to-print comparison

It is customary to view a monitor display under dim surround and a hard copy image under bright surround. ISO 12646 (2006) specifies that the ambient illumination of the monitor shall be low, i.e., less than 32 lux. ISO 3664 (2006) specifies that the viewing illumination of the hard copy shall conform to ISO viewing condition P2 or 500 ± 125 lux.

In a pilot study, many observers found it difficult to evaluate display-to-print color match with the display under dim surround and print under bright surround. The inability of human visual system to fully adapt to both viewing conditions is a major cause of the difficulty. The work of Katoh [1995] elaborates on the phenomenon, known as partial adaptation.

To overcome the difficulty of adaptation, this research modified a viewing booth to accommodate the display-to-print comparison in a common bright surround. As shown in Figure 4, a GraphicLite viewing station, manufactured by GTI Graphic Technology, Inc., was modified so that a hard copy (A) is placed next to a 20" Apple Cinema Display (B) surrounded by a gray mask (C). A second monitor, located outside the viewing booth, is used for logistic purposes. The 20" Apple Cinema Display is referred to as the soft proofing monitor in this research.

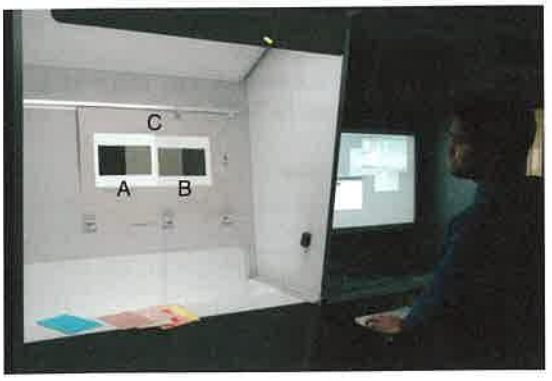


Figure 4:
Display-to-print comparison under bright surround

To configure the viewing condition and pre-media settings between display and print under bright surround, the following steps were carried out in this research:

1. A digital printer was profiled using the IT8.7/4 profiling target and X-Rite ProfileMaker 5. A grayscale print, as shown in Figure 4, was made as a reference.
2. The soft proofing monitor was calibrated and profiled under a number of white point and gamma combinations using the X-Rite Eye-One Pro. In a preliminary test, the grayscale print was compared to a number of displays of the grayscale PDF file using different monitor profiles. The monitor profile with D50 and 2.0 gamma was found to yield the best display-to-print match.
3. Both the monitor profile and the printer profile were placed in the ColorSync folder.
4. In the pre-media color settings dialog box, (a) the soft proofing monitor ICC profile acts as the RGB working space; (b) the digital printer ICC profile acts as the CMYK working space; (c) the color rendering intent was set to *absolute colorimetric*. This color setting was synchronized in all Adobe CS components using Adobe Bridge.
5. The grayscale PDF file was opened in Adobe Acrobat Pro and displayed on the soft proofing monitor. Go to Advanced / Print Production / Output preview and verified that (a) the correct printer ICC profile was chosen under "Simulation Profile," and (b) the "Simulate Paper Color" option was checked.
6. The observer was asked to adjust the intensity of the ambient light in the viewing booth so that the white point and intensity of the hard copy matched that of the monitor.

2.2 Validating the predictability of process color between display and print

The strategy for validating the experimental viewing setup is to test the display-to-print agreement using printed process (CMYK) color as the reference and multiple display conditions, as permitted by the pre-media software, as samples. Colorimetric coordinates of printed process colors, e.g., magenta and yellow, are inside the monitor color space. The display-to-print agreement is determined by paired comparison, a psychometric analysis technique [Rickmers, 1973]. Below is a description of the validation process with an illustration (Figure 5) to show how the experimenter interacts with a print reference and two display samples in the modified viewing booth.



Figure 5:
Paired comparison between a print reference and two display samples

1. Place a print reference (left-hand-side) in the viewing booth.
2. Prepare the digital file in four PDF "Output Preview" conditions, i.e., one with correct and the other three with incorrect "Proofing Simulation" profiles, as shown in Table I.
3. Display two of the four proofing simulations in the proofing monitor (middle and right).
4. A total of 10 observers are asked to select one display that matches closer to the print reference.
5. There are six possible display pairs with four display settings. The paired comparison procedure is repeated for all possible combinations of display pairs in random sequence.
6. The above steps are repeated for a total of four references (or scenarios), i.e., magenta solid, yellow solid, M+Y (50 %) overprint, and M+Y (100%) overprint, as shown in Table I.

Table I: Sample preparation of process color

Process Colors	Display Samples			
Magenta	FOGRA 28 ICC profile	Japan Newspaper ICC profile	Eps_4k SWOPv2_ Siml ICC profile	SWOP v2 ICC profile
Yellow				
M+Y - 50 % tint				
M+Y - 100 % tint				

Among the four display samples, the SWOP simulated Epson SP 4000 profile represents the correct simulation profile. In three out of four 'paired comparison' scenarios, the results showed that the best simulation profile for display-to-print match is the SWOP simulated Epson Stylus Pro 4000 profile.

The only exception is the M+Y (red) overprint where the SWOP v2 simulation profile was judged to provide the best display-to-print match. Upon colorimetric analysis, the colorimetric difference between the SWOP simulated Epson SP 4000 profile and the SWOP v2 profile is small. There are two lessons learned: (a) experimental errors occur when there is no real difference between the correct and the incorrect pre-media settings, and (b) such an error could be avoided by selecting proofing simulation profiles that are sufficiently different to begin with.

2.3 Testing the predictability of spot color solid between display and print

Spot colors are any number of specially formulated inks. Pantone color library provides color swatch books along with a unique number and a recipe. For example, Pantone 1788C is a bright red color and is mixed by "14 parts of Pantone Warm Red and 2 parts of Pantone Rubine Red." In this research, we created a test target

consisting two spot color solids, their 50% tints as well as their overprints of 50% tints and solids. Two pairs of spot colors were selected in the experiment. The first pair, Pantone 1788C (red) and Pantone 7466C (turquoise), and their overprints are shown in the Adobe Illustrator CS3 (Figure 6). The second pair of spot colors was Pantone 493C (pink) and Pantone 577C (green).

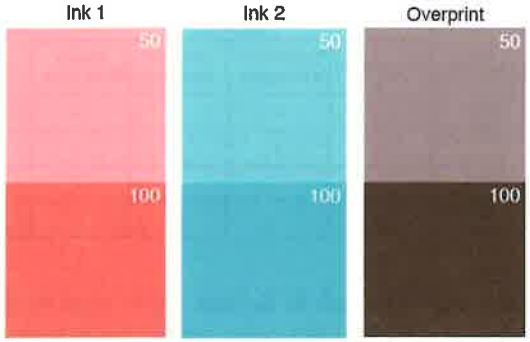


Figure 6: Spot color solids and overprints

These spot colors were printed in two different ink sequences using a Heidelberg Speedmaster 74 sheet-fed offset press and certified Pantone inks. Printed hardcopies then serve as references in the subsequent cross-media color matching experiment. The procedure below only describes how predictability of spot color solid between display and print is tested.

To test the predictability of spot color solid between display and print, four spot colors were created in the Adobe Illustrator (Table II). For each spot color selected, four different "input" (or spot color-to-PCS) conditions are defined, i.e., (a) correct PMS number and correct substrate, (b) incorrect (adjacent) PMS number and correct substrate, (c) incorrect PMS number and incorrect substrate, and (d) measured CIELAB values from the print reference.

Table II: Sample preparation of spot color solids

Spot Color Solids	Display Samples			
High Chroma 1 (7466 C)	Correct PMS Color and Correct Substrate	Hardcopy CIELAB Color	Incorrect PMS Color and Correct Substrate	Incorrect PMS Color and InCorrect Substrate
High Chroma 2 (1788 C)				
Moderate Chroma 3 (577C)				
Moderate Chroma 4 (493 C)				

The paired comparison procedure, as mentioned in Section 2b, is used to find out if a particular monitor display condition provides the best display-to-print color match. To hypothesize, the predictability of spot color solid should hinge on the pre-media settings for the "correct PMS number on correct substrate" yielding the best display-to-print match.

2.4 Testing the predictability of spot color overprints between display and print

To test the predictability of spot color overprint between display and print, the two high-chroma spot colors (Pantone 1788C and Pantone 7466C) were overprinted in two ink sequences; and the two moderate-chroma colors (Pantone 493C and Pantone 577C) were overprinted in two ink sequences.

There are five pre-media settings to display overprint colors, i.e., (a) Overprint Fill, (b) Overprint Fill with Opacity, (c) CIELAB measurement from hard copy reference, (d) Multiply blending mode, and (e) Photoshop Duotone. Only four display samples were chosen from the five "input" or display conditions for each of the overprint references, as shown in Table III. Specifically, Overprint Fill is the 'official' overprint setting given

by the Adobe Creative Suite software for any two overlapping color objects or layers. The rest of the overprint settings are chosen from their "simulation" possibilities, such as the Multiply blending mode, Overprint Fill with Opacity to account for ink trapping, and how duotone colors are defined in Photoshop.

Table III: Pre-media sample preparation of spot color overprints

Tint of Overprint	Type of Spot Color	Illustrator				Photoshop
		Overprint Fill	Overprint Fill with Opacity	LAB from Hardcopy	Multiply blend mode	Duotone
Solid Overprint	High chroma	x	x	x		x
	Moderate chroma	x	x	x	x	
50% Tint Overprint	High chroma	x		x	x	x
	Moderate chroma	x		x	x	x

The paired comparison procedure, as mentioned in Section 2b, is used to find out if a particular monitor display condition provides the best display-to-print color match. To hypothesize, the predictability of spot color overprint should hinge on whether any of the four pre-media settings yields the best display-to-print match. If, however, the pre-media setting from the measured CIELAB values is selected as the best display-to-print match, it is an indication that there is no mechanism in today's pre-media software to predict spot color overprint accurately.

3. Results

This research builds on the understanding of color management in pictorial color image reproduction and extends the understanding to including color management of spot colors and their overprints. A modified viewing condition was constructed to accommodate display and print comparison under bright surround. Display-to-print color match in the modified viewing condition was validated by means of paired comparison with the use of printed process color and the correct pre-media display settings. The same display-to-print viewing condition and paired comparison technique were used to test the predictability of spot colors and their overprints.

3.1 Predictability of individual spot color solids

A total of four spot color solids were tested for predictability. Two spot colors, 1788C (red) and 7466C (turquoise), are high chromatic colors; the other two, 493C (pink) and 577C (green), are moderate chromatic colors. Each spot color was configured with four pre-media settings. By means of paired comparison, two of the four display settings were shown to the judge at a time. The judge was asked to pick the display that matches the reference print. If every judge picks a particular display every time, the sample will receive a maximum of 4 points. On the other hand, if no judge picks a particular display, the sample will receive a minimum of one point. Table IV shows the average scores from paired comparison testing.

Table IV: Pre-media settings of individual spot color solids and paired comparison scores

Color Definition	Sample	Average Scores for Spot Color Solids			
		493 C	577 C	1788 C	7466 C
Correct PMS Color and Correct Substrate	A	2.8	1.1	3.6	2.0
CIELAB measure from hardcopy reference	B	1.2	3.1	2.9	1.1
Incorrect PMS Color and Correct Substrate	C	2.3	2.9	1.0	3.4
Correct PMS Color and Incorrect Substrate	D	3.7	2.9	2.6	3.4

The paired comparison scores indicate that there was no particular pre-media setting that would yield the best display-to-print match. The correctly named spot color that provides the best display-to-print match only occurred once, i.e., Pantone 1788C. Reasons that contribute to different display-to-print match outcome include (a) the similarity between the printed spot color reference and the colorimetric definition of the digital color swatch, (b) the similarity between the correct (coated) substrate and incorrect (matt) substrate, and (c) the similarity between the colorimetric definition of the correct color and the measured CIELAB values from the spot color print.

3.2 Predictability of spot color overprints

Four spot color overprints were also tested for color predictability, i.e., overprint solid and overprint tint at 50% tint of the Pantone 1788C-7466C pair and the Pantone 493C-577C pair. Table V summarizes the overprint settings and paired comparison results for the Pantone 1788C-7466C color pair only.

Table V: Pre-media overprint solid settings and paired comparison scores for Pantone 1788C-7466C

Overprint Definition	T+R (100%)	
	Sample	Average Score
Oveprint Fill	A	1.7
Photoshop Duotone	B	1.9
CIELAB measure from hardcopy reference	C	3.7
Oveprint Fill with Opacity	D	2.7

The paired comparison scores in Table V indicate that none of the pre-media settings yields the best display-to-print match of overprint solids. The display sample using the measured CIELAB values provides the best display-to-print color match. Paired comparison scores from the other three spot color overprints indicate the same outcome as the Pantone 1788C-7466C scenario. This is indicative that there is a gap in pre-media software's ability to predict solid color overprint accurately.

When conducting the spot color press run, CIELAB values of the resulting spot color overprint solid vary as a function of ink sequence used. As shown in Figure 7, C1 and C2 represent the Pantone 1788C (red) and Pantone 7466C (turquoise) respectively. The spot color overprint solid, C3, is printed with the Pantone 1788C (red) on top of the Pantone 7466C (turquoise). And the spot color overprint solid, C4, is printed the other way around. There are three important findings: (a) the color difference between C3 and C4 is quite large (23 ΔE_{ab}) and visible; (b) the hue of the overprint, C3, with the Pantone 1788C (red) ink overprint on top of the Pantone 7466C (turquoise) ink, looks bluer; and (c) the hue of the overprint, C4, with the Pantone 7466C (turquoise) ink printing on top of the Pantone 1788C (red) ink, looks redder. The last two findings are rather counter-intuitive, i.e., the last-down ink has less influence on the hue of its overprint. Ink trapping is suspected to be the cause.

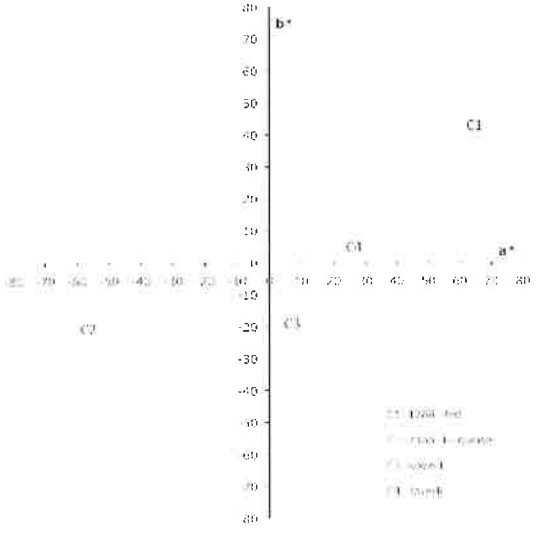


Figure 7: Colorimetric plots of Pantone 1788C, Pantone 7466C, and their overprints

The color difference of spot color overprints due to ink sequences decreases when either moderate-chroma spot color solids are printed (3 ΔE_{ab}) or when tints of high-chroma spot colors are printed (3.8 ΔE_{ab}). Nevertheless, ink and press related factors, such the effect of ink sequence on spot color overprint, have not been taken into consideration in current pre-media software. This has limited the ability of pre-media software to predict spot color overprint accurately.

4. Conclusions

This research places the predictability aspect of the color management under scrutiny. The display-to-print match succeeded for process color applications. The combination of the monitor profile, the CMYK printer profile, a well-defined viewing condition, and the correct pre-media color settings make display-to-print comparison under a common bright surround valid.

The display-to-print match failed completely for spot color overprint applications. Spot color overprints, defined by CIELAB measurement of the hardcopy reference, is chosen as the best match in all four scenarios. None of the pre-media settings renders spot color overprints accurately.

Overprint is defined as a Boolean flag in the third edition of the PostScript Language Manual [Adobe, 1999]. Page 248 of the Manual states, "If the overprint flag is false (default), painting a color in any color space causes the corresponding areas of unspecified colorants to be erased. If the overprint flag is true and the output device supports overprinting, anything previously painted in other colorants is left undisturbed. The effect produced by such overprinting is not defined by the PostScript language." Adobe Acrobat Reader may be used, via Advanced / Print Production / Overprint Preview, to display the effect of the 'Overprint Fill' of spot colors, but the resulting display is incorrect because there is no device-to-PCS (A-to-B) color conversion for spot color overprints.

Soft proofing performance ought to be judged visually. Paired comparison analysis techniques are effective in finding the best visual agreement between print and the display representing correct pre-media settings. The choice of spot color and pre-media settings can influence the outcome of paired comparison. For examples, a spot color is outside of the display gamut; colorimetric values of multiple pre-media color settings are too close to one another.

To improve the predictability of spot colors and their overprints in a pre-media environment, device-to-PCS color conversion must exist to include ink- and print-related parameters, e.g., paper color, ink color, ink transparency, ink tack, ink-down sequence, and ink trapping. Since there are more than 1,000 spot colors in the spot color library, it will be difficult, if not impossible, to obtain colorimetric values of all combinations of two-color overprints.

While there is a void in the prediction of spot color overprints in current pre-media software package, we encountered a few commercial software packages, e.g., X-Rite ProfileMaker 5 MultiColor Package, AVA CAD/CAM, Artworks Display Ink, that provide solutions for a limited number of spot colors. In general, predictability of spot color overprints with accuracy is likely to remain as a void in shrink-wrapped premedia software for some time to come.

Acknowledgments

The authors wish to thank Mr. Franz Sigg, RIT School of Print Media, for his effort in modifying the gti viewing booth for display-to-print comparison under bright surround, and the RIT Printing Applications Laboratory for implementing the spot color press run.

References

1. Adobe Systems Incorporated (1999) PostScript Language Reference Manual (3rd Edition). Reading, MA: Addison-Wesley, ISBN 0-201-37922-8
2. ISO/DIS 12646 (2006) Graphic technology - Displays for colour proofing - Characteristics and viewing conditions
3. ISO/WD 3664 (2006) Viewing conditions - Graphic technology and photography
4. Katoh, Naoya (1995), "Appearance Match between Soft Copy and Hard Copy under Mixed Chromatic Adaptation," 3rd IS&T/SID Color Imaging Conference, Scottsdale, Arizona, p. 22-25, ISBN 0-89208-188 - 0
5. Pantone (n.d.) Pantone Spot Color vs. Process Color. http://www.colorguides.net/pantone_spot_color.html (retrieved on June 18, 2008)
6. Rickmers, A. (1973) Paired Comparison, Course Notes on Statistics, Rochester Institute of Technology, Rochester, NY

Quality control and colour assessment for flexography and gravure printing based on machine vision

Andrés Navarro-López, José F. Caballero-Aroca, José J. Esteve-Taboada, Juan Hervás-Juan, Emilio Ribes-Gómez

AIDO - Technological Institute for Optics, Colour and Imaging, Machine Vision Department
Parque Tecnológico, C/Nicolás Copérnico, 7, 46980 Paterna (Valencia), Spain
E-mail: anavarro@aido.es

Abstract

Nowadays in-line machine vision systems for quality control are becoming popular, allowing automation of human tasks, lowering costs and improving quality control in many industrial processes. There are many applications for machine vision systems in the printing industry. Flexography and gravure are maybe the most critical tasks due to the speed and inspection width (up to 2 meters) considered in the printing jobs. Existing commercial systems for web-press printing are based on matrix sensor cameras with a strobe moving through an axis in a direction normal to the printing line, forming a mosaic of samples and acting as a simple visual aid to the operator. Thanks to the progress on current imaging hardware quality control, the authors propose an innovative, dual BN-RGB inspection system which implements high-speed, high-resolution linear cameras and adaptive calibration algorithms, allowing 100% inspection of the paper sheet.

Keywords

Colour assessment, machine vision, printing quality control, 100 % inspection

1. Introduction

The main objective of this research is to build a modular machine vision system for flexography and gravure printing, introducing improvements to the already existing ones by using colour linear cameras combined with greyscale linear cameras so that several current challenging problems can be solved. This project started as a request from a company which develops and commercialises systems for the printing industry, focusing on 100% inspection and colour assessment in flexography and gravure printing.

The challenges posed are:

- 100% Flaw detection in web-press printing, (spots, lack/poor impression, scratches/holes on the printed material). Commercial systems performing flaw detection and colour assessment are limited by the technology used for capturing colour: capture frequency and resolution get reduced drastically yielding poorer flaw detection by means of getting a combined colour and flaw detection solution.
- Colour assessment.
- Automatic pressure control.
- Automatic cylinder alignment control.

For this purpose a novel machine vision system has been developed, consisting of:

- A combined imaging solution based on a tri-linear high speed colour camera (3 chip and prism) and high-speed/high-resolution monochrome camera.
- A high-speed-computing computer.
- A diffuse and uniform lighting based on fluorescent tubes and reflectors.
- Communication input/output cards in order to send information to the printing machine and correct possible sources of error.
- A rotary encoder.
- A frame grabber for image acquisition.
- Special software for machine vision algorithmics.

Several aspects must be taken into account when using these optical and electronic devices:

- Electric noise due to the CCD (charge-coupled device) technology used by the camera: electromagnetic noise, white noise, thermal noise.

- Optic aberration from the camera optics
- Incorrect lighting (either too low or too strong) will introduce errors when performing colour assessment. Besides, several materials are used for printing, which reflect light in different ways and producing saturated areas on the image. On the other hand, a change in lighting conditions may introduce important variations in the colour temperature.
- Fluorescent tubes are not a stable light source (they "blink" at a rate of 100 Hz). This fact introduces both chromatic and intensity variations, requiring the use of digital ballast for stabilising the lighting source (otherwise such "blink" affects the grabbed images by the cameras, since they operate at higher rates).
- The amount of data to be processed is large due to the printing speed (up to 500 meters per minute) and sheet width (up to 2 meters).
- In colour assessment there are many factors that may introduce errors: Lighting aging, temperature, ambient lighting conditions.

Moreover, the printing method also introduces problems because of the material stretching introducing deformations on the acquired image.

2. Methods

A machine vision system is constructed by simulating the output of a flexography/gravure printing machine in a conveyor belt.

The cameras are situated in an axis perpendicular to the printing direction and the fluorescent tubes illuminate the caption using reflectors for increasing light intensity.

The way a camera grabs an image is by capturing line by line of the printed material, which is moving below the camera until a complete sample is taken. The speed these lines are taken with is given by the rotary encoder which gives a number of pulses according to the speed of the conveyor belt. In this way variations in the transport will not introduce large errors, because the capture is synchronized with the movement.

Two acquired images (greyscale and colour) are sent to the computer via Camera Link (this bus allows high speed and broad band); one image will be used for flaw detection and the other one for colour assessment. Once the images are received at the computer they are pre-processed in order to correct stretches due to variations on the printing speed, then several areas of the images are processed in order to find out possible printing errors, colour deviation or malfunction with either the printing cylinders alignment or pressure control.

If any problem is encountered, the computer sends several signals through the input/output card to the printing machine for correction, and shows the errors on the graphic interface, while processing the next sample.

The way to detect errors on the printed work is selecting one of the samples being printed as a "master sample" and setting parameter tolerances, then every subsequent captured image is compared with this master in order to find differences and hence errors.

A prototype with the following core parts has been developed for printing inspection:

a) Colour assessment for CMYK colour patches and whole printed area colour image comparison.
b) Greyscale flaw detection (printing errors: spots, lack/poor impression, scratches/holes...).
c) Pressure control.
d) Register control.

The system gets two different data flows: color and monochrome (grayscale) information, in this way color deviations on the image are processed in parallel with printing errors, pressure and register control processing as seen on figure 1.

a) Colour assessment for CMYK colour patches and whole printed area colour image comparison

A 4096 pixel 3-chip (with prism) colour line scan camera working at a 40 MHz rate is used. Colour assessment is made by inspecting printed colour patches on the margins of the printed samples. Variations on these patches will produce deviations in the whole print, as these patches represent the ink standards being

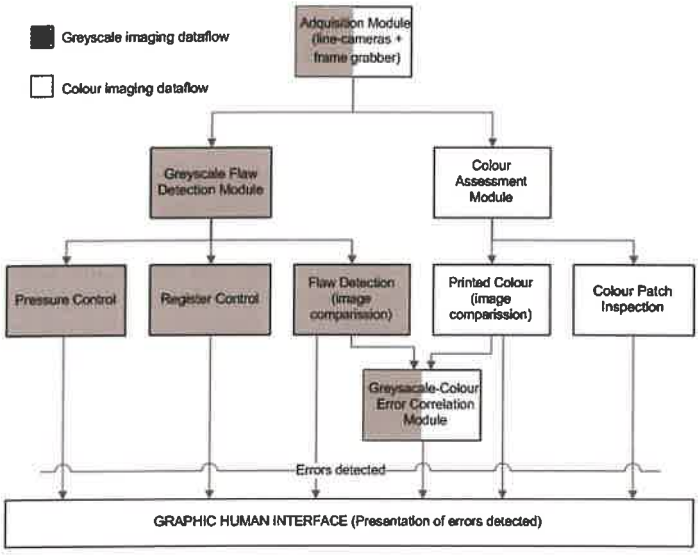


Figure 1:
Quality control and colour assessment system architecture for a prototype based on machine vision

used. In order to locate such patches on the acquired image, a region of interest is taken (knowing they are printed on the margins) and within this region, a pattern with a pre-defined shape is searched, in our case the prototype looks for four square-shaped patches (CMYK) on the margins. Since lighting variations would produce colour deviations in the acquired image we have to make sure that the lighting is uniform and remains stable over time, as powerful lighting is required due to the high capturing frequency employed. High-power fluorescent tubes have been chosen for this purpose, setting reflectors pointing to the scene of interest and stabilizing the tubes with electronic ballast in order to keep lighting properties as much stable as possible. Since our image acquisition hardware is RGB (line-scan 3-chip colour camera) we have to convert every pixel to CIE Lab standard colour space coordinates. This allows us to separate luminance as well as chromatic information, 2^{nd} and D65 illuminant have been chosen for the correlation matrix according to the position between our lighting and cameras.

After calibrating the camera (this depends on manufacturer specifications) using the lighting tubes and covering the whole system to avoid errors due to external illumination, the colour image is obtained from the 3 chip camera, the camera yields a flow of pixels in RGB (one colour per chip). Then the values of every pixel are transformed into XYZ and later into CIE Lab (EasyRGB at the Web) using transformation formulae. The CIE Lab values are processed in two different ways: The colour patches location is isolated from the rest of the image and every patch is processed pixel by pixel in order to obtain the CIE Lab average. The average of every one of the patches will be the value to be compared, between the master (giving the pattern to be followed) and the currently printed sheets. Such comparison yields a DeltaE value which is compared to the tolerance set by the user to check whether the printed work has invalid colour deviations. In parallel, the whole image CIE Lab colour pixel values are compared to the master samples in order to obtain colour deviations. The colour deviations outputs are shown in a graphic interface by means of DeltaE values.

b) Flaw detection (spots, lack/poor printing, scratches/holes)

A 4096 pixels monochrome line scan camera is used for this module (model spL4096-140k with an 80 MHz pixel clock). This module processes the dataflow obtained from the greyscale camera comparing the printed samples with the one set as master sample in the same way as mentioned before with colour.

Usually the maximum printing area for web-press is around 2 meters width and 1 meter long. This means that for the system resolution the images are 4096 x 8340 pixels (0.12 mm/px). Since the printing speed is not completely regular the material may stretch, producing differences with the master sample and giving false printing errors even though this effect is reduced by the rotary encoder. The samples printed under different speed can have a length variation, and because of this, some pre-processing is applied onto the image, by means of an algorithm for stretching effect correction, all this done prior to start searching for printing errors. For such purpose, several small areas of the image are taken as a reference and the distance between these areas is saved in order to compare these values between the sample and the master sample. The amount of areas to be saved as a reference is a parameter that is set in advance. These areas must be spread all around the

image in a uniform way in order to detect irregular stretching. In order simplify this algorithm part, the reference areas are chosen by the user directly through the GUI. He or she must select areas that are not uniform and not repetitive on the image since this could lead to errors making the system "believe" that there is a different stretch than the real one.

When this module receives the image sample (already pre-processed for stretching correction), the image is compared and matched with the standard in search for printing errors (occurrences printed in one of the images which are not printed in the other one). The operation used is pixel-by-pixel subtraction, where, for the perfect case, the result should be 0 for every pixel; in case that the obtained value is different than 0 this means that there is a difference between the master sample and the printed sample. With the greyscale module this subtraction gives information about printing errors with high contrast. With the colour module this subtraction gives colour deviations in CIE Lab. Even though the theoretical minimum size for error detection is 0.014 mm^2 according to the cameras resolution (8 pixel/mm) such a small defect cannot be detected, because of the pre-processing needed by this approach and the intrinsic modulation transfer functions of the optical components used, which limits the spatial resolution achieved for the given working distance - see results in section 3.

c) Pressure control

For pressure control a common pressure control patch has been selected as input, having one circular patch for every colour (CMYK). The patch tells the amount of pressure being made when printing by deficient or excessive presence of ink in the centre of it. For this module the way for searching within the image is similar to the one for colour patch inspection: search of known model (a circle in this case) within a pre-defined area (margin of the printed sample). This area is isolated and once the patch has been found, concentric circles are virtually drawn decreasing their radii. Then several saw-shaped graphs are obtained where transitions can be counted, knowing in advance how many transitions must have a correct pressure control patch. A variation of this value computes an error, therefore it can be known if there is less pressure than needed or the opposite (absence / small number of transitions).

d) Register control

We have supposed an experimental register control based on a line of dots and a matrix. The algorithm consists of drawing straight lines joining together the points and checking if the lines are parallel.

3. Results

These are the results obtained for each of the developed modules.

3.1 Colour assessment

In order to check the reliability of the system the results obtained have been compared with a spectrodensitometer, the model is an x-rite 530 with a measuring geometry of 45°/0°, D65 illuminant and CIE defined observer of 2° (according to our system). For the experiment 6 printed samples of the same digital file have been chosen, the samples are from a commercial printing machine in order to achieve results as close as possible to a real environment test. The samples have colour deviations between them, one of them is taken as the master sample. Then DeltaE is calculated for every pair of patches from their CIE Lab colour values using the spectrodensitometer (the ones on the master sample compared to the ones on the rest of the samples). Later on the samples are introduced in the system simulating a gravure printing machine output in order to compare the DeltaE values calculated from the system and the ones calculated with the spectrodensitometer - see figure 2 and table I.

This module does not intend to measure colour but only detecting colour deviations between patches of the same colour in different samples as well as colour deviation all over the sample not just particular areas like many other commercial systems (see section 4).

It has been detected differences of 3 DeltaE on average after doing 5 repetitions for every sample (4 colour patches on every repetition), so we can say that the approximation is good enough for detecting the exact instant when the colour differences are higher to a certain tolerance. Far from measuring colour these differences are not absolute but relative.

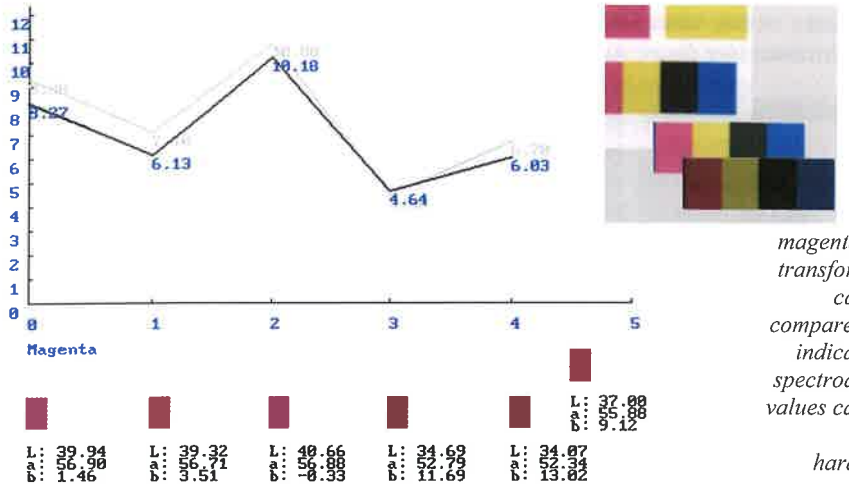


Figure 2: Output of the system comparing 5 printed samples with another one taken as "master", the software recognizes the location of the magenta colour patches on the image, then transforms the RGB values to CIE Lab and calculates the DeltaE for every patch compared to the "master", the brighter line indicates the values obtained by an x-rite spectrodensitometer and the darker one the values calculated by the system for the same samples captured through imaging hardware and processed with machine vision algorithms

Table I: CIELab values obtained for magenta colour patches on 5 different printed samples using a x-rite spectrodensiometer, the deltaE is calculated compairing them to another sample taken as master, the right-most column shows the results obtained with the system using machine vision

Sample no.	L	A	B	dE (Spectrodensitometer)	dE (Machine Vision System)
0	53,53	64,54	-9,94	**9,3**	**9,27**
1	52,5	66,1	-8,69	**7,1**	**6,13**
2	54,27	63,81	-11,03	**10,8**	**10,18**
3	47,7	69,87	0,17	**4,5**	**4,64**
4	46,63	71,24	2,05	**6,7**	**6,03**
Master sample	**L**	**A**	**B**		
	49,1	70,33	-4,1		

3.2 Flaw detection

The size of the printing errors detected has been around 1.2 mm, the systems detects small colour variations which would not be detected by the monochrome camera as well as high contrasted printing errors thanks to having two cameras, monochrome and colour, working in parallel.

The colour sub-system detected small variations on coloured areas of around 1.2 mm (taken with the 3-chip colour camera). Since variations in the printing speed as well as material stretching introduce errors, the image needs to be pre-processed before searching for differences. The bigger the image is the worse the error search algorithm behaves due to the corrections needed for deformation correction. On the other hand the greyscale line-scan sub-system allows error detection with more contrast and more resolution since the capture rate for the monochrome camera is twice the colour camera.

For system commercialisation, further research needs to be done with monochrome camera spL8192-70k having a pixel resolution of 8192 instead of 4096 pixels, in order to decrease number of cameras needed to achieving 100% width inspection.

3.3 Register control

The algorithm for register control performes well, as long as the marks are correctly printed. The presence of scratches in the register marks prevents the measeurement of register deviations.

3.4 Pressure control

The results have been satisfactory and when the patch has been found the pressure measuring was successful. The algorithm does not work if printing problems may cause critical deformations of the patch circular shape

or large scratches on this area may occur, since this may prevent the successful circular centre finding, required for good algorithm performance (see figure 4).

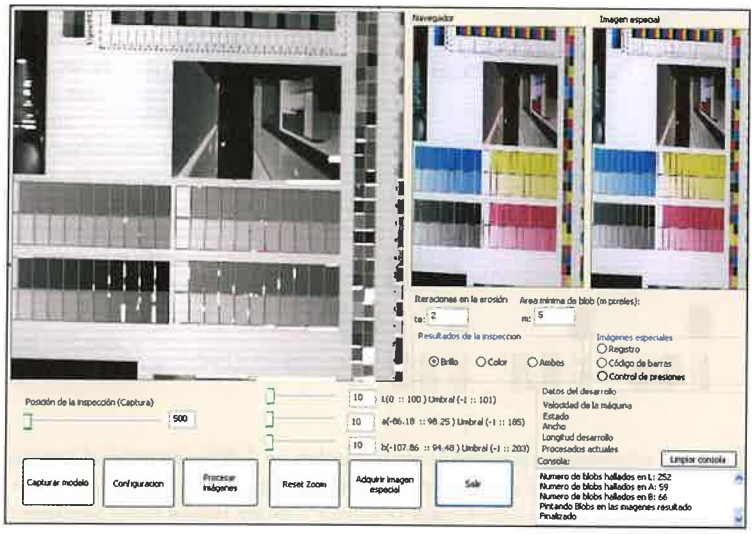


Figure 3: Snapshot of the system interface showing printing errors, for this case the reference areas for stretching correction were not selected in order to study the impact on the printing error detection (white gaps are false printing errors detected by the system)

The algorithm works fine for the experimental test but presents some limitation: the accuracy for cylinder alignment can not be bigger than the camera resolution (1 pixel). Since our pixels are 0.12 mm width, this is the theoretical limit for cylinder alignment.

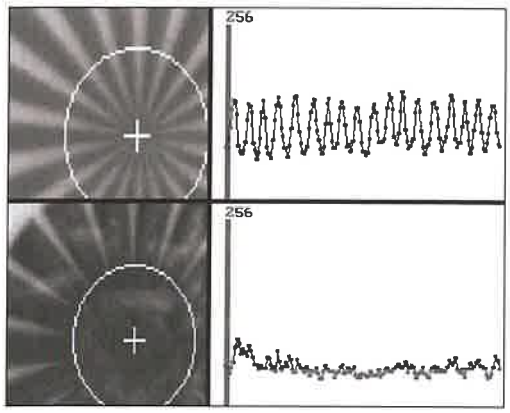


Figure 4:
Snapshot of the system showing a patch with the right pressure (above) and another one with too much pressure, the system detects this errors by counting the transitions on the pixel values all along the drawn circle perimeter

4. Discussion

After studying other systems it is observed that the colour assessment results are satisfactory. The system allows comparing colour for the whole captured area (500 mm) within the printed sample, although due to the processing time required for every single sample it is not possible to inspect all of them. Nevertheless, inspection of 100% (up to 2 m) may be possible by expanding the system with several line-scan cameras (500 mm per camera).

The task of selecting the reference areas for stretching correction is quite important in order to obtain good results (see figure 3). This implies that the amount of areas to be saved and the non-uniformity/not repetition of them should be carefully selected. The area selection could be automated, by implementing a variance detection algorithm [William K. Prat, 2001]. After finding a grid formed by sufficient reference areas covering the whole image, the algorithm would have to check that the areas, now acting as small images by themselves, are different enough between them. For such task, a pattern matching recognition algorithm could be used [Rafael Gonzalez/Paul Wintz, 1987].

It has been observed that many of the problems when detecting printing errors come from deformations (irregular stretching) on the printed surface (i.e. deformation on the material from the roll) to which the algorithm is still sensitive when it comes to detect small printing errors over the entire image. Nevertheless, the system performance is acceptable since the size of the "acceptable" error can be set as a parameter. Once the system is properly calibrated for a determined speed and the right lighting, which must be uniform over time, the printed materials must not suffer too much deformation or, in case they do, this should be constant to a certain extent in case small printing error detection is desired.

A further research could be made in order to check compatibility of the system for other types of printing procedures like sheet-fed printing.

4.1 Situation of the solution in the market

Information about several commercial systems has been gathered in order to compare the results obtained with the market state of the art.

4.2 Colour

Current commercial solutions offer either machine vision colour inspection, comparing areas of the image, or spectrodensitometer based solutions for machine feedback tuning. The ones based on spectrodensitometer are dedicated systems. In addition, this kind of instrumentation is far more expensive than stand-alone cameras, in contrast, systems based on machine vision usually only work with colour comparison in defined areas. The exception comes with the solution given by Isravision offering a line-scan based solution including colour assessment. BST Promark claims to be the only one having a system (based on matrix scan cameras) with an "almost perfect" correlation between the system output and a spectrodensitometer confirmed by an independent studio. As it has been shown in the results, the solution here presented offers superior correlation with a spectrodensitometer, and, since the system is based on line-scan cameras, this means that the area to be inspected can be drastically increased (400 mm x 330 for the BST Promark system and 500 mm x 1000 mm for ours).

Moreover, since our solution is a combined grayscale-colour approach, the system performs a correlation between the printing errors detected in Grayscale with much higher resolutions and colour deviations on the whole image. The limitation when using only a colour camera is that the maximum resolution for this hardware in the market is smaller than resolution for monochrome line-scan cameras

Table II: Comparative of commercial systems and the prototype exposed

Company	Commercial name	Camera	Inspection area	Printing error detection	Colour assessment	100% single sample inspection	100% production inspection	Scalability
BST Promark	PROScan3000	3 ccd x 440.000 pixels matrix	235 x 178 mm	no	yes			yes (up to 2)
BST Promark	PremiusDigital 3 chip	3 chips (1360 x 1024) matrix	440 x 330 mm	yes	yes	no	no	yes (up to 2)
BST Promark	Shark	monochrome line scan with posibility of upgrading to colour line scan	500 mm width	yes	yes	yes	yes	no
Isravision	x	only colour line scan	1000 mm width	yes	yes	yes	yes	yes
Elmo	Harmonica	colour matrix		yes	yes	no	no	no
AIDO	Prototype	line scan monochrome 4096 px line scan colour 4096 px	500 mm width	yes	yes	yes	no	yes

4.3 Printing errors

Matrix scan cameras are usually used for printing error detection. The scanning camera moves along the printed area to construct a mosaic for 100% printed image inspection. This method, however, does not allow total inspection of every printed image sample. The exception here is the Shark system from BST Promark which uses a line-scan solution for real-time 100% inspection of production (i.e. all samples are 100% inspected) with the possibility of upgrading the system for doing colour assessment of pre-defined areas. This system is far more complex than the one proposed in this paper. Our system could cover the needs of a market sector requiring a more fitted solution than the available matrix scan based ones. Besides the correlation between the errors obtained with the monochrome and colour camera is superior to that offered by any of the systems found during our research. Our system could arrive to inspect 100% of a sample but not 100% of production due to the required processing time for the algorithms developed. This makes that random errors between samples can't be guaranteed to be detected, but as said before, this may not be a critical issue, since in many applications repetitive errors may be more important than random ones.

The table II is a list of commercial solutions for printing quality control. The selected systems are those considered by the authors as more representative and /or competitive.

The presented systems currently covers 500 mm of image and usually flexography and gravure reach up to 2 meters. In order to achieve extended inspection area the system can be expanded by means of increasing the number of line-scan cameras.

5. Conclusion

Colour detection by means of the system proposed in this paper is superior to many market competitors', and satisfactory for the purpose of fast, direct and robust error detection and colour assessment in flexography and gravure printing. The results show the achievement of a DeltaE of 3 on average respect to densitometry measurements, making such system a very suitable solution to printing quality control, combining colour assessment and printing error detection using, optimizing hardware usage. For an absolute colour assessment there are commercial solutions based on densitometer instead of machine vision. Such solutions are, however, costly, and less adequate in applications where inspection by comparison is required to be fast and versatile. The system presented here can be used as a practical, versatile solution to printing quality control by comparison.

Acknowledgements

The authors would like to thank the Graphic Arts Department of Aido for their support and advice given during this research project.

References

1. Wintz, R. G. P., (2001). *Digital Image Processing. Addison-Weley Publishing Company. 5, 12, 331*
2. Prat, W. K., (2001). *Digital Image Processing. John Wiley & Sons, Inc. 17, 138, 139, 220, 224*
3. Hunt, R. W. G., (1991). *Measuring colour. Ellis Horwood limited*
4. Hunt, R. W. G., (1987). *The reproduction of color in photography, printing & television. Fountain Press*
5. Pitas, I., (2000). *Digital Image Processing and applications. John Wiley & Sons*

More information on the Internet:
www.bstpromark.com
www.easyrgb.com
www.gmicolor.com
www.isravision.com
www.inelme.com

Developing a test-procedure for newsprint color quality evaluation

Fons Put

Flemish Innovationcenter for Graphic Communication
Campus Blairon 5, 2300 Turnhout, Belgium
Email: fons.put@vigc.be

Abstract

The adoption of the ISO 12647 printing standard is increasing significantly. Especially in commercial offset the ISO 12647-2 printing standard is the subject of standardization and certification projects. Also for newsprint the trend for standardized printing is clear. To assure consistent exchangeable color quality the gathered Belgian newspaper publishers promote the use of the ICC-profile "ISOnewspaper26v4.icc" as the color space for ad delivery. This color profile is based on the ISO 12647-3 printing standard. Customers are also becoming aware of the existence and advantages of standardized printing. We noticed several "open counter public bidding"-projects in which printing according to standards was included for objective color quality assesments.

Keywords

ISO 12647-3, newspaper printing, standardization

1. Introduction

During the last year VIGC has evaluated more than 30 printing companies according to the ISO 12647-2 printing standards. In this particular case a customer was looking for a printing company that offers standardized newsprint. Standardized newspaper printing is described in the international standard ISO 12647-3, Coldset lithography on newsprint. Equipped with our experience with ISO 12647-2 certification we have conducted a research in which we investigated 4 newspaper publishers on the capabilities to print according the ISO 12647-3 print standard. The motive for the project is a print customer who was willing to supply a printing order to the company that meets with the demanded requirements. Only if the printer meets with all demanded requirements, he becomes a candidate to achieve the printjob.

The objectives of the research presented in this paper are:

- *Inventory of the necessary criteria to match standardized newsprint;*
- *Development of a printing test form;*
- *Investigation of the quality of color measuring equipment;*
- *Collection of the printed samples;*
- *Measuring, evaluating and reporting.*

2. ISO 12647-3 quality criteria

Analog to the ISO 12647-3 standard, the printed copies are divided in 2 parts: OK-prints and Production prints. The OK-prints are copies that are gathered after full adjustment of the printing press (registration, inking, dampening, etc). These copies serve as approval for the customer's demands. The production prints are the copies printed after the stage of full adjustment. They show the degree of color stability and variation that the printer can reach during a complete print run.

This leads us to following required printing parameters. Printers must be able to accomplish following tasks to assure visually acceptable results.

- *Print correct ink colors;*
- *Control the variation of the ink colors during production;*
- *Print within the minimum tone value reproduction limits;*
- *Print with correct dot gain;*

- *Control the variation of the dot gain during production;*
- *Print with correct registration.*

Notice that demands on the print substrate color are not implemented, although this is marked as a required parameter in the standard. Certification projects in commercial offset showed that almost none of the commonly used coated wood-free papers fulfill this requirement. The use of optical brighteners have caused significantly higher b* values according to the standard values. Nevertheless the use of appropriate inks makes it possible to print with the correct ink colors on these substrates.

Secondly registration is added, although this is not mentioned in the standard. We believe good registration is essential to obtain visually acceptable results.

These criteria were communicated in advance with the different printing plants to enable them to prepare and adjust their production processes towards the specifications.

3. Test form

A test form of 20 pages with different test-targets and images was prepared. The most important element of the pages is the certification target. This target enables to measure and evaluate most of the necessary print parameters according to the requirements. It is repeated 12 times to obtain reliable averaged measuring results. At least 5 copies are measured for the OK-prints what implies that the final results are based on 60 measurements.



Figure 1: The Certification target serves as a basis for evaluation

More elements were added to supply additional information:

- *Adjusted ECI2002 test chart (maximum ink coverage 260%);*
- *Tone value reproduction limits;*
- *Detailed dot gain;*
- *Gray-balance;*
- *Customer Spot colors;*
- *Critical skin tone picture;*
- *Picture with different sharpness/contrast settings;*
- *LUCHS registration targets.*

Imposition is organized in such a way that all targets have a unprinted verso-side what assures neutral measurements. The testpages were delivered as certified PDF-X1 files to the different printing plants.

4. Sample collection

The samples were collected on the following manner:

- *First all the different print settings had to be adjusted as best as possible. Then 50 nicely printed copies were gathered. (OK-print)*
- *Then the rest of the copies were printed and every 100 copies one copy was selected as a representative for the production printing (Production-print).*
- *At last 100 sequential copies were gathered to evaluate the press registration.*

5. Color measuring equipment

It is essential to guarantee that the measured values are of confident and exchangeable. In a related project the measurement repeatability and accuracy of 20 handheld spectrophotometers of different vendor and type were compared.

Measurement repeatability

A white and blue patch was measured 12 times (5 seconds interval) without displacement.

Measurement accuracy

This was done by measuring 13 color patches of a valid reference color chart (NetProfiler). The mean deviation ΔE*ab against the reference colors was calculated. Secondly the CMYK process colors are reported separately because this will be the focus of the evaluation.

Table I: Comparison of 20 handheld spectrophotometers

		colour difference ΔE*ab			
basis: 20 handheld instruments		Average	StDev	Best	Worst
repeatability	White patch	**0.08**	**0.04**	**0.00**	**0.44**
	Blue patch	**0.06**	**0.01**	**0.01**	**0.25**
Accuracy	13 color testchart	**0.94**	**0.74**	**0.37**	**2.74**
	cyaan	**1.21**	**0.99**	**0.30**	**3.22**
	magenta	**1.23**	**0.77**	**0.40**	**2.88**
	yellow	**1.39**	**0.97**	**0.19**	**3.72**
	black	**0.61**	**0.51**	**0.18**	**1.98**

Notice that there can be rather large deviations between the different instruments. To exclude discussions regarding measurement equipment the gretagmacbeth Netprofiler test chart, together with the software package, was used to certify the used spectrophotometers (SpectroEye, i1).

Table II: Repeatability and accuracy of a calibrated handheld spectrophotometer

basis: Calibrated SpectroEye		(ΔE*ab)
repeatability	White patch	**0.02**
	Blue patch	**0.02**
Accuracy	13 color testchart	**0.27**
	cyaan	**0.17**
	magenta	**0.15**
	yellow	**0.38**
	black	**0.10**

Repeatability and accuracy have improved significantly. The calculated repeatability falls within the expected tolerances of 0.02 (repeatability white), 0.03 (repeatability blue), 1.0 (accuracy).

6. Measuring, evaluating and reporting

6.1 Print substrate color

Table III: Print substrate color evaluation of the 4 competitors

Print substrate colour	Measurement according to ISO 12617-1: D50, 2 degree, geometry 1:50, no polarisation filter, black backing.										
	Reference			OK-print			Devintion OK-print / Reference				
	L	a*	b*	L	a*	b*	ΔE*ab			tolerance	status
Competitor 1	82	0	3	86.0	-0.6	1.1	**4.5**	ΔL	4.00	3	FAIL
								Δa*	-0.56	2	PASS
								Δb*	-1.89	2	PASS
Competitor 2				87.4	-0.2	1.1	**5.7**	ΔL	5.40	3	FAIL
								Δa*	-0.21	2	PASS
								Δb*	-1.94	2	PASS
Competitor 3				84.8	-0.3	0.7	**3.7**	ΔL	2.84	3	PASS
								Δa*	-0.34	2	PASS
								Δb*	-2.30	2	FAIL
Competitor 4				85.6	0.4	-2.8	**6.9**	ΔL	3.60	3	FAIL
								Δa*	0.35	2	PASS
								Δb*	-5.82	2	FAIL
ISO 12647-2 type 1 certification	93	0	-3	93.8	0.8	-5.6	**2.8**	ΔL	0.81	3	PASS
								Δa*	0.81	2	PASS
								Δb*	-2.55	2	FAIL

Results show that none of the competitors fulfilled all ISO 12647-3 criteria regarding paper substrate color. Especially the L-coordinates is significantly higher due to the slightly higher mass-per-area of the used papers (50 g/m^2). Competitor 4 used a paper with a degree of optical brighteners that caused the highest deviation due to a negative b* coordinate. Analog to the ISO 12647-2 print standardization, the print substrate color will not be considered as a requirement.

6.2 Ink set colors

To calculate the colorgamut the 60 measured points of the OK-prints are averaged into a single La*b* coordinate.

*6.2.1 ΔE*ab colour deviations*

*Table IV: Colour deviation ΔE*ab of the process colors according to standard*

Ink set colours Deviation	Measurement according to ISO 12647-1, D50, 2 degree, geometry 45/0, no polarisation filter, black backing				
	Tol.	Deviation OK-print / Reference			
	ΔE*ab	ΔE*ab CYAN	ΔE*ab MAGENTA	ΔE*ab YELLOW	ΔE*ab BLACK
Competitor 1	5.0	5.3	4.8	5.4	0.9
Competitor 2	5.0	7.3	7.3	9.3	0.6
Competitor 3	5.0	6.7	6.7	5.3	2.5
Competitor 4	5.0	11.9	11.9	10.4	6.3

Except for black, competitors did not print the process inks within the tolerance ΔE*ab = 5.

6.2.2 ΔH, ΔS, ΔL deviations

For more detailed evaluation, the color difference ΔE*ab is split up in a hue (ΔH), saturation (ΔS), and lightness (ΔL) component.

*Table V: Cyan colour deviation ΔE*ab and detailed components ΔH, ΔS, ΔL*

CYAN Colour deviation	Measurement according to ISO 12647-1: D50, 2 degree, geometry 45/0, no polarisation filter, black backing				
	Tol.	Deviation OK-print / Reference			
	ΔE*ab	ΔE*ab CYAN	ΔH	ΔS	ΔL
Competitor 1	5.0	5.3	0.4	3.8	3.7
Competitor 2	5.0	7.3	3.6	6.4	0.5
Competitor 3	5.0	6.7	3.4	5.8	0.2
Competitor 4	5.0	11.9	-8.2	7.9	-3.4

In case of the Hue-component, the 4 competitors shows extreme different results, especially competitor 4 is printing a complete different cyan hue. Furthermore the saturation of all competitors is significantly higher than standard, probably due the improved newsprint paper quality. With these differences in mind the next relevant question pops up: are the competitors able to print within the standard, just by adjusting the print density?

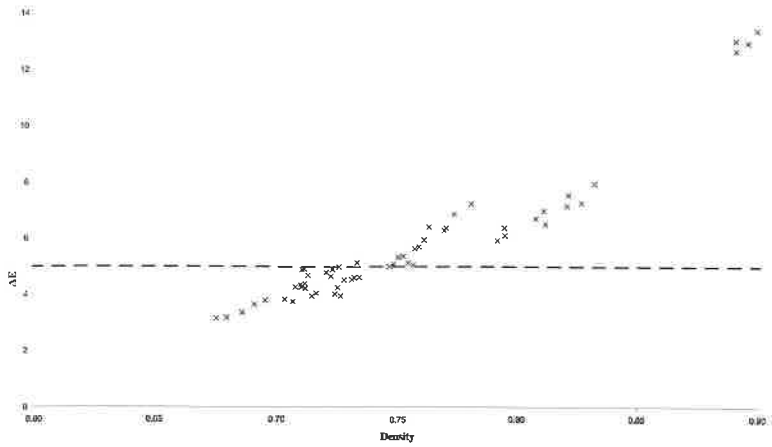


*Figure 4: Magenta ΔE*ab of the measured OK-prints*

Except for Cyan it seems that with an appropriate density, printing within standards is possible. As seen on the color gamut's it can be of interest to allow the competitors to print beyond the standard. This would mean that they still have to print the correct hue and lightness values, but a positive saturation difference will not contribute to the color deviation.

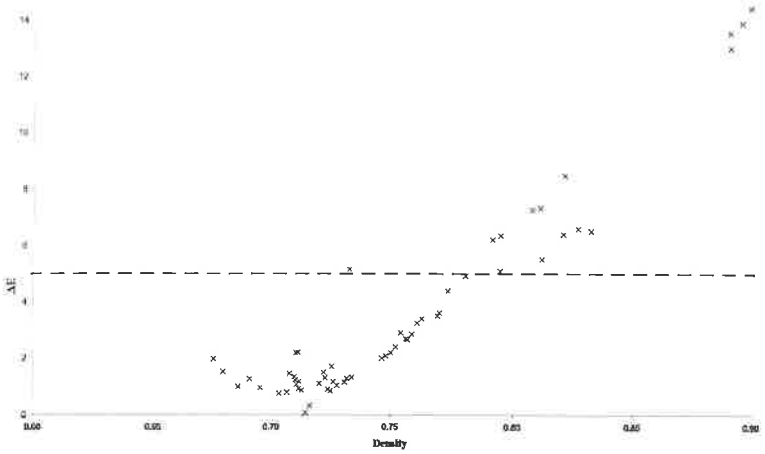


Figure 5: Magenta densities that minimize Lightness-Hue differences

*6.2.3 ΔE*ab colour variations*

When the printer has reached a target color in his OK-print, it is required to maintain this color in the production copies. For this reasons the participants were asked to sample a printed copy every 100 copies.

Table VI: Ink set color variation of the different competitors

Ink set colours Variation	Measurement according to ISO 12647-1: D50, 2 degree, geometry 45/0, no polarisation filter, black backing. The standard deviation between the production prints and average printed colour is calculated Note that for Yellow the tolerance value is 5.				
	Tol.	Standard Deviation Production prints			
	ΔE*ab	ΔE*ab CYAN	ΔE*ab MAGENTA	ΔE*ab YELLOW	ΔE*ab BLACK
Competitor 1	**4.0**	**2.6**	**2.6**	**3.5**	**1.2**
Competitor 2	**4.0**	**1.9**	**2.7**	**4.1**	**1.6**
Competitor 3	**4.0**	**1.7**	**3.1**	**3.1**	**1.1**
Competitor 4	**4.0**	**2.7**	**5.1**	**6.2**	**1.2**

Variation was mostly not an issue. Only competitor 4 who prints with higher pigmented inks is more vulnerable to color variation in his production process.

6.3 Dot gain

6.3.1 Deviation 40% and 80%

Dot gain was measured on a 40% and an 80% patch that was present in the certification target. This implies that the resulting dot gain is the average of 60 measurements across the different pages.

Tables VII & VIII: Dot gain difference compared to standard of the different competitors

Dot gain 40% Deviation	The densities for calculation of the dot gain are measured with a ISO Status E respons, with polarization filter and paper white as reference.							
	Tone value increase difference OK prints / reference				Certification Status			
	Cyan	Magenta	Yellow	Black	C	M	Y	K
Competitor 1	**-0.6%**	**-1.3%**	**-2.7%**	**-0.6%**	**PASS**	**PASS**	**PASS**	**PASS**
Competitor 2	**-6.5%**	**-6.9%**	**-7.7%**	**-9.6%**	**FAIL**	**FAIL**	**FAIL**	**FAIL**
Competitor 3	**0.7%**	**-2.5%**	**-0.5%**	**1.2%**	**PASS**	**PASS**	**PASS**	**PASS**
Competitor 4	**-6.0%**	**-0.4%**	**-5.1%**	**5.9%**	**FAIL**	**PASS**	**FAIL**	**FAIL**

Dot gain 80% Deviation	The densities for calculation of the dot gain are measured with a ISO Status E respons, with polarization filter and paper white as reference							
	Tone value increase difference OK prints / reference				Certification Status			
	Cyan	Magenta	Yellow	Black	C	M	Y	K
Competitor 1	-5.4%	-6.1%	-6.9%	-5.1%	FAIL	FAIL	FAIL	FAIL
Competitor 2	-5.8%	-6.5%	-7.7%	-15.3%	FAIL	FAIL	FAIL	FAIL
Competitor 3	-4.3%	-5.2%	-5.8%	-4.7%	FAIL	FAIL	FAIL	FAIL
Competitor 4	-8.3%	-2.2%	-6.0%	-0.6%	FAIL	FAIL	FAIL	FAIL

In the results can be seen that 2 competitors could print the 40% patch correctly. In case of the 80% dot, all competitors prints the shadow tonal values too light. In case of production printing, results show no significant change with the OK prints.

6.3.2 Mid-tone spread

Besides tone value increase deviation, the ISO 12647 print standard restricts the mutual difference between chromatic colors. Large differences in mid-tone spread will result in unacceptable color shifts.

Table IX: mid-tone spread of the 40% tone value in OK and Production prints

	OK prints			Production prints		
Midtone spread	result	tolerance	status	result	tolerance	status
Competitor 1	2.0%	5.0%	PASS	2.7%	6.0%	PASS
Competitor 2	1.2%	5.0%	PASS	3.6%	6.0%	PASS
Competitor 3	3.1%	5.0%	PASS	3.6%	6.0%	PASS
Competitor 4	5.6%	5.0%	FAIL	5.9%	6.0%	FAIL

6.3.3 Dot gain variation

For production printing the variation in dot gain is bounded.

Table X: dot gain variation of the 40% tone value in Production prints

Dot gain 40% Variation	The densities for calculation of the dot gain are measured with a ISO Status E respons, with polarization filter and paper white as reference.							
	Tone value increase difference OK prints / reference				Certification Status			
	Cyan	Magenta	Yellow	Black	C	M	Y	K
Competitor 1	3.2%	3.4%	3.4%	1.6%	PASS	PASS	PASS	PASS
Competitor 2	2.4%	1.6%	3.0%	1.8%	PASS	PASS	PASS	PASS
Competitor 3	2.1%	4.8%	5.1%	4.6%	PASS	PASS	FAIL	PASS
Competitor 4	3.4%	9.2%	10.0%	5.8%	PASS	FAIL	FAIL	FAIL

6.4 Registration

Registration evaluation is divided into 2 parts. First, the absolute registration of 7 pages was measured through videomicroscopy. These registration measurements are divided into 3 categories:

- *Category I: CMY-registration within ±100 μm.*
- *Category II: CMY-registration within ±200 μm.*
- *Category III: CMY-registration within ±300 μm.*

Table XI: absolute registration of 7 pages

Registration quality absolute registration	Measurement method: Visual inspect through videomicroscope. The number of pages that fall within a category are counted.		
	Cat I	Cat II	Cat III
Competitor 1	2	4	1
Competitor 2	3	4	0
Competitor 3	0	3	4
Competitor 4	2	5	0

Secondly, the registration of 20 sequencing sheets was measured at 4 reference points with the LUCHS Passer Measurement device. This to assure that the mechanical components and paper transport are working properly. This assures that the absolute registration can be maintained during production.

Table XII: Calculated standard deviation of the registration of 20 sequencing prints

Registration quality sequencing registration	Measurement method: measurement of 20 sequencing sheets with the LUCHS registration system. The standard deviation of the sequencing measurements is calculated.					
	lateral direction			axial direction		
	Cyan	Magenta	Yellow	Cyan	Magenta	Yellow
Competitor 1	**4**	**5**	**4**	**3**	**3**	**3**
Competitor 2	**13**	**15**	**9**	**13**	**13**	**5**
Competitor 3	**6**	**6**	**7**	**4**	**4**	**9**
Competitor 4	**4**	**7**	**8**	**3**	**8**	**23**

7. Conclusions

None of the competitors succeeded in meeting with al required criteria for achieving good predictable newsprint color quality. This is confirmed by a visual comparison of printed images in the test and by evaluating the cumulative frequencing curve.

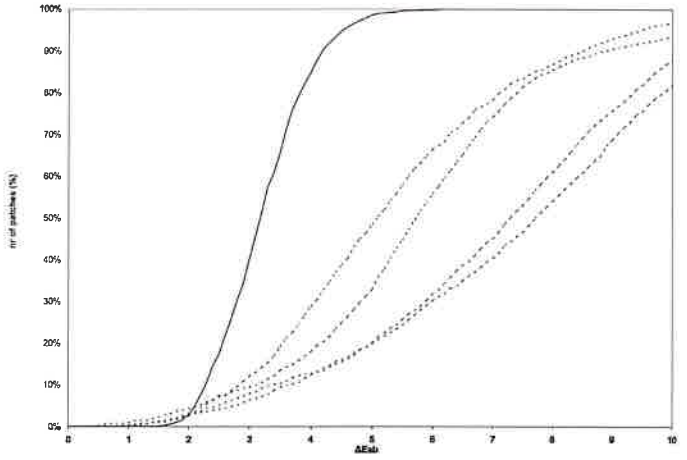


Figure 6: The Cumulative Frequency Curve of a printed ECI2002 test chart of certified ISO 12647-2 prints (FOGRA39) and newsprint (IFRA30L)

In a cumulative frequencing curve, based on the ECI 2002 testchart, the achieved results of the different participants can be compared. This same test has been carried out for the ISO 12647-2 certification program. It is clear that for newsprint further improvement is possible by tuning there production processes. Except for cyan, the target ink colors could be reproduced with the aid of a proper target-density in production. For the dot gain, competitors could nicely match the 26% dot gain at a 40% tone value, but failed to reproduce the 80% tone value correctly.

References

1. Rich, D. C., Okumura, Y., Lovell,V., *The Effect of Spectrocolorimeter Reproducibility on a Fully Color-managed Print Production Workflow*
2. IFRA, *Newsprint ISOnewspaper26v4 ICC Profile*
3. DIS/ISO 12647-3:2004, *Newspaper offset (coldset) and proof printing on standard newsprint*
4. ECI working group, *The new "ECI 2002" target*
5. LUCHS register measurement system
6. RIT, Test targets 5.0, *Dimitris Ploumidis, Device link profiling*



Use of static and dynamic device link profiles: incidence on colorimetric accuracy and ink savings

Amélie Trichon[1], Lionel Chagas[1], Elie Khoury[2], François Fournié[2], Nadia Hassissi[1]

[1] Pagora (the French Engineering School for Papermaking and Printing), formerly EFPG
BP 65 - Domaine Universitaire - F-38402 Saint-Martin d'Hères Cedex, France
E-mail: lionel.chagas@inpg.fr

[2] Alwan Color Expertise
The Graphic Industry Standardization Company
5 allée Alban Vistel, 69110 Sainte Foy lès Lyon, France

Abstract

ICC Profiles are standardized files that describe the color characteristics of devices, images and graphics using colorimetric standards. A digital document may be describe in various type of color formats. There are various classes of ICC Profiles. One of them is the class of DeviceLink Profiles. These contain a color transformation from an initial device color space directly into a second device color space. By using device link profile we can pay attention to printability specifications like color purity, TAC (Total Area Coverage). In this way, two options exist: a static or a dynamic device link profile. A static profile will apply the same adjustment to all the files whereas a dynamic device link profile will check the content of the file and optimize functions of the result. The aim of this study is to identify the interest of using device link profiles and to compare the dynamic device link profile and the static one in terms of colorimetric rendering, contrast and ink savings in case of inkjet printers. Until now it seems that dynamic profiles are better. The effect of device link profile was tested on different visual images and charts in format tiff and pdf with different kinds of settings, in one hand to test colorimetric accuracy and in the other hand to evaluate ink savings possibilities.

Keywords

Colorimetric accuracy, dynamic device link profile, ICC profile, ink savings, static device link profile

1. Introduction

ICC profiles are standardized files that describe the color characteristics of devices, images and graphics using colorimetric standards. A digital document may be described in various types of color formats. There are various classes of ICC profiles. Input profiles describe image scanners and digital cameras, monitor profiles describe luminous or projection output devices and output profiles describe printing processes. There are four other profile classes in addition to the device profiles. One of them is the class of device link profiles (DVLP). These contain a color transformation from an initial device color space directly into a second device color space. This clearly distinguishes them from the profiles previously mentioned, which transform the input or output color space into a device independent color space (PCS, Profile Connection Space). This means that there are always two profiles required in order to transform data from one device color space into another device color space.

There are different types of applications of DVLP. They may be used for process conversion, process calibration, ink saving and area coverage application.

Process conversion is used when a transformation is to be carried out between two different processes. This includes conversions between different printing processes, such as offset and gravure printing, but also applies to conversions within a printing process, for example between coated and uncoated papers or different applications such as commercial and newspaper.

Process calibration is used when a transformation is to be made between two similar processes. This includes conversions within a printing process in which, for example, different sets of printing inks or different dot gains need to be compensated for and where these calibrations cannot be carried out by "one-dimensional" dot gain corrections. In process calibration there is no fundamental change in the color composition or gamut mapping.

An other application is use DeviceLink Profiles to save inks and therefore reduce the cost of printing. This involves a transformation between two identical processes where the colored inks used to produce the dark areas are replaced by black using gray component replacement in the color separation. This reduces the total area coverage for tertiary colors in chromatic images.

A fundamental part of the color conversion process is the black printer generation. Several algorithms can be used. The most common are called UCR (Undercolor Removal) when applied to neutral colors only and GCR (Gray Component Replacement) when applied to all colors. The aim of the operation is to replace CMY inks by black ink, to extend the gamut of colors achievable in the darkest areas, to make the color control easier on the press and to save ink.

Calculations are often based on addition of densities. There are many ways to calculate but in GCR, a monotonic increasing function is always achieved (cf. figure 1)

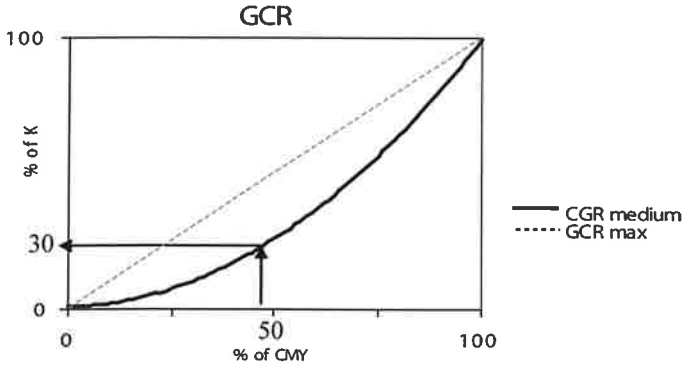


Figure 1:
GCR function : on this example, 50% of CMY inks are replaced by 30% of black ink. Next the color will be completed by a new percentage of CMY inks

An other process to replace CMY inks by black ink is called "maximum black". It consists of searching, for each color (that is to say each L*a*b* combination), the one which owns the couple (max (K), min (CMY)), among all the possible C-M-Y-K output values for a same color.

This model seams more efficient if one wants save ink, but, on the contrary of a classical UCR/GCR process, this operation is not necessarily continuous especially for graduated elements.

It is already possible to take into account the maximum area coverage by a suitable choice of parameters when calculating ICC profiles. These profiles are designed to preserve black and carry out a reduction in the chromatic inks if the total area coverage is exceeded.

The disadvantages of device link profiles are that: a DVLP is a unidirectional transformation and at the present time DVLP are not supported by all applications or RIP.

The classical ICC profiles do not take into account any printability specifications. During an ICC transformation, the input CMYK pixel values are converted to L*a*b* thanks to the source device profile and then the obtained L*a*b* values are converted to destination CMYK values thanks to the destination device profile. This operation can create problems on the press because specific informations can be lost. For example, with an ICC profile, an original black text will be converted in four colors (CMYK) like all the others elements of the document. So, it will complicate the registration on the press. To avoid this kind of problems, we can use an ICC device link profile. This is a specific type of profile that allows connecting two profiles. By using device link profile we can pay attention to printability specifications like color purity, TAC (Total Area Coverage). In this way, two options exist: a static or a dynamic device link profile. A static profile will apply the same adjustment to all the files, whereas a dynamic device link profile will check the content of the file and optimize functions of the result.

The aim of this study is to identify the interest of using device link profiles and to compare the dynamic device link profile and the static one in terms of colorimetric rendering, contrast and ink savings in case of inkjet printers. Until now it seems that dynamic profiles give better results. The effect of device link profile was tested on different images and charts in format tiff and pdf with different kinds of settings, on one hand, to test colorimetric accuracy and on the other hand, to evaluate ink savings possibilities.

2. Methods

The aim of the study is to evaluate and compare the performances of two methods of creating device link profiles for CMYK to CMYK transformations, especially color matching and ink savings. The first one is called static and use Link Profiler and the second one is called dynamic and use CMYK Optimizer. The main difference between a standard (static) and dynamic device link profile is that the last does not apply a transformation systematically but does a preliminary analysis of the file before changing something. The dynamic DVLP software analyses each pixel of the file and studies its inking and particularly TAC. According to the results the dynamic DVLP can optimize the color separation depending on the destination space.

The project is divided into three parts: in the first part, tests have been done on images in format Tiff, in the second part on documents in format PDF and in the last part, the documents created (in part two) have been printed with an inkjet press and analyzed.

In the dynamic treatment there is an analysis of the file before applying transformations. On CMYK optimizer this dynamic analysis depends of the "DTAC" parameter. The TAC can be calculated. region by region. On the application there are two main settings:

- "Tolerate excess TAC up to" (cm^2): represents an area that will be tolerate during the analysis even if its TAC is superior to the nominal TAC choose in the separation tab. Generally, this surface is little and corresponds to details. For example, if you print a portrait on a newspaper (TAC = 240), you can tolerate that a part of the subject like middle of the eyes have a TAC superior to 240.
- "Keep nominal TAC up to" (cm^2): represents the surface beyond TAC will be more decrease than other areas depending on the DTAC force cursor setting. So if the file contents a large dark area, the TAC will be more decrease.

For these two parameters, the surface is global and is calculated by adding all the pixels of all the document and not necessarily pixels that forms a unique area on the picture so the dynamic effect can be seen at several place on the page depending of the original separation. So this parameters allows adjusting and optimizing the transformation to the original file.

To evaluate color matching, the transformed file was compared with the original file by the software Colorpursuit. After proofing, original and transformed printed files have been also compared with spectrophotometers. The ΔE94 formula was used to compare the different files.

To evaluate ink savings, the reports generated by the software CMYK Optimizer were used. As a matter of fact CMYK Optimizer allows accessing to the values of inking. The ink amounts after optimization for each color can be found in the reports delivered after treatment by CMYK Optimizer.

Finally, a visual evaluation was made. A panel of seven persons has been asked to observe the proofing. They compared the static and the dynamic optimization and said whether they see a difference.

Part one: tests on tiff images

To be representative, the tiff images have been divided into two parts: the TC 3.5 chart that contains 432 patches for colorimetric measurements and a visual part.

We have attributed five different CMYK spaces to the test form: Isocoated V2, Isowebcoated, Isonewspaper26v4, Japan 2001 coated, Swop 2006 coated 5V2.

In each case we have converted into five different CMYK destination spaces. For each conversion we have used both dynamic and static device link profile and different settings concerning the Gray Component Replacement (GCR) and the Total Area Coverage (TAC).

Part two: test on PDF

A PDF X3/2002 test form has been created by using "In Design" software. The document is composed of two pages with parts for numerical and visual evaluations. The document includes several different colorimetric spaces: Adobe RGB 98, Isocoated V2, Isowebcoated, Isonewspaper26v4, Japan 2001 coated, Swop 2006 coated 5V2.

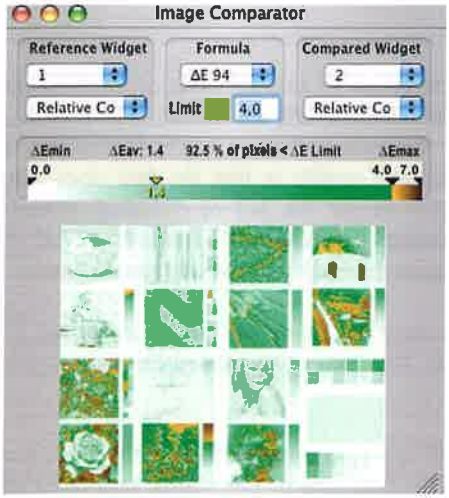


Figure 2:
The comparator window calculates the ΔE



Figure 3: the PDF test form created for the tests (left: page1; right: page2)

So the document includes several different colorimetric spaces as shown on figure 5. The first column of parts 1, 2, 3, 4 and parts 5, 7 and 8 will be used for numerical evaluation and the second and third columns of parts 1, 2, 3, 4 and part 6 will be used for a visual evaluation.

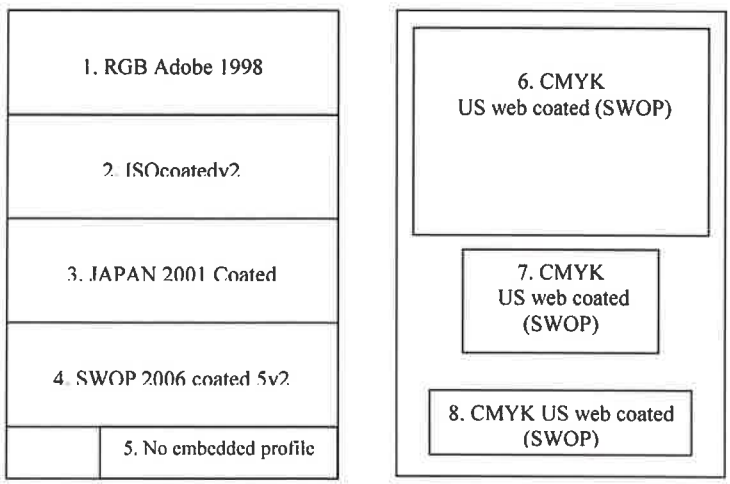


Figure 4: Scheme of the composition of the PDF test form

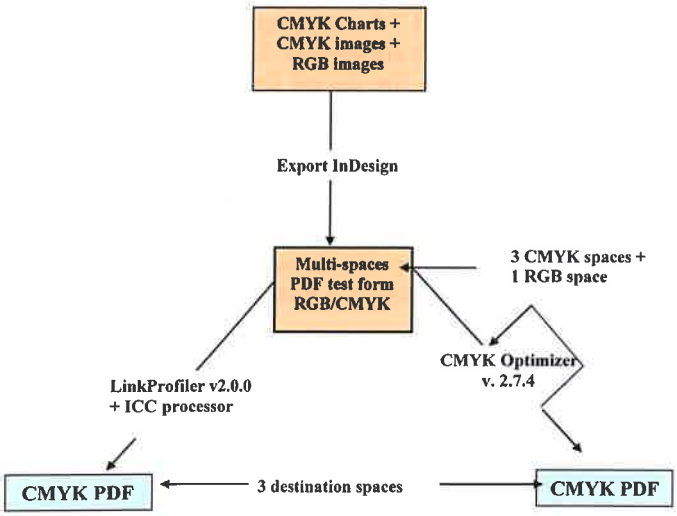


Figure 5:
Schema of the process for the test on PDF document test form

3. Results and discussion

3.1 Colorimetric accuracy

For all transformations the colorimetric accuracy is rather good. Even in the cases we introduce a strong value for the GCR, the average of ΔE94 does not exceed 4. This value is greater when we used the newspaper profile.

When we compare the use of dynamic and static profiles a trend emerges: the dynamic transformation confers a best ΔE94 than the static one. Because the dynamic transformation takes into account the content of the image, it can adapt colors and make a difference between strong inking areas and less inking areas on the contrary of static transformations.

The same data than for tests on tiff images were collected in the case of pdf images. The dynamic device link profiles take into account the input separation on different areas of the page and adapt its optimization. Initially it was important to measure the effect of a strong GCR. On figure 6 the input and output spaces are identical. The variations of ΔE 94 are lower than 2 for paper webcoated and lower than 0.5 for the others.

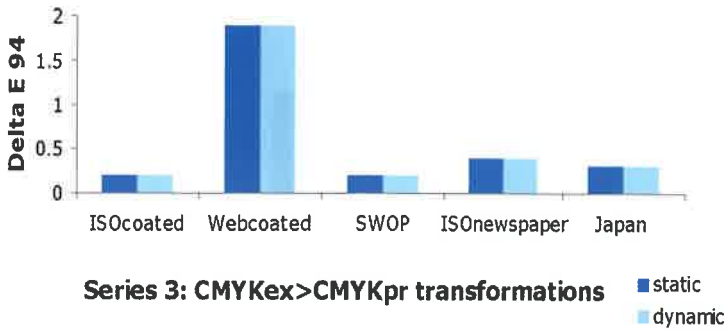


Figure 6: Medium ΔE94 on the TC3.5 chart with a strong GCR (1.0) settings - input and output spaces are identical

There are hardly any colorimetric differences between the two ways of treatment static and dynamic when the surface parameter of DTAC is not adapted to the size of the test form files.

For the standard GCR case, we begin to see a difference between the static and the dynamic method at Keep nominal TAC up to = 24 cm^2.

For the maximum black generation case, we begin to see a difference between the static and the dynamic method at Keep nominal TAC up to = 1 cm^2. So it seems that the hypothesis was probably true: the parameter" Keep nominal TAC up to" has an influence on the fact that in the tests we do not see the "dynamic" effect of CMYK Optimizer. To validate this fact, other test was done: a multi-page PDF from the

TC3.5 chart in ISOcoatedv2 was built so a file with 30 pages of the TC3.5 chart page was obtained and the same settings than case 1 on the "standard GCR ink savings settings" were applied. So I the "Keep nominal TAC up to" value was kept at 25 cm^2. And now, when analyzing the file we see that there is a difference between the treatment of 1 page and of the 30 same pages. So it seem confirm that the surface of 25 cm^2 is not adapted for the size of the image but is probably adapted for a bigger file like printers use everyday. So we can expect that, although we don't see an effect on one image, we will see a "dynamic" effect on an entire file. This note will be confirmed by the tests on PDF test form.

If we observe one image in particular, for example, the image of the car, we can see that we save more ink with the dynamic treatment and we see previously that we have nevertheless a better colorimetric accuracy. Moreover, this trend seems confirm by the visual evaluation.

These values can be dependant on the images. New tests with other documents were conducted. Several dark images were included. The results are presented on figure 7. The colorimetric differences between the files before and after treatment are more important. The colorimetric variations are slightly lower than 4 (for the dynamic transformations only).

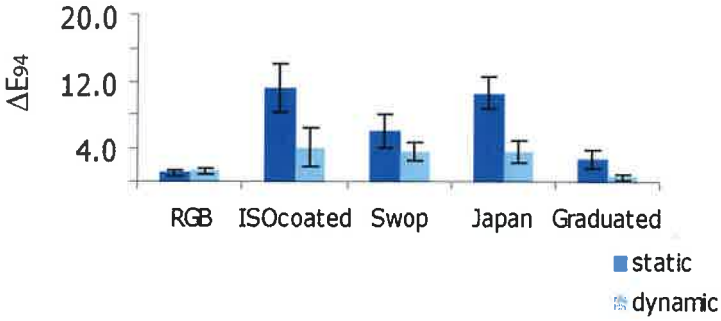


Figure 7:
Medium ΔE94 on images from page1 of PDF test form with a strong GCR (maximum black)

It was interesting to see the effect of more complex transformations on the colorimetric values. On figure 8, for each bar, the first name corresponds to the input CMJN space and the second to the output CMJN space. The transformations are realised by applying at the same time a gray component replacement (GCR). The case of the newspaper profile is to be put aside because the gamut is very different from the others. For the other cases the colorimetric difference between the original file and the output file is closer ($\Delta E94 < 2$ for a GCR of 2.4). The results are similar for a strong GCR. The ΔE94 are slightly higher. The rendering intent used is the colorimetric mode.

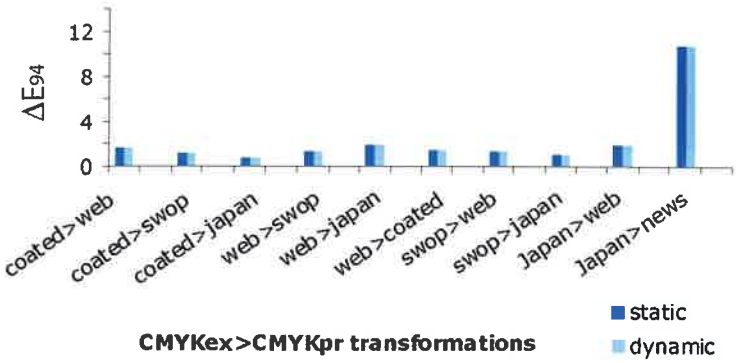


Figure 8:
Medium ΔE94 on the TC 3.5 chart with the "GCR (2.4) settings"

3.2 Ink saving

The amounts of cyan, magenta, yellow and black have been measured separately and compared to the initial ink amounts. We can determine three values:

$\Delta K = K_{final} - K_{initial}$ where K_i is the percentage of black plate ink coverage.
$\Delta CMY = CMY_{final} - CMY_{initial}$ where CMY_i is the sum of percentage of cyan, yellow and magenta plates ink coverage.
$\Delta CMYK = CMYK_{final} - CMYK_{initial}$ where $CMYK_i$ is the sum of percentage of cyan, yellow, magenta and black plates ink coverage.

To evaluate only the separation modification due to ink savings, few tests with transformation from one CMYK space into the same CMYK space have been done.

The results presented on figure 9 are to be observed in parallel with those of figure 6. The measures are made on the TC 3.5 test form. The ink saving varies from 5% to 20%.

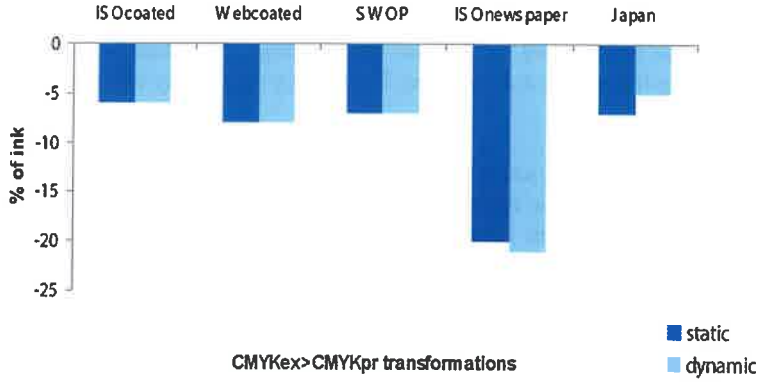
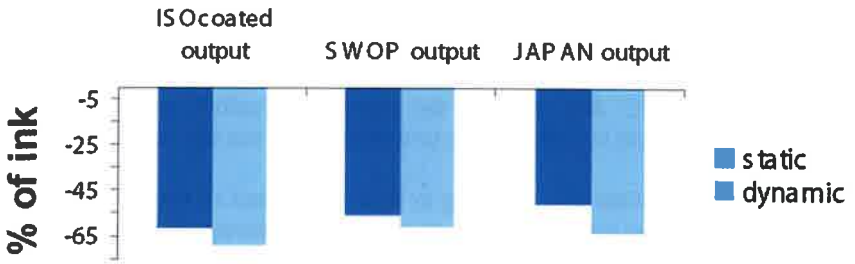


Figure 9: ink saving on TC 3.5 with the maxi GCR (1.0) settings

In the second time we have conducted the same tests on the car (page 2 of figure 3). The results are presented on figure 10. The image of the car is very dark. In this case the ink saving is much more important. We reach values from 50% to 70%.



Figures 10: ink saving on car image from PDF test form for a strong GCR (maximum black)

We observe, on figure 11, that the decrease of global inking is not systematic. The decrease is function of input and output profiles.

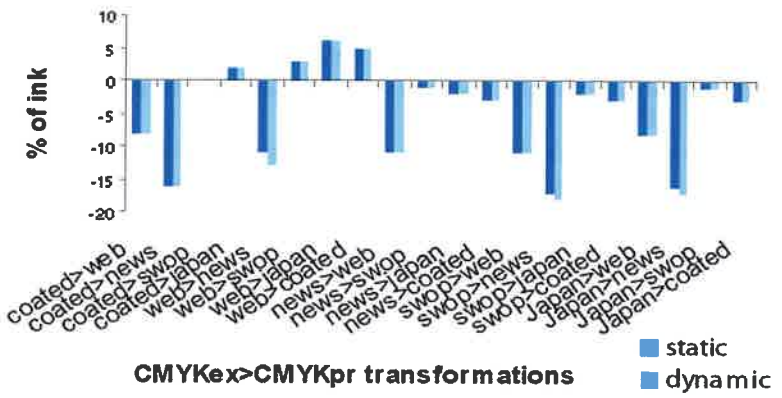


Figure 11: ink saving on TC 3.5 with the GCR (2.4) settings

We can see that we save more ink with the dynamic treatment and nevertheless we reach a better colorimetric accuracy. Moreover, this trend seems to be confirmed by the visual evaluation.

Dynamic link profiles give always a lower level of inking than static link profiles. The differences of inking level are significant between static and dynamic treatment. Moreover, save more ink does not produce larger colorimetric distortion.

3.3 Visual evaluation

A panel of seven persons has been asked to observe the proofing. They had to compare the static and the dynamic optimization and say if they see a difference. If yes, they should say which one is the most faithful to the original proof.

In a majority of cases (7/10), observers see a difference between the two treatments. And in only 1/9 case, they find that the static optimized proof is more faithful than the dynamic one to the original proof. Either we have visually a better sensation with the dynamic optimization, or we don't see visually a big difference between the two proofs. So it could be considered as an advantage because the dynamic treatment provides a better colorimetric accuracy and saves more ink. So, it seems that it does not lead to visual distortion.

To summarize:

- 74% of people say they see a difference between proofs treated by static profile and proofs treated by dynamic profile.
- 75% of people who saw a difference find the use of dynamic device link profile rendering nearer than static link profile.

4. Conclusions

In this study we wanted to bring to light the influence of the colorimetric conversions. More and more the manufacturers use the profiles ICC and multiply the changes of colour spaces. To preserve essential information, to realize ink savings and to obtain better printability they use device link profiles.

Through this systematic study we were able to bring to light the impact of conversions on the colorimetric accuracies and on ink savings. It was also interesting to validate the interest of the use of the dynamic device link profiles allowing adapting the treatment of colour according to the analyzed document.

References

1. Sharma, B., *(2003). Digital Color Imaging handbook, color fundamentals for digital imaging. CRC press, chapter one, pp. 34 - 40*
2. Lino and Berns *(1998), Building Color Management Modues Using linear optimization. Journal of Imaging Science and Technology, vol.42, March/April, p. 106*
3. Johnson, T., *(1996), Colour management in graphic arts and publishing. Pira technology series, pp. 31 - 32*
4. Bala, R., *(2003). Digital Color Imaging handbook, color fundamentals for digital imaging. CRC press, chapter four, pp 269 - 385*
5. Starr, B., *(2005), DeviceLinkProfiles/Repurposing CMYK. Progressive Color Media LLC*
6. International Color Consortium Specification ICC, *1:2004-10, <http://www.color.org/iccv42_2006-05.PDF > consulting 15/02/07*
7. Alwan Color Expertise, *http://www.alwancolor.com consulting 10/02/07*

Estimating the spectral reflectance of fluorescent offset papers for varying illuminants

Eva Maria Löffler[1], *Phil Green*[2]

[1] Stuttgart Media University, Germany
Nobelstraße 10, D-70569 Stuttgart
E-mail: loeffler@hdm-stuttgart.de

[2] London College of Communication
Elephant & Castle, London, SE1 6SB, United Kingdom

Abstract

In this study a method will be introduced for estimating the spectral reflectance factor of fluorescent offset papers, illuminated by either a physical source or a standard illuminant. The method was developed in two steps. Initially a range of 80 commercially available offset papers was classified according to their amount of fluorescence emission. The fluorescence characteristics were determined by calculating the 'difference area' between spectral reflectance factors measured both with a UV-Cut-Filter and without. For this classification process a GretagMacbeth Spectrolino was used. The total bi-spectral radiance factors of eight papers representing approximately the steps from lowest to highest fluorescence efficacy were then measured with a double monochromator instrument, and a model was developed using these measurements, based on the observation that the fluorescence characteristics of different offset papers have similar shapes and can therefore be defined by a scaleable model spectrum. The model was evaluated by finding the CIEDE2000 colour differences between L*a*b*-values calculated from measured bi-spectral data and estimated bi-spectral data. The mean colour differences for the illuminants A, D50 and D65 were 0.40, 0.51 and 0.62 respectively.

Keywords

Bi-spectral, fluorescent whitening agents, fluorescence, illuminant, offset paper

1. Introduction

The appearance and measurement of fluorescent substrates depends strongly on the UV-amount in the source illuminating a fluorescent sample. Most offset papers contain fluorescent whitening agents (FWA). Sources utilised in spectrophotometers related to the graphic industry show differing amounts of UV content [Dolezalek & Kraushaar, 2005; Pertler & Bertholdt, 2006]. This leads to ambiguity and misunderstandings in colour measurements as well as in the visual assessment of colour proofs and production prints. CIE Publication 163 shows how the varying UV content in different instruments influence the inter-instrument agreement between colour measurements made on fluorescent samples.

The only procedure to measure the reflectance factor of a fluorescent sample independently of the illumination source is to utilise a double monochromator spectrophotometer. Such devices allow monochromatic illumination as well as monochromatic detection and therefore provide bi-spectral measurements [Donaldson, 1954]. However, the majority of these instruments are expensive purpose-built laboratory devices and conducting measurements is time-consuming.

Different methods for estimating the fluorescence characteristics by the use of one-monochromator instruments are described in the literature, by Eitle & Ganz [1986], Allen [1973], Allman & Billmeyer [1977], and Grum & Costa [1977]. All these methods assume that the spectral power distribution of the source in the spectrophotometer is known. These methods are not practicable where the spd of source is not known, or where low-cost intruments are needed. Similarly, more recent approaches e.g. from Motta & Farrel [1993], Emmel & Hersch [1998], and Gil [2003], require complex measurement configurations and the measurement procedures are laborious.

This project is an attempt to develop a practicable method for estimating the source-independent fluorescence characteristics of offset papers.

The project was divided into two steps:

1. Developing a method for easily classifying the degree of paper fluorescence.
2. Deriving a model to predict the total bi-spectral radiance factor.

The latter step is based on the observation that the fluorescence characteristics of different offset papers have similar shapes and can therefore be defined in terms of scaleable model spectra

2. Methods

2.1 Measurements methods

The development of the introduced method is based on two kinds of spectral measurements. The classification method relies on measurements undertaken with a GretagMacbeth Spectrolino. This instrument is equipped with a diffraction grating placed between sample and detector, therefore allowing polychromatic illumination and monochromatic detection.

For the determination of source-independent fluorescence characteristics the BAM 2MM spectrophotometer was used. This instrument is a laboratory spectrophotometer equipped with two monochromators. The first monochromator irradiates the specimen with monochromatic light. The second monochromator analyses the radiation leaving the specimen.

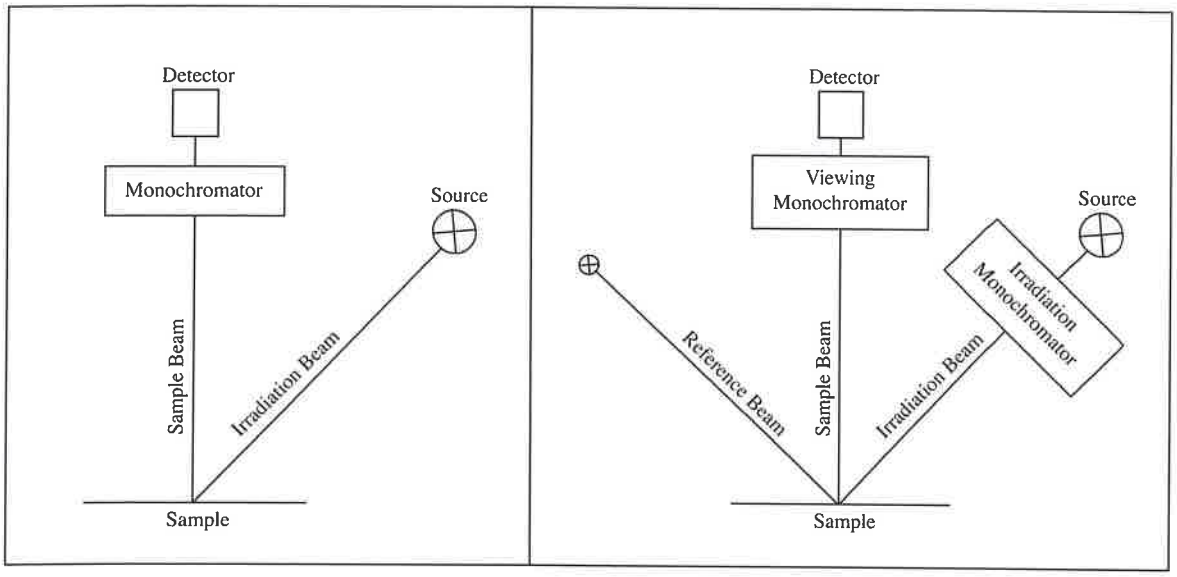


Figure1: Left: schematic design of the single-monochromator setup of the handheld spectrophotometer; right: schematic design of the BAM 2MM double monochromator setup

2.2 Method for classifying the degree of paper fluorescence

The estimation of the total bi-spectral radiance factor with the model described is based on a fluorescence identifier, ascertained by a classification method. A suitable value describing the degree of paper fluorescence results from the comparison of spectral reflectance factors measured with a common handheld spectrophotometer. One measurement is done with a UV-Cut filter and one measurement without such a filter. The UV-Cut filter suppresses the radiance of the source below 410 nm. The difference between both measurements can then be expressed in the difference spectrum and the area between the first and the second intersection point as difference area (Fig. 2). Hence the size of the difference area is directly caused by the FWAs, and this value can be used as a fluorescence identifier. The larger the size of the difference area, the greater is the degree of paper fluorescence.

The spectral reflectance factor of 80 commercially available offset papers was measured, with and without a UV-Cut filter. In order to range the offset papers according to their degree of fluorescence, the difference spectrum and the difference area was computed for all samples. For this classification process a GretagMacbeth

Spectrolino was used. Eight papers representing approximately the steps from lowest to highest fluorescence efficacy were selected as reference offset papers. These papers were sent to BAM Germany, for measuring the total bi-spectral radiance factor with a double monochromator instrument. These measurements were used to develop a model to estimate the source-independent, total bi-spectral radiance factor based on the classification method described above.

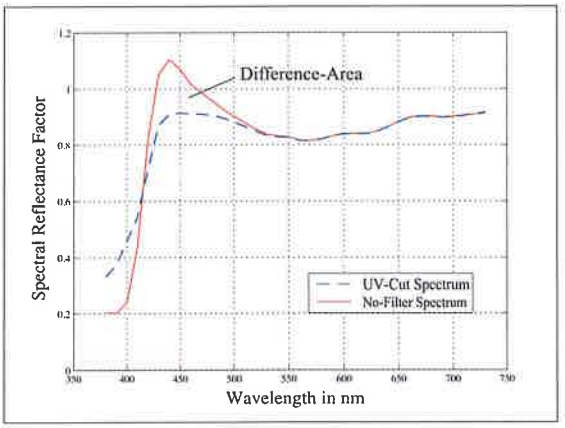


Figure 2: Spectral reflectance factors of an offset paper, measured with and without an UV-Cut Filter

2.3 Modelling the total bi-spectral radiance factor

For modelling the fluorescence characteristics of offset papers, two parts of the total bi-spectral radiance factor had to be examined separately: the three-dimensional fluorescence emission (bi-spectral luminescence radiance factor, $\beta_L(\lambda_{em}/\lambda_{ex})$) and the absorption range of the spectral reflected radiance factor $\beta_S(\lambda_{em})$ (Fig. 3).

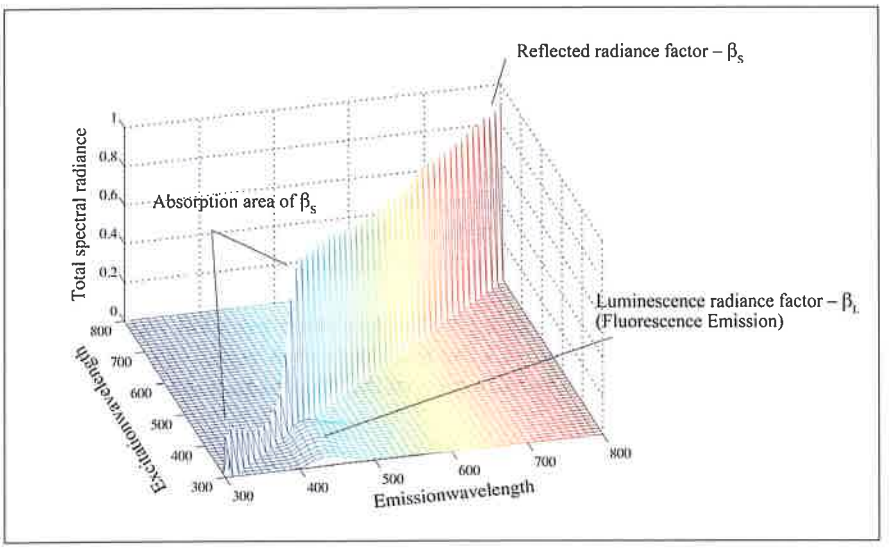


Figure 3: Total bi-spectral radiance factor of a fluorescent offset paper

2.3.1 Modelling the fluorescence emission

The fluorescence emission is described by emission and excitation spectra. Each emission spectrum belongs to a single excitation wavelength and each excitation spectrum belongs to a single emission wavelength. Figure 4 illustrates the direction of excitation and emission spectra. The approach to model the fluorescence emission of offset papers is based on two assumptions:

The excitation and emission spectra can be regarded as independent vectors.
The single excitation and emission spectra have similar shape.

The assumption of independent functions implies that the fluorescence emission can be described either by the single excitation spectrum or by the single emission spectrum. The second assumption implies that the single excitation- and emission spectra can be reconstructed by scaling an excitation or emission model spectrum. The emission model spectrum represents the general shape of all single emission spectra. The excitation model spectrum represents the general shape of all single excitation spectra.

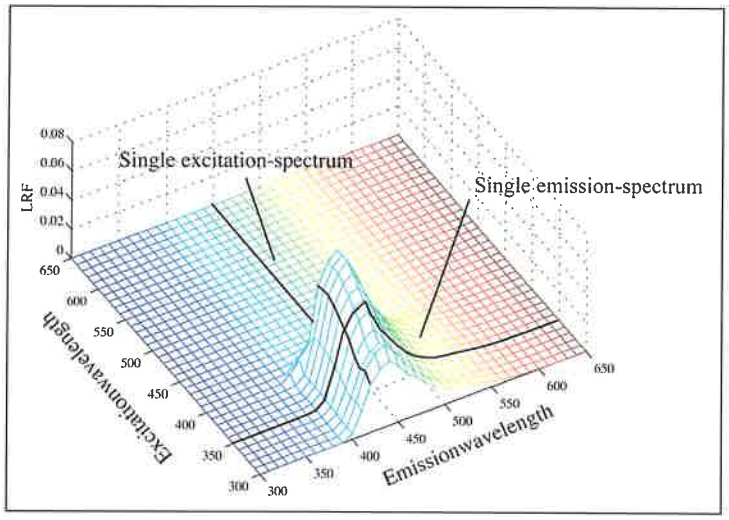


Figure 4: Luminescence Radiance Factor of a fluorescent offset paper; the black lines show the direction of emission and excitation spectra

The scaling factors for calculating the single target spectrum can be described with a scaling vector. On this basis the estimation of the fluorescence emission can be traced back to the dyadic product of two vectors, whereas the model spectrum is a column vector and the scaling vector is a row vector. The result of the vector-vector multiplication is a matrix representing the fluorescence emission. Depending on whether model spectrum or scaling vector is used, two models can be derived: an Emission model (Em-Model) and an Excitation model (Ex-Model). In the Em-Model, the fluorescence emission is estimated by the use of a general emission model spectrum and a general emission-scaling vector. In the Ex-Model, the fluorescence emission is estimated by use of a general excitation spectrum and a general excitation-scaling vector. The general emission model spectra, the general excitation model spectra as well as the corresponding general scaling vectors were derived from the bi-spectral reflectances of the eight reference offset papers. Figure 5 shows the general emission and excitation model spectra calculated from the bi-spectral measurement data.

Single factors (SF) for pre-scaling the general scaling vector to a sample-related vector were calculated. These scaling factors were brought into relationship with the difference area value. Since the relationship between these is linear, two equations which enable reconstruction of the fluorescence emission could be developed:

Em-Model:

$$\beta_{L(\lambda_{em},\lambda_{ex})} = EmMSg_{(\lambda_{em})} \otimes \left(EmSVg_{(\lambda_{ex})} \times \left((a \times Diffarea) + b\right)\right) \quad (1)$$

Ex-Model:

$$\beta_{L(\lambda_{em},\lambda_{ex})} = ExMSg_{(\lambda_{ex})} \otimes \left(ExSVg_{(\lambda_{em})} \times \left((a \times Diffarea) + b\right)\right) \quad (2)$$

where:

β_L = bi-spectral luminescence radiance factor (nxn-matrix)
λ_{em} = emission wavelength
λ_{ex} = excitation wavelength
$EmMSg$ = general model emission spectrum (nx1 vector)
$ExMSg$ = general model excitation spectrum (nx1 vector)
$EmSVg$ = general emission scaling vector (nx1 vector)
$ExSVg$ = general excitation scaling vector (nx1 vector)

Diffarea = fluorescence identifier; the difference area between UV-Cut- and No-filter-measurement of an offset paper
a, b = coefficients of the relationship between scaling factor (*SF*) and fluorescence identifier (*Diffarea*)

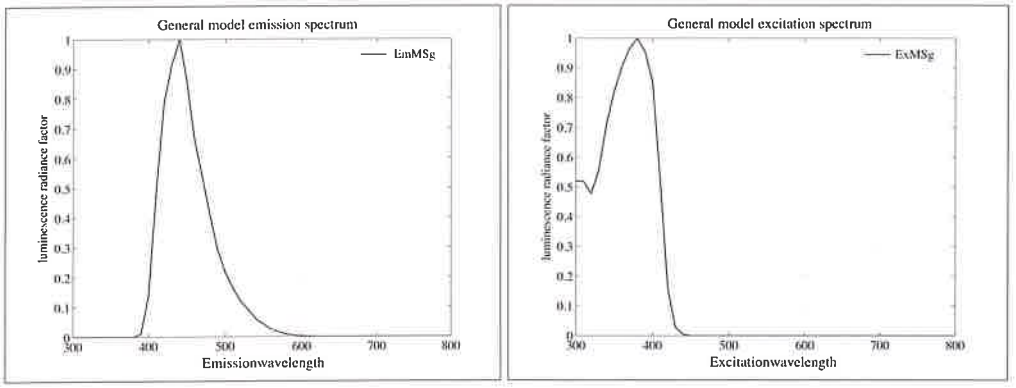


Figure 5: Right: general model emission spectrum; left: general model excitation spectrum

2.3.2 Modelling the absorption area

Similar to the approach of estimating the luminescence radiance factor, the absorption area of the reflected radiance factor was modelled by scaling a model spectrum representing the absorption area. This model spectrum was again derived from the BAM measurements. The scaling factors (SF) needed to reconstruct the paper-related absorption areas were brought into relationship with the difference area value and also showed a linear relationship, enabling estimation of the absorption area based on the fluorescence classification. The absorption area was modelled from 300 to 470 nm. At 470 nm the modelled absorption area was added to the measured reflected radiance of the respective paper. The method for estimating the absorption area is called Ab-Model. The calculation of the absorption area can be expressed as follows:

$$\beta_{S,E\left(\lambda_{em_n}-470nm\right)} = \left(AMS \times \left(\left(a \times Diffarea\right)+b\right)+1\right) \times \beta_{S,M(470nm)} \tag{3}$$

where:

$\beta_{S,E}$ = reflected radiance estimated = estimated absorption area
$\beta_{S,M}$ = reflected radiance originally measured
AMS = model spectrum representing the absorption area
Diffarea = fluorescence identifier; the difference area between UV-Cut- and No-filter-measurement of an offset paper
a,b = coefficients of the relationship between scaling factor (*SF*) and fluorescence identifier (difference area)
n = begin of wavelength range

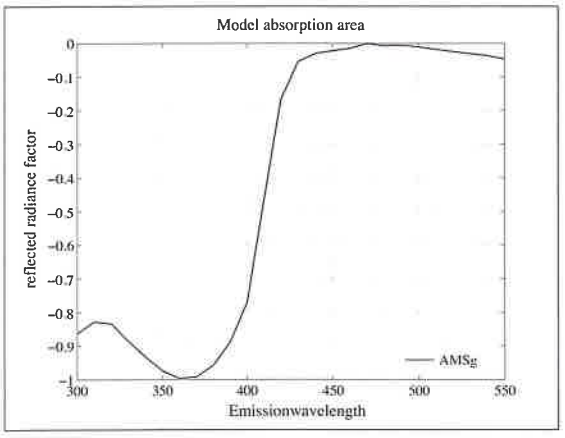


Figure 6: Model spectrum representing the absorption area

2.3.3 Assembling the total spectral radiance factor

For calculating the total spectral radiance factor of a fluorescent sample for arbitrary physical sources or illuminants three components are necessary:

- the estimated source-independent luminescence radiance factor
- the estimated absorption area
- the residual reflectance factor measured with a common spectrophotometer

The calculation can be expressed as follow:

$$\beta_{T(\lambda_{em},\lambda_{ex})} = \beta_{S,E(\lambda_{em_i=470nm})} + \beta_{S,M(470nm+k\cdots\lambda_{em_n})} + \frac{\sum \beta_{L(\lambda_{em},\lambda_{ex})} S_{(\lambda_{ex})} \Delta\lambda_{ex}}{S_{(\lambda_{em})}} \quad (4)$$

where:

β_T = total spectral radiance factor
β_L = bi-spectral luminescence radiance factor
$\beta_{S,E}$ = the modelled absorption area of β_S
$\beta_{S,M}$ = the reflected radiance of the original measurement
S = relative spectral power distribution of a light source or an illuminant
λ_{em} = emission wavelength
λ_{ex} = excitation wavelength
k = wavelength steps
i = begin of wavelength range
n = end of wavelength range

3. Results

Initially the best fluorescence model was determined. For modelling the fluorescence emission of offset papers, two different approaches were developed. If the emission model (Em-Model) is used, the fluorescence emission is basically described by the model emission spectrum. The excitation model (Ex-Model) works the other way round. A third option is to calculate the bi-spectral luminescence radiance factor with both models and determine a mean matrix afterwards. This option is called EmEx-model. The three variations were compared by calculating CIEDE2000 colour differences between CIELAB L^*, a^*, b^*-values based on the BAM-measurements and L^*, a^*, b^*-values based on the estimated total spectral radiance. In each case, only the spectral luminescence radiance factor was estimated. The calculations were performed for all reference offset papers and the illuminants A, D50 and D65. The greater the UV-content of the illuminant, the larger were the colour differences. Generally the differences were related to the paper and not the model. The three fluorescence models showed minor differences, with the EmEx-Model showing the smallest mean colour differences. Figure 7 shows a bar plot of the mean CIEDE2000 colour differences and ΔL^*-, Δa^*, Δb^*- values of Em-, Ex- and EmEx-Model.

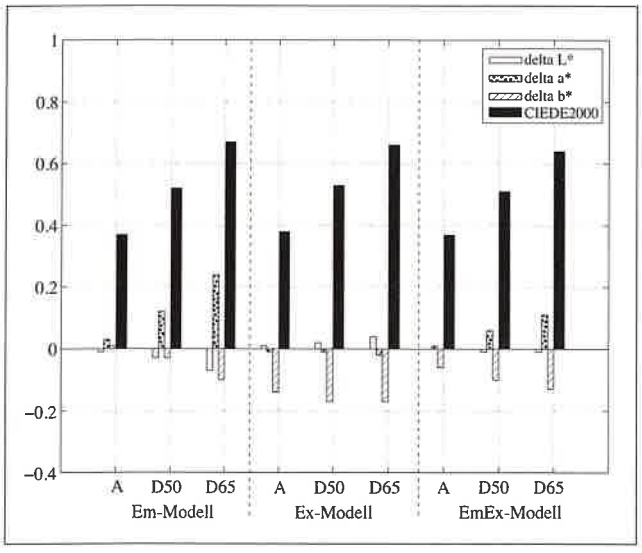


Figure 7:
Bar plot showing the mean CIED2000 colour differences and ΔL^*-, Δa^*-, Δb^*- values of the three fluorescence models

In a second evaluation step, the EmEx-Model was used in combination with the Ab-Model. The estimated absorption area as well as the estimated fluorescence emission were added to the normal reflection measured by BAM. In a third step, the estimated fluorescence emission and the estimated absorption area were added to reflection measurements undertaken with a GretagMacbeth Spectrolino. Neither evaluation step significantly increased the mean CIEDE2000 colour differences between measured and estimated data. Figure 8 shows a bar plot, which compares the results of EmEx-model with the results of the other evaluation steps. The result of the third evaluation step shows the performance of the model. The mean CIEDE2000 colour differences between measured and estimated data were 0.40, 0.51 to 0.62 for the illuminants A, D50 and D65 respectively.

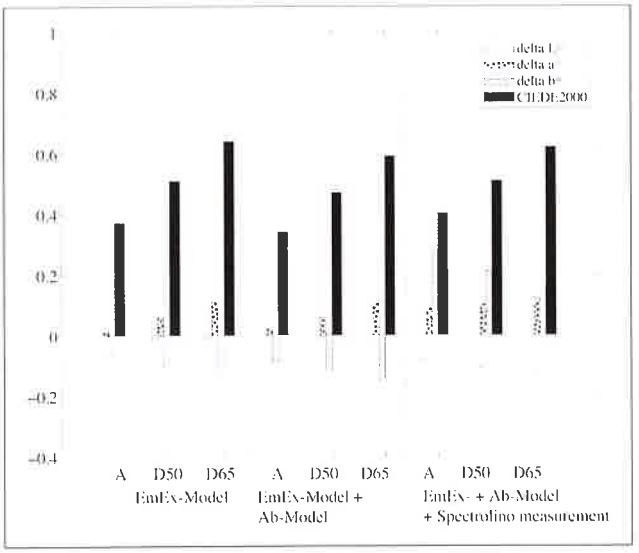


Figure 8: Bar plot showing the mean CIED2000 colour differences and ΔL- ,Δa*-, Δb*- values for all offset papers of all evaluations steps*

4. Discussion

The model described in the present paper does not cover the complex problem of estimating the fluorescent characteristics of fluorescent inks or fluorescing substrates different from those investigated, but it does introduce a method for estimating the source-independent fluorescence emission of offset papers without the need of specialist measurement equipment. With a simple classification method the degree of paper fluorescence was determined by computing the difference area between reflectance factor measurements undertaken with and without an UV-Cut filter. These measurements were conducted with a GretagMacbeth Spectrolino.

Three points regarding the performance and the application of the model should be considered:

1. The calculated scaling factors depend on the UV-characteristics of the spectrophotometer used for obtaining the difference area value. For obtaining repeatable results with different spectrophotometers two methods can be suggested:
   - the relationship between difference area and scaling factor has to be calculated for every instrument used to obtain difference area values;
   - a simple calibration with a scale of different, non-ageing, fluorescing standards representing a reference difference area value.
2. The model developed allows the estimation of source-independent fluorescence characteristics of unprinted offset paper. It does not cover the behaviour of the fluorescence characteristics of printed ink on offset papers. This will be a point of future work. Nevertheless, the outcome of the project can be used for white point adaptation transformations within soft proof applications, or for the estimation of fluorescence characteristics in the context of other methods, such as the method from Emmel and Hersch [1998].
3. The model spectra developed represent the fluorescence characteristics of a particular group of substrates. The application of the general model idea relating to other substrate groups has to be evaluated. There are certainly substrates or materials whose fluorescence characteristics can only be estimated by the use of

complex methods referred to above, but it is possible that there are also substrate groups showing similar characteristics. In this context it would be very helpful to gather bi-spectral measurements of printing, and other materials in a database freely available to researchers, as also suggested by Gonzales and Fairchild [2000].

5. Conclusion

A method has been developed to estimate the total spectral radiance factor of fluorescent offset papers, illuminated by either a physical source or a standard illuminant. The method is based on a classification method and scaleable model spectra. The fluorescence classification can be undertaken with the use of a common handheld spectrophotometer. The model was evaluated by finding the CIEDE2000 colour differences between $L^*a^*b^*$-values calculated from measured bi-spectral data and estimated bi-spectral data. The mean colour differences were 0.40, 0.51 to 0.62 for the illuminants A, D50 and D65 respectively.

The model developed allows the estimation of source-independent fluorescence characteristics for a limited group of substrates: unprinted offset papers. It does not cover the behaviour of the fluorescence characteristics of printed offset papers or fluorescent inks, which will be a point of future work. It would also be interesting to consider the application of the general model approach to other substrate groups in future research.

The model developed introduces a new method for estimating fluorescence characteristics of offset papers and therefore provides a contribution to current work in the context of fluorescence colorimetry.

Acknowledgement

Special thanks to BAM - Germany, in particular to Dipl.-Ing. Bernd Günther, Dr. Carsten Steckert, Dipl.-Phys. Klaus-Peter Gründer for providing the bi-spectral measurements. The authors would like to thank also, Dr. Johannes Hoffstadt (GMG GmbH & Co. KG), Andreas Kraushaar (Fogra, Germany) and Prof. Ronald Schaul (Stuttgart Media University, HdM) for providing useful comments on the project.

References

1. Allen, (1973), *Separation of the Spectral Radiance Factor Curve of Fluorescent Substances into Reflected and Fluoresced Components. Applied Optics 12 (2), 289 - 293*
2. Alman & Billmeyer, (1977), New Method for the Colorimetric Measurement of Opaque Fluorescent Samples, *Color research and application 2* (1), 19 - 25
3. CIE Publication 163:2004, *The effects of fluorescence in the characterization of imaging media,* CIE Central Bureau, Vienna
4. Dolezalek & Kraushaar, (2005), *Korrektur von Messfehlern bei Farbmessgeräten, Fogra Forschungsbericht Nr. 52.034. München: Fogra*
5. Donaldson, (1954), *Spectrophotometry of fluorescent pigments, British Journal of Applied Physics, 5, 210 - 214*
6. Eitle & Ganz, (1968), *Eine Methode zur Bestimmung von Normfarbwerten, Textilveredelung, 3 (8), 389 - 391*
7. Emmel & Hersch, (1998), *Spectral Colour Prediction Model for a Transparent Fluorescent Ink on Paper, Proceedings of the 6th IS&T and SID's Color Imaging Conference, Scottsdale Arizona, 116 - 122*
8. Gil, (2003), *A Practical Approach to Measuring and Modelling Paper Fluorescence for Improved Colorimetric Characterisation of Printing Processes, Proceedings of the 11th IS&T and SID's Color Imaging Conference, Scottsdale Arizona, 248 - 254*
9. Gonzalez, S. and Fairchild, M.D. (2000), Evaluation of Bispectral Spectrophotometry for Accurate Colorimetry of Printing Materials, *IS&T/SID 8th Color Imaging Conference,* Scottsdale, 39 - 43
10. Grum & Costa, (1977), *Color evaluation by fluorescence measurements without the need of multiple illumination sources, Tappi 60 (8), 119 - 121*
11. Motta & Farrel, (1993), *A Simplified Method for the Colorimetric Characterization of Fluorescent Inks, Proceedings of the 1st IS&T and SID's Color Imaging Conference, Transforms and Transportability of Color, Scottsdale Arizona, 83 - 84*
12. Pertler & Bertholdt, (2006). Colour comparison and Colour matching in fluorescing samples in the printing industry, Fogra Forschungsbericht Nr. 60.053. Munich:Fogra

Improving inter-instrument agreement in colour and density measurement

Andrew Williams

IFRA
Washingtonplatz 1
D-64287 Darmstadt, Germany
E-mail: williams@ifra.com

Abstract

One of the reasons why densitometry has failed the user in printing is the multitude of standards and the lack of a common agreement about how density should be measured. All the factors which contribute to measurement differences apply regardless of which of the major printing processes is used. The objectives were to improve measurement accuracy and precision for colour and density, to improve inter-instrument agreement and to maintain repeatability for hand-held spectrophotometers and densitometers.

The novelty of the paper lies in the compilation of the main factors that influence colour and density measurement together with a comprehensive study of the ISO graphic arts standards and TC130 documentation regarding these measurement instruments.

Further novelty has been added by some general observations and recommendations.

Keywords

Colour, density, ISO standards, measurement

1. Introduction

There are many factors that influence colour or optical density measurement, the accuracy of the results and how well they can be repeated by another instrument. Generally, these factors can be considered as belonging to one of the following groups:

- Instrument design
- Effect of time and the environmental conditions
- Measurement instrument set-up and technique

A study has been made of these influences and part of this study is reported here.

In the case of instrument design, measurements were made on the effect of directional illumination on colour and density measurement on newsprint, the effect of different ISO standardised colour filter sets and the effect of adding a cross-polarising filter set to the measurements.

Another part of the study reviewed the effect of thermochromism on colour measurement.

Finally, spectral data from the inks of the major four-colour printing processes were compared to show that an agreement on the specification of a single set of colour filters for optical density measurement is the most practical way to significantly improve inter-instrument agreement for density.

In order to achieve this agreement, certain ISO standards, particularly ISO 13656, relating to density measurement and print process control, need to be rationalised. Next, only the spectrodensitometers that conform to the agreed standard should be used for process control. Differences in the measurement results caused by the measurement conditions and method are more easily overcome. ISO status E colour filters with cross-polarising filters are recommended as the basis for a single density filter set for print process control.

2. Spectrodensitometer with directional illumination

Here the instrument illumination follows the 0° illumination, 45° collection geometry, but collection is made at one cardinal point only. The machine direction measurements mean that the reflected light is collected at a 90° azimuth angle to the long direction of the paper fibres and at a 45° elevation.

These measurement were made on newspaper samples of the 10 best of 200 individual newspapers in which measurements of the print quality control test strips came closest to the ISO 12647-3 printing process standard. Each value in the data collection is the respective average of three machine direction (md) or three cross-machine direction (cd) measurements of the same printed area. All colour measurements used the CIELAB, D50, 2°, absolute white reference setting and without polarisation filters. The maximum variation is that from the average md and cd paired values of the same individual newspaper samples.

Status T density measurements were not made. ISO/ANSI status T filters are identical to ISO/ANSI status E filters in the case of the red filter (cyan ink), green filter (magenta ink) and visual filter (black ink). Only the blue filter (yellow ink) has a different spectral response curve in that it is even wider in bandwidth than the wide-band ISO/ANSI status E blue filter.

Table I: Directional colour measurements on newsprint- CIELAB, D50, 2°, ABS and without polarisation filters

	Machine Direction (md)			Cross Direction (cd)			Ave.	Max
Colour	L*	a*	b*	L*	a*	b*	ΔE	ΔE
Red	52.39	41.77	22.89	50.84	42.96	23.56	2.06	2.82
Green	52.98	-35.57	15.32	52.06	-36.92	16.00	1.77	3.24
Blue	41.47	7.37	-23.92	39.29	7.31	-25.50	2.68	4.16
Black (Mono)	35.25	0.62	3.43	33.59	0.34	2.98	1.74	3.24
Cyan	57.70	-22.88	-27.59	56.25	-24.18	-28.31	2.07	3.06
Magenta	54.67	44.32	-2.19	52.44	45.79	-3.27	2.88	4.00
Yellow	78.46	-4.60	58.45	77.57	-4.74	60.18	1.95	2.55
Black (4-c)	34.02	0.25	1.76	31.67	-0.12	1.27	2.44	3.56
Cyan 50%	68.24	-13.65	-14.27	67.30	-14.27	-14.71	1.20	1.81
Magenta 50%	65.92	24.12	-2.12	64.58	24.67	-2.55	1.51	1.97
Yellow 50%	79.38	-3.94	33.20	78.60	-4.05	34.02	1.13	1.68
Black 50%	58.69	-0.10	2.76	57.41	-0.25	2.61	1.29	2.24
Paper	81.13	-0.41	2.73	80.0	-0.49	2.70	1.09	2.26

3. Results

Depending on the surface structure of the newsprint, the difference between md and cd measurements can cause a CIELAB ΔE of 4.0 or a density difference of 0.10.

It is to be noted that this type of measurement may be a simulation of real-world conditions in that printed copy is often illuminated or viewed with a directional bias. Texture and gloss are just two of the psycho-physical effects that can be investigated and quantified through directional measurement. Printing, however, is usually on higher quality papers than newsprint and texture and gloss are not usually an issue for newspapers.

In the case of relative density measurements and polarising filters, for status E and status I filters, the variation in the measured density values was very slightly greater than those for the status E absolute measurements without polarising filters. That is, without polarisation filters, the measurements were very slightly more consistent. However, the difference between the average md and cd measurements were more than halved by using polarising filters. This effect was particularly noticeable for the printing primary colours of CMYK.

Table II: Directional density measurements using different density references and filter combinations

Density md Den_E_NP_Abs	Ave. D	s.d.	C.o.V.%	Density cd Den_E_NP_Abs	Ave. D	s.d.	C.o.V.%	Density Changes Ave. ΔD	Density Changes Max ΔD
Black (Mono)	1.06	0.05	4.38	Black (Mono)	1.11	0.03	3.12	0.05	0.08
Cyan	0.87	0.04	4.96	Cyan	0.92	0.04	4.33	0.05	0.08
Magenta	0.87	0.03	3.71	Magenta	0.92	0.04	4.50	0.06	0.09
Yellow	0.93	0.04	3.99	Yellow	0.98	0.04	3.64	0.05	0.07
Black (4-c)	1.10	0.05	4.34	Black (4-c)	1.16	0.04	3.82	0.06	0.10
Red	0.99	0.02	2.06	Red	1.03	0.02	1.45	0.05	0.07
Green	0.93	0.04	4.42	Green	0.96	0.03	3.08	0.03	0.07
Blue	0.92	0.04	4.31	Blue	0.97	0.04	3.87	0.06	0.08
Cyan 50%	0.54	0.03	4.85	Cyan 50%	0.56	0.03	5.10	0.02	0.04
Magenta 50%	0.53	0.03	4.88	Magenta 50%	0.56	0.03	4.57	0.02	0.03
Yellow 50%	0.59	0.03	4.95	Yellow 50%	0.62	0.02	3.79	0.02	0.04
Black 50%	0.57	0.03	4.88	Black 50%	0.60	0.03	4.72	0.02	0.04
Paper md	0.23	0.02	7.16	Paper cd	0.25	0.01	4.25	0.01	0.03
			4.53			Ave.	3.87		

Density md Den_E_P_Rel	Ave. D	s.d.	C.o.V.%	Density cd Den_E_P_Rel	Ave. D	s.d.	C.o.V.%	Density Changes Ave. ΔD	Density Changes Max ΔD
Black (Mono)	1.10	0.08	7.39	Black (Mono)	1.10	0.07	6.60	0.01	0.03
Cyan	0.83	0.05	6.58	Cyan	0.84	0.05	6.11	0.01	0.02
Magenta	0.86	0.05	5.77	Magenta	0.87	0.05	5.42	0.01	0.04
Yellow	0.88	0.05	5.63	Yellow	0.89	0.05	5.88	0.01	0.03
Black (4-c)	1.23	0.08	6.74	Black (4-c)	1.24	0.08	6.71	0.01	0.02
Red	0.96	0.03	3.06	Red	0.96	0.03	3.08	0.01	0.02
Green	0.90	0.04	4.02	Green	0.89	0.03	3.76	0.01	0.02
Blue	0.94	0.04	4.22	Blue	0.94	0.04	4.16	0.01	0.03
Cyan 50%	0.37	0.03	8.62	Cyan 50%	0.36	0.04	9.83	0.01	0.03
Magenta 50%	0.37	0.03	7.95	Magenta 50%	0.37	0.03	8.70	0.01	0.03
Yellow 50%	0.38	0.03	7.74	Yellow 50%	0.38	0.03	8.09	0.01	0.02
Black 50%	0.40	0.03	7.87	Black 50%	0.40	0.03	8.41	0.01	0.02
		Ave.	6.30			Ave.	6.40		

Density md Den_I_P_Rel	Ave. D	s.d.	C.o.V.%	Density cd Den_I_P_Rel	Ave. D	s.d.	C.o.V.%	Density Changes Ave. ΔD	Density Changes Max ΔD
Black (Mono)	1.10	0.08	7.24	Black (Mono)	1.10	0.07	6.74	0.01	0.02
Cyan	0.87	0.06	6.45	Cyan	0.88	0.05	5.74	0.01	0.03
Magenta	0.90	0.07	8.00	Magenta	0.91	0.08	8.28	0.01	0.03
Yellow	0.91	0.05	5.09	Yellow	0.92	0.05	5.22	0.01	0.02
Black (4-c)	1.23	0.08	6.53	Black (4-c)	1.24	0.08	6.82	0.01	0.02
Red	0.98	0.06	5.98	Red	0.99	0.06	6.01	0.01	0.02
Green	0.93	0.03	3.70	Green	0.93	0.03	3.55	0.01	0.03
Blue	0.95	0.04	4.17	Blue	0.95	0.04	3.91	0.01	0.02
Cyan 50%	0.38	0.03	8.81	Cyan 50%	0.38	0.03	9.11	0.01	0.02
Magenta 50%	0.38	0.03	8.55	Magenta 50%	0.38	0.04	9.45	0.01	0.02
Yellow 50%	0.39	0.03	8.58	Yellow 50%	0.39	0.03	7.87	0.01	0.02
Black 50%	0.39	0.03	8.38	Black 50%	0.40	0.03	7.88	0.00	0.01
		Ave.	6.79			Ave.	6.72		

The abbreviations in the table (p. 415) refer to the following:

Abs - absolute white reference;
Rel - relative optical density to substrate;
E or I - ISO colour density filter spectral responses;
NP or P - no polarising filters or polarising filters;
s.d. - statistical standard deviation;
C.o.V. - statistical coefficient of variation;
ΔD. - density change (average and maximum).

4. Thermochromism effect

Thermochromism refers to a colour change with temperature change. According to Azom [1], suppliers of CERAM ceramic colour standards, all highly coloured materials show degrees of thermochromism under standard daylight conditions.

Ceramic tile issues

Thermochromism occurs, among others, with some tiles that contain selenium.Compton [2] reported that when a tile is heated from 25°C to 35°C - a typical temperature change in the instruments using prolonged polychromatic irradiation common at that time - the effect is a small reduction in reflectance with an increase in temperature. She observed that in general thermochromism occurs on steep spectral profiles.

Hewlett Packard researchers took a spectrophotometer with a tungsten lamp and measured a green CCS II tile 30 times at the instrument's maximum rate. With a precision thermometer, when the tile's temperature increased by 0.2°C, it introduced an error of approximately 0.01 CIELAB ΔE^*_{ab} units due to thermochromism [3].

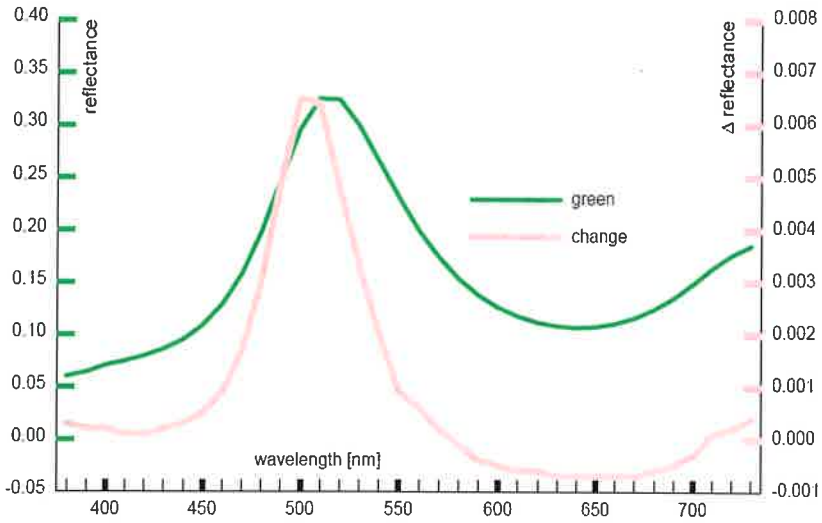


Figure 1: Difference in reflectance due to thermochromism

In Fig. 1, the green curve shows the spectral reflectance data of a green reference tile measured at 24.4°C ± 0.7°C. The pink curve plots the National Physical Laboratory (NPL) data for the difference in reflectance caused by a 10°C (25°C to 35°C) change in temperature (units on right axis).

For this reason, HP kept the tiles at the same ambient temperature as the instrument during its normal use; if the tiles were kept in a box or drawer, it would be opened half an hour prior to use [4].

Fairchild and Grum [5] conducted a similar experiment with an instrument of 0°:45° geometry. For the same temperature change they observed a ΔE^*_{ab} value of 0.7 for a green tile. However, they observed much larger changes for the orange (1.6) and red (1.5) BCRA CCS II tiles.

The following table shows the thermochromic characteristics when the BCRA colour tile changes 10°C from the room temperature (ΔE^*_{ab}) [6].

Table III: Change of colour of BCRA CCS II ceramic tiles with 10°C increase in temperature

BCRA Tile	ΔE^*_{ab}
White	0.01
Pale grey	0.02
Mid grey	0.05
Diff grey	0.05
Deep grey	0.05
Deep pink	0.60
Orange	1.52
Red	1.32
Yellow	0.92
Green	0.92
Diff green	0.91
Cyan	0.46
Deep blue	0.17
Black	0.02

More recently NPL has released a comprehensive collection of spectral reflectance and thermochromism data [7]. on the NPL Master Set of the BCRA CCS II tiles.

If the temperature is stable for a period of 30 minutes (the time for a ceramic tile to adapt to a small temperature change) or longer, and an accurate thermometer is available, for example a mercury in glass thermometer graduated in 0.1°C intervals, then highly accurate measurements can be made by correcting the spectral data for the temperature difference before the colorimetric quantities are computed. The correction data is listed in the reference Fairchild and Grum.

Pantone inks on paper

Hiltunen [8]. investigated the thermochromic behaviour of Pantone ink on paper samples using an Elmer double beam spectrophotometer. Although the samples were initially heated up to 94°C, steps were taken to isolate the instrument to prevent the heat from affecting its normal temperature. The results indicated a change of 0.093 ΔE^*_{ab}/°C for this paper sample.

Table IV: CIELAB values for the Pantone Red 032 U sample at four surface temperatures. The colour difference ΔE was calculated from the lowest temperature curve

°C	L*	a*	b*	ΔE^*_{ab}
28	55.75	58.42	27.63	
35	55.46	58.17	27.26	0.53
40	55.20	57.98	26.88	1.03
45	55.00	57.78	26.55	1.46

Under normal operating conditions, both the materials and the instrument are exposed to the same temperature change. Normally, it is unknown how much of the change in the colour measurement is due to thermochromism of the material and how much is due to uncorrected thermal drift of the measuring instrument. Both would have an effect, though manufacturers pay particular attention to the thermal stability of their instrument and build-in self-compensating circuitry as well as ensuring adequate cooling in the design. This is one of the reasons why a frequent white reference calibration should be made during the measuring. Nevertheless, as can be seen from the examples above, there is no satisfactory automatic compensation for temperature in spectrophotometry when the exact thermal properties of the materials are unknown. Correction values are dependent on the instrument, the colour and the material characteristics. Temperature control of the laboratory is a better solution.

A practical temperature chosen by many QC labs for colour measurement of printed samples is 23°C ± 2°C. The means of measuring temperature range from the straightforward laboratory mercury-in-glass thermometer to the microprocessor-driven, digital thermometer.

The objective is to have a temperature reading with approximately a 0.1°C precision. The temperature of both the samples and spectrophotometer or spectrodensitometer measuring instrument should both be allowed to stabilise in the controlled environment for at least 30 minutes before measuring.

Glass thermometers are easier to keep clean in a printing environment, while silicone tipped probes prevent scratches when checking the temperature of ceramic tiles. Obviously adding a silicone tip to a thermometer has the same effect. In any case, the room temperature is the most important item that needs to be controlled.

Interestingly, a glass thermometer with a limited temperature range of 19°C - 27°C and a scaling in steps of 0.1°C, can be more accurate than the much more expensive electronic version with the thermocouple connected. Adding the thermocouple can reduce the accuracy to 0.7°C or worse.

For each measurement performed for certification purposes, both the current temperature and the thermometer's tolerance are recorded.

5. Hygrochromism - relative humidity variation effects on measured colour

When ink on paper is measured, it is also necessary to record the current humidity, because humidity changes the way ink interacts with paper. The change of colour with humidity is known as *hygrochromism*.

The effect of humidity on the physical properties of paper are well documented. Data regarding the effect of humidity on printed colour seems to be restricted to digital printing and photo print finishing, where pigmented toners are more stable compared to dye toners which can show lateral 'bleeding' and dot gain when the prints are stored under high humidity[9],[10],[11]. There is some reliable data on the effect of changes in humidity on the colour of dyed natural and synthetic textile fibres [12].

Environmental conditions must be specified and continually controlled so as to minimise colour measurement variation for all samples to be evaluated.

6. The densitometer filter dilemma

The final selection of a densitometer or density measurement filter set is still bewildering and the choice is often based on arbitrary judgements rather than matching the ink spectral characteristics to the colour filter spectral responses in order to fulfil the main function of a densitometer - ink film thickness measurement for printing process control.

The variety of standard filter sets, Status E, T or I is a barrier to global standardised printing. This is especially the case in recent years, since the ISO 2846 1-5 ink standards for the different print processes mean that the basic colorants, pigments and spectral curves are almost the same, whichever conventional printing process is involved. The spectral curves for each of the cyan, magenta, yellow and black process inks used in the sheet-fed and heat-set offset, coldest offset (newspaper), gravure, screen and flexography printing processes are shown below:

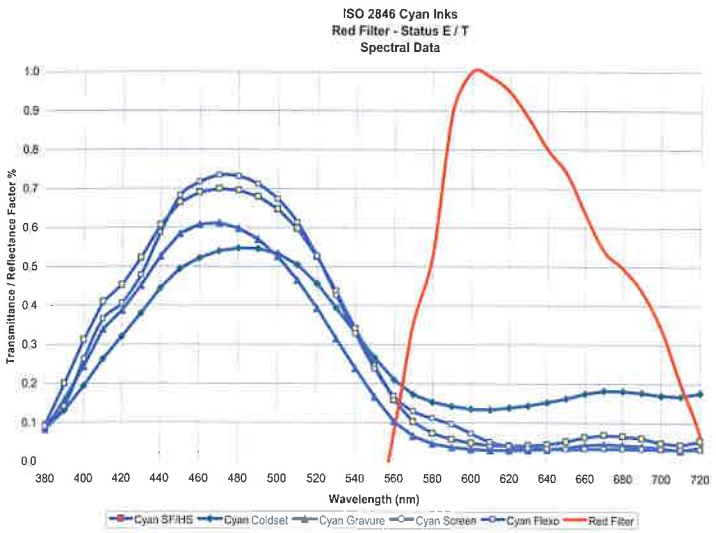


Figure: 2 ISO 2846 cyan ink spectral data and ISO 5-3 status E/T filter response

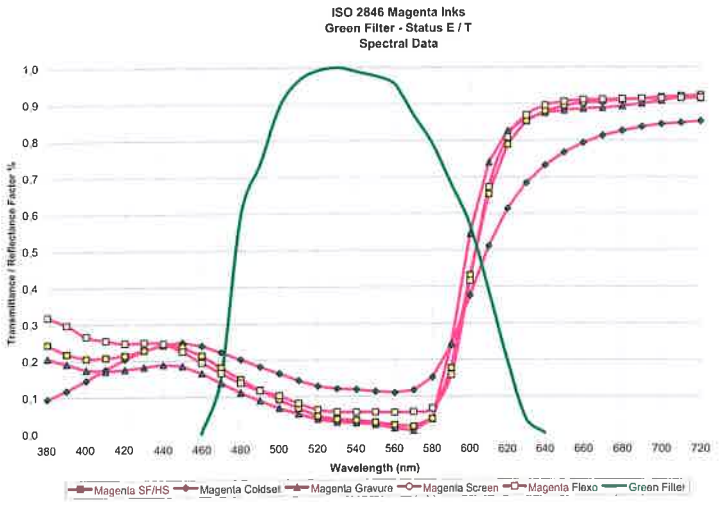


Figure 3:
ISO 2846 magenta ink spectral data and ISO 5-3 status E/T filter response

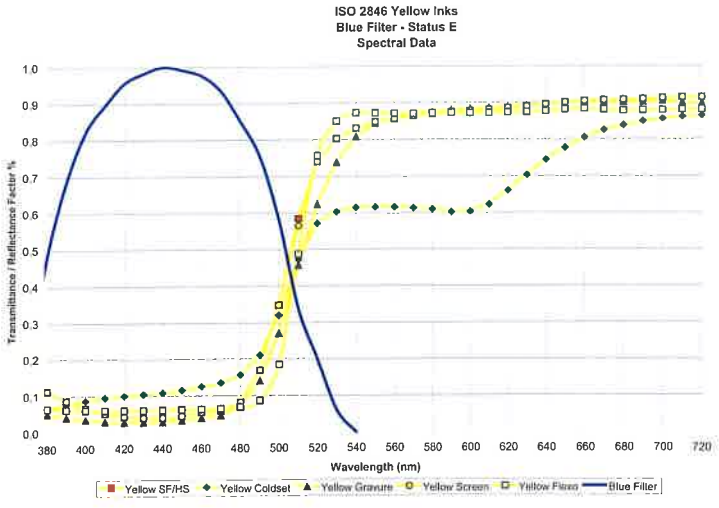


Figure 4:
ISO 2846 yellow ink spectral data and ISO 5-3 status E filter response

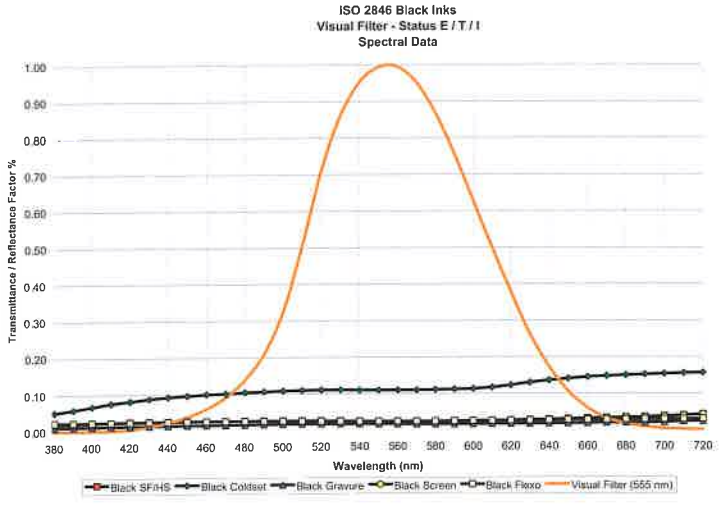


Figure 5:
ISO 2846 black ink spectral data and ISO 5-3 status visual filter response

The data for these spectral response curves is given in the recently revised ISO 2846 series of standards and are measured according to a D50 light source (0°:45° geometry, 2° observer, absolute measurement). It is unknown if the spectral curves would appear very different to a densitometer's light source, illuminant A, or another standardised light source.

In effect, a single class of densitometer filter set would work well for all the standard inks and common paper types encountered in both commercial and newspaper printing. A common agreement on ISO status E colour filter response would satisfy process control requirements for ISO 2846 1-5 standard process inks.

ISO 14981:2000 and ISO 13656, which are for densitometer print process control and related specifications for polarising filter performance, should be revised to point to ISO 5-3 [13] and stipulate the ISO status E filter set with additional UV and polarising filters.

References

1. http://www.ceram.com/colour-standards
2. Compton, Spring 1984, J.A. "The Thermochromic Properties of the Ceramic Colour Standard", in Color Research & Application, 9 1, pp. 15 - 22.
3. Reniff, L., October 1994, "Transferring the 45/0 Spectral Reflectance Factor Scale", in Colour Research and Application , 19, 5, pp. 332 - 340.
4. Beretta, Giordano, 1999, "Spectrophotometer Calibration and Certification".
5. As for reference 10.
6. Anon, 1998, Konica Minolta "Precise Color Communication".
7. Fairchild, M.D. and Grum, F., November 1985, "Thermochromism of Ceramic Reference Tiles", in Applied Optics, 24, 21, pp. 3432 - 3433.
8. Hiltunen, J., 2002, "Accurate Color Measurement", Uni. of Joensuu, DoP, Väisälä Lab.
9. McCormick-Goodhart, M., and Wilhelm, H., 2000, Wilhelm Imaging Research, "Humidity-Induced Color Changes and Ink Migration Effects in Inkjet Photographs in Real-World Environmental Conditions", IS&T's NIP16:2000 Int. Conference on Digital Printing Technologies.
10. Image Permanence Institute, 2004, "A Consumer Guide to Traditional and Digital Print Stability", http://www.imagepermanenceinstitute.org/shtml_sub/consumerguide.pdf (Good bibliography.)
11. Indigo Technology, "Digital Offset Technology", www.colorline-usa.com/Digital_Offset_color.pdf
12. Butts, K., 2002, Datacolor International, "Effects of Relative Humidity Variation on Measured Color", http://www.datacolor.com/index.php
13. ISO 5-3:1995 Photography - Density Measurements - Part 3: Spectral Conditions.

Causes of matt/gloss effects ("ghosting") in sheet-fed offset

Uwe Bertholdt, Gina Sommer

Fogra e.V. Forschungsgesellschaft Druck
Streitfeldstrasse 19
D-81673 München, Germany
E-mail: bertholdt@fogra.org

Abstract

Ghosting in sheet-fed offset printing refers to both matt/gloss effects and back side yellowing. These image defaults are caused by aldehydes liberated during the oxidative ink drying within the printed stack after the print run. The focus of this work is on matt/gloss effects. A laboratory method, which shows a very good predictive ability for production printing, could be developed to reproduce ghost effects. Slower drying inks ghost more strongly. Papers contribute to the occurrence of ghost effects through their influence on the drying speed of the inks. Drying of first side printing inks in the stack results in temporary pre-conditioning of paper sides to be perfected. Trials with paper prepared separately with hexanal demonstrate a correlation between hexanal and the appearance of the ghost effect. Tests about the drying speed of the inks show a faster drying on pre-conditioned paper. The contact phenomena known as ghost effects in sheet-fed offset printing thus result from varying in situ drying speeds of inks.

Keywords

Aldehydes, drying speed, ghosting, laboratory method, matt/gloss effects

1. Introduction

Ghost effects in sheet-fed offset printing first made an appearance with the emergence of high quality coated papers. These are reverse-side yellowing on the one hand and matt/gloss effects on the other hand. Reverse-side yellowing especially occurs on the blank reverse-sides of print jobs, where the front of the underlying sheet in the pile has been printed. Here, the image of the front shows up yellow on the reverse-side of the sheet lying over it. Matt/gloss effects normally occur in uniformly strong (dark) printed images as matt or glossy areas that exhibit the image of the print on the back of the sheet. Here too, marking occurs in the solid tone areas through contact of the respective printed front and reverse sides of consecutive sheets in the pile. The term "ghost" originates from both the light marking and the unpredictable occurrance of the phenomenon under seemingly constant conditions.

The oxidative drying process of sheet-fed offset inks results in the liberation of aldehydes due to side reactions [Schreiner 1957, Tremain 1957]. According to more recent investigations using simulator molecules for the wide variety of different natural fatty acids to be used as backbones of oxidative drying ink vehicles a huge variety of different small molecules was identified as side products of drying ink films [Muizebelt et al. 1997].

Simulations of the interactions between drying ink films in front and reverse printing in piles of paper resulted in the identification of both acceleraton and deceleraton of drying speeds for the ink. Acceleration was caused by volatile side products of the oxidative drying process in the early stages of the reaction (possibly peroxides), while deceleration originates from non-volatile side products (possibly organic acids) evolving during later stages of the drying process [Hartsuch 1960].

Time intervals between front and reverse side printing were found to be decisive for the occurance of matt/gloss effects [Schreiner 1967].

The ghost effects in sheet-fed offset printing may be avoided by separation of the printed sheets after printing [Schreiner 1967] and might sometimes be eliminated by varnishing.

2. Methods

2.1 Press run

The printing test was carried out on a sheet-fed offset-printing press, HEIDELBERG Speedmaster CD 74-5. The printing forme contained 200% and 300% solid tones and was subdivided into four sections allowing for different reverse-side printing intervals between the printed front-side and the blank reverse-side. Thus, print runs with very short contact time (front and reverse-side printing within a few hours in two print passes), as well as such with one, two and three days reverse-side printing intervals were performed. According to industry experience two black inks and three papers forming one conspicuous, two inconspicuous and three differing mixed combinations were tested. The press run was performed at 21°C and 50% relative humidity.

2.2 Simulation method

Test prints were carried out using a *prüfbau* printability tester. Two different printing formes were used (Figure 1), the one for the first test print (out of two per test) printed two stripes, the second was a standard forme. The amount of ink applied was fixed at 2,5 g/m². The first test print (two stripes) was carried out, and after an initial ink setting of 5 minutes this test print was covered by an unprinted paper stripe of the same paper quality. Both were stored as a sandwich in a pile of copy paper (10 cm high) for a defined time (perfecting interval). The second test print was performed using the paper stripe stored with the first test print and using the paper side having been in contact with the printed side of the first test print. Both the first and the second test print were arranged again to form a sandwich after an initial ink setting of the second test print (5 minutes) and again stored in the pile of copy paper for a defined time (converting interval). Visual evaluation of the second test print was performed. All test printing was conducted at 21°C and 50% relative humidity.



Figure 1: Printing formes of the prüfbau printability tester: left forme for 1st test print, right forme for 2nd test print

2.3 Visual assessment

Visual evaluations took place using CIE illuminant A with an illumination angle of 45° from the back of the evaluator and an illumination of 1400 lx at the sample surface. The samples were tilted in order to maximize the contrast. Print samples and test prints were evaluated by pair-wise comparison. Eleven levels of chemical ghosting were identified. These were arranged to form a visual assessment scale to be used for further evaluations.

2.4 Drying time determination

The drying times of inks 4 - 9 were determined using test prints with an ink film of 2,5 g/m² printed on aluminium coated paper and a *prüfbau* drying time tester.

2.5 Oxygen consuption during ink drying

12 test prints with an ink film of 1,8 g/m² each were placed in a glass vessel with a volume of 661 ml. An oxygen sensor of the company Electrovac was used to determine the decrease of the oxygen content in the closed vessel.

3. Results

3.1 Press run

Figures 2 and 3 show typical results of the press run after a converting interval of 24 hours. It is clearly recognisable that the individual ink/paper combinations have differing tendencies with regard to the development of ghost effects. It becomes clear that the effects increase significantly with increasing layer thickness of the ink. Further, the effects increase significantly from the front- and reverse-side printing towards the second reverse-side printing. A decline in ghosting was indicated after the second and third reverse-side printing.

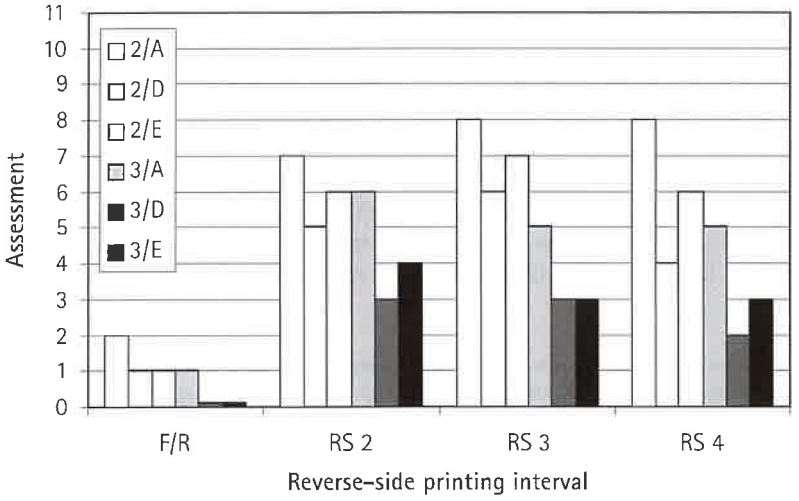


Figure 2: Assessment of printed sheets with area coverage of 200% depending on the perfecting interval (inks 2 and 3; papers A, D, E; F/R: immediate perfecting, RS 2, 3, 4: perfecting after 24, 48 and 72 hours respectively)

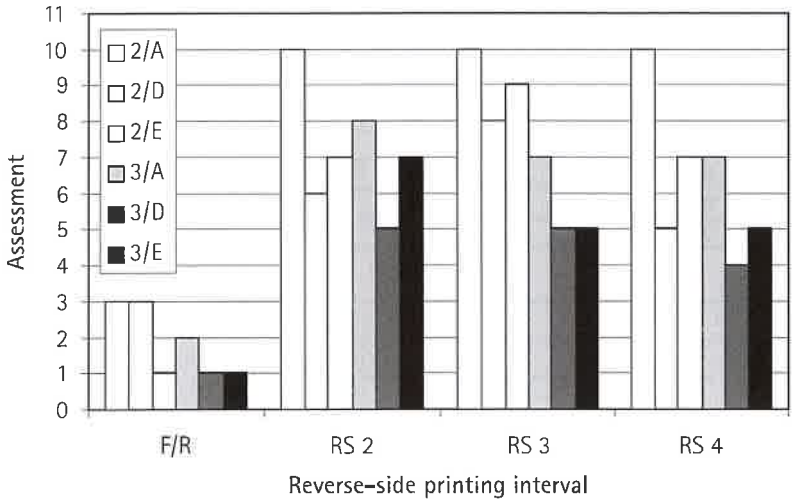


Figure 3: Assessment of printed sheets with area coverage of 300% depending on the perfecting interval (inks 2 and 3; papers A, D, E; F/R: immediate perfecting, RS 2, 3, 4: perfecting after 24, 48 and 72 hours respectively)

3.2 Comparison of the results of the press run with the simulation method

In order to test the reliability of the simulation method, test prints were produced in all material and time combinations of the production printing trial and assessed. For each material combination the assessments were compared for each combination of perfecting and converting interval and were found to be of good concurrence. Table I lists the sum of the ghost evaluations of each material combination.

Table I: Ink/paper matrix of commercial inks and papers that were used in the laboratory tests and in the printing test and their assessment

Test prints			Production prints		
Ink	Paper	Assessment (totalled)	Ink	Paper	Assessment (totalled)
2	A	32	2	A	33
3	A	23	3	A	24
2	D	21	2	D	22
3	D	16	3	D	15
2	E	22	2	E	24
3	E	15	3	E	18

The good concurrence of the results allowed reliable investigations using the simulation method.

3.3 Investigation of model inks with graduated compositions

In order to be able to examine the influence of different ink components, black inks with graduated compositions were investigated using the simulation method and paper A. The composition of the inks is summarized in Table II, and the results of the ghosting evaluations for the 24 hours converting interval is given in Figure 4.

Table II: Composition of model inks (Co: elementary content of cobalt from cobalt octoate; Mn: elementary content of manganese from manganese octoate; HQ: content of hydroquinone; BHT: content of 1,6-di-tert-butyl-4-methylphenol; L: content of linseed oil or linseed oil alkyd; S: content of soy oil or soy oil alkyd; T: content of tung oil; FAE: presence of fatty acid ethyl ester; M: presence of mineral oil)

	drying-catalysts [%]		drying-inhibitors [%]		varnish [%]			oil		
ink	**Co**	**Mn**	**HQ**	**BHT**	**L**	**S**	**T**	**FAE**	**M**	**oxidative drying**
4	0,04	0,13	0,27	-	40	-	-	+	+	+
5	0,01	0,0325	0,27	-	40	-	-	+	+	+
6	0,065	-	0,27	-	40	-	-	+	+	+
7	-	0,13	0,27	-	40	-	-	+	+	+
8	0,04	0,13	-	0,03	40	-	-	+	+	+
9	0,04	0,13	-	-	40	-	-	+	+	+
10	0,04	0,13	0,27	-	14	-	-	+	+	+
11	0,04	0,13	0,27	-	-	11	-	+	-	+
12	0,04	0,13	0,27	-	14	-	12	+	+	+
13	0,04	0,13	-	-	-	-	-	+	-	-
14	0,04	0,13	-	-	-	-	-	+	+	-

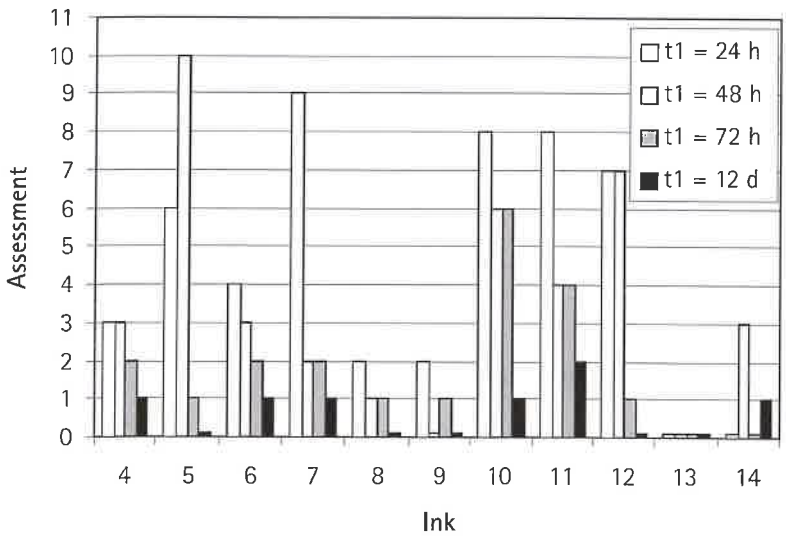


Figure 4: Assessment of sandwiches printed with model inks after a conversion interval of 24 hours depending on the perfecting interval t1

For all conversion intervals, the inks 5, 6, 7, 10, 11 and 12 show clear ghost effects. With an increasing perfecting interval, the ghost effect normally becomes less pronounced for all inks of this comparison series. Already after a perfecting interval of more than 24 hours, the occurrence of the ghost effect begins to recede.

The inks 4 to 9 belong to an ink group, in which only the amounts of the drying catalysts and drying inhibitors were varied. This leads to differing drying speeds and differing delays in the onset of drying of the inks. The occurrence of the ghost effects using inks 4 to 9 correlates well with the drying speeds and delays in the onset of drying such that quicker drying and earlier onset of drying lead to weaker ghost effects. This is further demonstrated in Figure 5.

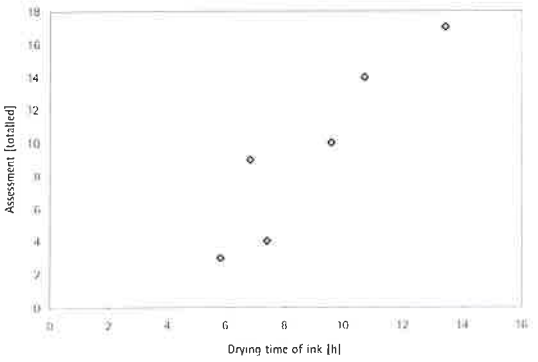


Figure 5:
Drying times of inks 4 - 9 vs. totalled ghost assessments for the conversion interval of 24 hours

The types and percentages of the drying oils were varied in the other ink group (10, 11, 12). The oil types differed especially in the number of multiple bonds in the carbon chain, in whose immediate vicinity the chemical (oxidative) drying reaction occurs. Tung oil dries faster than linseed oil and both dry much faster than soybeen oil. Somewhat unexpectedly, no distinctive dependence on the type of natural oil is displayed here.

Inks 13 and 14 contain no drying components and show no (ink 13) or distinctly weak ghosting (ink 14) in comparison.

When the influence of the different inks on the development of the ghost effect at constant perfecting intervals and variable converting intervals is compared, it becomes clear that as a rule, the ghost effect for all inks of this comparison series increases with a raising converting interval.

3.4 Infuence of drying times on the occurance of ghost effects

Test prints of the commercial inks 2 and 3 and the commercial papers A and D were investigated with respect of drying times using a closed vessel and an oxygen sensor. Figure 6 shows the decreasing oxygen content in a closed vessel for the ink/paper combinations 2/A (strong ghosting) and 3/D (medium ghosting). Combination 3/D consumed lesser oxygen in a shorter time and with a shorter onset than combination 2/A and therefore dries more quickly. Figure 7 shows combinations 2/A (strong ghosting) and 2/B (lesser ghosting). Here, also the quicker drying combination showed the lesser ghosting. In addition a possible reason for a paper influence is indicated. Figure 8 shows combination 2/A where the test prints were performed both on fresh paper and on paper having been in contact with drying ink from a print (like in a pile of paper). This comparison indicates a more quick drying of ink on paper having been in previus contact with drying ink.

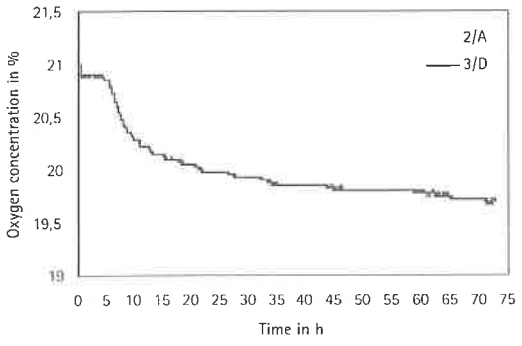


Figure 6:
Comparison of the decline in the oxygen concentration during the oxidative drying of two ink/paper combinations

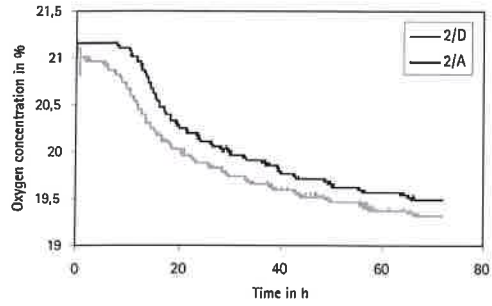


Figure 7:
Temporal decline of the oxygen content of paper A and paper D with ink 2

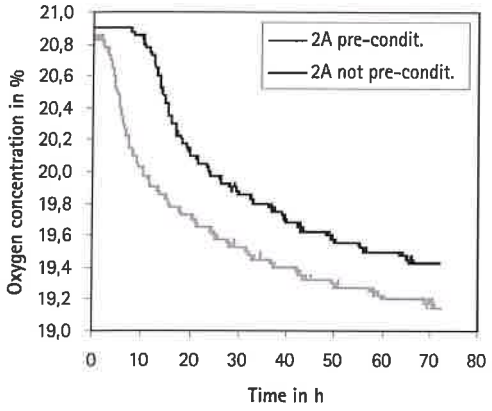


Figure 8:
Temporal decline of the oxygen content in the print samples on pre-conditioned and unconditioned paper A

3.5 Influence of aldehydes on chemical ghosting and ink drying times

A transition of aldehydes was identified from drying ink films to unprinted papers within a pile of paper by means of GCMS. In order to put the aldehydes directly in connection with the occurance or increasement of chemical ghosting, tests based on the simulation method with prepared papers were carried out. In this context, fresh paper A was selectively coated in situ with a 10% solution of hexanal. After evaporation of the solvent, printing with ink 2 as well as a 24h pre-conditioning and subsequent printing and 24h storage over another test print was carried out. Table III contains the ghosting assessments in dependance of the hexanal volume.

Table III: Assessment of chemical ghosting on paper A after preconditioning with hexanal

Hexanal volume [µl]	1	2	3	4	5	10
Assessment of directly printed paper	-	8	8	9	10	11
Assessment after pre-conditioning of printed paper	0	2	-	-	6	8

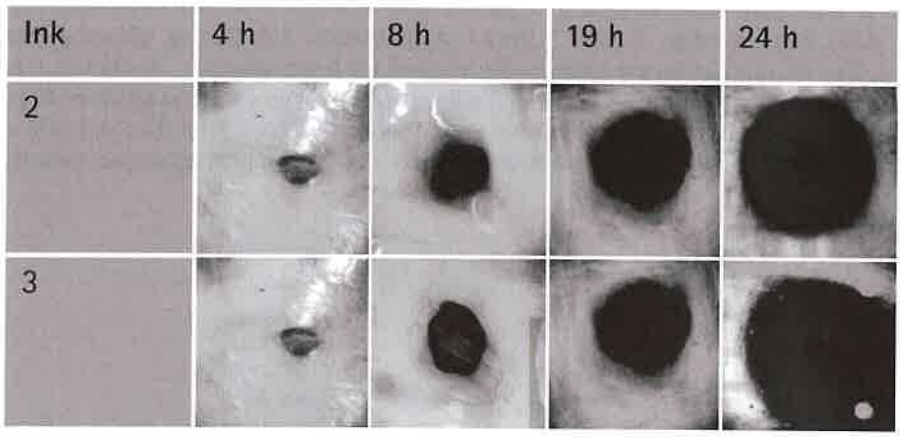


Figure 9: Ink dried in situ with hexanal vapores on previously completely inked in glass plates

To test the acceleration of drying of ink layers through aldehydes an old test [Hartsuch, 1960] was adapted in the way that ink layers (thickness 2.5 µm analog to the test prints) were applied on the surface of glass plates and these placed as upper plates in glass plate sandwiches (two glass plates, held at a distance of 3 mm using separators). Here, instead of ink films, hexanal drops (volume 10 µl) were applied to the lower glass plates using inks 2 and 3. The test times were 4, 8, 19 and 24 hours. After opening the sandwiches, the ink layer was wiped off with a dry cloth. The ink film opposite the hexanal drop had always dried and adhered to the glass plates; in the other areas the ink had not dried and could be wiped off. The size of the circular and dried ink areas increased with increasing test duration and was larger at least for ink 2 as against ink 3 after 4 and 19 hours.

The acceleration of the ink drying by aldehydes results from the cobalt or manganese catalized slow radical oxidation of the aldehydes thus delivering radicals to speed up the ink oxidative drying [Maslov, Bluymberg, 1976].

4. Conclusions

The development of ghost effects can be described as follows. Front-side printing emits aldehydes during the drying of ink after a certain induction phase. These are absorbed by the reverse-side of the opposite sheet (pre-conditioning, Fig. 10).

After reverse printing, the image-related drying accelerators already present on or in the reverse-printing side accelerate the drying of the freshly applied ink at the interface paper/ink effectively from below. This early drying of the underside of the ink film can thus hamper or prevent a possible later levelling of the entire ink film i.e. adaptation to the surface profile of the paper as well as late setting). Simultaneously, aldehydes still degassing from the front side can accelerate the surface drying of the ink in the area of the later ghost image and also result in a quicker film formation here (Fig. 11).

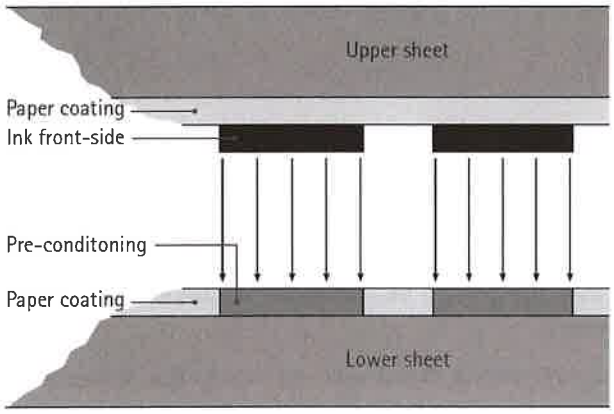


Figure 10: Situation after front-side printing and turning of the pile. Front-side pre-conditions reverse-side

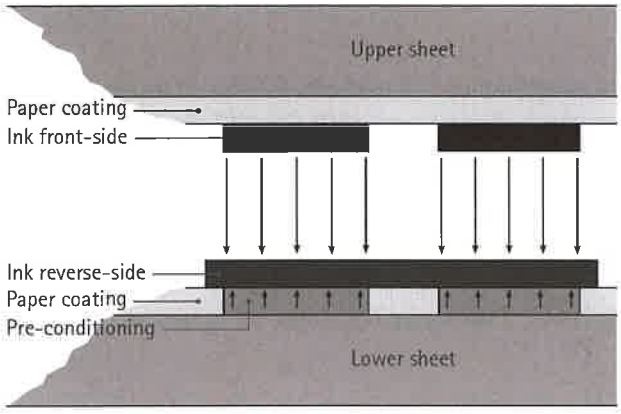


Figure 11: Selectively accelerated drying of ink

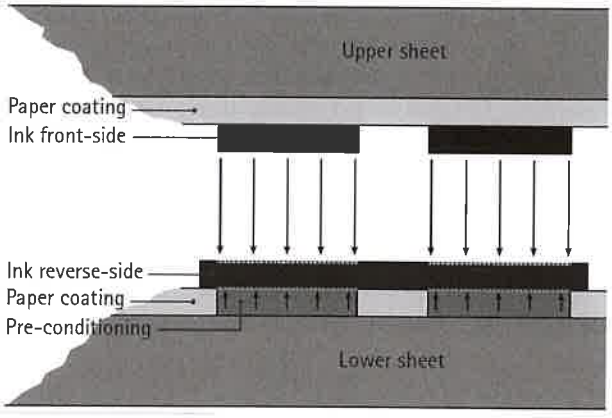


Figure 12: Ghost effect

The faster dryed sections of a bigger printed area will consequently show a smoother surface, which leads to stronger reflection (and lower scattering) of incident light, and the ghost areas thus appear to be darker.

Evidently, slow oxidative-drying inks of the same binder composition are therefore more predestined to give rise to matt/gloss effects as their faster drying equivalents, because the (front-side image dependent) drying acceleration - on a relative scale - can have a stronger effect for slow drying inks in comparison to their faster drying counterparts. The drying acceleration can apparently be attributed to the degassing aldehydes in the oxidative ink drying.

Contact appearances in sheet-fed offset printing known as ghost effects thus result from different in situ drying speeds of the inks.

Acknowledgements

We thank M-Real Zanders (Bergisch Gladbach) and Lecta Germany (Munich) for their donations of paper for the printing tests.

We are obliged to Epple-Druckfarben (Neusäß) and Flint Group Germany (Stuttgart) for providing printing inks for the test and production prints and specially Michael Huber Munich for the manufacture of specimen printing inks with graduated compositions.

We also express our thanks to Electrovac (Klosterneuburg) for providing an oxygen sensor.

This project was supported by funds from the budget of the Federal Ministry of Economics and Technology (BMWi) through the Association of Industrial Research Institutes (AiF, No 14366N).

References

1. Schreiner, (1957), Härtungseffekt bei Caseinstrichen, FOGRA-Mitteilungen, 13, p 1 - 3
2. Tremain, (1957), "Odourless" alkyds, Journal of the Oil and Colour Chemists Ass., 40, p 737 - 740
3. Muizebelt et al., (1997), Mechanistic study of drying of alkyd resins using (Z,Z) - and (E,E) - 3,6 nonadiene as model substance, Progress in Organic Coatings 31 p 331 - 340
4. Hartsuch, (1960), Drying of overprinted ink films, TAGA Proceedings, p 47 - 54
5. Schreiner, (1967), Unerwünschte Glanzbildung bei Mehrfarbendrucken, München: FOGRA, (5.003), Instituts-Mitteilung
6. Maslov, Bluymberg, (1976), Liquid-phase Oxidation of Aldehydes, Russian Chemical Reviews 45 (1976) Nr. 2, S. 155 - 167

Measurement possibilities of interference layers on a paper

Marta Klanjšek Gunde[1], *Maša Žveglič*[1], *Nina Hauptman*[1], *Gorazd Golob*[2]

[1] National Institute of Chemistry
Hajdrihova 19, SI-1000 Ljubljana, Slovenia
E-mail: marta.k.gunde@ki.si

[2] University of Ljubljana, Faculty of natural Sciences and Engineering
Department of Textile, Snežniška 5, SI-1000 Ljubljana, Slovenia

Abstract

Extended interference films can form optically variable devices which are highly important in optical document security area. A layer with similar properties can be deposited also on a paper substrate. We present here that such a layer may show an iridescent colour due to interference of light waves. If the layer is applied on a black substrate, the effect is very clearly seen and can be recorded in reflectance spectrum also by standard measurement geometry applied in printing industry. Much trouble happens on the white substrate where special measurement equipment is needed to measure the interference effect. The optical properties of reflection on such a considerably irregular interference sample are studied and the measurement possibilities to resolve the interference effect are analysed in particular. The possibilities to measure the layer thickness are shown as well.

Keywords

Interference layer, iridescent colour, reflectance measurement

1. Introduction

Most of objects in our surroundings show a colour that does not vary significantly with viewing angle. This is the effect of microscopic randomness, the common state of matter, which gives rise to diffuse reflectance and colour constancy. Such a colour is named an optically invariable colour. When material have a considerable degree of order on the scale of wavelength of the visible light, the interaction with light might cause iridescence that depends on observation and illumination angles. One of the most important properties of such an object is that its colour cannot be represented by diffuse (intrinsic or optically invariable) colours. Such ordered matter is frequently named also optically variable matter. It is applied in the so-called optically variable devices which play an important role in optical document security because such visual effects are impossible to be copied by any photographic technique [van Renesse, 2005]. Such a device could be either a grating or an interference structure which both provide special interaction with visible light, giving the iridescent or rainbow colours.

We are interested here in interference layers, i.e. a colourless material which gives iridescent colours due to reinforcement and extinction of light waves successively reflected from the front and rear surfaces of a thin layer. It may happen on flat surfaces of a transparent layer if it is thin and uniform enough so that the path differences between subsequent reflections does not exceed the coherence length of the light source. For white light this length is a few micrometers.

The phenomenon is known from Newton's time and remains one of the basic principles in modern optics [Born and Huang, 2006; Fowles, 1989]. It can be found in several industrial applications serving for functional purposes such as security printing and optical filters as well as for decorative purposes such as cosmetics, eye-catching promotional and automotive applications. Transparent extended films are required for most application in the first group whereas the so-called effect paints are applied in the second group. Here, the effect is achieved on interference (iridescent) pigment particles inside a suitable binder.

The optical properties of interference pigments and effect paints are reasonably well studied due to their broad application area [e.g. Bolomey and Greenstein, 1972; Pfaff and Reynders, 1999; Nadal and Early 2004; Hupp and Dörsam, 2007]. Most research is devoted to goniometric measurement geometry and its suitability to control the product where an effect paint or ink was applied.

Our research was focused on extended interference film, a transparent non-scattering and non-absorbing uniform layer with submicrometer thickness which was applied on a paper substrate. The basic question was what result we obtain by standard spectroscopic measurement techniques that are widely applied in graphic technology. A paper substrate is not an optically flat surface required for interference filters or in security printing application. Therefore the measurements and procedures well known from this area might not be appropriate for an adequate application. Spectrophotometric measurements were done with standard measuring geometry which serves to control process colour inks and more sophisticated geometry for research in the area of optically invariable colours. Reflectance spectra were measured also at specular (mirror) conditions. The comparison of results, obtained this way, show under which circumstances the effects of iridescent colour on a paper substrate can be measured and quantified.

2. Methods

Transparent interference layers were prepared on black and white matt paper (180 g/m^2). A clear lacquer was used for this purpose. The thickness of the layer was kept well below 1 μm, so that the interference of light reflected successively from the front and rear surfaces of the transparent layer could produce iridescent colours.

The appearance of equally thick layers applied on the black substrate is completely different from that on the white one, as seen by naked eye. The iridescent colours are seen very clearly and easily on the black background whereas on the white paper a very large viewing angle and well-directed illuminating light have to be applied to observe the colour. The interference effect on these two layers showing blue iridescent colour was analysed by spectral reflectance in different measuring geometries. Two spectrophotometers, the EyeOne (GretagMacbeth) and the Lambda 950 (Perkin-Elmer) were applied for this purpose. The latter was equipped with two accessories, the integrating sphere and the variable angle reflectance accessory. Four measurement geometries achieved this way are shown in Figure 1.

The standard measuring geometry (45°:0°) was measured applying the EyeOne (GretagMacbeth) spectrophotometer. A beam of directional light is incident on a sample surface at 45° and the amount of light reflected in 0° reflection angle is measured (Figure 1a). This is standard spectral measurement geometry which is frequently used for quick measurements in graphic technology. The EyeOne measures only in the visible part of the spectrum (380-730 nm).

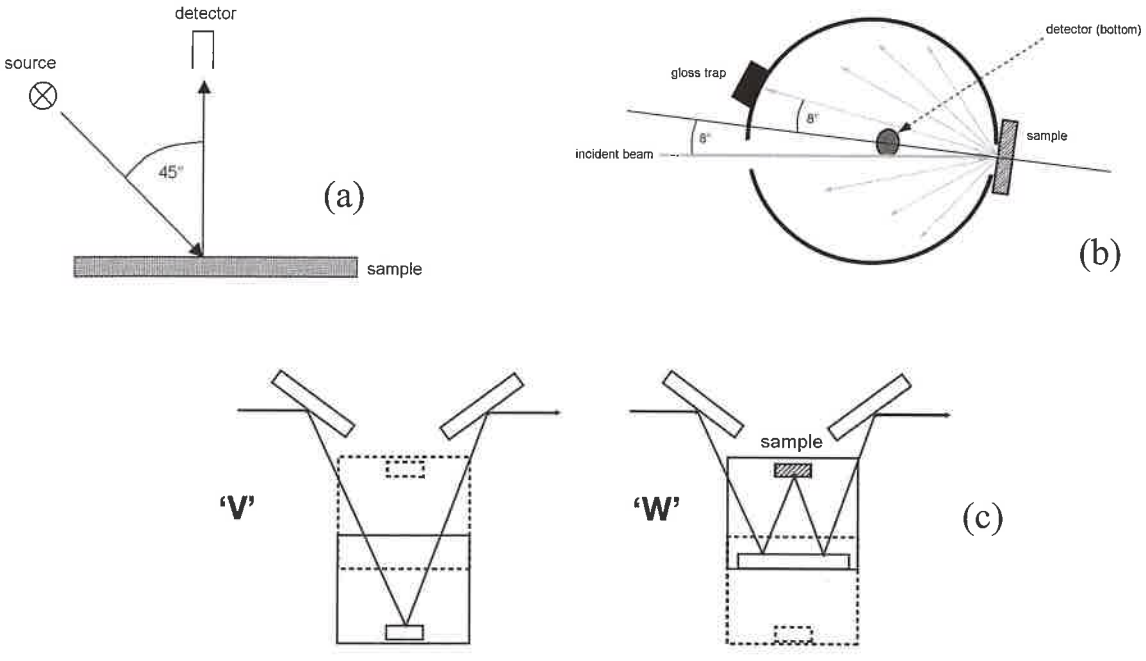


Figure 1: Sampling arrangement in the applied measuring geometries: (45°:0°), (a); total reflectance (8°:di,) (b); and absolute specular reflectance - VW method, (c). The diffuse reflectance (8°:de) was measured in geometry (b) with opened gloss trap

The Lambda 950 (Perkin-Elmer) spectrophotometer equipped with integrating sphere enables the total reflectance (8°:di) and its diffuse part (8°:de) to be measured (Figure 1b). The notation (8°:di) means the light impinges at 8° angle and reflected diffusely, the specular component is included. The (8°:de) measurement geometry is different only in specular component which is excluded when the gloss trap is opened (Figure 1b). Both measurements are possible applying integrating sphere. Such laboratory measurements are used for precise analysis and research in the field of optically invariable colours. The integrating sphere applied in our research is 150 mm in diameter and has the reflective surface constructed by Spectralon®, a highly diffuse reflecting material. Specular reflectance spectra at 10°, 20°, 30°, 40°, 50° and 60° incident angles were measured on the same spectrophotometer applying the Universal reflectance accessory (URA, Perkin-Elmer) It was mounted in the Lambda 950 spectrophotometer instead of integrating sphere. The absolute reflectance is measured by the help of the V-W reflectance geometry (Figure 1c). The incidence angle can be varied between 8° and 70° by proper adjusting the direction of the two side mirrors. The Lambda 950 spectrophotometer was applied in the 200-1500 nm spectral region in 2 nm steps. All spectral measurements were done on the blue colour shade on black and white backing. No polarization was used.

The topography of interference layers was analysed by scanning electron microscopy (SEM). The field emission microscope Karl Zeiss Supra 35 VP was applied for this purpose.

Reflection from a thin film on a substrate depends on coherent multiple reflections of the light beam inside the layer. The theory shows how the intensity of specular reflectance (i.e. if the incident angle is equal to the reflected angle) can be calculated from physical data of the layer and of the substrate. If all the interfaces are perfectly smooth, then the specular reflectance at angle α depends on layer thickness and refractive indices of the layer and the substrate. In general, refractive index is a complex quantity, where the real part (n) determines the refraction of light at the interface between vacuum and the considered medium, whereas the imaginary part (k) indicates the absorption of the light wave propagating through the material. In non-absorbing materials the imaginary part of complex refractive index is very close to zero and is usually neglected. The equation describing the reflectance of an interference layer on a substrate is the simplest for non-absorbing materials:

$$R = \frac{r_1^2 + r_2^2 + 2r_1 r_2 \cos\delta}{1 + r_1^2 r_2^2 + 2r_1 r_2 \cos\delta} \tag{1}$$

where δ is the phase change of the beam with incident angle α and wavelength λ when traversing transparent film with thickness d and refractive index n_1:

$$\delta = \frac{2\pi d}{\lambda}\sqrt{n_1^2 - \sin^2\alpha} \tag{2}$$

r_1 and r_2 are the Fresnel's amplitude reflection coefficients for the air-layer and layer-substrate boundaries, respectively. The r_1 depend on n_1 and α, the r_2 depend on n_1, n_2 (refractive indices of the layer and of the substrate, respectively) and α. Both reflection coefficients, the r_1 and r_2, are independent on λ. The positions of interference maxima and minima can be derived from Equation (1) by differentiating with respect to λ. This way a simple formula is obtained that express the thickness d as a function of the adjacent maximum (λ_{max}) and minimum (λ_{min}) in the reflectance:

$$d = \frac{\lambda_{min}\lambda_{max}}{4(\lambda_{min} - \lambda_{max})\sqrt{n_1^2 - \sin^2\alpha}} \tag{3}$$

It has to be pointed out that all above equations are valid for non-absorbing materials only, what is hardly ever completely fulfilled. The layer is supposed to have uniform thickness d with no variation across the sample. Both boundaries of the layer are supposed to be perfectly smooth so that no light is scattered off of the beam direction which is defined by Snell's laws. The best approximation to such tight conditions might be optical interference filters and some special interference-based security structures [Fowles, 1989; van Renesse, 2005].

The refractive index of a transparent material (n_1) depends on λ and its imaginary part (k_1) is never exactly zero. Nevertheless, most transparent polymers have refractive indices in the visible spectral region between 1,4 and 1,5 and their value does not diminish appreciably from the shortest up to the largest wavelength in the visible region. The refractive index of the substrate n_2 - in our case the refractive index of a paper - is more complicated. There are only few data in the literature for refractive index of a paper. The most important and complete data were published recently for unprinted white paper and paper printed with different process

colours [Bakker, 2004]. According to these data, the refractive index n_2 of a white paper varies between 1,38 and 1,41 whereas the absorption coefficient k_2 from 0,04 up to 0,08. The black-printed white paper have similar real part of refractive index ($1,37 < n_2 < 1,41$) but much larger imaginary part ($0,2 < k_2 < 0,27$) [Bakker, 2004]. With these data the specular reflectance of a perfectly smooth and uniform layer on a paper can be calculated applying equation 1, if the absorption coefficient of the paper is neglected. The error made this way is very large for the white substrate, but even larger for the black one.

3. Results

SEM micrographs of cross-cuts (Figure 1) show that the interference lacquer layer is not perfectly bonded to the substrate. The bottom optical interface of the layer is not unique but consists of layer-paper and layer-air interfaces. The front and the bottom interfaces are not smooth. The thickness of the layer is also not perfectly uniform. Similar micrographs were obtained for thin layers on both substrates.

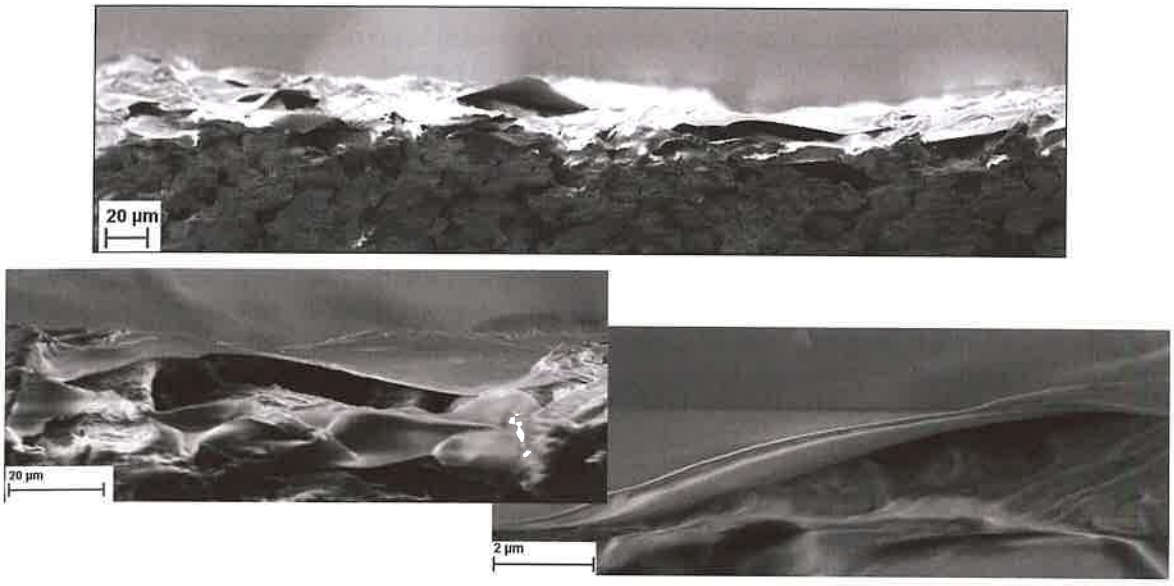


Figure 2: SEM micrographs of the interference layer on paper. The thickness of the layer is from 123 up to 288 nm (as measured on the bottom micrograph)

Reflectance spectra of the interference layer in the (45°:0°) and (8°:di) measuring geometries are shown in Figure 3. Similar reflectance of the black substrate was measured in both geometries. Interference fringes were obtained in reflectance spectra of the layer on black substrate in both measuring geometry. The interference effect is large in the (8°:di) geometry and much smaller in the (45°:0°) geometry.

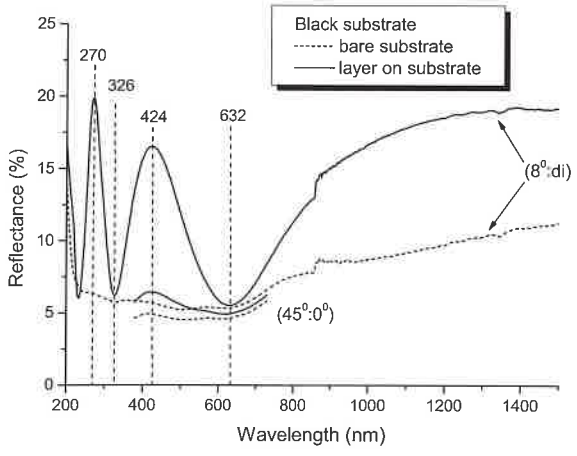


Figure 3:
Reflectance spectra of the interference layer on the black paper measured in the (45°:0°) and (8°:di) measurement geometries. Wavelengths of the successive interference maxima and minima are denoted on the picture

The positions of interference fringes shown in Figure 3 are not suitable enough to be applied in the equation (3) to calculate the thickness of the layer while the basic condition of specular reflectance is not fulfilled at all. This could be approached when the so-called gloss trap is opened (the (8°:de) geometry) and the difference between the (8°:di) and (8°:de) reflectance is calculated. This is the so-called spectral secular gloss, or more precisely, the spectral dependence of the specular gloss component. This spectrum is also shown in figure 4. The specular contribution to the total reflectance is very small compared to the diffuse reflectance. It indicates a large scattering of the light on both interfaces of the layer, the air-layer and the layer-substrate. The well-resolved first interference fringe (λ_{max} = 284 nm, λ_{min} = 342 nm) was applied in equation (3) to calculate the thickness d of the layer. Other data: n_l = 1,45, α = 8°. It gives d = 290 nm.

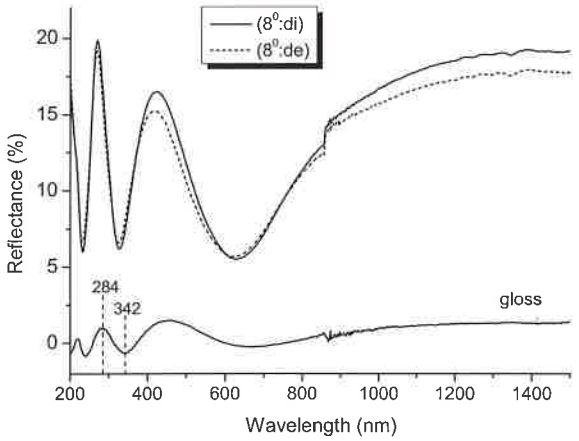


Figure 4: Reflectance spectra of the interference layer on the black substrate in total reflectance (8°:di) and in diffuse reflectance (8°:de) measurement geometry. The difference between them is the spectral specular gloss. The indicated wavelengths were applied in equation (3) to calculate the layer thickness

Reflectance spectra of the interference layer on the white paper are shown in Figure 5. They are completely different from that on the black paper. No interference fringes were obtained in both geometries, the (45°:0°) and (8°:di). Reflectance of the layer is very similar to the reflectance of the bare substrate. The effect could be assigned to the large diffuse reflectance of the white substrate which causes a large spread of the optical differences between the successively reflected light waves inside the interference layer. The effect is large also because of two types of bottom interfaces, layer-paper and layer-air (see Figure 1) which additionally spread the reflectance directions of the light waves at reflection on the bottom interface.

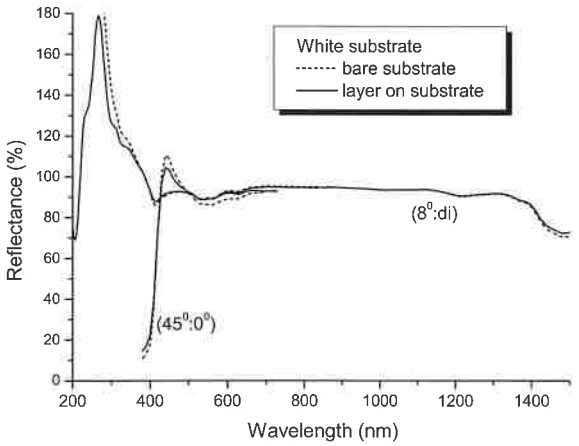


Figure 5: Reflectance spectra of the interference layer on the white paper in the (45°:0°) and (8°:di) measurement geometries

The specular reflectance spectra were measured applying a special reflectance accessory (URA) instead of integration sphere. The spectra of the bare black and white substrates are shown in Figure 6. The reflectance of the white substrate is higher than of the black one, but the difference is not as high as it is in the (45°:0°) and (8°:di) measuring geometry. The specular reflectance is low for both substrates due to surface scattering and is lower for the black substrate due to higher absorption. The specular reflectance of the black substrate increases with incident angle α. This is usual optical effect – at grazing angle the specular reflectance of perfectly flat surface approaches 100%. Such an effect was not obtained on the white substrate where the reflectance diminishes with α. It indicates that the white substrate gives rise to more complicated optical effects than the black one.

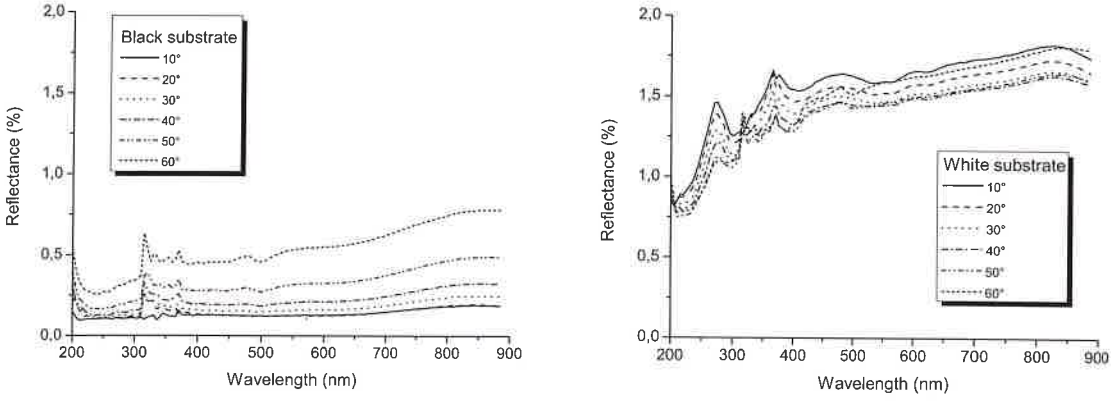


Figure 6: Specular reflectance spectra of the black (left) and white substrates (right) measured for the indicated incident angles

The specular reflectance spectra of the interference layer on both substrates are shown in Figure 7. As expected, the interference effect was obtained in both cases. Nevertheless, the specular reflectance tends to be higher for the layer on the black substrate where also the interference fringes are more clearly resolved. The reason for that could be similar as for the other non-specular measuring geometries applied in this study (see Figure 5). Some explanation could also be given on the basis of the optical peculiarities of the white substrate as shown in Figure 6.

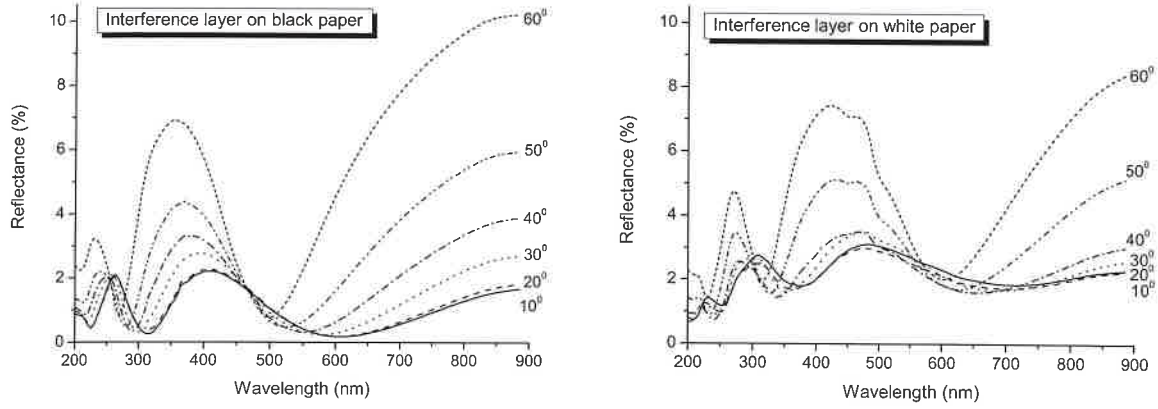


Figure 7: Specular reflectance spectra of the interference layer on the black (left) and white substrates (right) as recorded for the indicated incident angles

The first interference fringe (at $\alpha = 10°$ it is located at $\lambda_{max} = 260$ nm for the layer on the black substrate and at $\lambda_{max} = 310$ nm for the layer on the white substrate) was applied in equation (3) to calculate the thickness d of the layer. The thickness d calculated with position of this fringe slightly increases with α and gives values between 280 and 340 nm on the black substrate and between 310 and 400 nm for the white substrate.

4. Discussion

The theoretical approach that describes the specular reflection of the light on a supported interference layer (equation 1-3) requires several conditions to be valid. None of our measurement fulfils all of them. The samples are not perfect and could be hardly fitted into the required optical criteria. Specular reflectance measurements, which best approach the simplified theory, gives interference fringes that vary with angle. This shows that the sample is an optically variable one and confirms that its colour is really an iridescent one. The simplified theory cannot serve well for such a sample. This is evident through different thickness values that were calculated applying equation (3) for the same interference fringe in specular reflectance at different incident angles.

Some reasons for such a result are evident from SEM micrographs on Figure 1. The layer is not smooth, the bottom interface is not unique, and the substrate is rough and porous.

The thickness of the layer could be measured on SEM micrograph. The precise values obtained this way show thickness of the selected position on the sample. This procedure can give several results. The calculation of the thickness from reflectance spectra would give reasonable averaging over the beam spot of the light. The results obtained by our analysis are shown in Table I.

Table I: Thickness of interference layer, obtained by different methods. For the details see the text

Method	Layer thickness (nm)
SEM micrograph (Figure 1)	123 – 288
Spectral specular gloss, (Figure 4), $\alpha = 8°$, Eq. (3)	290
Interference fringes, black substrate, different α (Figure 7), Eq. (3)	280 - 340
Interference fringes, white substrate, different α (Figure 7), Eq. (3)	310 - 400

The interference effect is much more pronounced on the black substrate than it is on the white one. We may conclude that the diffuse reflectance at the bottom interface play an important role in diminishing the interference of the light waves. When the white paper is applied, the effect is so large that it can be observed only when the directional light in specular reflectance geometry is applied.

5. Conclusions

An interference layer on a paper show iridescent colour, which occur as a consequence of interference of light waves. The effect is clearly seen on a black substrate where it is obtained also in a diffuse lighting. When a similar layer is prepared on a white paper, a special observation condition and directional lighting is needed to see the effect.

The iridescent colour of a layer on a black substrate can be shown in all of the applied measurement geometries, the (45°:0°), the (8°,di), the (8°:de) and specular reflectance. This confirms that interfering light waves spread over a wide angle, but most of these waves are confined within a 45° cone. Therefore a small effect is obtained also beyond this angle and gives rise to slightly pronounced spectral dependence of reflectance in the (45°:0°) measurement geometry. The absorption of the light on the layer-black paper interface prevent larger scattering of light and thus enable the interference effect to prevail in reflectance spectra.

It is very hard to measure the iridescent colour of a layer on a white paper. The strong light scattering on the layer-substrate interface prevents the effect to be seen in all measurement geometry but the specular reflectance.

None of the measured spectra obey the tight conditions of optical theory of interference on thin layer. This is especially true for the simplified non-absorbing approximation shown here. The extension of the theory towards complex refractive indices for the layer and for the substrate would solve one of the assumptions. Our study was performed on samples that possess appreciable microscopic randomness, so that the term "optically variable matter" could be questionable here. We have shown that the interference effect is still present and that it could prevail if the ordered material (transparent lacquer) is applied on a black paper.

Acknowledgements

We thank Miss Andreja Jelen for measurements applying EyeOne spectrophotometer.

Rerefernces

1. Bakker, J. W. P., Brynste, G., Arwin, H., (2004) *Determination of refractive index of printed and unprinted paper using spectroscopic ellipsometry, Thin Solid Films vol. 445-456, pp. 361 - 365*
2. Bolomey, R. A. and Greenstein L. M. (1972), Optical characteristics of iridescence and interference pigments, J. Paint Technol., vol. 44, No 566, pp 39 - 50
3. Born, M. and Wolf, E. (2006), *Principles of Optics, 7th (expanded) edition, 4th printing, Cambridge University Press, Cambridge, ..., first published 1959 by Pergamon Press Ltd, London*
4. Fowles, G. R. (1989), *Introduction to Modern Optics, Second Edition, Dover Publications, New York*
5. Hupp, H., Dörsam, E. (2007), *Quality control for printed interference colours – investigation for basic measurement geometry, Iarigai 2007, Session 8B: Special printing*
6. Nadal, M. E. and Early, E. A. (2004), *Color measurements for pearlescent coatings, Color Research and Applications, vol. 29, No 1, pp 38 - 42*
7. Pfaff, G. and Reynolds, P. (1999), *Angle-dependent optical effects deriving from submicron structures of films and pigments, Chem. Rev. vol. 99, pp. 1963 - 1981*
8. van Renesse, R. L. (2005), *Optical Document Security, Third Edition, Artech House Boston, London*

Index of authors

Adams, Richard M. 69
Anayath, Rajendrakumar 67
Antikainen, Hannele 91
Aspler, Joe 119
Aurela, Birgit 237

Bakke, Arne M. 365
Baumann, Reinhard R. 9
Behm, Katri 27
Bertholdt, Uwe 421
Beynon, David G. 181
Bjurstedt, Anders 137
Bollström, Roger 147
Bonev, Slavtcho 207
Bould, D. C. 299

Caballero-Aroca, José F. 381
Casagrande, Elena-Magdalena 245
Chagas, Lionel 397
Cheng, Hui-Wen 333
Chung, Robert 373
Claypole, T. C. 181, 299

de Gracia, Vicente 5, 19
Deng, Nina 119
Dubé, Martin 279
Dörsam, Edgar 263

Engisch, Lutz 9
Esteve-Taboada, José J. 381

Fardim, Pedro 155
Farup, Ivar 365
Fleming, Paul D. 289
Forsström, Ulla 231
Fournié, François 397
Fujisawa, Naoko 189

Gaal, Zoltan 129
Gane, Patrick A. C. 249
Gerstner, Philip 249
Golob, Goraz 209, 429
Green, Phil 405
Gregor-Svetec, Diana 209
Gundlach, Mark 69

Hakola, Elina 231
Hamblyn, Simon M. 181
Hamel, Jean 119
Hardeberg, Jon Y. 365
Hassissi, Nadia 397
Hauptman, Nina 429
Hervás-Juan, Juan 381
Hladnik, Aleš 341
Horvat, Romana 107
Horvath, Csaba 129
Hörner, Andreas 245
Hrehorova, Erika 289
Hsieh, Yung-Cheng 333
Hübner, Gunter 313

Iglesias, Juan Carlos 5, 19
Ilmonen, Anu 237

Jabrane, Tarik 279
Jahn, Stephan F. 9
Jeaidi Jawad, 279
Jewell, E. H. 299
Joyce, Margaret K. 289

Kaplanová, Marie 213
Kariniemi, Merja 237
Kaulitz, Thomas 263
Kawamura, Eiji 189
Kenttä, Eija 237
Kerekes, Katalin 129
Khoury, Elie 397
Klanjšek Gunde, Marta 429
Kortekangas, Atte 79
Koskinen, Jorma 231
Kuusipalo, Jurkka 195
Kuusisto, Olli 91
Kuznetsov, Yuri V. 323, 347

Lahti, Johanna 195
Lazar, Miha 341
Lestelius, Magnus 169
Lindqvist, Ulf 101
Löffler, Eva Maria 405

Manfred, Tony 119
Mangin, Patrice J. 279
Mejtoft, Thomas 37, 45, 55
Miettinen, Päivi 355
Moilanen, Pertti 101
Možina, Klementina 107
Muck, Tadeja 209, 213

Navarro-López, Andrés 381
Nordin, Åsa 37
Nors, Minna 27
Nurmi, Olli 79
Nylander, Kenneth 147

Oittinen, Pirkko 231
Olsson, Robert 169
Otáhalová, Lenka 213
Otero, Susana 5, 19
Ozaki, Yasushi 189

Rebros, Marian 289
Reinhold, Ingo 9
Ribes-Gómez, Emilio 381
Riordan, Michael 373
Roberts, S. R. 299

Packmohr, Sven 55
Pajukanta, Janne 91
Pajula, Tiina 27
Pap, Klaudio 273
Parent, Frédéric 119
Pekarovicova, Alexandra 289
Peltonen, Jouko 147
Pérez, David 5, 19
Petersen, Ingmar 313
Pfletschinger, Markus 313
Pihkola, Hanna 27
Prakhya, Sri 373

Prayagi, Kiran P. 67
Preston, Janet 147, 155
Put, Fons 389
Pykönen, Maiju 155

Saukkoriipi, Kristiina 355
Silvaani, Hanna 155
Sommer, Gina 421
Sundqvist, Satu 237

Toivakka, Martti 147, 155
Trichon, Amélie 397
Tuominen, Mikko 195

Viluksela, Pentti 27
Viström, Magnus 45

Wessman, Helena 27
Williams Andrew, 413
Williams, Scott 223
Wirnitzer, Bernhard 307
Wixforth, Achim 245

Yang, Li 169

Zheludev, Denis E. 347

Žiljak Vujić, Jana 273
Žiljak, Ivana 273
Žveglič, Maša 429

Also available from iarigai:



Advances in Printing Science and Technology - Vol. XXX
261 pages, full colour, hard cover, price 95,00 €

Advances in Printing Science and Technology - Vol. XXXI
253 pages, full colour, hard cover, price 95,00 €

Advances in Printing and Media Technology - Vol. XXXII
306 pages, full colour, hard cover, price 105,00 €

Advances in Printing and Media Technology - Vol. XXXIII
306 pages, full colour, hard cover, price 145,00 €

Advances in Printing and Media Technology - Vol. XXXIV
306 pages, full colour, hard cover, price 165,00 €

More information and orders at www.iarigai.org
or from: iarigai.office@grf.hr



Your partner in networking for the print and media research

iarigai
The International Association of Research Organizations
for the Information, Media and Graphic Arts Industries

Washingtonplatz 1, D-64287 Darmstadt, Germany

www.iarigai.org